National Research Council Canada
Conseil national de recherches Canada

NRC · CNRC

Canadian Journal of Fisheries and Aquatic Sciences

Journal canadien des sciences halieutiques et aquatiques

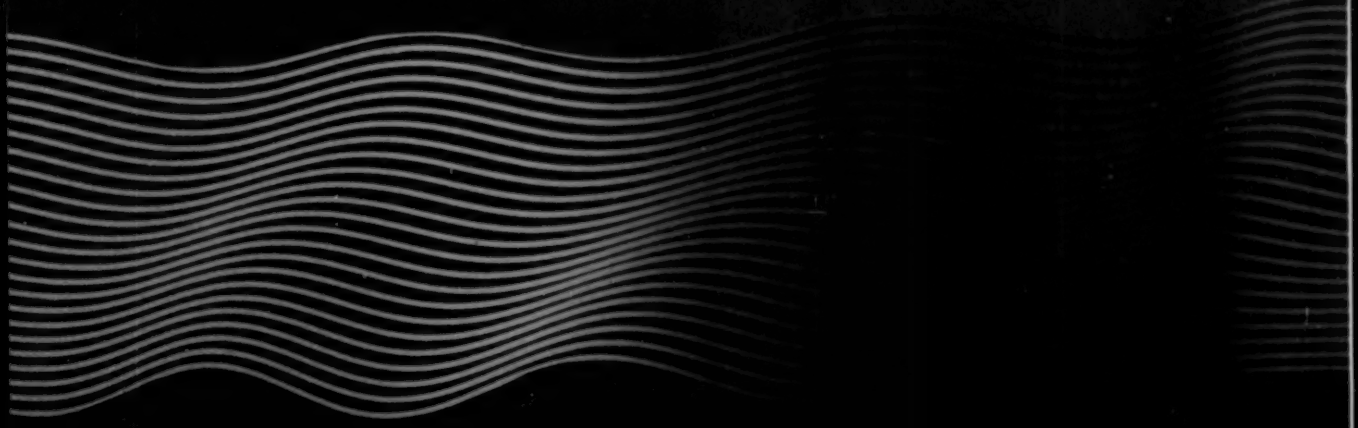

ISSN 0706-652X / CJFSDX 55(5) 1051–1306 (1998)

The *Canadian Journal of Fisheries and Aquatic Sciences*, previously published as *Contributions to Canadian Biology* 1901–1925, *Contributions to Canadian Biology and Fisheries* 1926–1934, *Journal of the Biological Board of Canada* 1934–1937, and *Journal of the Fisheries Research Board of Canada* 1938–1979, is issued monthly to form annual volumes of 12 numbers plus supplements.

Editorial policy: The Journal publishes original research articles, perspectives (syntheses, critiques, re-evaluations), discussions (comment and reply), and rapid communications. Manuscripts may concern cells, organisms, populations, communities, ecosystems, or processes that affect aquatic systems. They may cover a range of disciplines including biology and ecology of marine and freshwater organisms, limnology, oceanography, physiology, toxicology, genetics, economics, disease, and management. Preference will be given to manuscripts that emphasize understanding of observed phenomena and interpretation of experimental results. The Journal encourages papers that lead from clearly stated purpose or rationale and from testable hypotheses, concepts, or questions to identifiable conclusions or syntheses. Such papers may amplify, modify, question, or redirect accumulated knowledge embodied in contemporary perceptions of a particular state of aquatic sciences. The Journal discourages papers that are essentially descriptive, except in emerging disciplines; have only site-specific or local applications (a certain year, place, taxon, chemical compound, etc.); only confirm previously established principles; or apply standard techniques without breaking new methodological ground.

Manuscripts for publication should be submitted to the Editors, Canadian Journal of Fisheries and Aquatic Sciences, Department of Zoology, University of Guelph, Guelph, ON N1G 2W1, Canada (519-824-4120 ext. 2646; fax: 519-767-9798; e-mail: cjfas@uoguelph.ca).

Submissions in either English or French are acceptable. The information must be original, that is, not copyrighted, published, or submitted elsewhere except in abstract form or unless by written consent of the Editor. NRC accepts no responsibility for statements or opinions expressed by a contributor. Acceptance of an advertisement, announcement, or other material does not imply endorsement by either the *Journal*'s Editors or NRC. The use of proprietary names does not imply endorsement of the product or company.

Correspondence concerning accepted manuscripts and corrected proofs should be sent to NRC Research Press, National Research Council of Canada, Ottawa, ON K1A 0R6, Canada.

Instructions to Authors are published once a year in the first issue of each volume. Copies are available from NRC Research Press or from our Web site. The **Publication Policy** of NRC Research Press is also available at our Web site:
http://www.nrc.ca/cisti/journals/rj.html

Microfilm: Issues from 1934 through the current volume can be purchased on 16- or 35-mm microfilm. Photocopies of individual articles or issues can be purchased from University Microfilms International, 330 North Zeeb Road, Ann Arbor, MI 48106, U.S.A.

U.S. periodical postage paid at Champlain, N.Y., and at additional mailing offices. Attention U.S. POSTMASTER: Send address changes to **Canadian Journal of Fisheries and Aquatic Sciences**, c/o USACAN Media Distribution Center, P.O. Box 2888, Plattsburg, NY 12901, U.S.A.

Publié sans interruption depuis 1901, le *Journal canadien des sciences halieutiques et aquatiques* a paru sous plusieurs titres : *Contributions to Canadian Biology* 1901–1925, *Contributions to Canadian Biology and Fisheries* 1926–1934, *Journal of the Biological Board of Canada* 1934–1937, et *Journal of the Fisheries Research Board of Canada* 1938–1979. Le *Journal* paraît tous les mois, formant ainsi un volume de 12 numéros, et offre en plus jusqu'à deux suppléments par année.

Politique éditoriale : On publie, dans le Journal, des articles rendant compte de recherche originale, des perspectives (synthèses, critiques et réévaluations), des discussions (commentaires et réponses) et des communications rapides. Les documents peuvent porter sur les cellules, organismes, populations, communautés, écosystèmes ou processus qui affectent les systèmes aquatiques. Ils peuvent relever de divers domaines y compris la biologie et l'écologie des organismes marins et d'eau douce, la limnologie, l'océanographie, la physiologie, la toxicologie, la génétique, l'économie, la pathologie et la gestion. On accorde la préséance aux articles qui contribuent à la compréhension de phénomènes observés et à l'interprétation de résultats expérimentaux. On invite les auteurs à soumettre des articles ayant des objectifs précis ou relevant d'hypothèses, de concepts ou de questions vérifiables et se terminant par de solides conclusions ou d'utiles synthèses. Ces articles enrichissent, changent, mettent en question ou réorientent les connaissances acquises sur divers aspects des sciences aquatiques. On décourage toutefois la soumission d'articles simplement descriptifs (à moins qu'il ne s'agisse de nouvelles disciplines), d'application très limitée (applicables à une seule année, une seule région ou un seul taxon, portant sur un unique composé chimique, etc.); d'articles qui ne font que reprendre les principes énoncés dans des articles précédents; et d'articles rendant compte de l'application de normes sans gain de méthodologie.

Les auteurs voudront adresser leurs **manuscrits** aux directeurs scientifiques, Journal canadien des sciences halieutiques et aquatiques, Département de Zoologie, University of Guelph, Guelph, ON N1G 2W1, Canada (519-824-4120 poste. 2646; télécopieur : 519-767-9798; adresse électronique : cjfas@uoguelph.ca).

Les contributions peuvent être en anglais ou en français. Elles doivent être originales, c.-à.-d. qu'elles ne doivent pas avoir fait l'objet d'un copyright, avoir été publiées ou soumises ailleurs, sauf sous forme abrégée ou avec le consentement du rédacteur. Le CNRC ne se tient en aucune façon responsable des opinions exprimées par un collaborateur ou des déclarations qui pourrait faire ce dernier. La publication d'annonces publicitaires, d'avis et autres n'implique pas l'endossement de leur contenu par les directeurs du *Journal* ou du CNRC. L'utilisation des noms de marques de commerce ne signifie aucunement une sanction du produit en question ou de la compagnie qui le fabrique.

La correspondance ayant trait aux manuscrits acceptés et les **épreuves corrigés** doivent être envoyées aux Presses scientifiques du CNRC, Conseil national de recherches du Canada, Ottawa, ON K1A 0R6, Canada.

Recommandations aux auteurs sont publiés une fois par année dans le premier numéro de chaque volume. Des copies, ainsi que la **Politique de publication**, sont disponibles auprès des Presses scientifiques du CNRC ou au site Web :
http://www.nrc.ca/cisti/journals/rj.html

Microfilms : On peut acheter sur microfilms de 16 ou 35 mm tous les numéros depuis 1934. Des photocopies d'articles ou de numéros individuels sont aussi en vente auprès de University Microfilms International, 330 North Zeeb Road, Ann Arbor, MI 48106, É.-U.

This journal is indexed or abstracted in / Ce journal est signalé ou résumé dans
Aquatic Sciences and Fisheries Abstracts, Biological & Agricultural Index, CAB Abstracts (Centre for Agriculture and Biosciences), Chemical Abstracts, Current Awareness in Biological Sciences, Current Contents, FAO Freshwater and Aquaculture Contents Tables, FAO Marine Science Contents Tables, GEOBASE – Geo Abstracts, Meteorological and Geoastrophysical Abstracts, Oceanic Abstracts, Science Citation Index, Biological Abstracts, Environment Abstracts, Environmental Periodicals Bibliography, GEOREF, Life Sciences Collection, ABSEARCH, and PASCAL Database

Volume 55, Number 5, May 1998

Canadian Journal of Fisheries and Aquatic Sciences

Published by the National Research Council of Canada

Volume 55, numéro 5, mai 1998

Journal canadien des sciences halieutiques et aquatiques

Publié par le Conseil national de recherches du Canada

Editors / directeurs scientifiques John C. Roff and Moira M. Ferguson

Assistant to the Editors / adjointe aux directeurs scientifiques **Holly Foster**

Associate Editors / Directeurs scientifique associés

D. Boisclair, *Université de Montréal*
U. Borgmann, *Environment Canada, Burlington*
S.E. Campana, *DFO/MPO, Dartmouth*
B. de Young, *Memorial University of Newfoundland*
D.G. Dixon, *University of Waterloo*
A.E. Dizon, *National Marine Fisheries Service, La Jolla, Calif.*
J.J. Dodson, *Université Laval*
J.A. Downing, *Iowa State University*
K.T. Frank, *DFO/MPO, Dartmouth*
F.A. Huntingford, *University of Glasgow*
J.A. Hutchings, *Dalhousie University*
G.S. Jamieson, *DFO/MPO, Nanaimo*
B. Jonsson, *Norwegian Institute for Nature Research, Oslo, Norway*
L. Legendre, *Université Laval*
R.M. Peterman, *Simon Fraser University*
E.E. Prepas, *University of Alberta*
T.P. Quinn, *University of Washington, Seattle, Wash.*
R.D. Robarts, *Environment Canada, Saskatoon*
P.F. Sale, *University of Windsor*
D.W. Schindler, *University of Alberta*
S.J. Smith, *DFO/MPO, Dartmouth*
W.G. Sprules, *University of Toronto*
R.J. Thompson, *Memorial University of Newfoundland*
C.J. Walters, *University of British Columbia*
R.D. Ward, *CSIRO Division of Fisheries, Australia*
C.M. Wood, *McMaster University*

NRC Research Press / Presses scientifiques du CNRC

Editor-in-chief / directeur général **Bruce P. Dancik**
Assistant Editor-in-chief / directeur général adjoint **Iain E.P. Taylor**

Journals Program / Programme des revues

(Fax / télécopieur : 613-952-7656; e-mail / adresse électronique : research.journals@nrc.ca;
URL: http://www.nrc.ca/cisti/journals/)

Director / directrice **Aldyth Holmes**
Business Manager / gestionnaire des affaires **Paul McClymont**
Manager, Journals Program / gestionnaire, Programme des revues **Susan R. Strahlendorf**
Senior Publication Officer / agente principale de publication **Jennifer Douglas**
Publication Officer / agente de publication **Jennifer McColl (613-993-4500)**
Advertising / annonces publicitaires **Judy Heyman (613-993-0151)**
Reprints / tirés à part **Roxanne Landriault (613-990-2254)**
Subscriptions / abonnements **Helen Goulet (613-993-9084)**

© National Research Council of Canada 1998. World rights reserved.

No part of this publication may be reproduced, stored, or transmitted in any form or by any means, without the written permission of the publisher, except as stated below.

The National Research Council of Canada grants **permission*** to individuals to make single copies of articles for personal use. Any person may reproduce short excerpts from articles in the journal for any purpose that respects the moral rights of authors, provided that the source is fully acknowledged. As a courtesy, the consent of authors of such material should be obtained directly from the author.

Authorization to reproduce items for other than personal use, as stated above, is granted by the National Research Council of Canada provided that the copyright fee of $7.00 per copy is paid directly to the Copyright Clearance Center (CCC) Transactional Reporting Service, 222 Rosewood Drive, Danvers, MA 01923, U.S.A. 0706-652X/98 $7.00 + 0.00.

*The above permission does not extend to other kinds of copying, such as copying for general distribution, for advertising, or promotional purposes, for creating new collective works, or for resale. For such copying, arrangements must be made with the publisher, National Research Council of Canada, Ottawa, ON K1A 0R6, Canada.

© Conseil national de recherches du Canada 1998. Tous droits réservés.

Il est interdit de reproduire, de sauvegarder ou de transmettre quelque partie de la présente publication dans quelque format ou de quelque façon sans le consentement écrit de l'éditeur, à l'exception des conditions suivantes.

Le Conseil national de recherches du Canada accorde aux particuliers le droit de faire des copies individuelles pour leur usage personnel. Toute personne peut reproduire de courts extraits des articles de la Revue pour autant que les droits moraux de l'auteur soient respectés et que la mention de provenance soit clairement indiquée. Il est de convenance de demander le consentement de l'auteur avant de faire mention de son travail.

On obtiendra l'autorisation de reproduire des articles à d'autres fins que l'usage personnel (tel qu'on l'a décrit ci-dessus) auprès du Conseil national de recherches du Canada pour autant que des redevances de droits d'auteurs de 7,00 $/copie soient versées au Copyright Clearance Center (CCC) Transactional Reporting Service, 222 Rosewood Drive, Danvers, MA 01923, U.S.A. 0706-652X/98 7,00 $ + 0,00.

*La permission ci-dessus ne s'applique pas à la reproduction à grande échelle, telle que la reproduction aux fins de distribution générale, publicitaire ou promotionnelle, de compilation de nouveaux ouvrages collectifs ou de revente. Dans de tels cas, il faudra ratifier une entente particulière avec l'éditeur, le Conseil national de recherches du Canada, Ottawa, ON K1A 0R6, Canada.

Subscription information

The *Canadian Journal of Fisheries and Aquatic Sciences* (ISSN 0706-652X) is published monthly by the National Research Council of Canada. 1998 annual subscription rates (second class postage) for Canada are $516CAN institutional and $165CAN personal, for US & foreign $516US institutional and $175US personal. For air mail add $150US to foreign rate. Canadian customers please include 7% GST (business no. 12149 1807 RT 0275). In Quebec please add the QST to the total price including GST (QST no. 1006178088). Subscriptions are entered for the calendar year. Remittances should be made payable to the Receiver General for Canada credit NRC. Price for regular single issues: institutional, $60.00; personal, $25.00. Supplements will be priced separately. Special rates apply to members of Canadian scientific and engineering societies if they subscribe through their respective societies.

There are no refunds on cancelled subscriptions once delivery has begun. Claims for missing issues should be made within four months (N. America) or six months (outside N. America) following the date of publication. The publisher expects to supply missing issues only when losses have occurred in transit and when the reserve stock will permit. For change of address and subscription enquiries: Subscription Office, NRC Research Press, National Research Council Canada, Ottawa, ON K1A 0R6, Canada; tel: 613-993-9084; fax: 613-952-7656; e-mail: research.journals@nrc.ca.

Microform backfiles are available from UMI, P.O. Box 1346, Ann Arbor, MI 48106-1346, U.S.A., and Micromedia Ltd., 20 Victoria St., Toronto, ON M5C 2N8, Canada.

The 1998 issues of the *Canadian Journal of Fisheries and Aquatic Sciences* are available on the Web. Pricing information can be found at

http://www.nrc.ca/cisti/journals/

Renseignements sur l'abonnement

Journal canadien des sciences halieutiques et aquatiques (ISSN 0706-652X) est une publication mensuelle du Conseil national de recherches du Canada. Le prix de l'abonnement annuel au Canada (courrier de deuxième classe) est de 516 $CAN pour les organismes et de 165 $CAN pour les particuliers. À l'étranger (y compris les É.-U.), le prix de l'abonnement est de 516 $US pour les organismes et de 175 $US pour les particuliers. L'expédition par avion exige des frais de 150 $US en sus du prix d'abonnement à l'étranger. Les clients du Canada doivent ajouter la TPS de 7% (numéro d'entreprise 12149 1807 RT 0275). Au Québec, il faut ajouter la TVQ au prix total, TPS comprise (nº de TVQ 1006178088). Les abonnements sont pour l'année civile. Tout paiement doit être adressé au Receveur général du Canada, crédit du CNRC. Le prix par numéro est de 60 $ pour les organismes et de 25 $ pour les particuliers. Le prix des hors-série varie. Les membres des sociétés canadiennes de sciences et de génie bénéficient de taux préférentiels en s'abonnant via leurs sociétés respectives.

Aucun remboursement ne sera accordé ni aucune annulation acceptée une fois que les livraisons auront commencé. Les réclamations de numéros manquants devront être soumises dans les quatre mois (Amérique du Nord) ou dans les six mois (à l'extérieur de l'Amérique du Nord) suivant la date de publication. L'éditeur ne fournira de numéros manquants que si le document a été perdu pendant l'expédition et que si le stock le permet. Adressez tout changement d'adresse ou toute question quant à l'abonnement au : Bureau des abonnements, Presses scientifiques du CNRC, Conseil national de recherches Canada, Ottawa, ON K1A 0R6, Canada; téléphone : 613-993-9084; télécopieur : 613-952-7656; adresse électronique : research.journals@nrc.ca.

On peut obtenir les fichiers rétrospectifs sur **microforme** auprès de UMI, P.O. Box 1346, Ann Arbor, MI 48106-1346, É.-U., et auprès de Micromedia Ltée, 20 rue Victoria, Toronto, ON M5C 2N8, Canada.

Les numéros de 1998 de *Journal canadien des sciences halieutiques et aquatiques* sont accessibles sur le Web. On trouvera des renseignements sur les tarifs à

http://www.nrc.ca/cisti/journals/rjfr.html

Benthic invertebrate distributions in the San Joaquin River, California, in relation to physical and chemical factors

Harry V. Leland and Steven V. Fend

Abstract: The invertebrate fauna of nontidal portions of the lower San Joaquin River and its major tributaries is described in relation to water quality and habitat using canonical correspondence analysis, autecological metrics, and indicator species analysis. A large-scale (basin-wide) pattern in community response to salinity (sulfate–bicarbonate type) was detected when standardized, stable substratum was sampled. Community structure, taxa richness, and EPT (ephemeropterans, plecopterans, and trichopterans) richness varied with dissolved solids concentration (55–1700 mg total dissolved solids·L^{-1}), and distributions of many taxa indicated salinity optima. Distinct assemblages associated with either high or low salinity were evident over this range. Large-scale patterns in community structure were unrelated to pesticide distributions. Structure and taxa richness of invertebrate assemblages in sand substratum varied both with salinity and with microhabitat heterogeneity. The benthic fauna generally was dominated by a taxa-poor assemblage of specialized psammophilous species, contributing to a weaker relationship between community structure and water quality than was observed using standardized substratum. Habitat types and associated dominant species were characterized using indicator species analysis. Species assemblages did not vary substantially with irrigation regime or river discharge, indicating that structure of invertebrate communities was a conservative measure of water quality.

Résumé : La faune des invertébrés des tronçons sans marée du cours inférieur de la San Joaquin et de ses principaux affluents est décrite par rapport à la qualité de l'eau et de l'habitat au moyen de l'analyse de correspondance canonique, de paramètres autoécologiques et de l'étude des espèces indicatrices. L'analyse d'échantillons de substrat stable et normalisé a mis en évidence un profil à grande échelle (échelle du bassin hydrographique) de la réaction de la communauté à la salinité (type sulfate–bicarbonate). La structure des communautés, la richesse taxinomiques et la richesse des EPT (éphéméroptères, plécoptères et trichoptères) variaient en fonction de la concentration des matières dissoutes (55 – 1 700 mg matières dissoutes totales·L^{-1}), et la distribution de nombreux taxons a montré des valeurs optimales de salinité. On observait des groupements distincts associés à une salinité élevée ou faible dans cette plage. Les profils à grande échelle de la structure des communautés n'étaient pas liés à la distribution des pesticides. La structure et la richesse taxinomique des groupements d'invertébrés dans le sable variaient en fonction de la salinité et de l'hétérogénéité du microhabitat. En général, la faune benthique était dominée par un groupement comptant peu de taxons d'espèces psammophiles spécialisées, ce qui donnait une relation entre la structure des communautés et la qualité de l'eau plus faible que celle observée à l'aide d'un substrat normalisé. Les types d'habitat et les espèces dominantes associées ont été caractérisés par l'étude des espèces indicatrices. Les assemblages d'espèces ne variaient guère avec le régime d'irrigation ou le débit du cours d'eau, ce qui montre que la structure des communautés d'invertébrés donnait une idée modérée de la qualité de l'eau.
[Traduit par la Rédaction]

Introduction

The increasing salinity and potential toxicity of Se and other trace elements to fish and wildlife of surface waters in arid and semiarid regions due to agricultural practices are of great concern to water resources managers (e.g., Engberg and Sylvester 1993). Unfortunately, little information exists on responses of aquatic communities in rivers to concentrations of soluble salts commonly encountered. Lacking are comprehensive biological data from benchmark surveys on rivers undergoing salinization or community-level studies of rivers with clear gradients in salinity. The range in salinity of the San Joaquin River, California, and its major tributaries gave us an opportunity to provide information on the latter topic. This range is representative of other rivers in similar hydrogeologic areas (alkaline seleniferous soils, low precipitation, and high evaporation rates) of western North America. Agricultural areas where deposits of Cretaceous marine shales have weathered to produce seleniferous soils occur also in parts of Arizona, Nevada, Utah, Colorado, New Mexico, Wyoming, Montana, North Dakota, South Dakota, Nebraska, and Kansas (Presser et al. 1994).

The San Joaquin Valley has serious agricultural drainage problems potentially affecting over 450 000 ha. High concentrations of dissolved solids and inadequate drainage of subsurface water threaten the productivity of this important agricultural region (Moore et al. 1990). In some locations the

Received May 29, 1996. Accepted November 6, 1997.
J13489

H.V. Leland[1] **and S.V. Fend.** Water Resources Division, U.S. Geological Survey, 3215 Marine Street, Boulder, CO 80303, U.S.A.

[1] Author to whom all correspondence should be addressed. e-mail: hvleland@usgs.gov

© 1998 NRC Canada

Fig. 1. Location of sample reaches in the San Joaquin River and its major tributaries.

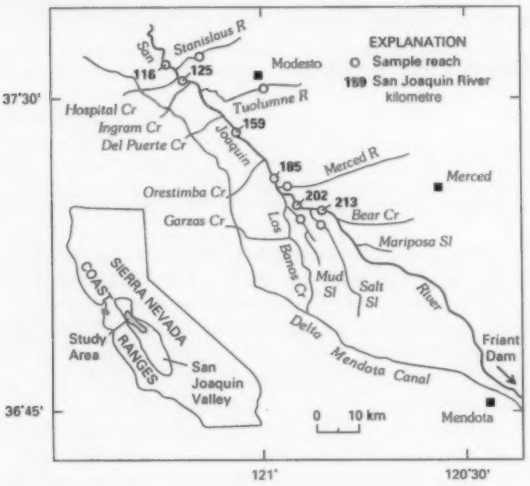

drainage water also contains elevated levels of several trace elements, of which Se exceeds quality criteria for the protection of aquatic life and B and Mo exceed criteria for their use in irrigation (USEPA 1986, 1987). Fertilizer and pesticide usage in agriculture is heavy and of continuing environmental concern. Past practices of disposal of agricultural drainage water have resulted in widespread degradation in the quality of surface waters and shallow groundwaters of the valley (Deverel and Fujii 1988) and in the contamination of scarce fish and wildlife habitat (Presser et al. 1994). This is the first investigation of the invertebrate fauna in nontidal (freshwater) portions of the lower San Joaquin River, the only natural outlet for surface water from the valley, and its tributaries. Assessments of the benthic fauna in tidal portions of the San Joaquin River related community composition to salinity and sediment composition (Siegfried et al. 1980; Markmann 1986).

We describe patterns in the distribution of benthic invertebrates of the San Joaquin River and its major tributaries in relation to water quality and physical characteristics of the drainage as elucidated by indicator species analysis, canonical correspondence analysis (CCA), and autecological metrics. This combination of analytical techniques provides an objective and informative procedure for delineating assemblages that respond differentially to a set of complex environmental variables (Leland 1995). Specifically, (*i*) relationships among species abundances and environmental variables are determined quantitatively using CCA or partial CCA, (*ii*) salinity is shown by weighted-averaging regression to consistently provide a greater degree of predictability in species–environment relationships than other measured environmental variables, (*iii*) dissolved solids optima for common species in the San Joaquin River and its tributaries are compared with halobion indices reported for the same, or closely related, taxa in other rivers, and (*iv*) two-way indicator species analysis is used to define habitat types and associated species assemblages in the basin. Comparable information on habitat types and associated dominant species is rare for rivers in western North America and is virtually nonexistent for sand-bed rivers in this region.

Study area

The San Joaquin River flows northward through the semiarid San Joaquin Valley of California and terminates in the Sacramento – San Joaquin Delta, which discharges to San Francisco Bay. During much of the year, water in the San Joaquin River is largely diverted for agriculture or substantially diluted with Sacramento River water, which is delivered from the Delta by way of the Delta Mendota Canal. During the irrigation season (usually March–September), subsurface drainage and drainage water from irrigated fields are a major part of the flow.

The study area is the perennial-flow portion of the San Joaquin River upstream of the backwater influence of the Sacramento – San Joaquin Delta (Fig. 1). About 800 000 ha of irrigated land drains directly or indirectly into this part of the river. Bear Creek, a tributary receiving water only from Sierra Nevada drainage and alluvium derived from this mountain range, joins the San Joaquin River at km 219. Salt Slough and Mud Slough join the river at km 206 and 195, respectively. These two tributaries originate on the valley floor and derive most of their discharge from groundwater seepage, irrigation return flows, and subsurface drainage. Major tributaries downriver of the confluence with Mud Slough are the Merced, Tuolumne, and Stanislaus rivers. Each originates in the Sierra Nevada and is impounded in the foothills for regulation of discharge. Streams draining the Coast Ranges and flowing into the San Joaquin River in this portion of the river (km 195–116) are both intermittent and unregulated.

Bedrock geology and mineral composition of derived soils significantly affect water quality in the study area. The Sierra Nevada are composed primarily of pre-Tertiary granitic rocks and are separated from the San Joaquin Valley by a foothill belt of Mesozoic metavolcanic rocks. The low solubility of dominant minerals (quartz and feldspars) in these rocks and derived soils results in runoff of a low dissolved solids concentration. In contrast, the Coast Ranges are composed primarily of rocks and sediments of marine origin. These rocks and derived soils are enriched in soluble salts and several trace elements, including B, Mo, and Se. The sparse precipitation on the eastern side of the Coast Ranges further contributes to runoff which is enriched in these constituents.

The study area is in the Central California Valley ecoregion, which is characterized by flat plains, recent alluvial soils, and irrigated cropland and pasture. The reaches sampled represent major sources of water, including river segments above and below confluences of the five major tributaries (Fig. 1). The rivers are low gradient and meandering. All tributaries were sampled far enough upriver that backflow from the San Joaquin River did not occur.

Sand is the dominant substratum in all river reaches sampled. Coarseness and sorting of particles increase downriver in the mainstem as the three major tributaries draining the Sierra Nevada contribute flow to the San Joaquin River. Snags are the primary stable habitat for benthic invertebrates, but root wads and macrophytes also are locally abundant.

© 1998 NRC Canada

Methods

Chemical and biological analyses

Sampling of river water for physical and chemical characteristics was conducted on alternate weeks from June 1985 through May 1986 and monthly for the remainder of the study (through September 1987). Determinations reported are for depth-integrated, discharge-weighted composite samples of the river cross section. Discharge was measured continuously at all sites. Analytical methods for inorganic constituents in river water are described in Fishman and Friedman (1985). Suspended algal mass was estimated from chlorophyll *a* determinations and based on a cellular organic C to chlorophyll *a* ratio of 40:1. Laboratory analyses of river water were conducted at the National Water Quality Laboratory of the U.S. Geological Survey.

Benthic invertebrate communities were sampled about every 2 months for 1.5 years (June 1985 – November 1986), except during an unusually high-flow period (February–May 1986). Hester–Dendy multiple-plate samplers were used to represent snags, a habitat with high species diversity and biomass but difficult to sample. The multiple-plate samplers also provided for standardization of substratum. Three replicate samplers were positioned 15 cm from the streambed in nondepositional areas (using concrete blocks) at an initial velocity of about 30 $cm \cdot s^{-1}$ and were colonized for 2 months (colonization time determined to be optimal in similar habitats, e.g., Mason et al. 1973). Some samples were lost to vandalism or streambed movement. Formalin (10%) was used to preserve the samples upon retrieval. All surfaces of the multiple-plate sampler (total area of 0.1 m^2) were scraped. Large organisms were removed before subsampling.

At least one-fourth of the total sample retained by a 210-µm-mesh screen was identified to the lowest taxon possible and enumerated. Densities of "bryozoans" were estimated from volumetric measurements. Rose bengal staining facilitated sorting. Identification of taxa generally was by reference to standard taxonomic monographs.

Ponar grab samples (0.02 m^2) were taken at three equidistant positions along the river cross section in the vicinity of the multiple-plate samplers and preserved in formalin (10%). A 100-mL subsample was retained for sediment particle size analysis. The remainder of the preserved sample was elutriated using a 210-µm-mesh screen. Otherwise, grab samples and multiple-plate samples were preserved and processed by the same methods.

Summarization and analysis of data

Community composition and enumeration data for individual months were summarized primarily by detrended correspondence analysis (DCA), an indirect-gradient ordination (Hill 1979), and CCA, a direct-gradient method (ter Braak and Verdonschot 1995). Stratification by month was used to reduce temporal variation in invertebrate abundances and environmental constituents to focus on large-scale spatial patterns. It is doubtful that life history patterns of the resident taxa are linked functionally to seasonal changes in concentration of anthropogenic constituents, so stratification by month was a conservative way to avoid spurious temporal relationships. Both DCA and CCA are based on reciprocal averaging (RA), a particularly useful method because site scores are positioned at the weighted averages of species scores and species scores are positioned at the weighted averages of site scores. This is analogous to scoring systems based on known species attributes (e.g., Armitage et al. 1983).

DCA was used to determine the major variation in species composition data and to elucidate patterns in community structure without incorporating data on environmental variables. CCA was used to explore relationships between the benthic invertebrate distributions and measured abiotic factors. In CCA, axes are selected as linear combinations of environmental variables that maximize the dispersion of species scores, so species are related directly to a set of abiotic factors. The order of site scores was the same in DCA and CCA, and eigenvalues for axis 1 in the two ordinations generally were identical. Eigenvalues for axes 2 and 3 decreased by 0.02 to 0.10 in the separate (monthly) ordinations if environmental variables were included (comparing RA and CCA results), and the percent variance of species–environment relationships increased on all axes (by >30% on axis 1). Thus, interpretations of patterns in community structure based on DCA and CCA were consistent, and measured environmental variables accounted for a significant portion of the explained variance in CCA. Both ordination analyses were performed using the computer program CANOCO 3.1 (ter Braak 1990). Species abundance data were transformed (natural logarithm) to reduce effects of highly variable population densities on ordination scores. Rare species (<10 individuals in the entire sample set (<0.1%) for a given date) were excluded, so summary distributions emphasize the more commonly occurring and abundant taxa. Minimum-spanning trees based on χ^2 distances (the distance measure used in reciprocal averaging) were constructed and plotted together with CCA site scores to indicate nearest neighbors (similarity) and to highlight possible distortions.

Forward selection of environmental variables and Monte Carlo permutations were used in CCA to identify a subset of the measured variables (Table 1) that exert significant and independent influences on the benthic invertebrate distributions. Environmental variables with high variance inflation factors (>20) in CCA (ter Braak 1990) were eliminated. The computer program WACALIB 3.3 (Line et al. 1994) was used to calculate optimum concentrations (based on weighted averages) of dissolved solids (TDS) for commonly occurring species colonizing multiple-plate samplers. A TDS model consistently provided a greater degree of predictability than other significant environmental variables identified in CCA. As both TDS concentration and species abundances varied substantially at most sites, median TDS optima for the resident taxa are reported to characterize their response during colonization. Thus the reported TDS optima do not represent maximum values for the period of record and should not be interpreted as physiological tolerance limits. For the same reason, weighted-averaging calibration was not used to infer TDS concentration from observed invertebrate abundances.

Two-way indicator species analysis (TWINSPAN), a divisive classification method based on correspondence analysis, was used to define species assemblages and the fidelity of species to an assemblage. Arranged data matrices for each month were examined initially together with DCA species ordinations to determine consistent patterns in assemblage structure. Ordination implies that a single continuum or gradient model is appropriate for describing species distributions throughout the study area. A complementary way to depict species distributions in a basin-scale study is as species assemblages, wherein classification is used to define co-occurring taxa (e.g., Leland 1995). Inclusion of results from all sampling dates would expand the discussion beyond reasonable limits. Therefore, TWINSPAN results presented here are based instead on the entire data set (all sampling dates, but multiple-plate fauna and benthic fauna were analyzed independently) to facilitate discussion of habitat types and associated dominant species. The analysis was based on natural logarithms of species abundances. The results are presented as median-abundance category or frequency of occurrence in groups, with taxa included if the minimum frequency in any group was 50% or greater. The significance of differences among site groups in taxa richness and selected environmental variables was determined by a Kruskal–Wallis ANOVA by ranks, followed by pairwise Mann–Whitney (ranked *t*) tests.

Results

Environmental variables

Concentrations of TDS, major ions, and trace elements in the San Joaquin River generally were low at km 213 (Table 1;

© 1998 NRC Canada

Table 1. Major, minor, and trace constituents (range in means of biweekly or monthly samples for the five sampling periods) in waters of the San Joaquin River and its major tributaries.

	San Joaquin River kilometre						Stanislaus River	Tuolumne River	Merced River	Mud Slough	Salt Slough
	116	125	159	185	202	213					
Discharge ($m^3 \cdot s^{-1}$)	56–160	40–140	22–67	17–51	6.3–24	0.79–12	12–40	6.6–43	6.0–9.9	0.51–3.4	3.4–10
Water velocity ($cm \cdot s^{-1}$)	20–35	25–59	19–41	16–43	22–35	26–60	23–24	10–24	22–40	17–43	21–53
Water temperature (°C)	12–22	12–24	12–24	11–24	11–25	12–26	12–17	13–26	11–25	12–25	11–23
Dissolved oxygen minimum ($mg \cdot L^{-1}$)	6.7–8.2	6.4–8.0	6.5–8.5	6.8–8.0	6.6–8.2	4.4–8.6	8.3–9.6	6.8–9.5	7.4–9.0	5.8–7.5	5.3–8.8
pH	7.7–7.9	7.8–8.0	7.8–8.1	7.8–8.1	7.7–8.0	7.6–8.4	7.6–7.7	7.4–8.1	7.5–7.9	8.1–8.4	7.9–7.9
Dissolved solids ($mg \cdot L^{-1}$)	250–350	270–540	420–690	420–740	410–970	200–620	54–78	55–140	74–140	1300–1700	650–1200
Ca ($mequiv. \cdot L^{-1}$)	1.1–1.7	1.2–2.3	1.8–2.7	1.6–3.0	1.8–4.3	0.97–3.4	0.38–0.64	0.22–0.75	0.47–0.80	3.0–7.1	2.7–5.6
Mg ($mequiv. \cdot L^{-1}$)	0.85–1.4	0.78–1.8	1.3–2.4	1.3–2.5	1.2–4.0	0.61–2.5	0.21–0.42	0.15–0.59	0.25–0.43	3.5–5.8	2.0–4.9
Na ($mequiv. \cdot L^{-1}$)	1.9–3.4	1.8–4.7	3.4–7.1	3.5–7.4	3.3–11.	1.5–7.4	0.12–0.25	0.12–0.70	0.44–0.95	11–19	5.4–14
K ($mequiv. \cdot L^{-1}$)	0.05–0.10	0.05–0.12	0.08–0.20	0.06–0.10	0.08–0.15	0.06–0.10	0.03–0.10	0.03–0.10	0.03–0.06	0.11–0.13	0.10–0.16
Cl ($mequiv. \cdot L^{-1}$)	1.4–3.0	1.5–3.8	2.4–5.4	2.5–5.4	2.9–8.8	0.61–5.4	0.05–0.15	0.23–0.43	0.23–0.57	7.0–12	4.3–11
SO_4 ($mequiv. \cdot L^{-1}$)	1.1–1.9	1.2–2.3	2.2–3.9	2.1–4.3	2.1–6.9	0.41–5.6	0.06–0.16	0.12–0.18	0.20–0.30	8.2–14	3.6–9.2
HCO_3 ($mequiv. \cdot L^{-1}$)	1.1–1.7	1.2–2.1	1.6–2.5	1.2–2.1	1.7–3.0	1.3–2.6	0.54–0.85	0.46–1.3	0.65–1.2	2.3–3.9	2.1–3.2
Suspended matter ($mg \cdot L^{1}$)	47–99	56–200	46–160	66–340	53–170	33–67	10–27	6.5–25	17–36	73–240	68–240
Particulate organic C ($mg \cdot L^{-1}$)	1.2–2.2	1.4–5.4	1.2–2.0	1.0–2.4	1.0–1.3	1.6–2.4	0.60–2.3	0.58–4.1	0.53–1.5	1.0–1.6	0.8–2.6
Algal mass ($mg\ C \cdot L^{-1}$)	0.17–0.58	0.12–0.64	0.24–0.64	0.26–1.7	0.28–0.88	0.41–0.91	0.02–0.18	0.02–0.08	0.04–0.18	0.18–1.7	0.16–1.0
Major nutrients											
Organic N + NH_4 ($mg\ N \cdot L^{-1}$)	0.68–1.2	0.65–1.7	0.92–2.0	0.97–1.3	0.95–1.3	0.75–1.6	0.30–0.55	0.43–0.63	0.40–0.63	1.3–1.7	1.1–1.9
$NO_2 + NO_3$ ($mg\ N \cdot L^{-1}$)	1.1–1.8	1.1–2.2	1.6–2.2	1.2–2.5	0.77–2.5	0.07–0.53	0.12–0.72	0.40–0.73	0.75–1.6	0.39–8.7	1.4–2.7
Total P ($mg\ P \cdot L^{-1}$)	0.12–0.34	0.15–0.43	0.24–0.59	0.19–0.35	0.19–0.34	0.23–0.37	0.04–0.08	0.05–0.25	0.07–0.09	0.23–0.42	0.19–0.42
Dissolved P ($mg\ P \cdot L^{-1}$)	0.07–0.23	0.08–0.29	0.16–0.44	0.09–0.21	0.11–0.17	0.13–0.27	0.03–0.06	0.02–0.22	0.04–0.06	0.10–0.29	0.06–0.17
Si ($mg\ SiO_2 \cdot L^{-1}$)	15–20	11–21	15–20	14–19	15–20	12–19	12–17	13–25	13–16	16–18	17–21
Trace constituents (<0.45 μm fraction)											
NH_3, unionized ($\mu g \cdot L^{-1}$)	<1–5	1–12	4–21	1–9	1–7	1–12	<1–4	<1–8	<1–4	3–12	3–7
B ($\mu g \cdot L^{-1}$)	180–380	210–430	380–740	430–850	420–930	48–190	6.7–18	18–28	16–28	1600–3300	670–1100
Mo ($\mu g \cdot L^{-1}$)	2–5	2–4	2–5	2–7	3–8	2–12	<1–1	<1–2	<1–2	7–17	5–9
Se ($\mu g \cdot L^{-1}$)	<1–1	1–2	2–4	2–5	1–5	<1–1	<1	<1	<1	3–27	1–8

Note: Chemical determinations are for depth-integrated, discharge-weighted composite samples from the river cross section. Water velocity was measured at the location and depth of the multiple-plate samplers. Minimum dissolved oxygen concentrations are the lowest recorded early-morning (before 08:00) measurements (adapted from Shelton and Miller 1988).

© 1998 NRC Canada

Fig. 2. Temporal variation in TDS concentrations (residue at 180°C). (A) San Joaquin River and tributaries draining the valley floor. TDS concentrations in Mud Slough generally were higher and more variable than in Salt Slough and were omitted for sake of clarity. (B) Major tributaries draining the Sierra Nevada.

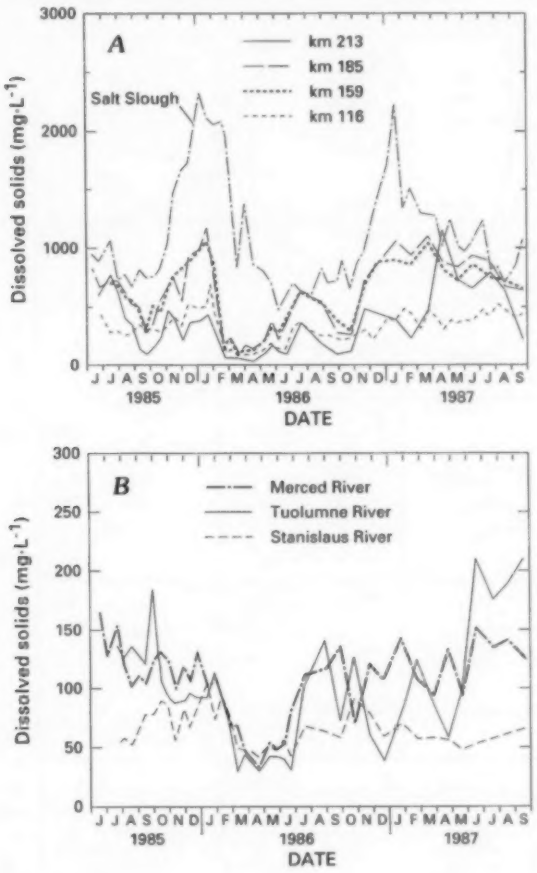

Fig. 2), reflecting the Sierra Nevada origin of Bear Creek water. However, when soils of the Bear Creek basin were irrigated, concentrations of these constituents at km 213 equalled or exceeded concentrations in the lower reaches (km 125 and 116) of the San Joaquin River. TDS concentrations in the San Joaquin River increased markedly when combined with the flows of Salt Slough and Mud Slough. In the more saline subsurface drainage and irrigation return flows of the southern/western portions of the San Joaquin Valley, the dominant cations are Na and Mg and the dominant anion is SO_4, a dissolution product of the thenardite (Na_2SO_4), bloedite ($MgNa_2(SO_4)_2 \cdot 4H_2O$), and other hydrolyzable salts present in abundant amounts in salt-affected soils (Presser et al. 1990). Thus, concentrations of Ca, Mg, Na, Cl, and SO_4 in the San Joaquin River also increased substantially downriver of the two sloughs (Table 1). Similar enrichment of B and Se occurred.

The ionic composition of the Merced, Tuolumne, and Stanislaus Rivers is dominated by bicarbonates of Ca and Mg; however, irrigation return flows also contribute substantial salinity to the river water. TDS concentrations generally were greater and more variable in the Merced and Tuolumne rivers than in the Stanislaus River (Fig. 2). Below the confluence of Mud Slough, the saline waters (sulfate–bicarbonate type) of the San Joaquin River are diluted progressively along its length by the less saline waters of the three Sierra Nevada drainages.

Concentrations of TDS, major ions, and trace elements declined initially (September–October) each year after the irrigation season (March–September) (Fig. 2), but then, concentrations increased as greater proportions of the surface flow originated from subsurface drainage and groundwater seepage. In 1986, concentrations of TDS, major ions, and trace elements in the San Joaquin River were less during the irrigation season than in 1985 or 1987. From mid-February through May 1986, water levels throughout the study area were exceptionally high due to record snowpacks in the Sierra Nevada the previous winter. Concentrations of these constituents were unusually low during this high-water event.

Inorganic N (NO_2-N + NO_3-N) concentrations varied more spatially and temporally than did other major nutrients (Table 1) because of its extensive usage in agriculture. Concentrations at km 213 in the San Joaquin River were low except when soils of Bear Creek basin were irrigated. Concentrations in Salt Slough were exceptionally high during the preirrigation season (January–March) due to leaching of soils to remove accumulated salts and in Mud Slough during the primary irrigation season. Inorganic N concentrations substantially increased between km 185 and 159 due to the volume of agricultural return flow discharged to this segment of the river and were higher and more variable in the Merced and Tuolumne rivers than in the other major tributary (Stanislaus River) draining the Sierra Nevada.

Relationships among benthic invertebrate distributions and environmental variables

Multiple-plate fauna

CCA biplots of abundance data for multiple-plate fauna primarily expressed intersite variation in assemblage structure (Figs. 3A–3C). Composite site scores for the two or three multiple-plate samplers from each reach are plotted because intrasite variation was low. For each sampling date, the loading on axis 1 is substantially larger than on succeeding axes, and axis 1 always expresses the same gradient. Mud Slough is consistently at one extreme on axis 1, and the tributaries draining the Sierra Nevada are at the other end. San Joaquin River reaches most impacted by Mud Slough and Salt Slough (km 202–185) tend to segregate from reaches (km 159–116) located further downriver. The position of km 213 in ordination space varies, reflecting the variable water source and lower TDS concentration during the irrigation season in 1986 than in 1985 (Fig. 2). Until July 1986, faunal assemblages at km 213 resembled those of other upriver reaches; however, the prolonged period of high discharge in spring–summer 1986 resulted in an assemblage by late summer similar to that of reaches located further downriver. Succeeding CCA axes primarily express differences in faunal assemblages of two or more tributaries. The nearest-neighbor analysis indicates dissimilar faunal assemblages at tributary sites despite a consistent relation to CCA axis 1.

© 1998 NRC Canada

Fig. 3. (A–C) Site ordinations (CCA) of abundance data for multiple-plate fauna in the San Joaquin River and its major tributaries. (D–F) Site ordinations (CCA) of abundance data for benthic fauna. (G–I) Site ordinations (partial CCA) of abundance data for benthic fauna. The biplots indicate significant water quality variables (arrows). The axis scale is the average standard deviation of species turnover (ter Braak 1990), and the eigenvalues (λ_1 and λ_2) indicate the maximized dispersion of species scores along the axes. Site scores are linked by their minimum-spanning tree for multiple-plate fauna (see text) to indicate nearest neighbors (similarity). The line lengths of the minimum-spanning tree represent minimum distances, not absolute distances.

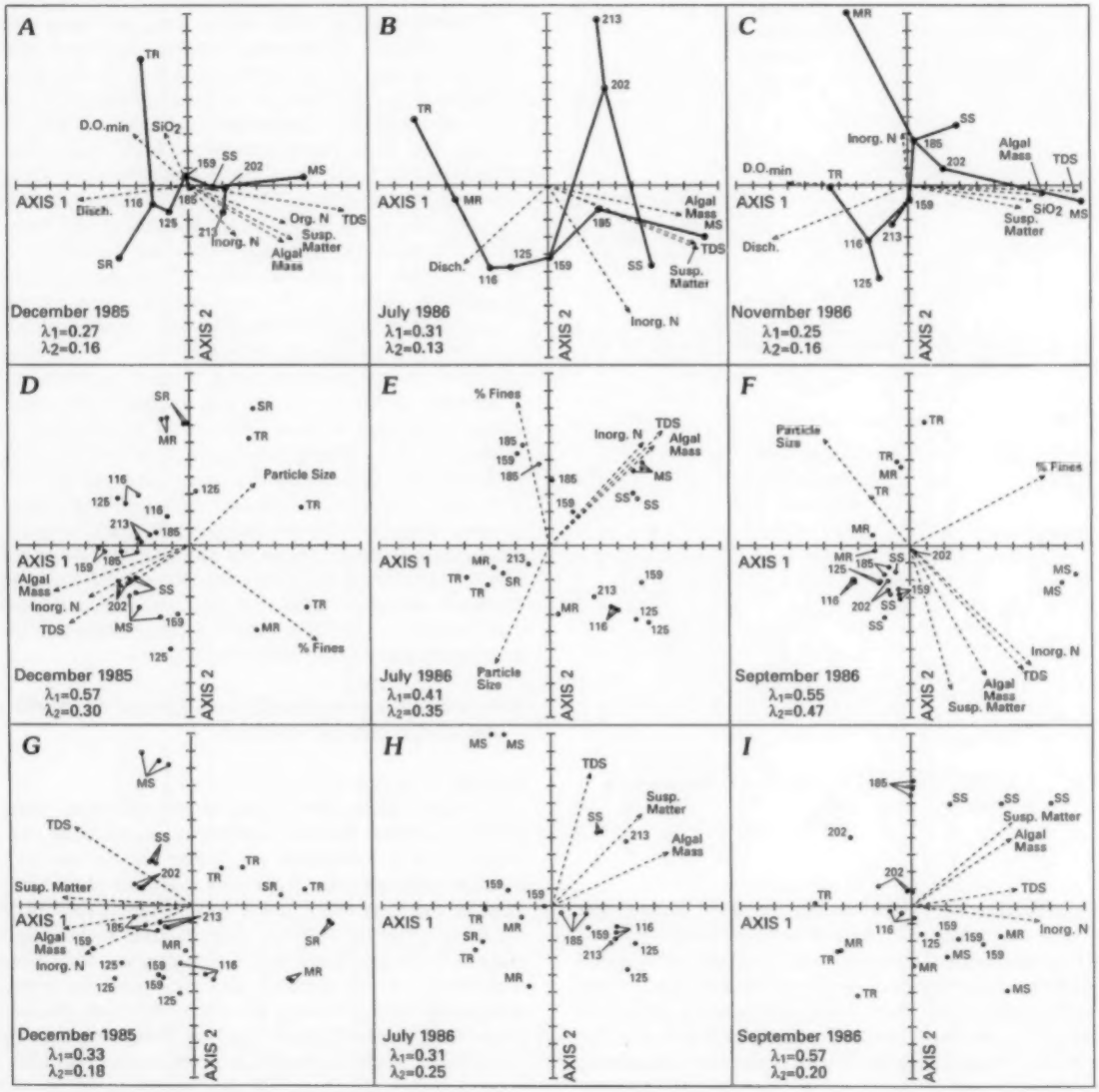

Concentrations of TDS, suspended matter, inorganic N, and algal mass were related ($p < 0.01$) independently to community summary statistics (CCA site scores) on all sampling dates (Table 2). Correlations between ordination axes and the environmental variables indicate that the dissolved oxygen minima during the postirrigation season (October–December) varied negatively with concentrations of TDS, suspended matter, and algal mass (axis 1). The variance in inorganic N, discharge, and SiO_2 concentration generally was expressed on two or more axes. Axis 1 accounted for 32–46% of the explained variance, axis 2 for 19–22% of the variance, and axis 3 for 12–16%. Ratios (λ_1/λ_2) of the constrained eigenvalue for TDS, suspended matter, and algal mass (constituents with consistently high loadings on axis 1) to the sum of all canonical eigenvalues ranged from 0.45 to 0.60, indicating that other environmental variables also strongly influence faunal assemblages of the study area.

Most abundant or frequently occurring invertebrate taxa in

© 1998 NRC Canada

Table 2. Weighted correlation matrices showing the relationship between species axes and environmental variables.

Axis	Discharge	Suspended matter	Dissolved oxygen (minimum)	Dissolved solids	Inorganic N	Organic N	Si	Algal mass	Eigenvalue	% variance of species–environment relationship
Multiple-plate fauna (CCA)										
Oct. 1985										
1	–0.33	0.57	–0.80	0.96	0.70	—	–0.28	0.61	0.30	34
2	0.35	0.11	0.26	0.07	0.04	—	–0.23	0.22	0.18	18
3	–0.36	–0.34	0.19	0.02	0.23	—	–0.46	–0.59	0.14	17
4	0.12	0.19	0.24	–0.07	0.17	—	–0.72	0.14	0.12	13
Dec. 1985										
1	–0.63	0.60	–0.31	0.90	0.27	0.56	–0.13	0.55	0.27	35
2	–0.07	–0.20	–0.54	–0.10	–0.34	–0.25	–0.70	–0.46	0.16	20
3	–0.12	–0.41	0.04	–0.20	–0.46	–0.34	0.00	–0.57	0.13	16
4	–0.58	–0.55	0.76	–0.16	–0.55	–0.53	–0.18	–0.14	0.08	11
July 1986										
1	–0.48	0.87	—	0.86	0.48	—	—	0.78	0.31	49
2	–0.10	–0.03	—	0.39	0.65	—	—	–0.26	0.13	21
3	0.39	0.42	—	0.13	0.43	—	—	0.21	0.09	14
4	0.68	0.03	—	0.12	0.07	—	—	0.34	0.06	9
Sept. 1986										
1	0.11	–0.87	—	–0.82	–0.59	—	0.20	–0.82	0.35	45
2	–0.79	0.26	—	0.45	0.41	—	0.58	0.25	0.18	23
3	–0.40	–0.14	—	–0.24	–0.61	—	–0.56	–0.22	0.11	13
4	–0.23	–0.15	—	–0.14	0.11	—	–0.40	–0.04	0.09	11
Nov. 1986										
1	–0.77	0.64	–0.68	0.95	–0.02	—	0.70	0.78	0.25	34
2	–0.45	–0.62	0.48	–0.20	–0.49	—	–0.21	–0.05	0.16	22
3	–0.06	0.12	–0.25	0.08	0.63	—	0.09	–0.12	0.11	15
4	–0.36	0.16	0.02	–0.10	–0.43	—	–0.42	0.53	0.09	13
Benthic fauna (partial CCA)										
Oct. 1985										
1	—	–0.68	—	–0.89	–0.55	—	—	–0.95	0.27	51
2	—	–0.28	—	–0.17	0.13	—	—	0.08	0.12	22
Dec. 1985										
1	—	–0.88	—	–0.77	–0.63	—	—	–0.85	0.33	51
2	—	0.05	—	0.47	–0.26	—	—	–0.14	0.18	27
July 1986										
1	—	0.61	—	0.25	—	—	—	0.81	0.31	46
2	—	0.66	—	0.91	—	—	—	0.39	0.25	38
Sept. 1986										
1	—	0.68	—	0.86	0.94	—	—	0.73	0.28	44
2	—	0.57	—	0.14	–0.11	—	—	0.50	0.17	26

Note: Environmental variables listed exerted significant ($p < 0.05$) and independent influences on faunal distributions.

the study area are found in more saline environments (Table 3), indicating that osmotic tolerance limits were not exceeded for most taxa. However, an ordering of taxa by TDS optimum (based on weighted averages) corresponds ($p < 0.01$, Spearman rank order) to an ordering based on their optimal salinity range (from distributions in other river basins). Thus, distributions of many of the resident taxa reflect, at least in part, their physiological fitness for saline conditions.

Benthic fauna

Results of CCA of abundance data for the benthic fauna (Ponar samples) indicated that intrasite variation was greater than for the multiple-plate fauna (Figs. 3D–3F). Intrasite differences in substratum were not visually apparent at the time of sampling. However, the microhabitat proved to be heterogeneous, and site scores for the three benthic samples from each reach are plotted. In contrast with CCA of the multiple-plate fauna, wherein axis 1 consistently expressed a large-scale gradient in water quality, biplots of the benthic fauna expressed a complex gradient (on axes 1 and 2) of water quality and habitat heterogeneity (based on particle size and percent fines of sediments). Benthic faunal assemblages

© 1998 NRC Canada

Table 3. Dissolved solids optimum and tolerance (standard deviation of the optimum) for taxa colonizing multiple-plate samplers in the San Joaquin River and its major tributaries.

Taxon	Dissolved solids ($mg \cdot L^{-1}$)		Halobion index[a]
	Optimum	Tolerance	
Aulodrilus limnobius (Tubificidae)	110	11	1–2
Nectopsyche sp. (Trichoptera)	120	11	—
Dubiraphia giuliani (Coleoptera)	130	24	1
Hydroptila sp. (Trichoptera)	130	27	—
Cricotopus tremulus gr. sp. 2 (Chironomidae)	130	18	—
Phenopsectra sp. (Chironomidae)	140	35	—
Tanytarsus sp. 1 (Chironomidae)	160	21	—
Tricorythodes cf. *minutus (Ephemeroptera)*	160	26	—
Pristinella acuminata (Naididae)	160	35	1
Amphichaeta nr. *leydigi* (Naididae)	160	23	—
Hydra sp. (Coelenterata)	160	41	—
Polypedilum cf. *halterale* (Chironomidae)	170	30	1
Stylaria lacustris (Naididae)	190	67	1
Simulium spp. (Simuliidae)	190	53	0–1
Paralauterborniella sp. (Chironomidae)	200	50	1–2
Polypedium cf. *illinoense* (Chironomidae)	200	30	1–2
Cricotopus tremulus gr. sp. 1 (Chironomidae)	200	31	—
Synorthocladius sp. (Chironomidae)	210	17	—
Parakiefferiella sp. (Chironomidae)	230	14	—
Ablabesmyia mallochi (Chironomidae)	240	31	1
Ferrissia sp. (Gastropoda)	260	23	—
Nais behningi (Naididae)	260	16	—
Dugesia sp. (Turbellaria)	280	67	—
Cladotanytarsus vanderwulpi gr. (Chironomidae)	280	50	—
Thienemanniella sp. (Chironomidae)	280	37	—
Fallceon quilleri (Ephemeroptera)	290	26	0–1
Dicrotendipes spp. (Chironomidae)	290	29	3
Heptagenia elegantula (Ephemeroptera)	300	21	—
Argia sp. (Odonata)	300	36	—
Rheotanytarsus sp. (Chironomidae)	320	32	1
Orthocladius or *Cricotopus* spp. (Chironomidae)	330	23	1–2
Caenis sp. (Ephemeroptera)	330	51	0–1
Dero furcata (Naididae)	350	24	2
Ophidonais serpentina (Naididae)	360	28	—
Thienemannimyia sp. (Chironomidae)	360	28	—
Hemerodromia sp. (Empididae)	390	35	3
Corynoneura sp. (Chironomidae)	390	56	0–1
Enchytraeidae (Oligochaeta)	390	100	—
Nais communis (Naididae)	390	37	2
Dero nivea (Naididae)	390	21	2
Chaetogaster diastrophus (Naididae)	400	72	—
Nais pardalis (Naididae)	400	54	2
Slavina appendiculata (Naididae)	400	39	1–2
Macrostomum sp. 1 (Turbellaria)	410	60	—
Pristinella osborni (Naididae)	410	64	1–2
Nanocladius bicolor gr. spp. (Chironomidae)	420	76	3
Hydropsyche californica (Trichoptera)	420	56	0–1
Corbicula fluminea (Pelecypoda)	430	98	—
Aeolosoma spp. (Aphanoneura)	440	86	2–3
Nais variabilis (Naididae)	440	47	2
Cricotopus bicinctus (Chironomidae)	440	96	3
Pristina leidyi (Naididae)	460	47	2

© 1998 NRC Canada

Table 3 (*concluded*).

Taxon	Dissolved solids ($mg \cdot L^{-1}$)		Halobion index[a]
	Optimum	Tolerance	
Limnodrilus hoffmeisteri (Tubificidae)	460	150	3
Pristinella jenkinae (Naididae)	470	17	2
Glyptotendipes cf. *barbipes* (Chironomidae)	480	50	3
Prostoma sp. (Nemertea)	480	77	2
Chaetogaster diaphanus (Naididae)	490	50	3
Pristina aequiseta (Naididae)	520	45	—
Urnatella gracilis (Entoprocta)	530	33	1
Paratanytarsus sp. (Chironomidae)	560	95	3
Parachironomus arcuatus gr. (Chironomidae)	630	83	3
Cricotopus sp. 1 (Chironomidae)	640	70	3
Parachironomus frequens gr. (Chironomidae)	670	70	3
Corophium spinicornae (Amphipoda)	670	60	3–4
Bratislavia unidentata (Naididae)	690	48	1
Plumatella repens (Bryozoa)	760	60	—
Cordylophora lacustris (Coelenterata)	850	72	4
Paranais frici (Naididae)	870	74	4
Tanytarsus sp. 2 (Chironomidae)	890	25	3
Apedilum subcinctum (Chironomidae)	1100	91	—
Cladotanytarsus mancus gr. (Chironomidae)	1300	53	3
Nais elinguis (Naididae)	1300	120	3
Goeldichironomus sp. (Chironomidae)	1300	92	—

Note: Concentrations listed are medians for the five sampling periods (see text). Tolerance values were corrected for bias by taking into account the effective number of occurrences.

[a]Halobion index classification: freshwater taxa (0 = not recorded at >1000 mg $TDS \cdot L^{-1}$; 1 = tolerates 1000–2000 mg $TDS \cdot L^{-1}$; 2 = tolerates 2000–5000 mg $TDS \cdot L^{-1}$); euryhaline freshwater taxa (3 = tolerates 5000 – 10 000 mg $TDS \cdot L^{-1}$); brackish water taxa (4 = tolerates >10 000 mg $TDS \cdot L^{-1}$). References used to determine halobion indexes may be obtained from Leland (1998).

varied on a scale too small to be summarized adequately by a large-scale environmental gradient. The apparent large-scale complex gradient generally was dominated by one or two sites (Tuolumne River, Merced River, or Mud Slough), and the order of sites was not consistent.

Partial CCA was used to eliminate effects of covariables (ter Braak 1990) primarily expressing microhabitat heterogeneity (particle size and percent fines of sediment) and to relate the residual variation to water quality constituents. As expected, eigenvalues for axes 1 and 2 decreased markedly with partialling-out of the variance (Figs. 3D–3I) associated with microhabitat heterogeneity; however, species–environment correlations remained high (CCA axis 1: 0.31–0.40; CCA axis 2: 0.21–0.34; partial CCA axis 1: 0.44–0.51; partial CCA axis 2: 0.22–0.38). For each sampling date, samples from tributaries draining the Sierra Nevada tended toward one end of the primary gradient (Figs. 3G–3I). San Joaquin River reaches most impacted by Mud Slough and Salt Slough (km 202–185) tended to segregate from reaches (km 159–116) located further downriver. The position of Salt Slough in ordination space was always near that of upriver reaches (km 202–185) of the San Joaquin River whereas the position of Mud Slough in ordination space was highly variable. The position of km 213 also was variable, reflecting the changing water source and lower TDS concentration during the irrigation season of 1986 than of 1985 (Fig. 2). Succeeding CCA axes were dominated by one or two sites (Mud Slough, Salt Slough, San Joaquin River km 159).

Concentrations of TDS, suspended matter, and algal mass were related ($p < 0.05$) independently to community summary statistics (partial CCA site scores) on all sampling dates (Table 2). Inorganic N was a significant environmental variable on most sampling dates. Axis 1 accounted for 44–51% of the explained variance (after fitting covariables) and axis 2 for 22–38%. Partialling-out variance associated with measured variables expressing microhabitat heterogeneity improved the ability to detect large-scale patterns in response of the benthic community to water quality. However, the pattern among sites in ordination space was less consistent for benthic fauna than for multiple-plate fauna, indicating in part a greater degree of habitat specialization. Because the orderings among sites and species in partial CCA were inconsistent, TDS optima for the benthic fauna are not reported.

Benthic invertebrate distributions

Multiple-plate fauna

Faunal assemblages on multiple-plate samplers were diverse (150 taxa identified) and dense (generally 2000 –10 000 individuals·0.1 m^{-2}). Animal biomass (visual estimate) generally was dominated by a few taxa, notably the arthropods *Hydropsyche californica* and *Corophium spinicornae*, the

© 1998 NRC Canada

cnidarian *Cordylophora lacustris*, and (or) the "bryozoans" *Plumatella repens* and *Urnatella gracilis*. These sessile filterers increased habitat complexity by building retreats or by "vegetative growth."

Six site (sample) groups were identified (Table 4) using TWINSPAN (and corroborating patterns in DCA) by including samples from all dates in the analysis and limiting the classification to major TWINSPAN divisions (levels 1–3). At level 3, site groups identified corresponded to apparent groupings expressed by DCA and geographic categories, with little segregation of samples based on sampling date. Groups 1 and 2 are the major tributaries draining the Sierra Nevada, and group 3 is the lower San Joaquin River (km 125–116). Median TDS concentrations in these reaches were different ($p < 0.01$) from those in other reaches of the study area (Fig. 4). Group 4 consists primarily of samples from the upper San Joaquin River (km 213 and 185–159). Group 5 is dominated by Salt Slough and reaches of the San Joaquin River (km 202–185) most impacted by Salt Slough and Mud Slough. Mud Slough (group 6) is the most saline reach in the study area.

Taxa richness and EPT (ephemeropterans, plecopterans, and trichopterans) richness, commonly used water quality indices, were greater for the lower San Joaquin River and tributaries draining the Sierra Nevada than elsewhere. In groups 1–3, EPT richness differed ($p < 0.01$) from that of groups 4–6, and taxa richness differed from that of groups 5 and 6. Mud Slough had fewer taxa (total and EPT) than other reaches sampled.

Taxa characteristic of an ecological group defined by TWINSPAN (Table 4) either occurred consistently with other taxa in the ecological group or were abundant in samples from an associated site group. These taxa also were identified in DCA as primary contributors to the explained variance in species abundances. Characteristic taxa in ecological groups A and B include several EPT species (*Ephemerella* sp., *Nectopsyche* sp., and *Tricorythodes* cf. *minutus*), chironomids (*Cricotopus tremulus* gr., *Parakiefferella* sp., *Polypedilum* cf. *illinoense*, *Tanytarsus* sp. 1 and *Synorthocladius* sp.), and pollution-intolerant oligochaetes (*Nais behningi* and *Pristinella acuminata*) that occurred regularly at some sites but were rarely numerical dominants (>100 individuals·0.1 m^{-2}). Taxa in ecological groups C and D also occurred more frequently in site groups 1–3 than elsewhere, but they were common residents of the upper San Joaquin River and Salt Slough (groups 4 and 5). These include the ephemeropterans *Caenis* sp., *Fallceon quilleri*, and *Heptagenia elegantula*, the chironomids *Ablabesmyia mallochi*, *Thienemanniella* sp., and *Thienemannimyia* sp., and the odonate *Argia* sp.

Taxa in group E exhibited little site affinity, but some rarely occurred in Mud Slough. Many taxa in this group, including most common oligochaetes of the study area, were numerical dominants in several reaches. The only non-chironomid insect was *Hydropsyche californica*.

Ecological group F consists of taxa that were most abundant in the upper San Joaquin River and tributaries draining the valley floor (groups 4–6). Characteristic taxa include *Corophium spinicornae*, *Parachironomus arcuatus* gr., and *Paranais frici*, species described as halophilic or pollution tolerant in other distributional studies (Table 3). Ecological group G contains taxa that were most abundant in Mud Slough and Salt Slough and reaches of the San Joaquin River (km 202–185) most impacted by flow from these tributaries. Characteristic taxa commonly associated with saline conditions in other surveys include *Cordylophora lacustris* and the chironomids *Cladotanytarsus mancus* gr., *Glyptotendipes* cf. *barbipes*, and *Parachironomus frequens* gr. Occurrence of the "bryozoans" *Urnatella gracilis* and *Plumatella repens* is not associated generally with saline conditions, so their abundance may indicate a plentiful suspended food supply.

Benthic fauna

Faunal assemblages in sand substratum were generally less diverse than multiple-plate assemblages (Fig. 4). In addition, sites were not differentiated consistently by TWINSPAN, indicating that small-scale habitat characteristics (including heterogeneity of substratum) impose an important constraint on community structure. Six site (sample) groups were identified (Table 4). Although strongly differentiated by faunal assemblage, groups 1 and 6 are both composed of samples from major tributaries draining the Sierra Nevada. Most samples from the Merced and Stanislaus rivers are in group 1 and most Tuolumne River samples in group 6. Taxa richness and percent fines (<0.63 μm) of sediment were greater ($p < 0.01$) in group 6 samples than in group 1 (Fig. 4).

Group 2 consists of samples from the San Joaquin River, with no consistent difference in faunal assemblage among upper and lower reaches. Taxa richness was low (median = 10), as in groups 1, 3, and 4. The particle size (medium to coarse sand) of sediment was similiar to that of most other site groups. The percent fine fraction was less than that of groups 3–6 ($p < 0.01$), indicating a more erosional environment. Group 3 is a small transition group similar to group 2.

Most samples from Mud Slough and Salt Slough were assigned to the same site group (4). Taxa richness of this group was low. Particle size (medium sand) was smaller than that of groups 1, 2, and 6. Group 5 consists of samples from the upper San Joaquin River (km 213–185), Salt Slough, and Mud Slough. Taxa richness was much higher than in groups 1–4 ($p < 0.01$). The larger fine fraction (median of 1.35%) of sediments indicates a less erosional environment.

Ecological group A contains many taxa ubiquitous in the study area (Table 4). Although not separated at level 3 by TWINSPAN, benthic assemblages of the San Joaquin River and the major tributaries draining the Sierra Nevada are distinct. *Paratendipes* cf. *basidens*, *Kloosia* nr. *pusilla*, *Macrostomum* sp. 2, and *Monhystera* sp. are more abundant in the San Joaquin River; *Chaetogaster parvus* and *Robackia demeijerei* occur more frequently in the tributaries. These taxa (with the exception of immature *Corbicula fluminea*) rarely occurred on multiple-plate samplers and are adapted to a shifting-sand habitat.

Group B consists of taxa that occurred most frequently in Mud Slough and Salt Slough and includes *Limnodrilus hoffmeisteri* and several unidentified microturbellarians. Group C contains ubiquitous taxa that occurred most frequently in the Tuolumne River or elsewhere in less erosional habitat (group 5). *Aulodrilus pigueti*, *Paracladopelma* cf. *nereis*, and *Paranais frici* are part of the river-margin assemblage of the lower San Joaquin River. *Prostoma* sp., *Cladotanytarsus mancus* gr., *Cladotanytarsus vanderwulpi* gr.,

© 1998 NRC Canada

Table 4. Median abundances (or frequency of occurrence) of fauna in TWINSPAN site groups.

	Multiple-plate fauna					
	Site group					
	1	2	3	4	5	6
Taxon group A						
Ephemerella sp.	*	2	*	*		
Nais behningi	*	3	4	*	*	
Chelifera sp.	*	2	*			
Polypedilum fallax gr.		1	**	*		
Tanytarsus sp. 1	3	2	2	*	*	
Synorthocladius sp.	3	3	3	*	*	
Cricotopus tremulus gr.	*	3	**	*		
Tricorythodes cf. *minutus*	3	3	2	**	*	
Corynoneura sp.	*	2	*	*	*	**
Simulium spp.		2	2	*		**
Parakiefferiella sp.	1	3	3	**		*
Orthocladius/Cricotopus spp.	**	3	3	2		*
Polypedilum cf. *illinoense*	**	3	2	**	*	
Undetermined Tardigrada	**	**	2	*	*	
Hydra sp.	2	2	**	**	*	*
Taxon group B						
Nectopsyche sp.	3	1	*	*	*	
Dubiraphia giulianii	2	**	*	*	*	
Ferrissia sp.	3	*	*	*	*	
Pristinella acuminata	3	*		*	*	
Dugesia sp.	2	**	**	*	**	**
Taxon group C						
Heptagenia elegantula	1	3	4	3	*	
Enchytraeidae	**	*	2	*	*	**
Thienemanniella sp.	3	4	3	3	2	*
Fallceon quilleri	2	3	3	3	**	
Undetermined Acari	2	3	3	3	*	*
Ablabesmyia mallochi	3	2	2	2	**	
Taxon group D						
Caenis sp.	3	*	**	**	**	**
Undetermined Ostracoda	2	1	*	**	*	2
Thienemannimyia sp.	*	1	**	2	*	
Argia sp.	2	2	**	2	2	

	Benthic fauna					
	Site group					
	1	2	3	4	5	6
Taxon group A						
Chaetogaster parvus	2	**		*		**
Chaetogaster sp. 1	2	2	*		*	**
Kloosia nr. *pusilla*	**	3	2	**	1	
Paratendipes cf. *basidens*	*	3	2	*	**	*
Macrostomum sp. 2	**	2	2	**	1	*
Monhystera sp.	*	4	4	3	3	*
Robackia demeijerei	3	**		*	*	3
Corbicula fluminea	4	3	4	4	3	4
Taxon group B						
Mononchus spp.		*	*	2	*	*
cf. *Tobrilus* spp.	*	*	*	*	2	2
Polycystidae sp.	*	*	2	2	**	*
Limnodrilus hoffmeisteri	*	**	2	2	3	2
Amphichaeta nr. *leydigi*	*	*	2	*	**	**
Taxon group C						
Prostoma sp.	**	*	**	**	**	3
Aeolosoma spp.	2	**	1	**	3	3
Undetermined Acari	**	**	*	**	**	3
Cladotanytarsus vanderwulpi gr.	*	*	*		*	3
Cypridopsis spp.	*	*	*	*	**	2
Cricotopus bicinctus	*	*	*	**	**	2
Cladotanytarsus mancus gr.	*	*	**	**	3	**
Paracladopelma cf. *nereis*	*	*	**	*	2	*
Aulodrilus pigueti		*	*	*	**	**
Paranais frici			*	*	1	*
Taxon group D						
cf. *Phaenocora* sp.			*	*	2	*
Undetermined Cytheridae	*	*	*	*	1	**
Cryptochironomus spp.	*		*	**	2	3
Nanocladius bicolor gr. spp.	*	*	*	*	1	2
Chaetogaster diastrophus	*	*			**	2
Nais pardalis	*	*	*	*	1	3
Nais variabilis	*	*			**	2

© 1998 NRC Canada

Table 4 (*continued*).

	Multiple-plate fauna						Benthic fauna					
	Site group						Site group					
	1	2	3	4	5	6	1	2	3	4	5	6
Taxon group E							*Pristinella acuminata*	*	*	*	*	**	3
Hemerodromia sp.	2	3	3	3	3	*	*Mermithoidea* spp.		*			*	3
Dicrotendipes spp.	3	2	3	3	3	**	*Macrostomum* sp. 1					*	1
Rheotanytarsus sp.	3	4	4	4	3	*	*Pristinella osborni*	*	*			**	3
Slavina appendiculata	3	2	4	3	3	*	*Slavina appendiculata*	*	*		*	*	1
Nais pardalis	4	4	4	4	4	2	*Aulodrilus limnobius*	*	*			*	3
Nais communis	2	3	2	3	2	*	*Bothrioneurum vejdovskyanum*	*		*	*	*	2
Macrostomum sp. 1	3	2	2	3	3	**	*Tricorythodes* cf. *minutus*	*	*	*	*	*	2
Corbicula fluminea	3	3	3	2	2	2	*Dubiraphia giuliani*	*					2
Cricotopus bicinctus	3	3	4	3	3	4	*Nectopsyche* sp.	*				*	2
Pristinella osborni	4	3	3	3	3	3	*Tanytarsus* sp.	*	*	*		*	3
Chaetogaster diastrophus	4	4	4	4	3	4	Group sample size						
Nanocladius bicolor gr. spp.	4	3	4	4	4	4	Tuolumne River	4					13
Hydropsyche californica	3	4	5	5	4	3	Stanislaus and Merced rivers	19	1			1	2
Undetermined Harpacticoida	2	**	3	3	4	4	San Joaquin River (km 125–116)		24	2		2	
Nais variabilis	3	3	3	3	3	2	San Joaquin River (km 213–159)		46	7	1	9	
Chaetogaster diaphanus	**	2	3	3	2	2	Salt Slough		1	3	13		
Aeolosoma spp.	4	3	4	4	4	5	Mud Slough			2	10	5	
Undetermined Nematoda	3	3	4	4	4	4	Total	23	72	14	24	17	15
Prostoma sp.	3	2	2	2	3	3							
Taxon group F													
Cypria spp.	2		**	2	3	3							
Parachironomus arcuatus gr.	*	*	**	**	**	3							
Corophium spinicornae			4	4	4	5							
Paranais frici	**		**	**	2	3							
Pristina aequiseta	2	*	2	3	3	2							
Dero nivea	*	2	**	3	2	*							
Urnatella gracilis	**	**	1	1	2	1							
Taxon group G													
Cordylophora lacustris			*	**	3	5							
Parachironomus frequens gr.	*			*	**	1							
Bratislavia unidentata			*	**	1	*							
Plumatella repens	*	*	*	1	2	3							
Cladotanytarsus mancus gr.	*			**	*	3							
Glyptotendipes cf. *barbipes*				**	2	*							

© 1998 NRC Canada

Table 4 (*concluded*).

	Multiple-plate fauna						Benthic fauna					
	Site group						Site group					
	1	2	3	4	5	6	1	2	3	4	5	6
Group sample size												
Stanislaus, Tuolumne, and Merced rivers	14	9			1							
San Joaquin River (km 125–116)			14	5								
San Joaquin River (km 213–159)			1	24	17							
Salt Slough				2	8							
Mud Slough						12						
Total	14	9	15	32	25	12						

Note: Data for all five dates and 11 river reaches sampled were included in the analysis. Taxa listed occurred in 50% or more of the samples of at least one site group. Abundance categories (individuals·0.1 m^{-2} for multiple-plate fauna and individuals·0.02 m^{-2} for benthic fauna (Ponar samples): 1 = 1; 2 = 1–10; 3 = 10–100; 4 = 100–1000; 5 = >1000. Taxa occurred in >50% of samples. Frequency categories: *taxon occurred in <25% of samples; **taxon occurred in >25% but <50% of samples.

Aelosoma spp., and *Paranais frici* also occurred commonly on the multiple-plate samplers as well as in sand substratum.

Group D is a large assemblage, accounting for the taxa richness of site groups 5 and 6. Many of these taxa also are common members of the multiple-plate fauna, indicating that they are not strongly psammophilous. Taxa unique to the major tributaries draining the Sierra Nevada are included.

Discussion

Water quality gradients of potential biological importance

Other investigators have considered the distribution of invertebrates in rivers in relation to salinity, but few were concerned with the concentration range (55–1700 mg TDS·L^{-1}) represented by the San Joaquin River and its major tributaries. This is surprising because typical increases in salinity due to agricultural drainage water in similar hydrogeologic areas range from <300 mg TDS·L^{-1} to between 300 and 1500 mg TDS·L^{-1} (Williams 1987; Engberg and Sylvester 1993). Based on a review of saline discharges to streams and wetlands, Hart et al. (1991) concluded that 1000 mg TDS·L^{-1} may be a critical threshold beyond which adverse effects occur.

Many of the numerically dominant multiple-plate species (Table 4, taxa group E), including most common oligochaetes, showed little variation in occurrence with salinity in the San Joaquin River and its major tributaries. However, more complex measures of community structure, taxa richness, and proportional representation of major taxonomic groups (EPT richness) varied with TDS concentration. This variable accounted for a large part of the explained variance in multiple-plate assemblages over all seasons, flow conditions, and irrigation regimes. However, the degree to which salinity alone limited distributions of resident taxa is not clear. Most of the common taxa are found in more saline environments (Table 3), indicating that osmotic tolerance limits were not exceeded for these taxa. (Information in the literature on osmotic tolerance limits is sparse and largely anecdotal.) However, an ordering of taxa based on abundance in sample reaches corresponds to an ordering based on their salinity tolerance. This suggests that distributions of many of the resident taxa reflect their optimal salinity range. Further documentation of their salinity optima in other rivers or detailed experimental work on salinity tolerances of the resident fauna is required for a more complete assessment.

Surveys of invertebrate assemblages in rivers undergoing salinization that can be compared directly with our findings are rare. Metzeling (1993) observed no relationship between salinity and taxa richness, faunal abundance, or proportional representation of major taxonomic groups at TDS concentrations ranging from 51 to 1100 mg·L^{-1} in a study of naturally saline river basins. However, invertebrate species in those basins were adapted to saline conditions. Nevertheless, distinct communities associated with either low or high salinity were evident over this range. Harrell and Dorris (1968) observed little effect of salinity at these concentrations on stream pool communities. Short et al. (1991) found taxa richness of invertebrate communities to decrease with increasing salinity at higher concentrations (<10 000 mg TDS·L^{-1}) in a basin chronically impacted by oilfield brines. Ephemeropterans

© 1998 NRC Canada

Fig. 4. Taxa richness, EPT richness, TDS concentration, and sediment particle size and percent fines of site groups (defined by TWINSPAN) in the San Joaquin River and its major tributaries. Richness is expressed as the median number of taxa per sample (0.02 m^2 for benthic fauna and 0.1 m^2 for multiple-plate fauna). The significance of differences among site groups was determined by a Kruskal–Wallis ANOVA by ranks, followed by pairwise Mann–Whitney (ranked *t*) tests.

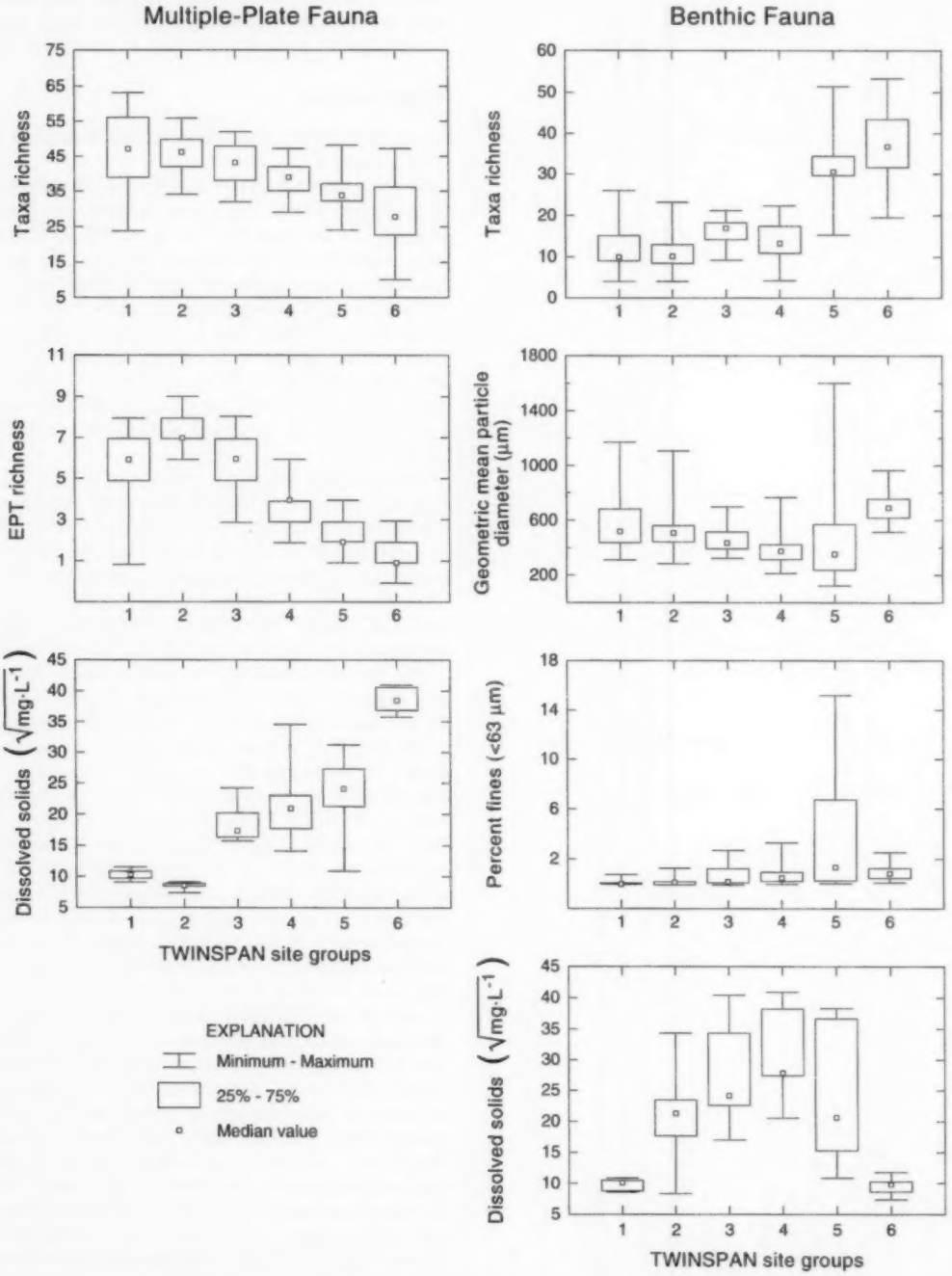

© 1998 NRC Canada

did not tolerate salinities >2000 mg TDS·L^{-1}. Ephemeropterans in the San Joaquin River rarely occurred at salinities >1000 mg TDS·L^{-1}. Below about 2000 mg TDS·L^{-1}, abundances of individual species are apt to be a better indicator than presence or absence (Williams 1987; Metzeling 1993).

Concentrations of Se and B in riverwater were strongly correlated ($r^2 > 0.60$) with TDS on most sampling dates, adding some uncertainty about effects of salinity on distributions of the resident fauna. Concentrations of Se (predominantly SeO_4) in Mud Slough, Salt Slough, and upper reaches of the San Joaquin River commonly exceed the water quality criterion (5 µg Se·L^{-1}, USEPA 1987) for protecting aquatic life resources. The few existing experimental data on direct toxicity of Se to aquatic invertebrates are contradictory. Se concentrations in tissue resulting in decreased growth of *Chironomus decorus* larvae in experimental chambers (Malchow et al. 1995) are two orders of magnitude less than concentrations found in dipterans from saline evaporation ponds in the study area. Furthermore, *Daphnia magna* tolerates dietary concentrations, without effects on reproduction, growth, or survival (e.g., Boyum and Brooks 1988), that greatly exceed Se concentrations in suspended matter of the San Joaquin River and its tributaries (Leland and Scudder 1990).

Concentrations of As, B, and Mo in the study area are substantially less than concentrations known to be toxic to fish and aquatic invertebrates (e.g., Naddy et al. 1995), indicating that direct effects of these trace elements on community structure are unlikely.

Unionized ammonia was not present during the period of study at concentrations known to be toxic to aquatic invertebrates. Measured concentrations did not exceed 0.05 mg NH_3·L^{-1}. The published response range for invertebrate species in acute toxicity tests is 0.53–23 mg NH_3·L^{-1}, and chronic (life cycle) tests of two species of *Daphnia* indicate that toxicity occurs at 0.3–1.2 mg NH_3·L^{-1} (USEPA 1986).

Synoptic surveys conducted in autumn 1985 and spring 1986 of commonly used triazine and chlorophenoxy herbicides, carbamate and organophosphorus insecticides, and purgeable organic compounds indicated that residues of these compounds in river water rarely exceeded legally acceptable limits or analytical detection limits (USEPA 1986; Shelton and Miller 1988). Of 51 compounds determined in samples from 28 river reaches, only diazinon (four reaches) and Dicamba (one reach) were detected and only diazinon exceeded the legally acceptable limit (in Orestimba Creek). Concentrations of chlorinated hydrocarbon compounds in bed sediment (Gilliom and Clifton 1990) and animal tissue (*Corbicula fluminea*) (Leland 1998) were greater in downriver reaches (km 175–116) of the San Joaquin River (and tributaries to this part of the river) than in upriver reaches. The concentrations typically were low, but several insecticides (chlorpyrifos, DDT, and toxaphene) were elevated in tributaries draining the Coast Ranges and in the mainstem downriver of these tributaries.

As solute pesticide concentrations during the study period were largely censored and chlorinated hydrocarbon residues in bed sediment and animal tissue were sampled only once (September–October 1985), these data were not included in the CCA. However, the data are inconsistent with large-scale spatial trends in water quality indicated by the structure of invertebrate communities. Pesticide concentrations during the study period and in subsequent surveys (springs of 1988 and 1989) of ambient toxicity (Foe and Connor 1991) were greater in downriver reaches (km 175–116) of the San Joaquin River (and tributaries to this part of the river) than in upriver reaches. In contrast, analyses of community structure revealed a different water quality gradient. The multiple-plate fauna in Mud Slough, Salt Slough, and reaches of the San Joaquin River (km 202–185) most impacted by these tributaries were less diverse and more indicative of degraded water quality conditions than in reaches located elsewhere in the study area.

The above discussion considers distributions of invertebrates in relation to single-constituent concentrations, but organisms respond to a complex of factors, not single constituents. Dissolved solids concentrations in the San Joaquin River and its major tributaries are not large compared with known salinity tolerances of resident species, but distributions of many of these taxa reflect, at least in part, their physiological fitness for saline conditions. Local abundances of some species in the drainage also may be limited by other water quality constituents (suspended matter, pesticides) or biotic factors (predation, competition). There is a paucity of literature on the effects of soluble salts on invertebrate communities over the observed salinity range, due in part to an inability to dissociate effects of salinity from those of other environmental factors.

Habitat type and dominant associated species

Multiple-plate fauna

Multiple-plate samplers were used to represent snags, the dominant stable substratum in the study area; qualitative sampling of snags supported this approach (see also Mason et al. 1973). Communities on stable and unstable substrata were highly dissimilar, an expected finding in light of other comparisons of faunal assemblages in sand-bed rivers (e.g., Benke et al. 1984). Biomass of the multiple-plate fauna was dominated by sessile filterers, species requiring both substratum stability and water flow. The microhabitat (near-surface velocity, substratum texture) of the samplers was modified by these animals, and interactions among species presumably affected community structure. Cover and Harrell (1978) noted an increase in oligochaete abundance with colonization time due to algal growth. It was common to find multiple-plate samplers densely covered with *Hydropsyche californica* retreats in the lower San Joaquin River and with *Cordylophora lacustris* colonies or *Corophium spinicornae* tubes at upriver sites and in Salt Slough and Mud Slough.

Benthic fauna

Benthic faunal assemblages of the San Joaquin River and its major tributaries resemble those of other sand-bed rivers. Although comparable data are rare for rivers in western North America, similar invertebrate assemblages, characterized by low taxa richness and psammorheophilic or psammobiontic specialists, have been reported for other regions. Common species include immature *Corbicula fluminea* (e.g., Beckett et al. 1983), chironomids of the "*Harnischia* complex" (e.g., Jankovic 1979; Soluk 1985), and very small annelids and microturbellarians (e.g., Fomenko 1972; Benke et al. 1984).

© 1998 NRC Canada

Kloosia and *Robackia*, in common with other members of the *Harnischia* complex, have a narrow body form adapted for burrowing. Field observations of *Kloosia* nr. *pusilla* and *Paratendipes* cf. *basidens*, the dominant psammorheophilic chironomids in the San Joaquin River, indicate active use of silk to resist displacement; this behavior also characterizes *Robackia demeijerei* (Soluk 1985). Other numerically dominant members of this assemblage (*Chaetogaster parvus*, *Chaetogaster* sp. 1, and *Macrostomum* sp. 2) are smaller than congeners on stable substratum or in less erosional sand habitat, a frequently noted characteristic of the fauna of sand-bed rivers.

Occasional samples of the benthic fauna had substantially more species than others and included taxa that colonized the multiple-plate samplers. Although river margins or pools were not sampled, patches of less erosional habitat were indicated by a greater silt–clay content of sediment. Assemblages in these patches resembled those of depositional habitat in other sand-bed rivers, including a greater representation of less specialized chironomids, tubificids, and naidids (e.g., Beckett et al. 1983; Benke et al. 1984). Greater abundances or biomass of individuals and greater taxa richness of assemblages are reported generally for silty, marginal areas than for midchannel, unstable substratum.

Habitat characteristics controlling diversity and abundance of invertebrate assemblages in sand substratum include particle size, heterogeneity, and organic matter content of sediments. Rae (1985) observed differences among chironomid species in preference for each of these attributes in a medium to coarse sand river reach. Species–species pair comparisons of the 17 most abundant taxa indicated that most taxa have a unique distribution. As systematic sampling of midchannel habitat was used in the present study to examine large-scale distributions of common taxa, statistical analyses of microhabitat preference were not feasible. However, communities associated with dominant habitats of the study area were defined.

Elucidation of large-scale (basin) patterns in community structure

A consistent large-scale pattern in community structure was observed with stable substrates standardized for small-scale habitat conditions. (Small-scale in this usage refers to variability within a reach, such as substratum patches, and large-scale to interreach variability.) Use of multiple-plate samplers provided similar substratum, water depth, and water velocity at all sites. A large-scale gradient related to water quality was evident in multiple-plate assemblages over all seasons, flow conditions, and irrigation regimes, despite substantial temporal variability (but consistent spatial trends) in water quality and seasonal cycles in abundance of dominant organisms such as *Plumatella repens* and *Cordylophora lacustris*.

Sampling of the benthic fauna was standardized partially by collecting only from medium to coarse sand habitat in the center three fourths of the channel. However, more detailed observation of the substratum indicated both small-scale and large-scale habitat heterogeneity. Measured sediment characteristics (particle size and percent fines) were related significantly to structure of the benthic community, and unmeasured habitat attributes (sediment stability and organic matter content) may have varied on the same scale. Attempts to eliminate effects of covariables expressing microhabitat heterogeneity using partial CCA were only partly successful. Most samples of the benthic fauna were dominated by a taxa-poor assemblage of psammorheophilous species rarely found on multiple-plate samplers. The small number of taxa and degree of habitat specialization of the benthic fauna contributed to a weaker relationship between community statistics and water quality gradients than was observed using standardized, stable substratum.

Rivers in semiarid and arid regions often develop complex salinity gradients. Most investigators have ignored or infrequently measured the impact of these complex gradients on structure of aquatic communities. However, concentration and composition of soluble salts in surface waters of these areas may be a more important large-scale constraint on benthic invertebrate distributions than the variable flow rates, sources of detritus, or anthropogenic contaminants that vary on a seasonal basis. Investigations of intensively irrigated agricultural drainages often begin with the assumption that pesticides and sediment erosion are the primary factors limiting invertebrate distributions. These factors clearly are important locally in the lower San Joaquin River and its tributaries, but salinity is the principal large-scale gradient expressed in invertebrate community structure.

Acknowledgments

Financial support for this study was provided in part by the U.S. Department of the Interior's San Joaquin Valley Drainage Program. We thank Barbara C. Scudder and Raymond L.J. Wong of the U.S. Geological Survey for their assistance in sample collection and acknowledge Robert J. Gilliom and Larry R. Shelton, also of the U.S. Geological Survey, for sharing data on water chemistry with us. Constructive reviews of the manuscript were provided by Larry R. Brown, Thomas F. Cuffney, and Terry M. Short.

References

Armitage, P.D., Moss, D., Wright, J.F., and Furse, M.T. 1983. The performance of a new biological water quality score system based on macroinvertebrates over a wide range of unpolluted running-water sites. Water Res. **17**: 333–347.

Beckett, D.C., Bingham, C.R., and Sanders, L.G. 1983. Benthic macroinvertebrates of selected habitats of the lower Mississippi River. J. Freshwater Ecol. **2**: 247–261.

Benke, A.C., Van Arsdall, T.C., Gillespie, D.M., and Parrish, F.K. 1984. Invertebrate productivity in a subtropical blackwater river: the importance of habitat and life history. Ecol. Monogr. **54**: 25–63.

Boyum, K.W., and Brooks, A.S. 1988. The effect of selenium in water and food on *Daphnia* populations. Arch. Environ. Contam. Toxicol. **17**: 555–560.

Cover, E.C., and Harrell, R.C. 1978. Sequences of colonization, diversity, biomass, and productivity of macroinvertebrates on artificial substrates in a freshwater canal. Hydrobiologia, **59**: 81–95.

Deverel, S.J., and Fujii, R. 1988. Processes affecting the distribution of selenium in shallow ground water of agricultural areas, western San Joaquin Valley, California. Water Resour. Res. **24**: 516–524.

Engberg, R.A., and Sylvester, M.A. 1993. Concentrations, distribution and sources of selenium from irrigated lands in the western United States. J. Irrig. Drain. Eng. **119**: 522–536.

Fishman, M.J., and Friedman, L.C. (*Editors*). 1985. Methods for determination of inorganic substances in water and fluvial

© 1998 NRC Canada

sediments. Chap. A1, Book 5. *In* Techniques of water-resources investigations of the United States Geological Survey. Open-File Rep. U.S. Geological Survey, Denver, Colo. pp. 85–495.

Foe, C.G., and Connor, V. 1991. San Joaquin watershed bioassay results, 1988–90. Central Valley Regional Water Quality Control Board, Sacramento, Calif.

Fomenko, N.V. 1972. Ecological groups of oligochaeta in the Dnieper Basin. *In* Aquatic oligochaete worms: taxonomy, ecology, and faunistic studies in the USSR. *Edited by* G.M. Belyaev. Nauka Publishers, Moscow, Russia. pp. 105–118.

Gilliom, R.J., and Clifton, D.G. 1990. Organochlorine pesticide residues in bed sediments of the San Joaquin River, California. Water Resour. Bull. **26**: 11–24.

Harrell, R.C., and Dorris, D.C. 1968. Stream order, morphometry, physico-chemical conditions, and community structure of benthic macroinvertebrates in an intermittent stream system. Am. Midl. Nat. **80**: 220–251.

Hart, B.T., Bailey, P., Edwards, R., Hortle, K., James, K., McMahon, A., Meridith, C., and Swadling, K. 1991. A review of the salt sensitivity of the Australian freshwater biota. Hydrobiologia, **210**: 105–144.

Hill, M.O. 1979. DECORANA —a fortran program for detrended correspondence analysis and reciprocal averaging. Release B. Ecology and Systematics, Cornell University, Ithaca, N.Y.

Jankovic., M.J. 1979. Communities of chironomid larvae in the Velika Morava River. Hydrobiologia, **64**: 167–173.

Leland, H.V. 1995. Distribution of phytobenthos in the Yakima River Basin, Washington, in relation to geology, land use, and other environmental factors. Can. J. Fish. Aquat. Sci. **52**: 1108–1129.

Leland, H.V. 1998. (1) References used to determine halobion indexes (Table 3), and (2) organochlorine insecticides in soft tissue of *Corbicula fluminea* from the San Joaquin River and its major tributaries – 1985. Available on the World Wide Web at http://water.usgs.gov/lookup/get?crresearch/projects

Leland, H.V., and Scudder, B.C. 1990. Trace elements in *Corbicula fluminea* from the San Joaquin River, California. Sci. Total Environ. **97/98**: 641–672.

Line, J.M., ter Braak, C.J.F., and Birks, H.J.B. 1994. WACALIB version 3.3 — a computer program to reconstruct environmental variables from fossil assemblages by weighted averaging and to derive sample-species errors of prediction. J. Paleolimnol. **10**: 147–152.

Malchow, D.E., Knight, A.W., and Maier, K.J. 1995. Bioaccumulation and toxicity of selenium in *Chironomus decorus* larvae fed a diet of *Selenastrum capricornutum*. Arch. Environ. Contam. Toxicol. **29**: 104–109.

Markmann, C., 1986. Benthic monitoring in the Sacramento – San Joaquin Delta. Results from 1975 through 1981. Interagency Ecological Study Program for the Sacramento – San Joaquin Estuary. Tech. Rep. 12, California Department of Water Resources., Sacramento, Calif.

Mason, W.T., Weber, C.I., Lewis, P.A., and Julian, E.C. 1973. Factors affecting the performance of basket and multiplate macroinvertebrate samplers. Freshwater Biol. **3**: 409–436.

Metzeling, L. 1993. Benthic macroinvertebrate community structure in streams of different salinities. Aust. J. Mar. Freshwater Res. **44**: 335–351.

Moore, S.B., Winckel, J., Detwiler, S.J., Klasing, S.A., Gaul, P.A., Kanim, N.R., Kesser, B.E., DeBevec, A.B., Beardsley, K., and Puckett, L.K. 1990. Fish and wildlife resources and agricultural drainage in the San Joaquin Valley, California. Vol. 1. San Joaquin Valley Drainage Program, California Water Resources Control Board, Sacramento, Calif.

Naddy, R.B., LaPoint, T.W., and Klaine, S.J. 1995. Toxicity of arsenic, molybdenum and selenium combinations to *Ceriodaphnia dubia*. Environ. Toxicol. Chem. **14**: 329–336.

Presser, T.S., Swain, W.C., Tidball, R.R., and Severson, R.C. 1990. Geologic sources, mobilization, and transport of selenium from the California coast ranges to the western San Joaquin Valley: a reconnaissance study. Water Resour. Invest. Rep. 90-4070. U.S. Geological Survey, Denver, Colo.

Presser, T.S., Sylvester, M.A., and Low, W.H. 1994. Bioaccumulation of selenium from natural geologic sources in western states and its potential consequences. Environ. Manage. **18**: 423–436.

Rae, J.R. 1985. A multivariate study of resource partitioning in soft bottom lotic Chironomidae. Hydrobiologia, **126**: 275–285.

Shelton, L.R., and Miller, L.K. 1988. Water-quality data, San Joaquin Valley, California, March 1985 to March 1987. Open-File Rep. 88-479. U.S. Geological Survey, Denver, Colo.

Short, T.M., Black, J.A., and Birge, W.J. 1991. Ecology of a saline stream: community responses to spatial gradients of environmental conditions. Hydrobiologia, **226**: 167–178.

Siegfried, C.A., Kopache, M.E., and Knight, A.W. 1980. The benthos of a portion of the Sacramento River (San Francisco Bay estuary) during a dry year. Estuaries, **3**: 296–307.

Soluk, D.A. 1985. Macroinvertebrate abundance and production of psammophilous Chironomidae in shifting sand areas of a lowland river. Can. J. Fish. Aquat. Sci. **42**: 1296–1302

ter Braak, C.J.F. 1990. CANOCO: a FORTRAN program for canonical community ordination by (partial) (detrended) (canonical) correspondence analysis, principal components analysis and redundancy analysis. Update notes: CANOCO version 3.1. Agricultural Mathematics Group, Wageningen, The Netherlands.

ter Braak, C.J.F., and Verdonschot, P.F.M. 1995. Canonical correspondence analysis and related multivariate methods in aquatic ecology. Aquat. Sci. **57**: 255–264.

USEPA (U.S. Environmental Protection Agency). 1986. Quality criteria for water. EPA 440/5-86-001. Office of Water Regulations and Standards, USEPA, Washington, D.C.

USEPA (U.S. Environmental Protection Agency). 1987. Ambient water quality criteria for selenium. EPA 440/5-87-006. USEPA, Office of Water Regulations and Standards, Washington, D.C.

Williams, W.D. 1987. Salinization of rivers and streams, an important environmental hazard. Ambio, **16**: 180–185.

© 1998 NRC Canada

Does annual variation in growth and sexual maturation of white sucker (*Catostomus commersoni*) confound comparisons between pulp mill contaminated and reference rivers?

Dany Bussières, Marthe Monique Gagnon, Julian Dodson, and Peter V. Hodson

Abstract: A previous study on the effect of pulp and paper effluents on white sucker (*Catostomus commersoni*), conducted in 1991 and 1992, in both effluent-exposed and reference rivers showed that fish grew faster at downstream sites than at upstream sites. However, in contrast with fish from a reference river, fish exposed to effluent showed no decrease in age or size at first maturity or increase in gonad size or fecundity in response to greater growth. The objective of the present study, conducted in 1993, was to test if differences in measures of growth and sexual maturation between fish populations in exposed and reference rivers would vary from year to year and whether such variation would affect conclusions concerning the effects of pulp mill effluents. Although size at age, fecundity, and age at first maturity varied between the two studies, patterns of demographic responses to pulp mill effluents, relative to reference populations, remained the same, i.e., conclusions about effects of pulp mill effluents did not change despite variation in demographic variables between years and sites. This study reaffirmed the view that only by including the fish populations in a reference river could effects due to bleached kraft mill effluent be separated from effects due to nutrient gradients.

Résumé :Une étude antérieure concernant l'effet des effluents d'usine de pâte et papier sur les meuniers noirs (*Catostomus commersoni*), menée en 1991 et 1992 dans des cours d'eau exposés aux effluents et des cours d'eau témoins, a montré que les poissons croissaient plus rapidement aux sites d'aval qu'aux sites d'amont. Toutefois, à la différence des poissons d'un cours d'eau témoin, il n'y a pas eu chez les poissons exposés aux effluents de diminution de l'âge ou de la taille à la première maturité ni d'augmentation de la taille des gonades ou de la fécondité liées à leur taux de croissance accrue. L'objectif de la présente étude, menée en 1993, était de vérifier si les différences dans les mesures de la croissance et de la maturation sexuelle entre les populations de poissons de cours d'eau exposés et témoins variaient d'année en année, et si cette variation pouvait avoir un impact sur les conclusions relatives aux effets des effluents d'usines de pâte. Bien que la taille selon l'âge, la fécondité et l'âge à la première maturité aient varié d'une étude à l'autre, les profils de réponses démographiques aux effluents d'usines de pâte, par rapport aux populations témoins, sont demeurés les mêmes; c'est-à-dire que les conclusions concernant les effets des effluents des usines de pâte n'ont pas changé malgré une variation dans les variables démographiques entre les années et les sites. Cette étude confirme l'idée suivant laquelle on ne peut distinguer les effets dus aux effluents d'usine de pâte kraft blanchie des effets dus aux gradients de nutriants qu'en prenant en considération les populations de poissons d'un cours d'eau témoin.
[Traduit par la Rédaction]

Introduction

Recent North American studies of the effects of pulp and paper mill effluents discharged to the aquatic environment have revealed a variety of effects on fish, from biochemical disturbances to changes in population dynamics. These effects include bioaccumulation of chlorophenolic compounds (Gagnon et al. 1994), induction of the mixed function oxygenase (MFO) system (Adams et al. 1992; Ahokas et al. 1993; Gagnon et al. 1994), lowered steroid sex hormone concentrations (Munkittrick et al. 1992; Gagnon et al. 1994), disrupted fecundity–weight relationships (Gagnon et al. 1994), delayed age at maturity and increased size at maturity (Munkittrick et al. 1991; Gagnon et al. 1994, 1995*a*), and increased growth rates (Adams et al. 1992; Gagnon et al. 1994, 1995*a*; Haley et al. 1995). Although observed in many case studies, the pattern and extent of these responses appear to be site specific and may not be easily extrapolated to all situations.

In 1989, an extensive survey of the St. Maurice River, Québec, was initiated to investigate the validity of different parameters to be used in the Canadian Federal Environmental Effects Monitoring (EEM) program on pulp and paper mill

Received August 6, 1996. Accepted December 17, 1997.
J13594

D. Bussières, M.M. Gagnon, and J. Dodson. Département de biologie, Université Laval, Ste-Foy, QC G1K 7P4, Canada.
P.V. Hodson.[1] Director, School of Environmental Studies, Department of Biology, Queen's University, Kingston, ON K7L 3N6, Canada.

[1] Author to whom all correspondence should be addressed.
e-mail: hodsonp@biology.queensu.ca

© 1998 NRC Canada

Fig. 1. Stations sampled on the St. Maurice and Gatineau rivers. On the St. Maurice River, white sucker populations are separated by hydroelectric dams at La Tuque and Grand-Mère. A pulp mill located at La Tuque is the major industry discharging effluent to the river. On the Gatineau River, dams were also located immediately downstream of stations 1 and 3, but no major industries occur in the study area. (Adapted from Gagnon et al. 1995*a*.)

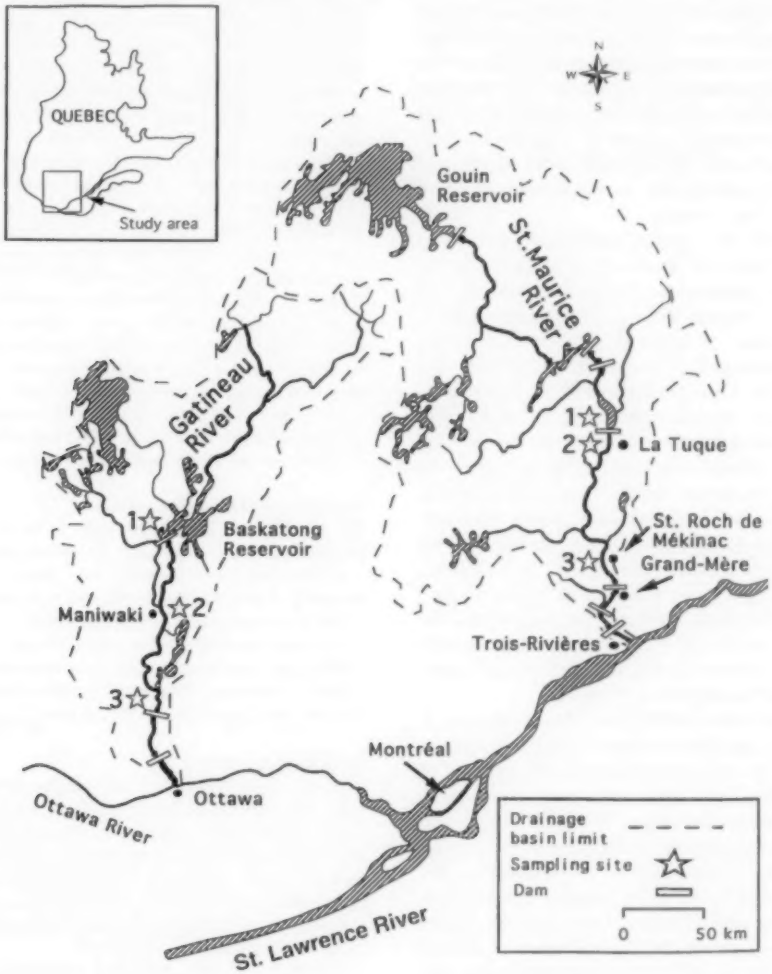

effluents (Environment Canada 1992). At the beginning of the study, the St. Maurice River received more than 10 t of chlorinated organic chemicals per day from a bleached kraft mill situated at La Tuque (Fig. 1) (Hodson et al. 1992). The mill adopted a new sequence of bleaching in September 1988, changing from C_DNE_HD to C_DE_O(DED) (mill manager, Cartons St-Laurent, La Tuque, Québec, personal communication). In September 1992, the mill converted to chlorine dioxide substitution to reduce elemental chlorine use.

In earlier studies, we sampled white sucker (*Catostomus commersoni*), one of the most widespread and abundant fishes in North America (Scott and Crossman 1973), from the St. Maurice River in 1991 at three sites extending over 100 km of river. The purpose was to assess the impact of the effluent on white sucker demographics and the spatial extent of that impact. A gradient of productivity was expected over such a distance (Vannote et al. 1980), and river morphology varied from reservoir (lake) to riverine conditions among sites. The river was also used for log driving. A second, uncontaminated river, the Gatineau River, Québec, was chosen as a reference river. It had a similar morphology and distribution of sampling sites as well as a log drive. White sucker were sampled from the Gatineau River in 1992 on similar dates and under similar conditions as for the St. Maurice River (Gagnon et al. 1995*a*).

In both rivers, we observed accelerated growth of white sucker that occurred between 2 and 10 years of age at downstream stations relative to upstream stations, suggesting gradients of nutrient enrichment independent of bleached kraft mill effluent (BKME) contamination (Gagnon et al. 1995*a*, 1995*b*). Despite enhanced growth at downstream stations in both rivers, the reproductive response was markedly different. Gatineau River fish exhibited increased reproductive effort in response to enhanced growth, as shown by reduced

© 1998 NRC Canada

length and age at first maturity, and increased gonad size and fecundity relative to body size (Gagnon et al. 1995*a*). The impacts of BKME exposure in the St. Maurice River were expressed as reduced reproductive effort in spite of enhanced growth at downstream stations, as revealed by greater length at maturity, reduced gonad size of females, and more variable fecundity relative to body size (Gagnon et al. 1995*a*). The reduction in potential reproductive performance was not obvious in simple upstream–downstream comparisons of the St. Maurice River, but became evident by comparison with fish from the uncontaminated Gatineau River which showed increased reproductive performance in response to enhanced growth rates (Gagnon et al. 1995*a*).

The EEM program for the pulp and paper industry requires each mill to study the impacts of its activities on the receiving environment. The EEM program is a series of monitoring and interpretation cycles, including field sampling repeated every 3 years, with comparisons of a recent cycle with previous cycles to assess temporal trends in environmental quality. The BKME-contaminated St. Maurice River and the uncontaminated Gatineau River provided an opportunity to test whether annual variations in demographics of white sucker populations would obscure effluent-associated changes that the EEM program wishes to detect. Both rivers exhibited very similar physicochemical and biotic characteristics, but interannual variations in demographic parameters among stations could affect previous conclusions. Although the mill changed its bleaching process in 1992, we did not anticipate new patterns in downstream fish population demographics in 1993 relative to 1991. Given the age of fish sampled (generally 4 years or older), the demographics in 1993 would likely reflect conditions from the previous 4–6 years.

The objective of this study was to determine if patterns of responses within rivers and between rivers previously documented were sufficiently strong to transcend the "noise" of natural annual variability and support the same conclusions about the effect of effluent exposure. Were the changes in demographics attributed to effluent exposure real and repeatable, or were they simply coincidental? We simultaneously sampled the Gatineau and St. Maurice rivers in 1993 during the spawning season of white sucker. Our previous results were based on data from the St. Maurice River in 1991 and from the Gatineau River in 1992. We compared these data sets to see if conclusions about the effect of effluent exposure would be altered by annual variation in fish demographics.

Materials and methods

Study areas

The St. Maurice and Gatineau rivers, located in the province of Québec (Fig. 1), exhibit similar watershed characteristics in terms of vegetation, soil types, weather conditions, and fish communities (Gagnon et al. 1995*a*). Overall, the St. Maurice River differs from the Gatineau River primarily in the discharge of BKME and a greater average flow rate of water associated with a greater watershed area. Fish communities were dominated by white sucker in both rivers.

The uncontaminated reference station 1 of the St. Maurice River was 10 km upstream of the mill and isolated from downstream stations by a hydroelectric dam situated beside the mill. Station 2 was located immediately downstream of the mill and next to the town of La Tuque, and station 3 was located 95 km downstream of the mill in a reservoir created by a second dam at Grand-Mère (Fig. 1). The primary sources of contamination in the study area were the pulp mill (chemicals, nutrients) and the town of La Tuque (nutrients). The effluent was diluted in the river to about 1% (v/v), and mixing was complete within 2 km of the discharge due to the hydroelectric dam and rapids downstream. At this rate of dilution, there were no measurable temperature differences among sites (Hodson et al. 1992). The 1993 sampling was performed 7 months after the conversion to chlorine dioxide substitution. However, because white sucker are long-lived, any significant demographic alterations observed in this study most likely reflect longer term exposure to effluent. There was continuous log floating at all three stations during the 2 years of sampling.

Three stations were also sampled on the Gatineau River (Fig. 1). The upstream station 1 was located in the Baskatong reservoir. The second station was located 30 km downstream of the dam near the town of Maniwaki. Station 3 on the Gatineau River was in a second reservoir located 105 km downstream from station 1. Most log floating was stopped during the summer of 1992, but some log floating persisted in 1993 while river banks were being cleared of logs.

In 1993, white suckers were collected simultaneously by two teams using gill nets in the two rivers immediately prior to spawning from May 3 to 13. The sampling procedure was similar for the two teams, following the methods used in 1991 and 1992 (Gagnon et al. 1995*a*). In the St. Maurice River, 1007 white sucker were collected in 1993 compared with 1301 in 1991, and in the Gatineau River, 854 white sucker were collected in 1993 compared with 723 in 1992.

Sample collection and analyses

For all fish, the fork length and the weights of the whole body, gonads, viscera, and carcass (whole body minus gonads and viscera) were recorded. Female gonads were preserved in Gilson's fluid and fecundity was measured by the method described in Gagnon et al. (1994) (egg counts of a dried subsample). For all fish, the first fin ray of the right pectoral fin was taken for age determination (Beamish 1973). Age was determined by the method described in Gagnon et al. (1995*a*). Validation of age estimates from fin rays with fish of known age has been established for white sucker (Chalanchuk 1984).

Statistical analyses

Five fish were considered the minimum number necessary to calculate a representative value for statistical analyses of any parameter at a given station in a given year. When a parameter did not satisfy the minimum sample requirement, we excluded that year and station from the statistical analysis. Normality and homogeneity of variances of all data sets were tested with a Shapiro–Wilk test and a Bartlett test, respectively. Log-transformation was used to correct for normality and heteroscedacity (Zar 1984).

For each river, an analysis of covariance (ANCOVA) with two classification factors (station, year) was used to compare fish size, gonad size, and fecundity, with age as the covariate of fish size and carcass weight (body weight minus gonads) as the covariate of gonad size and of fecundity (SAS 1988). The homogeneity of slopes relating the dependent variable and the covariable was tested and found to be similar ($P > 0.05$) in all cases. Therefore, the subsequent ANCOVAs were repeated excluding the interaction term (station × year × covariable) between the factors and the covariable (SAS 1988). We used contrast tests as a posteriori hypotheses to locate which station was significantly different from the others. In the case where there was a significant effect between the station and year (station × year), we analysed each station separately for year comparisons and each year for station comparisons. For all the analyses, we used a significance level of 0.05. The ANCOVA tables are summarized in the Appendix.

Age and size at maturity were determined by visually inspecting age – percent maturation curves as recommended by Trippel and Harvey (1991), since white sucker populations showed an abrupt transition from immaturity to reproductive maturity. Age and size at first maturity were defined as that age or size at which 50% or more

© 1998 NRC Canada

Fig. 2. Interannual and interstation comparisons of age-adjusted mean length of female and male white sucker captured during the spawning run in the Gatineau and St. Maurice rivers. Open squares, 1993 sampling (both rivers); solid squares, 1991 (St. Maurice River) or 1992 (Gatineau River) sampling. Asterisks indicate a significant difference between years ($P < 0.05$). Different letters indicate a significant difference among stations ($P < 0.05$). Horizontal lines indicate that interstation comparisons are based on pooled annual data. When annual data cannot be pooled (because of a significant year × station interaction), differences among stations are expressed by two different sizes of letter representing annual comparisons. Vertical bars indicate confidence limits.

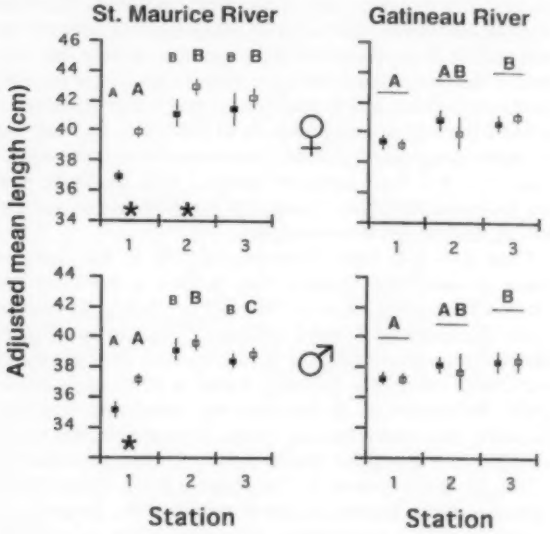

of fish examined were mature. Statistical analyses were precluded because analytical methods for binomial data, such as probit analysis, require partial responses (i.e., >0 but <100% mature); in about 50% of comparisons, there were no partial maturities at one or more sites. Comparisons between years and among stations were limited by the low numbers of younger and smaller fish captured in 1993. In both years, most fish captured were aged 4 years or older.

Results

Growth

In the St. Maurice River, the results of the ANCOVA for females aged between 5 and 10 years revealed that the changes in length among stations varied between years as shown by the significant difference ($P = 0.0037$) of the interaction term (station × year). The contrast test on adjusted mean length indicated that female white sucker at stations 1 and 2 were significantly longer ($P < 0.01$) in 1993 than in 1991 whereas those captured at station 3 were of similar length during the 2 years (Fig. 2). Despite these annual differences, female white sucker were smaller at the upstream station relative to those sampled downstream in both sampling years. For male white sucker, fish aged between 5 and 10 years also varied in length among stations between years as shown by the significant difference ($P = 0.0152$) of the interaction term (station × year). The contrast test on adjusted mean length indicated that only male white sucker at station 1

Fig. 3. Interannual and interstation comparisons of weight-adjusted mean gonad weight of female and male white sucker captured during the spawning run in the Gatineau and St. Maurice rivers. Open squares, 1993 sampling (both rivers); solid squares, 1991 (St. Maurice River) or 1992 (Gatineau River) sampling. Asterisks indicate a significant difference between years ($P < 0.05$). Different letters indicate a significant difference among stations ($P < 0.05$). Horizontal lines indicate that interstation comparisons are based on pooled annual data. Vertical bars indicate confidence limits.

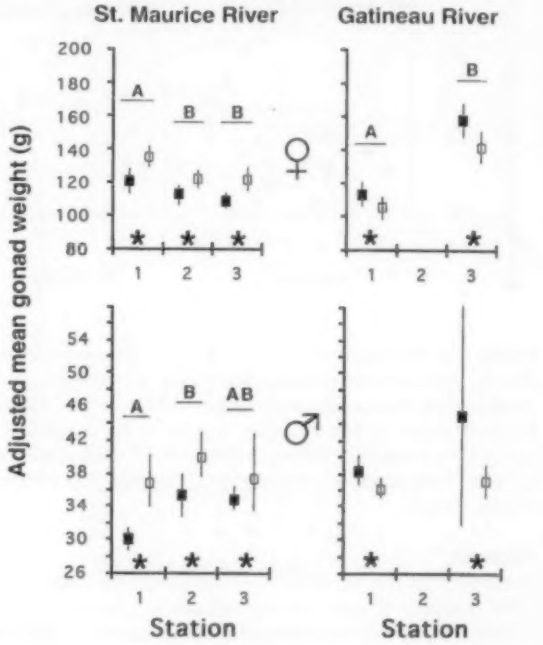

were significantly ($P < 0.05$) longer in 1993 relative to 1991 (Fig. 2). As in the case of females, males from the upstream station were significantly ($P < 0.05$) smaller than those from the two downstream stations in both sampling years despite annual differences in length at age.

In the Gatineau River, female and male white sucker aged 5–10 years were not significantly different in length ($P > 0.05$) between 1992 and 1993 at all stations. White sucker were significantly smaller ($P < 0.05$) at the upstream station relative to at least one downstream station in both sampling years (Fig. 2). The magnitude of changes in length among stations was smaller than observed in the St. Maurice River.

Gonad size

In the St. Maurice River, mature female and male white sucker exhibited greater gonad weights in 1993 than in 1991, relative to carcass weight. Females from the upstream station had bigger gonads per unit carcass weight than those from downstream stations (Fig. 3). In contrast, the gonad weights of male fish sampled at station 2 in 1993 were higher ($P < 0.05$) than those of fish located at the upstream reference station (Fig. 3).

In the Gatineau River, the gonad weights of mature female white sucker relative to carcass weight were lower ($P <$

© 1998 NRC Canada

Fig. 4. Interannual and interstation comparisons of weight-adjusted mean fecundity of female white sucker captured during the spawning run in the Gatineau and St. Maurice rivers. Open squares, 1993 sampling (both rivers); solid squares, 1991 (St. Maurice River) or 1992 (Gatineau River) sampling. Asterisks indicate a significant difference between years ($P < 0.05$). Different letters indicate a significant difference among stations ($P < 0.05$). Horizontal lines indicate that interstation comparisons are based on pooled annual data. Vertical bars indicate confidence limits.

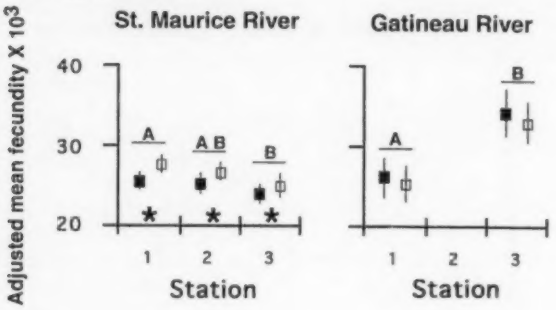

0.0001) in 1993 relative to 1992, and in both years, females from the downstream station 3 had higher ($P < 0.0001$) gonad weights than those sampled at station 1 (Fig. 3). The statistics for male white sucker indicated that the testis weights were lower ($P = 0.0385$) in 1993 relative to 1992 at stations 1 and 3, but in both years, no differences ($P > 0.05$) were observed among stations.

Fecundity

Females from the St. Maurice River produced a larger ($P < 0.001$) number of eggs per unit carcass weight in 1993 relative to 1991, and females from the upstream reference station had a higher fecundity ($P < 0.001$) relative to at least one downstream station in both sampling years (Fig. 4).

In the Gatineau River, the number of eggs produced was similar between 1993 and 1992 for all sites ($P = 0.091$). Females sampled at the upstream station 1 produced fewer eggs ($P < 0.0001$) than females from station 3 in both sampling years (Fig. 4).

Age and size at maturity

In the St. Maurice, the youngest females and males captured in 1993 at the upstream reference station were 5 years old and all were sexually mature (Figs. 5 and 6). Therefore, age at first maturity would be 5 years of age or less. At the downstream stations 2 and 3, females reached first maturity at 5 and 6 years, respectively (Fig. 5), and males reached first maturity at 4 and 6 years, respectively (Fig. 6). There were too few fish from stations 1 and 2 in 1993 to establish size at maturity for females or males, but it is clear that male fish at station 3 reaching first maturity at length class 36–37 cm were longer relative to males at first maturity captured at station 1 (Fig. 6). While size at maturity of males and females could not be measured at stations 1 and 2 in 1993, the trend was similar to that seen in 1991, where fish of both sexes from the reference station 1 matured at a much smaller size.

Compared with 1991, female and male white sucker from the reference station of the St. Maurice River appeared to mature at least a year earlier in 1993. At the downstream station 3, the age (6 years) and size (38–39 cm) at first maturity of females were the same for the two sampling years (Fig. 5). Males at station 3 reached first maturity at the same age (6 years), but were slightly longer in 1993 compared with 1991 (Fig. 6). There were too few male fish captured at station 2 to compare between years.

In the Gatineau River, females sampled in 1993 at stations 1 and 2 reached first maturity between 5 and 6 years of age. At the downstream station 3, the youngest females captured were 4 years old and 100% were mature (Fig. 7). Female white sucker at station 1 reached first maturity at length class 34–35 cm (Fig. 7). Although there were too few fish from stations 2 and 3 to make a valid comparison, it appears that mature fish from station 1 were longer than mature fish sampled at the downstream station 3. Male white sucker from the upstream station 1 and downstream station 3 were spawning at 5 and 3 years of age, respectively, in 1993 (Fig. 8). Male fish from the downstream station 3 were smaller at first maturity relative to fish from upstream station 1 (Fig. 8). There were too few male fish from station 2 to compare age at maturity among stations and between years.

Compared with 1992, sampling in 1993 in the Gatineau River revealed that females were mature at the same age (station 1) or a year older in 1993 (station 2) (Fig. 7) whereas males from stations 1 and 3 matured a year earlier (Fig. 8). Males from stations 2 and 3 were longer in 1993 compared with males captured at the same station in 1992. Most importantly, the pattern of station-to-station differences remained the same: fish at downstream station 3 matured earlier and at a smaller size than fish from the upstream reference station.

Overall, the fish from the St. Maurice River showed little variation among stations in age at maturity, but matured at a greater length at downstream stations in 1993. In contrast, white sucker of both sexes in the Gatineau River were spawning at younger ages and smaller sizes at the downstream stations in 1992, and there were variations in the age and size at first maturity for both sexes and stations in 1993 relative to 1992.

Discussion

Interstation variability

The results of the 1993 sampling campaign led us to the same conclusions as reached in the previous study (Gagnon et al. 1995*a*) concerning gradients of fish growth and reproductive effort as a function of river gradient and BKME exposure. The trends within the St. Maurice River remained the same over 2 years of sampling: white sucker from upstream (*i*) grew slower relative to white sucker from downstream as shown by size at age, (*ii*) exhibited greater reproductive effort (females only) as shown by greater gonad size and fecundity relative to body size, and (*iii*) matured at a younger age (in 1993) or at the same age (in 1991) relative to downstream sites. In comparison, white sucker from the upstream station of the Gatineau River (*i*) grew slower relative to white sucker from downstream as shown by size at age, (*ii*) exhibited reduced reproductive effort (females only) as shown by reduced gonad size relative to body size and fecundity, and (*iii*) matured at an older age relative to downstream sites.

In accordance with better growth, female fish from the

© 1998 NRC Canada

Fig. 5. Age and length at first maturity for female white sucker from the St. Maurice River. The numbers represents the station, and the thick line represents the upstream station 1. The vertical dotted lines indicate age and size at maturity. Samples sizes for each point ranged from 5 to 52 fish.

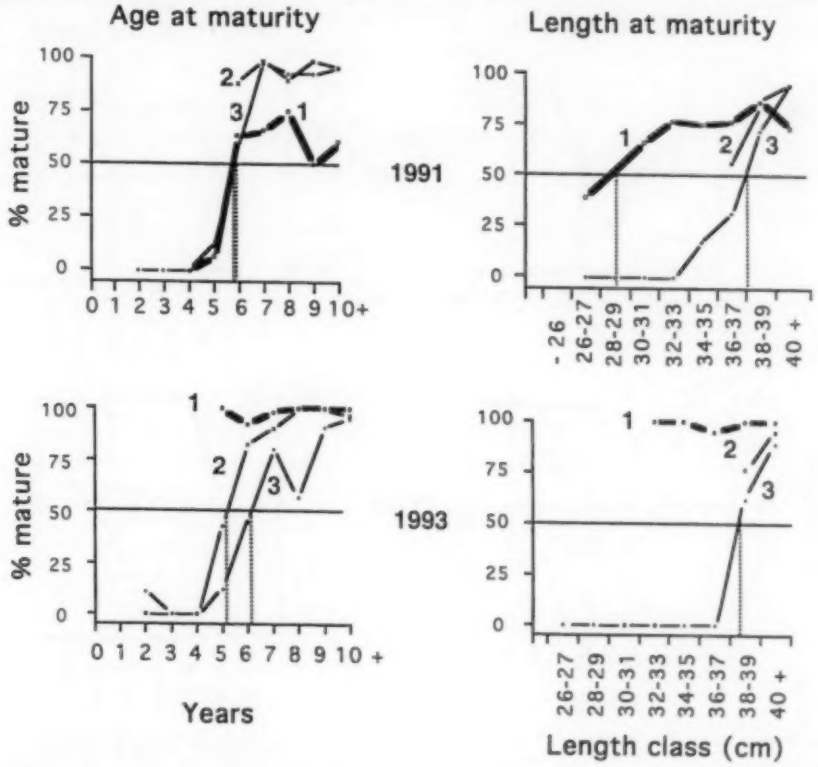

downstream stations of the Gatineau River had bigger gonads and higher fecundity relative to females of a similar carcass weight from the upstream station. This was consistent with a larger investment of energy in egg production because of greater nutrient availability at downstream stations. The fact that female white sucker from the downstream stations of the St. Maurice River did not develop bigger gonads and higher fecundity despite their larger size supports previous conclusions of negative impacts of BKME exposure on female gonad development (Munkittrick et al. 1991; Gagnon et al. 1994, 1995*a*). Only male fish from the St. Maurice River exhibited a bigger gonad weight relative to carcass weight at the BKME-exposed downstream station 2.

While age at first maturity exhibited great variability, fish from the BKME-exposed stations exhibited the same (1991) or delayed (1993) age at maturity relative to the reference upstream station of the St. Maurice River. In comparison, fish from the downstream stations of the Gatineau River reached maturity precociously relative to fish from the upstream station.

In the St. Maurice River, BKME may have also contributed to faster growth either directly or indirectly. Even the very low nitrogen and phosphorus levels of secondary-treated kraft effluent can be sufficient to alter the river's trophic status and cause algal blooms in receiving waters (Bothwell 1992). Rainbow trout (*Oncorhynchus mykiss*) exposed to secondary-treated effluents in experimental streams demonstrated increased growth relative to control rainbow trout, which is believed to result from a stimulation of benthic invertebrate biomass in effluent-exposed habitats (Haley et al. 1995). Similarly, recent experiments concluded that mayflies (*Eatis tricaudatus* Dodds) exposed to pulp mill effluent had 20–50% greater body weights than control benthic invertebrates (Lowell et al. 1995). The presence of juvabione-type compounds (juvenile hormone) in woody plants such as pine, fir, and spruce trees used by the pulp and paper industry could be responsible for stimulating the growth of benthic invertebrates. The juvenile hormone inhibits morphogenesis and differentiation of reproductive organs, allowing continued somatic growth of the insects (Lowell et al. 1995), resulting in an increased food biomass available to fish. The potential effects of juvabione-like compounds on fish growth are presently unknown, but may contribute to the increased growth of BKME-exposed fish.

Nevertheless, increased growth at downstream stations relative to the upstream station observed in both contaminated and reference rivers indicates gradients of productivity, and hence food availability, independent of BKME. Nitrogen and phosphorus contents of municipal effluents located along the rivers are expected to be higher than those associated with BKME and are the most likely cause of greater fish growth at downstream stations. In both rivers, growth of fish was better at downstream stations, indicating gradients of productivity independent of BKME contamination.

© 1998 NRC Canada

Fig. 6. Age and length at first maturity for male white sucker from the St. Maurice River. The numbers represents the station, and the thick line represents the upstream station 1. The vertical dotted lines indicate age and size at maturity. Samples sizes for each point ranged from 5 to 66 fish.

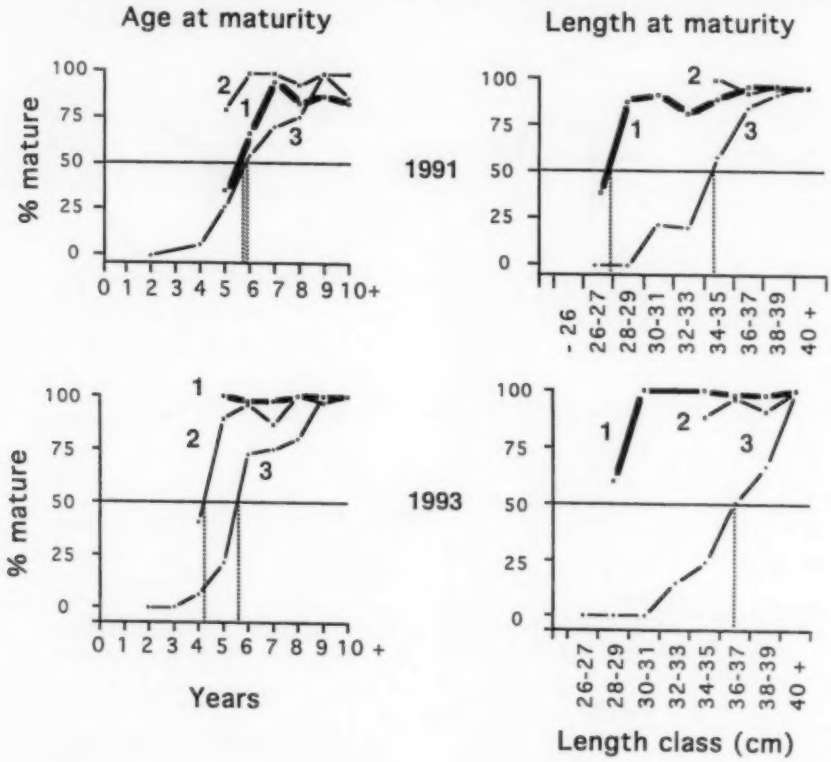

Annual variability within stations

The similarity in trends within and between rivers observed in the present and former studies was evident despite significant annual variability in demographic variables within stations. In the St. Maurice River, there was a significant enhancement in growth rates and reproductive effort in 1993 compared with 1991 at the upstream reference station. Female and male white sucker at station 1 (*i*) grew faster in 1993 as shown by direct observation of size at age, (*ii*) exhibited greater reproductive effort in 1993 as shown by greater gonad size and fecundity relative to body size, and (*iii*) were younger at first maturity. At stations 2 and 3 located downstream of the mill, females and males (*i*) did not grow faster in 1993 as shown by direct observation of size at age (except station 2, females), (*ii*) exhibited better reproductive effort in 1993 than in 1991 as shown by greater gonad size and fecundity relative to body size, and (*iii*) exhibited the same age at first maturity. Therefore, groups of white sucker sampled in the St. Maurice River exhibited significantly different within-station variability in growth and gonad investment in 1993 relative to 1991.

The enhanced gonad size and fecundity observed in 1993, associated with enhanced growth rates, resulted in a reduced age at maturity at the upstream station 1 of the St. Maurice River. Improved growth conditions may have led to greater energy allocation to reproduction and maturation at a younger age, in concordance with the findings of Trippel and Harvey (1989), Chen and Harvey (1994), and Gagnon et al. (1995*a*). But this was not the case at the downstream stations 2 (except females) and 3. Despite overall enhanced gonad size and fecundity, the growth and age at first maturity of the exposed fish did not change.

In comparison, growth rates and reproductive effort of white sucker from the reference Gatineau River demonstrated a different pattern of variation between years. Female and male white sucker located at the upstream station in 1993 (*i*) grew at the same rate as in 1992 as shown by no interannual difference in size at age, (*ii*) exhibited reduced reproductive effort as shown by reduced gonad size relative to body size, and no variation in fecundity, and (*iii*) matured at the same age and size. At the stations located downstream (Fig. 1), females and males (*i*) grew at the same rate as in 1992 as shown by no difference in growth at age, (*ii*) exhibited reduced reproductive effort as shown by reduced gonad size relative to body size (station 3), and no variation in fecundity (station 3), and (*iii*) were mature at a younger (station 3) or older (station 2, females only) age and at a larger size (station 3, males).

Thus, in the Gatineau and St. Maurice rivers, we observed annual differences within stations in growth rate, gonad investment, and age at first maturity. But these variations were not sufficient to alter our previous conclusions about the effects of BKME exposure. This demonstrates that the impact of BKME discharge on the reproductive investment of white sucker was evident despite the "noise" of natural annual

© 1998 NRC Canada

Fig. 7. Age and length at first maturity for female white sucker from the Gatineau River. The numbers represent the station, and the thick line represents the upstream station 1. The vertical dotted lines indicate age and size at maturity. Samples sizes for each point ranged from 5 to 84 fish.

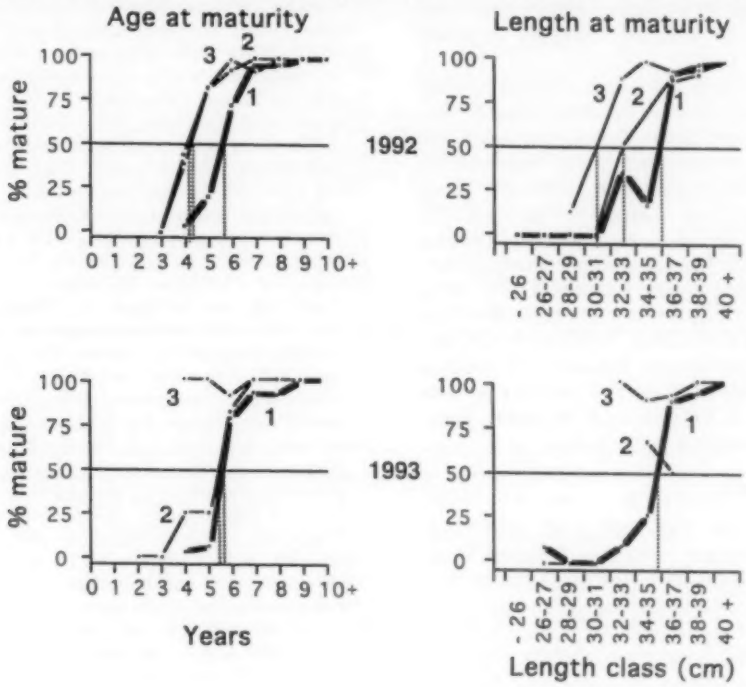

Fig. 8. Age and length at first maturity for male white sucker from the Gatineau River. The numbers represent the station, and the thick line represents the upstream station 1. The vertical dotted lines indicate age and size at maturity. Samples sizes for each point ranged from 5 to 60 fish.

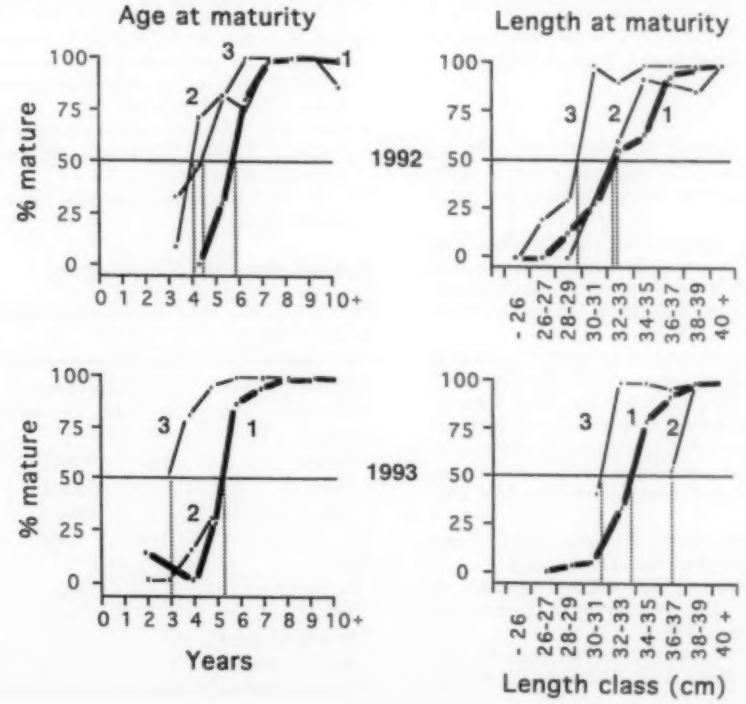

© 1998 NRC Canada

variability. This study suggests that in cases where BKME has a significant impact on reproductive investment, the multiple sampling cycles of the EEM program should detect such an impact despite naturally occurring variability in growth and reproduction.

These results also illustrate a useful statistical tool for EEM programs. The ANCOVAs showing the distribution of relative variability among main factors demonstrate significant differences in responses attributable to years. However, the "year effect" was generally smaller than effects due to site and fish size. Most importantly, there were no significant site × year interactions in any factor except growth, indicating that the main effects of site had not changed between years. For monitoring, the interactive term provides a very useful way to identify significant temporal changes in the effects of pulp mill effluents on fish populations. In this particular case, the lack of year × site interactions indicates that chlorine dioxide substitution, implemented in 1992, had no effects on population demographics in 1993, as might be expected considering the relatively long life of white sucker.

Acknowledgements

We thank Catherine Couillard, Marie-Hélène Michaud, Denis Thivierge, Francine Bélanger, Stéphane Plourde, Paul Robichaud, and Serge Higgins for technical assistance. This project was funded by the Department of Fisheries and Oceans (Institut Maurice Lamontagne), the Natural Sciences and Engineering Research Council of Canada (Strategic Grants and Research Partnerships Program), and Environment Canada (Centre Saint-Laurent). Scholarships to M.M. Gagnon were provided by Fonds pour la Formation des Chercheurs et l'Aide à la Recherche (FCAR), the Association des Femmes Diplomées des Universités (AFDU), Environment Canada, and Gauthier et Guillemette Consultants Inc. This is a contribution to the program of the Groupe Interuniversitaire de Recherche Océanographique du Québec (GIROQ).

References

Adams, S.M., Crumby, W.D., Greenley, M.S., Jr., Shugart, L.R., and Saylor, C.F. 1992. Responses of fish populations and communities to pulp mill effluents: a holistic assessment. Ecotoxicol. Environ. Saf. **24**: 347–360.

Ahokas, J.T., Holdway, D.A., Brennan, S.E., Goudey, R.W., and Bibrowska, H.B. 1993. MFO activity in carp (*Cyprinus carpio*) exposed to treated pulp and paper mill effluent in Lake Coleman, Victoria, Australia, in relation to AOX, EOX, and muscle PCDD/PCDF. Environ. Toxicol. Chem. **13**: 41–50.

Beamish, R.J. 1973. Determination of age and growth of populations of the white sucker (*Catostomus commersoni*) exhibiting a wide range of size at maturity. J. Fish. Res. Board Can. **30**: 607–616.

Bothwell, M.L. 1992. Eutrophication of rivers by nutrients in treated kraft pulp mill effluent. Water Pollut. Res. J. Can. **27**: 447–472.

Chalanchuk, S.M. 1984. Aging a population of the white sucker, *Catostomus commersoni*, by the fin-ray method. Can. Tech. Rep. Fish. Aquat. Sci. No. 1321.

Chen, Y., and Harvey, H.H. 1994. Growth, abundance, and food supply of white sucker. Trans. Am. Fish. Soc. **124**: 262–271.

Environment Canada, 1992. Pulp and paper effluent regulation. *In* Canada Gazette. Part 2. Vol. 126. Department of Fisheries and Oceans, Ottawa, Ont. pp. 1967–1997.

Gagnon, M.M., Dodson, J.J., Hodson, P.V., Van Der Kraak, G., and Carey, J.H. 1994. Seasonal effects of bleached-kraft mill effluent on reproductive parameters of white sucker (*Catostomus commersoni*) populations of the St. Maurice River, Québec, Canada. Can. J. Fish. Aquat. Sci. **51**: 337–347.

Gagnon, M.M., Bussières, D.B., Dodson, J.J., and Hodson, P.V. 1995*a*. White sucker (*Catostomus commersoni*) growth and sexual maturation in pulp mill-contaminated and reference rivers. Environ. Toxicol. Chem. **14**: 317–327.

Gagnon, M.M., Bussières, D.B., Dodson, J.J., and Hodson, P.V. 1995*b*. Letter to the editor: secondary treatment of bleached-kraft mill effluent. Environ. Toxicol. Chem. **14**: 1455–1456.

Haley, R.K., Hall, T.J., and Bousquet, T.M. 1995. Effects of biologically treated bleached-kraft mill effluent before and after mill conversion to increased chlorine dioxide substitution: results of an experimental stream study. Environ. Toxicol. Chem. **14**: 287–298.

Hodson, P.V., McWhirter, M., Ralph, K., Gray, B., Thivierge, D., Carey, J.H., Van Der Kraak, G., Whittle, D.M., and Levesque, M.-C. 1992. Effects of bleached-kraft mill effluent on fish in the St. Maurice River, Québec. Environ. Toxicol. Chem. **11**: 1635–1651.

Lowell, R.B., Culp, J.M., and Wrona, F.J. 1995. Stimulation of increased short-term growth and development of mayflies by pulp mill effluent. Environ. Toxicol. Chem. **14**: 1529–1541.

Munkittrick, K.R., Portt, C.B., Van Der Kraak, G.J., Smith, I.R., and Robson, D.A. 1991. Impact of bleached-kraft mill effluent on population characteristics, liver MFO activity, and serum steroid levels of Lake Superior (*Catostomus commersoni*) population. Can. J. Fish. Aquat. Sci. **48**: 1371–1380.

Munkittrick, K.R., McMaster, M.E., Portt, C.B., Van Der Kraak, G.J., Smith, I.R., and Dixon, D.G. 1992. Changes in maturity, plasma sex steroid levels, hepatic MFO activity and the presence of external lesions in lake whitefish exposed to bleached kraft mill effluent. Can. J. Fish. Aquat. Sci. **49**: 1560–1569.

SAS. 1988. SAS user's guide: statistics, version 6.02. SAS Institute Inc., Cary, N.C.

Scott, W.B., and Crossman, E.J. 1973. Freshwater fishes of Canada. Bull. Fish. Res. Board Can. No 184.

Trippel, E.A., and Harvey, H.H. 1989. Missing opportunities to reproduce: an energy dependent or fecundity gaining strategy in white sucker (*Catostomus commersoni*). Can. J. Zool. **67**: 2180–2188.

Trippel, E.A., and Harvey, H.H. 1991. Comparison of methods used to estimate age and length of fishes at sexual maturity using populations of white suckers (*Catostomus commersoni*). Can. J. Fish. Aquat. Sci. **48**: 1446–1459.

Vannote, R.L., Minshall, G.W., Cummins, K.W., Sedell, J.R., and Cushing, C.E. 1980. The River Continuum Concept. Can. J. Fish. Aquat. Sci. **37**: 130–137.

Zar, J.H. 1984. Biostatistical analysis. 2nd ed. Prentice-Hall, Englewood Cliffs, N.J.

Appendix. ANCOVA tables

Table A1. ANCOVA for comparisons of white sucker length in the St. Maurice River.

Source of variance	df	Sum of squares	*F* ratio	*P*
Female				
Station	2	1096	69.9	0.0000
Year	1	231	29.6	0.0000
Age (covariable)	1	1048	133	0.0000
Station × year	2	89.1	5.69	0.0037
Males				
Station	2	849	68.5	0.0000
Year	1	96.9	15.63	0.0001
Age (covariable)	1	1502	242	0.0000
Station × year	2	52.3	4.217	0.0152

© 1998 NRC Canada

Table A2. ANCOVA for comparisons of white sucker length in the Gatineau River.

Source of variance	df	Sum of squares	*F* ratio	*P*
Female				
Station	2	199	13.56	0.0000
Year	1	4.824	0.6561	0.4183
Age (covariable)	1	1971	268	0.0000
Station × year	2	13.56	0.9221	0.3983
Males				
Station	2	70.1	6.353	0.0019
Year	1	2.241	0.4059	0.5243
Age (covariable)	1	758	137	0.0000
Station × year	2	2.522	0.2284	0.7959

Table A3. ANCOVA for comparisons of gonad weight of white sucker in the St. Maurice River (CW, carcass weight).

Source of variance	df	Sum of squares	*F* ratio	*P*
Female				
Station	2	0.1913	12.27	0.0000
Year	1	0.2029	26.02	0.0000
log CW (covariable)	1	9.364	1201	0.0000
Station × year	2	0.0054	0.3459	0.7077
Males				
Station	2	0.1895	5.822	0.0031
Year	1	0.2807	17.25	0.0000
log CW (covariable)	1	4.970	305	0.0000
Station × year	2	0.0442	1.358	0.2578

Table A4. ANCOVA for comparisons of gonad weight of white sucker in the Gatineau River (CW, carcass weight).

Source of variance	df	Sum of squares	*F* ratio	*P*
Female				
Station	1	0.010	164	0.0000
Year	1	0.1121	1823	0.0000
log CW (covariable)	1	5.065	823	0.0000
Station × year	1	0.0022	0.3645	0.5464
Males				
Station	1	0.0338	2.121	0.1463
Year	1	0.0688	4.319	0.0385
log CW (covariable)	1	5.273	330	0.0000
Station × year	1	0.0202	1.271	0.2605

Table A5. ANCOVA for comparisons of fecundity of female white sucker in the St. Maurice and Gatineau rivers (CW, carcass weight).

Source of variance	df	Sum of squares	*F* ratio	*P*
St. Maurice River				
Station	2	0.0663	5.187	0.0060
Year	1	0.0794	12.42	0.0005
log CW (covariable)	1	2.763	432	0.0000
Station × year	2	0.0153	1.196	0.3035
Gatineau River				
Station	1	0.6926	105	0.0000
Year	1	0.0189	2.882	0.0910
log CW (covariable)	1	2.487	378	0.0000
Station × year	1	0.0001	0.0116	0.9143

© 1998 NRC Canada

Measurement of primary production and community respiration in oligotrophic lakes using the Winkler method

Richard Carignan, Anne-Marie Blais, and Chantal Vis

Abstract: The precision of the Winkler method can reach 2 $\mu g \cdot L^{-1}$ if a potentiometric end-point detection method if used and if minor modifications to standard protocols are made. The major sources of variability encountered at this precision level are due to the gradual decrease (1–3 $\mu g \cdot L^{-1} \cdot h^{-1}$) in apparent O_2 which occurs after reagent addition and to thermal expansion and contraction of the samples during storage. These sources of error can, however, be easily minimized or eliminated. The precision of the proposed protocols for Winkler determinations and metabolic rate measurements allows the detection of gross primary production and community respiration rates as low as 0.7 mg $C \cdot m^{-3} \cdot h^{-1}$ after 4-h incubations. The methods are therefore adequate for metabolic studies in oligotrophic lakes, where epilimnetic production and respiration rates range between 5 and 50 mg $C \cdot m^{-3} \cdot h^{-1}$.

Résumé : La précision de la méthode de Winkler peut atteindre 2 $\mu g \cdot L^{-1}$ en utilisant une méthode potentiométrique pour détecter le point de virage et en apportant quelques modifications mineures aux protocoles conventionnels. Les principales source de variabilité rencontrées à ce niveau de précision sont dues à la perte graduelle (1–3 $\mu g \cdot L^{-1} \cdot h^{-1}$) de O_2 apparent survenant après l'ajout des réactifs, ainsi qu'à l'expansion et à la contraction des bouteilles pendant l'entreposage. Ces sources d'erreur peuvent cependant facilement être diminuées ou éliminées. La précision des méthodes proposées pour les mesures d'oxygène et de taux métaboliques abaissent le seuil de détection des taux de production primaire brute et de respiration du plancton à 0,7 mg $C \cdot m^{-3} \cdot h^{-1}$ pour des incubation ayant une durée de 4 h. Ces méthodes sont donc adéquates à l'étude du métabolisme des lacs oligotrophes, où les taux de production et de respiration épilimnétiques sont de l'ordre de 5 à 50 mg $C \cdot m^{-3} \cdot h^{-1}$.

Introduction

The two most common methods used to measure primary production in lake waters are those based on dissolved O_2 changes and ^{14}C incorporation in clear and dark bottles. However, the limited sensitivity and precision of O_2 determinations using the Winkler method (20–50 $\mu g \cdot L^{-1}$) have, in the past, restricted the use of the O_2 method to productive waters. In oligotrophic lakes, such as those occurring on the Canadian Shield, the ^{14}C method has, until now, remained the only way to estimate primary production.

Although more sensitive, the ^{14}C method is not without problems. Production rates measured with ^{14}C are often ambiguous, since they can stand anywhere between gross primary production (GPP) and net primary production (NPP), depending on several factors including light and nutrient availability, phytoplankton size, and incubation time (e.g., Tilzer et al. 1977; Andersen and Sand-Jensen 1980; Peterson 1980). Furthermore, the ^{14}C method cannot measure community respiration (R_{com}). In some cases, production rates obtained using the O_2 and the ^{14}C methods have been found to differ by as much as one order of magnitude. As a consequence of the shortcomings of the ^{14}C method, fundamental properties of oligotrophic aquatic systems such as GPP, NPP, and R_{com} have remained poorly known. For the same reasons, recent estimates of the production–respiration balance of marine and freshwaters (del Giorgio and Peters 1994) should be considered with caution.

Our interests in the production–respiration balance of aquatic systems has led us to investigate whether the Winkler method could be adapted to the determination of GPP, NPP, and R_{com} in unproductive systems such as large rivers and oligotrophic lakes. In the lakes of the Canadian Shield, for example, O_2 changes expected in light or dark bottles during a typical 4-h incubation are of the order of 20–100 $\mu g \cdot L^{-1}$. Such low metabolic rates require that to be useful, Winkler determinations must reach a precision of about 10% of the lowest value, or 2 $\mu g \cdot L^{-1}$.

Several well-known sources of error contribute to decrease the precision of Winkler determinations in lake waters. These include the loss of volatile I_2 during sample manipulation and titration, the thermal expansion and contraction of samples in BOD bottles before or after reagent addition, the photochemical oxidation of iodide to I_2 at low pH, the time-dependent reduction of I_2 to iodide by organic matter, temperature variations of the titrant, and O_2 losses or gains that occur when filling replicate bottles. The following sections show that a few precautions to minimize or eliminate

Received August 25, 1997. Accepted November 19, 1997.
J14183

R. Carignan,[1] A.-M. Blais, and C. Vis. Département de sciences biologiques, Université de Montréal, C.P. 6128, Succ. Centre-Ville, Montréal, QC H3C 3J7, Canada.

[1] Author to whom all correspondence should be addressed. e-mail: carignar@ere.unmontreal.ca

© 1998 NRC Canada

these effects increase the precision of the Winkler method sufficiently to make it applicable for metabolic studies in almost any water.

Study site

Epilimnetic production and respiration rates were measured in Croche and Cromwell lakes (Station de Biologie des Laurentides, 70 km north of Montréal, altitude 340 m). The two lakes exhibit contrasting limnological conditions encountered in unperturbed Shield lakes. Croche Lake is a small (20 ha) headwater seepage lake with a mean depth of 4.8 m, a drainage ratio of 5.1, and a water residence time of 2.3 years. Macrophytes are virtually absent in the lake. Its water chemistry is typical of oligotrophic Shield lakes, with an average total phosphorus, chlorophyll *a*, and dissolved organic carbon of 4 $\mu g \cdot L^{-1}$, 1.1 $\mu g \cdot L^{-1}$, and 3.5 $mg \cdot L^{-1}$, respectively. In contrast, Cromwell Lake (11 ha) has a mean depth of 2.6 m, a large drainage ratio (91), and a much shorter residence time (0.07 years). The lake receives water from two larger lakes (Croche and Pilon) and from several extensive marshes and beaver dams. As a result, Cromwell Lake has higher concentrations of total phosphorus (10 $\mu g \cdot L^{-1}$), chlorophyll *a* (3.8 $\mu g \cdot L^{-1}$), and dissolved organic carbon (5.2 $mg \cdot L^{-1}$); it also has a well-developed littoral macrophyte belt dominated by *Utricularia vulgaris* and *Nymphoides cordata*.

Methods

Precision

Precision is defined here as the coefficient of variation and equals 1 SD of a sample composed of n replicate determinations ($n - 1$ degrees of freedom), expressed as a percentage of the mean. The uncertainty of the mean of n determinations is calculated as ± 1 SE where $SE = SD/(n)^{1/2}$. The precision of O_2 analyses was evaluated in two ways. First, the instrumental precision was measured by performing replicate titrations of a 0.0250 N iodate standard as described in the Appendix. The precision of O_2 measurements in lake water was determined on air-equilibrated (bubbled overnight) water taken from Croche Lake. Fifteen to 20 replicate BOD bottles were filled from a 40-L carboy by delivering 800–1000 mL (about three volumes) of water at the bottom of the bottles. The bottles were fixed with the three Winkler reagents, stored 4 h in the dark, and titrated in triplicate during the next 3 h.

Loss of I_2 and O_2 equivalents during storage

The decrease in O_2 equivalents during storage of fixed samples was measured in both lakes. A 50-L carboy of lake water was bubbled overnight with air at 23.7°C and the water delivered into 40 bottles. The manganous and alkaline iodide reagents were added to the bottles. Twenty bottles were immediately acidified with the H_2SO_4 reagent, while the remaining ones were left alkaline. All bottles were then stored at 23.7°C in a dark 800-L water tank kept in a basement to prevent temperature fluctuations. Every few hours, four acidified bottles were titrated, and four alkaline bottles were acidified and titrated immediately. To eliminate any effect due to daily temperature fluctuations in the field laboratory (25–29°C) the thiosulfate was standardized in triplicate before titrations for each sampling time.

Primary production and community respiration

Primary production and respiration were measured in clear and dark bottles at in situ temperatures (±1°C) using an incubator similar to the one described by Shearer et al. (1985). The incubator accommodated six 300-mL BOD bottles per rotating wheel and provided six light intensities (photosynthetically active radiation) decreasing geometrically between 1100 and 25 μeinsteins $(E) \cdot m^{-2} \cdot s^{-1}$, as measured inside the bottles with a Biospherical QSL-101 quantum meter.

Twenty to 40 L of water was collected with a 4-L Van Dorn bottle in the upper, middle, and lower epilimnia between 07:00 and 09:00 for production measurements and during midday for some respiration measurements. The water was poured into opaque 20-L polyethylene carboys and transported to the laboratory in coolers to minimize temperature changes. Within 30 min of collection, the carboys were transferred into a 50-L polyethylene tank fitted with a floating polyethylene hard cover designed to minimize gas exchange between air and water while replicate BOD bottles were filled. We have calculated, using a stagnant film boundary layer of 100 μm and a diffusion coefficient of 2×10^{-5} $cm^2 \cdot s^{-1}$ for O_2, that if the dissolved O_2 concentration inside a 40-L carboy deviates by only 1% from saturation, it can change by as much as 5 $\mu g \cdot L^{-1}$ during the 10–15 min needed to fill 20–30 replicate BOD bottles. The tank was stirred and the bottles were filled as rapidly as possible by delivering 800–1000 mL (about three volumes) of water at the bottom of the bottles from a rubber tube (1-cm diameter) fixed to a spigot located near the bottom of the tank.

The mass of water and dissolved O_2 contained in a Pyrex 300-mL BOD bottle varies appreciably with temperature (about $0.02\% \cdot °C^{-1}$). At the time of reagent addition, small temperature differences between bottles used for initial O_2 determinations and incubated bottles can therefore introduce significant errors when measuring small changes in O_2 concentration that occur during the incubation. Care was thus taken to bring the initial bottles to the same temperature as the incubated bottles before adding the Winkler reagents. We determined that the half-time necessary for 300-mL BOD to reach thermal equilibrium, after immersion in water having a different temperature, is 4.3 min (in air, this half-time increases to 45 min). Consequently, all bottles were placed in the incubator (with the light source blocked) for 15 min before the beginning of the incubation and before reagent addition to the initial bottles. Duplicate or triplicate bottles were incubated during 2–6 h at each light intensity. Initial O_2 concentrations for production or respiration measurements were determined on three or four replicate bottles. Clear bottles from a given production experiment were titrated randomly the next day to eliminate the possibility of systematic biases due to storage time effects (see below) and to temperature variations during the day. GPP was calculated by adding R_{com} to NPP, assuming equal respiration rates in clear and dark bottles. Addition and subtraction errors in the calculation of R_{com}, GPP, and NPP were calculated as $SE_{A \pm B} = (SE_A^2 + SE_B^2)^{1/2}$.

The effects of incubation time on GPP and R_{com} were investigated in both lakes by incubating duplicate clear bottles for 2, 4, and 6 h for production measurements and triplicate bottles for up to 27 h for respiration measurements.

Results and discussion

Precision

The average precision of 15 successive thiosulfate standardizations routinely performed in triplicate at our field laboratory in June and July 1997 was 0.019%. This precision is close to the resolution of the Metrohm titrator (±1 μL) and corresponds to the maximum instrumental precision attainable when the titrator is used with a Pt Titrode and programmed as described in the Appendix. We found the standardization procedure of the Appendix particularly precise compared with those found in most water analysis handbooks. The procedure thus provides an excellent test for the evaluation or comparison of titrator, electrode, and method performance. Investigators should not engage in production and respiration measurements of oligotrophic waters unless a precision of at least 0.04% is consistently achieved at this stage.

© 1998 NRC Canada

Table 1. Precision of successive triplicate titrations of lake water taken from Croche Lake and equilibrated with air at 22.2°C on July 3 and at 20.6°C on July 8, 1997.

July 3, 1997					July 8, 1997				
Time (h)	T(°C)	Dissolved O_2 ($mg \cdot L^{-1}$)	Mean dissolved O_2 ($mg \cdot L^{-1}$)	Precision (%)	Time (h)	T(°C)	Dissolved O_2 ($mg \cdot L^{-1}$)	Mean dissolved O_2 ($mg \cdot L^{-1}$)	Precision (%)
15:30	23.2	8.155	8.155	0.012	21:30	23.5	8.534	8.536	0.020
		8.156					8.537		
		8.154					8.537		
16:02	23.8	8.160	8.157	0.032	21:46	23.7	8.536	8.532	0.042
		8.156					8.531		
		8.155					8.529		
16:48	24.3	8.156	8.157	0.014	22:25	23.6	8.531	8.529	0.024
		8.156					8.530		
		8.158					8.527		
17:30	24.8	8.150	8.152	0.035	23:34	23.6	8.534	8.534	0.007
		8.150					8.534		
		8.155					8.535		
18:25	24.8	8.158	8.158	0.012	00:14	23.7	8.533	8.530	0.041
		8.157					8.526		
		8.159					8.530		

Note: Titrations were initiated 4 h after reagent addition and conducted over a 3-h interval. Titrant temperatures (T) were measured with a thermistor fastened to the burette wall.

The average precision obtained for triplicate lake water samples titrated successively was 0.024%, or 2 $\mu g\ O_2 \cdot L^{-1}$ (Table 1). The precision obtained with the iodate standard is expected to decrease somewhat when actual water samples are titrated, since they are subject to additional sources of variability including I_2 volatilization, I_2 reduction by organic matter, small differences in O_2 concentrations in the replicate samples, and pipetting errors. Nevertheless, this precision represents a substantial improvement over most previously reported values using visual, colorimetric, or electrometric end-point detection. For instance, Strickland and Parsons (1972) found a standard deviation of 24 $\mu g \cdot L^{-1}$ for Winkler determinations carried under "near ideal" laboratory conditions. These authors added that precision is not improved by the use of electrometric end-point detection methods. A standard deviation of 50 $\mu g \cdot L^{-1}$ is quoted in American Public Health Association (1992). Golterman (1983) obtained a coefficient of variation of 0.4% (equivalent to 40 $\mu g \cdot L^{-1}$) using automated dead-stop titration and an amperometric end-point detection technique. Talling (1973) reported a precision of 20 $\mu g \cdot L^{-1}$ for amperometric techniques. Although better precision has been reported from time to time, it was obtained using equipment that is unpractical for field work (Potter and Everitt 1959) or was based on limited evidence (Bryan et al. 1976).

Loss of I_2 and O_2 equivalents during storage

The loss of I_2 during storage of fixed samples of Croche and Cromwell lakes can be a major source of error at the 10 $\mu g \cdot L^{-1}$ level (Fig. 1). In both lakes, I_2 loss in acidified samples was rapid (2.3 and 3.4 $\mu g\ O_2 \cdot L^{-1} \cdot h^{-1}$) during the first 12 h and decreased progressively afterwards. After 12 h, the loss rates decreased to 1.5 and 2.0 $\mu g\ O_2 \cdot L^{-1} \cdot h^{-1}$ in Croche and Cromwell lakes, respectively. The problem was not eliminated by delaying the H_2SO_4 addition until just before titration, as sometimes recommended. Replicate samples stored under alkaline conditions and acidified before titration lost O_2 equivalents as rapidly as acidified samples did during the first 12 h. Note, however, that after 12 h, alkaline samples lost fewer O_2 equivalents than acidified samples. The chemical reaction responsible for the loss of O_2 equivalents in alkaline samples is unknown, but probably involves the production of a reactive compound that reduces the I_2 as soon as it is formed after H_2SO_4 addition. Similar tests performed on Montréal tapwater showed no significant loss of O_2 equivalents after 48 h in acidified bottles, suggesting that organic matter present in natural waters is involved in these reactions.

These results have two major implications regarding the accuracy and precision of Winkler determinations in Shield lakes. First, although many protocols (Hitchman 1978) recommend titration within a few hours following acidification and I_2 formation, Fig. 1 clearly shows that titrations cannot be delayed by more than a few minutes to achieve a 10 $\mu g \cdot L^{-1}$ accuracy. Since individual Winkler determinations usually take 4–8 min, regardless of the end-point detection method, only a few samples can be accurately titrated at a time. Second, if precision is more important than accuracy, as is the case for metabolic measurements, and if several samples are to be processed, it is preferable to delay the titrations for 12–24 h after reagent addition, when the loss of I_2 and O_2 equivalents with time becomes less pronounced.

These interferences are large enough to affect the precision of production and respiration measurements in oligotrophic waters. They can, however, be minimized if the

© 1998 NRC Canada

Fig. 1. Loss of O_2 equivalents during storage in the dark and at constant temperature after reagent addition to water samples taken in Croche and Cromwell lakes. Replicate samples were stored after alkaline iodide (open symbols) or H_2SO_4 (solid symbols) addition. Error bars represent ±1 SE of four determinations.

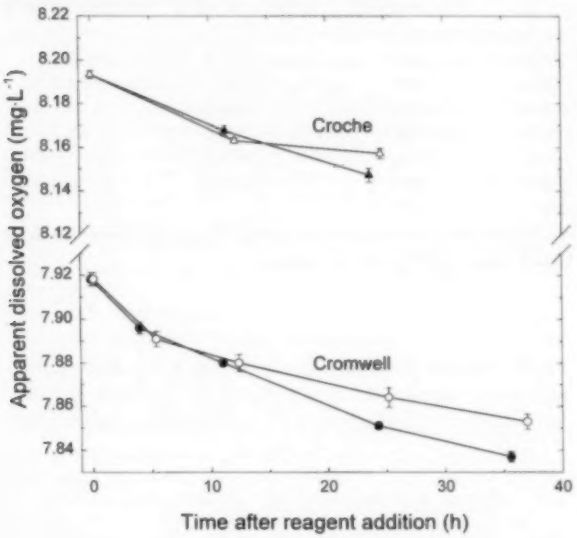

sampling chronology is respected during titration. For example, in our routine production and respiration measurements, we begin the incubation and fix replicate initial bottles at 10:00 and terminate the incubation of the clear and dark bottles at 14:00 and 17:00, respectively. The bottles are titrated 20–22 h later in the same sequence. Although some procedures recommend preservation of the samples by stopping biological activity with H_2SO_4 and (or) NaN_3, we found it simpler to conduct the titrations during the next day and to keep constant (within 2–3 h) the time interval between reagent addition and titration.

Production and respiration rates

Gross and net primary production measurements performed in the least productive lake (Croche) (Table 2; Fig. 2) show that the precision of the method is sufficient to accurately measure photosynthetic parameters and daily areal production rates. The average SE and precision of triplicate O_2 determinations were 1.7 $\mu g \cdot L^{-1}$ and 0.04%, respectively. The average SE of NPP estimates, which are calculated from the differences between the initial and clear bottles, was 0.55 mg $O_2 \cdot m^{-3} \cdot h^{-1}$. The minimum NPP and R_{com} rate that can be detected at the 95% confidence level after a 4-h incubation therefore amounts to 2.2 mg $O_2 \cdot m^{-3} \cdot h^{-1}$ (±2 SE). This quantity represents about 0.7 mg $C \cdot m^{-3} \cdot h^{-1}$ (using a photosynthetic quotient of 1.2) and is well below the ^{14}C production rates observed in the epilimnion of other Shield lakes (5–100 mg $C \cdot m^{-3} \cdot h^{-1}$, Schindler and Holmgren 1971).

The integrated epilimnetic (Z = 2.75 m) daily areal production calculated (Fee 1990) in Croche Lake on July 4 from the production versus irradiance curve of Fig. 2 amounts to 432 mg $O_2 \cdot m^{-2} \cdot day^{-1}$. Only 26% of the normal incident radiation was received during that day. Nevertheless, GPP was equivalent to the epilimnetic community respiration (440 ± 20 mg $O_2 \cdot m^{-2} \cdot day^{-1}$) calculated from the 4-h dark respiration rate (Table 2) and extrapolated to 24 h. This result and the positive epilimnetic production–respiration balance usually observed in this lake and in 11 other Laurentian Shield lakes (unpublished data) contrast with the highly negative balances reported for oligotrophic lakes by del Giorgio and Peters (1994).

Production measurements derived from ^{14}C uptake generally decrease when the incubation time increases. This problem is inherent to the ^{14}C method and has been attributed to several processes including the time-dependent reassimilation of respired $^{14}CO_2$ by algae and the respiration of organic ^{14}C by bacteria and zooplankton (Peterson 1980). The importance and kinetics of these processes are expected to vary widely; consequently, there is little agreement in the literature regarding optimal ^{14}C incubation times. Contrary to the ^{14}C method, production rates measured by the O_2 method appear to be independent of incubation time in the 2- to 6-h range (Fig. 3). In Cromwell Lake, incubation time had no significant effect (ANOVA) on GPP rates measured at all irradiance levels. These results suggest that the sensitivity and precision of the O_2 method can be further increased by simply increasing the incubation time.

The effect of incubation time on R_{com} was explored in both lakes (Fig. 4, note different scales). The R_{com} measured after a 4-h incubation time was much lower in the more oligotrophic Croche Lake (5.7 ± 0.9 mg $O_2 \cdot m^{-3} \cdot h^{-1}$) than in Cromwell Lake (25.6 ± 1.7 mg $O_2 \cdot m^{-3} \cdot h^{-1}$). Both O_2 versus time curves suggest that R_{com} decreases with time and that the effect is more pronounced in the more oligotrophic lake. Because R_{com} is small in unproductive waters, it is often measured after 24- to 48-h incubations to improve measurement accuracy. Our preliminary results indicate that in some cases, long (>12 h) incubation times could underestimate R_{com}. In Croche Lake, for example, the 27-h R_{com} estimate amounts to only 80% of the values measured after 4 and 12 h (Fig. 3). Because natural planktonic communities are exposed to 8- to 14-h-long dark periods, the use of comparable incubation times to measure R_{com} may represent a good compromise in terms of measurement sensitivity and ecological realism. Note, however, that algal respiration may vary considerably during a 24-h cycle (Harris 1973). Successive dark respiration measurements carried out at 4- to 6-h intervals during complete diel cycles may be necessary to produce realistic estimates of R_{com}. Furthermore, it should be stressed that GPP measurements using the O_2 method assume that light and dark respiration rates of the phytoplankton are equal. This assumption has been tested, but with conflicting results (Bidwell 1977; Harris and Piccinin 1977). Since algal respiration represents only a fraction of R_{com}, errors incurred by assuming equal light and dark algal respiration rates in R_{com} measurements are probably minor.

Conclusions

The O_2 method was virtually abandoned decades ago in favor of the more sensitive ^{14}C method in primary production and carbon flow studies. However, because the ^{14}C method cannot measure R_{com} and cannot distinguish GPP from NPP, our knowledge on fundamental aspects of the carbon flow in aquatic systems has remained limited and controversial. The

© 1998 NRC Canada

Table 2. Raw data, production, and respiration (NPP at zero irradiance) rates calculated from triplicate clear and dark bottles of epilimnetic water taken in Croche Lake, July 4, 1997.

Irradiance ($\mu E \cdot m^{-2} \cdot s^{-1}$)	Raw data ($mg\ O_2 \cdot L^{-1}$)				Precision (%)	GPP ± SE ($mg\ O_2 \cdot m^{-3} \cdot h^{-1}$)	NPP ± SE ($mg\ O_2 \cdot m^{-3} \cdot h^{-1}$)
	Replicate 1	Replicate 2	Replicate 3	Average ± SE			
0	8.033	8.032	8.033	8.033±0.000	0.01	0±0.4	–6.7±0.3
38	8.054	8.056	8.051	8.054±0.001	0.03	5.3±0.6	–1.4±0.5
68	8.081	8.068	8.074	8.074±0.004	0.08	10.4±1.0	3.8±1.0
151	8.112	8.106	8.107	8.108±0.002	0.04	18.9±0.6	12.3±0.5
420	8.128	8.134	8.132	8.131±0.002	0.04	24.7±0.6	18.0±0.5
999	8.123	8.117	8.120	8.120±0.002	0.04	21.8±0.6	15.2±0.5
Initial bottles	8.061	8.057	8.060	8.059±0.001	0.03		

Note: The clear and dark bottles were incubated during 4 h, fixed with the three Winkler reagents, and titrated the next day.

Fig. 2. GPP and NPP versus irradiance measured after a 4-h incubation of the epilimnetic water taken in Croche Lake, July 4, 1997. Error bars represent ±1 SE of triplicate determinations.

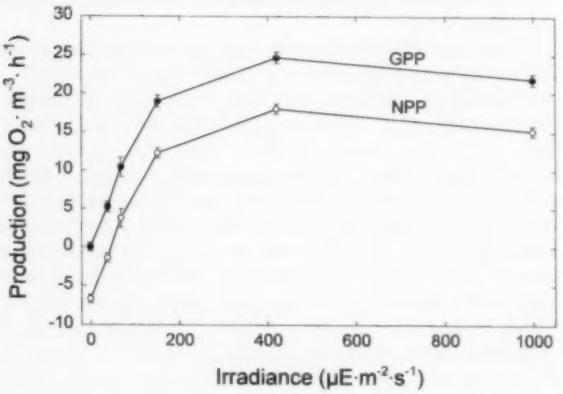

Fig. 3. GPP in Cromwell Lake versus irradiance, as measured after 2-, 4-, and 6-h incubations. Error bars represent the range of duplicate determinations. The 2- and 6-h symbols have been offset on the *x*-axis by –20 and +20 $\mu E \cdot m^{-2} \cdot s^{-1}$, respectively.

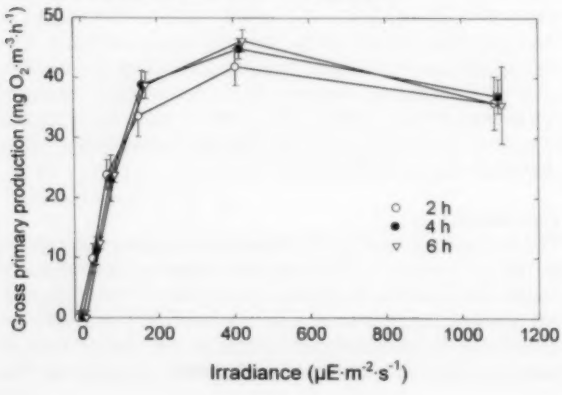

Fig. 4. Evolution of O_2 concentrations in dark bottles versus time in epilimnetic water samples taken in Croche and Cromwell lakes on July 6, 1997. Error bars represent ±1 SE of triplicate determinations.

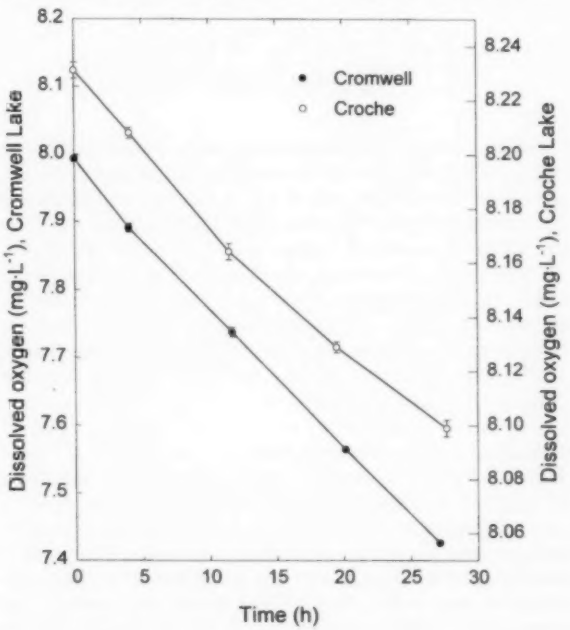

interpretation problems associated with ^{14}C production measurements (Peterson 1980) and the improved precision of the O_2 method argue for a thorough reconsideration of the pros and cons of both methods by limnologists and oceanographers. Our results show that the precision of the Winkler method is now entirely adequate for production and community respiration studies in Shield lakes and, possibly, in many other types of lakes and in the sea. Finally, the precautions and restrictions imposed by the use of radioactive tracers complicate or preclude the use of ^{14}C in the field and in the laboratory, especially by unexperienced students. For these

© 1998 NRC Canada

reasons, we believe that the potential of the Winkler method has not yet been fully exploited and that recent and future improvements of the technique are likely to replace the ^{14}C method in most situations.

References

American Public Health Association. 1992. Standard methods for the examination of water and wastewater. 18th ed. American Public Health Association, Inc., New York.

Andersen, J.M., and Sand-Jensen, K. 1980. Discrepancies between the O_2 and ^{14}C methods for measuring phytoplankton gross photosynthesis at low light levels. Oikos, **35**: 359–364.

Bidwell, R.G.S. 1977. Photosynthesis and light and dark respiration in freshwater algae. Can. J. Bot. **55**: 809–818.

Bryan, J.R., Riley, J.P., and Williams, P.J. 1976. A Winkler procedure for making precise measurements of oxygen concentration for productivity and related studies. J. Exp. Mar. Biol. Ecol. **21**: 191–197.

Carritt, D.E., and Carpenter, J.H. 1966. Comparison and evaluation of currently employed modifications of the Winkler method for determining dissolved oxygen in seawater; a NASCO report. J. Mar. Res. **24**: 286–318.

del Giorgio, P.A., and Peters, R.H. 1994. Patterns in planktonic *P:R* ratios in lakes: influence of lake trophy and dissolved organic carbon. Limnol. Oceanogr. **39**: 772–787.

Fee, E.J. 1990. Computer programs for calculating *in situ* phytoplankton photosynthesis. Can. Tech. Rep. Fish. Aquat. Sci. No. 1740.

Golterman, H.L. 1983. The Winkler determination. *In* Polarographic oxygen sensors. *Edited by* E. Gnaiger and H. Forstner. Springer-Verlag, New York. pp. 346–351.

Harris, G.P. 1973. Diel and annual cycles of net plankton photosynthesis in Lake Ontario. J. Fish. Res. Board Can. **30**: 1779–1787.

Harris, G.P., and Piccinin, B.B. 1977. Photosynthesis by natural phytoplankton populations. Arch Hydrobiol. **80**: 405–457.

Hitchman, M.L. 1978. Measurement of dissolved oxygen. Wiley, New York.

Peterson, B.J. 1980. Aquatic primary productivity and the ^{14}C-CO_2 method: a history of the productivity problem. Annu. Rev. Ecol. Syst. **11**: 359–385.

Potter, E.C., and Everitt, G.E. 1959. Further advances in dissolved oxygen microanalysis 1. Small-scale water sampling vessels and amperometric titrations. J. Appl. Chem. **9**: 642–645.

Schindler, D.W., and Holmgren, S.K. 1971. Primary production and phytoplankton in the Experimental Lakes Area, northwestern Ontario, and other low-carbonate waters, and a liquid scintillation method for determining ^{14}C activity in photosynthesis. J. Fish. Res. Board Can. **28**: 189–201.

Shearer, J.A., De Bruyn, E.R, DeClercq, D.R., Schindler, D.W., and Fee, E.J. 1985. Manual of phytoplankton primary production methodology. Can. Tech. Rep. Fish. Aquat. Sci. No. 1341.

Strickland, J.D.H., and Parsons, T.R. 1972. A practical handbook of seawater analysis. Revised. Bull. Fish. Res. Board Can. No. 167.

Talling, J.F. 1973. The application of some electrochemical methods to the measurement of photosynthesis and respiration in freshwaters. Freshwater Biol. **3**: 335–362.

Tilzer, M.M., Hillbricht-Ilkowska, A., Kowalczewski, A., Spodniewska, I., and Turczynska, J. 1977. Diel phytoplankton periodicity in Mikolajskie Lake, Poland, as determined by different methods in parallel. Int. Rev. Gesamten Hydrobiol. **62**: 279–289.

Appendix. Precise Winkler determinations

The volumes of the BOD bottles (≈300 mL) must first be determined with a precision better than 0.005%. We measure the volume of our bottles gravimetrically (±0.01 mL) near 20°C, after filling them with degassed (boiled 10 min and cooled) distilled water. Bottle volumes decrease significantly after repeated use due to the wear of ground glass surfaces. We recalibrate our bottles annually. Since the procedure's precision approaches 1 $\mu g\ O_2 \cdot L^{-1}$, particular care should be taken to avoid contamination of the glassware and working space by trace amounts of thiosulfate, iodate, I_2, and manganese. We use the reagents recommended by Carritt and Carpenter (1966) and titrate whole bottles (less 15.00 mL) to minimize the loss of volatile I_2 and the oxidation of iodide to I_2 at low pH.

Reagents

(1) Manganous chloride solution: dissolve 600 g of $MnCl_2 \cdot 4H_2O$ in 600 mL of distilled water. Bring to 1 L.

(2) Alkaline iodide solution: dissolve 320 g of NaOH and 600 g of NaI in 400 mL of distilled water. Cool and bring to 1 L.

(3) H_2SO_4 solution: slowly add 280 mL of concentrated H_2SO_4 to 700 mL of distilled water. Cool and bring to 1 L.

(4) Thiosulfate, 0.050 N: dissolve 12.41 g of $Na_2S_2O_3 \cdot 5H_2O$ in a 1-L volumetric flask. The thiosulfate is standardized with KIO_3 according to the procedure described below. Although the use of preservatives (chloroform, NaOH) is often recommended, we found that they are not necessary if the thiosulfate is standardized weekly.

(5) Iodate standard, 0.025 N: dissolve 0.8917 g of analytical-grade KIO_3 dried at 105°C in a 1-L volumetric flask. Alternatively, dissolve 0.8124 g of $KH(IO_3)_2$ dried 24 h over $MgClO_4$.

Procedure

(1) Gently dispense 2.0 ± 0.1 mL of $MnCl_2$ just below the water surface and 2.0 ± 0.1 mL of alkaline iodide just above the water surface using positive displacement pipettors. The pipettors should be washed with distilled water every 1–2 days to prevent valve and plunger malfunction due to salt crystallization.

(2) Immediately close the bottle and shake vigorously. Allow the precipitate to settle for about two thirds of the bottle and shake again to resuspend the precipitate a second time. If room temperature is more than 1°C below sample temperature, immediately add a water seal to the neck of the bottle; this will prevent air suction by the contracting sample.

(3) When the precipitate has settled to the lower third of the bottle, add 2.2 ± 0.1 mL of H_2SO_4. The H_2SO_4 must be allowed to flow gently along the neck of the bottle. Close and shake vigorously. If titration must be delayed, store the samples in darkness and at a temperature equal to or slightly lower than the temperature of the samples. Storage at temperatures above the sample temperature will cause the loss of I_2 due to the thermal expansion of the solution (0.06 $mL \cdot °C^{-1}$). Avoid poorly thermostated incubators and refrigerators that have large (>0.5°C) temperature oscillations. In the field, a pit dug in the ground and covered with polystyrene insulation provides a stable temperature.

Titration

Whole bottles are titrated using a Metrohm DMS 716 titrator equipped with a 10-mL burette and a Metrohm Pt Titrode. The Pt ring of the electrode should be polished weekly. The titrator

© 1998 NRC Canada

is used in the dynamic equivalence point titration (DET) mode, with a measuring point density of 1, a 20-µL minimum increment, and a 2 $mV \cdot min^{-1}$ signal drift condition. In this method, the solution's potential (controlled by the I_2/I^- and $S_2O_3^{2-}/S_4O_6^{2-}$ redox couples) is monitored after successive additions of titrant, where optimal increment volumes are calculated by the titrator's software. The size and rotation speed of the magnetic stirring bar must be adjusted in such a way that complete mixing of the I_2 generated during standardization occurs in 3–4 s, without vortex formation. We found that mixing speed is critical to obtain high measurement precision. Large (35 × 10 mm) stirring bars and slow rotation speeds (2–2.3 on the Metrohm 728 stirrer) yield the best results. To reduce the titration time (6–8 min) and I_2 volatilization, an initial volume of titrant equivalent to 85–90% of the expected O_2 concentration is added at the beginning of the titration. Because the molar volume of water and the normality of the titrant vary appreciably with temperature, care must be taken to standardize the titrant and conduct all titrations of a given batch of samples at constant temperature (±1°C). We found that a 5°C temperature difference in titrant temperature causes a dissolved O_2 error of about 10 $\mu g \cdot L^{-1}$. If titrant temperature cannot be controlled, it should be measured with a thermocouple fixed to the side of the burette, and the titrant volume should be corrected to a constant temperature using density-temperature tables for distilled water.

(1) Remove the stopper of the BOD bottle and, using a washbottle fitted with a 200-µL pipette tip, rinse the I_2 present on the side and conical part of the stopper into the BOD bottle with 1–2 mL of distilled water.

(2) An exact amount of titrate must be removed from the BOD bottle to make room for the electrode and the titrant. We use a clean (internally hydrophillic) volumetric pipette lowered 4–5 cm beneath the surface to withdraw 15.00 mL of titrate. During titrations, the volumetric pipette must be placed on a vertical stand for at least 5 min to allow it to drain in a reproducible manner. Alternatively, if a top-loading balance (±1 mg) is available, excess titrate can be removed with an automatic pipette, weighed, and converted to an exact volume using the specific gravity of the titrate (≈1.006 $g \cdot cm^{-3}$ at 20°C for freshwater plus Winkler reagents).

(3) Using plastic or stainless steel forceps, insert the stirring bar into the bottle.

(4) Immerse the delivery tip and the electrode, turn the stirrer on, begin the titration, and rinse the neck of the bottle with 1–2 mL of distilled water while the initial titrant volume is being delivered. The electrode must not touch the neck of the bottle. Note the equivalence point volume (V_T).

Standardization (modified from Carritt and Carpenter 1966)

Use a clean BOD bottle and clean glassware dedicated to this purpose. Adjust the initial titrant volume to 4.5 mL.

(1) Insert a stirring bar in the BOD bottle. Measure 270 ± 10 mL of distilled water in a graduated cylinder. Transfer about 200 mL of the water into the BOD bottle and pour the remaining water into a washbottle.

(2) Place a suitable weighing dish or weighing funnel in a precision balance (±0.1 mg), tare the balance, and gently add about 10 mL of the iodate standard using an automatic pipette. Immediately note the exact weight of the solution. This operation must be carried out quickly to minimize weighing errors due to evaporation. Beaker-shaped, plastic weighing dishes are ideal for this purpose. Transfer quantitatively the standard into the BOD bottle by rinsing the dish three times with 10 mL of distilled water. Rinse the neck of the bottle with some of the remaining distilled water.

(3) Add 2.0 mL of the H_2SO_4 reagent and, without mixing, 2.0 mL of the alkaline iodide reagent. Place the bottle on the magnetic stirrer and then rinse again the neck of the bottle with the remaining distilled water.

(4) Insert the electrode and the delivering tip, turn the mixer on, count 3 s, and then start the titration. The I_2 must be homogenously mixed before thiosulfate delivery begins.

(5) The normality of the thiosultate is calculated as

$$N_T = \frac{0.025 \times \text{gSTD}}{\text{EP} \times 1.0007}$$

where gSTD is the weight (grams) of 0.025 N KIO_3 used, 1.0007 is the density of 0.025 N KIO_3, and EP is the equivalence point (millilitres) of the titration.

Blank determination (modified from Carritt and Carpenter 1966)

Correction for titration blank and subtraction of the O_2 added with the reagents are not necessary when performing differential measurements, as in production and respiration studies. However, if highly accurate dissolved O_2 determinations are desired (better than 0.05 $mg \cdot L^{-1}$), titration blanks should be performed as follows.

(1) Set the titrator's initial titrant volume to zero. Using a precise (±0.002 mL) pipette, transfer 1 mL of the KIO_3 standard to a clean BOD bottle and 280 ± 5 mL of lake water. Add 2.2 mL of H_2SO_4 and 2.0 mL of the alkaline iodide solution, mix, and then add 2.0 mL of $MnCl_2$.

(2) Titrate and note the equivalence point volume. Repeat steps 1 and 2 three times and note the average equivalence point volume (EP1).

(3) Repeat step 1, but this time, set the titrator's initial titrant volume to the equivalence point found above. Start the titration sequence, but stop it just after the addition of the initial titrant volume. Reset the titrator's initial volume to zero, add another 1 mL of KIO_3, and start the titration again. Repeat three times and note the average equivalence point volume (EP2).

(4) The titration blank (blk, millilitres of thiosulfate) is the difference between EP1 and EP2.

Calculations

The O_2 concentration (milligrams per litre) is calculated as

$$O_2 = \frac{8000(N_T - \text{blk})V_T}{V_s\left(\frac{V_B - 4}{V_B}\right)} - 0.024$$

where N_T and V_T are the normality and volume (millilitres) of thiosulfate, V_B is the volume (millilitres) of the bottle, V_S is the volume (millilitres) titrated (V_B - 15.00 mL), blk (millilitres) is the titration blank, and the constant 0.024 is the O_2 (milligrams per litre) added with the reagents.

© 1998 NRC Canada

Sexual difference in polychlorinated biphenyl accumulation rates of walleye (*Stizostedion vitreum*)[1]

Charles P. Madenjian, George E. Noguchi, Robert C. Haas, and Kathrin S. Schrouder

Abstract: Adult male walleye (*Stizostedion vitreum*) exhibited significantly higher polychlorinated biphenyl (PCB) concentrations than similarly aged female walleye from Saginaw Bay (Lake Huron). To explain this difference, we tested the following three hypotheses: (*i*) females showed a considerably greater reduction in PCB concentration immediately following spawning than males, (*ii*) females grew at a faster rate and therefore exhibited lower PCB concentrations than males, and (*iii*) males spent more time in the Saginaw River system than females, and therefore received a greater exposure to PCBs. The first hypothesis was tested by comparing PCB concentration in gonadal tissue with whole-body concentration, the second hypothesis was tested via bioenergetics modeling, and we used mark–recapture data from the Saginaw Bay walleye fishery to address the third hypothesis. The only plausible explanation for the observed difference in PCB accumulation rate was that males spent substantially more time in the highly contaminated Saginaw River system than females, and therefore were exposed to greater environmental concentrations of PCBs. Based on the results of our study, we strongly recommend a stratified random sampling design for monitoring PCB concentration in Saginaw Bay walleye, with fixed numbers of females and males sampled each year.

Résumé : Dans la baie Saginaw (lac Huron), les mâles adultes du doré jaune (*Stizostedion vitreum*) montrent des teneurs en polychlorobiphényles (PCB) sensiblement plus élevées que les femelles adultes d'âge semblable. Pour expliquer cette différence, nous avons testé les trois hypothèses suivantes : (*i*) par rapport aux mâles, les femelles montrent une réduction considérablement plus marquée de la teneur en PCB immédiatement après la fraye, (*ii*) les femelles grossissent à un rythme plus rapide que les mâles et montrent donc des teneurs en PCB moins élevées et (*iii*) les mâles passent plus de temps que les femelles dans le réseau de la Saginaw et sont donc plus exposés aux PCB. Nous avons testé la première hypothèse en comparant le teneur en PCB des gonades à la teneur corporelle totale, la deuxième, par modélisation bioénergétique, et la troisième, à l'aide de données de recapture après marquage recueillies dans le cadre de la pêche du doré jaune dans la baie Saginaw. La seule explication plausible de la différence observée dans le taux d'accumulation de PCB était que les mâles passaient beaucoup plus de temps que les femelles dans le réseau très pollué de la Saginaw et qu'ils étaient par conséquent exposés à des teneurs plus élevées de PCB dans l'environnement. D'après les résultats de notre étude, nous recommandons fortement un échantillonnage aléatoire stratifié du doré jaune de la baie Saginaw pour contrôler les teneurs en PCB chez cette espèce, le nombre de femelles et de mâles échantillonnés chaque année étant fixes.
[Traduit par la Rédaction]

Introduction

Contaminant accumulation rate in piscivorous fish may be influenced by a myriad of factors, including the gross growth efficiency of the piscivorous fish, contaminant concentrations in prey fish, and release of gonadal material during spawning by the predator fish (Masnado 1987; Borgmann and Whittle 1992; Larsson et al. 1993; Madenjian et al. 1993, 1994; Rodgers 1996). Because contaminant accumulation rate can be affected by multiple factors, the principal determinants of contaminant accumulation rate can vary among species or among ecosystems for a given fish species. Identification of the important determinants of contaminant accumulation rate may be useful in managing a fishery to reduce contaminant exposure for people consuming fish (Stow et al. 1995) and may lead toward development of a more efficient sampling

Received July 2, 1997. Accepted December 11, 1997.
J14088

C.P. Madenjian[2] and G.E. Noguchi.[3] U.S. Geological Survey, Biological Resources Division, Great Lakes Science Center, 1451 Green Road, Ann Arbor, MI 48105, U.S.A.
R.C. Haas. Michigan Department of Natural Resources, Lake St. Clair Fisheries Station, 33135 S. River Road, Mt. Clemens, MI 48045, U.S.A.
K.S. Schrouder. Michigan Department of Natural Resources, 503 North Euclid Avenue, Suite 1, Bay City, MI 48706, U.S.A.

[1] This article is Contribution 1009 of the U.S. Geological Survey Great Lakes Science Center.
[2] Author to whom all correspondence should be addressed. e-mail: chuck_madenjian@usgs.gov
[3] Present address: U.S. Fish and Wildlife Service, Division of Environmental Contamination, 4401 Fairfax Drive, Suite 330, Arlington, VA 22203, U.S.A.

© 1998 NRC Canada

design for monitoring contaminant concentrations in fish (Sheffy 1980; Masnado 1987).

Among the factors influencing polychlorinated biphenyl (PCB) accumulation in piscivorous fish, gross growth efficiency (gge) represents the effect of bioenergetics on PCB accumulation (Madenjian et al. 1994). The gge is the amount of growth by a fish divided by the amount of food eaten to attain that growth. All other factors being equal, fish with a higher gge will accumulate contaminants at a lower rate than fish with relatively low gge (Madenjian et al. 1994).

For certain species, the effect of gonadal release during spawning has a huge impact on PCB accumulation rate. Larsson et al. (1993) showed that the PCB concentration in northern pike (*Esox lucius*) females declined after the females attained maturity whereas the PCB concentration in male northern pike did not show any such decrease with age. These researchers attributed this difference to a sharp decrease in female whole-body PCB concentration immediately after spawning because the PCB concentration in ovaries was about 100 times higher than the whole-body PCB concentration.

PCB concentrations in prey fish are also crucial in determining the PCB accumulation rates in predatory fish (Borgmann and Whittle 1992; Madenjian et al. 1993). Masnado (1987) showed that PCB concentrations of brown trout (*Salmo trutta*) were higher in Green Bay than in the main basin of Lake Michigan. The higher PCB concentrations in Green Bay were attributed to a higher contaminant exposure, presumably due to higher PCB concentrations in alewife (*Alosa pseudoharengus*) from Green Bay than from Lake Michigan's main basin. Madenjian et al. (1993) attributed a portion of the variability in PCB concentrations of lake trout (*Salvelinus namaycush*) from Lake Michigan to spatial variability in the PCB concentrations of prey fish, especially alewife.

The Saginaw River, which is the major tributary to Saginaw Bay of Lake Huron, has been intensively investigated for contaminant sources and loads during the last 15 years because the river has been contaminated with inorganic and organic materials released from industries (Giesy et al. 1997). The walleye (*Stizostedion vitreum*) population in Saginaw Bay was successfully rehabilitated during the 1980s through a stocking program that began in the mid-1970s (Mrozinski et al. 1991). The bulk of spawning activity for this population is believed to occur in the Tittabawassee River, which is the major tributary to the Saginaw River (Mrozinski et al. 1991). Female walleye grow faster than males (Johnson et al. 1996). The Michigan Department of Natural Resources has undertaken a walleye tagging program, from 1981 to present, in an attempt to understand movements of walleye throughout the Saginaw Bay system, including the Saginaw River system (Mrozinski et al. 1991). Typically, walleye were tagged in the Tittabawassee River during their spawning run.

Our preliminary data indicated that the whole-body PCB concentration of male walleye ≥6 years old in 1990 from Saginaw Bay was about 2.5 times higher than that of similarly aged females. We postulated three possible explanations for this difference: (*i*) the females lose such a large portion of their body burden after spawning that their whole-body PCB concentration undergoes a substantial decrease, (*ii*) the females show a higher gge than males, and therefore accumulate PCBs at a slower rate, or (*iii*) males spend more time in the heavily contaminated Saginaw River system, and therefore exhibit higher PCB concentrations than females, which spend most of their time in the less-contaminated Saginaw Bay. The objectives of our study were the following: (1) verify that the sexual difference in PCB concentrations of walleye from the Saginaw Bay system that was observed in 1990 was still present in 1996 by sampling male and female walleye from the Tittabawassee River in April 1996 and determining the PCB concentrations of those fish, (2) if the sexual difference in PCB concentrations was still evident in 1996, then test the above-mentioned three hypotheses and select the most plausible explanation for the observed difference, and (3) discuss management implications of these findings with regard to monitoring PCB concentrations of walleye.

Methods

Field sampling

During April 1990, five male and five female walleye were electrofished from the Tittabawassee River just below Dow Dam. This dam is situated 58 river km from the mouth of the Saginaw River at Saginaw Bay. Total length (to the nearest millimetre) and weight (to the nearest gram) of each fish were measured. Scales were taken from each fish for ageing. The gonads of each fish were then removed, weighed to the nearest gram, wrapped in solvent-rinsed aluminum foil, placed in contaminant-free plastic bags, and frozen. Each walleye (without gonads) was also wrapped in solvent-rinsed aluminum foil, placed in contaminant-free plastic bags, and frozen.

During April 1996, 11 male and 10 female walleye were electrofished from just below the Dow Dam. Again, total length and weight of each fish were measured and scales were taken for ageing. Each whole walleye was wrapped in solvent-rinsed aluminum foil, placed in contaminant-free plastic bags, and frozen.

Laboratory analysis

For each walleye caught in 1990, the gonads were homogenized and analyzed for total PCBs following the protocol described by Schmidt and Hesselberg (1992). The somatic tissue for each individual walleye was also homogenized and analyzed for total PCBs using the same procedure. Appropriate quality control samples (blanks, matrix spikes, duplicates, and dilutions when necessary) were used to ensure the accuracy and precision of the analyses (see Giesy et al. 1994). Whole-fish PCB concentration was reconstructed by summing the product of PCB concentration in somatic tissue and somatic tissue weight with the product of PCB concentration in gonad tissue and gonad tissue weight and then dividing by the whole-body weight of the walleye (see Niimi 1983).

Each whole walleye caught in 1996 was homogenized and analyzed for total PCBs using the Schmidt and Hesselberg (1992) procedure with the appropriate quality control measures. Lipid concentration was determined for each walleye using the methods described in Rottiers and Tucker (1982).

Statistical analysis of PCB data

We estimated the average change in whole-fish PCB concentration due to spawning for both male and female walleye following the calculations outlined by Niimi (1983) and using the 1990 PCB measurements. We applied a two-sample *t*-test to our 1996 data to determine whether the male whole-fish mean PCB concentration was significantly higher than the female whole-fish mean PCB concentration. We also estimated the standard deviation for both male and female whole-fish PCB concentrations from the 1996 data.

Bioenergetics modeling

To determine whether the average female walleye exhibited a higher gge than the average male, we estimated food consumption by

© 1998 NRC Canada

Fig. 1. Average daily water temperature of intake water to the Bay Metropolitan Water Treatment Plant, Bay City, Mich., 1969–1995. The opening of the intake pipe was located in Saginaw Bay about 6 km north of Bay City State Park. Day 1 corresponded to 1 January.

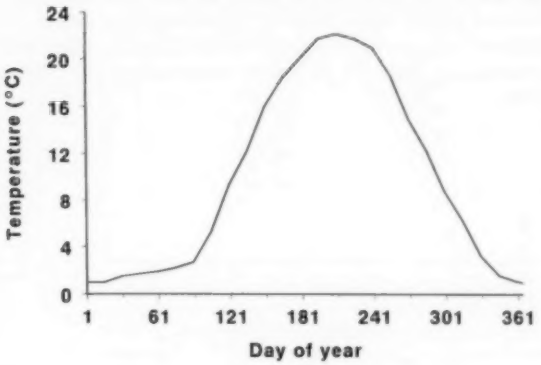

walleye using the "Wisconsin" bioenergetics model developed by Kitchell et al. (1977) and coded into a computer program by Hewett and Johnson (1992). This approach calculates energy losses as a function of water temperature and walleye size and then estimates the amount of food consumption that was necessary for a walleye to achieve the observed size (weight) at a given age. We assumed that males and females were equally active, and we assigned a value of 1.0 to the activity multiplier (Kitchell et al. 1977). The model time step was 1 day.

Model inputs included walleye growth, water temperature, walleye diet, and caloric densities of prey and predator (walleye). Fishery biologists for the Michigan Department of Natural Resources have caught walleye using gill nets, with stretch mesh sizes ranging from 19 to 102 mm, in Saginaw Bay during October each year since 1989 (Johnson et al. 1996; D. Fiedler, Michigan Department of Natural Resources, Alpena, Mich., personal communication). The average day of year for the gillnet deployment was 15 October. Based on these data for years 1989–1995, we estimated the average weight for both male and female walleye of ages 1–9 in mid-October. Comparison of lengths of aged walleye taken in mid-October with those caught during early spring of the following year at Dow Dam revealed that net growth was minimal over the winter (Johnson et al. 1996; D. Fiedler, personal communication). Therefore, in our bioenergetics model application, we assumed zero net growth between 16 October and 30 April. Thus, 1 May through 15 October marked the growing season in our simulations. Day 1 of our bioenergetics model simulations corresponded to 16 October.

The water temperature regime used in the bioenergetics model was taken from records of the water intake temperatures at Bay City (Fig. 1), located on the southwestern shore of Saginaw Bay. The diet schedule used in our simulations was based on the data presented by Schaeffer (1994), who examined stomach contents of Saginaw Bay walleye from May through October in 1988. For our simulations, we interpolated between the October diet of an age-class and the May diet of the next-older age-class to estimate winter diet. Data were only available for walleye up to age 3, and therefore, we assumed that the diet of walleye older than age 3 was similar to the diet of age 3 walleye. This assumption appeared to be reasonable based on the findings by Hartman and Margraf (1992) for Lake Erie walleye. The caloric density of age 1 and older walleye was assigned a value of 4605.5 J/g wet weight (Hartman and Margraf 1992). All caloric densities reported in this paper are based on wet weight. Because caloric density data specifically for prey fish from Saginaw Bay were not available, we used caloric density data from other Great Lakes populations. Alewife caloric density was assumed to follow a seasonal cycle, as described by Flath and Diana (1985). The caloric density of young-of-the-year (YOY) gizzard shad (*Dorosoma cepedianum*) was assumed to increase from a value of 4187 J/g in mid-August to 5443 J/g in mid-November, based on data from western Lake Erie (M. Kershner, Aquatic Ecology Laboratory, Ohio State University, Columbus, Ohio, personal communication). Rainbow smelt (*Osmerus mordax*) caloric density was assigned a value of 5700 J/g (Hartman and Margraf 1992). Shiners were assigned a value of 5008.7 J/g (Hartman and Margraf 1992). Finally, the caloric densities of YOY yellow perch (*Perca flavescens*), YOY white perch (*Morone americana*), and trout-perch (*Percopsis omiscomaycus*) were assigned values of 3822.5, 3759.7, and 3851.8 J/g, respectively, based on data from western Lake Erie (M. Kershner, personal communication).

Spawning was simulated on 4 April by the average male losing 2.9% of its whole-body weight and the average female losing 22.1% of its whole-body weight. These losses in body weight were estimated from our 1990 data. Spawning typically occurs in the Tittabawassee River during the last week of March through the first 2 weeks of April (D. Fiedler, personal communication), so we chose 4 April as a typical spawning date. In our simulations, the average male spawned at age 4 and each subsequent year whereas the average female began spawning at age 5. These maturity schedules were based on observations during the spring spawning run in the Tittabawassee River (D. Fiedler, personal communication).

To investigate the effect of seasonal movement between Saginaw Bay and the Saginaw River system on gge, we conducted an additional set of simulations. For age 3 and older males, we substituted the following temperature regime. For June–August, the Bay City water intake temperatures were used, but for September–May, water temperatures from the Saginaw River were used (Michigan Department of Natural Resources 1988). Thus, we simulated the growth of adult males moving from the river to the bay by June, spending most of the summer in the bay, and then returning to the river by September.

Mark–recapture analysis

The Michigan Department of Natural Resources initiated a tagging program for Saginaw Bay walleye in 1981 (Mrozinski et al. 1991). By December 1996, over 50 000 walleye had been tagged. Most of these fish were taken just below Dow Dam during the spring spawning run. These walleye were electrofished from the river, measured, sexed, marked with a numbered metal tag attached to their maxillary bones, and then released at the tagging site. By December 1996, almost 4000 of these tagged walleye had been recaptured by anglers fishing within the Saginaw River system, within Saginaw Bay, or at other locations outside Saginaw Bay.

To determine whether males spent more time in the river system than females, we estimated the probability of capturing adult walleye, by sex, in each of three areas: (*i*) within the Saginaw River system, (*ii*) within Saginaw Bay, and (*iii*) places other than the Saginaw River system or Saginaw Bay (this area included Lake Huron proper, Lake St. Clair, the Thames River, and western Lake Erie). These probabilities were estimated by dividing the number of recaptures in a particular area for a particular sex by the total number of recaptures for that sex; this ratio represented the maximum likelihood estimate (Brownie et al. 1985). The 95% confidence intervals about these probabilities were approximated by

$$(1) \qquad P_{ij} \pm 1.96\sqrt{\frac{P_{ij}(1-p_{ij})}{n_j}}$$

where p_{ij} is the estimate of the probability of recapturing a walleye of sex j in area i and n_j is the total number of recaptures for sex j (Brownie et al. 1985).

Previous studies of walleye movement in Lake Erie suggested

© 1998 NRC Canada

that females tend to increase their range of movements as they get larger (Thomas and Haas 1994). To investigate whether this same pattern was true for females from Saginaw Bay, we repeated the analysis for females, but only included females that were ≥610 mm in length at the time of tagging. To address this question of increased movement with increasing female size, it would have been preferable to partition the female recaptures by size or age at time of recapture, but these data were not available. Nevertheless, our approach did provide some resolution to this issue.

Sampling strategies for monitoring walleye PCB concentration

Presently, the Michigan Department of Natural Resources determines contaminant concentrations of 20 walleye from the Saginaw River –Saginaw Bay system each year, without regard to the sex of the 20 individuals (R. Day, Michigan Department of Natural Resources, Lansing, Mich., personal communication). These walleye were either captured during the spring spawning run in the Tittabawassee River or gillnetted in Saginaw Bay in the fall. We used our estimates of mean and standard deviation of PCB concentrations for both male and female walleye from our 1996 sampling below Dow Dam to evaluate sampling strategies for monitoring the mean PCB concentration in the Saginaw Bay walleye population. In particular, we wanted to see if the number of fish used to determine contaminant concentrations in the walleye could be reduced by following a stratified random sampling protocol, without sacrificing any precision in the estimate of mean PCB concentration.

First, we calculated the expected standard error of the mean based on simple random sampling of the PCB concentrations within the walleye population. We assumed equal numbers of males and females, and this assumption was supported by catches of both juvenile and adult walleye in gill nets fished in Saginaw Bay (D. Fielder, personal communication). By sampling theory (Cochran 1953), the expected standard error of the mean from simple random sampling, SE_{ran}, of a population composed of two distinct and equally sized subpopulations is given by

$$(2) \qquad SE_{ran} = \sqrt{\frac{\frac{\sigma_m^2 + \sigma_f^2}{2} + \frac{(\mu_m - \mu_f)^2}{4}}{n}}$$

where μ_m is mean PCB concentration of males, μ_f is mean PCB concentration of females, σ_m^2 is variance in PCB concentrations of males, σ_f^2 is variance in PCB concentrations of females, and n is the number of walleye sampled from the population. Again assuming equal numbers of males and females, the expected value of the mean, μ_{pop}, of a simple random sample of PCB concentrations from the walleye population is simply

$$(3) \qquad \mu_{pop} = \frac{\mu_m + \mu_f}{2}$$

with μ_m and μ_f representing the mean PCB concentrations of males and females, respectively (Cochran 1953). We calculated the standard error of the mean from eq. 2 for n ranging from 4 to 20.

The expected mean PCB concentration of the walleye population as estimated by stratified random sampling is identical to that estimated by simple random sampling, as illustrated in eq. 3. The expected standard error of the mean from stratified random sampling, SE_{str}, as presented by Cochran (1953), is given by

$$(4) \qquad SE_{str} = \sqrt{\frac{\frac{\sigma_m^2}{n_m} + \frac{\sigma_f^2}{n_f}}{4}}$$

where n_m and n_f are the numbers of males and females, respectively, sampled from the walleye population. Again, this estimator is based on equal numbers of males and females in the population.

Fig. 2. Whole-body PCB concentrations of male (open triangles) and female (open circles) walleye caught during April 1990 and whole-body PCB concentrations of male (solid triangles) and female (solid circles) walleye caught during April 1996. All walleye were caught in the Tittabawassee River just below Dow Dam (Midland, Mich.). Whole-body PCB concentrations of walleye caught in 1990 were reconstructed based on determinations of PCB concentrations in gonadal and somatic tissues, as outlined by Niimi (1983).

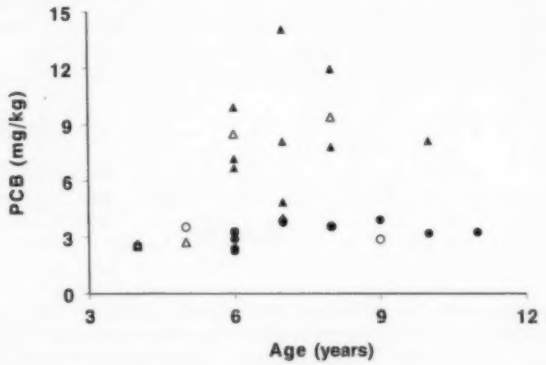

The total number of walleye sampled using the stratified random sampling procedure, n, is equal to the sum of n_m and n_f. To minimize SE_{str} (Cochran 1953), we used Neyman allocation to estimate n_m and n_f:

$$(5) \qquad n_m = \frac{n\sigma_m}{\sigma_m + \sigma_f}$$

$$(6) \qquad n_f = \frac{n\sigma_f}{\sigma_m + \sigma_f}.$$

To ensure that an estimate of the variance within a sex stratum could always be generated, we imposed the restriction that neither n_m nor n_f could be less than 2. Following this restriction and using eqs. 4, 5, and 6, we calculated SE_{str} for n ranging from 4 to 20. Finite population correction factors were not included in eq. 2 or 4 because the male and female populations of walleye in Saginaw Bay were sufficiently large that these factors could be ignored (Cochran 1953). Because our observed distributions of PCB concentrations in adult males and female walleye did not significantly differ from normal distributions (Shapiro–Wilk test (Shapiro and Wilk 1965), $P > 0.05$), we assumed that the adult female and male populations exhibited PCB concentrations that were normally distributed.

Results

Statistical analysis of PCB data

In 1990, males younger than age 6 exhibited relatively low PCB concentrations whereas the two males of age 6 and older showed PCB concentrations >8 mg/kg (Fig. 2). In contrast, all of the females (two younger than age 6, three older than age 6) caught in 1990 had PCB concentrations <4 mg/kg.

Ovary weight averaged 22.1% of total body weight whereas testes weight averaged only 2.9% of total body weight. On average, 18.6% of the female body burden was in the ovaries, and only 0.152% of the male body burden was in the testes. Therefore, spawning would be expected to cause an increase in PCB concentration of 4.5% in females and 2.8% in males.

© 1998 NRC Canada

Table 1. Cumulative consumption and cumulative gge, by age and sex, for walleye from Saginaw Bay.

	Males			Females		
Simulation year	Weight at end of year (g)	Cumulative consumption	Cumulative gge	Weight at end of year (g)	Cumulative consumption	Cumulative gge
1	410	1 010	0.280	425	1 042	0.300
2	817	2 806	0.246	835	2 871	0.252
3	1 084	4 754	0.201	1 334	5 308	0.230
4	1 370	7 139	0.174	1 699	8 123	0.195
5	1 607	9 795	0.151	2 059	11 915	0.163
6	1 726	12 512	0.128	2 309	16 023	0.137
7	1 832	15 348	0.111	2 668	20 700	0.124
8	2 069	18 568	0.105	2 738	25 330	0.104

Note: Consumption was estimated using the bioenergetics model developed by Kitchell et al. (1977). Growth data for 1989–1995 were used for the modeling. Each bioenergetics simulation year began on 16 October and ended on 15 October of the following year. The first simulation year began with age 0 walleye in October, when male weight averaged 127 g and female weight averaged 112 g. Cumulative gge was equal to the difference between the weight at end of year and the appropriate initial weight (127 g for males and 112 g for females) divided by cumulative consumption.

Table 2. Proportions of walleye recaptures, by sex, from each of three mutually exclusive areas during 1981–1996.

Sex	Size of walleye	Number of recaptures	Proportion of recaptures in Saginaw River system	Proportion of recaptures in Saginaw Bay	Proportion of recaptures outside Saginaw River – Saginaw Bay system
Male	All sizes	2188	0.61 (0.59, 0.63)	0.35 (0.33, 0.37)	0.05 (0.04, 0.06)
Female	All sizes	1550	0.34 (0.31, 0.36)	0.52 (0.49, 0.54)	0.15 (0.13, 0.17)
Female	Large	395	0.29 (0.25, 0.34)	0.51 (0.46, 0.56)	0.20 (0.16, 0.24)

Note: All of the tagging sites were within the Saginaw River – Saginaw Bay system, with the bulk of walleye tagged during the spring spawning run in the Tittabawassee River just below Dow Dam (Midland, Mich.). Large refers to walleye ≥610 mm in total length at time of tagging. The 95% confidence intervals for the proportions of recaptures are enclosed in parentheses. See the Methods section for more details.

The ages of the 21 adult walleye captured in 1996 ranged from 6 to 11 years (Fig. 2). In 1996, the mean PCB concentration of females was 3.17 mg/kg, with a standard deviation estimated at 0.53 mg/kg. Males averaged a PCB concentration of 7.95 mg/kg, with a standard deviation of 3.07 mg/kg. Mean PCB concentration of the males was significantly higher than mean PCB concentration of females (two-sample t-test with unequal variances, $P < 0.01$). Lipid concentrations of males and females, on a wet weight basis, averaged 7.1 and 7.7%, respectively; there was no significant difference in the mean lipid concentrations between sexes (two-sample t-test with equal variances, $P > 0.05$).

Bioenergetics modeling

Cumulative gge of walleye steadily decreased with age for both sexes (Table 1). At the start of simulation year 1, which began on 16 October, average male weight was 127 g and average female weight was 112 g; these walleye were fall yearlings. Females were 2.7 kg at the end of simulation year 8 whereas males were 2.1 kg at this point in development. Cumulative gge in males decreased from 0.28 at the end of simulation year 1 to 0.10 at the end of simulation year 8 whereas females experienced a decrease from 0.30 to 0.10 during this simulated period (Table 1). The greatest differences between the sexes in cumulative gge occurred at the end of simulation year 3, when female gge was 14.4% greater than male gge. Interestingly, the bioenergetics modeling results showed that by the end of simulation year 8, male gge was slightly higher than female gge (Table 1).

The additional set of bioenergetics model simulations for males exposed to a Saginaw River temperature regime from September through May and a Saginaw Bay temperature regime for the remainder of the year revealed that seasonal movements of males would have little effect on gge. The difference between the gge listed in Table 1 and the gge estimated from this additional set of simulations did not exceed 4.3% for any of the simulation years.

Mark–recapture analysis

Of the 1550 recaptures of female walleye that have been recorded, only 34% were in the Saginaw River system (Table 2). Most of the remaining female recaptures were in Saginaw Bay. In contrast, 61% of the 2188 male recaptures were in the Saginaw River system (Table 2). About 35% of

© 1998 NRC Canada

Fig. 3. Expected standard error of the mean PCB concentration of the adult walleye population in Saginaw Bay, as estimated from simple random sampling (eq. 2) and from stratified random sampling with Neyman allocation (eqs. 4, 5, and 6). For stratified random sampling, the further restriction that the number of males or females could not be less than 2 was imposed. Estimates of means and variances of PCB concentrations were based on 1996 data displayed in Fig. 2. See the Sampling strategies for monitoring walleye PCB concentration section under Methods for more details.

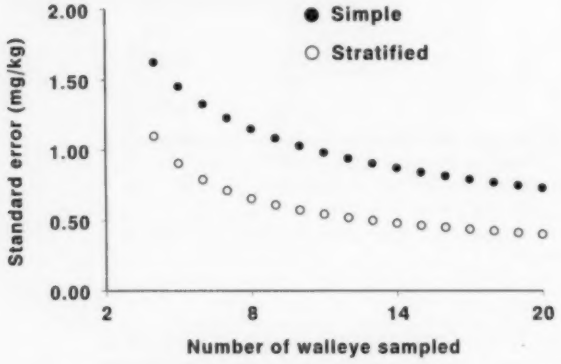

the male recaptures were in Saginaw Bay, and only about 5% of the recaptures were from other locations. Thus, the probability of a male recapture occurring in the Saginaw River system was almost twice as great as a female recapture there (Table 2). A higher percentage of female recaptures (15%) occurred outside the Saginaw River – Saginaw Bay system compared with male recaptures (only 5%) outside the system.

Considering only females that were ≥610 mm at time of tagging, the distribution of recaptures among the three location categories was somewhat different than the pattern for all females pooled (Table 2). The females that were of a larger size at tagging had a higher probability of being recaptured outside the Saginaw River – Saginaw Bay system. Therefore, it seemed that larger females were more likely to stray outside the system than smaller females. Also, the females of a larger size at tagging had a lower probability of being recaptured in the Saginaw River system than all females pooled (Table 2).

Sampling strategies for monitoring walleye PCB concentration

Regardless of the sampling procedure, the mean PCB concentration of the adult walleye population was estimated at 5.56 mg/kg. For a given sample size n, the expected standard error about the mean PCB concentration was substantially higher from simple random sampling than from stratified random sampling (Fig. 3). The expected standard error of the mean from simple random sampling was 0.73 mg/kg for a sample of 20 fish (Fig. 3) whereas the expected standard error of the mean from stratified random sampling was 0.71 mg/kg for a sample of just seven fish. Thus, a stratified random sample of just seven walleye from the adult population led to a more precise estimate of mean PCB concentration than a simple random sample of 20 walleye. The number of females sampled with our stratified random sampling protocol was two for n ranging from four to 16 fish and three for n between 17 and 20 fish. The disparity between the number of males and females sampled under stratified random sampling was due to the substantially greater variability in the male PCB concentrations than in female PCB concentrations (refer to eqs. 5 and 6).

Discussion

The act of spawning had little effect on PCB concentration in walleye. PCB concentration increased slightly in both males and females immediately following spawning. This finding agreed with Niimi (1983), who compared PCB concentration in ovaries with whole-body PCB concentration for rainbow trout (*Oncorhynchus mykiss*), white sucker (*Catostomus commersoni*), white bass (*Morone chrysops*), smallmouth bass (*Micropterus dolomieu*), and yellow perch. For three of these five species, PCB concentration in females was predicted to increase slightly after spawning, and PCB concentration would be expected to decrease slightly after spawning in the other two species. The changes in PCB concentration due to spawning did not exceed 10%, and therefore, Niimi (1983) concluded that spawning had little effect on PCB concentration in females of these five species. Perhaps the northern pike is one of the few fishes that exhibits a dramatic decrease in the PCB concentration of females following spawning.

PCB concentration in fish is inversely proportional to gge (Madenjian et al. 1994). Furthermore, it is reasonable to assume that the major pathway of PCB accumulation in piscivorous fish is by diet (Thomann and Connolly 1984; Madenjian et al. 1993). If a difference in gge was to successfully explain the 2.5-fold difference in PCB concentration between the walleye sexes, then there should be a 2.5-fold difference in gge between the sexes. Our bioenergetics modeling indicated that although females were more efficient growers than males for most of their lifetime, the difference in gge between the sexes was small (not greater than 15% for any age between 2 and 9 years), and this difference was negligible by the time the walleye were 9 years old. If females were slightly more active than males, as suggested by our mark–recapture data, then we may have overestimated the difference in gge between the sexes. We conclude that sexual differences in gge explain very little of the sexual difference in PCB accumulation rates of Saginaw Bay walleye.

Of the three hypotheses, sexual differences in migration patterns were the most plausible explanation for the observed sexual difference in PCB accumulation rates. According to our mark–recapture analysis, adult males appeared to spend most of their time in the Saginaw River system whereas adult females appeared to spend most of their time in Saginaw Bay and locations outside the Saginaw River – Saginaw Bay system. Our data suggested that male and female PCB concentrations were similar at onset of maturation. The sharp increase in PCB concentration of males following maturation may be attributable to an increased tendency to reside in the Saginaw River system. The lack of any trend toward increasing PCB concentration with increasing age following maturation in females could be due to an increase in the ranging of adult females with age. Our mark–recapture analysis suggested that as mature females grew in size, there was a greater tendency to travel outside the Saginaw River – Saginaw Bay system and to spend less time in the Saginaw River system. The

© 1998 NRC Canada

limited data on PCB concentrations in Lake Huron prey fish indicated that the PCB concentration of adult alewife in the main basin of Lake Huron is less than the PCB concentration of adult alewife in Saginaw Bay (Jones et al. 1993; Giesy et al. 1997; R. Day, personal communication). As described by Schaeffer (1994), large alewife are a major diet constituent of adult walleye in Saginaw Bay.

It appeared that the difference in prey fish PCB concentrations between Saginaw Bay and the Saginaw River system was sufficient to account for the difference in male and female walleye PCB concentrations. Adult alewife contained PCB concentrations of 1.22 mg/kg in the Tittabawassee River in spring 1990 whereas adult alewife from Saginaw Bay during the same time period averaged only 0.42 mg/kg (Giesy et al. 1997). It is possible that a subpopulation of adult alewife chiefly inhabited the Saginaw River system whereas another subpopulation chiefly resided in Saginaw Bay. PCB determinations of YOY alewife and YOY spottail shiner (*Notropis hudsonius*) from the lower Saginaw River further attested to elevated bioaccumulation rates in the river system. Giesy et al. (1997) reported an average PCB concentration of 0.86 mg/kg in YOY alewife from the mouth of the Saginaw River in August 1990, and Noguchi and Hesselberg (1991) measured an average PCB concentration of 1.20 mg/kg in YOY spottail shiner caught at the mouth of the Saginaw River during fall 1985.

Our documentation of the sexual difference in PCB accumulation rates of walleye from Saginaw Bay has management implications for monitoring contaminants in these fish. Our sampling strategy analysis showed that the level of precision in the estimate of mean PCB concentration was better under the stratified random sampling procedure for just two females and five males than under the simple random sampling procedure of 20 walleye. Thus, the number of walleye sampled for determination of PCB concentration each year could be reduced from 20 walleye sampled randomly from the adult walleye population to as few as seven walleye sampled by sex stratification without any sacrifice in precision of the mean PCB concentration estimate. The reduction in the number of fish sampled would reduce the cost of monitoring walleye. In the long run, the savings may be substantial, considering that the present cost of measuring a set of contaminants in one fish is $1000 (U.S. dollars in 1996) (D. Verbrugge, Michigan State University, East Lansing, Mich., personal communication). We strongly recommend that stratified random sampling be used to monitor the contaminant concentrations in Saginaw Bay walleye.

Some degree of spatial segregation of the sexes is not limited to walleye populations. A population of striped bass (*Morone saxatilis*) on the eastern coast of North America utilizes the Hudson River for spawning (Secor et al. 1995). The Hudson River has been heavily contaminated with PCBs, and preliminary data have suggested that adult males tend to reside in the Hudson River for much of the year, and the adult males exhibit significantly higher PCB concentrations than adult females (D. Secor, Center for Estuarine and Environmental Studies, University of Maryland, Solomons, Md., personal communication). Why do adult males show a propensity toward a river existence whereas adult females prefer to inhabit bays or lakes (or oceans) in populations of fish such as walleye and striped bass? The answer to this question is well beyond the scope of this study. Interestingly, the measuring of contaminant concentrations in fish has facilitated the discovery of this fascinating life history characteristic.

Our management recommendations for monitoring PCBs may be applicable to other fish populations exhibiting some degree of spatial segregation of the sexes. This would include other walleye populations as well as populations of other fishes. For example, the situation in Green Bay of Lake Michigan is somewhat similar to that in Saginaw Bay. The lower Fox River, which feeds into southern Green Bay, is heavily contaminated with PCBs (Velleux and Endicott 1994). Perhaps the male walleye of the Green Bay population also shift to a river lifestyle after maturing. Stratified random sampling, by sex, of the adult walleye from Green Bay may reveal a pattern similar to that for Saginaw Bay walleye. We would also recommend stratified random sampling for monitoring PCBs in the Hudson River striped bass population. In conclusion, we have shown that documentation of a sexual difference in PCB accumulation rates can be used to arrive at a more efficient sampling strategy for monitoring contaminants in these fish populations.

Acknowledgments

J. Adams and G. Fowler shared their expertise on sampling theory with us, and for their assistance we are very grateful. We thank L. Begnoche and L. Schmidt for determining the PCB concentrations in the walleye. This paper was greatly improved from reviews by J. Adams, J. Breck, J. Diana, T. Edsall, and L. Sweet. R. Shepherd is gratefully acknowledged for initiating the walleye tagging program in Saginaw Bay. D. Fielder and J. Johnson (Michigan Department of Natural Resources, Alpena, Mich.) kindly provided the growth data on Saginaw Bay walleye. We also thank J. Baker (Michigan Department of Natural Resources, Bay City, Mich.) and his crew for their help in obtaining the walleye from the site near Dow Dam and J. Allen, R. Quintal, and S. Wootke for their assistance in preparing the walleye samples. J. DeKam (Bay Metropolitan Water Treatment Plant, Bay City, Mich.) furnished the water temperature data.

References

Borgmann, U., and Whittle, D.M. 1992. Bioenergetics and PCB, DDE, and mercury dynamics in Lake Ontario lake trout (*Salvelinus namaycush*): a model based on surveillance data. Can. J. Fish. Aquat. Sci. **49**: 1086–1096.

Brownie, C., Anderson, D.R., Burnham, K.P., and Robson, D.S. 1985. Statistical inference from band recovery data — a handbook. U.S. Fish Wildl. Serv. Resour. Publ. No. 156.

Cochran, W.G. 1953. Sampling techniques. John Wiley & Sons, New York.

Flath, L.E., and Diana, J.S. 1985. Seasonal energy dynamics of the alewife in southeastern Lake Michigan. Trans. Am. Fish. Soc. **114**: 328–337.

Giesy, J.P., Verbrugge, D.A., Othout, R., Bowerman, W.W., Mora, M.A., Jones, P.D., Newsted, J.L., Bath, A.J., Vandervoort, C., Heaton, S.N., Auerlich, R.J., Bursian, S.J., Ludwig, J.P., Ludwig, M., Dawson, G.A., Kubiak, T.J., Best, D.A., and Tillitt, D.E. 1994. Contaminants in fishes from Great Lakes-influenced sections and above dams on three Michigan rivers: 1. Concentrations of organo-chlorine insecticides, PCBs, dioxin equivalents and mercury. Arch. Environ. Toxicol. Chem. **27**: 202–212.

© 1998 NRC Canada

Giesy, J.P., Jude, D.J., Tillitt, D.E., Gale, R.W., Meadows, J.C., Zajicek, J.L., Peterman, P.H., Verbrugge, D.A., Sanderson, J.T., Schwartz, T.R., and Tuchman, M.L. 1997. Polychlorinated-dibenzo-*p*-dioxins, -dibenzofurans, -biphenyls and 2,3,7,8-tetrachlorodibenzo-*p*-dioxin equivalents in fishes from Saginaw Bay, Michigan. Environ. Toxicol. Chem. **16**: 713–724.

Hartman, K.J., and Margraf, F.J. 1992. Effects of prey and predator abundances on prey consumption and growth of walleyes in western Lake Erie. Trans. Am. Fish. Soc. **121**: 245–260.

Hewett, S.W., and Johnson, B.L. 1992. Fish bioenergetics model 2 — an upgrade of a generalized bioenergetics model of fish growth for microcomputers. University of Wisconsin Sea Grant Tech. Rep. No. WIS-SG-92-250, Madison, WI.

Johnson, J.E., Schrouder, K., and Haas, R. 1996. Vital statistics of walleye in Saginaw Bay. *In* Michigan Dingell–Johnson Annual Reports, Projects F-35-R-21 and F53-R-12. Michigan Department of Natural Resources, Lansing, Mich. pp. 104–113.

Jones, P.D., Ankley, G.T., Best, D.A., Crawford, R., DeGalan, N., Giesy, J.P., Kubiak, T.J., Ludwig, J.P., Newsted, J.L., Tillitt, D.E., and Verbrugge, D.A. 1993. Biomagnification of bioassay derived 2,3,7,8-tetrachlorodibenzo-*p*-dioxin equivalents. Chemosphere, **26**: 1203–1212.

Kitchell, J.F., Stewart, D.J., and Weininger, D. 1977. Applications of a bioenergetics model to yellow perch (*Perca flavescens*) and walleye (*Stizostedion vitreum vitreum*). J. Fish. Res. Board Can. **34**: 1922–1935.

Larsson, P., Okla, L., and Collvin, L. 1993. Reproductive status and lipid content as factors in PCB, DDT and HCH contamination of a population of pike (*Esox lucius* L.). Environ. Toxicol. Chem. **12**: 855–861.

Madenjian, C.P., Carpenter, S.R., Eck, G.W., and Miller, M.A. 1993. Accumulation of PCBs by lake trout (*Salvelinus namaycush*): an individual-based model approach. Can. J. Fish. Aquat. Sci. **50**: 97–109.

Madenjian, C.P., Carpenter, S.R., and Rand, P.S. 1994. Why are the PCB concentrations of salmonine individuals from the same lake so highly variable? Can. J. Fish. Aquat. Sci. **51**: 800–807.

Masnado, R.G. 1987. Polychlorinated biphenyl concentrations of eight salmonid species from the Wisconsin waters of Lake Michigan: 1985. Wis. Dep. Nat. Resour. Fish Manage. Rep. No. 132.

Michigan Department of Natural Resources. 1988. Michigan Department of Natural Resources remedial action plan for Saginaw River and Saginaw Bay — area of concern. Mich. Dept. Nat. Resour., Surface Water Qual. Div., Great Lakes Environ. Assess. Section, Lansing, Mich.

Mrozinski, L.E., Schneider, J.C., Haas, R.C., and Shepherd, R.E. 1991. Rehabilitation of walleye in Saginaw Bay, Lake Huron. *In* Status of walleye in the Great Lakes: case studies prepared for the 1989 workshop. *Edited by* P.J. Colby, C.A. Lewis, and R.L. Eshenroder. Great Lakes Fish. Comm. Spec. Publ. 91-1. pp. 63–84.

Niimi, A.J. 1983. Biological and toxicological effects of environmental contaminants in fish and their eggs. Can. J. Fish. Aquat. Sci. **40**: 306–312.

Noguchi, G.E., and Hesselberg, R.J. 1991. Parental transfer of organic contaminants to young-of-the-year spottail shiners, *Notropis hudsonius*. Bull. Environ. Contam. Toxicol. **46**: 745–750.

Rodgers, D.W. 1996. Methylmercury accumulation by reservoir fishes: bioenergetic and trophic effects. *In* Multidimensional approaches to reservoir fisheries management. *Edited by* L.E. Miranda and D.R. DeVries. Am. Fish. Soc. Symp. **16**: 107–118.

Rottiers, D.V., and Tucker, R.M. 1982. Proximate composition and caloric content of eight Lake Michigan fishes. U.S. Fish Wildl. Serv. Tech. Pap. No. 108.

Schaeffer, J.S. 1994. Mechanisms regulating growth and food consumption of walleyes and yellow perch in Saginaw Bay, Lake Huron. Ph.D. thesis, University of Michigan, Ann Arbor, Mich.

Schmidt, L.J., and Hesselberg, R.J. 1992. A mass spectroscopic method for analysis of AHH- inducing and other polychlorinated biphenyl congeners and selected pesticides in fish. Arch. Environ. Contam. Toxicol. **23**: 37–44.

Secor, D.H., Henderson-Arzapalo, A., and Piccolo, P.M. 1995. Can otolith microchemistry chart patterns of migration and habitat utilization in anadromous fishes? J. Exp. Mar. Biol. Ecol. **192**: 15–33.

Shapiro, S.S., and Wilk, M.B. 1965. An analysis of variance test for normality (complete samples). Biometrika, **52**: 591–611.

Sheffy, T.B. 1980. The PCB monitoring program in Wisconsin — surveillance strategy and use of data. *In* Aquatic toxicology. *Edited by* J.G. Eaton, P.R. Parrish, and A.C. Hendricks. ASTM STP 707. American Society for Testing and Materials, Philadelphia, Pa. pp. 155–163.

Stow, C.A., Carpenter, S.R., Madenjian, C.P., Eby, L.A., and Jackson, L.J. 1995. Fisheries management to reduce contaminant consumption. BioScience, **45**: 752–758.

Thomann, R.V., and Connolly, J.P. 1984. Model of PCB in the Lake Michigan lake trout food chain. Environ. Sci. Technol. **18**: 65–71.

Thomas, M.V., and Haas, R.C. 1994. Status of yellow perch and walleye in Michigan waters of Lake Erie, 1989–93. Mich. Dep. Nat. Resour. Fish. Res. Rep. No. 2011.

Velleux, M., and Endicott, D. 1994. Development of a mass balance model for estimating PCB export from the lower Fox River to Green Bay. J. Great Lakes Res. **20**: 416–434.

© 1998 NRC Canada

Reconstruction of trophic state in Danish lakes using subfossil chydorid (Cladocera) assemblages

Klaus P. Brodersen, Melbourne C. Whiteside, and Claus Lindegaard

Abstract: Surficial sediments from 32 Danish lakes were screened for subfossil chydorid (Cladocera) assemblages. Two data sets from 1965 and 1992 were examined by cluster analysis and nonmetric multidimensional scaling (NMDS) for lake classification. The best environmental variable to explain the 1992 species data was total phosphorus (TP) ($r = 0.58$, Spearman rank correlation), and NMDS defined three lake classes that were significantly different in communities ($p < 0.01$, ANOSIM) and in TP values. Canonical correspondence analysis found a strong relationship between the species data and log(TP) (axis 1 eigenvalue = 0.30, total inertia = 0.85, log(TP) intraset correlation = 0.92). Environmental variables were tested by forward selection and six variables were found to be statistically significant by 99 unrestricted Monte Carlo permutations. Weighted averaging regression and calibration models were established from the 1992 chydorid data and corresponding contemporary log-transformed TP data. The model's predictive ability was assessed by the bootstrapped coefficient of determination and the bootstrapped root mean squared error of prediction ($r^2_{boot} = 0.79$, $RMSE_{boot} = 0.24$). The patterns of changes in chemical and biological variables (diversity, Bray–Curtis dissimilarity) over the 27-year period placed the 32 lakes in six different response groups.

Résumé : On a analysé les sédiments de surface de 32 lacs danois pour y recueillir des données sur des assemblages de chydoridés (Cladocera) subfossiles. On a traité deux ensembles de données (1965 et 1992) par analyse typologique et analyse multidimensionnelle non métrique en vue de classifier les lacs. La variable environnementale la mieux corrélée aux données sur les espèces de 1992 était le phosphore total (PT) ($r = 0{,}58$, corrélation de rang de Spearman), et l'analyse multidimensionnelle non métrique a défini trois classes de lacs qui étaient significativement différentes au chapitre des communautés ($p < 0{,}01$, analyse de similitude) et des valeurs de PT. L'analyse de corrélation canonique a établi l'existence d'une forte relation entre les données sur les espèces et log(PT) (valeur propre en axe 1 = 0,30, inertie totale = 0,85, corrélation intra-groupe pour log(PT) = 0,92). On a testé les variables environnementales par régression multiple ascendante, et on a établi que six variables étaient statistiquement significatives par 99 permutations de Monte Carlo sans contrainte. Des modèles de régression et de calibrage à moyenne pondérée ont été établis à partir des données sur les chydoridés de 1992 et des données contemporaines correspondantes de PT exprimées sous forme logarithmique. La capacité de prédiction du modèle a été évaluée au moyen du coefficient de détermination bootstrap et de l'erreur quadratique moyenne bootstrap de prédiction ($r^2_{boot} = 0{,}79$, $EQM_{boot} = 0{,}24$). Selon les types de changements observés dans les variables chimiques et biologiques (diversité, dissimilitude de Bray–Curtis) au cours de la période de 27 ans, on peut répartir les 32 lacs dans six groupes différents.
[Traduit par la Rédaction]

Introduction

D.G. Frey was among the first to recognize the importance of animal remains in lake sediments (Frey 1960). As a student of Professor Frey, M.C. Whiteside came to Denmark in 1965 to study the relationship between lake type and chydorid assemblages as reflected by their remains in lake sediments from Danish lakes (Whiteside 1970). In 1965, 77 lakes were grouped by Whiteside via multiple discriminant analysis and classified according to physical–chemical measurements into three groups: (1) clear-water lakes, (2) ponds and bogs, and (3) polluted, clear-water lakes. In most instances the relative abundance of chydorid assemblages correctly predicted the lake type (Whiteside 1970, table 12). The assemblages of chydorid remains from the surficial sediments of lakes were reliable indicators of lake conditions. The 1965 work provided the basis for this study, and 27 years later, we returned to these lakes to reanalyze their condition.

The development of computing power has resulted in several new and robust multivariate numerical methods to analyze biological community data. The most commonly used methods in palaeolimnology are canonical correspondence analysis (CCA) as an exploratory method (ter Braak 1986, 1987) and weighted averaging regression and calibration techniques for reconstruction models (Anderson 1993; Charles and Smol 1994; Birks 1995). Recently, Jeppesen

Received March 25, 1997. Accepted November 6, 1997.
J13933

K.P. Brodersen[1] **and C. Lindegaard.** Freshwater Biology Laboratory, University of Copenhagen, 51 Helsingørsgade, DK-3400 Hillerød, Denmark.
M.C. Whiteside. Biology Department, University of Minnesota, Duluth, MN 55812, U.S.A.

[1] Author to whom all correspondence should be addressed. e-mail: brodersen@ibm.net

© 1998 NRC Canada

Fig. 1. NMDS ordination of 32 Danish lakes on (A) 1965 chydorid species data and (B) 1992 chydorid species data. Lakes in both ordinations are marked according to the classification established by Whiteside (1970): W1, clear-water lakes; W2, ponds and bogs; W3, polluted clear-water lakes. Stress values were 0.11 and 0.13 for the ordinations in Figs. 1A and 1B, respectively. See Table 1 for lake abbreviations.

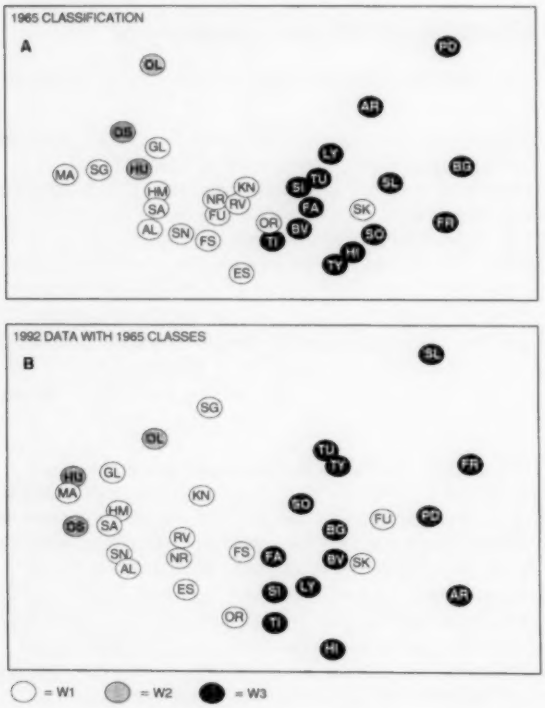

et al. (1996) applied these techniques to develop a calibration data set for reconstruction of planktivorous fish communities evaluated from sedimentary zooplankton fossils in 30 Danish lakes. In this study, we focused on the lakes studied by Whiteside (1970) with the aim of documenting the direction of lake ontogeny (Whiteside 1983) in some of the better-known lakes. Assuming total phosphorus (TP) to be a good indicator of trophic state in Danish lakes, we used the indirect chydorid response to increased nutrient richness (e.g., changing microhabitats, substrates, food availability, oxygen regimes) as a pollution proxy by inferring TP from subfossil assemblages. This study provided the opportunity to reevaluate the lake typology/ontogeny after 27 years with a complete replication of methods and subfossil identification done by the same person.

Methods

In 1992, 32 of the original lakes studied in 1965 were identified for study. The selection of these lakes was made in consultation with several scientists and was based on the scientific and (or) aesthetic value of the lakes. To make the comparisons between 1965 and 1992 as direct as possible, methods for collecting and processing chydorid remains were identical to those used in 1965 (Whiteside 1970). The single exception to this was in the laboratory preparation for 1992, where no HF treatment was used. Mud samples were collected with an Ekman dredge. From undisturbed samples with clear overlying water, the uppermost surficial muds were carefully scraped off and put into plastic bags until processed. No preservatives were added, since all samples were processed in the laboratory shortly after collection. Carapace, head shield, and postabdomen remains were identified and counted at 250× magnification.

The same variables that defined the original lake groups were used: transparency, *d* (see below), conductivity, pH, alkalinity, maximum depth, and area (Whiteside 1970). Additionally, summer mean values (May–September, both inclusive) for TP and Secchi depth were available for this study. Physical–chemical measures were taken from the literature, and supplemental chemical data were provided from published and unpublished data of the National Environmental Research Institute, Division of Freshwater Ecology, Silkeborg, Denmark. Surface water samples were obtained during July 1992; conductivity and transparency measures were made on these samples. Transparency was measured as percent transmittance with a spectrophotometer using 10-cm cells at 360 nm. A first measure was made on raw water taken directly from the surface-water sample. A second was made on lake water that had been centrifuged for 3 min. The difference between these two transmittance values for a given lake, which depends primarily on the amount of suspended material and the phytoplankton biomass in the water, was the *d* value, also called the "biomass" (Whiteside 1970).

In this study, 32 of the original 77 lakes were reanalyzed using less subjective techniques than multiple discriminant analysis (Whiteside 1970). Species data from 1965 and 1992 were first analyzed with nonmetric multidimensional scaling (NMDS, Clarke 1993) through the program package PRIMER (Clarke and Warwick 1994). Community similarities were calculated using the Bray–Curtis similarity coefficient (Bray and Curtis 1957) on double square root transformed species data standardized to percentages. The nonparametric Spearman rank correlations among distance matrices on six environmental variables (single and in combination) and similarity matrices on species associations were tested with the BIOENV procedure (Clarke and Ainsworth 1993). Ordination of species data constrained to environmental variables was carried out using CCA in the program package CANOCO (ter Braak 1992). Because there was a strong correlation between the 1992 species data and TP, it was possible to reconstruct the TP levels for 1965 data using a weighted averaging regression and calibration model (WACALIB, Line and Birks 1990; Line et al. 1994).

We used three classifications/groupings for this paper. The original (1–3) classification by Whiteside (1970) on 1965 data (termed W1–W3 in this study), the reevaluated classification on 1992 data (B1–B3, based on NMDS), and finally a grouping of lakes into patterns of changes (response) over the last 27 years (R1–R6).

Results

Classifications

Figure 1 shows the results of NMDS ordination of the species data for 1965 (Fig. 1A) and 1992 (Fig. 1B), where symbols indicate the 1965 classification established by multiple discriminant analyses. The NMDS classification of 1965 data was the same as that found by Whiteside (1970), except for Skanderborg Sø which in 1965 apparently was "misclassified" into the class originally assigned to clear lakes (W1). NMDS analysis of the 1992 species data to 1965 classes placed Furesø and Skanderborg Sø into the polluted lake class (Fig. 1B).

A more objective approach at establishing groupings based on chydorid relative abundances was used for the 1992 data. This was achieved through use of average-linkage clustering (van Tongeren 1987) on Bray–Curtis

© 1998 NRC Canada

Fig. 2. NMDS ordination of 32 Danish lakes on 1992 species data with the new classification. New groups were defined by average-linkage clustering of Bray–Curtis dissimilarities. See Table 1 for lake abbreviations.

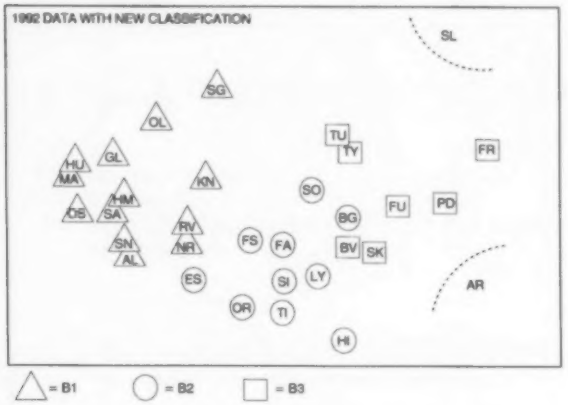

dissimilarities. Results of this technique suggested three major classes (B1, B2, and B3) and two potential outliers with similarities to class B3 (Fig. 2). The lakes to the left in the ordination were the most oligotrophic (B1), while those to the extreme right were the most eutrophic (B3); the lakes in the center had intermediate properties. Arresø and Søllerød Sø were grouped as outliers because of their very high percentages of *Chydorus sphaericus* (O.F. Müller) (98% in Arresø) or *Alona rectangula* Sars (46% in Søllerød Sø). Based on the ordination and the polluted nature of these lakes, they were considered as B3 lakes. The three lake groups were significantly different ($p < 0.01$) in chydorid species composition, as tested by the nonparametric permutation analysis of similarities, using 5000 permutations (ANOSIM, Clarke and Green 1988). Species diversity, as measured by the Shannon index, was greatest in B1 lakes. The range in Shannon diversity indices for B2 lakes was large (1.0–3.1). The Shannon indices for B3 sites were all low (<2.5) and communities were dominated by few, but very abundant, species (*C. sphaericus*, *A. rectangula*).

Changes in physical and chemical measures between 1965 and 1992 for these groupings are compared in Table 1. B1 lakes (primarily the "clear-water sites" of Whiteside 1970) had the highest transparencies and lowest biomasses (*d*), pHs, alkalinities, and conductivities of all the groups.

Most of the lakes of B2 formerly belonged in Whiteside's (1970) "polluted lakes" group. These sites are easily distinguished from B1 lakes based on chemical characteristics, and they are more similar to B3 sites. The parameters that separate B2 from B3 lakes are lower conductivities, alkalinities, and pHs (Table 1). Several B2 lakes had remarkable declines in transparency (Hinge Sø, Lyngby Sø, Silkeborg Langsø, and Ørnsø). Associated with these declines were increased biomass estimates.

The B3 lakes were characterized as being all highly productive, turbid, and without submerged vegetation. All non-stratified lakes in the study belong to this group. As with the other groups, we observed declined transparencies for B3 lakes. The large increase in biomass between years for B3 lakes was significant ($p = 0.01$). Among the B3 lakes, only Pedersborg Sø had improved transparency associated with a decline in biomass (*d*, Table 1).

Arresø and Søllerød Sø were positioned as outliers using chydorid taxa for cluster analysis (Fig. 2). These lakes were not similar to each other, although they were among the most polluted in Denmark. Søllerød Sø had high TP, yet low biomass (*d*, Table 1). Its conductivity had decreased dramatically (from 780 to 430 $\mu S \cdot cm^{-1}$), accompanied by a drop in pH. Arresø had the greatest biomass among all lakes studied in 1992 and was the least transparent lake except those that had humic waters.

In testing the correlation between environmental variables and species composition, we found TP concentrations ($r = 0.58$, Spearman rank) to be the environmental variable that best explained the groupings shown in Fig. 2 (Table 2). The best combination of environmental variables was TP + conductivity + alkalinity + *d* giving a correlation of $r = 0.64$. Class B1 was significantly different ($p < 0.01$) from classes B2 and B3 in all measured environmental variables, except for maximum lake depth ($p < 0.21$). Class B3 had significantly higher conductivity, alkalinity, and pH ($p < 0.03$) than class B2 and also a higher TP concentration ($p < 0.01$). The two outliers were only significantly different from class B3 with respect to maximum lake depth ($p < 0.04$)

To illustrate the degree of change between 1965 and 1992, we ran a NMDS ordination of both sets of data simultaneously (Fig. 3). The 1965 positions are shown with lake abbreviations and 1992 positions with the superimposed TP values for the lakes (arbitrary units); arrows show the direction of change over time. Under this procedure, it was evident that most of the change had been towards higher TP concentrations (horizontally to the right); most markedly for Store Gribsø, Furesø, and Søllerød Sø. Only three lakes, Bagsværd Sø, Sorø Sø, and Pedersborg Sø, moved in the opposite direction, i.e., decreased in trophic status (Fig. 3).

CCA

The results of CCA of the 1992 data constrained to environmental variables are summarized in Table 3. The species–environment correlation was high, indicating a strong relationship between six of the environmental variables and the 30 chydorid taxa (Table 3). The eigenvalue for the first ordination axis was high compared with those of the other axes, indicating that variation along the first axis is of greater importance than along the other three axes (Table 3). The first axis explained 35% of the species data and accounted for 70% of the chydorid–environment relationship. This axis mainly contrasted the TP concentration with a strong intraset correlation ($r = 0.92$), but the other five variables were also correlated with this axis and were found significant ($p < 0.01$) by forward selection and 99 unrestricted Monte Carlo permutations. Axis 2 was best explained by pH, although the correlation was weak ($r = -0.56$); however, this and the remaining two axes were relatively low in importance when compared with axis 1. The gradient length in detrended correspondence analysis was 2.0, which is in the range where both linear and nonlinear methods are appropriate (ter Braak and Prentice 1988).

Figure 4 shows the CCA ordination of the 1992 data constrained to the six environmental variables. The relationships

© 1998 NRC Canada

Table 1. Physical and chemical characteristics of Danish lake groupings using cluster analysis of subfossil chydorid species data.

	Transparency (%)		*d*		Conductivity (μS cm^{-1})		Alkalinity (mequiv. L^{-1})		pH		Maximum depth (m)	Area (ha)	TP (μg P L^{-1}), 1990–1992
	1992	1965	1992	1965	1992	1965	1992	1965	1992	1965			
B1 lakes													
Slåensø (SN)	84.0	91.0	5.7	0.3	220	212	1.08	1.23	6.8	7.2	12	18	16
Grane Langsø (GL)	89.4	92.1	0.3	0.0	65	49	0.01	0.10	4.9	4.9	11	11	17
Snabe-Igelsø (SA)	61.6	83.8	6.8	0.1	95	49	0.01	0.14	6.8	6.8	7	3	17
Almindsø (AL)	78.5	88.1	7.0	1.4	190	175	0.55	0.54	7.3	6.4	20	54	20
Hampen Sø (HM)	67.7	82.8	8.1	0.4	140	78	0.32	0.08	7.1	5.4	14	76	22
Hundsø (HU)	55.5	72.5	4.3	2.5	60	52	0.00	0.11	4.5	4.7	7	2	22
Nors Sø (NR)	74.2	80.0	6.0	2.0	220	223	1.22	0.94	7.9	7.3	19	357	23
Store Økssø (OS)	25.6	22.7	8.4	0.0	110	76	0.13	0.04	4.2	4.0	7	44	26
Knudsø (KN)	65.9	68.5	6.0	4.1	340	350	2.10	2.10	8.5	8.6	29	195	28
Ravnsø (RV)	50.3	66.0	12.3	0.9	350	358	1.85	1.82	7.9	9.0	33	183	28
Lille Økssø (OL)	0.0	0.0	0.0	0.0	115	88	—	0.44	3.8	4.0	6	1	33
Madum Sø (MA)	67.4	88.9	9.4	0.0	95	68	0.06	0.05	5.2	4.6	7	212	34
Store Gribsø (SG)	1.6	32.0	0.8	0.0	135	118	0.04	0.15	4.4	3.9	10	11	90
Average	55.5	66.8	5.8	0.9	164	144	0.61	0.60	6.1	5.9	14	90	29
B2 lakes													
Tissø (TI)	23.3	32.0	16.4	6.5	580	580	2.50	2.94	8.3	8.4	15	1353	85
Farum Sø (FA)	31.6	33.9	22.9	15.1	360	419	2.39	4.00	7.7	6.7	16	121	90
Fussing Sø (FS)	69.8	79.4	4.9	0.7	280	308	1.32	1.90	8.0	9.0	19	200	96
Ørnsø (OR)	36.8	62.5	21.0	5.1	175	165	0.78	0.76	7.2	7.1	11	43	116
Silkeborg Langsø (SI)	19.9	42.0	31.2	14.9	250	171	1.23	0.94	7.5	7.5	5	235	129
Esrom Sø (ES)	70.8	75.5	7.0	2.5	375	322	2.37	2.00	8.1	7.4	21	1730	130
Sorø Sø (SO)	45.2	33.6	11.8	20.4	380	367	4.60	2.16	7.5	7.7	13	217	143
Hinge Sø (HI)	9.0	41.6	25.9	9.5	310	275	1.05	1.60	7.6	8.2	5	115	170
Lyngby Sø (LY)	6.6	60.5	23.0	5.0	433	343	2.08	3.05	8.2	7.4	3	59	180
Bagsvaerd Sø (BG)	5.2	6.5	17.6	33.4	362	325	1.56	2.86	7.5	6.5	5	121	280
Average	31.8	46.8	18.2	11.3	351	328	1.99	2.22	7.8	7.6	11	419	142
B3 lakes													
Pedersborg Sø (PD)	37.8	11.4	14.5	20.4	350	393	2.60	2.56	8.8	7.0	7	19	138
Bavelse Sø (BV)	22.2	46.5	17.8	2.0	450	600	2.50	3.50	8.1	8.1	8	93	195
Tystrup Sø (TY)	27.5	46.5	17.2	1.4	550	620	2.50	3.18	8.1	7.5	18	662	195
Furesø (FU)	47.2	67.8	12.3	1.4	455	338	1.86	2.20	7.7	6.8	38	936	226
Skanderborg Sø (SK)	32.7	57.7	26.2	2.8	380	345	2.40	2.08	8.1	7.7	19	870	310
Tuel Sø (TU)	29.7	44.0	20.5	2.2	385	550	3.40	2.32	8.2	6.7	19	191	375
Frederiksborg S. (FR)	6.9	14.5	24.4	21.7	392	350	2.70	2.70	8.1	7.2	3	22	765
Average	29.1	41.2	19.0	7.4	423	457	2.57	2.65	8.2	7.3	16	399	314
Outliers													
Arresø (AR)	3.6	15.0	33.9	25.3	450	359	1.43	1.58	8.2	6.8	4	4063	316
Søllerød Sø (SL)	50.3	44.0	10.8	0.9	430	780	2.91	5.39	6.8	8.1	7	15	760
Average	27.0	29.5	22.4	13.1	440	570	2.17	3.49	7.5	7.5	6	2039	538

© 1998 NRC Canada

Table 2. Spearman rank correlation coefficients between chydorid species composition and environmental variables for the 1992 data.

Variable	r
TP	0.58
Conductivity	0.35
Alkalinity	0.34
d	0.33
pH	0.21
Transparency (%)	0.17
Secchi depth	0.08
Area	0.00
Maximum depth	0.00
Best combinations	
TP, *d*, conductivity	0.63
TP, *d*, conductivity, alkalinity	0.64

among sites and environmental variables are shown in Fig. 4A. There was good agreement between the NMDS and CCA ordinations. A majority of the clear-water lakes were positioned to the left of axis 2, while the most polluted lakes were positioned in the upper right and the remaining group in the lower right (Fig. 4A). One "outlier," Søllerød Sø, was at the extreme upper right, while the other, Arresø, was between the two groups located to the right (Fig. 4A). Figure 4B shows the relationship among species and environmental variables. Those taxa associated with the lake groupings are positioned in locations similar to lakes of Fig. 4A, i.e., chydorids tolerant of polluted sites (e.g., *C. sphaericus*) were located in the upper right and those associated with clear-water lakes to the left of axis 2 (Fig. 4B). The vectors of environmental variables suggest associations between taxa and variables (Fig. 4B).

The TP concentrations for the B1 lakes were <40 μg $P \cdot L^{-1}$. Of the taxa present in this group, 16 species had their weighted average TP optimum below this level. Eight of them (*Alona intermedia* Sars, *Alona guttata* Sars, *Alona rustica* T. Scot, *Alonopsis elongata* Sars, *Rhynchotalona falcata* (Sars), *Chydorus piger* Sars, *Alona nana* (Baird), *Alona excisa* (Fischer)) had their optimum at ~30 μg $P \cdot L^{-1}$ and their upper tolerance below ~60 μg $P \cdot L^{-1}$. These species were the first to be excluded when the lakes became more productive (section 1, Fig. 4B). The lakes within 60–140 μg $P \cdot L^{-1}$ were "intermediate" compared with Danish nutrient conditions and they all fell within class B2 (Fig. 4B). The level of ~140 μg $P \cdot L^{-1}$ was the upper tolerance limit of eight species (*Alona costata* Sars, *Graptoleberis testudinaria* (Fischer), *Monospilus dispar* Sars, *Disparalona rostrata* (Koch), *Acroperus harpae* Baird, *Eurycercus lamellatus* (O.F. Müller), *Camptocercus rectirostris* Schödler, *Alona affinis* Leydig) and thereby the next "threshold" level in the sample series (section 2, Fig. 4B). No species had a weighted average TP optimum >140 μg $P \cdot L^{-1}$ (see Fig. 6), and the species that characterize the lakes in class B3 were those for which the upper tolerance was above this level (*Alona quadrangularis* (O.F. Müller), *Pleuroxus uncinatus* Baird, *Pleuroxus trigonellus* (O.F. Müller), *Leydigia leydigi* Schödler, *Parachanta truncata* (O.F. Müller), *A. rectangula*, *Pleuroxus aduncus* (Jurine), *C. sphaericus*) (section 3, Fig. 4B).

Phosphorus reconstruction

The strong correlation between TP and species data suggests that a weighted averaging regression and calibration model (WA) to infer 1965 TP values from the 1992 data set could be attempted. The WA models were assessed in terms of the coefficient of determination (r^2) and the root mean square error of prediction (RMSE). Because all thirty-two 1992 lakes were included in the calibration data set, cross-validation of the models' predictive ability was not possible. Therefore, a bootstrapping technique was applied to obtain a more reasonable error estimation ($RMSE_{boot}$; Line et al. 1994). The best model in terms of $RMSE_{boot}$ and r^2_{boot} was found using simple weighted averaging, on square root transformed species data, log-transformed TP values, and inverse deshrinking (r^2_{boot} = 0.79, $RMSE_{boot}$ = 0.24). Calculation of species tolerance was weighted by effective number of occurrences (Hill's N2). The results of this model are shown in Fig. 5, in which the bootstrapped-inferred log TP values are plotted against the observed log TP values for all 32 lakes in the training set. A plot of the residuals showed a slight tendency to underestimate TP values at high phosphorus levels. Figure 6 shows the calculated optima and tolerances for the 24 chydorid species used in the model. The TP values for 1965 were inferred by running the species data from 1965 as passive samples simultaneously with the calibration samples (1992). New TP values were estimated and the changes from 1965 to 1992 were calculated (Fig. 7).

Discussion

The original grouping for the multiple discriminant analysis was based on subjective judgments of physical–chemical parameters (Whiteside 1970). The reanalysis of the 1965 species data using NMDS confirmed the early results, with the exception of one lake (Fig.1A; Whiteside 1970). NMDS analysis of the 1992 chydorid data using the original groupings of Whiteside (1970) also resulted in lakes belonging to the same groups with the exception of Furesø (Fig. 1B), which was now grouped with polluted lakes. However, the application of recently available multivariate methods to chydorid assemblages provided a more objective approach to establishing lake groups. This was followed by statistical analyses to determine clusters of lakes that were significantly different from each other.

Our results confirmed earlier work and that of several other investigators (Whiteside 1970; Beals 1976; Sprules 1977; Synerholm 1979; Crisman 1980; Roff et al. 1981; Cotten 1985; Herbert and Hann 1986; Keller and Pitblado 1989; Duigan and Kovach 1991), namely that zooplankton (including fossil chydorid assemblages) can be related to lake type. The environmental factors that were responsible for the Danish lake groupings were interrelated, but TP was highly correlated and explained much of the groupings (Table 2; Fig. 2).

Chydorid taxa and lake parameters

We have known for some time that as lakes became more eutrophic, some taxa became planktonic and more abundant

© 1998 NRC Canada

Fig. 3. NMDS ordination of 1965 and 1992 chydorid data simultaneously from 32 Danish lakes. The 1965 scores are shown by lake abbreviations (see Table 1) and 1992 scores by the superimposed TP concentrations. Arrows indicate the direction (and degree) of community changes over the 27-year period.

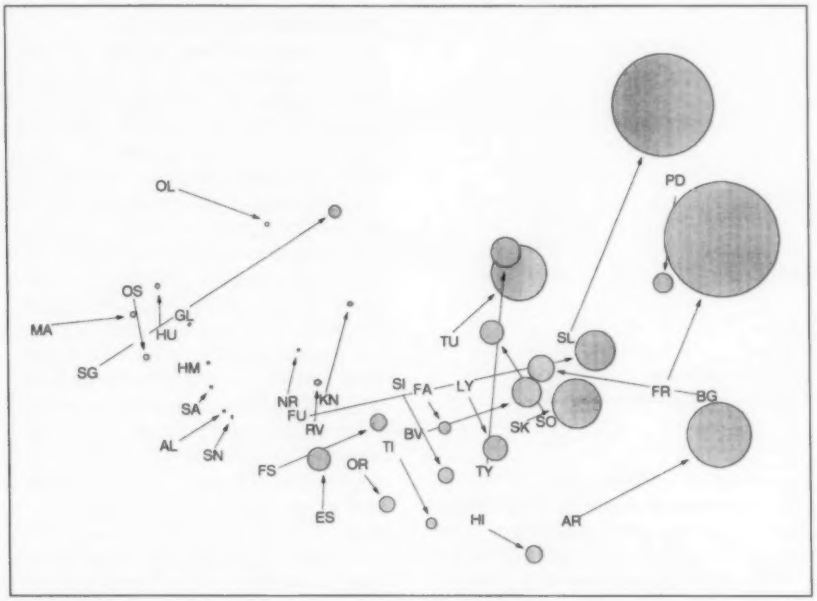

Table 3. Summary of the results of CCA of the 1992 chydorid species data constrained to six environmental variables.

	Axis 1	Axis 2	Axis 3	Axis 4
Eigenvalues	0.30	0.06	0.03	0.02
Species–environment correlation	0.97	0.74	0.77	0.59
Cumulative % variance of species data	35.1	41.5	45.5	47.5
Cumulative % variance of species–environment relationship	70.4	83.3	91.2	95.2

Total inertia	0.85
Sum of all constrained eigenvalues	0.42

(Frey 1979) and that species diversity declined with increased lake productivity (Whiteside and Harmsworth 1967). The exact nature of the decline in species diversity is unknown, and most likely the causes are complex and indirect. For example, increased algal productivity reduces light availability for rooted aquatic macrophytes, thus reducing the habitat for weed-dwelling chydorids. In such an abrupt event, the mud-dwelling taxa (*A. quadrangularis* and *L. leydigi*) and *C. sphaericus* and *A. rectangula*, which can be planktonic, could survive. By examination of the species optima and tolerances from CCA and WA results, it became evident that the changes in chydorid communities due to increased phosphorus loading do not follow a simple exclusion of species along the trophic gradient but rather a "stepwise" modification of the relative species composition (three levels, Fig. 6) (Hann et al. 1994). This could have been due to abrupt changes in biological structure at certain nutrient levels and alternative stable states as shown, for example, by Jeppesen et al. (1990) and Scheffer et al. (1993).

It is important for a good reconstruction model to be based on certain and well-defined taxonomy. Several species of North American chydorids have been revised, and it is possible that some of the European taxa should be reexamined (Frey 1980, 1982). However, in the interest of consistency between studies (1965 and 1992), we have not attempted to carry the systematics beyond that that is conventionally used. In spite of the potential taxonomic difficulties, the relative abundance and presence or absence of chydorid taxa have been linked to lake type and eutrophication by several workers (summarized by Whiteside and Swindoll 1988; Hann et al. 1994).

Lake changes, 1965–1992

Six response groups were formed based on physical and chemical changes, changes in chydorid assemblages as

© 1998 NRC Canada

Fig. 4. CCA biplots of 1992 chydorid assemblages from 32 Danish lakes. (A) Environmental variables and site scores (site scores × 0.5); (B) species biplot scores and their relation to the strongest environmental variable, TP (log TP). Vertical section limits indicate the upper tolerance (1*t*) of species groups important for the classification of 1992 data (Fig. 2, see Discussion). See Table 1 for lake abbreviations.

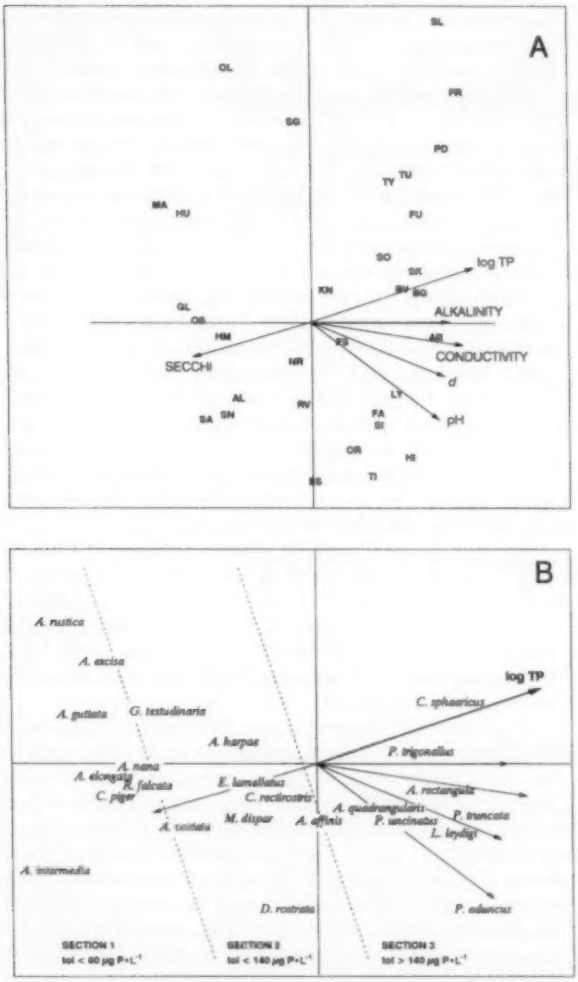

reflected by species diversity and Bray–Curtis dissimilarity, and changes in TP as modeled by WA (R1–R6, Fig. 7). Twelve of 13 B1 lakes fall into response group R1 (R1, Fig. 7). The lakes in R1 were either situated in forest, free of nutrient input, or were deep and stratified. The lakes of R1 had little change in TP and conductivity. Most had little or no decline in transparency and slight to moderate increases in biomass (*d*). Although their chydorid assemblages had changed, these changes were less than in the other study lakes. With the exceptions of Store Økssø, Hampen Sø, and Esrom Sø, community changes had resulted in lower species diversity (Fig. 7), yet diversity remained relatively high (>3). Most of the lakes of R1 belong to group B1, although four B2

Fig. 5. Calibration relationships for the chydorid TP WA model of 32 Danish lakes. (A) Bootstrapped-inferred versus observed TP values; (B) residuals (inferred minus observed) versus TP values.

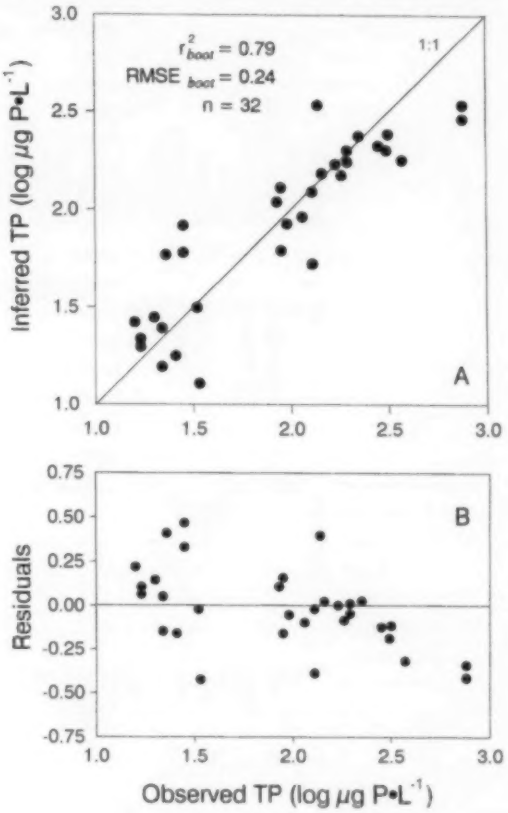

lakes (Fussing Sø, Tissø, Farum Sø, and Esrom Sø) were placed in this group (Fig. 7). Characteristic of these four lakes is the feature that they constituted the deepest, stratified lakes of class B2. In these lakes, the response in the littoral zone to increased phosphorus loading was less than that found in the small shallow lakes due to phosphorus loss during stratification (Jeppesen et al. 1997). Additionally, Jeppesen et al. (1996) examined subfossil material from surface sediments of Danish lakes and found that pelagic cladoceran communities were correlated with planktivorous fish stock, while littoral cladocerans were related to submerged macrophyte coverage. Thus, a well-developed littoral zone with submerged vegetation in the stratified lakes helped to sustain a diverse chydorid community, in spite of increased nutrients, as long as the changes in the composition of autotrophic components were low (Hann and Goldsborough 1997). In our study, this resulted in a reduced response in WA-inferred TP, and thereby placed these lakes in response group R1.

Grane Langsø, which was within this response group, deserves further mention. This small forest lake had undergone dramatic changes recently that are not evident in Fig. 7. Events in the catchment area in the 1980s had resulted in an increased water level. Riis and Jørgensen (1996) reported an increased water color due to inflow of humic substances, a

© 1998 NRC Canada

Fig. 6. Calculated species WA optima and tolerances for TP concentration (summer mean TP) for the 24 chydorid species used in the TP reconstruction model.

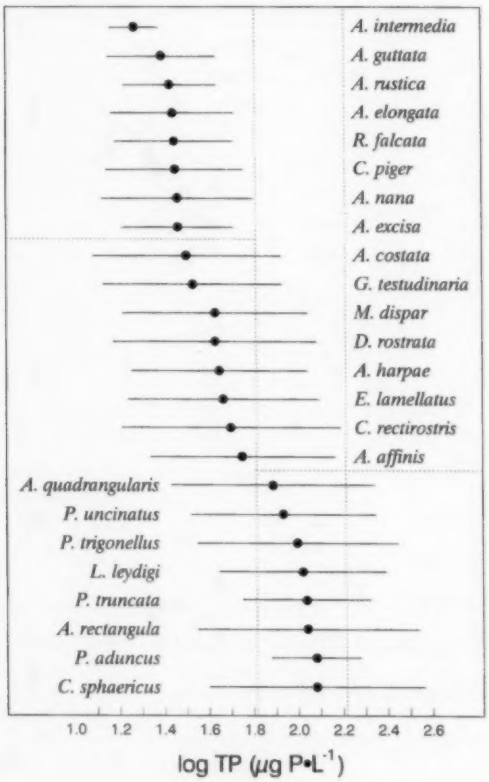

pronounced decline in water transparency, a decreased pH, and a decrease in the depth limits of submerged vegetation (Christensen et al. 1994; Riis et al. 1996). We noted in July 1992 that transparency was again relatively good (Table 1), but the submerged vegetation normally associated with this lake had not fully recovered. However, there was very little change in phosphorus concentrations associated with these changes. The small drop in chydorid diversity evident in Fig. 7 was caused by an increase in the relative abundance of a few taxa (*A. nana*: 9–33%; *C. piger*: 5–10%) and not by a loss of phosphorus-sensitive taxa.

The three lakes of response group R2 were characterized by improved conditions, such as declines in biomass for all the lakes and increased transparency for two of the three lakes (Fig. 7). Two of these were B2 lakes (Sorø Sø, Bagsværd Sø) and the third was a B3 lake (Pedersborg Sø). There was a moderate change in chydorid species composition to higher diversity and a lower or unchanged WA-inferred TP concentration. Sorø Sø and Bagsværd Sø received waste water through the 1960s and were at that time already highly productive. Our interpretation is that the lakes of group R2 have improved their status since the 1965 study.

The lakes of response groups R3–R6 have progressive increases in TP, greater biomass, and generally lower transparencies (Fig. 7). Most increased in conductivity and biomass and had lower species diversity. The first three lakes of R3 (Silkeborg Langsø, Hinge Sø, Lyngby Sø) were shallow B2 lakes. They were exceptional in that their diversity increased (Fig. 7). However, none of the increased diversity was due to a gain in taxa. In Lyngby Sø, there was no change in the number of taxa (13), while Hinge Sø and Silkeborg Langsø lost taxa. The 1992 assemblages generated higher diversity indices because they were more equitable in their distribution of species. The changes in taxa at Lyngby Sø were interesting; in 1965, *C. sphaericus* and *A. rectangula* were 27 and 54% of the chydorid community, respectively, but they switched dominance to 50 and 30%, respectively, in 1992. Ørn Sø, an R3 lake, was heavily impacted by sewage from the town of Silkeborg. In 1980, sewage was cut off, but phosphorus loading remained high due to fish-farming activities on the Funder River. Lately, large fluctuations in primary productivity during the summer have been observed, but the long-term trend has been towards lower transparencies during summer months so that submerged vegetation has not yet recovered in this lake. However, the change in chydorid assemblages was small (<20% dissimilarity), and consequently, there was only a slight indication of increased phosphorus concentration. The remaining two lakes of R3, Skanderborg Sø and Arresø, were among the "polluted" lakes; they had very high biomass values (Table 1) and low diversities. *Chydorus sphaericus* and *A. rectangula* made up over 90% of the chydorid communities; both taxa are phosphorus tolerant (Fig. 6) and characteristic of polluted sites (Fig. 4B; Whiteside 1970, table 13).

The three lakes of group R4 showed increases in biomass and TP and had lower species diversity. The conductivity of these three lakes ranked among the highest in 1965 (Table 1). The strong decline in conductivity suggested that the lakes were heavily exposed to nutrient input already in the mid-1960s, which has now been reduced, although the eutrophication process has continued.

Furesø and Store Gribsø were classified as R5 lakes, which were characterized by dramatic changes in species composition and diversity (Figs. 3 and 7). Furesø declined in water quality from the 1950s into the 1970s, until efforts to reduce nutrient inputs were initiated which reduced phosphorus loading from 37 to 3 $t \cdot year^{-1}$ (Sand-Jensen 1997). However, phosphorus was still available during summer stratification when the hypolimnion became anoxic, and the continued internal release of phosphorus resulted in no improvement in algal biomass as reflected by transparency and biomass. The chydorid assemblages indicated that the lake had not yet recovered from the nutrient loads of 1950–1980. The second lake, Store Gribsø, was the only B1 lake that had undergone dramatic changes in species composition and diversity over the years (Figs. 3 and 7). In 1965, *C. sphaericus* was <1% of the chydorids, but it was 84% of the community in 1992. *Alona nana* percentages decreased from 16 to <1%. These major shifts in chydorid taxa were reflected in the NMDS ordination of the species data (Fig. 3), where Store Gribsø moved further away from typical clear lakes. Additionally, the loss of transparency in Store Gribsø was dramatic. It was not caused by increased biomass (*d*), but, most likely, by increased color. A decrease in dissolved oxygen associated with increased color might have influenced the chydorid communities. Store Gribsø has always been a low-alkalinity lake (Berg and Petersen 1956).

© 1998 NRC Canada

Fig. 7. Summary of trends in biological and chemical changes in 32 Danish lakes from 1965 to 1992. Lakes are divided into response groups (R1–R6) according to type, degree, and direction of changes. Triangles, circles, and squares refer to the classification of 1992 chydorid assemblages (Fig. 2).

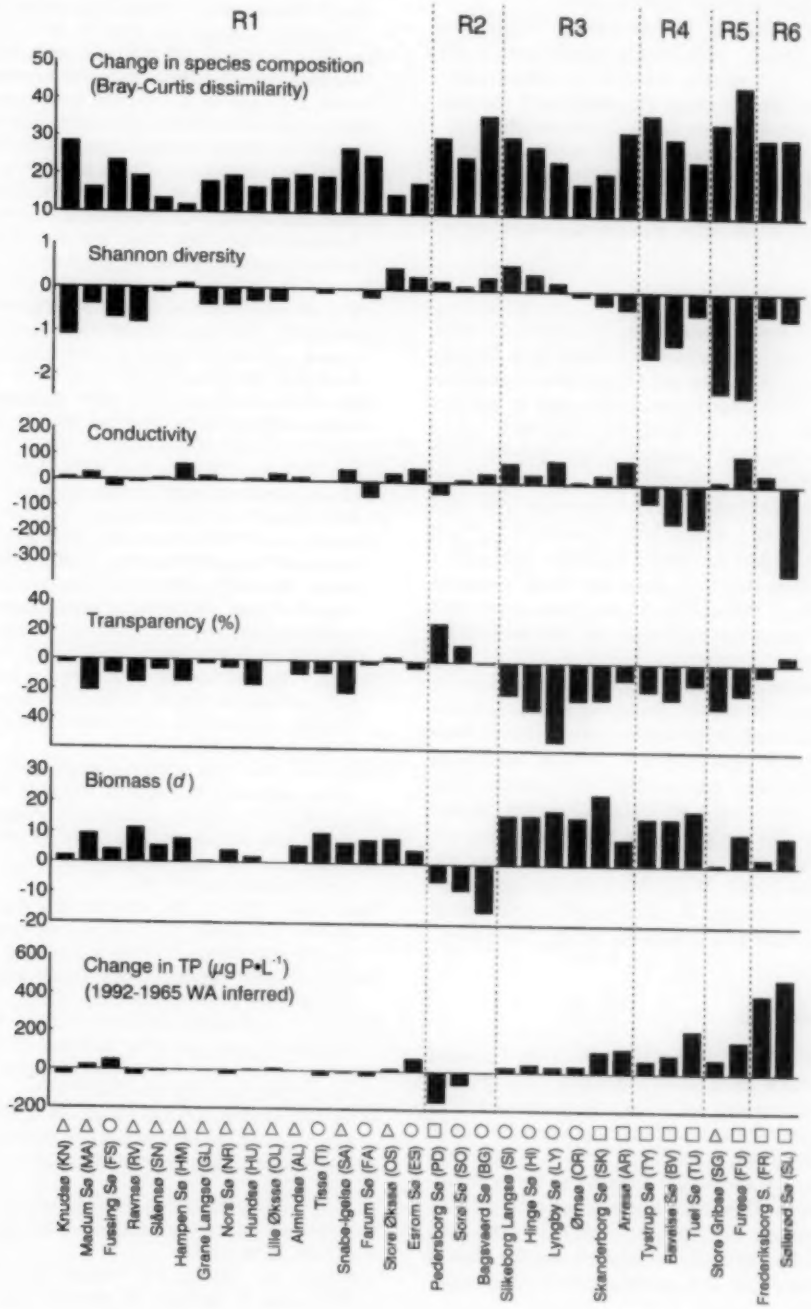

© 1998 NRC Canada

The lower alkalinity reported for 1992 and the dramatic change in chydorid assemblages might also be a result of acidification caused by both atmospheric deposition and events in the catchment area (Pedersen and Poulsen 1988).

The two lakes of group R6 (Frederiksborg Slotssø and Søllerød Sø) were already very highly productive in the 1960s. Although the WA results indicated increased phosphorus loading in the last 27 years, this additional increase had a slight effect on biomass (*d*) and species diversity. These lakes had the lowest diversity (<0.5) due to an almost complete dominance of *C. sphaericus*. The very significant decline in conductivity at Søllerød Sø clearly reflected the cutoff of waste water to the lake, but internal recycling of nutrients has kept the production at extreme levels.

Conclusions

Reexamination of chydorid assemblages by NMDS showed the Danish lake typology determined by Whiteside in 1970 to be reasonable. NMDS ordination made it possible to describe the direction and the relative degree of changes in species compositions between 1965 and 1992. CCA found a strong relationship between the 1992 species data and lake TP concentrations which allowed us to establish a reconstruction model to infer TP by weighted average regression and calibration techniques. The WA model was used to infer TP levels for the 1965 data set, and the results suggested that several "clear-water" lakes have declined, and a few have increased in water quality since 1965. There was good agreement between changes in species composition and measured environmental variables.

Lake sediments accumulate and integrate ecological information from both the entire water column and all lake habitats over time (Smol 1992), and surface-sediment samples of morphological fossil assemblages minimize what in traditional biological monitoring often are reported as "unusual (seasonal) events." The application of surface-sediment assemblages in monitoring fills the gap in the time frame between traditional monitoring and palaeoecological core studies, i.e., years and decades (Smol 1992); this study has confirmed that chydorid subfossils remain a valuable tool as biological indicators for trophic state and as markers for the "long-term" monitoring of lakes.

Acknowledgments

The authors wish to thank Erik Jeppesen from the National Environmental Research Institute in Silkeborg for providing chemical data. Thanks are also due to Lars Angantyr and Gildi Whiteside for assistance in the sampling program in 1992, and many thanks to John Birks, John Smol, and an anonymous reviewer for valuable comments and suggestions for improvement of the manuscript. This study was supported by a Ph.D. grant from the University of Copenhagen to K.P. Brodersen and by grants from the Fulbright Foundation and the Danish National Environmental Research Institute to M.C. Whiteside.

References

Anderson, N.J. 1993. Natural versus anthropogenic change in lakes: the role of the sediment record. Trends Ecol. Evol. **8**: 356–361.

Beals, P.W. 1976. Palaeolimnological studies of a Shropshire mere. Ph.D. thesis, Cambridge University, Cambridge, U.K.

Berg, K., and Petersen, I.C. 1956. Studies on the humic, acid Lake Gribsø. Folia Limnol. Scand. **8**: 1–273.

Birks, H.J.B. 1995. Quantitative palaeoenvironmental reconstructions. *In* Statistical modelling of quarternary science data. *Edited by* D. Maddy and J.S. Brew. Quarternary Research Association, Cambridge, U.K. pp. 161–254.

Bray, J.R., and Curtis, J.T. 1957. An ordination of the upland forest communities of southern Wisconsin. Ecol. Monogr. **27**: 325–349.

Charles, D.F., and Smol, J.P. 1994. Long-term chemical changes in lakes: quantitative inferences using biotic remains in the sediment record. *In* Environmental chemistry of lakes and reservoirs. *Edited by* L. Baker. Adv. Chem. Ser. **237**: 3–31.

Christensen, N., Paaby, H., and Holten-Andersen, J. 1994. Environment and society — a review of environmental development in Denmark. NERI Tech. Rep. No. 108, National Environmental Research Institute, Silkeborg, Denmark.

Clarke, K.R. 1993. Non-parametric multivariate analyses of change in community structure. Aust. J. Ecol. **18**: 117–143.

Clarke, K.R., and Ainsworth, M. 1993. A method of linking multivariate community structure to environmental variables. Mar. Ecol. Prog. Ser. **92**: 205–219.

Clarke, K.R., and Green, R.H. 1988. Statistical design and analysis for a "biological effects" study. Mar. Ecol. Prog. Ser. **46**: 213–226.

Clarke, K.R., and Warwick, R.M. 1994. Change in marine communities: an approach to statistical analysis and interpretation. Natural Environmental Research Council, U.K.

Cotten, C.A. 1985. Cladoceran assemblages related to lake conditions in eastern Finland. Ph.D. thesis, Indiana University, Bloomington.

Crisman, T.L. 1980. Chydorid cladoceran assemblages from subtropical Florida. *In* Evolution and ecology of zooplankton communities. *Edited by* W.C. Kerfoot. Am. Soc. Limnol. Oceanogr. Spec. Symp. **3**: 657–668.

Duigan, C.A., and Kovach, W.L. 1991. A study of the distribution and ecology of littoral freshwater chydorid (Crustacea, Cladocera) communities in Ireland using multivariate analyses. J. Biogeogr. **18**: 267–280.

Frey, D.G. 1960. The ecological significance of Cladocera remains in lake sediments. Ecology, **41**: 684–699.

Frey, D.G. 1979. Cladocera analysis. *In* Palaeohydrological changes in the temperate zone in the last 15 000 years. IGCP Project 158B, Lake and mire environments. Vol II. University of Lund, Lund, Sweden. pp. 227–257.

Frey, D.G. 1980. On the plurality of *Chydorus sphaericus* (O.F. Müller) (Cladocera, Chydoridae), and designation of a neotype from Sjælsø, Denmark. Hydrobiologia, **69**: 83–123.

Frey, D.G. 1982. Questions concerning cosmopolitanism in Cladocera. Arch. Hydrobiol. **93**: 484–502.

Hann, B.J., and Goldsborough, L.G. 1997. Responses of a prairie wetland to press and pulse additions of inorganic nitrogen and phosphorous: invertebrate community structure and interactions. Arch. Hydrobiol. **140**: 169–194.

Hann, B.J., Leavitt, P.R., and Chang, P.S.S. 1994. Cladocera community response to experimental eutrophication in Lake 227 as recorded in laminated sediments. Can. J. Fish. Aquat. Sci. **51**: 2312–2321.

Herbert, P.D., and Hann, B.J. 1986. Patterns in composition of Arctic tundra pond microcrustacean communities. Can. J. Fish. Aquat. Sci. **43**: 1416–1425.

Jeppesen, E., Jensen, J.P., Kristensen, P., Søndergaard, M., Mortensen, E., Sortkjær, O., and Olrik, K. 1990. Fish manipulation as a lake restoration tool in shallow, eutrophic temperate lakes 2: threshold levels, long term stability and conclusions. Hydrobiologia, **200/201**: 219–227.

Jeppesen, E., Madsen, E.A., Jensen, J.P., and Anderson, N.J. 1996. Reconstructing the density of planktivorous fish and trophic structure from sedimentary zooplankton fossils: a surface sediment

© 1998 NRC Canada

calibration data set from shallow lakes. Freshwater Biol. **36**: 115–127.

Jeppesen, E., Jensen, J.P., Søndergaard, M., Lauridsen, T., Pedersen L.J., and Jensen, L. 1997. Top-down control in freshwater lakes: the role of nutrient state, submerged macrophytes and water depth. Hydrobiologica, **342/343**: 151–164.

Keller, W., and Pitblado, J.R. 1989. The distribution of crustacean zooplankton in northern Ontario, Canada. J. Biogeogr. **16**: 249–259.

Line, J.M., and Birks, H.J.B. 1990. WACALIB version 2.1 — a computer program to reconstruct environmental variables from fossil assemblages by weighted averaging. J. Paleolimnol. **3**: 170–173.

Line, J.M., ter Braak, C.J.F., and Birks, H.J.B. 1994. WACALIB version 3.3 — a computer program to reconstruct environmental variables from fossil assemblages by weighted averaging and to derive sample specific errors of prediction. J. Paleolimnol. **10**: 147–152.

Pedersen, L.B., and Poulsen, M.S. 1988. Store Gribsø - forsuring. Stofbudgetter fortæller om ferskvandsforurening. Vand & Miljø, **5**: 18–23. (In Danish.)

Riis, T., and Jørgensen, T.B. 1996. Grane Langsø og Kalgård Sø - Tilstand og udvikling. Tech. Rep., County of Århus. (In Danish.)

Riis, T., Sand-Jensen, K., and Jørgensen, T.B. 1996. Danmarks reneste sø gennem 40 år. Vand & Jord, **5**: 199–203. (In Danish.)

Roff, C.J., Sprules, W.G., Carter, J.C.H., and Dadswell, M.J. 1981. The structure of crustacean zooplankton communities in glaciated eastern North America. Can. J. Fish. Aquat. Sci. **38**: 1428–1437.

Sand-Jensen, K. 1997. Eutrophication and plant communities in Lake Fure during 100 years. *In* Freshwater biology. Priorities and development in Danish research. *Edited by* K. Sand-Jensen and O. Pedersen. G.E.C. Gad, Copenhagen, Denmark. pp. 26–38.

Scheffer, M., Hosper, S.H., Meijer, M.-L., Moss, B., and Jeppesen, E. 1993. Alternative equilibria in shallow lakes. Trends Ecol. Evol. **8**: 275–279.

Smol, J.P. 1992. Paleolimnology: an important tool for effective ecosystem management. J. Aquat. Ecosyst. Health, **1**: 49–58.

Sprules, W.G. 1977. Crustacean zooplankton communities as indicators of limnological conditions: an approach using principal component analysis. J. Fish. Res. Board Can. **34**: 962–975.

Synerholm, C.S. 1979. The chydorid Cladocera from surface lake sediments in Minnesota and North Dakota. Arch. Hydrobiol. **86**: 137–151.

ter Braak, C.J.F. 1986. Canonical correspondence analysis: a new eigenvector technique for multivariate direct gradient analysis. Ecology, **67**: 1167–1179.

ter Braak, C.J.F. 1987. The analysis of vegetation–environment relationship by canonical correspondence analysis. Vegetatio, **69**: 69–77.

ter Braak, C.J.F. 1992. CANOCO — a FORTRAN program for canonical community ordination. Microcomputer Power, Ithaca, N.Y.

ter Braak, C.J.F., and Prentice, I.C. 1988. A theory of gradient analysis. Adv. Ecol. Res. **18**: 271–317.

van Tongeren, O.F.R. 1987. Cluster analysis. *In* Data analysis in community and landscape ecology. *Edited by* R.H.G. Jongman, C.J.F. ter Braak, and O.F.R. van Tongeren. Pudoc, Wageningen, The Netherlands. pp. 174–212.

Whiteside, M.C. 1970. Danish chydorid Cladocera: modern ecology and core studies. Ecol. Monogr. **40**: 79–118.

Whiteside, M.C. 1983. The mythical concept of eutrophication. Hydrobiologia, **103**: 107–111.

Whiteside, M.C., and Harmsworth, R.V. 1967. Species diversity in chydorid (Cladocera) communities. Ecology, **48**: 644–677.

Whiteside, M.C., and Swindoll, M.R. 1988. Guidelines and limitations to cladoceran paleoecological interpretations. Palaeogeogr. Palaeoclimatol. Palaeoecol. **62**: 405–412.

© 1998 NRC Canada

Sperm competition and paternity assurance during the first breeding period of female snow crab (*Chionoecetes opilio*) (Brachyura: Majidae)

Nicola Urbani, Bernard Sainte-Marie, Jean-Marie Sévigny, David Zadworny, and Urs Kuhnlein

Abstract: Two highly polymorphic microsatellite DNA loci were used to determine paternity of larvae of primiparous *Chionoecetes opilio* females. In addition, female spermathecal contents were genotyped at the two loci and histological analysis of the organs was carried out to elucidate patterns of sperm competition. Females carrying their first brood from controlled laboratory matings and from matings in the wild were examined. Spermathecal contents from wild-caught females were cut into several cross sections and each section genotyped individually. Both wild and laboratory females commonly mated with several males whose ejaculates were stored and stratified in the spermathecae. Genetic typing of the offspring of laboratory-mated females revealed single paternity and indicated that the last mate to inseminate a female before oviposition gained paternity of the clutch. The predominant mechanism ensuring single paternity appeared to be sperm stratification. In wild-caught females, the microsatellite typing of the offspring also revealed single paternity, but larvae appeared to be sired by males whose genotypes were found in the spermathecal cross sections towards the dorsal end (blind end) of the spermathecae. This suggested that they were the first males to mate with females that they guarded until oviposition, and females remated with other males thereafter.

Résumé : Deux loci d'ADN microsatellite hautement variables ont été utilisés pour déterminer la paternité des larves de femelles primipares de *Chionoecetes opilio*. De plus, la détermination des génotypes du contenu des spermathèques des femelles a été faite à partir de ces deux loci et l'analyse de coupes histologiques des organes a été réalisée dans le but d'élucider les modalités de compétition du sperme. Des femelles avec leur premières portées d'oeufs obtenues à partir d'accouplements contrôlés en laboratoire et d'accouplements en nature ont été examinées. Les spermathèques des femelles sauvages ont été coupées en plusieurs sections transversales et le génotype de chacune des sections a été déterminé. Les femelles sauvages ainsi que celles de laboratoire se sont accouplées avec plusieurs mâles dont le sperme était accumulé de façon stratifiée dans les spermathèques. La détermination du génotype de la progéniture des femelles accouplées en laboratoire a révélé qu'il y avait paternité unique et que le dernier mâle à inséminer une femelle avant la ponte des oeufs était le père. Le mécanisme prédominant assurant la paternité unique semble être la stratification des éjaculats. Chez les femelles sauvages, la détermination du génotype des larves a également démontré qu'il y avait paternité unique. Cependant, les oeufs semblaient avoir été fécondés par les mâles dont les génotypes se trouvaient dans les sections des spermathèques les plus éloignées de l'ouverture des organes. Ceci suggère qu'ils étaient les premiers à s'accoupler avec les femelles et qu'ils les auraient ensuite protégées jusqu'à ce qu'elles pondent. Les femelles se seraient donc ré-accouplées avec d'autres mâles uniquement après la ponte.

Introduction

Sperm competition is an important feature of the reproductive biology of numerous species that may explain many gamete and behavioral traits and is critical to the reproductive success of males (Parker 1970). Among taxa in which females are polygamous and have sperm storage organs, mechanisms of sperm competition often result in single paternity and fall into two broad categories called sperm stratification and sperm removal (Birkhead and Hunter 1990). In the former, sperm from the last male displaces previous ejaculates towards the blind end of the spermatheca, away from efferent ducts which

Received June 4, 1997. Accepted December 11, 1997.
J14044

N. Urbani, D. Zadworny, and U. Kuhnlein. Department of Animal Science, McGill University, Macdonald Campus, 21 111 Lakeshore Road, Sainte-Anne-de-Bellevue, QC H9X 3V9, Canada.
B. Sainte-Marie[1] and J.-M. Sévigny. Ministère des Pêches et des Océans, Institut Maurice-Lamontagne, Division des invertébrés et de la biologie expérimentale, 850 route de la Mer, CP 1000, Mont-Joli, QC G5H 3Z4, Canada.

[1] Author to whom all correspondence should be addressed. e-mail: sainte-marieb@dfo-mpo.gc.ca

© 1998 NRC Canada

lead from the ovary, so that this sperm may be the first to fertilize the eggs (e.g., Smith 1979). The latter category involves the elimination of previously deposited sperm from the female reproductive tract, either by extraction (e.g., Waage 1979) or by "flushing out" one ejaculate by a subsequent one (e.g., Rubenstein 1989).

While paternity has been studied in several terrestrial and freshwater arthropods with sperm storage organs, there is only limited information for marine forms that are principally crustaceans. It has been shown that impregnation by irradiated males of previously inseminated females resulted in the extrusion of unfertilized eggs in the crabs *Inachus phalangium* (Diesel 1990) and *Scopimera globosa* (Koga et al. 1993), indicating that the last mate fertilizes all or a very large fraction of the eggs. However, only in *I. phalangium* has the underlying mechanism ensuring single paternity been studied. Histological examination showed that putative ejaculates were segregated within the spermatheca and suggested that sperm stratification was the mechanism at play in *I. phalangium*, such that the ejaculate of the most recent mate occurred close to the oviduct opening and therefore had exclusive access to unfertilized eggs (Diesel 1989, 1991).

The snow crab *Chionoecetes opilio* (Brachyura, Majidae) may represent an ideal model species for the study of sperm competition and paternity assurance in marine crustacean decapods, by virtue of extensive information on anatomical, physiological, and behavioral aspects of its reproduction (Elner and Beninger 1992, 1995). The reproductive system of the female snow crab is bilaterally symmetrical, comprising two ovaries, each connected by an oviduct to separate expandable spermathecae. Each spermatheca forms a vast dorsal chamber, adjoining a small intermediate chamber (Beninger et al. 1988; Sainte-Marie and Sainte-Marie 1998). The spermatheca is of the ventral type (Diesel 1991) because the oviduct opens near its base, at proximity to the vagina. Mixing of female and male gametes is presumed to occur in the intermediate chamber (Beninger et al. 1993).

Female snow crab undergo a terminal molt to maturity and copulate for the first time while they are still soft-shelled (Watson 1972). Females in their first breeding period are called primiparous. In the laboratory, recently molted females often copulate serially with a single male or, provided the opportunity, with several different males (Sainte-Marie et al. 1997). After any number of copulations, and sometimes before the series of successive copulations has ended, eggs are extruded and attached beneath the abdomen where they are incubated (Sainte-Marie et al. 1997). Sperm stored in females of the genus *Chionoecetes* may not all survive between successive ovipositions. However, in some cases, sperm remaining from a previous mating period may be sufficiently abundant for partial or complete fertilization of a second egg clutch (Adams and Paul 1983; Sainte-Marie and Carrière 1995). To renew or supplement sperm stores, adult female snow crab may remate prior to extruding a new clutch of eggs (Taylor et al. 1985; Conan and Comeau 1986). Hence, in snow crab, there exists the possibility of competition between fresh sperm from different males at the first breeding period and between recent and old sperm in subsequent breeding periods. The former situation may be more conducive to intense sperm competition, as all sperm is recently deposited and thus may be equally viable.

It has been hypothesized for *Chionoecetes* species that the last male to inseminate a female before oviposition has precedence in fertilizing the eggs (Paul et al. 1983). Paternity for multiply-mated female *Chionoecetes* has been investigated only once, using isozymes as genetic markers. The limited data suggested that only the most recent sperm acquired after the second of two successive breeding periods was used to fertilize eggs, but no inference on the underlying mechanism was possible (Sévigny and Sainte-Marie 1996). The proposed mechanisms to ensure last-male sperm precedence in *Chionoecetes* species are (*i*) sperm stratification (Paul et al. 1983) and (*ii*) removal of rival sperm by the male's hook-shaped gonopods (Beninger et al. 1991).

In this study, two polymorphic microsatellite markers were used to determine the paternity of the embryos of primiparous females from controlled mating experiments and from the wild. In addition, female spermathecae were used for histological and genetic analysis to assess patterns of sperm storage. We demonstrate that progenies were fathered mainly or exclusively by a single male, even though ejaculates from several males were present in the spermathecae. The predominant or sole mechanism ensuring single paternity appears to be sperm stratification.

Materials and methods

Mating experiments

Maturing females of 40–60 mm carapace width (CW) and adult males of 65–132 mm CW were captured by beam trawl in the northwest Gulf of St. Lawrence in eastern Canada (50°06′N, 66°35′W) during October 1995. The crabs were held in laboratory tanks supplied with fresh flowing seawater subject to natural changes in temperature (–1.1 to 3.2°C) and salinity (28–31‰). Photoperiod was controlled to reflect natural light regimes. Females and males were kept in separate tanks with independent water supplies. Crabs were fed previously frozen northern shrimp (*Pandalus borealis*) or Atlantic herring (*Clupea harengus*) semiweekly. Tanks were checked for molting female crabs at least twice daily starting in January 1996.

Prior to experimentation, all captive males were individually tagged and had a mandibular palp excised for microsatellite genotyping (see below). This was done to ensure that experimental males had different genotypes at the loci studied. Females used in mating experiments were virgin and had either begun their maturity molt or completed their maturity molt less than 12 h before introducing a male. Mating experiments were conducted from February 5 to 28, 1996, in tanks with running fresh seawater at –0.5 to 0.3°C, following either one of two methods. In the first method ($n = 8$), a molting female was placed in a 500-L tank containing one, two, three, or four tagged males and monitored for 24 h using a ceiling-mounted low-light video camera (Panasonic Lunar Lite) and time-lapse VCR recorder (Panasonic AG-6720A) at one image per second. Video recordings were subsequently analyzed to determine the copulating sequence, identity of mates, and duration of copulations. However, the time of oviposition could not be determined from video recordings. In the second method ($n = 9$), a recently molted female was placed in a 50-L tank containing a single tagged male until copulation occurred and postcopulatory guarding was initiated by the male. She was then separated from her mate and transferred to another tagged male so that she might copulate anew. The time of oviposition was determined by direct examination of the females at each transfer. The values for duration of copulations for individual females obtained in this second set of experiments are less accurate, since video recordings were not taken and the observer was not always present at the start or end of copulatory bouts. Females from both types of experiments were individually tagged and then transferred and held in a female

© 1998 NRC Canada

communal holding tank until they were killed on April 1, 1996. Females and egg clutches were then processed for histological and genetic analyses as described below. The time delay between oviposition and processing was necessary to ensure that the developing embryos (about 256–1024 cells stage) yielded enough DNA for reliable polymerase chain reaction (PCR) analysis.

Collection of primiparous females in the wild

A total of 20 primiparous females carrying recently extruded, brilliant orange eggs were collected between April 27 and May 5, 1996, with the same equipment and at the same geographic site as above. These females had a clean, iridescent, and soft or brittle exoskeleton, indicating that they had molted to maturity in the past few weeks. They were immediately processed onboard ship for histological and genetic analyses.

Dissection of laboratory and wild-caught females

Females were killed and one pereopod and the egg clutch were removed and preserved separately in 100% ethanol for genetic analyses. An incision was then made along the posterior suture between carapace and sternites and the carapace was raised to reveal the internal organs. Spermathecae, intermediate chambers, and vaginas were dissected out without perturbing their contents. Because sperm delivery to paired spermathecae is usually balanced (Sainte-Marie and Lovrich 1994), the two spermathecae of an individual female were considered replicates and were used to assess complementary aspects of the reproductive process. In this study, the left spermatheca was used for genetic analysis and the right spermatheca was reserved for histological analysis.

The left spermatheca was prefixed for about 5 min in 100% ethanol to solidify the receptacle's wall and contents, after which the wall was carefully peeled away from the cohesive content. The content of the vagina and adjoining small intermediate chamber could not be isolated and was therefore not included in the genetic analysis. When the spermatheca was small, as occurred in the laboratory-mated females, its content was preserved whole in 100% ethanol. However, when the spermatheca was large, as occurred in most wild-caught primiparous females, some more or less distinct masses (putatively, different ejaculates) were apparent in the spermathecal content. Using a scalpel, we attempted to isolate these masses by cross-sectioning the spermathecal content more or less perpendicularly to its sagittal plane. The scalpel was carefully cleaned between each cut. Resulting cross sections were numbered sequentially from the dorsal to the most ventral (i.e., closest to the oviduct) location and preserved individually in 100% ethanol. The right spermathecae of laboratory-mated and wild-caught primiparous females were, respectively, fixed in Bouin for 48 h and then stored in 70% ethanol at 4°C for 4 months or fixed in Bouin added with 1.5% acetic and 1.5% trichloroacetic acids for 48 h and then stored in 70% ethanol at 4°C for 4 months. Spermathecae were embedded in paraffin and cut in mediosagittal sections 7 μm thick. Sections were stained using the technique of Dominici (Langeron 1949) and analyzed by light microscopy by an independent investigator (G. Sainte-Marie, Département de pathologie et biologie cellulaire, Université de Montréal, Montréal, Qué.) with no knowledge of the mating history of laboratory females or the results of genetic analyses.

DNA extractions

DNA for microsatellite analysis was extracted from male mandibular palps, female pereopods, spermathecal contents, and egg clutches. Because embryo development is very slow at the cold temperatures preferred by snow crab, embryos from wild-caught primiparous females had undergone only seven to nine cell divisions when they were caught in the late April to early May sampling period (B. Sainte-Marie, unpublished data). Consequently, for large clutches, DNA was extracted from a pool of about 10 000 embryos from each female. For each of these clutches, care was taken to sample embryos from each of the carrier pereopods. However, when the clutch was small (<10 000 embryos) the whole clutch was used to extract DNA.

Tissues preserved in 100% ethanol were vacuum dried, the dry weight of spermathecal contents was determined, and samples were crushed with a plastic pestle and resuspended in water. Total DNA was then isolated by SDS/proteinase K digestion followed by a phenol–chloroform–isoamyl extraction (Sambrook et al. 1989).

Microsatellite analysis

The two hypervariable loci used in this study, Cop3-4 and Cop24-3, are from a collection of microsatellites identified from a *C. opilio* genomic library (Urbani et al. 1998). They were chosen for having numerous alleles (22 and 13 in 20 unrelated individuals, respectively) and high levels of observed heterozygosity (94 and 90%, respectively) giving an average probability of 4.5×10^{-5} for two individuals to share a particular allelic combination by chance (Avise 1994). A test for deviation from Hardy–Weinberg equilibrium using 20 unrelated individuals according to Verheyen et al. (1994) showed that the observed and expected heterozygosities were not different for locus Cop3-4 ($\chi^2 = 3.8 \times 10^{-6}$, df = 1, $P > 0.99$) and locus Cop24-3 ($\chi^2 = 4.3 \times 10^{-5}$, df = 1, $P > 0.99$) (Urbani 1998).

The two loci are composed of repeats of the tetranucleotide-GACA motif and lead to low DNA polymerase slippage during PCR amplification compared with dinucleotide and trinucleotide repeats. However, locus Cop3-4 also contains short mononucleotide repeats of the $(C)_n$ and $(A)_n$ type so that its allelic variability is the result of the combined variability of its mononucleotide and tetranucleotide repeats. The low amount of slippage facilitated the scoring of bands, especially when analyzing cross sections of spermathecal contents where more than two alleles were present. The sequence (5′ to 3′) of the primers used for PCR for locus Cop3-4 were AACCGTGCTGGTGAGGCAAGG (forward) and GCTTCTTTGCCCAATGTCGGAG (reverse) and for locus Cop24-3 were GAGACATACAGACTGACA (forward) and CGGGTATCT-GAATTTTCC (reverse).

PCR was carried out in volumes of 12.5 μL according to Bowcock et al. (1993). Reactions for locus Cop3-4 were performed with 0.25 μM concentration of each primer, using 0.25 unit of *Taq* DNA polymerase (Pharmacia), 200 μM concentration each of dATP, dCTP, dGTP, and dTTP, and 1.5 mM $MgCl_2$. The forward primer was end-labelled with [γ-^{32}P]dCTP. Samples were overlaid with mineral oil, denatured for 2 min at 94°C, and amplified for 25–30 cycles of 1 min at 94°C, 1 min at an annealing temperature of 71°C, and 1 min at 72°C. Reactions for locus Cop24-3 were identical except that the primer concentrations were 0.5 μM, the $MgCl_2$ concentration 2.0 mM, and the annealing temperature 54°C. PCR products were resolved by electrophoresis on 6% denaturing polyacrylamide gels. The gels were dried and autoradiography was carried out at room temperature for 1–3 days.

Results

Sperm segregation and paternity in controlled mating studies

In the laboratory, females copulated between one and four times (median two times) with up to three different males. Total copulatory time for individual females varied from about 5 to 72 min and correlated positively with spermathecal dry weight ($r = 0.52$, $P = 0.039$). In 10 females, histological examination of the right spermatheca–intermediate chamber–vagina complex revealed the presence of two rather discrete structural units, arranged sequentially along the longitudinal axis of the organs (e.g., Fig. 1*a*). The seven remaining females had a single unit in their spermatheca. Each unit was usually composed of a concentration of spermatophores

© 1998 NRC Canada

Fig. 1. Light micrographs and schematics of mediosagittal sections of the right spermathecae of (*a*) female 977 from the controlled matings and (*b*) female A17 from the wild. The spermathecae contain several ejaculates (EJ), each with many spermatophores capped by amorphous matter. Spermatophores in the light migrographs are small circular structures either black or grey. The base of spermathecae is at the bottom of micrographs. RW, receptacle wall; C1, C2, and C3, approximate cutting sites on the corresponding left spermatheca yielding spermathecal cross sections 1, 2, 3, and 4.

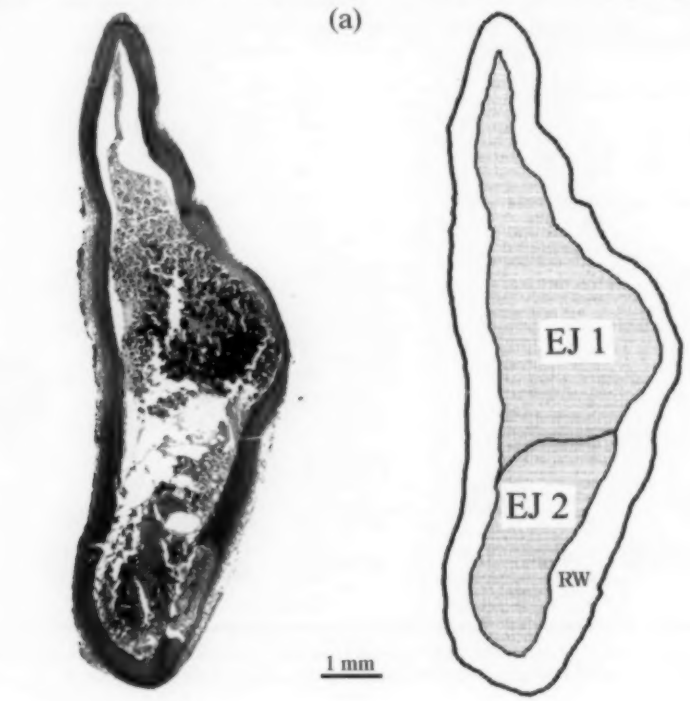

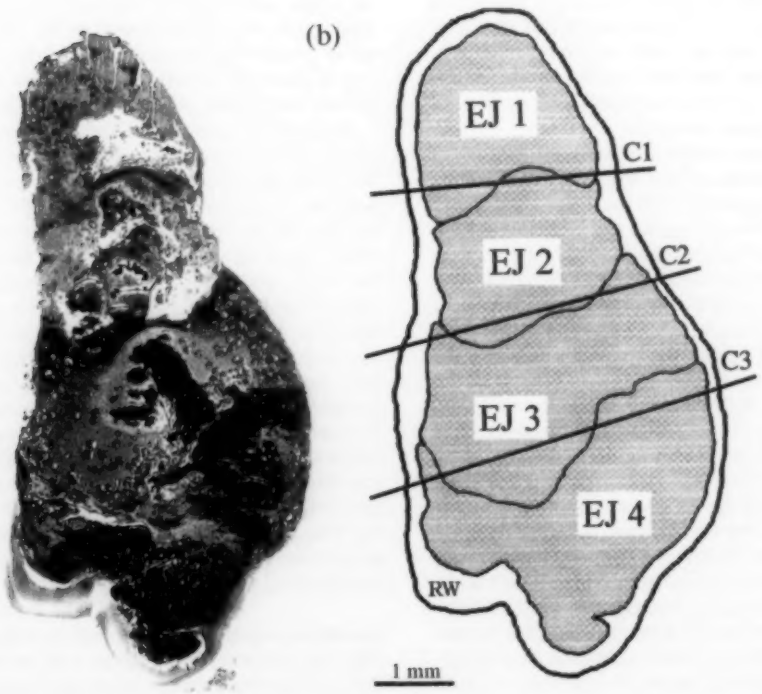

© 1998 NRC Canada

Table 1. Mating history and analysis of paternity in 11 broods of primiparous females subjected to controlled matings.

Female identity	Mate identity and order	Presence of male genotype		Duration of copulations (min)	Time (h) between copulations	Structural units in receptacle
		Spermatheca	Embryos			
976 (*v*)	P5	+	+	14		1
980 (*v*)	P2	+	+	11		1
961 (*v*)	PI	+	+	22	20.5	2
	P3	+	–	17		
966 (*v*)	P3	+	+	9	9.0	2
	P6	–	–	14		
979	P8	+	+	60	8.0	1
	P6	–	–	≈12		
962 (*v*)	P6	+	–	13	4.0	2
	P8	+	–	22	4.0	
	P8	+	–	23	3.75	
	P5	+	+	5		
965	P6	+	–	18	0.25	2
	P4	+	+	≈9		
970	P3	+	–	12	1.0	2
	P4	+	+	13		
973	P5	+	–	≈20	2.5	1
	P8	+	+	≈21		
975	P10	+	–	19	0.75	1
	P7	+	+	6		
977	P9	+	–	nd	3.0	2
	P2	+	+	20		

Note: A "*v*" indicates the matings that were videotaped, while in the other matings, females were observed directly and transferred between matings (see Materials and methods). nd, not determined; +, presence of genotype; –, absence of genotype.

dorsally capped by a relatively large amount of amorphous matter. In 13 of 17 cases (76.5%) the number of structural units in the spermatheca coincided with the number of copulations realized by the female, and there was no significant difference between number of structural units and number of copulations (Wilcoxon signed-ranks test, $P = 0.68$).

The results of the genetic analysis of the spermathecae of two singly- and nine multiply-mated laboratory females are shown in Table 1. Two females (976 and 980), which each mated with a single male, had a single male genotype in their spermatheca identical to the genotype of their mate, thus validating our methodology. Females 961, 962, 965, 970, 973, 975, and 977 mated with multiple males and the genotypes of all the males involved in the matings were present in the spermatheca. Exceptions were female 966 and 979 where only the genotype of the first of their two mates was present in the spermatheca. In the case of female 966, the video recording showed that the copulation by the second mate (male P6) was terminated prematurely by a sudden aggression initiated by male P3. Histology of the contents of her right spermatheca–intermediate chamber–vagina complex revealed that the spermatophore aggregate of one of the two distinct structural units was small and lodged in the intermediate chamber near the vagina, possibly due to the last mate's precipitous withdrawal. This aggregate was not included in our genetic analysis, since only the spermathecal content was sampled. In the case of female 979, a long copulation with male P8 was followed by one rather short copulation with male P6. Only one structural unit was evident in the spermatheca, suggesting that little sperm, if any, was passed by the second male. An example of genetic analysis at locus Cop24-3 of spermathecal content is shown for female 977 in Fig. 2*a*, where the alleles of her two mates were represented in her spermatheca.

Analysis of multiply-mated females indicated that one male fathered most or all of the embryos (Fig. 2*a*; Table 1). Two patterns of paternity with respect to male copulating sequence were apparent. In females 961, 966, and 979, it was the first of two successive mates that sired the progeny. In these cases, there was a long time lapse between matings (8–20.5 h) and extended female guarding by the first mate before copulation with the second male occurred. In females 962, 965, 970, 973, 975, and 977, it was the last of successive mates that fathered the progeny, coincident with a shorter time lapse of ≤4 h between copulations and interrupted female guarding (either by experimental manipulation or aggression by a rival male) before the following copulation. Oviposition occurred after the first copulation in female 979 and after the last copulation in females 965, 970, 973, 975, and 977, but was not observed for females 961, 966, and 962. For females for which oviposition was observed, the last male to inseminate a female before oviposition gained paternity of the offspring.

Sperm segregation and paternity in wild-caught females

Histological examination of the right spermathecae of seven wild primiparous females revealed the presence of two to six

© 1998 NRC Canada

Fig. 2. Alleles observed at locus Cop24-3 in (*a*) female 977 sequentially mated with males P9 and P2, her left spermathecal content (Sp.), and her embryos and (*b*) female A17, four cross sections of her left spermatheca, and her embryos. Spermathecal cross section 1 is at the dorsal end (blind end) of the receptacle and cross section 4 is close to the vagina. Allele sizes (bp) are indicated.

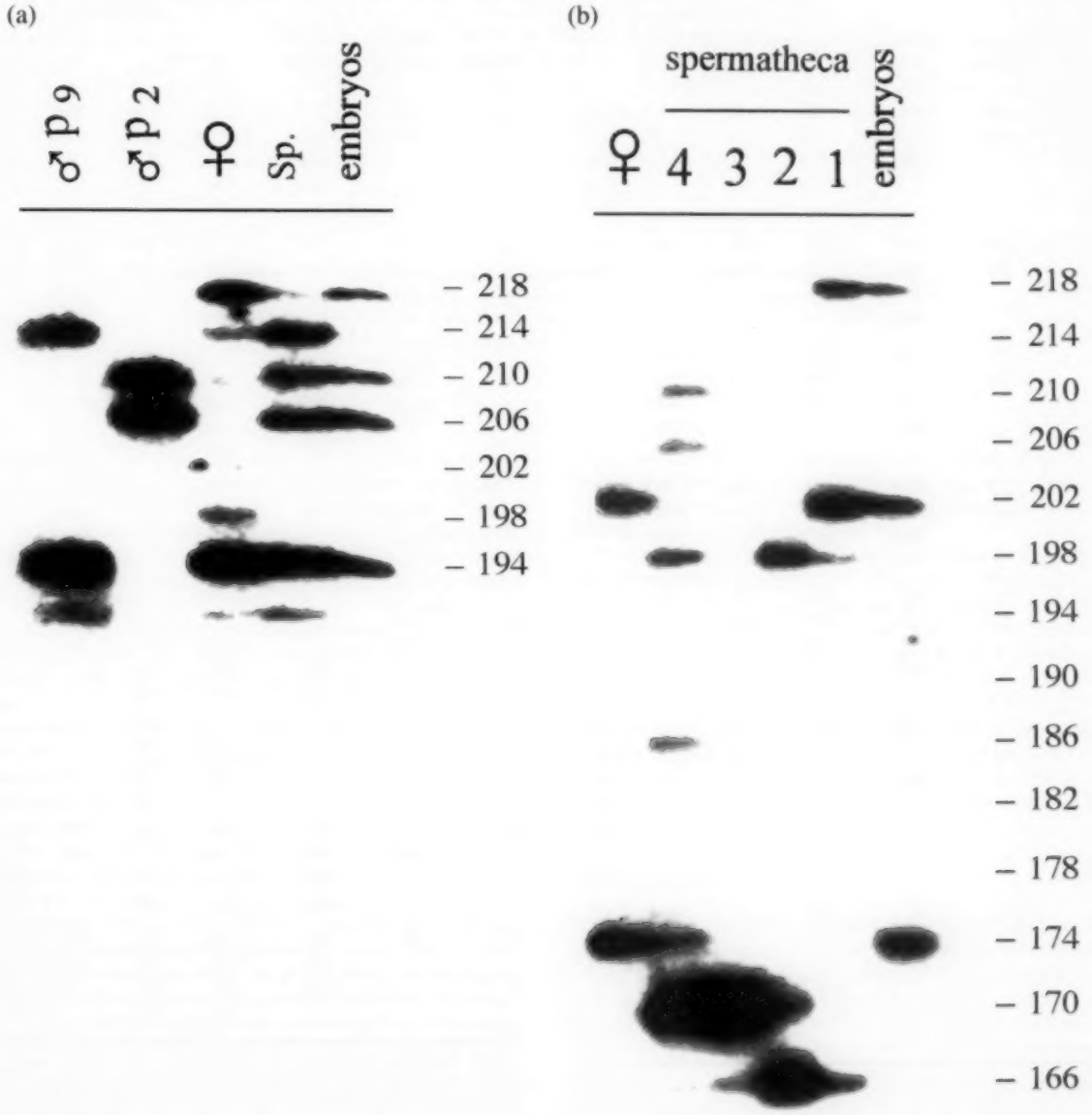

(mean 4.2) more or less discrete structural units arranged sequentially along the longitudinal axis of the organs (e.g., Fig. 1*b*). The outline of the units was often irregular. As was the case for laboratory-mated females, each unit was composed of an aggregate of spermatophores, usually capped by a larger volume of amorphous matter. Each of these units presumably represented individual ejaculates.

The genetic analysis of the spermathecal cross sections of seven primiparous females revealed the presence of more than two alleles at each locus for every spermatheca. The total number of male alleles was determined as the number of non-maternal alleles present in the cross sections (Tables 2 and 3). Since each male contributes one (homozygosity) or two alleles (heterozygosity), the least number of males that must have contributed to sperm content of a particular spermatheca is given by half the number of male alleles (rounded to the next integer in the case of an uneven number of alleles). The least number of males contributing to the sperm present in a spermatheca was determined from the locus that revealed the highest number of alleles. The actual number of males

© 1998 NRC Canada

Table 2. Alleles observed at locus Cop24-3 in spermathecal cross sections and embryos of seven wild-caught primiparous females.

Female	Female alleles	Embryo alleles	Alleles in spermathecal cross sections 1	2	3	4
A1	*190*	*190*	**182**	**182**	na	(218)
	166	*166*	174	174		(210)
		182	170	170		(202)
			166	166		(174)
						170
A5	*214*	*214*	198	178	186	218
	186	*186*	178	**(174)**	**174**	**174**
		190[a]	**174**			
		174				
A7	*190*	*190*	**(222)**	194	218	
	174	174	**186**	178	194	
		222	164		(190)	
		186			178	
					174	
A9	*210*	*210*	**186**	**(186)**	198	
	198	*198*	**174**	**(174)**	186	
		186	162	162	164	
		174			162	
A13	*186*	*186*	**214**	*186*	194	
	174	*174*	**202**	182	182	
		214	*186*	*174*		
		202	*174*	170		
			170			
A14	*210*	*210*	*(210)*	*(210)*	*(210)*	*(210)*
	166	*166*	**(202)**	**202**	**202**	206
		202	*(166)*	*(166)*	*(166)*	**(202)**
						198
						190
						186
						(166)
A17	*202*	*202*	**218**	198	170	(210)
	174	*174*	202	(170)		(206)
		218	(198)	166		(198)
			(166)			(186)
						(174)
						170

Note: The length of the alleles is indicated in base pairs. Alleles shared by females, their embryos, and spermathecal cross sections are indicated in italics. In the case of heterozygote females, alleles in spermathecal cross sections were considered to belong to the maternal genotypes only when both maternal alleles were observed. Non-maternal alleles shared by embryos and cross sections are indicated in boldface and indicate paternity. Alleles in parentheses indicate weak PCR amplifications. Left spermathecae of females A7, A9, and A13 were cut into three cross sections and those of the other females were cut into four cross sections. Cross section 1 was located at the dorsal end (blind end) of the receptacle and cross section 4 (cross section 3 for females A7, A9, and A13) was located at the base of the organs, close to the vaginal opening. na, no amplification.

[a]Allele not observed in the spermathecal cross sections.

Table 3. Alleles observed at locus Cop3-4 in spermathecal cross sections and embryos of seven wild-caught primiparous females.

Female	Female alleles	Embryo alleles	Alleles in spermathecal cross sections 1	2	3	4
A1	*276*	*276*	(282)	(266)	266	270
	270	*270*	(274)	**254**	250	258
		254	(266)	**250**		246
		250	**254**			238
			250			
A5	*279*	*279*	(276)	276	*(279)*	*(279)*
	260	*260*	266	(260)	266	266
		254	258	**(254)**	(263)	(263)
			(254)	251	*(260)*	*(260)*
			(251)		253	253
A7	*262*	*262*	*(262)*	287	(278)	
	256	*256*	**259**	250	*(262)*	
		259	*(256)*		259	
		251	**251**		*(256)*	
					250	
A9	268	na	267	na	266	
	263		260		252	
			252		236	
			236			
A13	*289*	*289*	**292**	**(292)**	279	
	273	*273*	*(289)*	*(289)*	266	
		292	(282)	282		
		279	**279**	**279**		
			(273)	*(273)*		
			(266)	266		
			254	254		
			251	251		
A14	*272*	*272*	**(279)**	**279**	**279**	**(279)**
	264	*264*	*(272)*	*(272)*	**260**	266
		279	*(264)*	*(264)*		**(260)**
		260	**(260)**	**260**		250
A17	*244*	*244*	(283)	283	263	283
		264	(270)	270	252	269
		261	**264**	263		263
			261	252		252

Note: The length of the alleles is indicated in base pairs. Alleles shared by females, their embryos, and spermathecal cross sections are indicated in italics. In the case of heterozygote females, alleles in spermathecal cross sections were considered to belong to the maternal genotypes only when both maternal alleles were observed. Non-maternal alleles shared by embryos and cross sections are indicated in boldface and indicate paternity. Alleles in parentheses indicate weak PCR amplifications. Left spermathecae of females A7, A9, and A13 were cut into three cross sections and those of the other females were cut into four cross sections. Cross section 1 was located at the dorsal end (blind end) of the receptacle and cross section 4 (cross section 3 for females A7, A9, and A13) was located at the base of the organs, close to the vaginal opening. na, no amplification.

© 1998 NRC Canada

Table 4. Genetic and histological data on the spermathecal contents of seven wild-caught primiparous females.

	Spermathecal contents			
Female	Number of alleles at locus Cop24-3	Number of alleles at locus Cop3-4	Least number of male genotypes	Number of structural units
A1	7[a]	9	5	6
A5	5	8	4	5
A7	6	5	3	2
A9	5	5[a]	3	4
A13	5	6	3	4
A14	5	4	3	nd
A17	9	7	5	4

Note: The least number of male genotypes per organ was determined from the highest number of non-maternal alleles seen at either locus Cop3-4 or locus Cop-24-3. A structural unit consists of a patch of spermatophores capped dorsally by amorphous matter and corresponds to one ejaculate observed in the histological slides. nd, not determined.

[a]Incomplete data.

contributing to the sperm present in a spermatheca might have been higher, since males could have shared certain alleles due to random allele sharing. The least number of male genotypes found in the seven spermathecae ranged from three to five (mean 3.7). The number of structural units determined from histology relative to the least number of mates estimated by genetic analysis was greater in the spermathecae of females A1, A5, A9, and A13 and less in females A7 and A17 (Table 4). Overall, the number of structural units was in agreement with the estimated least number of male genotypes.

Individual cross sections of spermathecae often revealed more than one male genotype, indicating that we were unsuccessful in fully separating individual units (Tables 2 and 3). Nonetheless, different combinations of alleles occurred in successive cross sections of the spermathecae of individual females, demonstrating that sperm deposits from different males were to some extent stratified within the spermathecae.

Paternity of pooled embryos was analyzed using both microsatellite loci. In each of the seven clutches, only three or four alleles were observed. Maternal alleles (usually two) were always observed in the progeny, while the remaining one or two alleles represented paternal genotypes (Tables 2 and 3). The results suggested that each brood had been sired by a single male. In each case, the paternal alleles seen in the offspring were also present in one or several sections of the spermatheca. The only exception was observed for female A5 at locus Cop24-3, where the 190 base pair (bp) paternal allele seen in the progeny was absent from the spermathecal cross sections. The analysis at locus Cop3-4 revealed that the paternal genotype (homozygote for the 254-bp allele) was present in spermathecal cross sections 1 and 2 but weakly amplified. This indicated that little sperm of the father was left in the spermatheca and suggested that the PCR failed to amplify the paternal genotype at locus Cop24-3. Instead, it must have amplified more abundant genotypes that shared at random the 174-bp allele with the paternal genotype. Alternatively, the presence of the 190-bp allele at locus Cop24-3 in the progeny of female A5 could be the result of a maternal mutation due to strand slippage during DNA replication, leading to the addition of one GACA repeat to the 186-bp maternal allele. In such a case, the father of the progeny would have been homozygote for the 174-bp allele.

The distribution of the paternal alleles within the spermathecae showed that the genotypes of the fathers of the embryos were often present in more than one cross section. However, the paternal alleles were represented mostly in the cross sections towards the dorsal end (blind end) of the spermathecae (i.e., first and second). This pattern can be seen in Fig. 2*b* with female A17, where the 218, 202, and 174 bp alleles observed in the embryos are shared with those of the mother (202 and 174 bp) and those in cross section 1 of the spermatheca (218 and 202 bp). Only three alleles were present in the progeny, since the 202 bp allele was shared between the parental genotypes.

Discussion

Histology revealed that spermathecal contents of primiparous females were composed of more or less discrete units ordered sequentially along the longitudinal axis of the spermatheca. The agreement between the number of such units and the number of copulations recorded for individual laboratory-mated females strongly suggests that they represented individual ejaculates. Furthermore, each individual unit was organized into a cluster of spermatophores usually capped dorsally by amorphous matter. This observation is consistent with reports stating that during ejaculation, male brachyurans first pass a relatively large volume of seminal plasma (i.e., the amorphous matter) followed by a relatively small volume of spermatophores (Ryan 1967; Diesel 1991). The units observed in the spermathecae of snow crab are similar to those seen in the majiid *I. phalangium*, which were also interpreted to be individual ejaculates (Diesel 1989, 1990).

Our results confirm the polyandrous nature of female snow crab during their first breeding period. As was the case in the study by Sainte-Marie et al. (1997), laboratory-mated females copulated several times with the same or different

© 1998 NRC Canada

males (Table 1). Wild-caught primiparous females had also copulated with at least three to five different mates (Table 4) which demonstrates that polyandry is not a laboratory artifact. There were some discrepancies between the number of ejaculates determined by histology and the number of male genotypes determined by microsatellite analysis (Tables 1 and 4). At least two natural causes could account for these differences. Delivery of sperm to left and right spermathecae can exceptionally be unbalanced (Sainte-Marie and Lovrich 1994; Sainte-Marie et al. 1997), which could give rise to different estimates of the number of sperm deposits based on histological and genetic analyses using alternative spermathecae. In the specific case of four wild-caught primiparous females, there were more ejaculates than genotypes, which might reflect repeated copulations with the same mate as often occurs in the laboratory (Sainte-Marie et al. 1997). However, the differences between genetic and histological data could also reflect some methodological limitations. First, some difficulties were encountered in resolving small ejaculates by histology. Second, the sperm used for genetic analysis was that obtained solely from the spermathecae. Any sperm present elsewhere in the female reproductive organs would not have been included in the genetic analysis. Third, our calculation of the least number of male genotypes per spermatheca could underestimate the real number of genotypes, depending on the degree of random allele sharing between males.

From the genetic analysis of the embryos of both laboratory and wild-caught primiparous females, it can be inferred that a single mate (of at least two) fathered most or all of the progeny of each primiparous female. Because we analyzed pooled embryos from each clutch, we cannot completely exclude the possibility that a minor fraction of the eggs of each female were fertilized by the sperm of competing mates. However, this seems unlikely for two reasons. First, PCR detected maternal alleles in some spermathecal cross sections, possibly due to the occurrence of desquamated epithelial cells originating from the spermatheca wall (Beninger et al. 1993; Sainte-Marie and Sainte-Marie 1998). Since we carefully peeled away the spermathecal wall, the maternal signal was probably caused by small quantities of tissues which suggests that our PCR detection procedure was very sensitive. Second, the analysis of 20 individual eggs containing well-developed embryos (i.e., about a year older than the eggs used in this study) from each of five multiply-inseminated wild primiparous females also revealed single paternity (N. Urbani, unpublished data). Thus, the paternity contribution of another male would be <5%.

The controlled laboratory experiments indicated that the last male to inseminate a female before oviposition gains paternity of the clutch. Considering (*i*) that the mass of spermathecal contents was positively correlated with total female copulatory time (also see Sainte-Marie et al. 1997), (*ii*) that ejaculates were sequentially ordered within the spermatheca, such that only one ejaculate was located close to the oviduct opening, and (*iii*) that the spermathecae contained sperm from every unsuccessful male predecessor, the most parsimonious mechanism to explain last-male sperm precedence in primiparous females is sperm stratification, i.e., displacement of rival sperm towards the blind end of the spermatheca where there is no access to unfertilized eggs. Seminal plasma is indeed thought to act as an internal sperm plug (Christy 1987; Diesel 1990) and, in the short term at least, it may be effective in sealing off sperm from rival males. Although we cannot completely exclude the possibility that males can extract some previously deposited sperm using their gonopods, as proposed by Beninger et al. (1991), that possibility seems quite remote considering the evidence above. Moreover, male gonopods appear to be only shallowly inserted into the female vagina, and there is no perceptible rocking motion of the male's abdomen (Sainte-Marie et al. 1997), as occurs, for example, in male odonates that extract rival sperm (Miller 1995). Since sperm from competing males obviously persisted in the spermathecae of female snow crab in relatively large amounts, the failsafe mechanism leading to last-male precedence must be rival sperm stratification and positional advantage of parental sperm.

The observation for wild-caught females that paternal sperm occurred in the most dorsal cross section(s) of spermathecal contents suggests that females remated after extruding their eggs. Such a behavior often occurs in the laboratory (Sainte-Marie et al. 1997) and has been observed directly in the field (B. Sainte-Marie, unpublished data). In nature, males are attracted to females up to 8–13 days prior to their maturity molt by semiochemicals released in the water (Bouchard et al. 1996). Over this period of time, male competition for females can be very intense and dominant males may gradually displace subordinate males (Sainte-Marie and Hazel 1992). In the genus *Chionoecetes*, male dominance is a complex function of maturity, body size, chela size, shell condition, and time elapsed since last molt (Stevens et al. 1993; Paul et al. 1995; Elner and Beninger 1995; Sainte-Marie et al. 1997). A dominant male may assist a female in molting, promptly inseminate her, and then guard her until she extrudes her eggs. Females are then released, and since they may remain attractive and receptive to males for several days after the maturity molt (Watson 1972), they may mate again. We hypothesize that these ulterior matings occur with subordinate males. While these males would have no immediate reward, their sperm might be mobilized to fertilize a second egg clutch in the event that females do not remate.

In conclusion, two mechanisms can lead to single paternity in primiparous female snow crab. The first is behavioral, through insemination and complete control of a virgin female by a dominant male until oviposition is completed. The second, which can operate to ensure single paternity in previously inseminated females, is mechanical and consists of stratification (displacement) of rival sperm, resulting in a positional advantage of the most recently deposited sperm.

Acknowledgments

This research was supported by a grant from the Natural Sciences and Engineering Research Council of Canada to U. Kuhnlein. The authors wish to thank G. Sainte-Marie for the preparation and interpretation of histological slides, P. Kuhnlein for help with the DNA extractions, É. Parent for useful technical advice, and Drs. S. Aggrey, P.G. Beninger, and F. Hayes and an anonymous referee for helpful comments on the manuscript.

© 1998 NRC Canada

References

Adams, A.E., and Paul, A.J. 1983. Male parent size, sperm storage and egg production in the crab *Chionoecetes bairdi* (Decapoda, Majidae). Int. J. Invertebr. Reprod. **6**: 181–187.

Avise, J.C. 1994. Individuality and parentage. *In* Molecular markers, natural history and evolution. *Edited by* J.C. Avise. Chapman and Hall, New York, London. pp. 141–190.

Beninger, P.G., Elner, R.W., Foyle, T.P., and Odense, P.H. 1988. Functional anatomy of the male reproductive system and the female spermatheca in the snow crab *Chionoecetes opilio* (O. Fabricius) (Decapoda: Majidae) and a hypothesis for fertilisation. J. Crustacean Biol. **8**: 322–332.

Beninger, P.G., Elner, R.W., and Poussart, Y. 1991. The gonopods of the majid crab *Chionoecetes opilio* (O. Fabricius). J. Crustacean Biol. **11**: 217–228.

Beninger, P.G., Lanteigne, C., and Elner, R.W. 1993. Reproductive processes revealed by spermatophore dehiscence experiments and by histology, ultrastructure, and histochemistry of the female reproductive system in the snow crab *Chionoecetes opilio* (O. Fabricius). J. Crustacean Biol. **13**: 1–16.

Birkhead, T.R., and Hunter, F.M. 1990. Mechanisms of sperm competition. Trends Ecol. Evol. **5**: 48–52.

Bouchard, S., Sainte-Marie, B., and McNeil, J.N. 1996. Indirect evidence indicates female semiochemicals release male precopulatory behaviour in the snow crab, *Chionoecetes opilio* (Brachyura, Majidae). Chemoecology, **7**: 39–44.

Bowcock, A., Osborne-Lawrence, S., Barnes, R, Chakravarti, A., Washington, S., and Dunn, C. 1993. Microsatellite polymorphism linkage map of human chromosome 13q. Genomics, **15**: 376–386.

Christy, J.H. 1987. Competitive mating, mate choice and mating associations of brachyuran crabs. Bull. Mar. Sci. **41**: 177–191.

Conan, G.Y., and Comeau, M. 1986. Functional maturity and terminal molt of male snow crab, *Chionoecetes opilio*. Can. J. Fish. Aquat. Sci. **43**: 1710–1719.

Diesel, R. 1989. Structure and function of the reproductive system of the symbiotic spider crab *Inachus phalangium* (Decapoda: Majidae): observations on sperm transfer, sperm storage, and spawning. J. Crustacean Biol. **9**: 266–267.

Diesel, R. 1990. Sperm competition and reproductive success in the decapod *Inachus phalangium* (Majidae): a male ghost spider crab that seals off rival's sperm. J. Zool. (Lond.), **220**: 213–223.

Diesel, R. 1991. Sperm competition and the evolution of mating behavior in Brachyura, with special reference to spider crabs (Decapoda: Majidae). *In* Crustacean sexual biology. *Edited by* R.G. Bauer and J.W. Martin. Columbia University Press, New York. pp. 145–163.

Elner, R.W., and Beninger, P.G. 1992. The reproductive biology of snow crab, *Chionoecetes opilio*: a synthesis of recent contributions. Am. Zool. **32**: 524–533.

Elner, R.W., and Beninger, P.G. 1995. Multiple reproductive strategies in snow crab, *Chionoecetes opilio*: physiological pathways and behavioral plasticity. J. Exp. Mar. Biol. Ecol. **193**: 93–112.

Koga, T., Henmi, Y., and Murai, M. 1993. Sperm competition and the assurance of underground copulation in the sand-bubbler crab *Scopimera globosa* (Brachyura: Ocypodidae). J. Crustacean Biol. **13**: 134–137.

Langeron, M. 1949. Précis de microscopie, Tome 1. Masson, Paris.

Miller, P.L. 1995. Sperm competition and penis structure in some libellulid dragonflies (Anisoptera). Odonatologica, **24**: 63–72.

Parker, G.A. 1970. Sperm competition and its evolutionary consequences in the insects. Biol. Rev. **45**: 525–567.

Paul, A.J., Adams, A.E., Paul, J.M, and Feder, H.H. 1983. Some aspects of the reproductive biology of the crab *Chionoecetes bairdi*. Univ. Alaska Sea Grant Rep. 83-1.

Paul, A.J., Paul, J.M, and Donaldson, W.E. 1995. Shell condition and breeding success in Tanner crabs. J. Crustacean Biol. **15**: 476–480.

Rubenstein, D.I. 1989. Sperm competition in the water strider, *Gerris remigis*. Anim. Behav. **38**: 631–636.

Ryan, E.P. 1967. Structure and function of the reproductive system of the crab *Portunus sanguinolentus* (Herbst) (Brachyura: Portunidae). I. The male system. *In* Proceedings of the Symposium on Crustacea, Ernakulam. Part III. Mar. Biol. Assoc. India. Bangalore Press, Bangalore, India. pp. 506–521.

Sainte-Marie, B., and Carrière, C. 1995. Fertilization of the second clutch of snow crab, *Chionoecetes opilio*, mated once or twice after their molt to maturity. Fish. Bull. U.S. **93**: 758–763.

Sainte-Marie, B., and Hazel, F. 1992. Moulting and mating of snow crabs, *Chionoecetes opilio* (O. Fabricius), in shallow waters of the northwestern Gulf of Saint Lawrence. Can. J. Fish. Aquat. Sci. **49**: 1282–1293.

Sainte-Marie, B., and Lovrich, G.A. 1994. Delivery and storage of sperm at first mating of female *Chionoecetes opilio* (Brachyura, Majidae) in relation to size and morphometric maturity of male parent. J. Crustacean Biol. **14**: 508–521.

Sainte-Marie, B., Sévigny, J.-M., and Gauthier, Y. 1997. Laboratory behavior of adolescent and adult males of the snow crab *Chionoecetes opilio* mated noncompetitively and competitively with primiparous females (Brachyura: Majidae). Can. J. Fish. Aquat. Sci. **54**: 239–248.

Sainte-Marie, G., and Sainte-Marie, B. 1998. Morphology of the spermatheca, oviduct, intermediate chamber and vagina of the adult snow crab (*Chionoecetes opilio*). Can. J. Zool. **76**.

Sambrook, J., Fritsch, E., and Maniatis, T. 1989. Molecular cloning: a laboratory manual. 2nd ed. Cold Spring Harbor Laboratory, Cold Spring Harbor, N.Y.

Sévigny, J.-M., and Sainte-Marie, B. 1996. Electrophoretic data support the last-male sperm precedence hypothesis in the snow crab, *Chionoecetes opilio* (Brachyura: Majidae). J. Shellfish Res. **15**: 437–440.

Smith, R.L. 1979. Repeated copulation and sperm precedence: paternity assurance for a male brooding water bug. Science (Washington, D.C.), **205**: 1029–1031.

Stevens, B.G., Donaldson, W.E., Haaga, J.A., and Munk, J.E. 1993. Morphometry and maturity of paired tanner crabs, *Chionoecetes bairdi*, from shallow and deepwater environments. Can. J. Fish. Aquat. Sci. **50**: 1504–1516.

Taylor, D.M., Hooper, R.G., and Ennis, G.P. 1985. Biological aspects of the spring breeding migration of snow crabs, *Chionoecetes opilio*, in Bonne Bay, Newfoundland (Canada). Fish. Bull. U.S. **83**: 707–711.

Urbani, N. 1998. Microsatellite DNA analysis of the mating system during the first breeding period of the female snow crab *Chionoecetes opilio* (Brachyura, Majidae). Ph.D. thesis, McGill University, Montreal, Canada.

Urbani, N., Sévigny, J.-M., Sainte-Marie, B., Zadworny, D., and Kuhnlein, U. 1998. Identification of microsatellite markers in the snow crab *Chionoecetes opilio*. Mol. Ecol. **7**: 357–358.

Verheyen, G.R., Kempenaers, B., Burke, T., Van den Broeck, M., Van Broeckhoven, C., and Dhondt, A. 1994. Identification of hypervariable single locus minisatellite DNA probes in the blue tit *Parus caeruleus*. Mol. Ecol. **3**: 137–143.

Waage, J.K. 1979. Dual function of the damselfly penis: sperm removal and transfer. Science (Washington, D.C.), **203**: 916–918.

Watson, J. 1972. Mating behavior in the spider crab, *Chionoecetes opilio*. J. Fish. Res. Board Can. **29**: 447–449.

© 1998 NRC Canada

Biomagnification and bioaccumulation of mercury in an arctic marine food web: insights from stable nitrogen isotope analysis

Lisa Atwell, Keith A. Hobson, and Harold E. Welch

Abstract: Several recent studies have shown that the use of $\delta^{15}N$ analysis to characterize trophic relationships can be useful for tracing biocontaminants in food webs. In this study, concentration of total mercury was measured in tissues from 112 individuals representing 27 species from the arctic marine food web of Lancaster Sound, Northwest Territories. Samples ranged from particulate organic matter through polar bears (*Ursus maritimus*). Using $\delta^{15}N$ values to identify trophic position, we found that total mercury in muscle tissue biomagnified in this food web. Polar bears were a notable exception, having a lower mean mercury concentration than their main prey, ringed seals (*Phoca hispida*). Most vertebrates showed greater variance in mercury concentration than invertebrates, and there was a trend in seabirds toward increased variability in mercury concentration with trophic position. Within species, we found no evidence of bioaccumulation of mercury with age in the muscle tissue of clams (*Mya truncata*) or ringed seals. Because stable nitrogen isotopes illustrated the relationship in this biome between trophic position and mercury level on a continuous, quantitative scale, we were able to determine that $\log_{10}$[Hg] (μg/g dry weight) = $0.2(\delta^{15}N) - 3.3$. The measurement of $\delta^{15}N$ values and mercury concentration allowed us to quantitatively assess mercury biomagnification within this extensive arctic marine food web.

Résumé : Plusieurs études récentes ont montré que l'utilisation d'une analyse du $\delta^{15}N$ pour caractériser les relations trophiques peut être utile pour suivre les biocontaminants dans les réseaux trophiques. Dans la présente étude, nous avons mesuré la concentration totale du mercure dans les tissus de 112 individus représentant 27 espèces appartenant au réseau trophique marin arctique du détroit de Lancaster, dans les Territoires du Nord-Ouest. Les échantillons allaient de particules de matière organique à des tissus prélevés sur des ours blancs (*Ursus maritimus*). En nous servant des valeurs de $\delta^{15}N$ pour déterminer la position trophique, nous avons mis en évidence une bioamplification de la teneur en mercure total dans les tissus musculaires dans ce réseau trophique. Les ours blancs constituaient une exception notable, car leurs tissus avaient une concentration moyenne en mercure plus faible que ceux de leur principale proie : le phoque annelé (*Phoca hispida*). Les concentrations de mercure notées chez la plupart des vertébrés ont montré une variance supérieure à celles obtenues pour les invertébrés; et on a observé chez les oiseaux marins une tendance à une variabilité accrue de la concentration de mercure en fonction de la position trophique. Au sein d'une espèce, nous n'avons trouvé aucune preuve de bioamplification du mercure en fonction de l'âge dans les tissus musculaires de la mye tronquée (*Mya truncata*) ou du phoque annelé. Puisque les isotopes stables de l'azote illustraient dans ce biome la relation entre la position trophique et la teneur en mercure selon une échelle quantitative continue, nous avons pu déterminer que $\log_{10}$[Hg] (μg/g de poids sec) = $0{,}2(\delta^{15}N) - 3{,}3$. La mesure des valeurs de $\delta^{15}N$ et de la teneur en mercure nous a permis d'évaluer quantitativement la bioamplification du mercure dans ce vaste réseau trophique marin arctique.
[Traduit par la Rédaction]

Introduction

Previous studies investigating the potential for mercury to biomagnify progressively through higher trophic levels of food webs have produced varied results. While several researchers have found evidence for biomagnification of mercury with trophic level (e.g., Riisgard and Hansen 1990; Futter 1994; Jarman et al. 1996), others have found no such relationship (Williams and Weiss 1973; Wagemann and Muir 1984). Disagreement in findings may be due, in part, to the difficulty of accurately characterizing trophic structure in complex food webs. Traditional methods of assessing trophic position have depended largely on inferred feeding behaviour or stomach content analysis (Rowan and Rasmussen 1992; Futter 1994). These methods can be limited, since they usually provide only a "snapshot" of feeding habits for a particular season, life

Received April 8, 1997. Accepted December 23, 1997.
J13956

L. Atwell. Department of Biology, University of Saskatchewan, Saskatoon, SK S7N 0W0, Canada.
K.A. Hobson.[1] Department of Biology, University of Saskatchewan, Saskatoon, SK S7N 0W0, Canada, and Canadian Wildlife Service, Prairie and Northern Wildlife Research Centre, 115 Perimeter Rd., Saskatoon, SK S7N 0X4, Canada.
H.E. Welch. Department of Fisheries and Oceans, Freshwater Institute, 501 University Crescent, Winnipeg, MB R3T 2N2, Canada.

[1] Author for correspondence at Canadian Wildlife Service, Prairie and Northern Wildlife Research Centre, 115 Perimeter Rd., Saskatoon, SK S7N 0X4, Canada. e-mail: Keith.Hobson@ec.gc.ca

© 1998 NRC Canada

history stage, or location. These snapshots may not necessarily reflect an organism's long-term feeding habits, which can ultimately influence its contaminant load. Changes in diets and varying degrees of omnivory in consumers can also confound the process of accurately assessing trophic position (e.g., Rowan and Rasmussen 1992; Futter 1994).

The measurement of stable isotopes of nitrogen ($^{15}N/^{14}N$) has recently become useful as an alternative method to characterize trophic level (reviewed by Michener and Schell 1994). Enrichment (i.e., an increase in relative abundance of ^{15}N) on the order of 3–5‰ generally occurs at each trophic transfer (DeNiro and Epstein 1981; Minagawa and Wada 1984; Hobson and Welch 1992). Measurement of the relative abundance of ^{15}N in organisms provides a continuous variable, then, by which trophic position can be *quantitatively* assessed. This method offers a useful alternative for characterizing food web structure because it is a time-integrated measure of dietary components and therefore not subject to the same temporal bias as stomach content analysis (DeNiro and Epstein 1981; Tieszen et al. 1983; Hobson and Clark 1992) . Moreover, trophic positioning of organisms by stable nitrogen isotope analysis is based on assimilated (not just ingested) food, and trophic estimates can reflect dietary integrations over many meals, depending on the tissue analyzed (e.g., Tieszen et al. 1983). The time frame over which the $\delta^{15}N$ value of a tissue represents the trophic position of an organism depends on the tissue's specific rate of turnover (e.g., Hobson and Clark 1992). However, caution should be exercised when comparing $\delta^{15}N$ values between food webs, since baseline $\delta^{15}N$ values may vary from system to system (Cabana and Rasmussen 1996). Often, $\delta^{15}N$ values can only be interpreted relative to other organisms in the same food web, or by comparison with a species common to all food webs under observation.

Several recent studies have used stable nitrogen isotope measurements to describe the biomagnification of lipophilic contaminants in freshwater and marine ecosystems (Cabana and Rasmussen 1994; Kiriluk et al. 1995). Kidd et al. (1995*b*) concluded that the regression slope of the logarithmic concentration of total dichlorodiphenyltrichloroethane (ΣDDT), total hexachlorocyclohexane (ΣHCH), and total chlorinated bronanes (ΣCHB) versus $\delta^{15}N$ represented the degree of biomagnification in a subarctic lake. Broman et al. (1992) and Rolff et al. (1993) developed biomagnification models of polychlorinated dibenzo-*p*-dioxins (PCDD) and dibenzofurans (PCDF) for two Baltic marine food webs using $\delta^{15}N$ as a numerical representative of trophic position. Recently, Jarman et al. (1996) used $\delta^{15}N$ analysis to investigate the behaviour of both lipophilic and metal contaminants in the marine food web of the Californian Gulf of the Farallones. Their study illustrated that mercury was strongly associated with $\delta^{15}N$ and hence trophic level, indicating that mercury biomagnified in that food web. Kidd et al. (1995*a*) found a similar association between mercury and $\delta^{15}N$ in fish from several freshwater lakes in Canada.

Previous investigations in the Canadian Arctic have revealed mercury levels in biota to be higher than might be expected in pristine environments (Smith and Armstrong 1975; Wagemann et al. 1983). Some researchers have found mercury contamination in the Arctic to be highest in upper trophic level biota from northwestern regions (Norstrom et al. 1986; Braune et al. 1991). As there are practically no sources of industrial mercury in the arctic environment, geologic sources and atmospheric transport from developed regions appear to be the most likely origins of mercury in arctic marine food webs (e.g., Braune et al. 1991).

Recently, Hobson and Welch (1992) used stable isotopes of nitrogen to examine trophic relationships among organisms from the marine food web of Lancaster Sound, Northwest Territories. Here, we extend their findings by examining the relationship between $\delta^{15}N$, as an indicator of trophic position, and mercury levels in the tissues of a subsample of those organisms. The demonstration that $\delta^{15}N$ characterized the structure of this complex food web was used to explore the magnitude of mercury biomagnification in 112 individuals representing 27 different species ranging from particulate organic matter (POM) and algae through polar bears (*Ursus maritimus*). As well, mercury concentration in two long-lived species, clams (*Mya truncata*) and ringed seals (*Phoca hispida*), was examined for evidence of bioaccumulation with age. To our knowledge, this is the most extensive food web for which mercury biomagnification has been assessed quantitatively.

Materials and methods

Sample collection

From the previous collections of Hobson and Welch (1992), we obtained tissues from 11 species of invertebrates, two species of fish, eight species of marine birds, two species of toothed whales, walrus (*Odobenus rosmarus*), and polar bear (summarized in Table 1) for which $\delta^{15}N$ had been determined. All samples were from the region of Lancaster Sound and collected between 1988 and 1990 (see Hobson and Welch 1992 for a description of sampling methods). Additionally, clams and ringed seals were collected from the region of Barrow Strait in 1990 to examine whether mercury accumulated with age. Seal tissue and teeth were provided by local Inuit hunters from unsexed animals. Clams and seals were aged at the Freshwater Institute, Winnipeg, Manitoba, by counting annular growth rings on shells and teeth. Both $\delta^{15}N$ and mercury analyses were performed on muscle tissue, except for small (<5 mm) invertebrates, where whole bodies were used.

Stable isotope analysis

Subsamples of whole-body composites of small invertebrates and muscle tissue of vertebrates and large invertebrates were freeze-dried and powdered. Whole-body invertebrate samples had been treated with 2 N HCl and dried (60°C) without rinsing to remove carbonates (see Bunn et al. 1995). Lipids were extracted from all samples using a Soxhlet apparatus with chloroform solvent for 4–6 h. Samples were converted to ammonia by Kjeldahl reaction and then reacted with LiBrOH to produce N_2 gas (Porter and O'Dean 1977). $^{15}N/^{14}N$ was analyzed using a Micromass 602E mass spectrometer with an analytical error of ±0.3‰ (see Hobson and Welch 1992 for a complete description of the procedure).

Stable nitrogen isotope values are expressed in δ notation as parts per thousand difference from a standard by the following equation:

$$\delta X = [(R_{sample}/R_{standard}) - 1] \times 1000$$

where X is ^{15}N and R is the ratio $^{15}N:^{14}N$. For nitrogen, $R_{standard}$ is atmospheric (AIR) nitrogen.

Metal analysis

Samples were excised from inner muscle with acid-washed tools to minimize the possibility of mercury contamination. Following stable-isotope analysis and prior to mercury analysis, samples were

© 1998 NRC Canada

Table 1. Food web components of Lancaster Sound, N.W.T., used in this study, their mean $\delta^{15}N$ values (±SE), and their mean mercury concentration (±SE).

Species	*n*	$\delta^{15}N$ (‰)	Total [Hg] (μg/g dry weight)
POM	1	5.4	<0.02
Invertebrates			
Mya truncata	7	8.8±0.2	0.07±0.01
Hiatella arctica	5	9.1±0.7	0.15±0.02
Unidentified sea cucumber	3	9.5±0.5	0.04±0.00
Strongylocentrotus sp.	2	9.9	0.18
Calanus hyperboreus	3[a]	10.2±0.6	0.06±0.01
Macoma calcarea	1	10.3	0.09
Leptastarias sp.	3	11.2±0.1	0.05±0.01
Onisimus glacialis	1[a]	11.4	0.10
Parathemisto libellula	2[a]	11.6	0.06
Mertensia ovum	2[a]	14.0	0.07
Anenome urticina	1	14.4	0.06
Crossaster papposus	2	16.1	0.03
Fish			
Boreogadus saida	9	14.7±0.1	0.19±0.03
Icelus bicornis	4	16.0±0.4	0.24±0.04
Marine birds			
Alle alle	1	12.5	0.33
Somateria mollissima	3	13.5±0.0	0.38±0.02
Sterna paradisaea	3	14.2±0.4	0.83±0.21
Cepphus grylle	6	15.0±0.4	1.57±0.65
Fulmarus glacialis	5	15.4±0.2	0.75±0.23
Rissa tridactyla	6	15.8±0.3	1.93±1.14
Uria lomvia	4	16.4±0.1	1.79±0.78
Larus hyperboreus	4	16.7±0.2	1.86±0.68
Marine mammals			
Odobenus rosmarus	3	12.8±0.4	0.41±0.08
Monodon monoceros	2	15.9	2.32
Phoca hispida	20	16.4±0.2	1.07±0.11
Delphinapterus leucas	4	16.4±0.3	2.25±0.97
Ursus maritimus	5	19.6±0.5	0.84±0.17

[a]Composite samples of >5 individuals.

stored for about 1 year in glass vials rinsed with nitric acid. Mercury concentrations in tissues were determined by cold-vapour flameless atomic absorption spectrometry at the Freshwater Institute (Hendzel and Jamieson 1976). Samples were oxidized at 180°C with a mixture of nitric and sulfuric acids in a graduated digestion tube, brought to a constant volume with distilled water, and analyzed using an atomic absorption spectrophotometer fitted with a modified (pneumatic) sampler. This method is rapid, cost effective, and eliminates the possibility of sample loss or contamination during transfer. Results are reported as micrograms of total mercury per gram dry weight.

Statistics

Model II reduced major-axis regression was used to analyze the relationship between $\delta^{15}N$ and mercury concentration in the whole food web and within subgroups, since the variables are measured on different scales and neither can be measured without error (Sokal and Rohlf 1995). Model I linear regression was used to assess the significance of mercury concentration with seal and clam age. Analysis of variance (ANOVA) was used to examine differences in mean mercury concentrations among species. Residuals were visually inspected to ensure that normality and homogeneity of variance assumptions were not violated. In all cases, $p < 0.05$ was considered significant. All statistical procedures were performed using SYSTAT software (Wilkinson 1991).

Results

A summary of the species examined, their mean $\delta^{15}N$ values, and their mean total mercury concentrations is presented in Table 1. Average $\delta^{15}N$ values for muscle of species ranged from 8.8‰ in *Mya truncata* to 19.6‰ in polar bears. Mercury concentration in tissues was more variable than $\delta^{15}N$, but was lowest in sea cucumber (unidentified species, 0.04 ± 0.01 μg/g) and starfish (*Crossaster papposus* and *Leptasterias* sp., 0.04 ± 0.02 μg/g) and highest in narwhal (*Monodon monoceros*, 2.32 μg/g) and beluga whales (*Delphinapterus leucas*, 2.25 ± 0.97 μg/g).

Our $\delta^{15}N$ measurements illustrate the continuous enrichment of ^{15}N with trophic position from the filter-feeding clam *Mya truncata* to polar bear at the top of the arctic food chain (see Hobson and Welch 1992). Because an ^{15}N enrichment of 3–5‰ between organisms has been shown to denote one full

© 1998 NRC Canada

Fig. 1. Mean (±SE) mercury concentrations in muscle tissue of species from the arctic marine food web of Lancaster Sound, N.W.T. (Hobson and Welch 1992). Species are arranged from lowest to highest trophic position as indicated by $\delta^{15}N$. Squares, POM; open circles, invertebrates; triangles, fish; diamonds, birds; solid circles, mammals. Refer to Table 1 for $\delta^{15}N$ SE.

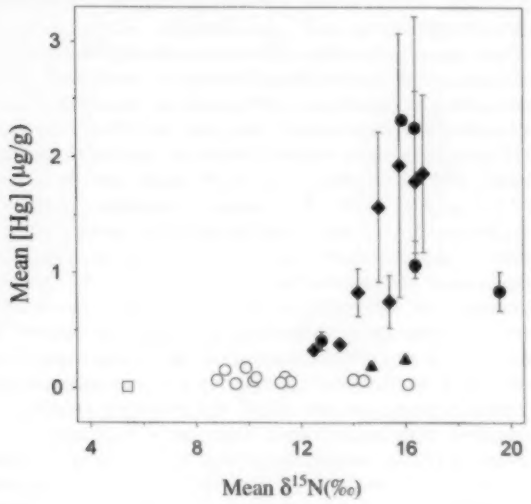

Fig. 2. Relationship between trophic level, determined by $\delta^{15}N$, and logarithm of mercury concentration in organisms from the arctic food web of Lancaster Sound, N.W.T. Squares, POM; open circles, invertebrates; triangles, fish; diamonds, birds; solid circles, mammals. Refer to Table 1 for $\delta^{15}N$ SE.

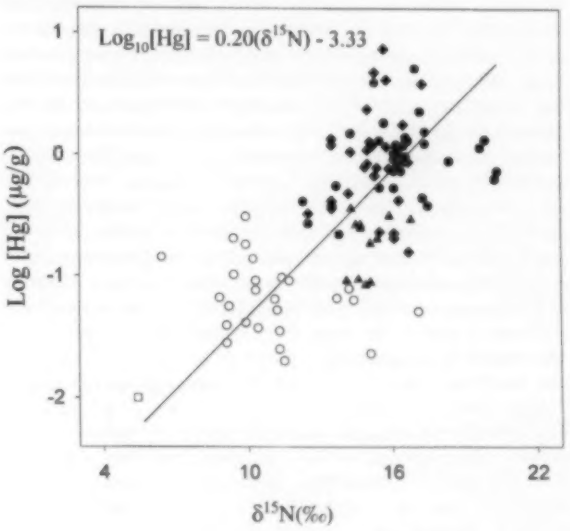

trophic level (Hobson and Welch 1992), the fine gradation of $\delta^{15}N$ values suggests extensive omnivory. However, an enrichment in ^{15}N of 3.4‰ (about one trophic step) was observed between POM and *Mya truncata*. Likewise, the enrichment of 3.2‰ between polar bear and its primary prey ringed seals also represents one trophic step.

Total mercury levels were quite variable. Interestingly, vertebrates showed notably more variation in mercury concentration in their tissues than did invertebrates (Fig. 1). We found a significant trend of increasing total mercury concentration with increasing trophic level through the food web (model II reduced major-axis regression; $\log_{10}[Hg]$ (µg/g) = $0.20(\delta^{15}N) - 3.33$) (Fig. 2).

Seabirds showed a clear pattern of ^{15}N enrichment with trophic level from largely planktivorous dovekies (*Alle alle*) to carnivorous glaucous gulls (*Larus hyperboreus*). Total mercury levels in bird muscle tissue increased in variance, but not in mean value, with increasing $\delta^{15}N$ (Fig. 1). Although there was no significant difference in total muscle mercury concentration among these seabird species (model II one-way ANOVA; $F = 0.424$, $p = 0.877$), lower trophic level seabirds (e.g., dovekie and eider (*Somateria mollissima*)) had mercury concentrations almost an order of magnitude lower (e.g., 0.33, 0.38 µg/g, respectively) than the two highest trophic position species, thick-billed murre (*Uria lomvia*) and glaucous gull (e.g., 1.79 and 1.86 µg/g, respectively).

Clams showed no significant linear relationship between age and muscle $\log_{10}[Hg]$ (model I regression; $r^2 = 0.003$, $p = 0.797$), even though the age range covered 42 years. Similarly, there was no statistically significant relationship between clam length and tissue mercury levels (model I regression; $r^2 = 0.005$, $p = 0.728$). Interestingly, we determined a marginally significant linear relationship between clam age and $\delta^{15}N$ (model I regression; $y = 0.05x + 7.65$, $r^2 = 0.491$, $p = 0.035$).

Ringed seals showed no correlation between age and the logarithm of total mercury concentration in muscle tissue (model I regression; $n = 17$, $r^2 = 0.160$, $p = 0.112$), although seals aged 0–1 year old had lower mean mercury levels (0.57±0.27 µg/g) than seals over 1 year old (1.31±0.45 µg/g). There was no significant change in $\delta^{15}N$ with age, suggesting that seals did not alter their diet as they aged (model I regression; $r^2 = 0.069$, $p = 0.325$). However, seals less than 1 year old had more variable $\delta^{15}N$ values (13.8–17.3‰, mean 15.9 ± 1.3‰) than older seals (14.3–17.4‰, mean 16.4 ± 0.9‰).

Discussion

The significant linear relationship between $\delta^{15}N$ values and total mercury concentration in organisms of this arctic marine food web indicate that an overall biomagnification of mercury occurred. We found the overall relationship between mercury and trophic position to be described by the model II regression equation $\log_{10}[Hg]$ (µg/g) = $0.20(\delta^{15}N) - 3.33$. The slope of this regression (i.e., 0.20) is an estimate of the biomagnification power of mercury in this food web and it is analogous to the term B in $Ae^{B\delta^{15}N}$ from Broman et al. (1992). $B > 0$ indicates that the transfer efficiency of a contaminant is greater than the biomass transfer efficiency (biomagnification), and $B < 0$ indicates a contaminant transfer efficiency less than that of the biomass transfer efficiency (Rolff et al. 1993).

The biomagnification power (0.20) of mercury observed in

© 1998 NRC Canada

this arctic marine food web is of similar magnitude to that observed in freshwater fishes (i.e., 0.2–0.3) from several lakes by Kidd et al. (1995*a*), who also determined trophic position using $\delta^{15}N$ values in muscle tissue. Kidd et al. (1995*a*) described mercury biomagnification in a subset of the food web (i.e., fishes) whereas the biomagnification power of 0.20 found in our study is the overall biomagnification of mercury through many groups (i.e., invertebrates, fish, birds, mammals). Our description of biomagnification does not reflect the potential of mercury to biomagnify in specific subsets of this food web. For example, invertebrates in our study, taken as a subset, showed no biomagnification with trophic position ($\log_{10}$[Hg] (μg/g) = $-0.04(\delta^{15}N) - 0.73$). Similarly, as reveiwed by Boudou and Ribeyre (1995), benthic invertebrate food webs in Swedish forest lakes did not biomagnify mercury, since detrivores had higher mercury levels than predatory invertebrates. This strongly suggests that there may be different transfer mechanisms occurring at different levels of the food web. Jarman et al. (1996) found the overall biomagnification power of mercury in the Gulf of the Farallones food web to be 0.32 (values in Jarman et al.'s (1996) table 2 converted from ln[Hg] to $\log_{10}$[Hg] for comparison with the results presented here). In Jarman et al.'s (1996) study, the Gulf of the Farallones food web was represented largely by marine birds which may assimilate mercury differently rate than metabolically less active organisms such as many invertebrates. It should be noted that Jarman et al. (1996) analyzed mercury concentration in a variety of tissues, including egg albumen, and their results may not be directly comparable with our findings based on muscle tissue. Boudou and Ribeyre (1995) suggested that omnivory or differences in metabolic rate or feeding ecology may influence the trophic transfer of mercury.

Mean mercury levels and $\delta^{15}N$ values of species showed a trend of increasing variability in mercury levels with increasing trophic position. In general, vertebrates had wider ranges of mercury concentrations in their tissues than did invertebrates (Fig. 1). Higher trophic level organisms are more likely to be migratory and to have larger foraging ranges than low trophic level organisms. Thus, among high trophic levels, individuals of the same species may encounter quite different levels of dietary mercury during certain seasons, or even during individual foraging excursions.

Mercury concentration among eight arctic seabird species showed notably more variation in upper trophic position birds. Although differences in mean mercury levels among species were not statistically significant, the dovekie and eiders at the lowest trophic levels had mercury levels almost an order of magnitude lower than the highest trophic level birds (gulls, murres, and black-legged kittiwakes). Birds incorporate mercury into feathers (e.g., Thompson et al. 1992), and Furness et al. (1986) suggested that feather moult reduces mercury body burdens through the loss of mercury bound to feather keratin (see also Thompson et al. 1991). Mercury sequestered in plumage may account for up to 93% of the total body burden (Braune and Gaskin 1987), and regular elimination of mercury during moult may reduce interspecific differences in accumulated mercury. Alternatively, mercury levels in seabirds may be more influenced by age than by trophic position. For example, Särkkä et al. (1978) found differences in total mercury content between muscle tissue of juvenile and adult aquatic bird species from a large lake in Finland. As well, Dietz et al. (1990) found a wide range of mercury concentrations in arctic marine birds in Greenland. However, both Hutton (1981) and Thompson et al. (1991) found no evidence of mercury accumulation with age in several seabird species and suggested that individual diet was the important factor affecting variability of mercury levels in soft tissues.

Polar bears had a mean $\delta^{15}N$ value 3.2‰ higher than their main prey, ringed seals. Mercury levels in polar bears, however, were generally lower than in ringed seals. Polar bears preferentially consume seal skin and fat (Norstrom et al. 1986) which, in many marine mammals, are low in mercury content relative to other tissues (Sergeant and Armstrong 1973; Muir et al. 1988). Polar bears are therefore exposed to less dietary mercury than other animals that consume whole bodies, or mostly muscle, of their prey. Muscle tissue contains more of the body burden of mercury than other tissues, including liver which has a higher concentration, because muscle is relatively more abundant (see Pentreath 1976*a*). As well, Dietz et al. (1990) noted the unusually high capacity of polar bear kidneys for storing mercury and suggested that this caused their blood mercury levels, and therefore muscle mercury levels, to be lower than in other marine mammals.

While previous studies suggest that mercury levels tend to be greater in tissues of higher trophic level organisms (e.g., Riisgard and Hansen 1990; Futter 1994), it is unclear to what extent this is a result of biomagnification through the food web or bioaccumulation within organisms over time. This can be difficult to discern, as higher trophic level organisms tend to be longer lived and therefore have more potential for accumulating mercury in their tissues. Some authors have suggested that mercury accumulates with age (e.g., Dietz et al. 1990; Wagemann et al. 1990) and that the food chain accounts for very little magnification of mercury (Williams and Weiss 1973), but we find no such evidence in either clams (age ranging over 42 years) or ringed seals (age ranging over 24 years). This discrepancy is possibly due to the type of tissue chosen for analysis. In marine mammals, mercury concentration in liver tissue is up to two orders of magnitude higher than in muscle (e.g., Sergeant and Armstrong 1973). Mercury also accumulates over time more readily in liver than in muscle, but experiments with rainbow trout (*Oncorhynchus mykiss*) indicate that muscle appears to retain the mercury burden for a much longer period during depuration (Boudou and Ribeyre 1995). Thus, liver may provide information only on short-term exposure to mercury or may accumulate mercury only when an organism is exposed to constant or increasing levels of dietary mercury. Smith and Armstrong (1975) found a weak, but inconsistent correlation of total mercury with age in muscle of ringed seals, and Wagemann et al. (1990) found no correlation between muscle mercury levels and age in beluga whales from the Canadian Arctic. However, Honda et al. (1983) observed that levels of total mercury in muscle tissue of striped dolphins (*Stenella coeruleoalba*) reached a plateau around 15 years of age.

There does not appear to be strong evidence that mercury accumulates in muscle tissue with age; however, for seals, this may be confounded by the fact that reproductive females reduce their toxicant loads during pregnancy and nursing (Wagemann et al. 1988; André et al. 1990). Small amounts of

© 1998 NRC Canada

mercury may be passed through milk while the pup is nursing during the first 5–7 weeks. However, the amount of mercury ingested with milk is not enough to account for the levels of mercury found in pup tissues (Wagemann et al. 1988). Milk is extremely high in fat, and mercury is found in relatively low levels in lipids (Sergeant and Armstrong 1973; Wagemann et al. 1983), so this is not likely to be a major pathway for mercury transfer. Alternatively, mercury transfer can occur during gestation between mother and fetus as methyl mercury (i.e., organic mercury) readily passes across the placental barrier (Jernelov 1986). This may result in increased pup mercury levels, with concurrent decreases in body burden of the mother. Honda et al. (1983) attributed a relatively wide variation of mercury levels in female striped dolphins of reproductive age to parturition and lactation.

Young-of-the-year seals displayed greater variability in $\delta^{15}N$ values (mean 15.9 ± 1.3‰) and lower mean mercury levels (0.57 ± 0.27 μg/g) than seals older than 1 year (16.4 ± 0.9‰ and 1.31 ± 0.45 μg/g, respectively). A decrease in $\delta^{15}N$ may occur upon weaning when the diet shifts from milk (i.e., same trophic level as adult seals) to fish, amphipods, euphausiids, and crustaceans, all at lower trophic positions (e.g., Hobson and Welch 1992). Mercury concentrations in muscle tissue of young seals may decrease after birth as the proportion of maternally derived fetal tissue decreases relative to diet-derived tissue. As well, ringed seals reach about 70% of adult length by age 1 (Frost and Lowry 1981), and this rapid rate of growth with no concomitant increase in dietary exposure to mercury may physically "dilute" mercury taken up through the diet (Boudou and Ribeyre 1995).

Clams did not show a significant accumulation of mercury with age or with size. However, an unexpected finding was the marginally significant correlation between age and $\delta^{15}N$ of clams. This suggests perhaps some physiological shift in food assimilation with age, or a change in the size and relative trophic position of particles filtered by larger clams. Conversely, Minagawa and Wada (1984) found $\delta^{15}N$ to be independent of age in two species of marine mussels up to about 8 years old. Again, further analysis of this relationship would be useful.

In this study, total concentrations of mercury were measured, but it should be noted that organic and inorganic species of mercury have very different dynamics within a food web. Most mercury present in seawater is in the inorganic form (Pentreath 1976*b*); however, benthic invertebrates take up organic mercury much more readily than inorganic mercury (Riisgard and Hansen 1990). Fish take up mercury directly from seawater (Pentreath 1976*b*) as well as diet (Riisgard and Hansen 1990) and show high concentrations of organic mercury in muscle tissue relative to both diet and seawater (Riisgard and Hansen 1990). Aquatic birds have also been found to have very high ratios of organic to inorganic mercury in muscle tissue (up to 100%, Särkkä et al. 1978; Thompson et al. 1991), and most mercury in marine mammal muscle is organic (Dietz et al. 1990). However, the ratio of organic to inorganic mercury in liver of fish (Pentreath 1976*a*), birds (Thompson et al. 1991; but see Thompson and Furness 1989), and marine mammals (e.g., Dietz et al. 1990) is low, relative to muscle tissue, and to overall body burdens in prey. Demethylation occurs in the liver, and so, it is the less toxic inorganic form that is sequestered in this organ; however, no mechanism has been found (Smith and Armstrong 1975 (seals); Thompson and Furness 1989 (birds); Dietz et al. 1990 (polar bears)).

Our $\delta^{15}N$ values in tissues from a broad range of arctic marine animals described their trophic position quantitatively on a continuous scale. Such an illustration of trophic positioning allowed for a more detailed account of the relationship between mercury and trophic position for this extensive food web. Mercury increased with trophic position at an overall biomagnification power of 0.20, and we did not find evidence that mercury accumulation in muscle tissue was linked with age. These findings indicate that total mercury burdens in muscle tissue are a result of biomagnification through the food web rather than bioaccumulation. Further studies on the dynamics of both organic and inorganic mercury would improve our understanding of mercury behaviour in food webs, and future work should concentrate on using the stable-isotope method to further explore the behaviour of both species of mercury.

Acknowledgements

We thank the Polar Continental Shelf Program for logistical support. Financial support to K.A.H. was provided by the Science Institute of the Northwest Territories, the Northern Studies Training Program, a Natural Sciences and Engineering Research Council of Canada (NSERC) Postgraduate Scholarship, and a University of Saskatchewan Graduate Fellowship. Stable-isotope analyses were conducted at the laboratory of Chris van Kessel, Department of Soil Sciences, University of Saskatchewan, Saskatoon, Sask., and mercury analyses were performed at the laboratory of Robert Hunt at the Freshwater Institute, Winnipeg, Man. We also thank Carolyn Ranson for assistance with mercury sample preparation and two anonymous reviewers for valuable comments on an earlier draft of this manuscript.

References

André, J.M., Ribeyre, F., and Boudou, A. 1990. Mercury contamination levels and distribution in tissues and organs of delphinids (*Stenella attenuata*) from the eastern tropical Pacific, in relation to biological and ecological factors. Mar. Environ. Res. **30**: 43–72.

Boudou, A. and Ribeyre, F. 1995. Mercury in the food web: accumulation and transfer mechanisms. *In* Metal ions in biological systems. *Edited by* A. Sigel and H. Sigel. Marcel Dekker, Inc., New York. pp. 289–319.

Braune, B.M., and Gaskin, D. 1987. Mercury levels in Bonaparte's gull (*Larus philadelphia*) during autumn moult in the Quoddy region, New Brunswick, Canada. Arch. Environ. Contam. Toxicol. **16**: 539–549.

Braune, B.M., Norstrom, R.J., Wong, M.P., Collins, B.T., and Lee, J. 1991. Geographical distribution of metals in livers of polar bears from the Northwest Territories, Canada. Sci. Total Environ. **100**: 283–299.

Broman, D., Näf, C., Rolff, C., Zebühr, Y., Fry, B., and Hobbie, J. 1992. Using ratios of stable nitrogen isotopes to estimate bioaccumulation and flux of polychlorinated dibenzo-*p*-dioxins (PCDDs) and dibenzofurans (PCDFs) in two food chains from the Northern Baltic. Environ. Toxicol. Chem. **11**: 331–345.

Bunn, S.E., Loneragan, N.R., and Kempster, M.A. 1995. Effects of acid washing on stable isotope ratios of C and N in penaeid shrimp and seagrass: implications for food-web studies using multiple stable isotopes. Limnol. Oceanogr. **40**: 622–625.

© 1998 NRC Canada

Cabana, G., and Rasmussen, J.B. 1994. Modelling food chain structure and contaminant biomagnification using stable nitrogen isotopes. Nature (Lond.), **372**: 255–257.

Cabana, G., and Rasmussen, J.B. 1996. Comparison of aquatic food chains using nitrogen isotopes. Proc. Natl. Acad. Sci. U.S.A. **93**: 10 844 – 10 847.

DeNiro, M.J., and Epstein, S. 1981. Influence of diet on the distribution of nitrogen isotopes in animals. Geochim. Cosmochim. Acta, **45**: 341–351.

Dietz, R., Nielsen, C.O., Hansen, M.M., and Hansen, C.T. 1990. Organic mercury in Greenland birds and mammals. Sci. Total Environ. **95**: 41–51.

Frost, K., and Lowry, L. 1981. Ringed, Caspian, and Baikal seals. *In* Handbook of marine mammals. Vol. 2. *Edited by* S. Ridgway and R. Harrison. Academic Press, New York. pp. 29–54.

Furness, R.W., Muirhead, S.J., and Woodburn, M. 1986. Using bird feathers to measure mercury in the environment: relationship between mercury content and moult. Mar. Pollut. Bull. **17**: 27–30.

Futter, M.N. 1994. Pelagic food-web structure influences probability of mercury contamination in lake trout (*Salvelinus namaycush*). Sci. Total Environ. **145**: 7–12.

Hendzel, M.R., and Jamieson, D.M. 1976. Determination of mercury in fish. Anal. Chem. **48**: 926–928.

Hobson, K.A., and Clark, R.G. 1992. Assessing avian diets using stable isotopes I: turnover of ^{13}C in tissues. Condor, **94**: 181–188.

Hobson, K.A., and Welch, H.E. 1992. Determination of trophic relationships within a high Arctic marine food web using $\delta^{13}C$ and $\delta^{15}N$ analysis. Mar. Ecol. Prog. Ser. **84**: 9–18.

Honda, K., Tatsukawa, R., Itano, K., Miyazaki, N., and Fujiyama, T. 1983. Heavy metal concentrations in muscle, liver and kidney tissue of striped dolphin, *Stenella coeruleoalba*, and their variations with body length, weight, age and sex. Agric. Biol. Chem. **47**: 1219–1228.

Hutton, M. 1981. Accumulation of heavy metals and selenium in three seabird species from the United Kingdom. Environ. Pollut. **26**: 129–145.

Jarman, W.M., Hobson, K.A, Sydeman, W.J., Bacon, C.E., and McLaren, E.B. 1996. Influence of trophic position and feeding location on contaminant levels in the Gulf of the Farallones food web revealed by stable isotope analysis. Environ. Sci. Technol. **30**: 654–660.

Jernelov, A. 1986. Ecological and human health effects of mercury. FAO Fish. Rep. No. 325. pp. 111–116.

Kidd, K.A., Hesslein, R.H., Fudge, R.J.P., and Hallard, K.A. 1995*a*. The influence of trophic level as measured by $\delta^{15}N$ on mercury concentration in freshwater organisms. Water Air Soil Pollut. **80**: 1011–1015.

Kidd, K.A., Schindler, D.W., Hesslein, R.H., and Muir, D.C.G. 1995*b*. Correlation between stable nitrogen isotope ratios and concentrations of organochlorines in biota from a freshwater food web. Sci. Total Environ. **160/161**: 381–390.

Kiriluk, R., Servos, M., and Whittle, D. 1995. Using ratios of stable nitrogen and carbon isotopes to characterize the biomagnification of DDE, Mirex, and PCB in a Lake Ontario pelagic food web. Can. J. Fish. Aquat. Sci. **52**: 2660–2674.

Michener, R.H., and Schell, D.M. 1994. Stable isotope ratios as tracers in marine aquatic food webs. *In* Stable isotope tracers in ecology and environmental science. *Edited by* K. Lathja and R.H. Michener. Blackwell Scientific Publications, Oxford, U.K. pp. 138–186.

Minagawa, M., and Wada, E. 1984. Stepwise enrichment of ^{15}N along food chains: further evidence and the relation between $\delta^{15}N$ and animal age. Geochim. Cosmochim. Acta, **48**: 1135–1140.

Muir, D.C.G., Wagemann, R., Grift, N., Norstrom, R.J., Simon, M., and Lien, J. 1988. Organochlorine chemical and heavy metal contaminants in white-beaked dolphins (*Lagenorhynchus albirostis*) and pilot whales (*Globicephala melaena*) from the coast of Newfoundland, Canada. Arch. Environ. Contam. Toxicol. **17**: 613–629.

Norstrom, R.J., Schweinsberg, R.E., and Collins, B.T. 1986. Heavy metals and essential elements in livers of the polar bear (*Ursus maritimus*) in the Canadian Arctic. Sci. Total Environ. **48**: 195–212.

Pentreath, R.J. 1976*a*. The accumulation of inorganic mercury from sea water by the plaice, *Pleuronectes platessa* L. J. Exp. Mar. Biol. Ecol. **24**: 103–119.

Pentreath, R.J. 1976*b*. The accumulation of inorganic mercury from sea water by the plaice, *Pleuronectes platessa* L. J. Exp. Mar. Biol. Ecol. **24**: 121–132.

Porter, L.K., and O'Dean, W.A. 1977. Apparatus for preparing nitrogen and ammonium chloride for nitrogen-15 determinations. Anal. Chem. **45**: 514–516.

Riisgard, H.U., and Hansen, S. 1990. Biomagnification of mercury in a marine grazing food-chain: algal cells *Phaeodactylum tricorntum*, mussel *Mytilus edulis* and flounders *Platichthys flesus* studied by means of a stepwise-reduction-CVAA method. Mar. Ecol. Prog. Ser. **62**: 259–270.

Rolff, C., Broman, D., Näf, C., and Zebhür, Y. 1993. Potential biomagnification of PCDD/Fs — new possibilities for quantitative assessment using stable isotope trophic position. Chemosphere, **27**: 461–468.

Rowan, R.J., and Rasmussen, J.B. 1992. Why don't Great Lakes fish reflect environmental concentrations of organic contamination? An analysis of between-lake variability in the ecological partitioning of PCBs and DDT. J. Great Lakes Res. **18**: 724–741.

Särkkä, J., Hattula, M., Passivirta, J., and Palokangas, R. 1978. Chlorinated hydrocarbons and mercury in birds of Lake Päijänne, Finland — 1972–74. Pestic. Monit. J. **12**: 26–35.

Sergeant, D.E., and Armstrong, F.A.J. 1973. Mercury in seals from eastern Canada. J. Fish. Res. Board Can. **30**: 843–846.

Smith, T.G., and Armstrong, F.A.J. 1975. Mercury in seals, terrestrial carnivores, and principal food items of the Inuit, from Holman, N.W.T. J. Fish. Res. Board Can. **32**: 795–801.

Sokal, R., and Rohlf, F. 1995. Biometry. 3rd ed. W.H. Freeman, New York.

Thompson, D.R., and Furness, R.W. 1989. The chemical form of mercury stored in South Atlantic seabirds. Environ. Pollut. **60**: 305–317.

Thompson, D.R, Hamer, K.C., and Furness, R.W. 1991. Mercury accumulation in Great Skuas *Catharacta skua* of known age and sex, and its effects upon breeding and survival. J. Appl. Ecol. **28**: 672–684.

Thompson, D.R., Furness, R.W., and Walsh, P.M. 1992. Historical changes in mercury concentrations in the marine ecosystem of the north and north-east Atlantic Ocean as indicated by seabird feathers. J. Appl. Ecol. **29**: 79–84.

Tieszen, L., Boutton, T., Tesdahl, K., and Slade, N. 1983. Fractionation and turnover of stable carbon isotopes in animal tissues: implications for $\delta^{13}C$ analysis of diet. Oecologia (Heidelb.), **57**: 32–37.

Wagemann, R., and Muir, D.C.G. 1984. Concentrations of heavy metals and organochlorines in marine mammals of northern waters: overview and evaluation. Can. Tech. Rep. Fish. Aquat. Sci. No. 1279.

Wagemann, R., Snow, N., Lutz, A., and Scott, D. 1983. Heavy metals in tissues and organs of the narwhal (*Monodon monoceros*). Can. J. Fish. Aquat. Sci. **40**(Suppl. 2): 206–214.

Wagemann, R., Stewart, R.E.A., Lockhart, W.L., Stewart, B.E., and Povoledo, M. 1988. Trace metals and methylmercury: associations and transfer in harp seal (*Phoca groenlandica*) mothers and their pups. Mar. Mammal Sci. **4**: 339–355.

Wagemann, R., Stewart, R.E.A., Beland, P., and Desjardins, C. 1990. Heavy metals and selenium in tissues of beluga whales, *Delphinapterus leucas*, from the Canadian Arctic and the St. Lawrence

© 1998 NRC Canada

Estuary. *In* Advances in research on the beluga whale, *Delphinapterus leucas*. *Edited by* T. Smith, D. St. Aubin, and J. Geraci. Can. Bull. Fish. Aquat. Sci. No. 244. pp. 191–206.

Wilkinson, L. 1991. SYSTAT 5.03. SPSS Inc., Chicago, Ill.

Williams, P.M., and Weiss, H.V. 1973. Mercury in the marine environment: concentration in seawater and in a pelagic food chain. J. Fish. Res. Board Can. **30**: 293–295.

© 1998 NRC Canada

Winter mortality of young-of-the-year Hudson River striped bass (*Morone saxatilis*): size-dependent patterns and effects on recruitment

Thomas P. Hurst and David O. Conover

Abstract: Winter mortality plays a significant role in the dynamics of some temperate fish populations and has been shown to be size-dependent for some species, but not for others. Our objective was to determine how winter mortality affects the recruitment dynamics of Hudson River striped bass (*Morone saxatilis*). We used catch-per-unit-effort data from three separate surveys targeting young-of-the-year (YOY), overwintering, and age 1 striped bass. Age 1 abundance was negatively correlated with the severity of winter. In contrast, the abundance of age 0 fish was not correlated with age 1 abundance, suggesting that winter mortality greatly modifies year-class strength. A progressive increase in the mean length of YOY fish, coupled with a decrease in the coefficient of variation in length, occurred during some winters. Laboratory experiments showed that growth in length requires temperatures in excess of 10°C; hence, these changes likely result from selective mortality of smaller fish. Direct evidence of size-dependent mortality was obtained from a laboratory experiment that exposed fish to ambient conditions throughout the winter. Accounting for interannual differences in the severity and size dependency of winter mortality may improve our ability to evaluate striped bass year-class strength in the Hudson River.

Résumé : La mortalité hivernale joue un rôle important dans la dynamique de certaines populations de poissons des régions tempérées, et on a montré qu'elle était fonction de la taille chez certaines espèces. Nous voulions déterminer comment la mortalité hivernale affecte la dynamique du recrutement du bar rayé (*Morone saxatilis*) de l'Hudson. Nous avons utilisé des données de captures par unité d'effort de trois relevés différents visant les jeunes de l'année, les poissons hivernants et les bars rayés d'âge 1. L'abondance des bars d'âge 1 était corrélée négativement avec la rigueur de l'hiver. Par ailleurs, l'abondance des poissons d'âge 0 n'était pas corrélée avec l'abondance des poissons d'âge 1, ce qui laisse penser que la mortalité hivernale modifie grandement l'effectif des classes d'âge. On a observé durant certains hivers un accroissement progressif de la longueur moyenne des jeunes de l'année, combiné à une baisse du coefficient de variation de la longueur. Des expériences de laboratoire ont montré que la croissance en longueur exige des températures supérieures à 10°C; ainsi, ces changements sont probablement dus à une mortalité sélective des poissons de plus petite taille. Une expérience de laboratoire dans laquelle on a exposé des poissons aux conditions ambiantes durant tout l'hiver a fourni une preuve directe du phénomène de mortalité liée à la taille. Le fait de tenir compte des différences interannuelles dans l'importance de la mortalité hivernale et dans la dépendance de cette dernière à l'égard de la taille peut accroître notre capacité d'évaluer l'effectif des classes d'âge du bar rayé dans l'Hudson. [Traduit par la Rédaction]

Introduction

Determining the factors that affect recruitment has been a primary focus of fisheries research for decades. Recruitment is known to be influenced by a wide variety of biotic and abiotic factors. Small changes in the rate of growth or mortality of eggs, larvae, and juveniles have been shown to substantially impact population recruitment (Houde 1987). Thus, it is suggested that much of the variability in recruitment is determined very early in the life history. This has led to a proliferation of abundance indices aimed at very early stages in the life history to be used as predictors of future recruitment (Bradford 1992). However, it is clear that recruitment to a population is rarely determined by a single process and that variable mortality rates among juveniles can also impact year-class strength (Shuter et al. 1980; Anderson 1988).

One factor that may cause recruitment variability is winter severity. Temperate organisms occupy habitats that alternate between periods of warm temperature and abundant food (summer) that enhance opportunities for growth and periods of low temperature and reduced food availability (winter) that cause individuals to lose energy. In addition to net energy loss, winter imposes additional stresses on fish such as increased osmotic stress at low temperatures (Belkovskiy et al. 1991; Johnson and Evans 1996). Mortality from energy depletion tends to be higher among smaller individuals due to the allometries of energy storage and metabolic rates, as does mortality from osmotic stress due to the scaling of gill surface area to body size (Johnson and Evans 1996). Therefore, mortality from these sources should be most pronounced during the first winter of life.

Much of the research on the mortality patterns of

Received October 1, 1996. Accepted December 19, 1997.
J13673

T.P. Hurst[1] **and D.O. Conover.** Marine Sciences Research Center, State University of New York, Stony Brook, NY 11794-5000, U.S.A.

[1] Author to whom all correspondence should be addressed. e-mail: hurst@msrc.sunysb.edu

© 1998 NRC Canada

overwintering temperate fishes has involved laboratory experiments exploring the potential for size-selective mortality (Oliver et al. 1979; Toneys and Coble 1979; Post and Evans 1989; Johnson and Evans 1990, 1991; Thompson et al. 1991). Studies of wild populations have been conducted over at most two winters (Adams et al. 1982; Conover and Ross 1982; Henderson et al. 1988; Post and Evans 1989; Miranda and Hubbard 1994) and therefore have not generally addressed the potential for interannual variation in the selective nature of mortality. In many cases where size-dependent mortality has been documented, continuous sampling throughout the winter was hindered due to migrations (Conover and Ross 1982) or ice cover (Post and Evans 1989). Comparison of a sample taken in the fall with one in the spring does not allow investigation into the timing of mortality, nor can growth be ruled out as the cause of changes in size distribution (see fig. 7 in Post and Evans 1989). In addition, comparison of a single sample before winter with a single sample after winter allows sampling error to significantly affect the conclusions drawn from these studies. Continuous sampling throughout the winter provides a more complete picture of the timing of selection and is less subject to sampling errors (Miranda and Hubbard 1994).

The striped bass (*Morone saxatilis*) has historically supported one of the most important commercial and recreational fisheries along the east coast of the United States. The Hudson River represents the northernmost of the major spawning stocks of striped bass in the United States (several smaller stocks occur in Canada). Spawning occurs at the head of the estuary in late May, with juveniles distributed throughout the estuary in summer (Dovel 1992). In late October, juveniles begin moving to the New York Harbor area, the only known area of wintering aggregation (Dovel 1992). As temperatures warm in the spring, fish disperse throughout the region, with concentrations occurring in the embayments surrounding the western end of Long Island (Young et al. 1994).

For purposes of forecasting year-class strength, indices of summer abundance of young-of-the-year (YOY) fish have been developed for several east coast populations, including the Hudson River and several subestuaries of Chesapeake Bay (McKown 1991; Goodyear 1985). Use of these indices as predictors of future recruitment assumes that year-class strength is fixed prior to the early juvenile stage when the index is calculated. Because these indices are calculated during the first summer of life, they necessarily neglect the effects of the first winter of life on year-class strength. An understanding of how the stresses associated with overwintering affect fish of varying sizes may significantly increase our understanding of population dynamics and our ability to predict recruitment to this and other commercially important fish stocks.

In this paper, we present evidence that year-to-year variations in winter severity may, in part, regulate recruitment of striped bass in the Hudson River stock. Our results are based on analyses of winter conditions and indices of abundance for eight year-classes. We also describe the size dependence of winter mortality in YOY striped bass and the interannual variation in the size-specific pattern of mortality over five winters. Finally, we present experimental evidence for size-dependent winter mortality and the temperature threshold for growth of YOY striped bass. These laboratory experiments clarify interpretation of field results by evaluating possible alternative explanations.

Methods

Recruitment

To assess the influence, if any, of winter conditions on recruitment dynamics of striped bass, we compared indices of winter severity with the change in the relative abundance of juveniles over the winter. Throughout this study, fish are referred to as YOY (or age 0) from the time of hatching until the end of the first winter and are thereafter classified as age 1. For clarity, winters will be referred to by the year in which they began. To determine the relative abundance of YOY striped bass, the New York State Department of Environmental Conservation (NYSDEC) conducts an annual beach seine survey in the Hudson River. The YOY index is calculated as the geometric mean catch-per-unit-effort (CPUE) of YOY striped bass captured at 25 sampling sites within the nursery area (river miles 22–42). These sites are sampled every 2 weeks from mid-July through late October (Young et al. 1994). NYSDEC also conducts a beach seine survey in the embayments of Long Island to tag age 1 and older striped bass. The age 1 index of abundance is the geometric mean CPUE of age 1 striped bass captured at multiple sites within three western Long Island embayments sampled biweekly from May through August. Both surveys are conducted with a 61 × 3 m beach seine (6-mm-mesh wings and 5-mm-mesh bag) deployed by boat (McKown 1991).

Weekly average river temperature data reported from the winter trawl survey of the Hudson River Electric Utilities (see survey description below) were used to calculate indices of winter severity. To discriminate winters of long duration from those with acute or chronically low temperatures, three measures of winter severity were used: (*i*) the lowest of the weekly average bottom temperatures recorded during the survey, (*ii*) the number of days that bottom water temperatures were below 4°C, and (*iii*) the sum of degree-days below 4°C (i.e., $\sum(4.0 - t_i)$, where t_i is the daily temperature for each day below 4°C). The latter two measures were calculated by assigning the weekly average temperature to each day of the entire week. We chose 4°C to assess the severity of winter because the winter trawl survey encompassed the entire time that river temperatures were below 4°C in all years.

To evaluate the role of winter in regulating recruitment, we first assessed the degree of correlation between the YOY index and age 1 index for the years 1984–1992 disregarding winter. We then examined the relationship between the age 1 index and our three indices of winter severity. Because there were no measures of winter severity for the winter of 1984, these analyses were restricted to the 1985–1992 year-classes. Stepwise linear regression was used to determine if adding YOY abundance to the individual measures of winter severity in a multiple linear regression model explained significantly more variation in age 1 abundance than single factor regressions. Potential spurious correlations between age 1 abundance and winter conditions were assessed by examining the relationships among winter indices and YOY abundance.

Size-dependent mortality

Field analysis

The Hudson River Electric Utilities has funded a hatchery evaluation and tagging program for striped bass in the lower Hudson River estuary each winter since 1985 (Normandeau Associates 1992). Fish were captured with a bottom trawl with a 9-m foot rope and 3.8-cm stretched mesh cod end, although other trawl designs were used sporadically throughout the survey (Normandeau Associates 1992). Trawls were conducted weekly, generally from mid-November to mid-April, and targeted the primary overwintering grounds of Hudson River striped bass (river miles 0–10). The size distributions of

© 1998 NRC Canada

Fig. 1. Relationships between age 1 index of abundance and (*a*) YOY index of abundance for year-classes 1984–1992, (*b*) minimum bottom water temperatures observed in the Hudson River, (*c*) cumulative number of degree-days below 4°C, and (*d*) number of days that bottom water temperatures were below 4°C for year-classes 1985–1992.

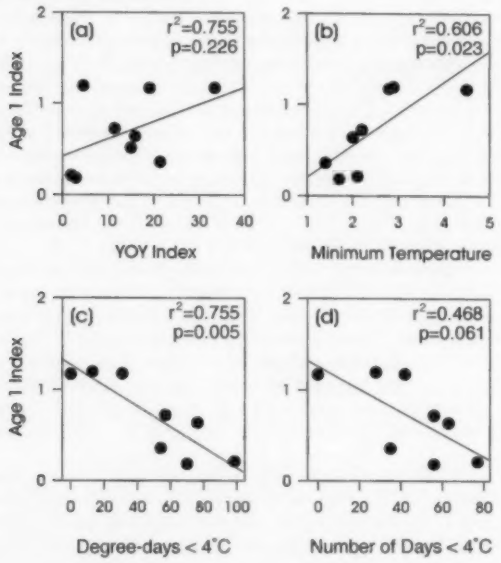

fish captured in this survey were used to assess the size-selective pattern of mortality of YOY striped bass during each of the winters of 1986–1990. For each of the five winters examined, the survey was subdivided into a series of 2-week intervals. A size–frequency distribution of fish in 1-mm intervals was created for each 2-week period. The abundance of fish in larger size-classes required adjustment due to the overlap in size between the 0+ and 1+ age-classes. This was done by determining the ratio of age 0 to age 1 fish in all overlapping size-classes. Percentage of age 1 fish in 10-mm size-classes was determined from a subsample of fish aged from scales. This correction would not have influenced our results, as all distributions within a year would have been affected similarly, and in most cases, less than 10% of all age 0 fish were in the region of overlap with age 1 fish. After this adjustment, the mean size and coefficient of variation in size (CV) of YOY striped bass within each 2-week period were determined from the resulting size–frequency distribution.

Mortality that selectively removes smaller fish from a population of nongrowing fish will increase the mean size and decrease the variance in size of the survivors (Ricker 1969; Post and Evans 1989). We used these criteria to identify the occurrence of size-dependent mortality. Mean size of YOY fish (weighted by the number of fish captured in the period) and CV (unweighted) for each sampling period were regressed against date to test the significance of changes in mean size and variation in size through the winter.

The occurrence of size-dependent mortality might be difficult to detect if there is a threshold size above which mortality rates are constant and the majority of fish in the population in a given year were above that size. Changes in less abundant size-classes may not be sufficient to affect the overall mean. Therefore, years when no significant change in mean size was evident were further examined by calculating the mean size of fish less than or equal to 120 mm. These means were then regressed against date as before. We used 120 mm to truncate the distributions because it removed the larger size-classes while leaving a sufficient portion of the distribution to analyze in all years. A significant increase in the size of fish in the smaller size-classes was interpreted as being consistent with the occurrence of size-dependent mortality, but weaker evidence than shifts in the entire distribution.

Overwintering experiment

We conducted a laboratory experiment during the winter of 1993 to gather direct information on the size-dependent patterns of mortality. YOY striped bass were collected by beach seine from the Hudson River in the area of Haverstraw Bay on 6 and 20 October 1993 prior to their down-estuary migration. The fish were transported to the Flax Pond Marine Laboratory, Stony Brook, New York, in river water and transferred to tanks of the same salinity located in a greenhouse. The salinity was raised to the ambient level of flow-through seawater in the laboratory (about 25 ppt) over 3 days following capture. Laboratory salinities were similar to those found in the overwintering areas (15–25 ppt). Fish experienced ambient temperature, photoperiod, and salinity and were fed frozen adult brine shrimp (*Artemia* sp.) daily until initiation of the experiments.

The experimental design incorporated treatments for fish size and food availability. Prior to the start of the experiment, a sample of fish was measured to estimate median size. All experimental fish were then measured to the nearest millimetre (total length) and randomly assigned to one of four replicates of each of two size-classes. Size range of all fish used in the experiment was 67–135 mm with a mean of 87.8 mm and the distribution skewed to the right. The small size-class treatment fish were 77.4 ± 4.4 mm and large size-class fish were 98.3 ± 11.0 mm (mean ± SD). There were no significant differences in size among the four tanks within either size-class (ANOVA: $p > 0.1$). Tanks were randomly assigned to one of two feeding treatments: (*i*) excess food (frozen brine shrimp) provided once daily or (*ii*) food withheld for the duration of the experiment. Each tank contained 19 fish, and each combination of size and feeding treatment had two replicates (eight tanks total). During the experiment, fish were kept under natural light in large (295 L) flow-through tanks that were periodically cleaned and checked twice daily for mortalities. Fish were held under these experimental conditions for 99 days from 22 December to 25 March.

Temperature threshold for growth

To verify that changes in length–frequency distributions through the winter could not be due to growth, we conducted an experiment to determine the minimum temperatures that permit increases in length and dry weight. YOY striped bass were captured from the lower Hudson River estuary on 3 February 1995. Fish were transported and acclimated to laboratory conditions as described above. On 23 February, 48 fish were weighed, measured, and randomly assigned to 5, 10, and 15°C temperature treatments (four fish per tank, four tanks per temperature). Temperatures were raised from 5°C (acclimation temperature) to test temperatures over 4 days and maintained for 26 days. Fish were fed frozen adult brine shrimp in excess of what they could consume twice daily. Brine shrimp were used because they are similar in size and morphology to *Gammarid* amphipods, the primary natural prey of YOY striped bass in winter (T.P. Hurst, unpublished data). At the end of the experiment, all fish were again weighed and measured. Fish were dried in a freeze-drier for 3 days for determination of dry weights. Initial dry weights were estimated from measured wet weights using the wet to dry weight ratio of all fish measured at the end of the experiment.

Due to variation in size of individuals within a tank (total size range in the experiment: 70–138 mm), it was possible to identify individual fish throughout the experiment without marking. We were thereby able to identify the initial sizes of the several fish that died during the course of the experiment and remove them from the analysis. The growth rates of fish in each tank were expressed as the mean change in size of fish from beginning to end of the experiment.

© 1998 NRC Canada

Table 1. Summary of winter characteristics.

Year-class	Index of YOY abundance[a]	Mean fish size at onset of winter[b]	Minimum temperature (°C)[c]	Degree-days <4°C[c]	Number of days <4°C[c]	Mean biweekly sample size	*r* from regression of mean size on date	*r* from regression of CV on date	Evidence of size-dependent winter mortality[d]
1986	2.9	120	1.7	70	56	306	0.453 ns	–0.574 ns	Partial
1987	15.9	108	2	76.3	63	261	–0.135 ns	–0.717**	None
1988	33.5	118	2.8	30.9	42	642	0.217 ns	–0.06 ns	None
1989	21.4	107	1.4	54.4	35	589	0.278 ns	–0.3 ns	Partial
1990	19.1	103	4.5	0	0	353	0.787**	–0.598*	Strong

Note: *Regression significant at $p < 0.05$; **regression significant at $p < 0.01$; ns, not significant at $p > 0.05$.

[a]From New York State Department of Environmental Conservation beach seine survey.

[b]Size predicted for 1 December from regression lines of mean size onto date shown in Fig. 3.

[c]From Hudson River Electric Utilities winter trawl survey.

[d]Strong, significant increase in mean size and decrease in CV; partial, significant increase in mean size of distributions truncated at 120 mm.

Results

Effects on recruitment

The relative abundance of age 1 fish was more highly correlated with the measures of winter severity than with the relative abundance of age 0 fish (Fig. 1). There was a significant positive correlation between the minimum water temperatures observed in the Hudson River and the age 1 index of abundance ($r^2 = 0.606$; $p = 0.023$). Winter severity measured as degree-days below 4°C was negatively correlated with age 1 abundance ($r^2 = 0.756$; $p = 0.005$) as was the number of days below 4°C ($r^2 = 0.468$; $p = 0.061$). The Hudson River YOY beach seine survey was not significantly correlated with the age 1 index of abundance ($r^2 = 0.221$; $p = 0.201$) for the years 1984–1992.

Combining the YOY index with each measure of winter severity into multiple linear regression models improved the fit slightly, but the improvements were not significant ($p > 0.10$ in all three cases; stepwise test for addition of independent factors). Spurious correlations between YOY abundance and winter severity indices were not responsible for the relationships between winter severity and age 1 abundance: the YOY index of abundance was not significantly correlated with any measure of winter severity (all $p > 0.30$). All three measures of winter severity were significantly correlated with each other (all $p < 0.036$).

Evidence of size-dependent mortality in the field

By all three indices of winter severity, the winter of 1990 was the mildest of the five years examined (Table 1). The winter of 1988 was also relatively mild by most measures. The other three years were generally more severe, in terms of either minimum temperature (1989) or duration of low temperature (1986 and 1987). The mean size of fish at the onset of winter (i.e., on 1 December, estimated from regression lines in Fig. 2) ranged from 103 to 120 mm in the five years examined (Table 1); it was relatively high in 1986 and 1988, low in 1990, and intermediate in 1987 and 1989.

Within winters, mean sizes of fish in consecutive sampling periods differed by as much as 15 mm (Fig. 2). Despite large samples used to estimate mean size (Table 1), these differences were most likely due to sampling error, rather than actual changes in mean size of individuals in the population. This variability demonstrates the potential problems associated with assessing mortality patterns from only two samples, such as before and after winter.

Analysis of mean size and variation in size over time indicated that winter mortality of YOY striped bass had a significant size-dependent component in some, but not all, years (Fig. 2). There were clear indications that winter mortality of the 1990 year-class was size selective. This is based on a significant increase in mean size ($p = 0.002$) and significant decrease in CV ($p = 0.040$) of YOY striped bass captured during the winter trawl survey (Fig. 2). The mean size of YOY fish in the population increased from 103 mm in late November to 116 mm in mid-March, while the CV declined from 19.2 to 15.5%. In none of the remaining four winters was the evidence sufficient to warrant classifying mortality as size dependent. Mean size increased in three of these winters and decreased slightly in 1987, but these changes were not significant ($p > 0.05$ all years; Table 1). In the winter of 1987, we observed a significant decrease in CV ($p = 0.009$), while there were no significant changes in CV in the remaining three winters ($p > 0.08$).

Analyses of the 1986–1989 distributions truncated at 120 mm indicated that mortality among smaller fish may have been higher than among larger fish in two of these four years. Regression analyses showed a significant increase in the mean size of fish in the truncated distribution during the winters of 1986 and 1989 ($p = 0.011$ and $p = 0.039$), lending some support to the size-dependent mortality hypothesis. Even after truncation, there was no indication of an increase in fish size during the 1987 and 1988 winters ($p > 0.05$ both years). When other sizes were used to truncate the distribution data (100, 103, and 130 mm), the results in all years were the same as above.

Visual examination of representative size distributions (dates marked by arrows in Fig. 2) from the beginning and end of each winter indicates that fish in the left-hand tail of the distribution are consistently more abundant in the beginning of winter than in the end of winter (Fig. 3). This difference is most evident in the distributions from the winter of

© 1998 NRC Canada

Fig. 2. Winter mean size and CV in size of YOY striped bass from the 1986–1990 year-classes. Circles represent mean size ± 1 SE with regression onto date weighted by sample size (solid line). Triangles represent CV in size of YOY striped bass with regression onto date (broken line). Arrows indicate sampling periods plotted as size–frequency distributions in Fig. 3.

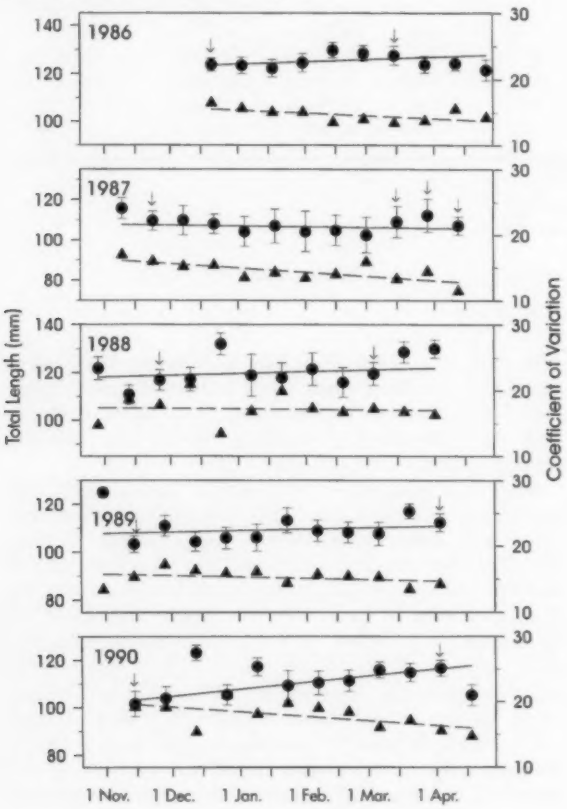

1990 where there was a pronounced shift in shape of the distribution as well as the mean. Changes in other years were less evident, with apparent changes confined to the smallest fish, suggesting that size-dependent mortality may have occurred but was not detected in the previous analyses.

Overwintering experiments

Fish size and food availability influenced survival rates of YOY striped bass in the experiment. Analysis of survival rates was conducted with 2 × 2 tests of independence with number of fish dying versus surviving as one factor and the desired comparison as the other (tank, size, or feeding treatment). One replicate of the large/fed treatment had nearly complete mortality of an episodic nature between 5 and 11 February (all but one fish died), while the other replicate had 37% survival over the entire winter. Because this unknown mortality agent appeared confined to a single tank, we removed this tank from the analyses. Mortality rates were not significantly different between replicates in the remaining three treatments ($p > 0.20$), allowing us to pool the fish from replicates of each treatment for analysis of survival rates. Survival of small fish was significantly higher in the fed treatment than in the unfed treatment (58 versus 34%; $p = 0.039$). Among unfed treatments, mortality was size dependent, with significantly more large fish surviving than small fish (55 versus 34%; $p = 0.047$). Sample sizes in the large/fed treatment were half those of the other treatments due to inclusion of only one replicate in the analyses. However, the survival rates in this treatment did not differ significantly from either the large/starved treatment ($p = 0.194$) or the small/fed treatment ($p = 0.138$).

Size-dependent mortality was also evident from the timing of mortality in the experiment. Pooling fish from all treatments (excluding those from the large/fed treatment tank with episodic mortality), there was a significant increase in the size of fish dying in the experiment as winter progressed (Fig. 4; regression of length of dead fish onto date: $p < 0.001$). A single line was used to describe the relationship, as ANCOVA indicated that regressions for fed and unfed treatments were not significantly different (slopes $p = 0.242$; intercept $p = 0.248$). Early deaths were mostly small fish, while later deaths included progressively larger fish.

Temperature threshold for growth

Nested ANOVA indicated that there were no significant differences in growth rates among tanks within temperature treatments (length $p = 0.56$; dry weight $p = 0.61$), but temperature did significantly affect growth rates (length $p = 0.002$; dry weight $p = 0.002$). At both 5 and 10°C, there was a loss in length during the experiment of 0.8 mm (Fig. 5). At 15°C, fish grew an average of 1 mm during the experiment (0.033 mm/day). Striped bass were able to sustain growth in dry weight at lower temperatures than for length. Striped bass lost an average of 0.01%/day at 5°C and grew at rates of 0.02 and 0.26%/day at 10 and 15°C. From these results, we suggest 5 and 10°C as conservative estimates of the minimum temperatures that permit growth in weight and length, respectively.

Discussion

Our results indicate that winter severity plays a fundamental role in regulating recruitment of fish to age 1 in the striped bass population of the Hudson River. Year-class strength is not yet fully determined in the juvenile stages that occur prior to winter, as is assumed by using field surveys of year-class abundance that target YOY juvenile fish in mid- to late summer. We also found evidence that mortality during the winter is size selective, but the magnitude of size selectivity varies from year to year. Detailed discussion is provided below.

Effects on recruitment

The relative abundance of age 1 striped bass was significantly correlated with several measures of winter severity. Age 1 abundance was most closely correlated with the number of degree-days below 4°C, an index that incorporates both the length and severity of winter conditions. This may indicate that winter mortality rates are determined by the cumulative exposure to low temperatures. However, cold winters tend to have longer durations and the three measures of winter severity were correlated with each other, precluding further analysis.

© 1998 NRC Canada

Fig. 3. Winter size distributions of YOY striped bass from the 1986–1990 year-classes. Frequencies are grouped into 5-mm size-classes. Distributions shown here are from the beginning and end of the survey period, representing the trend in size through the winter, and are indicated by arrows in Fig. 2. Three periods were used for the end of winter distribution in 1987 due to small sample sizes in individual periods.

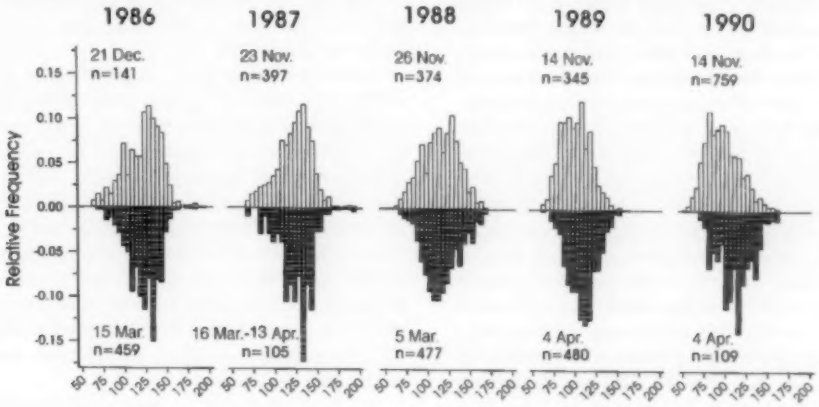

Fig. 4. Size-dependent pattern of mortality in the laboratory experiment. Circles and triangles represent fish from fed and unfed treatments, respectively. The line represents the regression of length of fish that died versus date of death.

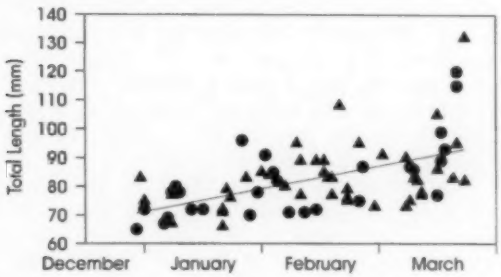

Fig. 5. (*a*) Length and (*b*) dry weight growth rates of YOY striped bass as function of temperature. Points represent mean growth rates for each tank. The solid line connects mean growth rates measured at three temperatures.

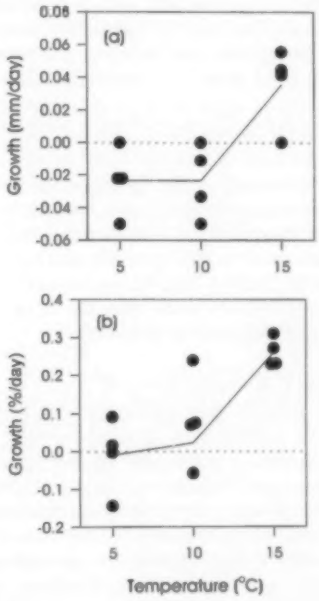

The importance of winter severity to recruitment can be illustrated clearly by tracking the 1989 year-class. This year-class was among the most abundant when assessed at age 0, but when it was assessed at age 1 after a particularly severe winter, it was among the least abundant. Because winter mortality can only modify the abundance of YOY fish through differential survival during the first winter of life, we calculated the deviation of each year-class from the regression line describing the relationship between age 0 abundance and age 1 abundance (in Fig. 1*a*) and compared these deviations with our measures of winter severity. Minimum winter temperature was positively correlated and the number of degree-days below 4°C was negatively correlated with these deviations ($p < 0.03$).

Our conclusion that winter severity affects recruitment is based on the assumption that the beach seine surveys conducted by NYSDEC provide accurate representations of the relative abundance of YOY and age 1 fish across year-classes. Therefore, effects of interannual variation in distributions and migration patterns on indices of abundance cannot be ruled out. However, in designing their surveys, NYSDEC personnel selected sites in the center of the geographical distribution where YOY and age 1 striped bass were consistently captured (B. Young, NYSDEC, personal communication). It is therefore likely that fluctuations in catch rates are reflective of actual changes in overall abundance.

Episodes of severe winter mortality have been documented in a variety of species, but the role of such events in recruitment regulation remains unidentified. Low winter temperatures and rapid rates of temperature decline have been implicated in recruitment regulation for northern populations of summer flounder (*Paralichthys dentatus*) (Malloy and Targett 1991; Szedlmayer et al. 1992) and Atlantic croaker

© 1998 NRC Canada

(*Micropogonias undulatus*) (Lankford 1997). These species breed during the fall and winter, and it is primarily the survival of larvae and early juveniles that is affected. In only a few other cases has winter severity been shown to be correlated with recruitment during later juvenile stages. Seelbach (1987) has shown that return rates of adults and survival rates of presmolt steelhead trout (*Oncorhynchus mykiss*) are negatively related to the severity of winter prior to smoltification, and Hunt (1969) found that survival of brook trout (*Salvelinus fontinalis*) was positively related to January temperatures.

Indices of abundance of the early life history stages have become an increasingly common tool by which fisheries managers attempt to predict future recruitment to local stocks (Bradford 1992). Use of this technique is based on the assumption that year-class strength is determined in the life history stages prior to the time of the survey. Such indices have been created for most of the major east coast populations of striped bass and are based on beach seine surveys of YOY fish conducted in mid- to late summer. Goodyear (1985) conducted the first statistical validation of these indices, comparing the Maryland Department of Natural Resources YOY indices of abundance with fishery harvest data. YOY abundances explained 57% of the variation in harvest levels. For the Hudson River stock, McKown (1991) found that abundance in the NYSDEC YOY beach seine survey was significantly correlated with the abundance of age 1 fish the following year for the 1984–1989 year-classes. Our reanalysis of the relationship between the YOY beach seine survey and the age 1 index, over the period 1984–1992, found that the indices were not as strongly correlated as earlier analyses suggested (McKown 1991). We suggest that prediction of year-class strength in Hudson River striped bass, and perhaps other populations, could be improved considerably if severity of winter was included in a recruitment model or if the assessment was based on postwinter abundance data. For other temperate species, indices of abundance calculated prior to completion of the first year of life should be viewed with caution unless effects of winter mortality on recruitment variability have been shown to be minimal.

Size dependence of winter survival

Our analyses indicate that size-dependent winter mortality occurs in YOY striped bass, at least in some winters. The significant increase in mean size of fish in the population and the reduction in CV during the winter of 1990 are consistent with predictions of size-dependent mortality. However, possible alternative explanations for increase in size of fish during the winter include growth of fish and sampling bias due to migration patterns. In previous studies, these alternatives have not been tested with independent field data or laboratory experiments.

We determined that YOY striped bass require temperatures in excess of 10°C to maintain positive growth in length and temperatures in excess of 5°C to maintain growth in weight. Karås (1990) observed a similar pattern in European perch (*Perca fluviatilis*), with positive growth in weight occurring at lower temperatures than growth in length. Our growth rate estimates are consistent with other information on growth of YOY striped bass. Hartman and Brandt (1995) found growth in weight to be near zero at 6.9°C, and field collections of YOY striped bass suggest that increases in length of wild fish slow markedly as water temperatures fall below 15°C (Young et al. 1994). During the winter of 1990, the change in mean length clearly could not be accounted for by growth, as bottom water temperatures were below the threshold for growth for more than 19 weeks, nearly the entire duration of the survey.

The overwintering experiment demonstrated size-selective winter mortality in captive YOY striped bass. Overall, survival rates of large fish were higher than those of small fish in the experiment when food was withheld, and there was a significant increase in the size of dead fish over time, independent of food availability. These patterns are similar to observations in laboratory experiments on other temperate fishes (Oliver et al. 1979; Post and Evans 1989; Johnson and Evans 1990). While we cannot rule out movement patterns or predation as contributing to the field patterns observed, the overwintering experiments demonstrate that size-dependent winter mortality can occur purely from exposure to typical winter thermal regimes.

Although we found an increase in the overall mean size of fish in the population in only one of five winters examined, the phenomenon of size-dependent mortality may be more common than this analysis indicates. The initial size range of a population undergoing mortality is likely to have a pronounced effect on the intensity of size selection. If the mean size of individuals in the population is large, there may be relatively few individuals in the lower tail of the distribution where size-selective mortality has the greatest potential impact. In this case, size-dependent mortality would lead to only minor changes in the mean size of the remaining population. Size distributions may appear to indicate the loss of small fish in some years, even though changes in mean size and CV are not significant (Figs. 2 and 3). Removing the larger fish from the distribution to magnify changes in the smaller size-classes provided additional evidence of size-dependent mortality in two of the five winters examined (1986 and 1989). Given that the mean sizes of YOY striped bass entering the winter vary substantially among years (Table 1), it is not surprising that the intensity of size selection also varies interannually. This degree of interannual variability has not previously been recognized, as studies of other species have followed natural populations through no more than two winters.

Size-dependent winter mortality of YOY striped bass was suggested by Conover (Conover 1990; Conover et al. 1997) as a possible force driving the evolution of among-population variation in growth capacity. This study supports the presumption that size-dependent mortality does occur among Hudson River YOY striped bass, but does not necessarily occur during every winter. Interannual variability in the pattern of winter mortality with regard to fish size does not eliminate it as the potential selective pressure favoring the evolution of countergradient variation in growth rates, so long as size-selective mortality occurs frequently enough to maintain differences in gene frequencies among populations (Endler 1977).

Most recruitment models that incorporate the effect of winter (e.g., Shuter et al. 1980; Johnson and Evans 1990; Shuter and Post 1990) assume that all mortality results from depletion of energy stores and is therefore inherently size dependent, but the actual mechanisms of mortality have yet to be

© 1998 NRC Canada

defined. While the most commonly cited cause of size-dependent overwinter mortality has been depletion of energy reserves (Oliver et al. 1979; Post and Evans 1989; Thompson et al. 1991), other possible causes are size-dependent predation, exposure to lethal temperatures (Adams et al. 1982), and osmoregulatory stress (Belkovskiy et al. 1991; Johnson and Evans 1996). While the causes of mortality and sources of variability in winter mortality patterns need further investigation, the overall results of this study demonstrate that interannual variation exists in the size-dependent vulnerability of year-classes to winter mortality and may influence recruitment. We suggest that a more comprehensive model of recruitment variability in Hudson River striped bass, and perhaps elsewhere, will require parameters describing the prewinter density of YOY fish, the body sizes and energy content of YOY fish, and how these factors interact with the severity of winter to determine survival through the first year of life.

Acknowledgments

We thank J. Buckel, N. Steinberg, E. Schultz, D. Fontes, S. Munch, and A. Ehtisham for assistance with field collections and laboratory experiments. Hudson River Electric Utilities' data were provided by J. Young of the Consolidated Edison Company of New York, Inc. and D. Dunning of the New York Power Authority. New York State Department of Environmental Conservation survey data were provided by K. McKown and B. Young. J. Buckel, N. Steinberg, E. Schultz, K. McKown, D. Lonsdale, P. Symons, and two anonymous reviewers provided comments on an earlier version of this manuscript. This research was funded by a graduate fellowship in Population Biology from the Electric Power Research Institute (to T.P.H.) and by research grants from the National Science Foundation (No. OCE 9217025) and the Hudson River Foundation for Science and Environmental Research (to D.O.C.). This is contribution No. 1074 of the Marine Sciences Research Center, State University of New York, Stony Brook.

References

Adams, S.M., McLean, R.B., and Huffman, M.M. 1982. Structuring of a predator population through temperature-mediated effects on prey availability. Can. J. Fish. Aquat. Sci. **39**: 1175–1184.

Anderson, J.T. 1988. A review of size dependent survival during pre-recruit stages of fishes in relation to recruitment. J. Northwest Atl. Fish. Sci. **8**: 55–66.

Belkovskiy, N.M., Lega, Y.V., and Chernitskiy, A.G. 1991. Disruption of water–salt metabolism in rainbow trout *Salmo gairdneri*, in seawater at low temperatures. J. Ichthyol. (Engl. Transl. Vopr. Ikhtiol.), **31**: 134–141.

Bradford, M.J. 1992. Precision of recruitment predictions from early life stages of marine fishes. Fish. Bull. U.S. **90**: 439–453.

Conover, D.O. 1990. The relation between capacity for growth and length of growing season: evidence for and implications of countergradient variation. Trans. Am. Fish. Soc. **119**: 416–430.

Conover, D.O., and Ross, M.R. 1982. Patterns in seasonal abundance, growth and biomass of the Atlantic silverside, *Menidia menidia*, in a New England estuary. Estuaries, **5**: 275–286.

Conover, D.O., Brown, J.J., and Ehtisham, A. 1997. Countergradient variation in growth of young striped bass (*Morone saxatilis*) from different latitudes. Can. J. Fish. Aquat. Sci. **54**: 2401–2409.

Dovel, W.L. 1992. Movements of immature striped bass in the Hudson Estuary. *In* Estuarine research in the 1980's. *Edited by* C.L. Smith. State Univiversity of New York Press, Albany, NY. pp. 276–300.

Endler, J.A. 1977. Geographic variation, speciation and clines. *Series Editor*: R.M. May. Monographs in population biology 10. Princeton University Press, Princeton, N.J.

Goodyear, C.P. 1985. Relationship between reported commercial landings and abundance of young striped bass in Chesapeake Bay, Maryland. Trans. Am. Fish. Soc. **114**: 92–96.

Hartman, K.J., and Brandt, S.B. 1995. Comparative energetics and the development of bioenergetics models for sympatric estuarine piscivores. Can. J. Fish. Aquat. Sci. **52**: 1647–1666.

Henderson, P.A., Holmes, R.H.A., and Bamber, R.N. 1988. Size-selective overwintering mortality in the sand smelt, *Atherina boyeri* Risso, and its role in population regulation. J. Fish Biol. **33**: 221–233.

Houde, E.D. 1987. Fish early life dynamics and recruitment variability. Am. Fish. Soc. Symp. **2**: 17–29.

Hunt, R.L. 1969. Overwinter survival of wild fingerling brook trout in Lawrence Creek, Wisconsin. J. Fish. Res. Board Can. **26**: 1473–1484.

Johnson, T.B., and Evans, D.O. 1990. Size-dependent winter mortality of young-of-the-year white perch: climate warming and invasion of the Laurentian Great Lakes. Trans. Am. Fish. Soc. **119**: 301–313.

Johnson, T.B., and Evans, D.O. 1991. Behavior, energetics, and associated mortality of young-of-the-year white perch (*Morone americana*) and yellow perch (*Perca flavescens*) under simulated winter conditions. Can. J. Fish. Aquat. Sci. **48**: 672–680.

Johnson, T.B., and Evans, D.O. 1996. Temperature constraints on overwinter survival of age-0 white perch. Trans. Am. Fish. Soc. **125**: 466–471.

Karås, P. 1990. Seasonal changes in growth and standard metabolic rate of juvenile perch, *Perca fluviatilis* L. J. Fish Biol. **37**: 913–920.

Lankford, T.E. 1997. Estuarine recruitment processes and stock structure in Atlantic croaker, *Micropogonias undulatus* (Linnaeus). Ph.D. dissertation, Graduate College of Marine Studies, University of Delaware, Newark, Del.

Malloy, K.D., and Targett, T.E. 1991. Feeding, growth and survival of juvenile summer flounder *Paralichthys dentatus*: experimental analysis of the effects of temperature and salinity. Mar. Ecol. Prog. Ser. **72**: 213–223.

McKown, K.A. 1991. Validation of the Hudson River young-of-the-year striped bass indices. Report to the Atlantic States Marine Fishery Commission. New York State Department of Environmental Conservation, Stony Brook, N.Y.

Miranda, L.E., and Hubbard, W.D. 1994. Length-dependent winter survival and lipid composition of age-0 largemouth bass in Bay Springs Reservoir, Mississippi. Trans. Am. Fish. Soc. **123**: 80–87.

Normandeau Associates. 1992. Hudson River striped bass hatchery evaluation/monitoring program, November 1990 – April 1991. Normandeau Associates, Bradford, N.H.

Oliver, J.D., Holeton, G.F., and Chua, K.E. 1979. Overwinter mortality of fingerling smallmouth bass in relation to size, relative energy stores, and environmental temperature. Trans. Am. Fish. Soc. **108**: 130–136.

Post, J.R., and Evans, D.O. 1989. Size-dependent overwinter mortality of young-of-the-year yellow perch (*Perca flavescens*): laboratory, in situ, and field experiments. Can. J. Fish. Aquat. Sci. **46**: 1958–1968.

Ricker, W.E. 1969. Effects of size-selective mortality and sampling bias on estimates of growth, mortality, production, and yield. J. Fish. Res. Board Can. **26**: 479–541.

Seelbach, P.W. 1987. Effect of winter severity on steelhead smolt yield in Michigan: an example of the importance of environmen-

© 1998 NRC Canada

tal factors in determining smolt yeild. *In* Common strategies of anadromous andcatadromous fishes. *Edited by* M.J. Dadswell, R.J. Klauda, C.M. Moffitt, R.L. Saunders, R.A. Rulifson, and J.E. Cooper. Symposium 1, American Fisheries Scoiety, Bethesda, Md. pp. 441–450.

Shuter, B.J., and Post, J.R. 1990. Climate, population viability, and the zoogeography of temperate fishes. Trans. Am. Fish. Soc. **119**: 314–336.

Shuter, B.J., MacLean, J.A., Fry, F.E.J., and Reiger, H.A. 1980. Stochastic simulation of temperature effects on first-year survival of smallmouth bass. Trans. Am. Fish. Soc. **109**: 1–34.

Szedlmayer, S.T., Able, K.W., and Roundtree, R.A. 1992. Growth and temperature-induced mortality of young-of-the-year summer flounder (*Paralichthys dentatus*) in Southern New Jersey. Copeia, 1992: 120–128.

Thompson, J.T., Bergersen, E.P., Carlson, C.A., and Kaeding, L.R. 1991. Role of size, condition, and lipid content in the overwinter survival of age-0 Colarado squawfish. Trans. Am. Fish. Soc. **120**: 346–353.

Toneys, M.L., and Coble, D.W. 1979. Size-related, first winter mortality of freshwater fishes. Trans. Am. Fish. Soc. **109**: 415–419.

Young, B.H., McKown, K.A., and Savona, P. 1994. A study of the striped bass in the marine district of New York. VII. New York State Department of Conservation Report, New York.

© 1998 NRC Canada

Increased deposition of organic matter, polychlorinated biphenyls, and cadmium by zebra mussels (*Dreissena polymorpha*) in western Lake Erie

Evan P. Dobson and Gerald L. Mackie

Abstract: Biodeposition of organic matter, polychlorinated biphenyls (PCBs), and cadmium (Cd) by zebra mussels (*Dreissena polymorpha*) was investigated at five stations in the western basin of Lake Erie during the summer of 1992. Biodeposition rates at the five stations were determined by using sediment traps and converted to per unit area values to facilitate comparisons with natural sedimentation rates. Biodeposition of suspended material by zebra mussels was up to 8 times greater than sedimentation in the traps. Concentrations of organic matter, PCBs, and Cd were determined for the biodeposits and the sedimented material. There were no significant differences in concentration of organic matter, PCBs, or Cd between the two types of material. Biodeposition rates per unit area of organic matter, PCBs, and Cd were 8–10 times greater than corresponding values for natural sedimentation; therefore, the natural sedimentation processes of these factors appear to be greatly accelerated in the presence of zebra mussels. Results support the possibility that zebra mussels are altering contaminant movement in western Lake Erie, as well as clarifying the water column by removing suspended material.

Résumé : On a étudié le biodépôt de matière organique, de polychlorobiphényles (PCB) et de cadmium (Cd) dû à la moule zébrée (*Dreissena polymorpha*) dans cinq stations du bassin ouest du lac Érie au cours de l'été 1992. Les taux de biodépôt ont été déterminés aux cinq stations à l'aide de pièges à sédiments et vonvertis en valeurs par unité de surface pour faciliter les comparaisons avec les taux de sédimentation naturelle. Dans les pièges, le biodépôt de matières en suspensions dû aux moules zébrées était jusqu'a 8 fois supérieur à la sédimentation observée. Les concentrations de matière organique, de PCB et de Cd dans les biodépôts et dans les sédiments ont été calculées. Elles n'étaient pas significativement différentes entre les deux types de dépôts. Les taux de biodépôt par unité de surface de la matière organique, des PCB et du Cd étaient 8 à 10 fois supérieurs aux valeurs correspondantes obtenues pour la sédimentation naturelle. Par conséquent, le processus de sédimentation naturelle de ces facteurs semble être grandement accéléré en présence de moules zébrées. Les résultats confirment que les moules zébrées peuvent modifier le mouvement des contaminants dans le lac Érie et qu'elles clarifient la colonne d'eau en fixant la matière en suspension.
[Traduit par la Rédaction]

Introduction

Zebra mussels (*Dreissena polymorpha*) are thought to alter the rate of organic matter and contaminant movements in the water column through their biodeposition processes. The overall objective of this study was to assess the ability of zebra mussels to remove organic matter and particulate bound total polychlorinated biphenyls (t-PCBs) and cadmium (Cd) from the water column through biodeposition. Kaustsky and Evans (1987) and Jaramillo et al. (1992) showed that biodeposition rates by bivalves is similar to, or greater than, natural sedimentation rates. Significant ecological impacts due to zebra mussel filtration and biodeposition have been reported by Stanczykowska et al. (1975) and Reeders et al. (1989) for European waters. Klerks et al. (1996) observed biodeposition by zebra mussels to be 50% greater than natural sedimentation in their experiments, as well as an increased organic content of deposited material with increasing zebra mussel density. Reeders and Bij de Vaate (1992) have shown zebra mussel biodeposits are more contaminated than suspended material. However, despite the many studies dealing with biodeposition of zebra mussels, few, if any, have quantified the mussel's biodeposition of organic matter and contaminants in relation to the sedimentation of organic matter and contaminants. We predicted that zebra mussels will significantly increase the deposition rate of organic matter, t-PCBs, and Cd over that of natural sedimentation in the western Lake Erie. If so, zebra mussels may be playing a key role in decreasing contaminant loads in the water column and in water clarification in the Great Lakes.

In the present study, we determined zebra mussel biodeposition rates, sedimentation rates, and contaminant concentrations of biodeposits and sedimented material using sediment traps suspended within the water column of western Lake Erie. Biodeposition rates of contaminants were converted to per unit area values by incorporating mussel density data collected off settlement racks and were compared with natural sedimentation rates of contaminants.

Received February 19, 1997. Accepted October 27, 1997.
J13881

E.P. Dobson[1] and G.L. Mackie. Department of Zoology, University of Guelph, Guelph, ON N1G 2W1,Canada.

[1] Author to whom all correspondence should be addressed.

© 1998 NRC Canada

Fig. 1. Western basin of Lake Erie showing the study locations, Coast Guard buoy names, and maximum depths.

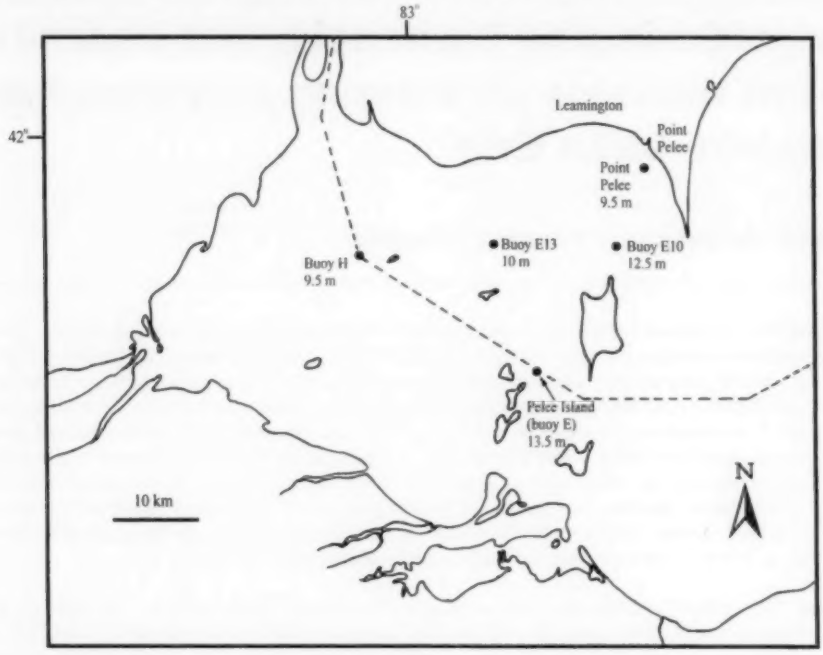

Materials and methods

Site location and sediment trap deployment

In August 1992, studies were conducted at five locations in the western basin of Lake Erie (Fig. 1) to determine the effects of zebra mussel biodeposition on PCB and Cd sedimentation. These locations were chosen to represent a gradient in contaminants in the basin (Farara and Burt 1993) downstream from the Detroit River. Locations with Coast Guard buoys (with the exception of Point Pelee, Fig. 1) were selected to facilitate relocation. At each location, two depths were used as individual sites: one near the top of the water column (3 m below the surface) and one near the bottom of the water column (1.5 m above the bottom, 8–12 m below the surface). Hence, there were 10 sites (two depths per location) used in the study. Locations were selected so that variability in contaminants (Cd and PCBs) among sites was maximized. Different depths were chosen as sites because variation in contaminant levels within the water column had been observed in our previous studies (unpublished data). Open-water locations were chosen to reduce problems of high resuspension of bottom sediments associated with shallow inshore locations (discussed below).

Sedimentation traps (Fig. 2) were used to determine the effects of zebra mussel biodeposition on PCB and Cd sedimentation. The efficiency of a sedimentation trap in trapping settling particles is dependent on a trap's aspect ratio (height:diameter) and the absolute diameter of the opening (Roff and Hopcroft 1985). The combination of the aspect ratio and the Reynolds number (Re) for a given trap design is the most reliable measure for determining the efficiency of a sedimentation trap in trapping settling material (Lau 1979). The Re, in the case of sediment traps, is equal to the inner trap diameter multiplied by the current velocity divided by the kinematic viscosity of the water (0.01 stokes (1 $mm^2 \cdot s^{-1}$) at 20°C) (Hawley 1988). The principle behind sedimentation trap design is to allow for water exchange between the inside and outside of the trap while also maintaining a nonturbulent bottom layer of water in the trap so that settled material will not resuspend. Lau (1979) observed that traps with an aspect ratio of 5:1 and Re < 7000 did not readily resuspend settled material.

In the present study, the aspect ratio of the sedimentation traps was 5.3:1. It is difficult to calculate the Re for these traps, since under field conditions the current velocity in the western basin of Lake Erie is highly variable. For this reason, few studies have examined the current patterns in the western basin. Current speeds are usually less than 20 $cm \cdot s^{-1}$ in the Great Lakes (Roff and Hopcroft 1985). MacIsaac et al. (1992) measured current speeds of 0.9–3.4 $cm \cdot s^{-1}$ at their study site in the western basin of Lake Erie but suggested that these values were probably recorded during calm periods. If the value of 3.4 $cm \cdot s^{-1}$ is doubled to account for any potential differences in currents between the present study and those from MacIsaac et al. (1992), then our traps would have an Re of 6434, which is under the limit suggested by Lau (1979) (<7000) for avoiding a turbulent bottom layer in the trap.

The traps were made out of 9.5-cm-diameter Plexiglas tubing. Each tube was 51 cm high. Holes were drilled at appropriate levels in each tube to allow for draw-off of water after retrieval. As well, one hole was drilled in the bottom to allow for sediment removal. All holes were plugged with rubber stoppers during deployment.

Eight traps were used at each site. Three traps were used for collection of sedimenting material (sedimentation traps), another three contained random samples of zebra mussels for the purpose of collecting biodeposits (biodeposition traps), and two other traps containing empty shells of zebra mussels were used as controls for the biodeposition traps (control traps). All mussels for the biodeposition traps were collected from the lake bottom at buoy E10 (Fig. 1). Each trap contained 300–500 mussels. The mussels were placed in a Plexiglas cage (Fig. 2) which fitted closely on the inside of the sediment trap. The cage was held in the trap about 10 cm from the top by pegs that ran through the tube. Prior to deployment, all traps and cages were thoroughly cleaned with soap and water and rinsed with hexane.

Despite the use of open-water sites in the present study,

© 1998 NRC Canada

Fig. 2. Design of the zebra mussel cage apparatus used to deploy all types of traps (refer to Materials and methods) in the western basin of Lake Erie, August 1992.

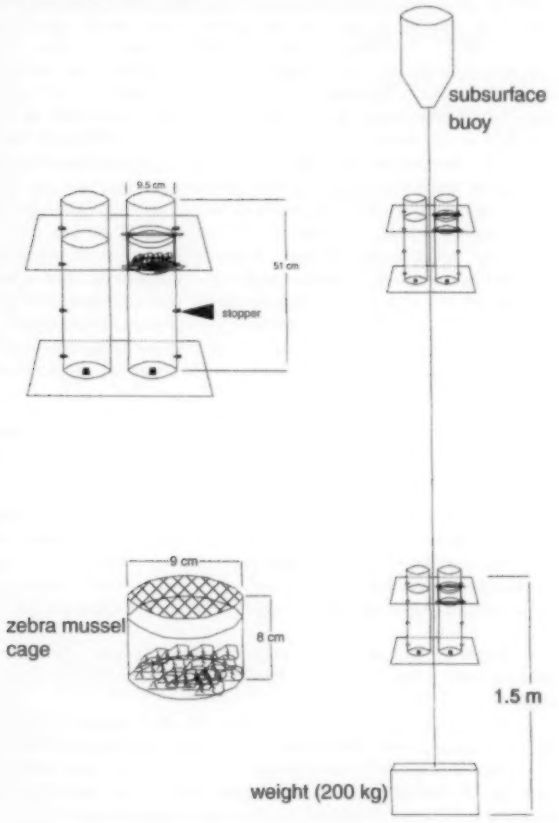

Fig. 3. Design of the settlement racks used in the western basin of Lake Erie for the purpose of determining the recruitment of zebra mussels, July–September 1992.

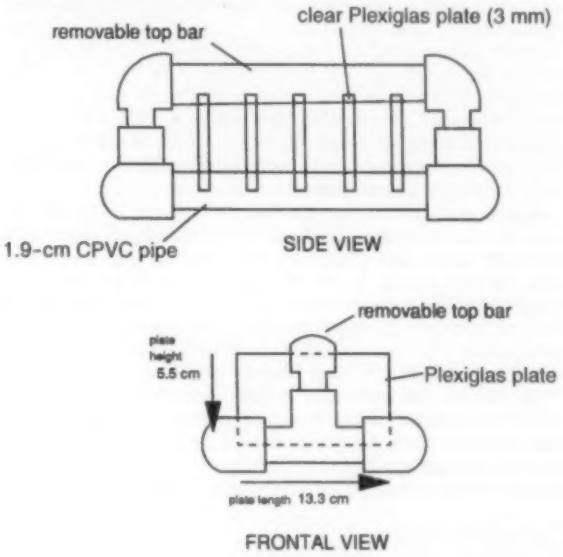

resuspended sediment was probably a major portion of the trap material. Our experimental design, however, enabled us to compare the three types of traps, since the effects of resuspension would have been constant for each.

The trap deployment structure at each site consisted of a large styrofoam buoy (473 × 321 mm) submerged 3 m below the surface of the water and anchored by about 200 kg of weight (Fig. 2). Sediment traps were attached onto fixed brackets and held in place with elastic cords attached to galvanized aircraft cable (3 mm in diameter). All attachments (at the buoy, anchor, and sediment trap brackets) were constructed so that complete 360° movement around the line was possible. The approximate upward lift created by the buoy was 50 kg, which caused minimal swaying motion of the apparatus. This design proved resistant to dislocation by waves and currents.

Trap deployment took place August 11, 12, and 18, 1992, and traps were left in the water undisturbed until September 12, 1992.

In previous studies, chloroform was used to reduce decomposition of trapped material (Broman et al. 1989; Baker et al. 1991). Sigg et al. (1987) suggested that chemical preservatives in traps may interfere with contaminant levels in the settled material. This may be particularly true with organic contaminants, since chloroform, for example, is an organic compound that may sorb contaminants from the sediments or water. Therefore, we did not use preservatives. Rubber stoppers used in plugging drainage holes were wrapped in hexane-rinsed aluminum foil to prevent any contamination/sorption caused by the rubber.

Settlement rack study

At eight of the 10 sites in the western basin (the exception being Point Pelee), several settlement racks (Fig. 3) were deployed in early June 1992 for the purpose of determining recruitment densities of mussels. Density estimates were later incorporated into calculations for biodeposition per unit area by zebra mussels (described later). The rack consisted of five Plexiglas plates (each plate 5.5 × 13.3 cm) mounted in a frame made of CPVC pipe (1.9 cm in diameter). One rack was removed about every 2 weeks by SCUBA divers, thus enabling recruitment density measurements to be determined for the entire rack deployment period (about 2 months). For each date, the number of mussels and the length–frequency distribution on each plate were determined. Length–frequency distributions were determined by digitizing 150–200 mussels per plate using a Hipad™ digitizing pad and an associated computer program developed by Mr. Russel Hopcroft, University of Guelph, Guelph, Ont. If total numbers of mussels on plates were less than 150–200, all mussels were digitized.

Trap removal and sediment sample collection

After the deployment period (about 3–4 weeks), traps were removed from the water by SCUBA divers. All traps were tightly capped while still attached to the line underwater to avoid any disturbance during ascent and transport back to shore. Although material in traps did not appear to be disturbed during retrieval and transport, all traps were left intact for a minimum of 5 h upon reaching shore so that material that may have been suspended in the trap water would settle. Very fine suspended material may not have settled during this time, but we assumed that most of the potential suspended material had done so. In addition, we assumed that the rate of settling of particles disturbed during retrieval was constant among trap types. Water was then drained off by removing successive stoppers from the top down each tube. The small amount of remaining water and all trapped material was removed by unplugging the bottom rubber stopper and draining the contents into a 1-L hexane-rinsed, acid-washed mason jar. Any excess material left in the trap was rinsed through the bottom opening with water that was previously drained from the tube. All jars were appropriately labelled and capped, with hexane-rinsed

© 1998 NRC Canada

aluminum foil used as a liner. Upon return to the laboratory, all jars were placed in a refrigerator (4°C) for at least 12 h to allow any remaining suspended material to settle. Water was then siphoned off and solid material was thoroughly mixed with a stainless steel, hexane-rinsed, acid-washed probe. A small subsample (about 100 mg) was removed and immediately frozen (–22°C) for the purpose of determining organic matter content of the trap sample. This was done by drying each subsample at 60°C until constant weight (about 24 h) and then weighing and ashing at 550°C for 2 h after gradually bringing the samples up to temperature over a 3-h period. After cooling down in a desiccator, samples were reweighed to determine the percent loss on ignition.

Upon retrieval of the apparatus, mussels in the biodepositional traps were removed and immediately placed on ice until return to the laboratory (same day) where they were frozen at –22°C. At a later date, the shell lengths of 150–200 mussels from each sample were determined using methods already described. The shell lengths were used to determine the length–frequency distribution of mussels in each sample. The dry weight (DW) of all mussel samples was determined by drying at 60°C until constant weight was attained (about 48 h). The ash-free dry weight (AFDW) of each sample was determined by gradually raising the temperature over a 3-h period and then ashing at 550°C for 2 h. Samples were placed in a desiccator prior to reweighing. These data were later used to calculate the amount of mussel biodeposition on a per unit weight basis.

Contaminant analysis

All sediment samples were analysed for t-PCBs and Cd by Ortech Corporation, Mississauga, Ont. For both t-PCB and Cd analysis, a separate portion of each sample was removed and accurately weighed. Moisture content was then determined. For t-PCB analysis, the sediment sample was triple extracted with 50% acetone in hexane. Cleanup procedures were performed on a 2% water-deactivated Florisil column. Total PCB determinations were carried out by a packed-column GC/EC technique. Aroclor 1254 was used as a PCB reference. For Cd analysis, the sample was digested twice with aqua regia (3 HCl : 1 HNO_3), filtered through Whatman 40 paper, and then diluted to volume. Analysis was carried out by flame atomic absorption spectroscopy.

For quality assurance and control (QA/QC), two randomly chosen samples were split and submitted as regular samples. Results for contaminant analysis showed similar values. As part of Ortech's own QA/QC, several samples were analysed twice, also showing very similar values. As well, for PCB analysis, a soil reference material (lot No. 9701) from Environmental Resource Associates was included, which gave 91% recovery.

Calculations and statistical analysis

Material produced by zebra mussels in the traps consisted of feces and pseudofeces, which were indistinguishable and therefore were included under the one term, biodeposits. "Biodeposition" refers to the process of zebra mussels depositing suspended material that they have filtered from the water column. "Sedimentation" here refers to the process of suspended material settling into the bottom of the sedimentation traps. "Deposition" refers to the process of suspended material settling into the bottom of traps through sedimentation and (or) biodeposition. Biodeposited material was also indistinguishable from sedimented material in the traps containing zebra mussels. Therefore, biodeposition rates by mussels were determined for a site by determining the difference between the mean weight of material in the biodeposition and control traps. Each value was then divided by the AFDW of the mussels in the biodeposition trap and by the number of deployment days to determine the biodeposition rate on a per unit tissue weight basis.

Biodeposition rates were compared with sedimentation rates to test if there was any significant effect caused by zebra mussels. This comparison was done by converting biodeposition and sedimentation rates to a per unit area basis (i.e., per square metre). Sedimentation rates in this respect were calculated by simple conversion from the area of the sediment trap opening. Biodeposition rates were converted to a per unit area value by first calculating the weight distribution of the mussels in the traps, using the length–weight regression $y = 0.007x^{2.982}$, described by Mackie (1993), where x is the shell length and y is the dry tissue weight. For each biodeposition trap, this weight was then multiplied by the number of mussels per square metre, determined from those found on the settlement racks on the last day of the sampling period (September 12, 1992), and then divided by the number of mussels in the trap. This calculated weight per square metre was multiplied by the biodeposition rate per unit weight of mussel tissue (calculation described previously) from the biodeposition traps for each site. If more settlement of mussels was to occur after this date, then at worst, these calculated values would be underestimates of the tissue weight of mussels per unit area. Biodeposition per unit area was compared with sedimentation per unit area using a paired Student t-test at $p \leq 0.05$ level of acceptance.

Organic matter and contaminant concentrations in the biodeposited material also could not be directly determined and were calculated using the following equation:

$$[X]_{pf} = \frac{[X]_{bd} \cdot [\text{weight}]_{bd} - [X]_{sm} \cdot [\text{weight}]_{sm}}{\text{weight of pf}} \quad (1)$$

where X is the contaminant or organic matter, "pf" is pseudofeces and feces produced by mussels, "sm" is sedimented material (mean of sediment and control trap concentrations, see above), "bd" is biodeposition trap material (i.e., "pf" and "sm" in trap containing mussels), and weight of "pf" is weight of "bd" minus mean weight of "sm".

Contaminant concentrations in the biodeposits and sedimented material were compared over all sites by using a paired Student t-test at the $p \leq 0.05$ level.

Biodeposition rates of organic matter and contaminants per unit weight of mussel were determined by multiplying the organic matter or contaminant concentration of "pf" by the biodeposition rate for each site. Sedimentation rates of organic matter and contaminants were also calculated by multiplying the sedimentation rate (weight of sediment trap material divided by the number of deployment days) by the organic matter or contaminant concentration of "sm" for each site.

Biodeposition and sedimentation rates of organic matter and contaminants were compared on a per unit area basis by multiplying biodeposition and sedimentation rates per square metre by the respective organic matter or contaminant concentrations at each site. Comparisons were then made using a paired Student t-test at the $p \leq 0.05$ level.

Results

Effects of zebra mussels on deposition

Control traps versus sedimentation traps

The presence of mussel shells did not significantly affect ($p > 0.05$) the amount of material deposited in the control traps, when compared with the amount of material in the sedimentation traps. As a result, weight data were combined for the control and sedimentation traps at each site, and these values were subsequently used in determining the biodeposition rates of the mussels.

Biodeposition versus sedimentation

When biodeposition rates of mussels were converted to a per unit area basis, the potential for mussels to greatly accelerate suspended matter deposition became apparent. The

© 1998 NRC Canada

Table 1. Adult zebra mussel abundances (mean ± 1 SD) calculated from mussels found on settlement racks at sites in the western basin of Lake Erie, September 12, 1992.

Site[a]	Abundance (number·m^{-1})
E13 top	1 082 263 ± 288 367
E13 bottom	732 208 ± 14 151
Pelee Island top	291 529 ± 115 296
Pelee Island bottom	200 456 ± 52 834
E10 top	224 072 ± 71 566
E10 bottom	214 010 ± 83 128
H top	206 775 ± 69 887
H bottom	319 264 ± 86 515

[a]Top: sampling apparati placed 3 m under the surface of the water; bottom: sampling apparati placed 1.5 m off the bottom of the lake. Refer to Fig. 1 for specific locations.

Table 2. Biodeposition rates (mean ± 1 SD) of suspended material by zebra mussels calculated from the biodeposition traps at all sites in the western basin of Lake Erie, August 1992.

Site[a]	Biodeposition rate (g DW biodeposits·g DW tissue·day^{-1})
E13 top	0.096±0.049
E13 bottom	0.055±0.011
Pelee Island top	0.142±0.098
Pelee Island bottom	0.446±0.054
Point Pclee top	0.471±0.112
Point Pelee bottom	0.799±0.037
E10 top	0.296±0.013
E10 bottom	0.383±0.106
H top	0.089±0.022
H bottom	0.179±0.050

[a]Top: sampling apparati placed 3 m under the surface of the water; bottom: sampling apparati placed 1.5 m off the bottom of the lake. Refer to Fig. 1 for specific locations.

biodeposition rate of mussels per unit area in the western basin is based on the zebra mussel densities (on racks) (Table 1) and on the biodeposition rate of mussels in the traps at each site (Table 2). When compared among sites (paired Student *t*-test), calculated biodeposition rates per unit area by zebra mussels were significantly greater ($p < 0.05$) than the sedimentation rates per unit area by, on average, over 8 times (Table 3). Average biodeposition rates ranged from 236 g DW biodeposits·m^{-2}·day^{-1} (site H top) to 2076 g DW biodeposits·m^{-2}·day^{-1} (site E13 top) whereas average sedimentation rates ranged from 77.9 g DW sediment·m^{-2}·day^{-1} (site H top) to 167.9 g DW sediment·m^{-2}·day^{-1} (site Point Pelee bottom).

Effects of zebra mussels on deposition of organic matter and contaminants

When compared among all sites, there were no significant differences between organic matter, PCB (Table 4), or Cd (Table 5) concentrations in the biodeposited and sedimented material. Organic matter content was about 7–16% of the total trap material. PCB concentration of the trap material ranged from 0.037 to 0.276 µg PCB·g DW deposition^{-1}. Cadmium concentration ranged from 0.35 to 0.80 µg Cd·g DW deposition^{-1}. However, when considering the obvious influence of mussels on deposition of suspended material (see previous results), the calculated biodeposition rates of organic matter (Table 6), PCBs (Table 7), and Cd (Table 8) per unit area were significantly greater (paired Student *t*-test, $p < 0.05$) than the sedimentation rates of these among sites in the western basin. These differences, on average, were about 8–10 times greater.

Discussion

Biodeposition versus sedimentation

Zebra mussels appear to increase the sedimentation rate of suspended material over natural sedimentation through their filtration and biodeposition processes. To quantify the effects of biodeposition on a lake, biodeposition rates must be converted to a per unit area basis so that direct comparisons can be made with sedimentation rates. Tsuchiya (1980) calculated biodeposition rates for blue *Mytilus edulis* in intertidal and subintertidal regions of Japan by developing a regression model of mussel shell length versus mussel biodeposition rates for different times of the year and then applying this to in situ mussels. In the present study, a different approach was taken where biodeposition rates determined from trap mussels were multiplied by the tissue weight of mussels on a per square metre basis given the density found on the settlement racks. We felt that this was the most appropriate approach here, since it takes into account the biodeposition rate of a mature population of mussels (mussels used in the biodeposition traps) and the density of the mussels found at the site of interest (newly settled mussels on the racks). However, this method may be overestimating the true biodeposition rate, since the density values of mussels are based on the settlement rack data, which may not be representative of natural densities. For example, mussels on racks suspended in the water column may have less predation exposure than in situ mussels on the bottom of the lake, resulting in a higher density estimate than that naturally found. Unfortunately, density measurements of in situ mussels were not taken in this study. Therefore, the settlement rack data are the best available estimates for determining specific site densities. Leach (1993) recorded densities of in situ zebra mussels at between 142 000 and 342 000·m^{-2} on reefs in western Lake Erie. The densities estimated from the settlement racks in the present study are similar to Leach's values. Therefore, results incorporating settlement rack data appear to be applicable to western basin locations with solid substrates, such as reefs.

Mussels appear to have a very large potential to increase the deposition of suspended material and increase water clarity, since the biodeposition rates alone in this study were found to be up to 8 times greater than corresponding sedimentation rates. The lake-wide implications of this are not decernable within the scope of our study; however, given that our zebra mussel densities are representative of solid substrates in the western basin, our calculated biodeposition rates per unit area could be considered estimates of mussel

© 1998 NRC Canada

Table 3. Calculated biodeposition rates (mean ± 1 SD) of suspended material by zebra mussels on a per square metre basis (refer to Materials and methods for calculation procedure) and sedimentation rates of suspended material on a per square metre basis at all sites in the western basin of Lake Erie, August 1992.

Site[a]	Biodeposition rate (g DW biodeposits·m^{-2}·day^{-1})	Sedimentation rate (g DW sediments·m^{-2}·day^{-1})
E13 top	2076±1062	90.3±6.8
E13 bottom	613±119	165.1±42.9
Pelee Island top	636±440	83.2±7.1
Pelee Island bottom	1379±169	105.8±9.3
Point Pelee top	—	121.9±7.1
Point Pelee bottom	—	167.9±17.5
E10 top	774±33	88.5±5.6
E10 bottom	896±248	150.1±0.6
H top	236±58	77.9±1 9.5
H bottom	645±181	91.7±14.7

[a]Top: sampling apparati placed 3 m under the surface of the water; bottom: sampling apparati placed 1.5 m off the bottom of the lake. Refer to Fig. 1 for specific locations.

Table 4. Calculated PCB concentrations (mean ± 1 SD) in the zebra mussel biodeposits from biodeposition traps (refer to Materials and methods for calculation procedures) and in settled material in sedimentation traps at all sites in the western basin of Lake Erie, August 1992.

Site[a]	PCB concentration in biodeposits (μg PCBs·g DW biodeposits^{-1})	Sedimentation rate (μg PCBs·g DW sediment^{-1})
E13 top	0.240±0.072	0.114±0.025
E13 bottom	0.090±0.028	0.154±0.038
Pelee Island top	0.276±0.058	0.202±0.121
Pelee Island bottom	0.037±0.015	0.220±0.112
Point Pelee top	0.163±0.122	0.098±0.015
Point Pelee bottom	0.104±0.071	0.083±0.010
E10 top	0.258±0.076	0.122±0.029
E10 bottom	0.212±0.076	0.122±0.019
H top	0.102±0.058	0.192±0.055
H bottom	0.177±0.023	0.154±0.026

[a]Top: sampling apparati placed 3 m under the surface of the water; bottom: sampling apparati placed 1.5 m off the bottom of the lake. Refer to Fig. 1 for specific locations.

biodeposition at such natural locations. Several studies have outlined the potential effects of zebra mussels on water clarification. Reeders et al. (1989) concluded that their experimental lakes could be filtered at least once a month by the existing zebra mussel population. In Lake Erie, Holland (1993) observed lower plankton levels in water samples taken after the zebra mussel invasion compared with preinvasion data. MacIsaac et al. (1992) also observed a depletion of chlorophyll *a* concentrations above *Dreissena* beds. These findings, in conjunction with the present results, strongly suggest that filtration and resulting biodeposition by zebra mussels in Lake Erie are great enough to significantly decrease water column biomass of suspended material. The extent of this would require long-term investigations on a lake-wide scale.

Organic matter, PCB, and Cd deposition

The results of this study support the prediction that zebra mussels significantly increase the deposition rate of organic matter, t-PCBs, and Cd over that of natural sedimentation. Results pertaining to PCB and Cd deposition by zebra mussels followed a similar trend and are discussed together.

Organic matter concentration in the biodeposits was not significantly different from that of the sedimented material, which does not reflect findings of other studies. Jaramillo et al. (1992) found that the biodeposits from mussels used in their study were, in general, higher in organic carbon content than the sedimented material. Kautsky and Evans (1987) found similar results. The latter study attributed this to the selection by mussels of particles that had high organic content. Pseudofeces production by mussels may be a response to

© 1998 NRC Canada

Table 5. Calculated Cd concentrations (mean ± 1 SD) in zebra mussel biodeposits from biodeposition traps (refer to Materials and methods for calculation procedure) and in settled material in sedimentation traps at all sites in the western basin of Lake Erie, August 1992.

Site[a]	Cd concentration in biodeposits (μg Cd·g DW biodeposits^{-1})	Cd concentration in sedimentation (μg Cd·g DW sediment^{-1})
E13 top	0.35±0.18	0.85±0.10
E13 bottom	0.51±0.12	0.96±0.20
Pelee Island top	1.08±0.19	0.48±0.14
Pelee Island bottom	0.69±0.05	0.72±0.22
Point Pelee top	1.52±0.67	0.84±0.09
Point Pelee bottom	0.80±0.07	0.83±0.08
E10 top	0.83±0.17	0.85±0.28
E10 bottom	1.31±0.75	0.77±0.13
H top	0.75±0.02	0.87±0.41
H bottom	1.41±0.36	0.61±0.22

[a]Top: sampling apparati placed 3 m under the surface of the water; bottom: sampling apparati placed 1.5 m off the bottom of the lake. Refer to Fig. 1 for specific locations.

Table 6. Calculated biodeposition rates (mean ± 1 SD) of organic matter on a per square metre basis and sedimentation rates of organic matter on a per square metre basis at all sites in the western basin of Lake Erie, August 1992.

Site[a]	Biodeposition rate of organic matter (g AFDW organic matter·m^{-2}·day^{-1})	Sedimentation rate of organic matter (g AFDW organic matter·m^{-2}·day^{-1})
E13 top	224.2±111.4	7.0±1.1
E13 bottom	101.3±31.8	13.9±4.8
Pelee Island top	73.0±50.8	7.2±0.8
Pelee Island bottom	133.2±26.2	9.6±2.8
E10 top	51.5±17.4	8.0±3.6
E10 bottom	79.6±23.1	11.8±0.6
H top	23.7±7.0	8.7±2.2
H bottom	88.3±38.2	9.3±1.5

[a]Top: sampling apparati placed 3 m under the surface of the water; bottom: sampling apparati placed 1.5 m off the bottom of the lake. Refer to Fig. 1 for specific locations.

overall high concentrations of suspended material which may clog the gills (Foster-Smith 1975; Sprung and Rose 1988; Reeders and Bij de Vaate 1992). Although total suspended solid concentrations in the present study were not exceedingly high (maximum of 6.4 mg·L^{-1} in the present study compared with a maximum of 86.4 mg·L^{-1} in Reeders and Bij de Vaate 1992), perhaps zebra mussels were producing pseudofeces in response to the concentrations of suspended solids. The sedimentation of suspended material will include organic and inorganic components. Therefore, we expected similar organic matter concentrations in biodeposited and sedimented material, since there would not be a specific selection for organic or inorganic particulates by mussels to be deposited as pseudofeces.

The concentrations of PCBs and Cd in the biodeposits were similar to those in the sedimented material. Reeders et al. (1993) observed a higher level of both of these contaminants in zebra mussel biodeposits than with suspended material. They attributed this to a selection for deposition of smaller particles, which would therefore have a greater surface area and greater contaminant concentration. The measurement of the size range of particles was not possible in the present study, since naturally sedimenting material and biodeposits were mixed in the traps. Both Cd and PCBs preferentially bind to organic matter, especially PCBs which are lipophilic (Allan 1986; Morfett et al. 1988; Servos and Muir 1989). Contaminant concentrations may not differ because of the similarity in the content of organic matter to which these contaminants are bound.

The greater rate of organic matter biodeposition per unit area over that of sedimentation may have particular importance, among other reasons, because increased deposition of organic matter due to zebra mussels may be providing other benthic invertebrates with an increased food source (Tsuchiya 1980; Kautsky and Evans 1987; Deslous-Paoli et al. 1992; Klerks et al. 1996). Kautsky and Evans (1987) pointed out that species diversity and biomass are generally higher in mussel beds than in areas without mussels. The

© 1998 NRC Canada

Table 7. Calculated biodeposition rates (mean ± 1 SD) of PCBs on a per square metre basis by zebra mussels (refer to Materials and methods for calculations) and sedimentation rates of PCBs on a per square metre basis for sites at sites in the western basin of Lake Erie, August 1992.

Site[a]	Biodeposition rate of PCBs ($\mu g\ PCBs \cdot m^{-2} \cdot day^{-1}$)	Sedimentation rate of PCBs ($\mu g\ PCBs \cdot m^{-2} \cdot day^{-1}$)
E13 top	480.3±228.1	8.8±1.0
E13 bottom	50.7±8.0	26.8±4.7
Pelee Island top	177.3±123.4	13.4±8.8
Pelee Island bottom	49.5±13.1	20.5±12.1
Point Pelee top	—	12.6±1.1
Point Pelee bottom	—	13.3±2.8
E10 top	197.9±51.9	9.6±0.9
E10 bottom	198.8±119.1	16.7±1.3
H top	25.2±15.6	13.8±1.3
H bottom	117.7±21.9	15.4±1.3

[a]Top: sampling apparati placed 3 m under the surface of the water; bottom: sampling apparati placed 1.5 m off the bottom of the lake. Refer to Fig. 1 for specific locations.

Table 8. Calculated biodeposition rates (mean ± 1 SD) of Cd on a per square metre basis by zebra mussels (refer to Materials and methods for calculation procedures) and sedimentation rates of Cd on a per square metre basis for sites in the western basin of Lake Erie, August 1992.

Site[a]	Biodeposition rate of Cd ($\mu g\ Cd \cdot m^{-2} \cdot day^{-1}$)	Sedimentation rate of Cd ($\mu g\ Cd \cdot m^{-2} \cdot day^{-1}$)
E13 top	609.8±145.8	79.4±18.5
E13 bottom	303.9±15.9	82.8±27.3
Pelee Island top	689.9±471.1	45.6±7.9
Pelee Island bottom	944.3±43.8	65.3±28.0
Point Pelee top	—	107.4±4.2
Point Pelee bottom	—	146.7±9.9
E10 top	637.4±105.4	80.7±8.1
E10 bottom	1083.0±344.0	154.9±36.7
H top	177.6±41.8	88.7±41.7
H bottom	885.1±191.7	55.6±9.3

[a]Top: sampling apparati placed 3 m under the surface of the water; bottom: sampling apparati placed 1.5 m off the bottom of the lake. Refer to Fig. 1 for specific locations.

same study found that *Mytilus edulis* increased deposition of organic matter to the bottom sediments. Izvekova and Lvova-Katchanova (1972) observed greater growth of chironomid larvae exposed to zebra mussel biodeposits than when exposed to other food sources. Therefore, zebra mussel biodeposition could be providing an additional food source for benthic animals.

Given that the biodeposits have organic matter and contaminant concentrations similar to those of the sedimented material, and biodeposition by mussels is significantly greater than sedimentation, it would be expected that the biodeposition of organic matter and contaminants would exceed sedimentation of contaminants on a per unit area basis. Following our argument previously, the potential for mussels to increase deposition of suspended material up to 8 times around lake substrates such as reefs would be applicable to organic matter and contaminant deposition also. Reeders and Bij de Vaate (1992) did not compare biodeposition rates of contaminants with sedimentation rates, although they suggested that zebra mussels may act as an excellent "biological filter" through the biodeposition of contaminants. Given the estimates generated by our study, this may be applicable to the Great Lakes as well.

When the biodeposition rates of organic matter and contaminants are converted to a per square metre basis, the potential effects of the presence of zebra mussels in western Lake Erie become evident; however, the influence of resuspension must also be considered. Increased deposition may be increasing food supply and contaminant transfer from pelagic areas to benthic food webs. Alternatively, much of the material biodeposited by zebra mussels could be resuspended, making it unavailable to benthic animals. Kautsky and Evans (1987)

© 1998 NRC Canada

stated that mussel biodeposits consist of packages of fine-sized particles that can easily be broken up and resuspended. This may be particularly true of pseudofecal pellets, since these are not as compacted as fecal pellets, and the mucus exterior can easily dissolve in water, thus allowing for easy breakup and resuspension (Deslous-Paoli et al. 1992). Kemp et al. (1977) observed a mean sedimentation rate for western Lake Erie of 5.92 $g \cdot m^{-2} \cdot day^{-1}$, which is considerably less than the sedimentation rate observed in the present study. This suggests that much of the material being trapped is from resuspension. If most of the biodeposition by zebra mussels consists of pseudofeces, as suggested earlier, then the net effect of biodeposition may not be as great as shown in the present study, since the resuspension factor was not considered. Further studies dealing with the effects of contaminant biodeposition on benthic animals and food web transfer are required to understand these processes. These studies should incorporate resuspension factors, since this is an important means by which contaminants can be reintroduced into the cycling process. The present study only examined the effects of zebra mussels on the flux of these contaminants through biodeposition. Knowing the extent of resuspension processes is important to better understand the overall effects of zebra mussels on contaminant dynamics in aquatic environments.

Acknowledgements

The authors wish to gratefully acknowledge the field and laboratory contributions of Todd Gillis, Tom MacDougall, Mick Legare, and Jim Godfrey. Funding was provided by the Ontario Ministry of Environment and Energy, Project 594G.

References

Allan, R.J. 1986. The role of particulate matter in the fate of contaminants in aquatic ecosystems. Sci. Ser. No. 142, Inland Waters Directorate, National Water Research Institute, Canada Centre for Inland Waters, Burlington, Ont.

Baker, J.E., Eisenreich, S.J., and Eadie, B.J. 1991. Sediment trap fluxes and benthic recycling of organic carbon, polycyclic aromatic hydrocarbons, and polychlorobiphenyl congeners in Lake Superior. Environ. Sci. Technol. **25**: 500–509.

Broman, D., Naf, C., Zebuhr, Y., and Lexen, K. 1989. The composition, distribution and flux of PCDDs and PCDFs in settling particulate matter (SPM) — a sediment trap study in the northern Baltic. Chemosphere, **19**: 445–450.

Deslous-Paoli, J., Lannou, A., Geairon, P., Bougrier, S., Raillard, O., and Heral, M. 1992. Effects of the feeding behaviour of *Crassostrea gigas* (Bivalve Molluscs) on biosedimentation of natural particulate matter. Hydrobiologia, **231**: 85–91.

Farara, D.G., and Burt, A.J. 1993. Environmental assessment of western Lake Erie sediments and benthic communities — 1991. Report prepared for the Ontario Ministry of Environment and Energy, Water Resources Branch, Great Lakes Section, by Beak Consultants Limited, Brampton, Ont.

Foster-Smith, R.L. 1975. The effects of concentration of suspension on the filtration rates and pseudofaecal productions for *Mytilus edulis* L., *Cerastoderma edule* (L.) and *Venerupis pullastra* (Montagu). J. Exp. Mar. Biol. Ecol. **17**: 1–22.

Hawley, N. 1988. Flow in cylindrical sediment traps. J. Great Lakes Res. **14**: 76–88.

Holland, R.E. 1993. Changes in planktonic diatoms and water transparency in Hatchery Bay, Bass Island area, western Lake Erie since the establishment of the zebra mussel. J. Great Lakes Res. **10**: 617–624.

Izvekova, E.I., and Lvova-Katchanova, A.A. 1972. Sedimentation of suspended matter by *Dreissena polymorpha* Pallas and its subsequent utilization by chironomidae larvae. Pol. Arch. Hydrobiol. **19**: 203–210.

Jaramillo, E., Bertran, C., and Bravo, A. 1992. Mussel biodeposition in an estuary in southern Chile. Mar. Ecol. Prog. Ser. **82**: 85–94.

Kautsky, N., and Evans, S. 1987. Role of biodeposition by *Mytilus edulis* in the circulation of matter and nutrients in a Baltic coastal ecosystem. Mar. Ecol. Prog. Ser. **38**: 201–212.

Kemp, A.L.W., MacInnis, G.A., and Harper, N.S. 1977. Sedimentation rates and a revised sediment budget for Lake Erie. J. Great Lakes Res. **3**: 221–233.

Klerks, P.L., Fraleigh, P.C., and Lawniczak, J.E. 1996. Effects of zebra mussels (*Dreissena polymorpha*) on seston levels and sediment deposition in western Lake Erie. Can. J. Fish. Aquat. Sci. **53**: 2284–2291.

Lau, Y.L. 1979. Laboratory study of cylindrical sedimentation traps. J. Fish. Res. Board Can. **36**: 1288–1291.

Leach, J.H. 1993. Impacts of the zebra mussel (*Dreissena polymorpha*) on water quality and fish spawning reefs in western Lake Erie. *In* Zebra mussels, biology, impacts, and control. *Edited by* T.F. Nalepa and D.W. Schloesser. Lewis Publishers, Boca Raton, Fla. pp. 381–397.

MacIsaac, H.J., Sprules, W.G., Johannsson, O.E., and Leach, J.H. 1992. Filtering impacts of larval and sessile zebra mussels (*Dreissena polymorpha*) in western Lake Erie. Oecologia (Heidelb.), **92**: 30–39.

Mackie, G.L. 1993. Biology of the zebra mussel (*Dreissena polymorpha*) and observations of mussel colonization on anoint bivalves in Lake St. Clair of the Great Lakes. *In* Zebra mussels, biology, impacts, and control. *Edited by* T.F. Nalepa and D.W. Schloesser. Lewis Publishers, Boca Raton, Fla. pp. 153–181.

Morfett, K., Davison, W., and Hamilton-Taylor, J. 1988. Trace metal dynamics in a seasonally anoxic lake. Environ. Geol. Water Sci. **11**: 107–114.

Reeders, H.H., and Bij de Vaate, A. 1992. Bioprocessing of polluted suspended matter from the water column by the zebra mussel (*Dreissena polymorpha* Pallas). Hydrobiologia, **239**: 53–63.

Reeders, H.H., Bij de Vaate, A., and Slim, F.J. 1989. The filtration rate of *Dreissena polymorpha* (Bivalvia) in three Dutch lakes with reference to biological water quality management. Freshwater Biol. **22**: 133–141.

Reeders, H.H., Bij de Vaate, A., and Noordhuis, R. 1993. Potential of the zebra mussel (*Dreissena polymorpha*) for water quality management. *In* Zebra mussels, biology, impacts, and control. *Edited by* T.F. Nalepa and D.W. Schloesser. Lewis Publishers, Boca Raton, Fla. pp. 439–464.

Roff, J.C., and Hopcroft, R.R. 1985. Determination of sediment traps with respect to their size and aspect ratio, and water velocity and particle size. Contract 01-SKW405-4-0039, Department of Supplies and Services, Ottawa, Ont.

Servos, M.R., and Muir, D.C.G. 1989. Effects of dissolved organic matter from Canadian shield lakes on the bioavailability of 1,3,6,8-tetrachlorodibenzo-*p*-dioxin to the amphipod *Crangonyx laurentianus*. Environ. Toxicol. Chem. **4**: 511–521.

Sigg, L., Strum, M., and Kistler, D. 1987. Vertical transport of heavy metals by settling particles in Lake Zurich. Limnol. Oceanogr. **32**: 112–130.

Sprung, M., and Rose, U. 1988. Influence of food size and food quality on the feeding of the mussel *Dreissena polymorpha*. Oecologia (Heidelb.), **77**: 526–532.

Stanczykowska, A., Lawacz, W., and Mattice, J. 1975. Use of field measurements of consumption and assimilation of evaluation of the role of *Dreissena polymorpha* Pall. in a lake ecosystem. Pol. Arch. Hydrobiol. **22**: 509–520.

Tsuchiya, M. 1980. Biodeposit production by the mussel *Mytilus edulis* L. on rocky shores. J. Exp. Mar. Biol. Ecol. **47**: 203–222.

© 1998 NRC Canada

Competition between larval lake herring (*Coregonus artedi*) and lake whitefish (*Coregonus clupeaformis*) for zooplankton

Bruce M. Davis and Thomas N. Todd

Abstract: Diet and growth of larval lake herring (*Coregonus artedi*) and lake whitefish (*Coregonus clupeaformis*) were compared in mesocosm experiments in a small mesotrophic lake in southeastern Michigan. Fish were sampled from single-species and mixed assemblages in 2-m^3 cages for 8 weeks during April and May. Both species initially ate mostly cyclopoid copepodites and small cladocerans (*Bosmina* spp.). Schoener's index of diet overlap showed considerable overlap (70–90%). Lake whitefish ate *Daphnia* spp. and adult copepods about 2 weeks earlier than did lake herring, perhaps related to their larger mean mouth gape. Lake whitefish were consistently larger than lake herring until the eighth week, especially in the sympatric treatments. Lake whitefish appeared to have a negative effect on the growth of lake herring, as lake herring in mixed-species treatments were smaller and weighed less than lake herring reared in single-species treatments. The diet similarities of lake whitefish and lake herring larvae could make them competitors for food in the Great Lakes. The greater initial size of lake whitefish could allow them to eat larger prey earlier and thereby limit availability of these prey to lake herring at a crucial period of development.

Résumé : Le régime et la croissance des larves de cisco (*Coregonus artedi*) et de grand corégone (*Coregonus clupeaformis*) ont été comparés dans le cadre d'expériences en mésocosmes menées dans un petit lac mésotrophe du sud-est Michigan. On a procédé pendant 8 semaines, en avril et mai, à un échantillonnage des poissons gardés dans des cages de 2 m^3 contenant une seule espèce ou un mélange des espèces. Au début, les deux espèces se nourrissaient principalement de copépodites cyclopidés et de petits cladocères (*Bosmina* spp.). Selon l'indice de Schoener, le chevauchement des régimes alimentaires était considérable (70–90%). Le grand corégone s'est nourri de *Daphnia* spp. et de copépodes adultes environ 2 semaines plus tôt que le cisco, peut-être en raison de la plus grande largeur moyenne de sa bouche. Les grands corégones ont eu une taille constamment supérieure aux ciscos jusqu'à la huitième semaine, en particulier lorsqu'ils étaient soumis au mode sympatrique. Les grands corégones ont semblé exercer un effet négatif sur la croissance des ciscos, car ces derniers, lorsque les espèces étaient mélangées, avaient une taille et un poids inférieurs aux sujets des groupes monospécifiques. En raison des similarités du régime alimentaire des larves du cisco et du grand corégone, ces deux espèces pourraient entrer en compétition alimentaire dans les Grands Lacs. La taille initiale plus grande des grands corégones pourrait leur permettre de consommer plus tôt des proies plus grosses, ce qui limiterait la possibilité pour le cisco de se nourrir de ces proies à une période cruciale de son développement.
[Traduit par la Rédaction]

Introduction

The coregonine fishes of the Great Lakes historically comprised a complex group of several species differentiated primarily by time and place of spawning (Smith and Todd 1984). Human impacts on the Great Lakes severely depleted stocks of all species, in particular, lake herring (*Coregonus artedi*), lake whitefish (*Coregonus clupeaformis*), and bloater (*Coregonus hoyi*), and resulted in the extinction of *Coregonus alpenae*, *Coregonus johannae*, *Coregonus nigripinnis*, and *Coregonus reighardi* (Todd and Smith 1992). Other factors contributing to the decline included predation from alewife (*Alosa pseudoharengus*, on larvae), rainbow smelt (*Osmerus mordax*, on larvae), and sea lamprey (*Petromyzon marinus*, on juveniles and adults) and competition from alewife, rainbow smelt, and other species of *Coregonus* (Smith 1972; Crowder et al. 1987). Recent declines in exotic fish populations and favorable climatic changes have resulted in the resurgence of lake whitefish and bloater populations to record levels (Fleischer 1992). The resurgence of lake whitefish and bloater populations in Lakes Michigan and Huron was not accompanied by a resurgence of lake herring populations (Fleischer 1992). The reason for the differential response is not known, in part because the causes of the resurgence itself are not well understood.

Factors affecting the early life history of these fishes are thought to be the most important in determining ultimate population abundance and stability (Taylor et al. 1987; Miller et al. 1988). Small changes in the initial cohort growth rate can change survival over the first 60 days of life 10- to 30-fold (Rice et al. 1993). Miller et al. (1990) suggested that the

Received October 21, 1996. Accepted December 19, 1997.
J13709

B.M. Davis[1] **and T.N. Todd.** Great Lakes Science Center, Biological Resources Division, 1451 Green Road, Ann Arbor, MI 48105, U.S.A.

[1] Author to whom all correspondence should be addressed. e-mail: bruce_davis@USGS.GOV

© 1998 NRC Canada

availability of appropriate sizes of zooplankton may have profound effects on the growth of juvenile fish and subsequent recruitment. Food availability and the consequences of its scarcity have affected growth and survival of both bloater and lake whitefish larvae (Taylor and Freeberg 1984; Rice et al. 1987). Competition between lake herring, bloater, and rainbow smelt also has been suggested as a contributing factor in the continuing low abundance of lake herring in Lakes Michigan and Huron (Davis and Todd 1992; Todd and Davis 1995). Hatch and Underhill (1988) suggested that larval mortality may be a reason for the continued low recruitment of adult lake herring. Lake whitefish substantially overlap lake herring in spawning and hatching times and locations (Cucin and Faber 1985), and lake whitefish larvae have been found associated with lake herring larvae (Faber 1970; Reckhan 1970).

The purpose of this study was to determine the degree of competition for food in larval lake herring and lake whitefish by (*i*) comparing their preference for particular prey species, sizes, and quantities of zooplankton and (*ii*) determining the extent of diet overlap between the two species.

Methods

Eggs were removed from mature adults of lake herring and lake whitefish and mechanically fertilized. Adult fecund lake herring were taken from gill nets in the St. Mary's River near Sault Ste. Marie, Michigan, in November 1988 and adult fecund lake whitefish were taken from gill nets in Grand Traverse Bay near Traverse City, Michigan, in November 1988. Fertilized embryos were placed in McDonald jars for incubation at mean temperatures of 2.4°C ± 0.05 (mean ± SE) for lake herring and 3.4°C ± 0.05 for lake whitefish. The embryos from the two species were incubated to synchronize hatching times.

On March 31, 1989, newly hatched lake herring larvae and lake whitefish larvae were evenly distributed among twelve 2-m^3 circular cages (500 per cage), 1.5 m in diameter, 1 m high, and made of 0.8-mm-mesh netting. The mesh was mainly selected to ensure retention of the fish at their smallest size. Four cages contained only lake herring, four contained only lake whitefish, and four contained equal mixtures of both species (250 each). Lake herring were about 11.3 mm and lake whitefish were about 14.5 mm at time of release in the cages. The cage experiments were conducted in Pickerel Lake, Washtenaw County, Michigan, a small mesotrophic lake that supports a population of native lake herring. Cages with fish larvae were randomly distributed in four rows and four columns along with four cages without fish (controls). We used the control cages to monitor the difference between potentially available prey species inside and outside the cages. This experimental setup provided five different treatments: single-species lake herring, single-species lake whitefish, mixed-species, no fish, and open lake.

Zooplankton and fish larvae were sampled beginning at dusk once a week. A 4.2-L Kemmerer bottle was used to sample zooplankton. Two replicates were taken in each cage during each visit. Two replicates were also taken in the open lake adjacent to each control cage during each visit. Samples were sieved through a 0.065-mm-mesh bucket, rinsed into 0.5-L glass jars, and preserved in 10% formalin. During each visit, 10 fish were taken from each cage with a dip net, narcotized in 1% MS 222, and then preserved in 10% formalin. Surface water temperature was routinely taken with a mercury thermometer and routine maintenance of the cages included a thorough scrubbing of the sides of the netting with a long-handled nylon brush 2 days preceding and the day after sampling.

In the laboratory, zooplankton were identified and measured to the nearest 0.1 mm with an ocular micrometer. Five fish per species were chosen at random from the 10 sampled from each cage on each date. All fish from the mixed-species cages were chosen. Nine to 18 fish per species on each date were selected from the remaining specimens for use in mouth gape measurements with a gape micrometer. Fish were weighed wet to the nearest 0.1 mg with a digital microbalance and measured to the nearest 0.1 mm with an ocular micrometer. Stomach contents were excised and all prey were identified and counted. Up to 20 individuals of each prey species were randomly selected and measured to the nearest 0.1 mm. Prey items were identified and prey biomass (dry weight) was estimated for each taxon from published length–weight regressions and values of mean dry weights (references available on request). For the few taxa for which no dry weight value was available, weights for taxa of similar shape and size were used. Prey species were combined into higher taxonomic groups for computing electivity indices for copepod nauplii, cyclopoid copepods, calanoid copepods, small cladocerans, large cladocerans, Rotifera, and miscellaneous invertebrates. Linear prey selection indices (Strauss 1979) for these groups as prey categories were computed for both lake herring and lake whitefish for each visit. Strauss' index = $(r_i - p_i)$, where r_i is the proportion of prey category i in the diet and p_i is the proportion of prey category i in the environment. Schoener's index of diet overlap (Schoener 1970) was also computed for each visit as

$$\alpha = 1 - 0.5\left(\sum_{x=1}^{n} |P_{xi} - P_{yi}|\right)$$

where P_{xi} is the proportion of prey category i in the diet of species x, P_{yi} is the proportion of prey category i in the diet of species y, and n is the number of prey categories. We used analysis of variance (ANOVA) with repeated measures to (*i*) compare the differences between the cages and the open lake for zooplankton density and size, (*ii*) test differences in lengths and weights of fish, and (*iii*) compare differences between species for amount and size of eaten prey. When interactions and treatment and time effects were significant, we performed an interaction contrast analysis and used the Scheffe adjustment to calculate a critical value for the F statistic to test for contrasts in treatment effects between the first 4 weeks and last 4 weeks of the experiment (Tabachnick and Fidell 1996) because a physical metamorphosis usually occurs between the fourth and fifth weeks of life. We also examined specific linear contrasts for various treatments when interaction contrasts were not significant (Tabachnick and Fidell 1996). We used analysis of covariance (ANCOVA) to remove the effect of fish size when testing for differences in mouth gape of fish. Instantaneous growth rates were calculated weekly following Ricker (1975) as

$$\mu = [\ln L_{t_2} \text{ (or } W_{t_2}) - \ln L_{t_1} \text{ (or } W_{t_1})]/(t_2 - t_1).$$

Computations were performed with the General Linear Model (GLM) procedure of SAS/STAT (SAS Institute Inc. 1989).

Results

Sixty invertebrate taxa excluding Rotifera were collected from Pickerel Lake and combined into larger taxonomic groups for analysis (Table 1). Rotifera were excluded from the analyses because they were less than 1% of the fish diets by number and weight. Zooplankton density decreased in the lake and all cages except the controls throughout the study (Fig. 1). The density in the control cages peaked in week 5 and thereafter declined to values similar to the start of the study. Overall, there was a significant difference in zooplankton densities among treatments ($F_{(4,15)} = 84.76$, $P < 0.05$). There was a significant time by treatment interaction ($F_{(28,33.87)} = 3.39$, $P < 0.05$), and patterns of change in the control cages differed

© 1998 NRC Canada

Table 1. Taxonomic groups of invertebrates occurring in Pickerel Lake in April–May 1989.

Cyclopoid copepods	
Acanthocyclops robustus	*Diacyclops thomasi*
Eucyclops agilis	*Macrocyclops albidus*
Mesocyclops edax	*Microcyclops varicans*
Tropocyclops prasinus	
Calanoid copepods	
Epischura lacustris	*Skistodiaptomus oregonensis*
Copepod nauplii	
Small cladocerans	
Acroperus harpae	*Alona costata*
Alonella spp.	*Bosmina longirostris*
Ceriodaphnia spp.	*Chydorus sphaericus*
Pleuroxus denticulatus	*Pleuroxus procurvus*
Scapholeberis kingii	
Large cladocerans	
Daphnia galeata mendotae	*Daphnia pulex*
Diaphanosoma brachyurum	*Eurycercus lamellatus*
Ophryoxus gracilis	*Polyphemus pediculus*
Simocephalus serrulatus	*Simocephalus vetulus*
Miscellaneous invertebrates	
Ceratium tripos	Ceratopogonidae
Chaoborus punctipennis	Chironomidae
Collembola	Ephemeroptera
Ergasilus spp.	Harpacticoida
Hyalella azteca	*Hydra* spp.
Hydracarina	Nematoda
Odonata	Oligochaeta
Ostracoda	Plecoptera
Trichoptera	

Fig. 1. Density of total zooplankton and major zooplankton groups in Pickerel Lake and study cages in April–May 1989. Symbols refer to cage type as follows: triangles, open lake; solid squares, control; open squares, lake whitefish; diamonds, lake herring; plus signs, mixed-species.

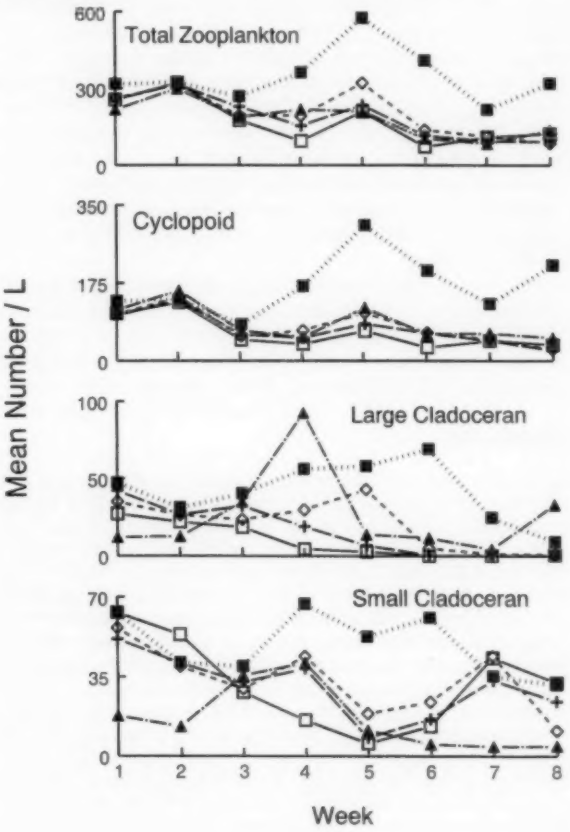

from those for the other treatments and these patterns were different before and after metamorphosis ($F_{(1,15)} = 56.14$, $P < 0.05$). The slopes were significant ($F_{(1,15)} = 154.03$, $P < 0.05$), indicating a significant linear trend in zooplankton density.

Density of the different zooplankton groups in the fish cages showed similar trends during the study. In general, cyclopoid copepod densities followed a pattern similar to total zooplankton density (Fig. 1). There was a significant time by treatment interaction ($F_{(28,33.87)} = 3.61$, $P < 0.05$), and patterns of change in the control cages differed from those for the other treatments and these patterns were different before and after metamorphosis ($F_{(1,15)} = 85.28$, $P < 0.05$). Overall, there was a significant difference in cyclopoid densities among treatments ($F_{(4,15)} = 63.56$, $P < 0.05$). The slopes were significant ($F_{(1,15)} = 41.39$, $P < 0.05$), indicating a significant linear trend in cyclopoid density. Copepod nauplii, the second most abundant group, showed a significant time by treatment interaction ($F_{(28,33.87)} = 1.94$, $P < 0.05$), and densities appeared to be cyclic. The variability in density of nauplii did not appear to be associated with differences in the control cages ($F_{(1,15)} = 1.39$, $P > 0.05$). The slopes were significant ($F_{(1,15)} = 343.35$, $P < 0.05$), indicating a significant linear trend in nauplii densities. Both cyclopoid copepod and copepod nauplii densities peaked in the fifth week. Calanoid copepod densities remained low throughout, although they did increase in the lake and control cages beginning in the fourth week.

Densities of large cladocerans steadily declined in most of the cages containing fish except for the fourth and fifth weeks in the cages with lake herring alone (Fig. 1). Densities in the lake and the control cages greatly increased before declining. There was a significant time by treatment interaction ($F_{(28,19.45)} = 2.42$, $P < 0.05$), and there was an overall significant difference among treatments ($F_{(4,15)} = 7.04$, $P < 0.05$). The variability in density of large cladocerans did not appear to be associated with differences in the control cages ($F_{(1,11)} = 3.48$, $P > 0.05$). The slopes were significant ($F_{(1,11)} = 27.08$, $P < 0.05$), indicating a significant linear trend in density of

© 1998 NRC Canada

Fig. 2. Mean (A) length and (B) weight of fish in cages in Pickerel Lake in April–May 1989. Symbols refer to fish type as follows: squares, single-species lake whitefish; diamonds, single-species lake herring; circles, mixed-species lake whitefish; triangles, mixed-species lake herring.

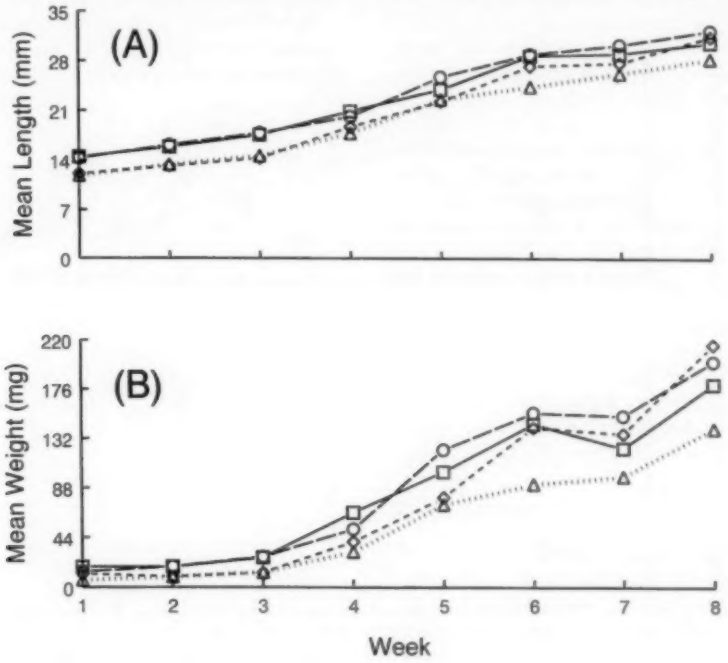

large cladocerans. Densities of small cladocerans in the fish cages declined greatly until the fifth week and then increased whereas in the control cages, they increased in the middle weeks before declining. There was a significant time by treatment interaction ($F_{(28,33.87)} = 4.13$, $P < 0.05$), and significant differences were detected among treatments ($F_{(4,15)} = 30.77$, $P < 0.05$), as patterns of change in the control cages differed from those for the other treatments ($F_{(1,15)} = 4.63$, $P < 0.05$). The slopes were significant ($F_{(1,15)} = 47.68$, $P < 0.05$), indicating a significant linear trend in density of small cladocerans. Miscellaneous invertebrates remained low until large increases occurred in the cages in the last 2 weeks. In most weeks, densities of the five major groups in fish cages were highest in the lake herring cages, lowest in the lake whitefish cages, and intermediate in the mixed-species cages.

Lake herring larvae and lake whitefish larvae grew at similar rates in the first 4 weeks whether they were in mixed- or single-species assemblages (Fig. 2). The length–weight regression equations were $\ln W = -5.68 + 3.17 \ln L$ ($r^2 = 0.94$) for single-species lake whitefish, $\ln W = -6.21 + 3.36 \ln L$ ($r^2 = 0.96$) for single-species lake herring, $\ln W = -6.30 + 3.35 \ln L$ ($r^2 = 0.98$) for mixed-species lake whitefish, and $\ln W = -6.78 + 3.50 \ln L$ ($r^2 = 0.96$) for mixed-species lake herring. In the last 4 weeks, single-species lake herring grew faster and became as large as single-species lake whitefish. Mixed-species lake whitefish grew slightly faster than mixed-species lake herring in the latter weeks. There was a significant difference in mean length among treatments ($F_{(4,15)} = 4.13$, $P < 0.05$), and the interaction contrasts showed that the differences were between combined lake herring and lake whitefish ($F_{(1,12)} = 112.20$, $P < 0.05$). The slopes were highly significant ($F_{(1,12)} = 2461.22$, $P < 0.05$), indicating a significant linear trend in fish growth. These differences were more pronounced with weight. Single-species lake herring weighed as much as single-species lake whitefish in the fifth week and were ultimately heavier by the eighth week. Mixed-species lake whitefish were much heavier than mixed-species lake herring by the end of the study. In fact, interaction contrasts showed mixed-species lake herring weighing significantly less than fish in the other treatments ($F_{(1,12)} = 36.59$, $P < 0.05$). A significant time by treatment interaction was observed ($F_{(21,17.78)} = 5.29$, $P < 0.05$), and patterns of change in weight of the mixed-species lake herring differed from those for the other treatments ($F_{(1,12)} = 11.35$, $P < 0.05$). The slopes were significant ($F_{(1,12)} = 544.32$, $P < 0.05$), indicating a significant linear trend in fish weight.

Instantaneous growth rates were generally highest early in the study and declined as the fish became larger (Fig. 3), in particular after metamorphosis. A sharp drop in rates occurred in both weight and length of fish in mixed-species cages in the fifth week that continued through the remainder of the study. This was observed after the fourth week in the single-species cages, especially for weight. Weight growth rate increased in all groups in the eighth week whereas length growth rate increased only in single-species lake herring.

Consumption of prey generally exhibited a significant linear increase throughout the study period ($F_{(1,12)} = 133.36$, $P < 0.05$) (Fig. 4). However, prey eaten by both single-species lake whitefish and lake herring declined sharply in the last week. A significant time by treatment interaction was

© 1998 NRC Canada

Fig. 3. Instantaneous growth rates in (A) length and (B) weight of fish in cages in Pickerel Lake in April–May 1989. Symbols refer to fish type as follows: squares, single-species lake whitefish; diamonds, single-species lake herring; circles, mixed-species lake whitefish; triangles, mixed-species lake herring.

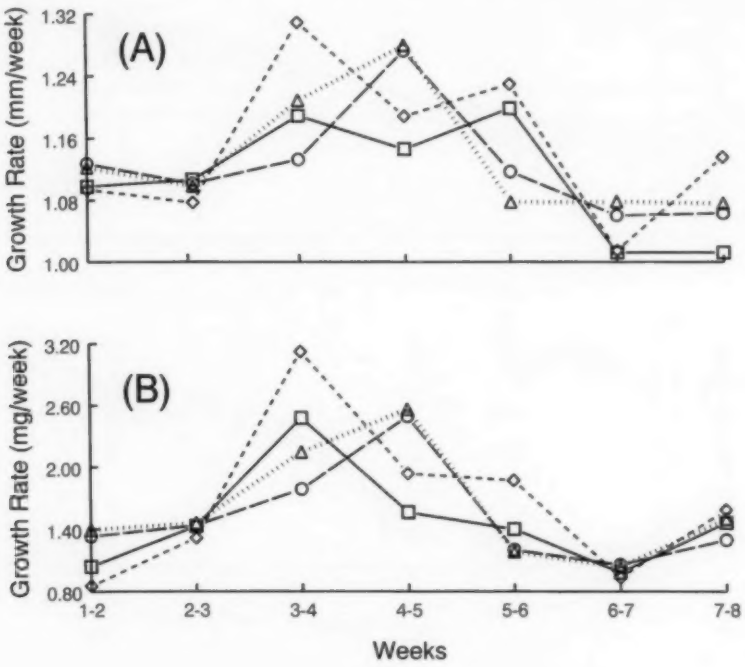

observed ($F_{(21,17.78)}$ = 2.37, $P < 0.05$). Overall, the mixed-species lake whitefish ate significantly more prey ($F_{(1,12)}$ = 15.93, $P < 0.05$), followed by single-species lake whitefish, mixed-species lake herring, and single-species lake herring. The variability in amount of prey eaten did not appear to be associated with differences in the mixed-species lake whitefish treatments ($F_{(1,12)}$ = 0.01, $P > 0.05$). Throughout the study, the most abundant prey in fish stomachs were cyclopoid copepods. Small cladocerans were also eaten frequently; fish ate *Bosmina longirostris* in the first 4 weeks and then switched to *Chydorus sphaericus* in the last 4 weeks. Copepod nauplii were eaten by all fish for the first 3 weeks. Large cladocerans (*Daphnia* spp.) were eaten by both species in varying degrees; lake whitefish began eating *Daphnia* 2 weeks earlier than lake herring. Single-species lake whitefish ate large cladocerans mainly from the second through the fifth week whereas they were eaten by single-species lake herring from the third through the sixth week. Large cladocerans were eaten by mixed-species lake whitefish from the second through the fifth week whereas they were eaten by mixed-species lake herring in the fourth and fifth weeks. Miscellaneous invertebrates were mainly eaten in the sixth and seventh weeks. One lake whitefish from the mixed-species cages had an empty stomach in the first week.

Mean lengths of eaten prey increased slightly in both mixed- and single-species fish (Fig. 4). There was a significant treatment ($F_{(3,12)}$ = 48.12, $P < 0.05$) and time effect ($F_{(7,84)}$ = 19.65, $P < 0.05$). The single-species fish and the mixed-species lake herring ate similar-sized prey, but prey of the mixed-species lake whitefish were significantly larger throughout the study ($F_{(1,12)}$ = 126.06, $P < 0.05$). The slopes were significant ($F_{(1,12)}$ = 182.75, $P < 0.05$), indicating a significant quadratic trend for length of prey eaten, but were not significantly different across treatments ($F_{(3,12)}$ = 2.51, $P > 0.05$). All fish except for lake herring in the first week ate, on average, prey that were larger than the size available in their environment.

The mean length of zooplankton in the lake and control cages increased slightly whereas zooplankton in the fish cages decreased in size (Fig. 4). Similar to density, mean length of zooplankton in the mixed-species cages was intermediate to that in the single-species cages. There was a significant treatment effect ($F_{(4,15)}$ = 26.68, $P < 0.05$), but the time by treatment interaction was also significant ($F_{(28,33.87)}$ = 3.33, $P < 0.05$), and patterns of change in zooplankton length density in the control cages and open lake differed from those for the fish cages ($F_{(1,15)}$ = 18.83, $P < 0.05$). The size of zooplankton in the lake and the control cages was significantly larger than in the fish cages ($F_{(1,15)}$ = 96.21, $P < 0.05$), and zooplankton in the lake herring cages were significantly larger than in the lake whitefish cages ($F_{(1,15)}$ = 9.15, $P < 0.05$) . The slopes were significant ($F_{(1,15)}$ = 8.50, $P < 0.05$), indicating a significant linear trend in mean length of zooplankton.

Mean weight of prey increased throughout the study similar to the pattern for mean number of prey consumed (Fig. 4). However, the peak in weight was about a week later than the peak in numbers for most fish. Overall, mixed-species lake

© 1998 NRC Canada

Fig. 4. Mean number of prey consumed per fish, mean length of prey consumed per fish, mean weight of prey consumed per fish by fish in cages, and mean length of total zooplankton in Pickerel Lake in April–May 1989. Symbols refer to fish type as follows: squares, single-species lake whitefish; diamonds, single-species lake herring; circles, mixed-species lake whitefish; triangles, mixed-species lake herring; plus signs, mixed-species.

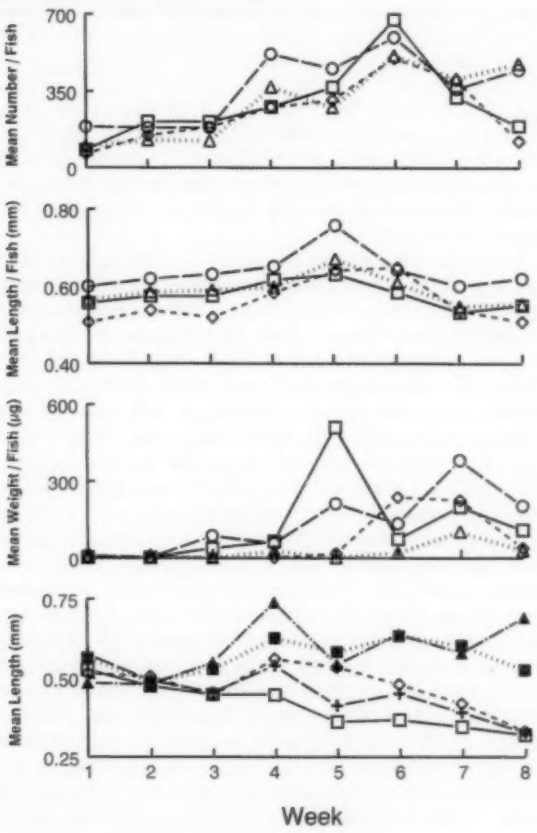

whitefish ate the most biomass followed by single-species lake whitefish, single-species lake herring, and mixed-species lake herring. However, except for a few instances, no significant differences were observed between treatments ($F_{(3,12)}$ = 2.89, $P > 0.05$); the prey of mixed-species lake whitefish were significantly heavier than the prey of fish in the other treatments ($F_{(1,12)}$ = 5.68, $P < 0.05$). There was also a significant time effect ($F_{(7,84)}$ = 2.44, $P < 0.05$). The slopes were significant ($F_{(1,12)}$ = 23.20, $P < 0.05$), indicating a significant linear trend in mean weight of prey.

The model relating mouth gape to fish length was significant ($F_{(2,168)}$ = 515.98, $P < 0.05$), and length was a significant factor ($F_{(1,168)}$ = 1029.26, $P < 0.05$). Although mean mouth gape of lake whitefish was larger than that of lake herring in the first 4 weeks (Table 2), mouth gape did not differ significantly between species ($F_{(1,168)}$ = 2.16, $P > 0.05$) when length was considered. The larger initial size of lake whitefish probably accounts for the larger mean mouth gape until metamorphosis.

Food selection values and overall trends for both species and assemblages were similar throughout the study. Cyclopoid copepods were the only prey items positively selected, and electivities remained essentially constant from week to week ($E = 0.475 \pm 0.02$); however, great variation was observed among the single-species lake herring cages in the last 2 weeks. Copepod nauplii were increasingly avoided throughout the study ($E = -0.327 \pm 0.02$), but great variation was observed in the lake herring cages in the fifth week. Calanoid copepods, large cladocerans, small cladocerans, and miscellaneous invertebrates were randomly selected during the study with electivities about 0, but for small cladocerans, great variation occurred among the single-species lake herring cages in the last 2 weeks.

The index of diet overlap was high throughout the study. Both single-species and mixed-species assemblages had over 70% overlap in the first week, peaking at over 95% in week 4. Slight decreases were observed in the last 4 weeks, although diet overlap remained above 80%. The mixed-species assemblages had a slightly higher mean overlap (89% vs. 87%), but the differences were probably not significant.

Discussion

The high diet overlap between the species indicates potential competition, especially considering the apparently high densities of potential prey. Index values greater than 60% suggest significant overlap, and overlap is usually highest among competing species when food is most abundant and becomes least when food is in short supply (Schoener 1982). However, in this study, food did not appear to be in short supply. Competition by definition requires that one of the competitors show negative effects from the interaction. Lake herring consumed less and grew less in the presence of lake whitefish even when a great surplus of zooplankton appeared to occur.

Intraspecific competition among lake whitefish could exist because lake whitefish when mixed with lake herring ate more and larger prey than lake whitefish alone. Although the differences were not significant, they were consistent. The lesser number of equally large and aggressive lake whitefish competitors could have allowed each mixed-species treatment lake whitefish to eat more large-sized prey, theoretically eating more for less effort and with less competitive stress.

Lake whitefish could outcompete lake herring for limited resources and thus leave them more vulnerable to predation from slower growth. Crowder et al. (1987) found that smaller zooplankton sizes induced reduced growth rates of larval bloater and a prolongation of vulnerability to predation, and Rice et al. (1993) demonstrated that mean growth rate and growth rate variation among individuals can interact strongly with size-dependent mortality to cause significant effects on the number, growth rates, and final sizes of survivors. The mixed lake herring showed reduced growth in length and especially weight after the third week compared with the single-species lake herring. Hoagman (1974) found that alewife only fed on lake whitefish smaller than 17 mm. When our mixed lake herring reached similar lengths, the single-species lake herring were by then already 1 mm longer and 10 mg heavier. However, the greatest differences in size occurred several weeks later. Lake herring may even then still be vulnerable to alewife predation because Davis and Foltz

© 1998 NRC Canada

Table 2. Mean gape (mm ± SE) of young lake herring and lake whitefish in Pickerel Lake in April–May 1989.

	Week							
	1	2	3	4	5	6	7	8
Lake herring	0.53±0.03	0.72±0.06	0.94±0.02	1.28±0.07	1.73±0.03	1.72±0.01	1.70±0.02	2.26±0.09
Lake whitefish	0.71±0.04	0.86±0.03	1.08±0.05	1.69±0.03	1.73±0.03	1.73±0.01	1.71±0.01	1.88±0.07

Note: Data were analyzed by ANCOVA and significance values are in the text.

(1991) found land-locked blueback herring (*Alosa aestivalis*) eating substantial numbers of juvenile fish (mean length 23.9 mm).

We raised *Coregonus* larvae in other years and obtained similar results (Davis and Todd 1992; Todd and Davis 1995). Lake whitefish and lake herring larvae had good growth and survival with 500 fish per cage. However, increasing densities of fish resulted in poorer growth and survival. Experiments in 1988 resulted in poorer growth for larvae of both *C. artedi* and *C. hoyi*. The poorer growth in 1988 was probably caused by unusually warm conditions and higher fish densities (1500 fish per cage) that led to excessive stress and mortality (Davis and Todd 1992). Karjalainen (1992) observed density-related responses in cage-reared vendace (*Coregonus albula*) and suggested that intraspecific competition for food or predation disturbance on the feeding of the larvae resulted in increased energy costs, weak growth, and ultimately decreased survival of the larvae. He also noted that vendace larvae were more dispersed in high-density situations and that this deterioration of the normal schooling behavior might have implications for foraging efficiency.

The lake herring and lake whitefish larvae should have had sufficient food for growth. Dabrowski (1976) reported the optimal feeding densities for Baltic whitefish (*Coregonus lavaretus*) larvae as 200–260 plankton individuals/L (199 994 – 259 992/m^3) (if weight is 4 μg/individual). Hoagman (1974) suggested that *C. clupeaformis* larvae require 10–20 copepods daily, which all of our fish greatly exceeded. Dabrowski (1976) found *C. lavaretus* larvae consuming 80–97 individuals daily at 13.5°C for the first 16 days of life. Our fish probably needed less food because temperatures averaged 7°C for the first 21 days of the study; McCormick et al. (1971) found that optimal growth for lake herring occurred at 13–18°C.

Taylor and Freeberg (1984) and Brown and Taylor (1992) observed slower growth rates for *C. clupeaformis* than we found in our fish. However, they experimentally fed their fish with varying rations up to 100 or 110 zooplankton per fish per day in addition to deliberately starving some of them. Our cage-raised fish generally consumed several hundred zooplankton daily and so obtained better growth. Our growth rates for lake whitefish were far higher than those measured in Lake Michigan by Freeberg et al. (1990) (≈29.8 mm compared with 17.9 mm total length after 7 weeks), but again, our fish ate far more zooplankton.

Exact comparisons between our experimental fish and larval fish in the Great Lakes may not be possible because of the high growth rate and zooplankton densities observed in the cages. However, the relative level of response was repeated in different tests with varied fish and zooplankton densities in other years of experimentation (Davis and Todd 1992; Todd and Davis 1995). Lake whitefish grew larger than lake herring in combined tests, but lower zooplankton densities or higher fish densities resulted in slower growth rates than those reported here.

Both lake whitefish and lake herring controlled the density and size of the zooplankton community by cropping off the largest zooplankton. The depletion of larger zooplankton such as daphnids and calanoids from the fish cages was also noted in 1988 and 1990 (Davis and Todd 1992; Todd and Davis 1995). We inferred that they were highly preferred as prey because they were scarce in fish cages and relatively more abundant in the open lake and control cages. Other workers have also noted that planktivores prefer larger zooplankton and rely on abundant cyclopoid copepods when daphnids and other cladocerans have been depleted (Bronisz 1979; Gunkel 1981; Karjalainen and Viljanen 1993; Link 1996). The gape measurements showed that both fish species could easily swallow most prey, providing they were eaten lengthwise. Even the largest *Daphnia* were no more than 1.6 mm wide, and the average lake whitefish could probably have handled that size prey item by week 4 and lake herring that size prey item by week 5. Cyclopoid copepods were preferred, but they were also more available than the other large zooplankton. In general, *Coregonus* larvae seem to ingest the most abundant prey size without selecting the biggest ones available, even if mechanically they were able to ingest them (Ponton and Müller 1990). John and Hasler (1956) found lake herring larvae preferring cyclopoids, and Reckhan (1970) and Freeberg et al. (1990) found lake whitefish larvae initially feeding on cyclopoid and calanoid copepods.

Zooplankton densities were near equilibrium with the external environment, as most taxa appeared in similar numbers in both the fish cages and the open lake. This may suggest a similar level of planktivory among the cages and the lake, or possibly that the cages provided an initial refuge for zooplankton and the high concentration of fish within decreased the densities to open-lake levels. Most zooplankton appeared to have flowed freely through the mesh, but passage was probably difficult for the larger individuals of calanoid copepods and large cladocerans. After the largest individuals were eaten, any smaller ones would also have been eaten once they attained similar sizes. However, as calanoids are a large and a very elusive prey, these young fish would probably still have preferred cyclopoids. Miller et al. (1990) found the diets of larval bloater dominated by copepods, and peak selectivity was for prey 0.6–0.8 mm in fish 20–40 mm. It was not until their fish were 60 mm that cladocerans were preferred and peak selectivity was for prey 1.3–1.8 mm. Any affects on our

© 1998 NRC Canada

fish by the lack of availability of the largest calanoids may have been masked by the high abundance of other prey.

In comparing Pickerel Lake zooplankton with that of some Great Lakes, we found major differences in abundance and species composition. Larval fish in our study had a veritable zooplankton soup to feed on compared with what they might normally encounter upon hatching in the Great Lakes. The cages with fish had average abundances ranging from 100 000 to 317 000/m^3 excluding rotifers. In lake-wide surveys, Makarewicz et al. (1989) found average zooplankton abundance from April to November in 1983–1985 to be 54 689/m^3 in Lake Michigan, 56 422/m^3 in Lake Huron, and 223 178/m^3 in Lake Erie. However, these samples were taken offshore and 40–70% of the total abundance was attributed to rotifers. Most crustacean zooplankton species in Lake Michigan are uniformly distributed in the spring (Gannon 1975). Roth and Stewart (1973) found inshore and offshore crustacean zooplankton (and the rotifer *Asplanchna*) ranging from 4000 to 32 000/m^3 in southeast Lake Michigan during April–June. Inshore densities were 10-fold higher (280 000/m^3) in mid-August.

The species composition of available zooplankton prey was also quite different from what these larval fish would normally encounter in the Great Lakes after hatch. However, except for certain calanoid copepods (*Leptodiaptomus* spp. and *Limnocalanus macrurus*), most of the major planktonic copepods occurring in the Great Lakes (Robertson and Gannon 1981) were found in Pickerel Lake. Cyclopoid copepods and nauplii were the most abundant organisms in the cages, but there were also sizeable numbers of both large and small cladocerans. Most studies report early spring zooplankton being dominated by both calanoid and cyclopoid copepods and nauplii (Roth and Stewart 1973; Gannon 1975; Evans et al. 1980; Makarewicz et al. 1989). Roth and Stewart (1973) reported smaller cladocerans (*Bosmina*) not appearing until May or dominating until mid-June, with larger cladocerans not becoming significantly abundant until August. Evans et al. (1980) reported that nearshore zooplankton in southeast Lake Michigan in early spring was dominated by copepods and nauplii, and although cladocerans were present in the shallower and warmer areas of the lake, they were rare.

Because of their time of hatch in the Great Lakes, larval lake herring and lake whitefish would have less access to cladocerans and would eat mainly cyclopoid and calanoid copepods. Lake herring and lake whitefish begin hatching in April, and the larvae in Lake Huron are associated along steep shorelines with larvae of burbot (*Lota lota*), rainbow smelt, and deepwater sculpin (*Myoxocephalus thompsoni*) (Reckhan 1970); all except rainbow smelt appeared directly after ice breakup (Faber 1970). Most cladocerans do not appear in the upper Great Lakes until after April (Balcer et al. 1984). However, we have found *B. longirostris* and *Daphnia galeata mendotae* in very low numbers from samples taken in Lake Michigan in mid-April 1993 (Great Lakes Science Center, unpublished data), and Gannon (1975) found the same species in very low numbers (<100/m^3) in samples taken from cross-lake transects in March and June.

Our study has shown that larval lake herring and lake whitefish favor the same type of food, and these diet similarities could make them competitors for food in the Great Lakes. Sandlund et al. (1991) observed competition between adult and juvenile vendace in which larger fish impacted the survival of the smaller fish, and Miller et al. (1992) demonstrated that foraging ability is heavily dependent on size differences. Possible competition should favor the lake whitefish whose greater initial size could allow them to eat larger prey earlier and thereby limit availability of these prey to lake herring at a crucial period of development. Additionally, Savino and Hudson (1995) have shown that larval lake whitefish are more aggressive feeders than lake herring. The net result of such competition would result in lake herring remaining at smaller, more vulnerable sizes for a longer period than lake whitefish with consequent increased mortality from predation, as has also been suggested for bloater (Rice et al. 1987) and vendace (Karjalainen 1991). Size differences of only tenths of a millimetre can confer considerable size advantages in resistance to starvation, and slight size differences may have important consequences to a fish's vulnerability to predators (Miller et al. 1988).

Acknowledgments

We thank John LaBossiere, Michigan Department of Natural Resources, Pinckney, Michigan, for allowing our study to be carried out in Pickerel Lake and Susan Walker, biologist for Grand Traverse Bay Tribe, Grand Traverse Bay, Michigan, for obtaining lake whitefish eggs. We also thank Marc Blouin, Cynthia Kolar, John Miller, Daniel Ropek, and Gentry Yearout for assistance in the field and for identification and enumeration of zooplankton samples and fish stomachs and Melissa Kostich for processing of gape measurements. We also thank Mary Fabrizio and Anthony Frank for their aid in statistical analysis. We also thank John Gannon, Jaci Savino, and Patrick Hudson for their review of this manuscript. Contribution 1005 of the Great Lakes Science Center of the Biological Resources Division of the U.S. Geological Service.

References

Balcer, M.D., Korda, N.L., and Dodson, S.I. 1984. Zooplankton of the Great Lakes. University of Wisconsin Press, Madison, Wis.

Bronisz, D. 1979. Selective exploitation of lake zooplankton by coregonid fry in cage culture. *In* Cultivation of fish fry and its live food. *Edited by* E. Styczynska-Jurewicz., T. Backiel, E. Jaspers, and G. Persoone. Spec. Publ. Eur. Maricult. Soc. **4**: 301–307.

Brown, R.W., and Taylor, W.W. 1992. Effects of egg composition and prey density on larval growth and survival of lake whitefish (*Coregonus clupeaformis* Mitchill). J. Fish Biol. **40**: 381–394.

Crowder, L.B., McDonald, M.E., and Rice, J.A. 1987. Understanding recruitment of Lake Michigan fishes: the importance of size-based interactions between fish and zooplankton. Can. J. Fish. Aquat. Sci. **44**(Suppl. 2): 141–147.

Cucin, D., and Faber, D.J. 1985. Early life studies of lake whitefish (*Coregonus clupeaformis*), cisco (*Coregonus artedii*) and yellow perch (*Perca flavescens*) in Lake Opeongo, Ontario. Ont. Fish. Tech. Rep. Ser. No. 16.

Dabrowski, K.R. 1976. How to calculate the optimal density of food for fish larvae. Environ. Biol. Fishes, **1**: 87–89.

Davis, B.M., and Foltz, J.W. 1991. Food of blueback herring and threadfin shad in Jocassee Reservoir, South Carolina. Trans. Am. Fish. Soc. **120**: 605–613.

Davis, B.M., and Todd, T.N. 1992. Diet overlap in larval lake herring (*Coregonus artedi*) and bloaters (*Coregonus hoyi*). *In*

© 1998 NRC Canada

Biology and management of coregonid fishes. *Edited by* T.N. Todd and M. Luczynski. Pol. Arch. Hydrobiol. **39**: 279–287.

Evans, M.S., Hawkins, B.E., and Sell, D.W. 1980. Seasonal features of zooplankton assemblages in the nearshore area of southeastern Lake Michigan. J. Great Lakes Res. **6**: 275–289.

Faber, D.J. 1970. Ecological observations on newly hatched lake whitefish in South Bay, Lake Huron. *In* Biology of coregonid fishes. *Edited by* C.C. Lindsey and C.S. Woods. University of Manitoba Press, Winnipeg, Man. pp. 481–500.

Fleischer, G.W. 1992. Status of coregonine fishes in the Laurentian Great Lakes. *In* Biology and management of coregonid fishes. *Edited by* T.N. Todd and M. Luczynski. Pol. Arch. Hydrobiol. **39**: 247–259.

Freeberg, M.H., Taylor, W.W., and Brown, R.W. 1990. Effect of egg and larval survival on year-class strength of lake whitefish in Grand Traverse Bay, Lake Michigan. Trans. Am. Fish. Soc. **119**: 92–100.

Gannon, J.E. 1975. Horizontal distribution of crustacean zooplankton along a cross-lake transect in Lake Michigan. J. Great Lakes Res. **1**: 79–91.

Gunkel, G. 1981. Untersuchungen zu den quantitativen und qualitativen Beziehungen innerhalb einer pelagischen Nahrungskette am Beispiel von *Coregonus fera*, *Daphnia pulicaria* und Phytoplankton. Verh. Ges. Ökol. **9**: 35–68.

Hatch, J.T., and Underhill, J.C. 1988. Abundance, distribution, growth, and mortality of larval lake herring in western Lake Superior. Am. Fish. Soc. Symp. **5**: 96–103.

Hoagman, W.J. 1974. Feeding by alewives (*Alosa pseudoharengus*) on larval lake whitefish (*Coregonus clupeaformis*) in the laboratory. J. Fish. Res. Board Can. **31**: 229–230.

John, K.R., and Hasler, A.D. 1956. Observations on some factors affecting the hatching of eggs and the survival of young shallow-water cisco, *Leucichthys artedi* LeSueur, in Lake Mendota, Wisconsin. Limnol. Oceanogr. **1**: 176–194.

Karjalainen, J. 1991. Survival, growth and feeding of vendace, *Coregonus albula* (L.), larvae in net enclosures. J. Fish Biol. **38**: 905–919.

Karjalainen, J. 1992. Food, ingestion, density-dependent feeding and growth of vendace (*Coregonus albula* (L.)) larvae. Ann. Zool. Fenn. **29**: 93–103.

Karjalainen, J., and Viljanen, M. 1993. Changes in the zooplankton community of Lake Puruvesi, Finland, in relation to the stock of vendace (*Coregonus albula* (L.)). Verh. Int. Ver. Limnol. **25**: 563–566.

Link, J. 1996. Capture probabilities of Lake Superior zooplankton by an obligate planktivorous fish — the lake herring. Trans. Am. Fish. Soc. **125**: 139–142.

Makarewicz, J.C., Lewis, T., and Bertram, P. 1989. Phytoplankton and zooplankton in Lakes Erie, Huron, and Michigan: 1985. U.S. Environmental Protection Agency Great Lakes National Program Office, Chicago, Ill. EPA-905/3-90-003.

McCormick, J.H., Jones, B.R., and Syrett, R.F. 1971. Temperature requirements for growth and survival of larval ciscoes (*Coregonus artedii*). J. Fish. Res. Board Can. **28**: 924–927.

Miller, T.J., Crowder, L.B., Rice, J.A., and Marschall, E.A. 1988. Larval size and recruitment mechanisms in fishes: toward a conceptual framework. Can. J. Fish. Aquat. Sci. **45**: 1657–1670.

Miller, T., Crowder, L.B., and Binkowski, F.P. 1990. Effects of changes in the zooplankton assemblage on growth of bloater and implications for recruitment success. Trans. Am. Fish. Soc. **119**: 483–491.

Miller, T.J., Crowder, L.B., Rice, J.A., and Binkowski, F.P. 1992. Body size and the ontogeny of the functional response in fishes. Can. J. Fish. Aquat. Sci. **49**: 805–812.

Ponton, D., and Müller, R. 1990. Size of prey ingested by whitefish, *Coregonus* sp., larvae. Are *Coregonus* larvae gape limited predators? J. Fish Biol. **36**: 67–72.

Reckhan, J.A. 1970. Ecology of young lake whitefish (*Coregonus clupeaformis*) in South Bay, Manitoulin Island, Lake Huron. *In* Biology of coregonid fishes. *Edited by* C.C. Lindsey and C.S. Woods. University of Manitoba Press, Winnipeg, Man. pp. 437–460.

Rice, J.A., Crowder, L.B., and Binkowski, F.B. 1987. Evaluating potential sources of mortality for larval bloater (*Coregonus hoyi*): starvation and vulnerability to predation. Can. J. Fish. Aquat. Sci. **44**: 467–472.

Rice, J.A., Miller, T.J., Rose, K.A., Crowder, L.B., Marschall, E.A., Trebitz, A.S., and DeAngelis, D.L. 1993. Growth rate variation and larval survival: inferences from an individual-based size-dependent predation model. Can. J. Fish. Aquat. Sci. **50**: 133–142.

Ricker, W.E. 1975. Computation and interpretation of biological statistics of fish populations. Bull. Fish. Res. Board Can. No. 191.

Robertson, A., and Gannon, J.E. 1981. Annotated checklist of the free-living copepods of the Great Lakes. J. Great Lakes Res. **7**: 382–393.

Roth, J.C., and Stewart, J.A. 1973. Nearshore zooplankton of southeastern Lake Michigan. Proc. Conf. Great Lakes Res. **16**: 132–142.

Sandlund, O.T., Jonsson, B., Naesje, T.F., and Aas, P. 1991. Year-class fluctuations in vendace, *Coregonus albula* (Linnaeus): who's got the upper hand in intraspecific competition. J. Fish Biol. **38**: 873–885.

SAS Institute Inc. 1989. SAS user's guide, version 6. SAS Institute Inc., Cary, N.C.

Savino, J.F., and Hudson, P.L. 1995. Feeding competition between larval lake whitefish and lake herring. Arch. Hydrobiol. Spec. Issues Adv. Limnol. **46**: 153–162.

Schoener, T.W. 1970. Nonsynchronous spatial overlap of lizards in patchy habitats. Ecology, **51**: 408–418.

Schoener, T.W. 1982. The controversy over interspecific competition. Am. Sci. **70**: 586–595.

Smith, S.H. 1972. Factors of ecological succession in oligotrophic fish communities of the Laurentian Great Lakes. J. Fish. Res. Board Can. **29**: 717–730.

Smith, G.R., and Todd, T.N. 1984. Evolution of species flocks of fishes in north temperate lakes. *In* Evolution of Fish species flocks. *Edited by* A.A. Echelle and I. Kornfield. University of Maine Press, Orono, Me. pp. 45–68.

Strauss, R.E. 1979. Reliability estimates for Ivlev's electivity index, the forage ratio, and a proposed linear index of food selection. Trans. Am. Fish. Soc. **108**: 344–352.

Tabachnick, B.G., and Fidell, L.S. 1996. Using multivariate statistics. 3rd ed. Harper Collins, New York.

Taylor, W.W., and Freeberg, M. 1984. Effect of food abundance on larval lake whitefish, *Coregonus clupeaformis* Mitchill, growth and survival. J. Fish Biol. **25**: 733–741.

Taylor, W.W., Smale, M., and Freeberg, M. 1987. Biotic and abiotic factors as determinants of recruitment to stocks of lake whitefish (*Coregonus clupeaformis* Mitchill) in northeastern Lake Michigan. Can. J. Fish. Aquat. Sci. **44**: 313–323.

Todd, T.N., and Davis, B.M. 1995. Effects of fish density and relative abundance on competition between larval lake herring and lake whitefish for zooplankton. Arch. Hydrobiol. Spec. Issue Adv. Limnol. **46**: 163–171.

Todd, T.N., and Smith, G.R. 1992. A review of differentiation in Great Lakes ciscoes. *In* Biology and management of coregonid fishes. *Edited by* T.N. Todd and M. Luczynski. Pol. Arch. Hydrobiol. **39**: 13–19.

© 1998 NRC Canada

The dead of winter: size-dependent variation and genetic differences in seasonal mortality among Atlantic silverside (Atherinidae: *Menidia menidia*) from different latitudes

Eric T. Schultz, David O. Conover, and Amir Ehtisham

Abstract: Genetic differences among populations of Atlantic silverside (*Menidia menidia*) are hypothesized to be evolutionary responses to intense, size-selective winter mortality at high latitudes. Three experiments were conducted to test features of winter mortality. In the first experiment, we varied size and whether food was provided or withheld; temperatures were permitted to follow ambient (New York) wintertime fluctuations. Mortality and depletion of energy reserves were more rapid in the units receiving no food. Small fish died before larger fish in these units, but not in the units receiving food. Energy depletion of fish in the no-food treatment resembled that of fish in the wild. In the second experiment, we varied size and population of origin, representing high-latitude (Nova Scotia), midlatitude (New York), and low-latitude (South Carolina) populations. These fish were provided food and showed minimal depletion of energy reserves, but mortality rates were high when water temperatures were low. Mortality did not vary with size in New York and South Carolina fish, but was highest in intermediate-size fish from Nova Scotia. There was a pronounced population difference in survival rate (Nova Scotia > New York > South Carolina). In the third experiment, food was withheld and extreme low temperatures were moderated. Energy depletion was rapid and small fish died before large fish. We conclude that populations in seasonal environments are likely to be subject to size-selective winter mortality when energy reserves are depleted and that juvenile growth rates have evolved in response to this selection pressure. In addition, high-latitude populations have evolved greater tolerance to other winter stresses associated with low temperatures.

Résumé : La mortalité hivernale est souvent fonction de la taille et peut contribuer à l'apparition de différences latitudinales dans la capacité de croissance des juvéniles. Nous présentons ici trois expériences sur des caractéristiques de la mortalité hivernale chez *Menidia menidia*. Dans la première expérience, nous avons fait varier la taille et l'apport de nourriture sous des températures hivernales ambiantes (New York). La mortalité et la perte d'énergie ont été plus rapides chez les poissons privés de nourriture, et les petits poissons sont morts avant les plus gros poissons en situation de privation alimentaire. Dans la deuxième expérience, nous avons fait varier la taille des poissons et la population tout en fournissant de la nourriture; l'expérience s'est déroulée à la température ambiante. Ces poissons ont montré une perte d'énergie minimale. Le taux de mortalité a varié selon la population (Nouvelle-Écosse > New York > Caroline du Sud), mais n'a pas varié en fonction de la taille, sauf qu'il a été le plus faible chez les plus petits poissons de la Nouvelle-Écosse. Dans la troisième expérience, nous avons privé les poissons de nourriture et modéré les basses températures extrêmes. La perte d'énergie a été rapide, et les petits poissons sont morts avant les gros. Nous concluons que dans les populations soumises à des conditions saisonnières, on peut s'attendre à observer une mortalité hivernale touchant les poissons de certaines tailles quand les réserves énergétiques sont réduites, et que les taux de croissance des juvéniles ont évolué en réponse à cette pression de sélection. De plus, les populations des hautes latitudes ont développé une plus grande tolérance aux stress liés au froid.
[Traduit par la Rédaction]

Introduction

Winter is typically a period of reduced growth, depletion of energy, and heightened mortality risk. Variance in the extent of winter mortality among young fish may contribute to fluctuations in recruitment to the adult population and year-class strength (Adams et al. 1982; Gutreuter and Anderson 1985; Henderson et al. 1988; Hurst 1995; Conover and Schultz 1997). Winter mortality may also be highly selective: individuals that are relatively large, energy rich, and cold tolerant may survive more readily than others. Here, we report experiments testing whether mortality during winter conditions is selective in the Atlantic silverside (*Menidia menidia*).

Characteristics that should be subject to selection during the winter season include energy storage patterns and thermal tolerance. The notion that energy storage is a strategy for coping with winter has recently been tested and confirmed by comparing the extent of energy storage in Atlantic silverside from different latitudes (Schultz and Conover 1997). Cold

Received January 17, 1997. Accepted October 30, 1997.
J13832

E.T. Schultz.[1] Department of Ecology and Evolutionary Biology, 75 N. Eagleville Rd., University of Connecticut, Storrs, CT 06269-3042, U.S.A.
D.O. Conover and A. Ehtisham. Marine Sciences Research Center, State University of New York, Stony Brook, NY 11794-5000, U.S.A.

[1] Author to whom all correspondence should be addressed.
e-mail: eschultz@uconnvm.uconn.edu

© 1998 NRC Canada

tolerance has been studied extensively in high-latitude fishes, and multiple mechanisms of individual acclimatization to changes in temperature are known (Cossins and Bowler 1987; Hazel 1993). However, there is surprisingly little evidence for intraspecific differentiation in cold tolerance (Garland and Adolph 1991; but see Hart 1952; Fletcher et al. 1985; Hew et al. 1988; Hayes et al. 1991).

Winter mortality also selects upon individual size, and therefore upon growth prior to winter. Winter mortality is often inversely size dependent (i.e., smaller fish more likely to die; references in Conover 1990, 1992; Schultz and Conover 1997; Sogard 1997). Size-dependent winter mortality (SDWM) may drive selection on size and growth rate in seasonal environments (Conover 1992; Conover and Schultz 1995). Previous work has shown that rapid somatic growth evolves in environments with short growing seasons among local populations of several fishes of the eastern coast of North America (Atlantic silverside: Conover and Present 1990; striped bass (*Morone saxatilis*): Conover et al. 1997; mummichog (*Fundulus heteroclitus*): Schultz et al. 1996). The research on winter mortality presented here is part of our effort to clarify the selective context of this evolutionary change.

We test the following predictions. (*i*) In experimentally imposed winter conditions, there will be SDWM. Smaller individuals are predicted to reach starvation relatively early; because of other factors that act in a size-dependent fashion, fed fish should show the same size-dependent patterns but die more slowly. (*ii*) Winter mortality should be population dependent. In experimentally imposed winter conditions, fish from southern populations should be more susceptible than northern fish because of higher starvation rates or lower tolerance of cold.

Study organism

The Atlantic silverside is common in estuaries and other shallow coastal waters from northern Florida, U.S.A. (about 30°N), to Newfoundland and the Gulf of St. Lawrence, Canada (about 46°N). All populations are essentially annual (<1% of breeding adults are 2+ years old; Conover and Ross 1982). Juveniles in northern populations have less than half as long to grow before winter than those in southern populations, both because they are spawned later and because the season ends earlier as waters cool (Conover and Present 1990). Individuals in northern population accumulate energy over the growing season at a higher rate and store large quantities of lipid prior to winter, relative to southern fish; these interpopulation differences in energy accumulation are at least partially genetic (Schultz and Conover 1997). At the end of the growing season, fish in northern populations move offshore, apparently to avoid low temperatures in shallow inshore waters (Conover and Murawski 1982). A portion of the population in New York remains in shallow water and can be collected by seine throughout the winter (Schultz and Conover 1997). From temporal changes in local abundance and size structure, overwinter mortality in northern populations appears to be high (about 99% decrease in local abundance) and size selective (Conover 1984; see Henderson et al. 1988 for similar results in a closely related species). In southern populations, no offshore migration occurs, winter mortality rates are low, and mortality is not size selective (Conover and Present 1990).

Materials and methods

We report here on three "winter analogue" experiments in which the goal was to mimic winter conditions found in the nearshore waters of New York. All fish in the experiments were acclimated to winter conditions before testing (details below). In each experiment, the water temperature in each tank was checked daily. Fish were recovered from tanks for analysis only upon death (except when experiments were terminated). Dead fish were measured for total length (TL, millimetres), individually bagged, and frozen.

Origin and care of experimental fish

The individuals utilized in these experiments were collected in the field, at the egg stage in the spring or as juveniles in the fall, and transported to the Flax Pond Marine Laboratory (FPML) of the Marine Sciences Research Center at Old Field, New York. Two of the experiments (described below) utilized wild fish collected in Great South Bay, Long Island, New York (40°45′N, 72°55′W). Fish were transported to FPML in aerated 120-L containers and suffered negligible mortality. Another experiment (see below) tested for genetic effects by comparing survival among three laboratory-reared populations: a low-latitude population near the southern limit (South Carolina (SC)), a high-latitude population near the northern limit (Nova Scotia (NS)), and the New York population (NY). See Schultz and Conover (1997) for information on the collection and rearing of these populations. These methods and the facilities at FPML have proven effective at rearing and breeding populations of Atlantic silverside for multiple successive generations. Handling of captive fish followed animal care protocols filed with the University at Stony Brook Institutional Animal Care and User's Committee (IACUC) and American Society of Ichthyology and Herpetology guidelines.

Experiment 1

The first experiment tested the effects of size and feeding on energy depletion and mortality during winter conditions. Wild NY juveniles collected on November 20, 1992, were immediately sorted into four groups. Each group, consisting of 65 individuals, was held in a 680-L round tank. The tanks were illuminated by fluorescent light fixtures set to a 9 h light : 15 h dark photoperiod. Water was continually pumped into each tank from Flax Pond (a salt marsh) after filtration through sand and was not heated. However, the building heat raised the water temperature in the tanks slightly (about 2°C).

During a 30-day acclimation period, all fish were offered frozen brine shrimp once per day to satiation. The four tanks were then randomly assigned to one of two treatments, fed or unfed. The fed tanks continued to receive a daily brine shrimp feeding for the duration of the experiment, even though appetite sharply decreased once temperatures fell below about 5°C. The experiment was initiated on December 23, 1992, and terminated on April 1, 1993.

Of the 260 individuals placed in the tanks at the beginning, 231 (89%) were recovered for analysis; of the remainder, 24 died before the experiment had begun (most shortly after the experiment was set up, probably associated with handling), and five were undetected mortalities during the experiment (e.g., fish jumped out). The length distributions of the fish collected over the experimental period did not differ among tanks (mean TL = 80–84 mm, SD = 8.7–10; one-way analysis of variance for tank differences in length, $F_{3,227} = 1.84$, $P = 0.14$).

We subsequently conducted a simple gravimetric analysis of the energy reserves in each fish. Briefly, after dissection of the specimen for sex determination and to remove gut contents, each specimen was refrozen and then tissue water was eliminated by freeze-drying.

© 1998 NRC Canada

Following determination of the dry weight of the specimen, neutral lipids were extracted in a Soxhlet apparatus, using petroleum ether as a solvent (for an analysis of the efficacy of this technique, see Dobush et al. 1985). Lipid was quantified by the difference between the dry weight after freeze-drying and the weight after extraction. Finally, the remaining lean tissue was destroyed by ashing in a muffle furnace at 600°C. The lean weight was quantified as the difference between the weight after lipid extraction and the weight after ashing. Further details of the analysis are provided in Schultz and Conover (1997). The total somatic energy in each individual was estimated as (Brett and Groves 1979)

$$\text{Total energy (kcal)} = 4.8 \cdot \text{lean weight (g)} + 9.45 \cdot \text{lipid weight (g)}.$$

Experiment 2

The second experiment tested the effects of size and population of origin on energy depletion and mortality during winter conditions in the absence of starvation. Individuals from three populations (SC, NY, and NS) were reared from hatching in the spring of 1993. Until September 23, 1993, the fish were held on a fixed 14 h light : 10 h dark photoperiod in flow-through seawater at 19–27°C. On that date, fish were transferred to 1300- or 250-L acclimation tanks in a greenhouse receiving flow-through seawater. In these tanks the fish experienced only natural illumination and ambient water temperatures. Throughout the rearing period, fish were fed to satiation twice daily with formulated feeds, live brine shrimp nauplii, and frozen brine shrimp.

The experiment was set up on December 20 and 21, 1993. The experimental array consisted of twelve 193-L tanks. These were placed in groups of four into 1260-L baths and were perforated so that each tank exchanged water freely with the bath. The four tanks within each bath were randomly allocated among four treatment populations: SC, NY, and two size ranges of NS, corresponding to the two egg samples (June 8 and 29, referred to henceforth as NS Lg and NS Sm, respectively). Fish drawn from the acclimation tanks were measured to the nearest 5 mm and distributed among the experimental tanks to provide close size matching (length statistics of recovered fish: NS Lg: mean = 86 mm, SD = 5.7; NS Sm: mean = 67 mm, SD = 6.4; NY: mean = 84 mm, SD = 4.7; SC: mean = 67 mm, SD = 6.8). Each tank was stocked with 53 fish for a total of 636 fish. Samples of at least 20 fish from each population were drawn from the acclimation tanks for analysis of initial energy content.

Experimental conditions were as follows. The fish in each tank were provided with brine shrimp (commercial frozen) once per day to satiation. Water temperatures in the tanks usually were close to ambient temperatures in Flax Pond because the incoming water and the air in the greenhouse were unheated (except daytime solar heating). Flow into the water baths was adjusted during cold spells to prevent freezing in the tanks. Individuals were preserved for compositional analysis only if they were in good condition (no obvious external signs of decay). Because of the large number of specimens, we systematically subsampled up to 10 individuals per tank from among the preserved specimens.

Experiment 3

The third experiment was designed to test the effect of size on mortality during moderated winter temperatures and starvation. By minimizing mortality due to extreme low temperatures (i.e., below about 2°C, as seen in experiment 2), we hoped to isolate the effects of mortality due to energy depletion alone. NY juveniles were collected on November 23, 1994, sorted roughly by size into two groups, and acclimated in two 1260-L tanks in the greenhouse for a month. Brine shrimp was furnished once per day to satiation. On December 21 and 22, eight 250-L tanks in the greenhouse were stocked with fish. Four tanks were stocked with 31 large fish (100–125 mm TL) each and four were stocked with 46 (one tank) or 51 (remaining three tanks) small fish (60–75 mm TL). For analysis of energy content changes, 24 additional fish from each size group were sacrificed immediately. Following the stocking of tanks, there was an additional week of acclimation and tank heater adjustment. Once the experiment was initiated on December 28, no food was provided.

Analysis of mortality data and energy data

To evaluate the effects of feeding, population, and size on the rate of mortality under winter conditions, we used survival analysis models (Chambers and Leggett 1989). We used rank tests (log-rank test and Wilcoxon test) to test the equivalence of survival curves among groups (i.e., experimental treatments such as population) and for association of survival time with fish length. Both test statistics quantify the discrepancy between the observed number and expected number of events (i.e., mortalities) in a unit of time and are examined via χ^2 tests. The log-rank and Wilcoxon tests yielded similar results, and we report results of only the latter test in each analysis.

The length effect on survival is predicted to be positive: fish that are larger should survive longer, if there is SDWM. This prediction was tested in two ways. Testing for the effect of covariates is a feature of the survival analyses described above (Elandt-Johnson and Johnson 1980). We also tested the Pearson correlation coefficient of length and mortality date to assess the strength of the association. Because the agreement between the analyses was good, we report only the correlation results for brevity. Changes in length over time can be attributed to size-dependent mortality and not growth because conditions in each experiment did not favor growth even when food was offered. Temperatures only rarely, and very briefly, exceeded the minimum temperature for growth in length (10–12°C; references in Schultz and Conover 1997).

To determine changes in energy stores over time, we divided the experimental periods into biweekly intervals and predicted the energy content for a fish of standard size in each interval. We derived this prediction from regressions of log-transformed energy versus log-transformed length, conducted on each biweekly interval separately. The standard size chosen for prediction was close to the average size of the individuals in each experimental group. We wished to compare the energy utilization patterns of fed and unfed fish in experiment 1 with energy patterns of wild fish, and so we selected a contemporaneous series of samples taken from Great South Bay (December 31, 1992, and February 5, March 8, and March 31, 1993: Schultz and Conover 1997).

Results

Experiment 1. Effects of size and feeding on mortality and energy reserves

Few fish survived the experimental treatment. Most of the mortality (61% of fed fish, 63% of unfed fish) occurred in the second month of the experiment, during which time the average water temperatures in the tanks remained low (2–4°C) (Fig. 1A). Temperatures briefly rose above 5°C in early March (days 71–75). By late March, temperatures were generally warmer than 5°C. When the experiment was terminated, nine fish remained alive, six of which had been fed throughout the experiment.

Both food provision and fish length affected survival rates. Fish in the unfed treatment died earlier than fish in the fed treatment (Wilcoxon $\chi^2 = 22$, df = 1, $P = 0.0001$) (Fig. 1A). The median difference in survival time was about 7 days (unfed tanks 43.5 and 47 days, fed tanks 51.5 and 52.5 days). There was no difference in survival times between tanks within each treatment (unfed treatment: Wilcoxon $\chi^2 = 0.59$, df = 1, $P = 0.44$; fed treatment: Wilcoxon $\chi^2 = 1.9$, df = 1,

© 1998 NRC Canada

Fig. 1. Experiment 1: effects of feeding level and size on survival rate and energy depletion. (A) Survival curves and temperature over time. Average temperature over all four tanks is represented as the solid line. Solid circles, fed treatment; open triangles, unfed treatment. (B) Average length (±1 SE) of fish that died in each 14-day period. The numbers indicate sample size for each sample group. Solid circles, fed treatment; open triangles, unfed treatment. (C) Energy content over time. The symbols indicate the predicted energy content for an 85-mm fish (±1 SE of mean predicted value) for fish in the two feeding treatments and among fish collected in the field. Sample sizes for the field fish are indicated; sample sizes for fish in the experiment are the same as in Fig. 1B. Solid circles, fed treatment; open triangles, unfed treatment; solid squares, field fish.

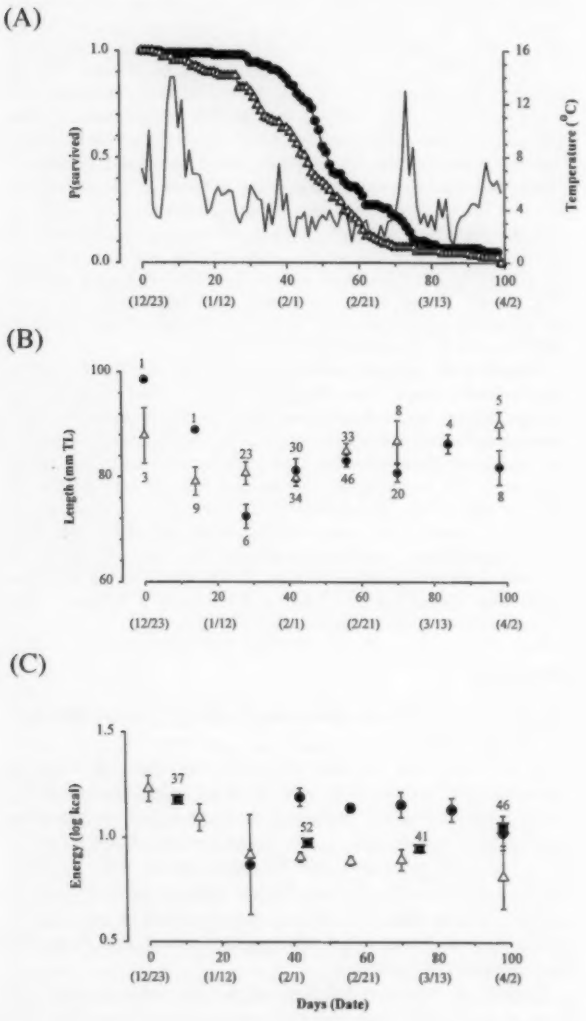

$P = 0.16$). Small fish died before large fish in the unfed treatment (correlation between length and date: Pearson $R = 0.24$, $P = 0.011$) but not in the fed treatment (Pearson $R = -0.0017$, $P = 0.98$) (Fig. 1B).

Energy reserves declined among individuals in the unfed treatment, but remained nearly steady or declined slightly among those in the fed treatment (Fig. 1C). Among unfed fish, reserves decreased over the first few weeks and then remained relatively constant for much of the experiment. In fed fish, reserves were higher than in unfed fish. Lipid levels, expressed as a percentage of somatic dry weight, were relatively constant over time among fed fish, averaging 13–14%. In contrast, lipid content among unfed fish decreased to about 5%.

Which treatment conforms more closely to the energy balance of wild fish? For much of the experiment, energy reserves in wild fish were similar to those in unfed fish in the experiment (Fig. 1C). In the last few weeks of the experimental period, energy reserves of the field fish recovered somewhat as temperatures in the shallow waters of Great South Bay increased above 5°C (unpublished data).

Fish in this experiment displayed several symptoms. Before dying, many of the fish developed a condition we called "lockjaw". The mouth was frozen in an open position (recorded for 31% of dissected fish). They typically lost equilibrium and bobbed at the surface head upwards. Often, fish in this experiment also had white fecal casts. Another symptom that these fish displayed at times was exophthalmia (protruding eyes, 7% of dissected fish). These symptoms developed early in the experiments, in the same week that we began withholding food from the unfed fish, in both fed and unfed tanks. The condition was reversed upon application of a broad-spectrum antibiotic, but returned shortly thereafter.

Experiment 2. Effects of population of origin and size on mortality and energy reserves

During this experiment, temperatures fluctuated and were at times quite cold, especially during winter storms. Shortly after the experiment was begun, the region experienced a severe cold snap. Water temperatures in the tanks declined from 5 to 0°C in 2 days (Fig. 2A). Temperatures returned to the 3–5°C range after 4 days. However, temperatures dropped to 1°C on January 7 and to zero and subzero levels in mid-January.

Survival analysis indicated a highly significant population difference (Wilcoxon $\chi^2 = 510$, df = 2, $P = 0.0001$). Fish from southern populations succumbed more rapidly than northern fish, but no fish survived the entire experiment. Each temperature drop was associated with major mortality events among fish from the SC and NY populations (Fig. 2A). About 75% of the SC population died following the first dip in temperature, and virtually all that remained died after the next cold spell. In contrast, 30% of the NY fish died following the first temperature plunge, and another 30% died in the second cold snap. Only 15% remained after the third cold snap in mid-January. Fish in the NS population were less susceptible than the NY and SC fish; more than half remained in mid-January. Most fish in one of the NS Sm tanks were lost early in the experiment when a valve froze and burst and the tank overflowed; the fish in this tank were excluded from analysis.

There was a complex effect of size on mortality rate in this experiment. If, as predicted, smaller fish in a population were more likely to die under winter conditions, then the mortality of the NS Sm group should have been higher than the NS Lg mortality rate. However, the two groups had nearly identical

© 1998 NRC Canada

Fig. 2. Experiment 2: effects of population and size on survival rate and energy depletion. Solid squares, NS fish, large cohort; open squares, NS fish, small cohort; solid inverted triangles, NY fish; open diamonds, SC fish. (A) Survival curves and temperature over time. Symbols represent the proportion alive on each day for four experimental groups; average temperature over all four baths is represented as the solid line. (B) Average length (±1 SE) of fish that died in each 14-day period. The numbers indicate sample size for each sample group. (C) Energy content over time. The symbols indicate the predicted energy content for an average-size fish (NS Lg, NY: 85 mm; NS Sm, SC: 65 mm; ±1 SE of mean predicted value). The numbers indicate sample size for each sample group.

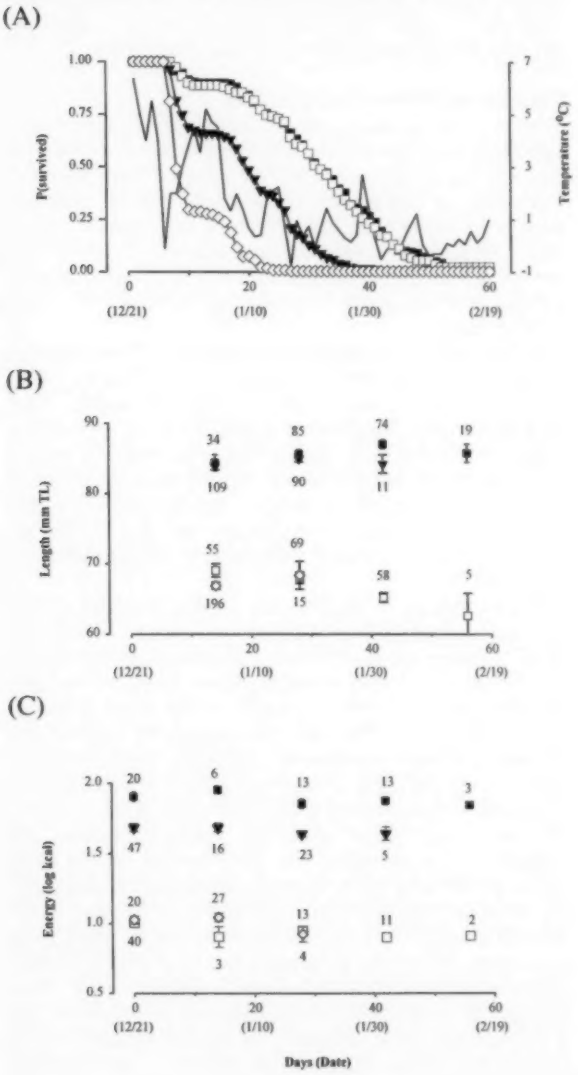

survival curves over the course of the experiment (Fig. 2A). Pursuing the possibility of size differences further, we analyzed relationships between size and death date within each population. In these analyses, we also included tank as a grouping variable. The null hypothesis that survival curves were homogenous across tanks within population was rejected (NS: Wilcoxon $\chi^2 = 64$, df = 6, $P = 0.0001$; NY: Wilcoxon $\chi^2 = 10$, df = 3, $P = 0.01$; SC: Wilcoxon $\chi^2 = 48$, df = 3, $P = 0.0001$). There was no significant association between length and survival among NS, NY, or SC fish. However, once analysis was performed on the separate NS size groups, we found that the smallest and largest fish survived best. Large fish died sooner than small fish in the NS Sm group (Pearson $R = -0.26$, $P = 0.0003$), while small fish died (non-significantly) sooner than large fish in the NS Lg group (Pearson $R = 0.11$, $P = 0.12$) (Fig. 2B).

Energy was not depleted in this experiment, or was depleted gradually (Fig. 2C). Lipid levels remained roughly constant throughout the experiment. Among NS fish, lipid levels averaged 34–39%, while among NY and SC fish, they averaged 28–30%.

Common symptoms associated with death were somewhat different from those of the first experiment. Hemorrhaging in the snout and around the mouth was noted in some fish (11% of specimens). Other fish had injuries to their mouth, such as breakage at the mandibular symphysis (6.4%). Some fish had water in their gut (4% of those dissected for energy analysis), but most of these fish did not have damaged noses.

Experiment 3: Effects of size on mortality under mild winter conditions

Temperatures remained moderate during this experiment. The submerged heaters maintained tank temperatures well above ambient to an average of 6.8°C (SD = 1.34), with no temporal pattern of variability (Fig. 3A).

The size effect built into the experimental design was compromised immediately following the setup. On the day after setup (5 days before the experiment began), 7% of the "large" fish died. Apparently the stress of handling during setup exacerbated a low-grade condition that had been restricted to the acclimation tank containing most of the large fish. In the following week, a syndrome developed among diseased fish, involving loss of the caudal fin and flesh of the caudal peduncle. Of 15 fish that were recorded as having this condition, only two were "small" fish (probably fish that had been acclimated before setup with the larger fish). Mortality involving these symptoms was confined to the first 3 weeks after setup. In the first 21 days after setup, 37% of the large fish died, a period in which only 2% of the small fish died. Because much of the large fish mortality was due to a factor extraneous to our experimental treatment, we elected to disregard these fish in the experiment and focused our analysis on the small fish.

In the first month of the trial, small fish mortality rates were quite low (Fig. 3A). Nearly 80% of the specimens died in the second 30-day period of the trial (median date of survival = 44 days). Two fish remained alive on March 12, when the experiment was discontinued.

Smaller fish within the small group died before larger fish in the experiment (Fig. 3B). Across the four tanks, survival curves were similar (Wilcoxon $\chi^2 = 5.4$, df = 3, $P = 0.14$). There was a significant positive effect of size on survival rate (Pearson $R = 0.35$, $P = 0.0001$).

Energy levels declined rapidly in this experiment (Fig. 3C). The change in energy reserves was similar to that seen in fish in experiment 1, consisting of initially rapid change followed

© 1998 NRC Canada

Fig. 3. Experiment 3: survival rate, size, and energy depletion. (A) Survival curve and temperature over time. Average temperature over all four tanks is represented as the solid line. (B) Average length (±1 SE) of fish that died in each 7-day period. The numbers indicate sample size for each sample group. (C) Energy content over time. The symbols indicate the predicted energy content (±1 SE of mean predicted value) for a 70-mm fish. The sample size for the analysis of initial energy content is shown; otherwise, sample size for each weekly group is the same as shown in Fig. 3B.

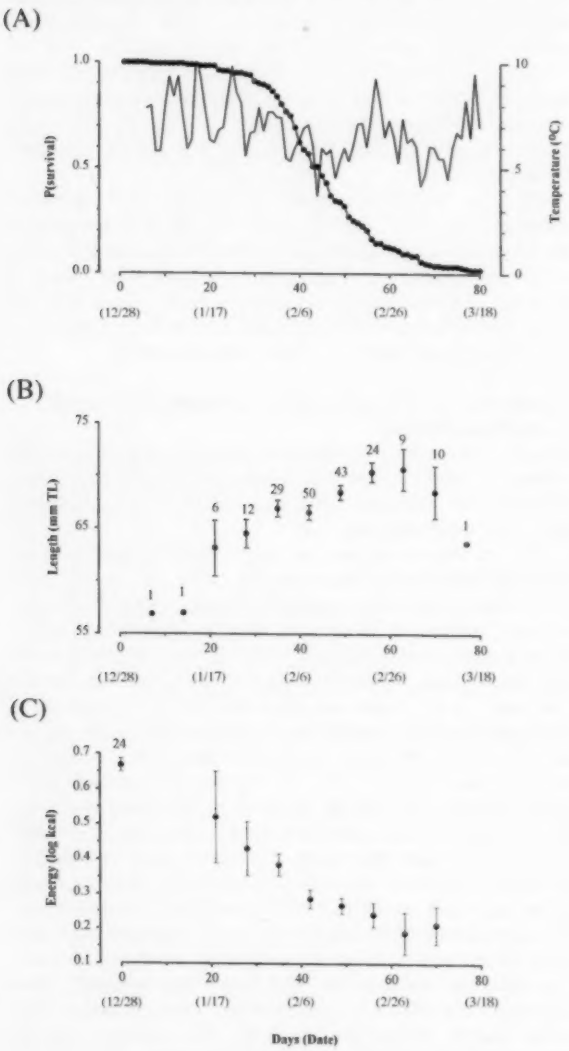

by a period of slower reduction. Tissue lipid content in the initial sample, as a percentage of somatic dry weight, averaged 14%. Lipid levels among dead fish dropped over the course of the experiment to 4–5% by day 50 and then remained constant.

Discussion

The experiments presented in this paper demonstrate that mortality among Atlantic silverside confined under winter conditions can be size and population dependent, depending on the experimental treatment. We found size-dependent mortality, in which larger fish survived for longer periods, when food was withheld and energy reserves were depleted. Another finding of the study is that fish from northern latitudes survive for longer periods in cold water. The existence of size-dependent mortality is important because it provides a selective explanation for latitudinal variation in growth capacity: winter mortality imposes directional selection favoring rapid growth as a juvenile in the first growing season. The existence of population-dependent mortality, independent of size, is important because it indicates that high-latitude Atlantic silverside populations have adapted to winter conditions in other ways, aside from the ability to grow rapidly. We discuss these points in greater detail below.

Evidence for SDWM and its causes

SDWM, in which small individuals were more likely to succumb than large individuals, was found in some but not all of the experiments reported here. We interpret these results as supporting our first prediction that smaller fish are more susceptible to winter mortality when they are depleting energy stores. Under other winter stresses, such as cold, there is no survival advantage in size. It should be noted that the survival advantages of larger size were relatively weak ($R < 0.5$) when SDWM occurred.

SDWM has been observed in a number of freshwater and marine fish species across a variety of taxa (Sogard 1997). Mortality rates in small fish are typically higher, when SDWM is found. A number of approaches have been used in studies of SDWM, and size-dependent mortality in general (see Sogard 1997 for references). Experimental work on captive animals has several advantages, such as control over confounding factors such as emigration and growth and the ability to test mechanistic explanations (manipulations of food level, etc.).

A disadvantage of experimental work is that confinement may add mortality factors that obscure natural mortality patterns. The mortality rates of fish in these experiments are relatively high, but it must be remembered that high overwinter mortality rates (e.g., 99% mortality over the winter in Massachusetts: Conover 1984) are characteristic of high-latitude Atlantic silverside populations. Moreover, captivity effects alone are not the cause of high mortality, given that the survival rates of fish confined in the same tanks, at similar densities, are much higher when the water is warmer. For comparison, we quantified the survival rates of fish being reared for breeding under the same conditions (similar stocking densities, feeding twice a day) and over the same winter months (January–February 1993–1995) but in warm water (i.e., above 20°C). The percentage that died over a 2-month period varied from 0 (three tanks) to 5 and 6%. In our winter experiments, many fish displayed an array of symptoms, and it is likely that these symptoms contributed to their demise. No size bias in the symptoms was detected. The exophthalmos and water retention in the gut are often indicative of ascites, resulting from bacterial infection of the kidneys (Dulin 1976). These and the other symptoms reported here have not been found in fish maintained in warmer water at FPML for more than 10 years of nearly continuous culture. Nor have we seen these symptoms in fish collected in the

© 1998 NRC Canada

wild. The syndrome may be less prevalent under natural conditions; it is also possible that as many fish suffer in the wild from these winter stresses and succumb before the condition has progressed to the same degree.

The evidence indicates that cold water is a threat to Atlantic silverside. In that regard, it is important to note that the thermal conditions imposed in these experiments were reasonable. The water temperatures recorded for bottom trawl stations at which Atlantic silverside have been found during winter were as low as 1°C, with most catches in 2–6°C water (Conover and Murawski 1982). Inshore, we have collected Atlantic silverside by seine in shallow water throughout the winter in Great South Bay, New York, and water temperatures were comparable with the minimum temperatures imposed in these experiments. In January 1994, we recorded a nearshore temperature of –1°C and collected fish at that site (this is the only occasion on which we collected a fish that was clearly already dead).

Mechanistic explanations for SDWM range from physiological (starvation, susceptibility to cold) to behavioral (e.g., migration) and ecological (e.g., predation). The experiments presented here are pertinent primarily to physiological mechanisms for SDWM. Our results indicate that energy depletion is one plausible factor, given the difference in results between the fed and unfed treatments in experiment 1 and the strong size-dependent mortality in experiment 3. SDWM is a predictable result when food is withheld, and energy reserves depleted at a rate comparable with that of fish in the field.

The greater susceptibility of smaller fish to starvation is generally believed to be the compound result of size differences in energy utilization rate and energy storage capacity. Allometry in resting and routine metabolic rates in fishes is well known (Fry 1957; Post and Lee 1996). This is likely to mean that small individuals will use their energy reserves relatively more rapidly than large individuals during periods of energy depletion (Shuter and Post 1990). Indeed, we have confirmed that such differences exist during winter starvation conditions in Atlantic silverside (E.T. Schultz, unpublished data). Small fish may also be at greater risk of starvation in the winter if they begin the winter with relatively low levels of energy reserves. If somatic stores of lipids or protein vary hyperallometrically (increase disproportionately with size), then small fish may exhaust these stores before large fish, even in the absence of allometry in metabolic rate. Many fish exhibit hyperallometry in lipid stores (Shul'man 1974; Larson 1991; Schultz and Conover 1997). However, this is not always the case (e.g., Miranda and Hubbard 1994), and this variability provides an opportunity to explore the association between size differences in energy storage and SDWM in the field.

Behavioral factors, such as winter habitat selection, may contribute to SDWM. Small fish may select different locations than large fish, which may place them at greater risk from biotic or abiotic stresses. For example, we have observed that small young-of-the-year Atlantic silverside in New York have a lesser tendency to move offshore as winter approaches (E.T. Schultz and D.O. Conover, personal observation). There are costs of migrating offshore, and costs of remaining inshore. Migration is likely to incur an energetic cost, resulting from greater activity and higher offshore temperatures, and may be associated with higher predation. Alternatively, we have shown that the risk of cold-induced mortality associated with remaining inshore, where temperatures tend to be variable and will drop to low levels when air temperatures are low, is likely to be great. Winter migration behavior may be conditional on size because small fish, with more limited energy reserves, can less afford the costs of migration than the costs of lower temperatures. Remaining inshore is making the best of a bad situation. In populations at higher latitude than New York, inshore winter waters are so cold that remaining inshore is not an option; size-dependent tactics might include variation in the timing or extent of migration.

In this paper, we have shown experimental evidence for a hypothesized selection pressure. Following the observation that there is a remarkable latitudinal cline in growth capacity, we hypothesized that this was an evolutionary response to a gradient in selection on size. Here, we confirm that directional selection on size occurs when fish are held in conditions analogous to winter. The conditions were restrictive, in that we found directional selection only when energy reserves were being depleted. Nonetheless, the predicted response occurred in each case that these conditions were met, and there is evidence that comparable rates of energy depletion occur in the wild. Winter selection on size has been documented before. In the analysis of winter mortality and the Atlantic silverside, we have shown how evolutionary changes in juvenile growth can arise from individual size-based differences in seasonal survival. The next step is to clarify what countervailing pressures may select against rapid juvenile growth to maintain the latitudinal cline.

Significance of population differences in susceptibility to winter conditions

Resistance to thermal stresses is undoubtedly favorable in seasonal environments. A number of physiological mechanisms improve the ability of individuals to tolerate seasonal changes in temperature (acclimatization), including changes in soluble enzymes, proteins that inhibit freezing, membrane viscosity, cell ultrastructure (Cossins and Bowler 1987), and partial or complete thermal compensation of vital rates (Bullock 1955). Adaptation to colder temperatures, following invasion of higher latitudes or climate change, may involve evolutionary changes in these mechanisms, genetically augmenting the plasticity. In some cases, genotypic (allelic) differences among populations or closely related species in different thermal environments have been found that clearly link metabolic enzyme kinetics to organism-level performance and thermal adaptation (Graves and Somero 1982; Graves et al. 1983; Powers et al. 1991). Arrays of biochemical adaptations that reduce the risk of freezing are known, including the production of antifreeze proteins. Interpopulation differences in the dosage of genes for antifreeze proteins, enabling high rates of protein production where the risk of freezing is great, are known for two families of demersal fishes from the east coast of North America (Fletcher et al. 1985; Hew et al. 1988; Hayes et al. 1991). The combination of individual plasticity and genotypic variability permits persistence in a wide thermal range, at the local and geographic scales. It is important to note that experiments demonstrating interpopulation variance in tolerances and other physiological traits often do not rear

© 1998 NRC Canada

individuals from the different populations in a common environment (e.g., Hart 1952). Given the potent influence of acclimatization on thermal tolerance, it is crucial to experimentally controi for prior individual experience. In experiment 2, individuals were reared in the same environment from the embryo stage. While we cannot rule out the possibility that environmental effects during embryogenesis induced interpopulation differences, this is unlikely. Naturally spawned eggs at high latitudes are not subjected to colder environments than eggs at low latitudes (Conover 1990).

With our evidence of geographic variation in the ability to tolerate winter stresses (Fig. 2), another trait may be added to the list of those that show genetic differences among latitudinal populations of Atlantic silverside (Conover and Schultz 1997). The level of differentiation among populations of this species is somewhat surprising, in light of potentially rapid gene flow: fishes in northern populations overwinter in waters of the continental shelf (Conover and Murawski 1982), and thus could potentially breed at some distance from their natal site. Analysis of allozyme distributions has indicated that gene flow has been sufficient to eliminate significant interpopulation differences (Johnson 1974, 1975). The question of the degree to which Atlantic silverside populations are geographically structured deserves a closer look, with attention to other polymorphic protein loci, nuclear, and mitochondrial genomes.

Acknowledgements

We thank those who cheerfully assisted with fish care on weekends and vacations and kept the lifeline from the frozen salt marsh flowing: J. Brister, J Buckel, D. Fontes, A. Green, B. Hanrahan, T. Hurst, J. Billerbeck, K. Reynolds, N. Steinberg, M. Wiggins, and B. Wise. B. Hanrahan, D. Hendrickson, J. Maul, and U. Sharma performed the dissections and energy reserve determinations. Thanks also to A. Gospodarek, D. Penick, and two anonymous referees for manuscript reviews. This research was supported by National Science Foundation grant OCE 9217025 to D.O.C. and E.T.S. This is contribution 1114 of the Marine Sciences Research Center.

References

Adams, S.M., McLean, R.B., and Huffman, M.M. 1982. Structuring of a predator population through temperature-mediated effects on prey availability. Can. J. Fish. Aquat. Sci. **39**: 1175–1184.

Brett, J.R., and Groves, T.D.D. 1979. Physiological energetics. *In* Fish physiology. Vol. 8. *Edited by* W.S. Hoar, D.J. Randall, and J.R. Brett. Academic Press, New York. pp. 279–352.

Bullock, T.H. 1955. Compensation for temperature in the metabolism and activity of poikilotherms. Biol. Rev. **30**: 311–342.

Chambers, R.C., and Leggett, W.C. 1989. Event analysis applied to timing in marine fish ontogeny. Can. J. Fish. Aquat. Sci. **46**: 1633–1641.

Conover, D.O. 1984. Adaptive significance of temperature-dependent sex determination in a fish. Am. Nat. **123**: 297–313.

Conover, D.O. 1990. The relation between capacity for growth and length of growing season: evidence for and implications of countergradient variation. Trans. Am. Fish. Soc. **119**: 416–430.

Conover, D.O. 1992. Seasonality and the scheduling of life history at different latitudes. J. Fish Biol. **41B**: 161–178.

Conover, D.O., and Murawski, S.A. 1982. Offshore winter migration of the Atlantic silverside, *Menidia menidia*. Fish. Bull. (U.S.), **80**: 145–150.

Conover, D.O., and Present, T.M.C. 1990. Countergradient variation in growth rate: compensation for length of the growing season among Atlantic silversides from different latitudes. Oecologia (Heidelb.), **83**: 316–324.

Conover, D.O., and Ross, M.R. 1982. Patterns in seasonal abundance, growth, and biomass of the Atlantic silverside, *Menidia menidia*, in a New England estuary. Estuaries, **5**: 275–286.

Conover, D.O., and Schultz, E.T. 1995. Phenotypic similarity and the evolutionary significance of countergradient variation. Trends Ecol. Evol. **10**: 248–252.

Conover, D.O., and Schultz, E.T. 1997. Natural selection and adaptation of growth rate: what are the tradeoffs? *In* Early life history and recruitment in fish populations. *Edited by* R.C. Chambers and E.A. Trippel. Chapman and Hall, London, U.K. pp. 305–332.

Conover, D.O., Brown, J.J., and Ehtisham, A. 1997. Countergradient variation in growth of young striped bass (*Morone saxatilis*) from different latitudes. Can. J. Fish. Aquat. Sci. **54**: 2401–2409.

Cossins, A.R., and Bowler, K. 1987. Temperature biology of animals. Chapman and Hall, London, U.K.

Dobush, G., Ankney, C.D., and Krementz, D.G. 1985. The effect of apparatus, extraction time, and solvent type on lipid extractions of snow geese. Can. J. Zool. **63**: 1917–1920.

Dulin, M.P. 1976. Diseases of marine aquarium fishes. TFH Publications, Neptune City, N.J.

Elandt-Johnson, R.C., and Johnson, N.L. 1980. Survival models and data analysis. John Wiley & Sons, New York.

Fletcher, G.L., Hew, C.L., Li, X., Katsuji, H., and Kao, M.H. 1985. Year-round presence of high levels of plasma antifreeze peptides in a temperate fish, ocean pout (*Macrozoarces americanus*). Can. J. Zool. **63**: 488–493.

Fry, F.E.J. 1957. The aquatic respiration of fish. *In* The physiology of fishes. Vol. 1. *Edited by* M.E. Brown. Academic Press, Inc., New York. pp. 1–63.

Garland, T.J., and Adolph, S.C. 1991. Physiological differentiation of vertebrate populations. Annu. Rev. Ecol. Syst. **22**: 193–228.

Graves, J.E., and Somero, G.N. 1982. Electrophoretic and functional enzyme evolution in four species of eastern Pacific barracudas from different thermal environments. Evolution, **36**: 97–106.

Graves, J.E., Rosenblatt, R.H., and Somero, G.N. 1983. Kinetic and electrophoretic differentiation of lactate dehydrogenases of teleost species-pairs from the Atlantic and Pacific coasts of Panama. Evolution, **37**: 30–37.

Gutreuter, S.J., and Anderson, R.O. 1985. Importance of body size to the recruitment process in largemouth bass populations. Trans. Am. Fish. Soc. **114**: 317–327.

Hart, J.S. 1952. Geographic variations of some physiological and morphological characters in certain freshwater fish. Univ. Toronto Biol. Ser. 60. University of Toronto, Toronto, Ont.

Hayes, P.H., Davies, P.I., and Fletcher, G.L. 1991. Population differences in antifreeze protein gene copy number and arrangement in winter flounder. Genome, **34**: 174–177.

Hazel, J.R. 1993. Thermal biology. *In* The physiology of fishes. *Edited by* D.H. Evans. CRC Press, Boca Raton, Fla. pp. 427–467.

Henderson, P.A., Holmes, R.H.A., and Bamber, R.N. 1988. Size-selective overwintering mortality in the sand smelt *Atherina boyeri* Risso, and its role in population regulation. J. Fish Biol. **33**: 221–233.

Hew, C.L., Wang, N.-C., Joshi, S., Fletcher, G.L., Scott, G.K., Hayes, P.H., Buettner, B., and Davies, P.L. 1988. Multiple genes provide the basis for antifreeze protein diversity and dosage in the ocean pout, *Macrozoarces americanus*. J. Biol. Chem. **263**: 12 049 – 12 055.

Hurst, T.P. 1995. Winter mortality of young-of-the-year Hudson River striped bass (*Morone saxatilis*). M.S. thesis, State University of New York, Stony Brook, N.Y.

Johnson, M.S. 1974. Comparative geographic variation in *Menidia*. Evolution, **28**: 607–618.

© 1998 NRC Canada

Johnson, M.S. 1975. Biochemical systematics of the atherinid genus *Menidia*. Copeia, 1975: 662–691.

Larson, R.J. 1991. Seasonal cycles of reserves in relation to reproduction in *Sebastes*. Environ. Biol. Fishes, **30**: 57–70.

Miranda, L.E, and Hubbard, W.D. 1994. Length-dependent winter survival and lipid composition of age-0 largemouth bass in Bay Springs Reservoir, Mississippi. Trans. Am. Fish. Soc. **123**: 80–87.

Post, J.R., and Lee, J.A. 1996. Metabolic ontogeny of teleost fishes. Can. J. Fish. Aquat. Sci. **53**: 910–923.

Powers, D.A., Lauerman, T., Crawford, D., Smith, M., Gonzalez-Villasenor, I., and DiMichele, L. 1991. The evolutionary significance of genetic variance at enzyme synthesizing loci in the teleost *Fundulus heteroclitus*. J. Fish Biol. **39A**: 169–184.

Schultz, E.T., and Conover, D.O. 1997. Latitudinal differences in energy storage: adaptive responses to seasonality in an estuarine fish (Atherinidae: *Menidia menidia*). Oecologia (Heidelb.), **109**: 516–529.

Schultz, E.T., Reynolds, K.E., and Conover, D.O. 1996. Countergradient variation in growth rate among newly hatched *Fundulus heteroclitus*: geographic differences revealed by common-environment experiments. Funct. Ecol. **10**: 366–374.

Shul'man, G.E. 1974. Life cycles of fishes. Wiley, New York.

Shuter, B.J., and Post, J.R. 1990. Climate, population viability, and the zoogeography of temperate fishes. Trans. Am. Fish. Soc. **119**: 314–336.

Sogard, S. 1997. Size-selective mortality in the juvenile stage of teleost fishes: a review. Bull. Mar. Sci. **60**: 1129–1157.

© 1998 NRC Canada

Strontium:calcium ratios in Atlantic salmon (*Salmo salar*) otoliths and observations on growth and maturation

Kevin D. Friedland, David G. Reddin, Nobumichi Shimizu, Ruth E. Haas, and Alan F. Youngson

Abstract: In this paper, we report on two data sets that have relevance to contemporary ideas on maturation in Atlantic salmon (*Salmo salar*): (*i*) an analysis of maturity rate of Atlantic salmon captured in the southern Labrador Sea and (*ii*) a study of otolith strontium:calcium ratios for maturing and immature Atlantic salmon. A discrimination function based on gonadosomatic indices was developed to classify maturation state of Atlantic salmon caught in Newfoundland and Labrador fisheries during the period 1985–1988. Atlantic salmon believed to be on feeding migrations were found to be in advanced states of sexual development. In an attempt to clarify the meaning of these data, chronological transects of Sr:Ca ratios from the otoliths of maturing and immature one-seawinter fish were collected. Sr:Ca ratios deposited during freshwater residency varied by stock and appeared to reflect the environmental availability of Sr. Sr:Ca ratios deposited during marine residency appeared to reflect somatic growth and sexual development. We detected no differences in the postsmolt Sr:Ca ratios for mature and immature Atlantic salmon from a hatchery stock originating in North America, suggesting that for this stock, little differentiation occurs between the maturity components. Mechanisms by which environment may contribute to the variation in maturation rate of North American Atlantic salmon are discussed.

Résumé : Le présent document est un rapport sur deux ensembles de données pertinentes pour les idées contemporaines sur la maturation du saumon atlantique (*Salmo salar*) : (*i*) une analyse du degré de maturité des saumons atlantiques capturés dans le sud de la mer du Labrador et (*ii*) une étude des ratios de la teneur en strontium et en calcium dans les otolithes de saumons atlantiques immatures et en voie de maturation. Nous avons mis au point une fonction de discrimination basée sur des indices gonadosomatiques afin de classer selon le degré de maturation les saumons atlantiques capturés dans les pêches de Terre-Neuve et du Labrador de 1985 à 1988. Des saumons atlantiques que l'on pensait être en migration trophique présentaient un stade de développement sexuel avancé. Afinde clarifier la signification de ces données, nous avons établi des transectes chronologiques des ratios Sr:Ca obtenus à partir des otolithes de saumons atlantiques unibermarins immatures et en maturation. Les ratios Sr:Ca qui se sont déposés durant le séjour en eau deuce variaient selon les stocks et semblaient refléter la disponibilité du Sr dans l'environnement. Les ratios Sr:Ca qui se sont déposés durant le séjour en mer semblaient refléter la croissance somatique et le développement sexuel. Nous n'avons décelé aucune différence dans les ratios Sr:Ca au stade de post-smolt chez des saumons atlantiques matures et immatues provenant d'une écloserie nord-américaine. Ces résultats indiquent que, pour ce stock, il y a peu de différences dans ce ratio entres les degrés de maturité. Nous analysons les mécanismes par lesquels l'environnement peut contribuer aux variations dans le taux de maturation chez les saumons atlantiques nord-américains.
[Traduit par la Rédaction]

Introduction

Elements are often differentially deposited in the hard body parts of an organism during the chronology of its life. The first interpretations of the elemental history of biological samples were made for corals and assumed to represent the temperature regime the animal experienced during growth (Schneider and Smith 1982). Fish species contain a number of different hard body parts that have been scrutinized for elemental signals; however, it has been the otoliths of fish that have yielded some of the most interesting results to date due to their resistance to chemical remodeling and stability during analysis (Campana

Received October 21, 1996. Accepted November 18, 1997.
J13712

K.D. Friedland[1] **and R.E. Haas.** Northeast Fisheries Science Center, National Marine Fisheries Service, 166 Water Street, Woods Hole, MA 02543, U.S.A.
D.G. Reddin. Department of Fisheries and Oceans, Science Branch, P.O. Box 5667, St. John's, NF A1C 5X1, Canada.
N. Shimizu. Woods Hole Oceanographic Institution, Woods Hole, MA 02543, U.S.A.
A.F. Youngson. SOAEFD Marine Laboratory, Victoria Road, Aberdeen, AB9 8DB, Scotland, U.K.

[1] Author to whom all correspondence should be addressed. e-mail: kevin.friedland@noaa.gov

© 1998 NRC Canada

and Neilson 1985; Gunn et al. 1992). A number of studies have ascribed elemental signals in otoliths to environmental variables such as temperature and salinity (Kalish 1990; Townsend et al. 1992; Farrell and Campana 1996). But recent studies suggest that while physical parameters are important, physiological mechanisms and their concomitant seasonal cycles, such as growth and sexual maturation, also influence chemical composition of otoliths (Kalish 1989, 1991; Gallahar and Kingsford 1992; Radtke and Shafer 1992; Sadovy and Severin 1992, 1994; Fowler et al. 1995; Fuiman and Hoff 1995). In the case of maturation, chemical composition of otoliths may reflect sexual development and spawning events and thus provide a record of the variation that occurs between individuals and populations. Otolith microchemistry may become an important tool in the study of maturation in fish populations (Gallahar and Kingsford 1992).

The maturation mechanism in Atlantic salmon (*Salmo salar*) is complex and has important consequences on the generational contribution of gametes to a population (Randall 1989). Although the physiology of maturation has been described (Thorpe 1994), the influence and interaction of stock genetics (Saunders et al. 1983), growth (Thorpe 1994; Friedland and Haas 1996), and environment (Scarnecchia et al. 1989) on the proportion of a cohort that matures annually are still poorly understood.

Atlantic salmon populations in the Northwest Atlantic exhibit variable maturation schedules that produce runs of predominately one-seawinter (1SW) and two-seawinter (2SW) Atlantic salmon (Saunders 1981). Postsmolts of these populations migrate from a wide latitudinal range and are found feeding as far north as the Labrador Sea after only a few months in the marine environment (Reddin and Short 1991). Most postsmolts are believed to overwinter in the vicinity of the Grand Banks, likely moving into this area in response to changes in water temperature and food availability (Reddin and Friedland 1993). After the overwintering period, some 1SW fish return to natal rivers to spawn. However, other 1SW fish migrate to feeding areas in the Labrador Sea and are concentrated along the Newfoundland and Greenland coasts (Møller Jensen 1990). These Atlantic salmon do not mature until the following year.

Atlantic salmon destined to sexually mature are believed to undergo physiological changes that differentiate them from the immature component of the cohort. It is also believed that the marine homing behaviors of maturing Atlantic salmon are specific, since the homing ability is so precise (Hansen et al. 1993). Ultimately, therefore, the process of sexual maturation and the return migration are intimately linked.

In this paper, we present observations of the age and apparent maturation state of Atlantic salmon migrating along the Newfoundland and Labrador coasts during summer. We then compare the otolith strontium:calcium ratios for maturing and immature 1SW Atlantic salmon on spawning and feeding migrations, respectively. These two sets of observations are complementary and form the basis of a discussion of migration and maturation mechanisms in Atlantic salmon.

Materials and methods

In overview, we examined Atlantic salmon specimens originating from both North America and Europe for two purposes. First, whole and gonad weights were taken from fish samples to train and test discriminant functions that assign maturation state. Following the successful development of the functions, Atlantic salmon of unknown maturation state, taken from commercial fisheries in Canada, were classified as mature or immature. Second, we analyzed the chemical composition of otoliths of Atlantic salmon of known maturation state. Immature fish came from samples taken in West Greenland whereas mature fish came from samples taken in natal rivers.

State of maturity of Atlantic salmon migrating in Canada

Discriminant analysis of gonadosomatic indices (GSI) was used to determine the maturity state of Atlantic salmon caught in the commercial fisheries of Newfoundland and Labrador. The indicator variable used in the discriminant analysis was GSI (GSI = gonad weight/whole weight) where whole weight was measured to the nearest gram and gonad weight was measured to the nearest 0.1 g. Discriminant functions were developed separately for male and female Atlantic salmon.

The sample of known-maturity Atlantic salmon consisted of immature 1SW fish taken in research vessel gillnet catches in the Labrador Sea each fall during 1987–1989 and maturing 1SW Atlantic salmon taken in gill nets and by anglers in the Conne River, Newfoundland (Fig. 1). Gonad and whole weight measurements were taken from all fish. Cross-validation results yielded a misclassification rate of 4.7% and an error rate of ±0.7% for the function classifying male Atlantic salmon and a misclassification rate of 7.7% and error rate of ±1.1% for the female function.

Samples of Atlantic salmon of unknown maturity were taken from commercial landings at Twillingate, Newfoundland, and Square Islands, Labrador, during 1985–1988 (Fig. 1). Samples consisted of scales for aging, whole weight, and gonad weight obtained daily from the commercial landing sites. A total of 3077 fish were analyzed, 1856 of which were males and 1221 females.

Elemental analysis of Atlantic salmon otoliths

Elemental analysis was limited to determining the ion counts of Sr (^{88}Sr) and Ca (^{40}Ca). Otoliths were surveyed for a number of elements, many of which showed trends in chronological deposition. We concentrated on Sr for two main reasons. First, Sr could be measured very reliably because of its relative abundance and ionic properties. Second, there is a wealth of comparative studies available on Sr deposition in otoliths allowing us to make more informed conclusions about this element than for others less well studied.

Elemental analysis was performed on the otoliths of 40 Atlantic salmon, 27 of which were from immature Atlantic salmon and 13 from maturing fish (Table 1). Immature fish were sampled from commercial catches at West Greenland during 1987 and 1988. Nineteen of these fish were tagged with coded-wire tags as juveniles, thus providing river and continent of origin. The nine other immature fish were of unknown origin and assumed to be a mixture of wild stocks originating from both North America and Europe. All fish at Greenland were immature 1SW Atlantic salmon and thus would not have spawned until the following year. Thirteen maturing fish were sampled from traps in two U.S. rivers in 1994 and 1995. A sample of eleven 1SW spawners were taken from the Penobscot River and two 2SW spawners were collected from the Merrimack River (Fig. 1). A sample of 10 smolt otoliths was also taken from fish in the Penobscot River in 1994 for morphological measurements only (i.e., not included in Table 1). In all samples, the sagittal otoliths were extracted and stored dry in envelopes or vials.

Secondary ion beam mass spectrometry was used to determine the concentrations of Ca and Sr in chronologically ordered locations in sagittal otolith cross sections. Otoliths were prepared for analysis by embedding them in epoxide resin and cutting them transversely through the otolith core with a low-speed saw. The posterior sections were then embedded in aluminum rings for polishing with submicron alumina. Preparation for mass spectrometry analysis was completed

© 1998 NRC Canada

Fig. 1. Map of the Northwest Atlantic area showing the location of Canadian fishing ports and rivers of sampled stocks. The cross-hatched area marks the region with Atlantic salmon stocks that produce fish aged 1 river-year (hatchery) and 2 river-years.

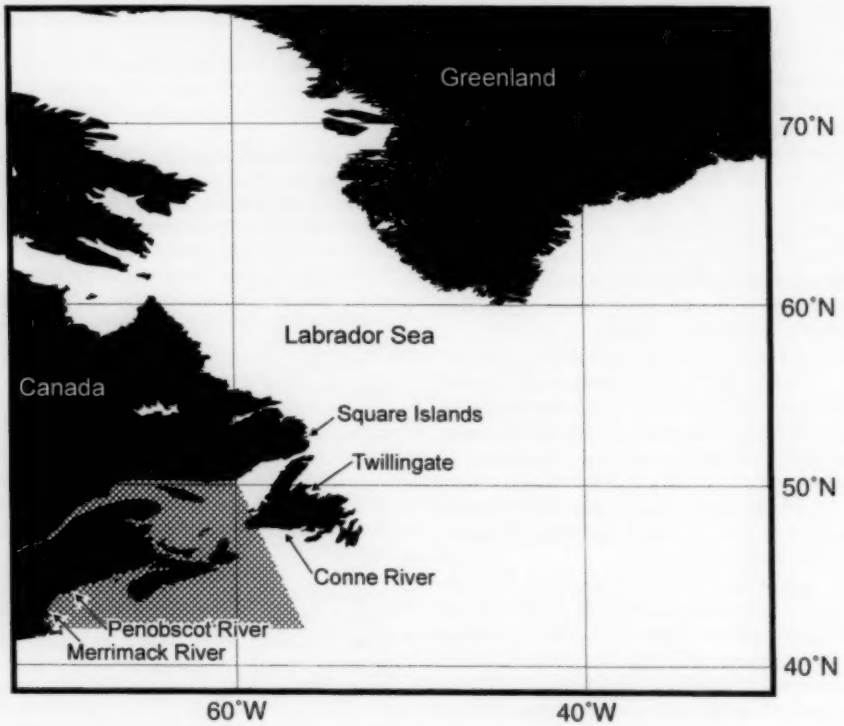

by sputter coating the samples with gold at a thickness of about 300 Å (30 nm).

A Cameca IMS 3f ion microprobe was used to measure secondary ion intensities of ^{40}Ca and ^{88}Sr. A primary beam of O^- ions was used with a net energy of 12.61 keV and an ion current of about 1 nA, focused to a spot of about 5–8 μm in diameter. The secondary positive ions released from the bombardment were accelerated to 4.41 keV and analyzed with combined electrostatic and magnetic analyzer sectors. Secondary ions were detected with a 17-stage Allen-type multiplier in pulse counting mode with a pulse amplifier/discriminator following TTL pulse counting. The energy bandwidth of the secondary ion analyzer was adjusted to ±10 eV.

Secondary ion intensities were measured on peak top intensities for ^{40}Ca and ^{88}Sr. For each analysis, five measurement cycles were made and an average intensity ratio against Ca was calculated based on four sets of doubly time-interpolated ratios. The coefficient of variation (CV) for Sr:Ca measurements was typically less than a percent; thus, confidence intervals were not plotted on the figures, since intervals would not exceed the dimensions of the point estimate markers.

Ion counts were collected from a standardized transect of the otolith cross section. First, a point on the proximal surface of the otolith (point *c* in Fig. 2A) was located midway between the dorsal tip (point *a*) and the dorsal edge of the sulcul groove (point *b*). The line between point *c* and the core (point *d*) represented the standard transect. However, it was not possible to take all samples along the standard transect due to an inability to accurately locate points and the desire to avoid surface imperfections on the polished otolith. While measurements were being made, vateritic otoliths were identified by both morphology and ion counts. These samples were then excluded from the study.

After the ion counts were completed, computer image processing was used to determine the positions of sample locations along the standard cross-section transect. Using reflected light optics, an image was captured that showed the surface topography of the otolith and the positions of ion beam burn spots. The distance from the otolith core to a site along the standard transect having the same chronology as a burn spot was determined using the topography of the otolith ring structure (Fig. 2B). These distances, in millimetres, are referred to as standardized positions and were used to facilitate comparisons among otoliths. However, standardized positions were not strictly equivalent among samples due to the different growth rates of otoliths, variation in the position of the otolith cross sections, and measurement error.

The transition between otolith material deposited before and after juvenile Atlantic salmon migrated to sea could be detected both visually and chemically. In most samples, a check was visible in the banding pattern observed in the otolith cross section. Likewise, the subject ion of the study, Sr, also showed changes in relative concentration around this transition zone. The average total length of the standard transects from a sample of 10 smolts (average = 0.54 mm) was used as a demarcation between freshwater and marine zones of the otolith. This average correlated well with the other landmarks indicating the transition zone.

Comparison of growth and elemental deposition

Marine growth was characterized by measuring the circuli spacing on scales. Circuli spacing was measured from the end of the freshwater zone to the outer edge of the scale. The spacings reflect growth during the postsmolt year and through the 1SW summer when the fish were caught (Friedland et al. 1996). Scales were prepared and circuli spacings measured following the methods of Friedland and Haas

© 1998 NRC Canada

Table 1. Sample information for otoliths used in analysis of Sr:Ca ratios.

Sample	Stock	Smolt year	FL (cm)	Origin and age[a]	Freshwater Sr:Ca ($\times 10^{-3}$) Min.	Freshwater Sr:Ca ($\times 10^{-3}$) Max.	Marine Sr:Ca ($\times 10^{-3}$) Min.	Marine Sr:Ca ($\times 10^{-3}$) Max.	Max.–edge difference
Immature Atlantic salmon									
A1	Ballyshannon, Ireland	1986	67	H1.1	1.020	1.310	2.540	2.170	0.370
A3	Wear, England	1986	69	W1.3	1.370	2.170	2.460	2.270	0.190
A5	Inniscarra, Ireland	1986	74	H1.–	0.510	0.660	2.080	1.770	0.320
G1	Inniscarra, Ireland	1986	66	H1.1			2.810	2.030	0.770
G2	Lussa, Scotland	1986	69	H1.–	0.760	0.780	2.020	1.720	0.290
G3	Galway, Ireland	1986	68	H1.1	0.400	1.280	2.410	1.890	0.520
G4	Tees, England	1986	70	H1.1	0.510	0.610	2.170		
Mean					0.760	1.130	2.360	1.980	0.410
B1	Penobscot, U.S.A.	1986	61	H1.1	0.960	1.230	2.220	1.900	0.320
B3	Penobscot, U.S.A.	1986	65	H1.1	1.120	1.390	2.400	1.860	0.540
F1	Nepisiguit, Canada	1986	67	H1.2	0.500	0.950	2.110	1.460	0.650
F2	Miramichi, Canada	1986	65	H1.–	0.440	1.190	1.870	1.690	0.180
F3	Penobscot, U.S.A.	1986	61	H1.1	0.940	1.250	2.110	1.740	0.370
F4	Nepisiguit, Canada	1986	64	H1.1			2.180	1.780	0.400
P1	Penobscot, U.S.A.	1986	62	H1.1			2.370	1.820	0.550
P2	Penobscot, U.S.A.	1986	61	H1.1			1.990	1.650	0.340
P3	Penobscot, U.S.A.	1986	63	H1.1			2.370	1.750	0.620
P4	Penobscot, U.S.A.	1986	63	H1.1			2.150	1.670	0.480
P5	Penobscot, U.S.A.	1986	59	H1.–			2.170	2.170	0.000
Mean					0.790	1.200	2.180	1.770	0.400
D2	Unknown	1987	68	W1.3	1.220	1.580	2.270	2.270	0.000
D3	Unknown	1987	65	W1.3	0.620	0.670	2.540	2.100	0.440
D4	Unknown	1987	60	W1.5	1.050	1.660	2.470	2.290	0.180
D5	Unknown	1987	68	W1.3	1.530	1.180	2.350	2.010	0.350
E1	Unknown	1987	64	W1.5			2.270	2.030	0.240
E2	Unknown	1987	68	W1.4			2.350	2.140	0.210
E3	Unknown	1987	65	W1.4			2.610	1.700	0.910
E4	Unknown	1987	63	W1.5			2.000	2.000	0.000
E5	Unknown	1987	61	W1.4			2.490	2.460	0.030
Mean					1.100	1.430	2.370	2.110	0.260
Maturing Atlantic salmon									
C1	Merrimack, U.S.A.	1992	80	W2.2	1.270	1.570	2.400	1.930	0.470
C3	Merrimack, U.S.A.	1992	75	W2.2	1.130	1.260	2.100	1.740	0.360
Mean					1.200	1.420	2.250	1.830	0.420
H1	Penobscot, U.S.A.	1994	52	H1.1	1.400	1.490	1.880	1.550	0.330
H2	Penobscot, U.S.A.	1994	57	H1.1	1.170	1.580	2.140	2.040	0.100
H3	Penobscot, U.S.A.	1994	54	H1.1			2.040	1.900	0.140
H4	Penobscot, U.S.A.	1994	52	H1.1	1.530	1.880	2.000	2.000	0.000
H5	Penobscot, U.S.A.	1994	57	H1.1			1.920	1.850	0.080
I1	Penobscot, U.S.A.	1994	51	H1.1			1.770	1.710	0.060
I2	Penobscot, U.S.A.	1994	57	H1.1			2.050	2.050	0.000
I3	Penobscot, U.S.A.	1994	58	W1.2			2.060	1.710	0.350
I4	Penobscot, U.S.A.	1994	53	H1.1			2.190	2.150	0.050
I5	Penobscot, U.S.A.	1994	54	H1.1			2.080	1.850	0.230
I6	Penobscot, U.S.A.	1994	52	H1.1			2.560	1.870	0.690
Mean					1.370	1.650	2.060	1.880	0.180

Note: Minimum and maximum Sr:Ca ratios from the freshwater portion of Atlantic salmon otoliths and maximum and outer edge Sr:Ca ratios from the 1SW marine portion of Atlantic salmon otoliths.

[a]H, hatchery-origin fish; W, wild-origin fish; age: sea-age.river-age.

© 1998 NRC Canada

Fig. 2. Polished cross-section of an Atlantic salmon otolith. (A) Location of the standardized transect. Point *c* marks a point on the dorsal surface midway between the dorsal tip (point *a*) and the dorsal edge of the sulcul groove (point *b*). The line between this point and the core (point *d*) represents the transect along which samples were taken. (B) Translations of ion beam burn locations to standardized locations along the standardized transect.

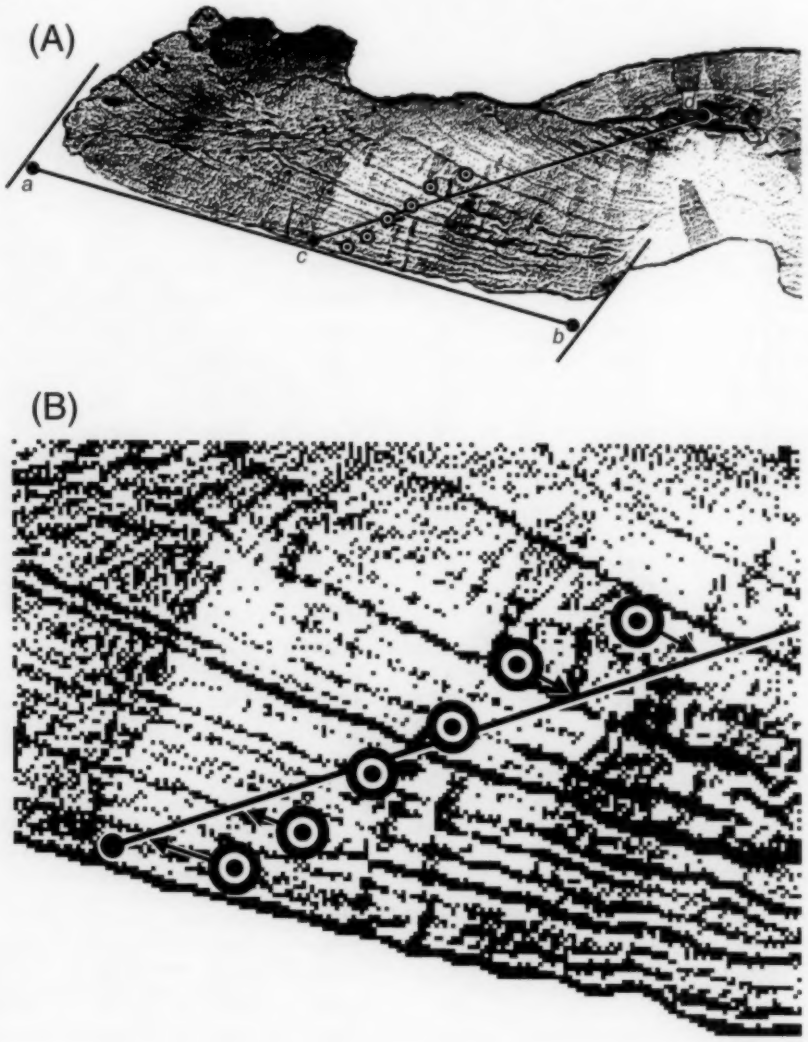

(1996) with the exception that four additional measurements were made over about a 15° sector centered on the 360° axis of the scale. The five independent measurements of circuli spacing were averaged by circuli pair and standard deviations computed.

Circuli spacing growth patterns were compared with patterns of Sr:Ca ratio in the otolith by plotting both data sets over standardized chronologies. The standardized chronology for the circuli spacing data was a scaling of the position of each spacing datum over the total length of the marine zone (the distance from the beginning of the marine zone to the outer edge of the scale). Thus, the first circuli spacing occurred at standardized chronology 0.0 and the last circuli spacing at standardized chronology 1.0. The standardized chronology for the Sr:Ca ratios was computed in a similar manner except that measurements less than 0.54 mm from the otolith core (average smolt standard transect total length) were assumed to be from the freshwater zone and thus excluded. Hence, the standardized chronology was computed by first subtracting 0.54 mm from each standardized position and then dividing by the new value for the outer edge position.

Results

State of maturity of Atlantic salmon migrating in Canada

Maturation rates estimated by discriminant function analysis for Atlantic salmon caught in the Newfoundland and Labrador commercial fisheries ranged from a low of 43% for female, river age 2 Atlantic salmon to a high of 100% for male, river age 6 fish (Fig. 3). Although the dates varied over the sampling period, the spring fishery generally peaked by

© 1998 NRC Canada

Fig. 3. Percent maturity of male (solid bars) and female (cross-hatched bars) Atlantic salmon sampled in Twillingate and Square Islands during 1985–1988 by river age and sex. Numbers above bars indicate sample size.

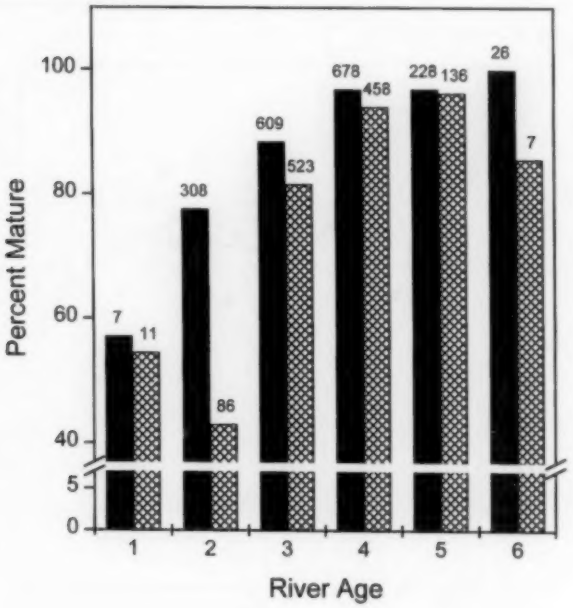

late June and was completed within a few weeks. The maturation rates of river age 1 and 2 Atlantic salmon were surprisingly high because most of these fish are thought to be destined to spawn in rivers south of Newfoundland the following year. As marked in Fig. 1, rivers tending to produce river age 2 Atlantic salmon are to the south of the sampling sites; thus, the feeding migration along the Newfoundland and Labrador coasts would take the fish in a northwesterly direction away from these rivers. Likewise, the river age 1 fish were from hatchery programs in Nova Scotia, New Brunswick, and the northeast United States and would also be unlikely to spawn until the following year.

Fig. 4. Sr:Ca ratio versus standardized position for (A) two immature North American 1SW Atlantic salmon (solid circles, sample B1; open circles, sample B3), (B) two immature European 1SW Atlantic salmon (solid circles, sample A3; open circles, sample A5), (C) two mature Penobscot 1SW Atlantic salmon (solid circles, sample I3; open circles, sample I6), (D) two mature Penobscot 1SW Atlantic salmon (solid circles, sample I2; open circles, sample I4), and (E) two mature Merrimack 2SW Atlantic salmon (solid circles, sample C1 female; open circles, sample C3 male). The vertical dotted line marks the average length of standardized transects of a sample of smolts.

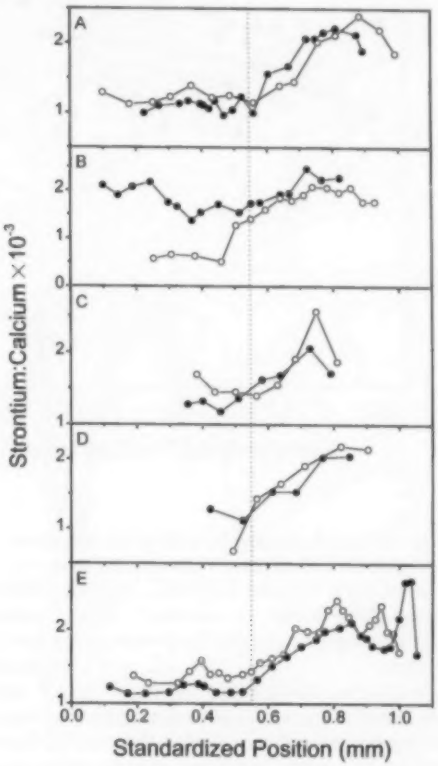

Elemental analysis of Atlantic salmon otoliths

Sr:Ca ratios in Atlantic salmon otoliths varied chronologically and systematically in patterns common to all individuals. Overall, Sr:Ca ratios averaged 1.65×10^{-3} and ranged from a low value of 0.40×10^{-3} to a high of 2.81×10^{-3} (Table 1). We considered Sr:Ca ratios deposited during the freshwater phase separately from those deposited during the marine phase. Using the standard position of 0.54 mm as an approximate demarcation between freshwater and ocean life, ratios in the freshwater region averaged 1.25×10^{-3} ($N = 140$, CV = 31%) whereas ratios deposited during the marine phase averaged 1.87×10^{-3} ($N = 242$, CV = 18%). Freshwater ratios varied over a broad range with little chronological patterning whereas marine ratios increased with standardized position or age of the fish. The data for individual otoliths provide important information for the interpretation of ion deposition and maturity data.

Freshwater Sr:Ca ratios for fish captured at West Greenland tended to vary by stock origin. Freshwater ratios for North American hatchery fish average 1.03×10^{-3} and ranged from 0.44×10^{-3} to 1.88×10^{-3} (Table 1). Ratios for hatchery fish varied little as illustrated in Fig. 4A; we assume that this reflects the constant environment of the hatchery. Ratio values in the freshwater zone of European-origin fish averaged 0.93×10^{-3} and ranged from 0.40×10^{-3} to 2.17×10^{-3} and also generally showed little ontogenetic pattern in this region of otolith, but there were some exceptions (Fig. 4B). Specimen A3, which was a wild-origin fish, had the highest mean and widest range of freshwater Sr:Ca ratios of all samples.

Marine Sr:Ca ratios for immature 1SW fish captured at West Greenland followed a pattern of monotonic increase to a peak level followed by a decrease before the fish were captured. Regardless of stock origin and freshwater Sr:Ca ratio levels, when the fish entered the marine environment the Sr:Ca ratios converged to a level of about 1.5×10^{-3} and

© 1998 NRC Canada

Fig. 5. Polynomial regression (with 95% confidence intervals) of the Sr:Ca ratio versus standardized position for immature (solid circles) and mature (open circles) Penobscot 1SW Atlantic salmon. The vertical dotted lines mark the average lengths of standardized transects for immature and mature fish.

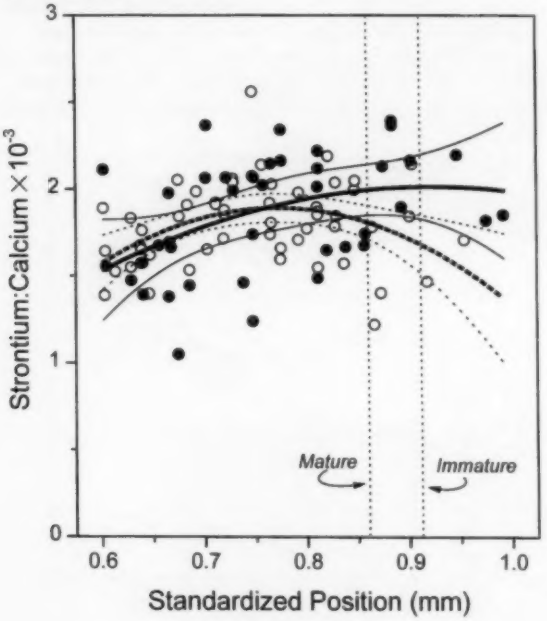

Fig. 6. Polynomial regression (with 95% confidence intervals) of the Sr:Ca ratio versus standardized position for immature Penobscot 1SW Atlantic salmon (solid circles) and immature wild 1SW Atlantic salmon of unknown stock origin (open circles). The vertical dotted lines mark the average lengths of standardized transects of Penobscot and wild fish.

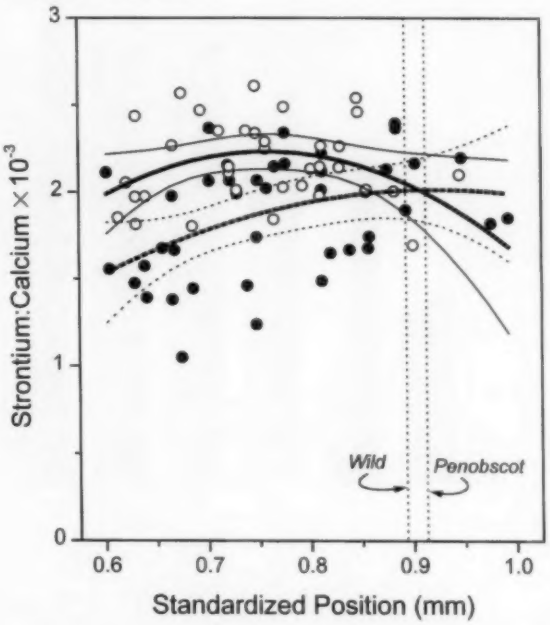

gradually increased during the period of postsmolt growth (Figs. 4A and 4B). Maximum values of the ratio were generally between 2.0×10^{-3} and 2.5×10^{-3}. Another feature of the Sr:Ca ratio chronologies for immature Atlantic salmon was the decline in the ratio before the fish were captured during late summer.

The Sr:Ca ratio values for the 11 maturing 1SW fish taken from the Penobscot River displayed two general patterns during their marine residency. All these fish had Sr:Ca ratios of about 1.5×10^{-3} at the beginning of their marine residency (Figs. 4C and 4D). However, about half the samples showed a distinct peak in Sr:Ca ratio immediately prior to entry into their natal river (Figs. 4C, 7A, and 7B) whereas the balance showed little evidence that the ratio ever peaked before capture (Fig. 4D). The overall extent of this phenomenon can be seen by differencing the maximum Sr:Ca ratio observed in the marine zone and the ratio observed near the edge of the otolith (Table 1). These differences averaged 0.4×10^{-3} for fish taken in Greenland whereas for this group of maturing fish the differences averaged 0.18×10^{-3}.

The Sr:Ca ratio decreases after the first sea summer but increases again before spawning, as evidenced by the otoliths of two maturing 2SW fish returning to the Merrimack River. The chronology of the Sr:Ca ratio for a female spawner can be seen in Fig. 4E. After the first peak in the Sr:Ca ratio, which appears in a position similar to that observed in fish captured at Greenland, the ratios decline to less than 2.0×10^{-3}. The second peak occurs in the year after the second winter at sea. A nearly identical pattern was observed in the male 2SW fish (Fig. 4E). Both Atlantic salmon were spawned and held in a hatchery an additional month before being sacrificed; this may explain the decline in the Sr:Ca ratio after the second peak. The freshwater zones for these fish showed relatively little fluctuation in the Sr:Ca ratio.

Marine Sr:Ca ratios for maturing and immature Penobscot River Atlantic salmon showed no systematic differences. We plotted the Sr:Ca ratios for mature and immature Penobscot fish in Fig. 5 and limited the range of the standardized positions to 0.6 mm and above to minimize the risk of including any values from otolith material deposited during freshwater residency. The patterns or trajectories of increasing Sr:Ca ratio were the same for the two groups (ANCOVA; assumption of homogeneity of slope plausible: $P = 0.12$, treatments were not significantly different: $P = 0.49$). We discount the divergence of the high end of the regressions at the greater standardized positions, since the mean standardized transect length of the maturing fish was much less than for the immature fish. The same data for the Penobscot immature fish were also compared with ratios from a mixture of immature, wild Atlantic salmon of unknown stock origin. The ratios for the nine 1SW wild-origin fish were higher than for the Penobscot stock (Fig. 6; ANCOVA; assumption of homogeneity of slopes plausible: $P = 0.07$, treatments were significantly different: $P < 0.01$).

Comparison of growth and elemental deposition

The chronology of marine growth as evidenced by circuli spacing patterns was similar for all samples. The beginning

© 1998 NRC Canada

Fig. 7. Sr:Ca ratio (solid circles) and circuli spacing (open circles) versus standardized chronology for mature Penobscot 1SW Atlantic salmon ((A) sample H5; (B) sample H2)) and for immature Penobscot 1SW Atlantic salmon ((C) sample B1; (D) sample B3)).

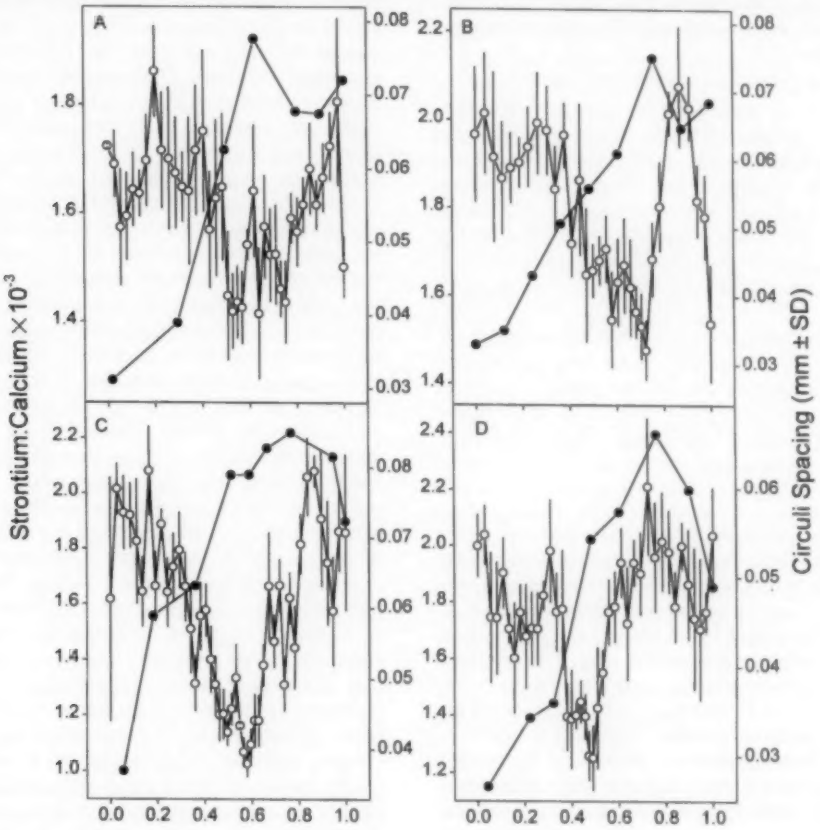

of the chronology was characterized by rapid growth rate associated with the first summer at sea for both maturing and immature examples plotted (Fig. 7). This was followed by a period of slow growth for the winter period and then followed by rapid growth associated with the second sea summer. In maturing fish, there is evidence that growth is arrested at the end of the chronology (Figs. 7A and 7B). However, growth remained at a high level right up until capture for immature fish (Figs. 7C and 7D). The chronologies of Sr:Ca ratios for the same fish reflected some of the properties of the growth data. Sr:Ca ratios reflected the inverse of the growth rates suggested by relative changes in the circuli spacing data; but absolute levels of the ratios and growth data are a poor match. Sr:Ca ratios are at their lowest values at the beginning of the chronology when growth rate is rapid; however, when growth rate returned to these high levels during the second sea summer, Sr:Ca ratios remained elevated. Despite the lack of correlation in overall trend, the two declines in growth seen in the maturing fish could be interpreted as matching the two increases in Sr:Ca ratio (Figs. 7A and 7B). Likewise, the decline in growth associated with winter for immature fish taken at West Greenland could be considered a match to the single inflections in the Sr:Ca ratio data (Figs. 7C and 7D).

Discussion

The Sr:Ca ratios in the marine region of Atlantic salmon otoliths appear to be a record of growth and sexual development during the postsmolt year. This assertion is based on our own observations and emerging research that correlates Sr deposition patterns to physiologic ontogeny (Kalish 1989, 1991; Gallahar and Kingsford 1992; Sadovy and Severin 1992, 1994; Fuiman and Hoff 1995). As recommended by Fowler et al. (1995), each species should be examined on a case by case basis to determine the mechanisms controlling the incorporation of chemical constituents into hard body parts. We were able to evaluate temperature, environmental Sr and salinity, and somatic growth as factors controlling Sr deposition by considering the freshwater and marine regions of the otolith separately and by correlation with known histories for individual otoliths.

The effect of water temperature on the Sr:Ca ratio was evaluated by considering the Sr:Ca ratio chronologies from fish that were resident in freshwater for multiple years and by contrasting ratio levels in freshwater versus the marine portion of the otolith. Temperature has been related to Sr deposition in otoliths for a number of species (Gauldie et al. 1986; Radtke 1989). From these studies, there appeared to be a

© 1998 NRC Canada

Fig. 8. Prefishery abundance of the North American immature or 2SW stock component (solid circles) and winter thermal habitat index for the Northwest Atlantic Ocean (open circles). The thermal habitat index is based on the distribution of sea surface temperature (from Anonymous 1997).

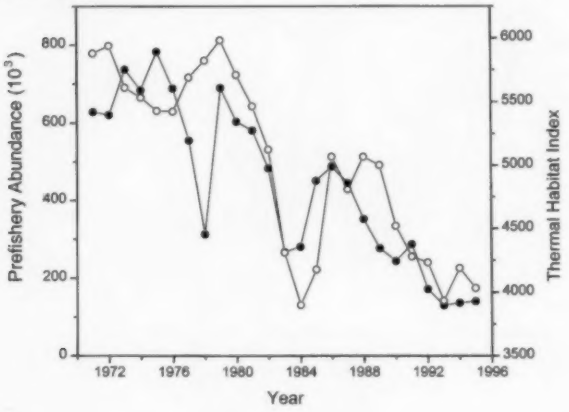

negative relationship between temperature and the Sr:Ca ratio. However, in most circumstances, this relationship is the result of growth effects that covary with seasonal temperature cycles (Kalish 1989; Sadovy and Severin 1994; Fowler et al. 1995; Gallahar and Kingsford 1996). Only in situations where growth and other environmental effects vary little can temperature be a stress factor producing significant change in the Sr:Ca ratio (Townsend et al. 1992). Data from our study are consistent with the body of evidence regarding temperature effects. The 2SW spawners from the Merrimack River were resident in freshwater for 2 years and thus experienced, at a minimum, a yearly 20°C excursion in water temperature while resident in freshwater streams. This is based on the assumption that water temperature during winter approached 0°C and exceeded 20°C during summer. These temperature changes are not reflected in the freshwater Sr:Ca ratios observed for these fish. Furthermore, the ocean temperature that the fish would have experienced would fall within the freshwater temperature range with an upper temperature likely lower than 20°C (Reddin and Friedland 1993), yet all marine Sr:Ca ratios for the fish are above those observed in freshwater.

Salinity and the environmental availability of Sr undoubtedly affect the concentration of Sr in Atlantic salmon otoliths and most likely account for differences in Sr:Ca ratios deposited during freshwater and marine residency. Environmental plasticity of Sr deposition in otoliths is reflected in how Sr levels can be manipulated for use as a chemical mark in otoliths. If simple immersion in a Sr-rich solution can load otoliths with high levels of Sr, differences in Sr levels in different freshwater drainages and between freshwater and marine environments would be expected do the same. We observed wide variation in the Sr:Ca ratio in the freshwater region of the otoliths, a period during which all juveniles would have been in 0 salinity waters with the exception of some presmolt migrants which may have utilized the estuary before migrating. Therefore, if salinity is the principal factor determining Sr:Ca ratios in Atlantic salmon, one would expect to see all the fish start at nearly the same ratio level; and perhaps some wild-origin fish have increasing Sr:Ca ratios in the section of the otolith considered to be the later part of the freshwater phase. However, this was not observed; instead, individual stocks tended to have specific ratio levels associated with them. Undoubtedly, variation in Sr availability due to local conditions, reflecting either indigenous substrates or pollution, must have caused these differences (Farrell and Campana 1996). Therefore, differences in the Sr:Ca ratio in the freshwater region of Atlantic salmon otoliths most likely reflect local availability of Sr.

The difference between Sr:Ca ratios in the freshwater versus marine regions of Atlantic salmon otoliths must in part be caused by water chemistry differences related to salinity. As has been demonstrated for a number of salmonids and clupeids (Kalish 1990; Limburg 1995), salinity is correlated with the concentration of Sr in otoliths. Examining our data, we see a general pattern of higher Sr:Ca ratios in the marine regions of the otolith, with only a few exceptions where freshwater ratios are as high. These data are consistent with the assertion that salinity and Sr concentration influence the general level of the Sr:Ca ratio in the otoliths. However, the chronologies of Sr:Ca ratios in the marine regions were highly patterned; ratios slowly increased to a maximum level. Atlantic salmon migrate to sea very rapidly, going from freshwater to ocean salinities in a matter of weeks. Sr:Ca ratio chronologies for individual Atlantic salmon did not show a discontinuity around the region of the otolith that would have been laid down during that transition. Therefore, water chemistry must play a significant role in influencing Sr:Ca ratio levels in freshwater versus the ocean. But in the marine environment, where environmental Sr levels are less variable, otolith Sr concentrations are clearly influenced by other factors.

The pattern of Sr:Ca ratios deposited in Atlantic salmon otoliths during the postsmolt year appears to reflect the combined effects of somatic growth and maturation. In general, an inverse relationship has been observed between the Sr:Ca ratio and somatic growth (Sadovy and Severin 1994; Gauldie et al. 1995; Halden et al. 1995). In our comparisons between the Sr:Ca ratio and growth rate from circuli spacing data, we observed time course changes in the Sr:Ca ratio that matched the changes observed in growth rate, thus supporting the inverse correlation observed elsewhere. However, maturation, which also causes change in the Sr:Ca ratio (Kalish 1989, 1991; Rieman et al. 1994; Fuiman and Hoff 1995; Gallahar and Kingsford 1996), results in an effect opposite to that caused by somatic growth. The onset of maturity in a fish will elevate the Sr:Ca ratio. Fuiman and Hoff (1995) suggested that other isotopes may be more responsive to physiologic changes in fishes during annual reproductive cycles, but that Sr deposition generally increases with age and maturity of the fish. The experimental work of Kalish (1991) explicitly showed that Sr levels in otolith endolymph are related to the presence of metal-binding proteins in the plasma associated with seasonal reproductive cycles. Although we found the pattern of change in the Sr:Ca ratio to be consistent with seasonal patterns of somatic growth, the overall levels of the Sr:Ca ratio increased with age and the most logical contributing factor would be maturation.

We draw two conclusions from our study that could influence the current thinking surrounding maturation in Atlantic

© 1998 NRC Canada

salmon. First, for the stock we studied in detail, the Penobscot, our evidence shows that the Sr:Ca ratio is similar in maturing and immature fish during the postsmolt year. Interpreting the Sr:Ca ratio as indicative of the state of growth and maturity of Atlantic salmon, these data indicate that maturity groups do not significantly differentiate in their growth and maturation trajectories during this period. Second, fish from southern rivers in North America appear in north-shore Newfoundland and Labrador summer fisheries in advanced states of maturation. These fish are in the wrong place, at the wrong time, and likely migrating in the wrong direction to mature that season; this is an unexpected result and deserves careful consideration.

The suggestion based on the Sr:Ca ratio that mature and immature fish do not differentiate during the postsmolt year is the same finding reported by Friedland and Haas (1996). In that study, growth signatures for 1SW versus 2SW Atlantic salmon were similar for postsmolt spring and summer seasons and only diverged during the winter period. This draws our attention to the winter period and to what importance it may hold in understanding maturation of North American Atlantic salmon. Winter climate effects have been related to the total abundance of North American Atlantic salmon (Friedland et al. 1993) and specifically to the abundance of immature Atlantic salmon, or those destined to mature at 2SW (Reddin and Friedland 1993; Reddin et al. 1993). Winter thermal habitat, based on the distribution of sea surface temperature, correlates significantly with stock abundance of the immature stock component of North American Atlantic salmon (Fig. 8 (data from Anonymous 1997)). To review, our data suggest that for at least some Atlantic salmon stocks, fish destined to mature at 1SW do not appear to differentiate during the postsmolt year from those destined to mature at 2SW. And, considering the relationship between stock abundance and environment, whatever does separate the maturity groups would appear to be related to events that occur during the first winter at sea. Is the unexpected appearance in Newfoundland and Labrador of maturing Atlantic salmon of southern North American stocks related to these observations?

Maturing Atlantic salmon originating from the southern stocks found along the Newfoundland coast may have been on a trajectory to mature, but, as a consequence of winter events, join feeding migrations that would likely result in regression of maturation. Atlantic salmon studied in the laboratory show evidence of sexual maturation as measured by peripheral steroid hormone levels, rather than pituitary or hypothamalic activity that precedes gonad activity, and still may not mature in the current reproductive current cycle (Hunt et al. 1982; Youngson et al. 1988; McLay et al. 1992). It is our contention that the events in Newfoundland parallel the phenomenon observed in the laboratory; the fish begin to mature and then regress.

Logically, our speculations focus on how climate change in winter could influence Atlantic salmon maturation. If maturity groups are poorly differentiated through most of the postsmolt year, winter conditions could influence a critical growth period that produces sufficient differences that allow some fish to mature. But this fails to explain why maturing fish from southern stocks appear in Newfoundland. Alternatively, the distribution of sea surface temperatures may simply influence migration by sending some fish that are ready to mature into feeding zones, which in turn initiates feeding migrations instead of homing behavior. The balance of the cohort would emerge from winter conditions in areas that facilitate homing behavior (Hansen et al. 1993). Although not well studied, there is a precedence for relating migration to maturity. Woodhead (1959) found that groups of immature cod (*Gadus callarias*) in the Barents Sea that followed different migration routes showed different patterns of sexual development. Furthermore, Atlantic salmon stocks originating from rivers located nearer to the feeding areas would be expected to have high 1SW maturation rates, since feeding and spawning migration routes are the same. This is generally true for stocks in Newfoundland and Labrador that tend to produce runs dominated by 1SW Atlantic salmon (Saunders 1981).

Further research with experimental animals and a wider range of Atlantic salmon populations will undoubtedly provide new insights into the dynamics of otolith development and maturity in Atlantic salmon. Specific deficiencies in our study involve the inaccuracies associated with relating the ontogeny of Atlantic salmon development to element deposition in the otoliths. Likewise, comparative studies of otolith composition in stocks with varying life history traits will be useful. Variation in maturation rate in Atlantic salmon continues to be an important issue in the management of wild and domestic Atlantic salmon populations. It is essential to combine the diversity of data available on maturation to come to a point of resolution on the critical factors controlling the process.

Acknowledgments

We thank K. Beland, V. Segarich, T. Sadusky, and T. Sheehan for their invaluable help in completing this study. We also thank F. Serchuk for a productive review of an early draft.

References

Anonymous. 1997. Report of the Working Group on North Atlantic Salmon. ICES CM 1997/Assess:10, Copenhagen, Denmark.

Campana, S.E., and Neilson, J.D. 1985. Microstructure of fish otoliths. Can. J. Fish. Aquat. Sci. **42**: 1014–1032.

Farrell, J., and Campana, S.E. 1996. Regulation of calcium and strontium deposition on the otoliths of juvenile talapia, *Oreochromis niloticus*. Comp. Biochem. Physiol. A Comp. Physiol. **115**: 103–109.

Fowler, A.J., Campana, S.E., Jones, C.M., and Thorrold, S.R. 1995. Experimental assessment of the effect of temperature and salinity on the elemental composition of otoliths using laser ablation ICPMS. Can. J. Fish. Aquat. Sci. **52**: 1431–1441.

Friedland, K.D., and Haas, R.E. 1996. Marine post-smolt growth and age at maturity of Atlantic salmon. J. Fish Biol. **48**: 1–15.

Friedland, K.D., Reddin, D.G., and Kocik, J.F. 1993. Marine survival of North American and European Atlantic salmon: effects of growth and environment. ICES J. Mar. Sci. **50**: 481–492.

Friedland, K.D., Haas, R.E., and Sheehan, T.F. 1996. Comparative post-smolt growth, maturation, and survival in two stocks of Atlantic salmon. Fish. Bull. U.S. **94**: 654–663.

Fuiman, L.A., and Hoff, G.R. 1995. Natural variation in elemental composition of sagittae from red drum. J. Fish Biol. **47**: 940–955.

Gallahar, N.K., and Kingsford, M.J. 1992. Patterns of increment width and strontium:calcium ratios in otoliths of juvenile rock blackfish, *Girella elevata* (M.) J. Fish Biol. **41**: 749–763.

© 1998 NRC Canada

Gallahar, N.K., and Kingsford, M.J. 1996. Factors influencing Sr/Ca ratios in otoliths of *Girella elevata*: an experimental investigation. J. Fish Biol. **48**: 174–186.

Gauldie, R.W., Fournier, D.A., Dunlop, D.E., and Coote, G. 1986. Atomic emission and proton microprobe studies of the ion content of otoliths of chinook salmon aimed at recovering the temperature life history of individuals. Comp. Biochem. Physiol. A Comp. Physiol. **84**: 607–615.

Gauldie R.W., West, I.F., and Coote, G.E. 1995. Evaluating otolith age estimates for *Hoplostethus atlanticus* by comparing patterns of checks, cycles in microincrement width, and cycles of strontium and calcium deposition. Bull. Mar. Sci. **56**: 76–102.

Gunn, J.S., Harrowfield, I.R., Proctor, C.H., and Thresher, R.E. 1992. Electron probe microanalysis of fish otoliths — evaluation of techniques for studying age and stock discrimination. J. Exp. Mar. Biol. Ecol. **158**: 1–36.

Halden, N.M., Babaluk, J.A., Campbell, J.L., and Teesdale, W.J. 1995. Scanning proton microprobe analysis of strontium in an arctic charr, *Salvelinus alpinus*, otolith: implications for the interpretation of anadromy. Environ. Biol. Fishes, **43**: 333–339.

Hansen, L.P., Jonsson, N., and Jonsson, B. 1993. Oceanic migration in homing Atlantic salmon. Anim. Behav. **45**: 927–941.

Hunt, S.M.V., Simpson, T.H., and Wright, R.S. 1982. Seasonal changes in the levels of 11-oxotestosterone and testosterone in the serum of male salmon, *Salmo salar* L., and their relationship to growth and maturation cycle. J. Fish Biol. **20**: 105–119.

Kalish, J.M. 1989. Otolith microchemistry: validation of the effects of physiology, age and environment on otolith composition. J. Exp. Mar. Biol. Ecol. **132**: 151–178.

Kalish, J.M. 1990. Use of otolith microchemistry to distinguish the progeny of sympatric anadromous and non-anadromous salmonids. Fish. Bull. U.S. **88**: 657–666.

Kalish, J.M. 1991. Determinants of otolith chemistry: seasonal variation in the composition of blood plasma, endolymph and otoliths of bearded rock cod *Pseudophycis barbatus*. Mar. Ecol. Prog. Ser. **74**: 137–159.

Limburg, K.E. 1995. Otolith strontium traces environmental history of subyearling American shad *Alosa sapidissima*. Mar. Ecol. Prog. Ser. **119**: 25–35.

McLay, H.A., Youngson, A.F., Wright, R.S., and Johnstone, R. 1992. Effect of rearing density on sexual maturation and growth on sea-cage reared Atlantic salmon, *Salmo salar* L. Aquacult. Fish. Manage. **23**: 353–365.

Møller Jensen, J. 1990. Atlantic salmon at Greenland. Fish. Res. **10**: 29–52.

Radtke, R.L. 1989. Strontium–calcium concentration ratios in fish otoliths as environmental indicators. Comp. Biochem. Physiol. A Comp. Physiol. **92**: 189–193.

Radtke, R.L., and Shafer, D.J. 1992. Environmental sensitivity of fish otolith microchemistry. Aust. J. Freshwater Res. **43**: 935–951.

Randall, R.G. 1989. Effect of sea-age on the reproductive potential of Atlantic salmon (*Salmo salar*) in eastern Canada. Can. J. Fish. Aquat. Sci. **46**: 2210–2218.

Reddin, D.G., and Friedland, K.D. 1993. Marine environmental factors influencing the movement and survival of Atlantic salmon. *In* Salmon in the sea. *Edited by* D.E. Mills. Fish News Books, Blackwell Scientific, Cambridge, Mass. pp. 79–103.

Reddin, D.G., and Short, P.B. 1991. Postsmolt Atlantic salmon (*Salmo salar*) in the Labrador Sea. Can. J. Fish. Aquat. Sci. **48**: 2–6.

Reddin, D.G., Friedland, K.D., Rago, P.J., Dunkley, D.A., Karlsson, L., and Meerburg, D.M. 1993. Forecasting the abundance of North American two-seawinter salmon stocks and the provision of catch advice for the West Greenland fishery. ICES CM 1993/M:43, Copenhagen, Denmark.

Rieman, B.E., Myers, D.L., and Nielsen, R.L. 1994. Use of otolith microchemistry to discriminate *Oncorhynchus nerka* of resident and anadromous origin. Can. J. Fish. Aquat. Sci. **51**: 68–77.

Sadovy, Y., and Severin, K.P. 1992. Trace elements in biogenic aragonite: correlation of body growth rate and strontium levels in the otoliths of white grunt, *Haemulon plumieri*. Bull. Mar. Sci. **50**: 237–257.

Sadovy, Y., and Severin, K.P. 1994. Elemental patterns in red hind (*Epinephelus guttatus*) otoliths from Bermuda and Puerto Rico reflect growth rate, not temperature. Can. J. Fish. Aquat. Sci. **51**: 133–141.

Saunders, R.L. 1981. Atlantic salmon (*Salmo salar*) stocks and management implications in the Canadian Atlantic Provinces and New England, USA. Can. J. Fish. Aquat. Sci. **38**: 1612–1625.

Saunders, R.L., Henderson, E.B., Glebe, B.D., and Lounderslager, E.J. 1983. Evidence of a major component in determination of the grilse : large salmon ratio in Atlantic salmon (*Salmo salar*). Aquaculture, **33**: 107–118.

Scarnecchia, D.L., Ísaksson, Á., and White, S.E. 1989. Effects of oceanic variation and the West Greenland fishery on age at maturity of Icelandic west coast stocks of Atlantic salmon (*Salmo salar*). Can. J. Fish. Aquat. Sci. **46**: 16–27.

Schneider, R.C., and Smith, S.V. 1982. Skeletal Sr content and density in *Porites* spp. in relation to environmental factors. Mar. Biol. **66**: 121–131.

Thorpe, J.E. 1994. Reproductive strategies in Atlantic salmon, *Salmo salar* L. Aquacult. Fish. Manage. **25**: 77–87.

Townsend, D.W., Radtke, R.L., Corwin, R.L., and Libby, D.A. 1992. Strontium–calcium ratios in juvenile Atlantic herring, *Clupea harengus* L., otoliths as a function of water temperature. J. Exp. Mar. Biol. Ecol. **160**: 131–140.

Woodhead, A.D. 1959. Variations in the activity if the thyroid gland of the cod, *Gadus callarias* L., in relation to its migrations in the Barents Sea. J. Mar. Biol. Assoc. U.K. **38**: 417–422.

Youngson, A.F., McLay, H.A., Wright, R.S., and Johnstone, R. 1988. Steroid hormone levels and patterns of growth in the early part of the reproductive cycle of adult Atlantic salmon (*Salmo salar* L.). Aquaculture, **69**: 145–157.

© 1998 NRC Canada

Phosphorus loading reductions needed to control blue-green algal blooms in Lake Mendota

Richard C. Lathrop, Stephen R. Carpenter, Craig A. Stow, Patricia A. Soranno, and John C. Panuska

Abstract: We evaluated the reductions in P loading needed to control blue-green algal blooms in Lake Mendota, Wisconsin. After developing a 21-year loading data set, we used a P mass balance model expressed as a difference equation with an annual time step indexed from mid-April. We defined and estimated a loss parameter λ as the proportion of the lake's April P concentration lost through sedimentation and outflow during the following year. Using the distribution of annual λ's and input loadings, we predicted the steady-state distribution of April P concentrations that would result from scenarios of altered inputs due to changes in management practices. These results were then linked to the probability of summer blue-green algal blooms. For no load reduction, the probability of a bloom (>2 mg algae·L^{-1}) on any summer day is about 60%. This probability decreases to 20% with a load reduction of 50%. Our approach illustrates how managers can consider reducing the frequency of extreme events like algal blooms, which may correspond more to the public's perception of lake water quality than average conditions.

Résumé : Nous avons évalué les réductions de la charge en P nécessaires pour éliminer les efflorescences d'algues bleues dans le lac Mendota, au Wisconsin. Après avoir établi une série de données sur la charge couvrant une période de 21 ans, nous avons utilisé un modèle du bilan massique de P exprimé sous la forme d'une équation à différences finies avec la mi-avril comme pas de temps annuel. Nous avons défini et estimé un paramètre de perte λ correspondant à la proportion de la teneur du lac en P au mois d'avril qui est perdue par sédimentation et par évacuation au cours de l'année suivante. En utilisant la distribution des λ annuels et des charges d'entrée, nous avons prédit la distribution en état d'équilibre des teneurs en P d'avril qui résulteraient de scénarios de modification de la charge suite à des changements dans les méthodes de gestion. Nous avons alors établi un lien entre les résultats obtenus et la probabilité d'efflorescences estivales d'algues bleues. Sans réduction de charge, la probabilité d'une efflorescence (>2 mg d'algues·L^{-1}) pendant n'importe quel jour d'été se situait à environ 60%. Cette probabilité diminue à 20% lorsque la charge est réduite de 50%. Notre approche illustre une façon pour les gestionnaires d'envisager la réduction de la fréquence d'événements extrêmes comme les efflorescences phytoplanctoniques, qui, aux yeux du grand public, peuvent sembler plus révélateurs de la qualité de l'eau d'un lac que les conditions moyennes.
[Traduit par la Rédaction]

Introduction

Despite decades of management and research, blooms of blue-green algae are still a major water quality problem in lakes and reservoirs (National Research Council 1992). Excessive inputs of P have been identified as the major cause of these eutrophication symptoms (Vollenweider 1968; Schindler 1977; Sas 1989). In the United States, nonpoint pollution from agricultural and urban runoff is the main source of P (National Research Council 1992). Because reducing nonpoint source P inputs can be costly, estimates of the benefits derived from various levels of P reduction are useful in decision making.

Eutrophication models frequently have been used to predict the lake response to P input reductions. Most of the models are deterministic and calculate seasonal or annual averages for P, chlorophyll, or algal concentrations, or for water transparency readings, as a function of P input (Reckhow and Chapra 1983; Cooke et al. 1993). These models, derived from cross-sectional analyses of many lakes (e.g., Dillon and Rigler 1974*a*; Vollenweider 1976; Canfield and Bachmann 1981; Reckhow and Chapra 1983), have large prediction uncertainties when applied to any one lake. For widely used models, errors in predicting P concentrations in a given lake can be as much as ±0.05 mg·L^{-1} (Cooke et al. 1993), which may be unacceptably large for decision making by managers.

More importantly, blue-green algal blooms are extreme and highly stochastic events whose occurrence can be masked in average conditions (Walker 1985; Paerl 1988; Havens 1994; Soranno 1997). It is these extreme events that are associated with episodes of toxicity, fish kills, anoxia, and generally noxious shoreline conditions resulting from wind-blown accumulations of algae. Thus, the public's perception of water quality

Received July 29, 1997. Accepted November 19, 1997.
J14143

R.C. Lathrop.[1] Wisconsin Department of Natural Resources, 1350 Femrite Dr., Monona, WI 53716, U.S.A., and Center for Limnology, 680 North Park St., University of Wisconsin, Madison, WI 53706, U.S.A.
S.R. Carpenter, C.A. Stow,[2] **and P.A. Soranno.**[3] Center for Limnology, 680 North Park St., University of Wisconsin, Madison, WI 53706, U.S.A.
J.C. Panuska. Wisconsin Department of Natural Resources, 1350 Femrite Dr., Monona, WI 53716, U.S.A.

[1] Author to whom all correspondence should be addressed. e-mail: rlathrop@facstaff.wisc.edu
[2] Present address: Nicholas School of the Environment, Duke University, Durham, NC 27708, U.S.A.
[3] Present address: Department of Fisheries and Wildlife, Michigan State University, East Lansing, MI 48824, U.S.A.

© 1998 NRC Canada

in lakes is often associated with the frequency of algal blooms. Prediction of these extreme events is inherently probabilistic. While various in-lake factors have been used to predict bloom frequencies or probabilities (Havens et al. 1994; James and Havens 1996; Soranno 1997), few attempts have been made to predict probabilities of algal blooms as affected by management of P inputs. Suitable models exist (Reckhow and Chapra 1983), but their calibration requires long-term data spanning a wide range of P input rates.

Lake Mendota, Wisconsin, affords an excellent opportunity to test the application of models linking P input rates to the probability of algal blooms. Extensive limnological and P loading data have been obtained for the lake and its watershed since the mid-1970s. During those years, runoff from the lake's watershed has varied greatly due to climate — periods of regional drought and flooding have occurred. The system's natural variability, therefore, can be used to simulate how the lake would respond to changes in P loading as a result of changes in land use practices. While we recognize that most lake eutrophication assessments do not have the advantage of extensive long-term data sets, we hope our analysis will help in the development, refinement, and (or) calibration of predictive models, as well as provide direction for local lake managers interested in improving Lake Mendota's water quality.

Background

Blue-green algal blooms have commonly occurred during the summer in Lake Mendota (A_0 = 40 km^2, z_{max} = 25.3 m) since at least the late 1800s (Brock 1985; Lathrop and Carpenter 1992). However, algal blooms were not a major concern until after World War II when P from sewage effluents entering via the lake's tributaries increased (Lathrop 1992). Even though these effluents were diverted in 1971, agricultural and urban runoff from the lake's large watershed (604 km^2) has continued to maintain high lake fertility. State and local governmental agencies from the mid-1970s through the 1980s identified the sources of nonpoint pollution, but attempts to reduce these inputs have proven unsuccessful because funding was limited, compliance by individual landowners and municipalities was voluntary, some of the installed practices were untested and unfortunately proved unreliable, and only a portion of the lake's watershed was targeted for action.

Recognizing that the only way to control the blue-green algal blooms in Lake Mendota was to conduct an aggressive nonpoint pollution reduction program, in 1993 the Wisconsin Department of Natural Resources (WDNR) designated the lake as a "Priority Watershed Project" (Betz et al. 1997). This designation allows the use of state funds to identify important sources of P pollution and to provide a significant amount of cost-sharing money to contract with both rural landowners and local municipalities to apply management practices that will reduce P loadings to the lake. In specific cases where pollution is excessive (e.g., animal feedlots), regulatory controls can be used.

As part of the initial planning phase of the project, we were charged with determining the P loading reductions needed to achieve identifiable water quality goals in the lake — a substantial reduction in the probability of summer blue-green algal blooms. These loading reduction recommendations were then incorporated into the final plan for implementation. Knowing the probability of reducing these blooms has been and will continue to be important for lake managers to accurately portray their program to the public.

Methods

In our analyses, we utilized Vollenweider's (1969) mass balance P model expressed as a difference equation with an annual time step:

$$(1) \qquad M_t - M_{t-1} = L_t - O_t - S_t$$

where M is P mass in the lake water column at the beginning of an annual time step, L is annual input loading mass of P to the lake from all external sources, O is the annual outflow mass of P, S is annual net sedimentation mass of P, and t is the annual time step indexed from April 16. All variates were calculated from extensive monitoring data for Lake Mendota except for S, which was calculated by difference. All mass loadings (L, O, and S) were calculated from April 16 of year $t-1$ through April 15 of year t. P masses and concentrations used throughout this paper refer to total P. A summary of methods for computing loadings and in-lake masses is given below. Detailed descriptions of data sources, laboratory analytical methods, and methods for computing loadings and in-lake masses are given in Lathrop (1998).

The P mass for April 16 of each year was calculated from long-term P concentration data that were generally obtained at 0 and 4 m water depths on a biweekly sampling schedule beginning soon after ice-out around early April. The average P concentration for April 16 was then interpolated from average P concentrations for sampling dates before and after April 16. The whole-lake P mass for that date was the interpolated average concentration multiplied by the lake volume (adjusted for lake level).

We chose April 16 as the annual time step index for two reasons. First, Stow et al. (1997) used April P concentrations to predict the probability of summer blue-green algal densities exceeding bloom threshold concentrations in Lake Mendota. Spring P as a predictor of summer chlorophyll also has been widely applied in lake trophic assessments (Dillon and Rigler 1974*b*; Cooke et al. 1993). Thus, we were able to make a straightforward linkage between external P loadings and summer algal densities in Lake Mendota. Second, mid-April occurs during spring mixis when P concentrations are relatively uniform throughout the water column. Whole-lake P masses could be reliably calculated for this period from surface water P concentration data. While we recognize that external loadings occurring after April 16 could influence that year's summer blue-green algal densities, choosing a summer date for in-lake P concentrations or masses would have invalidated our predictions of algal bloom probabilities. This is because summer P concentrations are a surrogate for algal densities; most of the eplimnetic P is incorporated in algae during the summer.

Outflow P loadings were calculated from daily flows at the lake outlet (Yahara River) multiplied by daily P concentrations interpolated from surface water P data for the central lake station (except for part of 1975 when outlet data were used). Daily flows for years since 1978 were determined from a flow rating model that utilizes daily lake level and tailwater elevations and operation records for the outflow gates, boat locks, and bypass pipes. Outflows for 1975–1977 were updated from estimates made by Lathrop (1979).

External P inputs

Major P inputs to Lake Mendota come from runoff carried by five inflowing streams draining mostly agricultural areas: Pheasant Branch Creek, Dorn Creek, Sixmile Creek, Yahara River, and Token Creek (Fig. 1; Table 1). While the urban area draining directly to the lake is much less than the rural area, two large storm sewer systems carry runoff from the City of Madison's southwest side: Spring Harbor and Willow Creek storm sewers. At various times during the past 25 years, continuous flow monitoring stations were maintained on all of these inputs (except Dorn Creek) by the U.S. Geological Survey

© 1998 NRC Canada

Fig. 1. Lake Mendota watershed including monitored subwatersheds. (Map prepared by Dave Fritzke, Dane County Land Conservation Department.)

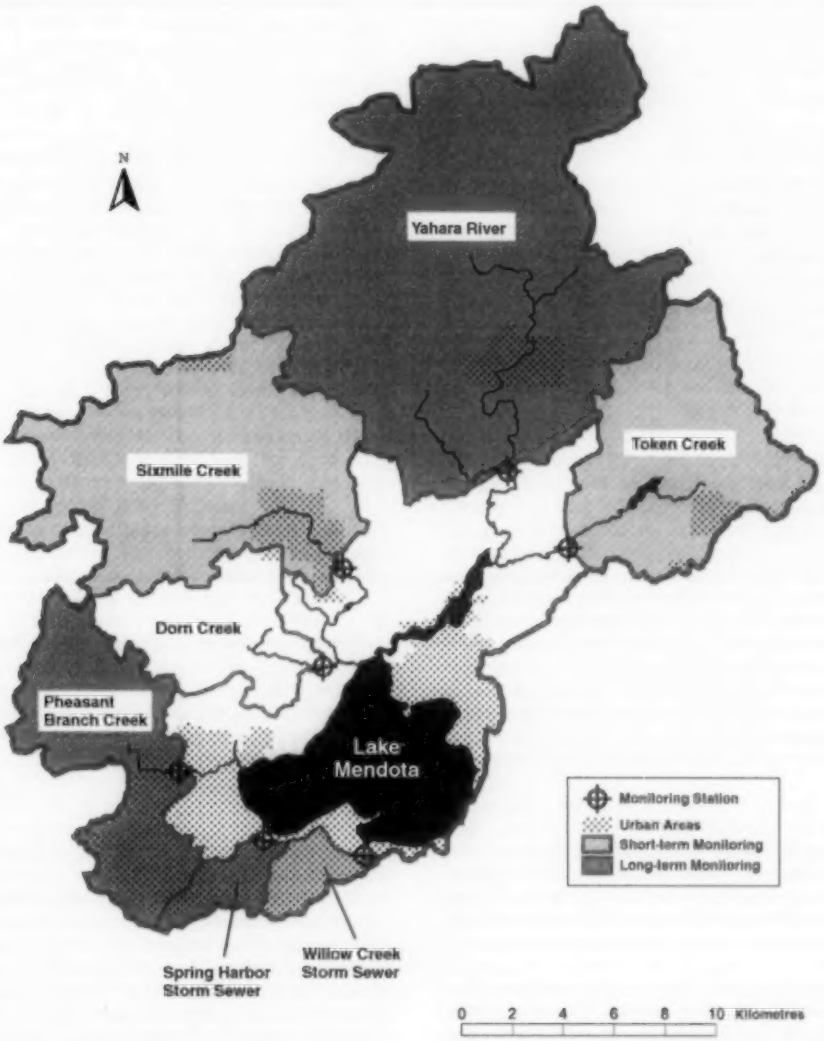

(USGS) at points upstream of the lake. P concentration data were also obtained at these stations, particularly during storm or snowmelt runoff events, with multiple water samples collected throughout each monitored event. All stations were monitored during 1976–1980. During that period, water samples were collected manually at the stream stations, while automatic samplers were used at the storm sewer stations. P analyses were performed by the WDNR.

Continuous flow monitoring has been maintained at three of these stations since 1980: Pheasant Branch Creek, Yahara River (excluding 1982–1989), and Spring Harbor storm sewer (Table 1). A limited number of runoff events were sampled each year for P during 1981–1991 at Pheasant Branch Creek; sampling was extensive during 1992–1996. Sampling has been extensive at the Yahara River station since 1990. Automatic water samplers were used for sampling runoff water; P analyses were performed by the USGS. Since 1980, P concentration data for the Spring Harbor storm sewer station were only available for 1992–1993 (P.A. Soranno, unpublished data).

Developing the annual external P loadings to Lake Mendota from 1975 to 1996 required a multistage procedure. P loadings for all monitored subwatershed stations during 1976–1977 had previously been calculated using a direct integration method that utilized each station's instantaneous flow records and P concentrations corresponding to instantaneous flow (Lathrop 1979). Instantaneous P concentrations were interpolated between actual measured concentrations obtained throughout the runoff events and during baseflow. Subwatershed loadings had only been calculated (using direct integration methods) for the Pheasant Branch Creek and Yahara River stations since the early 1990s (USGS Water Resources Data Wisconsin, annual reports). P concentration data were available for selected runoff events in other years as previously described, but event loadings had not been calculated. Also, for the Pheasant Branch Creek station during the 1980s, many runoff events were not sampled for P. Finally, while raw instantaneous flow data were available from the USGS, only summary flow data expressed as mean daily discharges had been processed for errors and published

© 1998 NRC Canada

Table 1. Drainage areas[a] and years of monitoring (ongoing monitoring indicated by arrows) for subwatersheds in the Lake Mendota drainage basin.

		Years of monitoring data	
	Area (km^2)	Continuous flow	P concentrations
Monitored rural streams	407.3		
Pheasant Branch Creek	47.4	1974[b]→	1976→
Contributing	43.4		
Noncontributing[c]	4.0		
Sixmile Creek	106.4	1976–1981	1976–1981
Yahara River	190.6	1976–1981, 1989[b]→	1976–1980, 1990→
Token Creek	62.9	1976–1980	1976–1980
Monitored urban storm sewers	16.68		
Spring Harbor	8.52	1976→	1976–1980, 1992–1993
Willow Creek	8.16	1973[b]–1983	1976–1983
Unmonitored area	139.6		
Dorn (Spring) Creek[d]	32.6		
Other rural	68.1		
Urban[e]	38.9		
Contributing	35.5		
Noncontributing[c]	3.4		
Lake Mendota	39.9		1976→
Lake outlet	603.5	1975[f]→	

[a]Drainage areas from Henrich and Daniel (1983).
[b]Continuous flow monitoring began midyear.
[c]Noncontributing drainage areas for Pheasant Branch Creek and for unmonitored urban land (Stricker's Pond and Tiedeman Pond) from USGS unpublished data.
[d]Monitoring conducted during 1976 using a rated staff gauge and grab sampling.
[e]Unmonitored urban drainage area determined from land use information for the mid-1990s provided by Dane County Land Conservation Department.
[f]Daily flows computed from model using outlet operation records.

in annual reports. Using the raw instantaneous flow data for calculating P loadings was not practical. Consequently, a method was developed to calculate loadings using the published mean daily discharge data along with the runoff P concentration data for discrete samples. These data were then used to estimate P loadings from the other unmonitored rural areas.

When mean daily flow records were available, daily loadings were computed by one of the following methods. If the loadings had already been computed via direct integration, those data were used. If no direct integration loadings had been calculated but P concentration data were available for a runoff event, we multiplied the mean of all P concentrations obtained for a given day times the mean daily flow. This proved to be an accurate unbiased way of calculating loadings (Lathrop 1998). When no P concentration data were available for a given day, daily P loadings were predicted using a second-order polynomial regression model with log mean daily discharge as the predictor variable and log daily P loading as the response variable. The model developed for each station was based on all the mean daily P concentration data and corresponding mean daily discharge data available for that station prior to 1996. The second-order polynomial models consistently had small, uncorrelated, and apparently normal residuals. A comparison of daily loading data obtained for the Pheasant Branch Creek station during the 1970s and 1990s indicated that land use changes were insufficient to alter the overall runoff – P loading relationship (Lathrop 1998).

In years when no flow data were available for the Yahara River station (1982–1989), monthly loads for that station were predicted from Pheasant Branch Creek monthly loads using a geometric mean functional relationship model of log-transformed data. The model was developed from monthly loading data when both stations were monitored. The geometric mean model minimizes the sum of triangular areas formed by connecting the measured data points to the estimated line with lines parallel to the coordinate axes (Barker et al. 1988). This approach was chosen over simple linear regression because the predictor variable (monthly Pheasant Branch Creek loads) was not measured more accurately than the response variable (monthly Yahara River loads). Similar models were developed for both the Pheasant Branch Creek and the Yahara River monthly loads (log transformed) as predictor variables and Sixmile Creek and Token Creek monthly loads (log transformed) as response variables. Both Sixmile Creek and Token Creek monthly loads were estimated from Yahara River monthly loads if those loads were derived from monitoring data. Otherwise, Sixmile Creek and Token Creek monthly loads were estimated from Pheasant Branch Creek monthly loads.

To improve the predictability of both high and low monthly loads at a given station, the monthly loading data of either the Pheasant Branch Creek or Yahara River (predictor variable only) station were stratified into periods with almost no runoff (i.e., dominated mostly by baseflow) and with runoff. Separate geometric mean models were thus developed. An analysis of residuals justified this approach. No such stratification was needed for predicting Token Creek loadings. The actual models (and associated statistics) used to predict P loadings at the monitored rural subwatersheds are given in Lathrop (1998).

Annual P loadings for urban areas not included in the monitored

© 1998 NRC Canada

rural subwatersheds were related to runoff volumes for the Spring Harbor storm sewer station. (Monthly runoff volumes for 1975 were estimated from Willow Creek storm sewer volumes.) Annual runoff volumes for the Spring Harbor storm sewer station were multiplied by an annual average P concentration derived from runoff monitoring data for that station. Average P concentrations of 0.97 and 0.26 mg·L^{-1} were used for 1975–1985 and 1986–1996, respectively. The earlier concentration was a volume-weighted average of monitoring data for 1976–1977 (Lathrop 1979). In 1985, the open channel section of the storm sewer system was stabilized to prevent bank erosion causing suspended sediment concentrations (monitored every year by the USGS) to drop considerably. The runoff P concentration of 0.26 mg·L^{-1} was an average for 1992–1993.

To compute annual P loadings for the Willow Creek storm sewer and for the other unmonitored urban area draining directly to Lake Mendota, the unit area runoff volume computed from the Spring Harbor storm sewer data for each year was multiplied by the unmonitored urban area (Table 1) times an average runoff P concentration of 0.80 mg·L^{-1}. This concentration was the volume-weighted average concentration for Spring Harbor, Willow Creek, and Olbrich Park (drains to Lake Monona downstream of Lake Mendota) storm sewers for 1976–1977 (Lathrop 1979). This average runoff P concentration for older neighborhoods may be high, but areas being developed would produce disproportionately higher P concentrations in runoff because of construction site erosion.

One major problem in estimating the annual P loading to Lake Mendota was determining the contribution for the unmonitored rural watershed areas (Fig. 1; Table 1). Loadings for the Dorn Creek subwatershed were estimated from the unit area Pheasant Branch Creek loadings multiplied by the Dorn Creek area. Loadings for the remaining unmonitored rural lands were computed by multiplying the land area times the unit area P loadings for the combined Pheasant Branch Creek, Sixmile Creek, Yahara River, and Token Creek subwatersheds. This unit area computation was justified because of results from a 16-month study where loads were monitored at the lake inlets of the Yahara River and Pheasant Branch Creek as well as their upstream stations. Even though both tributaries flow through extensive wetlands before entering the lake, unit area loads based on the upstream station monitored loadings were relatively good estimators for the remaining subwatershed area loadings (USGS, unpublished data).

In addition to P loadings entering Lake Mendota via streams and storm sewers, P can also enter via dry fallout, precipitation, and groundwater. Annual estimates for these sources were developed by Lathrop (1979) utilizing local monitoring data, although our groundwater estimate is slightly higher because of outlet flows that were updated from the original water budget calculations. The combined P loading estimate of 3800 kg from these other sources was added to each year's drainage basin loading estimate. Finally, a liquid fertilizer spill of 4000 kg of P into upper Pheasant Branch Creek was added to 1985's total loading.

Predicting effects of P load reduction

To predict effects of changes in P inputs, we coupled a dynamic model of the P budget with the model described by Stow et al. (1997) that predicts blue-green algal densities from April P concentrations. To predict mid-April P concentration changes, we divided both sides of our mass balance model (eq. 1) by the lake volume to convert masses to concentrations and added terms to identify the input loading that will be controlled by management actions:

$$[P]_t = [P]_{t-1} + (((1 - R)I_t + U)/V) - \lambda_t[P]_{t-1}. \quad (2)$$

In the dynamic model, [P] is the mid-April P concentration (milligrams per litre) for a given year, t, V is the average volume of the lake (505 × 106 m^3), and R is the reduction (as a proportion) of the drainage basin P input loading (I_t) to the lake after nonpoint pollution controls are implemented. R is determined by management policy. The proportion of I_t remaining after pollution controls is represented by $1 - R$. A negative value for R would signify an increase in loadings. The "uncontrollable" P loading, U (3800 kg·year^{-1}), from dry fallout, precipitation on the lake surface, and groundwater inputs was set as a constant; we considered U unaltered by nonpoint pollution controls. The empirical loss parameter λ (dimensionless) was calculated for each year from the long-term data as

$$\lambda_t = (O_t + S_t)/(V\,[P]_{t-1}) \quad (3)$$

where λ_t corresponds to the proportion of the mid-April P concentration in year $t - 1$ that is lost through both the outlet and sedimentation by mid-April of the following year, t. Dividing O (outlet) and S (net sedimentation) by V expresses the loss as a concentration. Initially, we computed loss parameters for O and S separately, but both terms were combined in our final analysis because results were nearly identical and one additional degree of freedom was gained by having only one parameter, λ.

The steady-state distribution of mid-April P concentrations, [P*], is

$$[P^*] = ((1 - R)I + U)/(\lambda V). \quad (4)$$

The distribution of [P*] was calculated by random sampling from the joint distribution of λ and the log of I for the 21 years of annual loading data. The distribution of [P*] was assumed to be a multivariate Student t distribution, with parameters estimated from the measurements of λ and log I (Gelman et al. 1995). This distribution corresponds to the posterior predictive distribution of I and λ derived from a Bayesian analysis with a noninformative prior and normal likelihood, assuming that the means of I and λ, their variances, and their covariance are unknowns to be estimated from the data. Normal probability plots and autocorrelation functions suggested that the residuals were normally distributed and independent, thereby supporting the assumption that a multivariate t model was appropriate. Sampling from the multivariate t distribution was done in Matlab using algorithms described by Ripley (1987) and Gelman et al. (1995).

Dynamic simulations with eq. 2 showed that P concentrations were close to steady state in 2–5 years. This time interval is reasonable given that the average P residence time calculated from the monitoring data is about 1.7 years. The time interval is also shorter than the proposed nonpoint pollution control project. Because the long-term distribution of P concentrations is of more interest than changes over a few years, our analysis focused on the steady-state distribution of April P concentrations.

We extended our model to predict the probability of blue-green algal blooms as a function of P inputs. Stow et al. (1997) provided $p(\text{BGA} < 2 \mid [P]_{\text{April}})$ and $p(\text{BGA} < 5 \mid [P]_{\text{April}})$ where BGA is the blue-green algal concentration measured in microlitres of cell biovolume per litre converted to milligrams of algae per litre, 2 and 5 mg·L^{-1} are threshold levels for nuisance blooms in Lake Mendota (Lathrop and Carpenter 1992), and $[P]_{\text{April}}$ is the mean April P concentration. Stow et al. (1997) also found that below the critical April P concentration of 0.074 mg·L^{-1}, the probability of blue-green blooms is less than 0.2. Thus, our mid-April P prediction links directly with the prediction of summer blue-green algal blooms.

For a given scenario of nonpoint P control (i.e., for a given value of R), we estimated $p([P^*] < 0.074)$, $p(\text{BGA} < 2)$, and $p(\text{BGA} < 5)$ as follows. A random value of [P*] was obtained by sampling from the joint distribution of λ and log I and then calculating [P*] from eq. 4. A probability distribution of [P*] values, $p([P^*])$, was constructed using 5000 such random draws. The proportion of [P*] values less than 0.074 is $p([P^*] < 0.074)$. The probability of blue-green algal concentrations <2 mg·L^{-1} was calculated as

$$p(\text{BGA} < 2) = \Sigma p([P^*])p(\text{BGA} < 2 \mid [P^*]))/\Sigma p([P^*]) \quad (5)$$

where the summations are over P concentrations ranging from 0 to

© 1998 NRC Canada

Fig. 2. Monthly P loadings for the Pheasant Branch Creek subwatershed from January 1975 through September 1996.

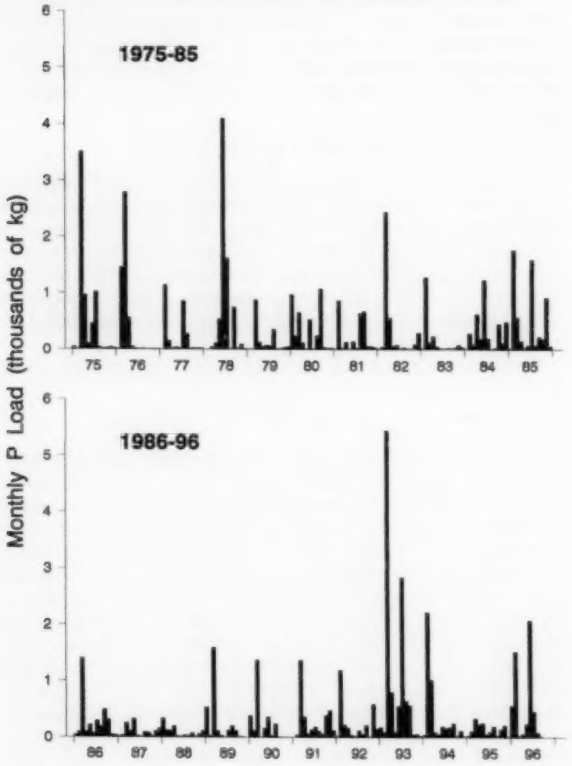

0.25 mg·L^{-1} with an interval of 0.01 mg·L^{-1}. The probability of blue-green algal concentrations <5 mg·L^{-1} was calculated in the same way.

Results

P loadings

The importance of climate as a driver of P loadings is highlighted in the monthly loading data for the Pheasant Branch Creek station during 1975–1996 (Fig. 2). Many years had high loadings in one or more spring months and lower loadings throughout the summer and fall. In a few years, spring loadings were low and summer loadings were high. The prolonged period of low monthly loadings during the Midwest drought years of 1987–1988 was also evident as well as the very high loadings in the late winter and summer of 1993, a year of severe flooding in the Midwest. The drought effect and the 1993 flood were less noticeable in the annual loadings (Table 2) because the mid-April index caused the calendar year loadings to split between two years.

Mid-April P changes between successive years indicated that Lake Mendota often responded rapidly to large changes in P loadings (Table 2). This is reasonable given that the average P residence time of 1.7 years is much shorter than the average water residence time of 4.6 years (Table 3). The lowest April P concentrations occurred during the second year of the drought in 1988 and reflected an overall decline from high concentrations in the 1970s when runoff was high (Lathrop 1992). By April 1994, in-lake P concentrations had increased by two and a half times in response to the very high loadings in 1993.

The long-term average annual P input was 34 000 kg, but annual inputs ranged between 15 000 and 67 000 kg (Tables 2 and 3). This long-term average was slightly less than an earlier long-term estimate of 38 000 kg, which was based on 1976–1977 monitoring data and adjusted for prior long-term runoff patterns (Lathrop 1979, 1992). Except for drought or flood years, outlet P loadings were relatively stable compared with input loadings. Net sedimentation P losses were variable year to year. In years when net sedimentation was low, the lake sediments may have supplied a relatively large proportion of P to the water column.

Predicted effects of nonpoint P reductions

We considered the effects of reducing nonpoint P inputs by various proportions (eq. 4). The consequences for the distribution of P input rates under a hypothetical scenario of a 50% load reduction ($R = 0.5$) are shown in Fig. 3. (The 50% reduction in the drainage basin average input loading, I, corresponds to a target annual P loading of about 19 000 kg, which includes the uncontrollable sources, U.) In comparison with the current scenario of no load reduction, a 50% load reduction shifts the probability distribution toward lower P input rates. The right-hand tail of extremely large P input rates is reduced in area, but there is still an appreciable probability of input rates above the current annual average of 34 000 kg. Even with nonpoint pollution controls, unusual events (e.g., very wet spring seasons) will occasionally yield large annual P inputs to the lake.

Probability distributions for April P concentrations ([P*]) indicated a substantial decrease between the no load and 50% load reduction scenarios (Fig. 4). (The probability distributions are jagged because they are obtained by random sampling.) Under current conditions, 80% of the probability mass or area (10% in each tail) is between an April P concentration of 0.069 and 0.203 mg·L^{-1}, which is similar to the 1975–1996 range (Table 2). With a 50% load reduction, 80% of the probability mass is between 0.038 and 0.113 mg·L^{-1} (Fig. 4). In this scenario, 64% of the probability mass is less than 0.070 mg·L^{-1}, the lowest April P concentration recorded during the long-term record.

Another observation is noteworthy when we superimpose the scenarios of no load reduction and 50% load reduction on curves for the probability of summer blue-green algal bloom concentrations >2 and >5 mg·L^{-1} (Fig. 4). In the case of no load reduction, a substantial area of the distribution of April P concentrations exceeds a 0.5 probability of blue-green algal blooms >2 mg·L^{-1}. In the case of 50% load reduction, the area exceeding that probability is substantially reduced. However, even with 50% load reduction, there is still some probability of April P concentrations high enough to cause summer blue-green blooms in Lake Mendota. This prediction makes sense because in high-runoff years, P loadings will still be excessive even with nonpoint pollution controls in place.

Predictions for a range of load reductions suggest that improvements in water quality scale almost linearly with load reductions up to about 60% of the current levels (Fig. 5).

© 1998 NRC Canada

Table 2. P input mass loadings from the drainage basin, total input mass loadings, outlet water volumes and P mass loadings, in-lake mid-April P masses and concentrations, net sedimentation mass loadings, and loss parameter values (λ) all derived from monitoring data for Lake Mendota, 1975–1996.

Year	Drainage basin input (kg)	Total input (kg)[a]	Outlet flow (10^6 m^3)	Outlet mass (kg)	April lake mass (kg)[b]	April lake P sedimentation mass (mg·L^{-1})	Net sedimentation mass (kg)	Loss parameter λ
1975	—	—	—	—	69 600	0.136	—	—
1976	52 700	56 500	154.3	15 400	66 100	0.13	44 600	0.874
1977	19 800	23 600	66.6	7 800	75 400	0.15	6 500	0.218
1978	11 700	15 500	62.8	8 500	79 500	0.16	2 900	0.150
1979	45 500	49 300	121.1	11 600	56 500	0.11	60 700	0.895
1980	27 300	31 100	110.1	10 000	71 200	0.14	6 400	0.293
1981	40 800	44 600	98.9	10 400	50 200	0.10	55 200	0.915
1982	35 500	39 300	114.3	10 000	46 000	0.091	33 500	0.861
1983	21 300	25 100	110.0	9 900	46 100	0.091	15 100	0.544
1984	12 100	15 900	105.7	9 500	36 100	0.073	16 400	0.564
1985	47 900	51 700	141.1	10 600	46 000	0.091	31 200	1.134
1986	35 500	39 300	145.9	16 100	45 600	0.090	23 600	0.864
1987	20 400	24 200	141.3	10 300	44 300	0.088	15 200	0.561
1988	18 000	21 800	113.9	7 200	35 400	0.070	23 500	0.691
1989	21 800	25 600	63.5	4 200	46 700	0.093	10 100	0.405
1990	22 300	26 100	74.1	5 200	57 200	0.113	10 400	0.332
1991	22 200	26 000	70.5	7 100	54 600	0.107	21 500	0.501
1992	19 600	23 400	79.1	7 300	49 100	0.098	21 600	0.535
1993	47 900	51 700	96.4	10 000	78 600	0.151	12 200	0.449
1994	63 200	67 000	188.6	29 300	88 900	0.177	27 400	0.744
1995	18 900	22 700	111.8	12 800	62 700	0.125	36 100	0.547
1996	28 100	31 900	113.4	11 300	61 000	0.121	22 300	0.532

Note: Input, outlet, and sedimentation mass loadings are from the previous April 16 to April 15 of the given year. In-lake data are for April 16 of the given year.

[a]Total input P mass loadings = drainage basin inputs plus other sources (U = dry fallout, precipitation, groundwater) that are considered unaltered by watershed management practices implemented in the watershed.

[b]In-lake P masses and P concentrations for April 16 interpolated from 0–4 m data for different April sampling dates during spring mixis.

Table 3. Long-term annual mean P loadings and corresponding standard deviations, and average residence times for water and P for Lake Mendota, 1976–1996 (21 years).

	Mean	SD
Input loading (all sources, kg P·year^{-1})	33 900	14 500
Drainage basin inputs (kg P·year^{-1})	30 100	14 500
Pheasant Branch Creek (kg P·year^{-1})[a]	3 700	2 300
Yahara River (kg P·year^{-1})[a]	6 200	3 900
Urban (kg P·year^{-1})[b]	6 300	1 800
Net sedimentation (kg P·year^{-1})	23 600	15 600
Outlet loading (kg P·year^{-1})	10 700	5 100
Outlet flow (10^6 kg P·year^{-1})	109	33
Mid-April P mass (kg)[c]	57 600	14 800
Mid-April P concentration (mg·L^{-1})[c]	0.114	0.029
Loss parameter λ	0.60	0.26
Water residence time (years)	4.6	—
Presidence time (years)	1.7	—

[a]Pheasant Branch Creek and Yahara River loadings are for USGS flow gauging station locations.

[b]Urban loading excludes urban area in monitored rural subwatersheds.

[c]Statistics for mid-April P mass and concentration are for 1975–1996 (22 years).

With no load reduction, the probability of blue-green algal densities >2 mg·L^{-1} on any summer day over the long-term is about 60%. If loads are reduced 50%, this probability decreases to 20%. Severe blooms >5 mg·L^{-1} occur with probabilities of 40 and 10% with no load and 50% load reductions, respectively. If loadings were to increase in future years as a result of deteriorating land use management, bloom probabilities increase, although not linearly. This is because P concentrations and input loads are already high enough to cause high probabilities of blue-green algal blooms. For example, if P loads increase by 20% (R = –0.2), blooms >2 and 5 mg·L^{-1} increase to probabilities of 70% (from 60%) and 50% (from 40%), respectively.

Discussion

Lake Mendota has experienced considerable variation in annual P loadings and in-lake P concentrations during 1975–1996. Most of the loading variation can be attributed to climatic variations — periods of drought or high precipitation. A result of this loading variation has been marked annual differences in summer blue-green algal densities (Lathrop and Carpenter 1992) that Stow et al. (1997) were able to link to lake P concentrations from the spring. Additional variation in summer algal densities occurs because of weather as it affects

© 1998 NRC Canada

Fig. 3. Probability distributions for scenarios of no P load reduction and 50% load reduction of annual surface water P inputs (excluding unalterable sources).

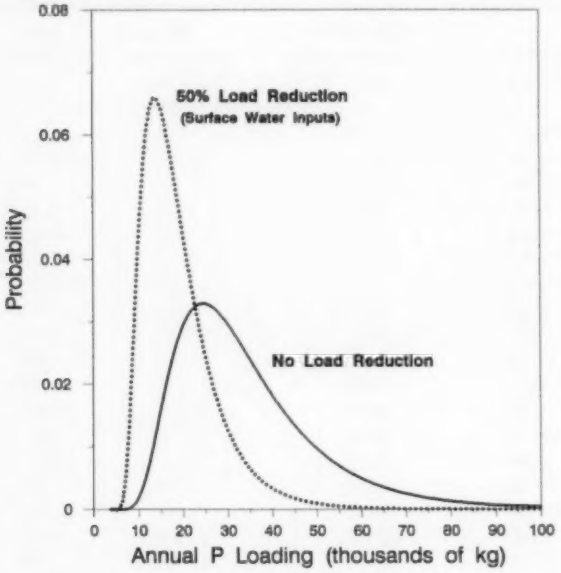

Fig. 4. Probability distributions of April P concentrations for scenarios of no load reduction (open circles) and 50% load reduction (solid circles), and probabilities of blue-green algal concentrations >2 $mg \cdot L^{-1}$ (solid line) and >5 $mg \cdot L^{-1}$ (dotted line) versus April P concentrations. Probabilities of April P are based on 5000 random samples from the model described in the text. Probabilities of blue-green algal blooms are from Stow et al. (1997).

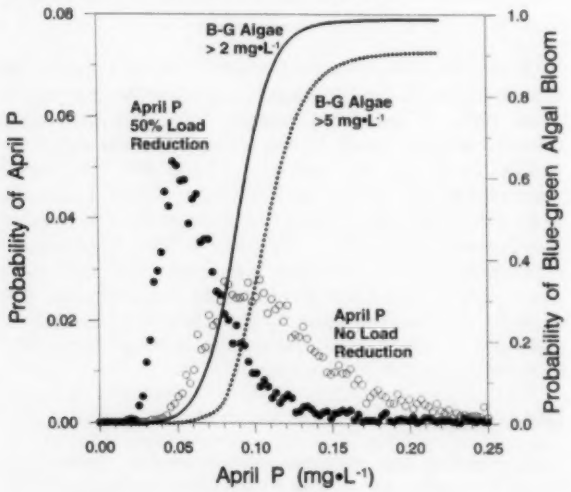

internal P recycling rates (Stauffer and Lee 1973; Soranno 1997; Soranno et al. 1997) and because of differences in grazing by *Daphnia* spp. (Lathrop et al. 1996). This paper focuses on P as a driver of blue-green algal blooms because we are evaluating management of P input rates. Any variance caused by factors that are not managed (such as weather-induced

Fig. 5. Probabilities of April P concentrations >0.074 $mg \cdot L^{-1}$ (asterisks), blue-green algal concentrations >2 $mg \cdot L^{-1}$ (open circles), and blue-green algal concentrations >5 $mg \cdot L^{-1}$ (solid circles) versus percentage change of the annual P load. Each point is based on 5000 random samples from the model described in the text. Probabilities for a 50% load reduction (surface water inputs excluding unalterable sources) are depicted by the dotted lines and arrows.

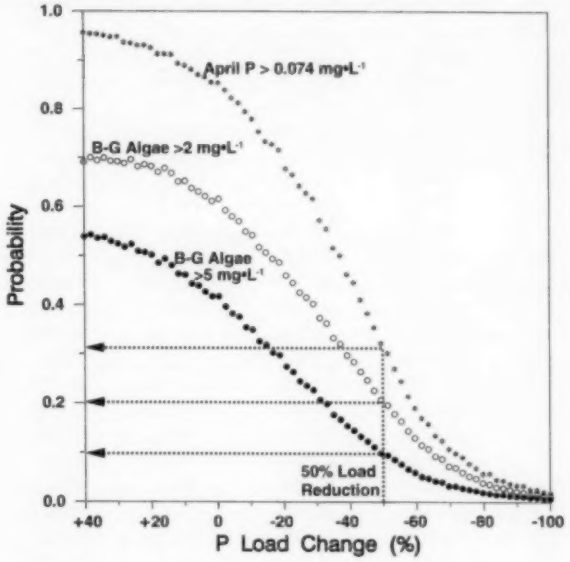

internal recycling and grazing) is represented by the stochastic terms of our model.

Because of the annual variability in P loadings, short-term monitoring can provide biased data for traditional P loading assessment models. An additional problem in determining P inputs to a lake like Lake Mendota is that P concentrations in inflowing streams increase as runoff flow increases. However, the relationship between P concentration and flow varies greatly between different events including the rise and fall of each event's hydrograph. Therefore, P input loadings calculated from minimal water quality data can produce significant underestimates even when continuous flow records are available. P loadings determined from monitoring data for Lake Mendota during the 1940s, and later used in Vollenweider's (1968) initial modeling efforts, were subject to this bias.

Vollenweider (1975) recognized that models predicting the relationship between P loadings and lake trophic state were highly sensitive to errors in loading estimates. He suggested that increased attention be focused on developing P loading databases for model verification, yet recognized that the high cost of long-term studies often precluded such studies. The database we present in this paper should be useful for that purpose.

One approach for computing average P loadings for lakes is the use of watershed export coefficients for watersheds in similar geographic regions (Reckhow et al. 1980). Many of these coefficients are derived from short-term monitoring of relatively small drainage areas. A large range in coefficient

© 1998 NRC Canada

values is commonly reported. Thus, application to a large hydrologically complex watershed like Lake Mendota's leads to large uncertainty in predicted loadings (Soranno et al. 1996). In the early 1970s, P input estimates that had been derived from export coefficients were too high because the lake's watershed is in a glacial region where many small, internally drained areas occur (Lathrop 1979). The total land area exporting P to the lake's tributaries is thus reduced, as was verified by a flow routing analysis using digital elevation data (Soranno et al. 1996).

The long-term record for Lake Mendota allowed us to predict the impact of nonpoint pollution controls in a more powerful, probabilistic way. While the mathematical basis of our model has long been known, suitable data for predicting probability distributions of future water quality in a single lake have not been combined with this modeling approach until the present study. Several important insights emerge. The variability observed over 21 years of study dominates our analyses. Traditional deterministic models would be misleading because "average" conditions rarely occur.

A few specific features of our mass balance model also are noteworthy. We avoided the "mixed reactor" modeling assumption of uniform P concentrations throughout the water column. This is not true for Lake Mendota, as P concentrations in surface waters are much lower than in bottom waters during summer and late winter (WDNR, unpublished data). In the more traditional models reviewed by Reckhow and Chapra (1983) and Cooke et al. (1993), the P concentration at steady state is mathematically derived from a mixed reactor average P concentration in the outlet and sedimentation terms. However, outlet P concentrations normally are from surface waters, not the entire water column. By using an empirical loss parameter λ that is derived from measured outlet and net sedimentation P loadings and April P concentrations, we were able to define steady state with respect to P concentrations in April when the water column is mixed. Because spring P is a good predictor of summer algal densities in lakes (Dillon and Rigler 1974*b*; Stow et al. 1997), relating P loadings to a steady-state April P concentration is limnologically meaningful.

Another important feature of our model relates to the steady-state definition. Lake Mendota never experiences a true steady state (i.e., invariant April P concentrations over many years) because annual P loadings are highly variable due to climatic variations. As a result, our steady-state April P is expressed in terms of a probability distribution of April P concentrations ([P*]) that the lake should experience given annually varying P loadings as influenced by a relatively constant set of watershed management practices and by varying climate. A new steady-state distribution of April P concentrations would be attained from major changes in land management practices such as would be implemented by the Lake Mendota Priority Watershed Project. This distribution would also change if future climatic conditions affecting runoff patterns were to change for some reason such as global warming. Modeling this linkage is beyond the scope of this paper, but future research in this area is warranted given the likelihood of global climate change.

One final comment about the steady-state April P distribution relates to its dependence on the distribution of λ's derived from the long-term data. As external P loadings decline because of land management improvements, P stored in the sediments of the lake and inflowing river channels may continue to be released in significant amounts. If internal loading remains high, then net sedimentation should decline, causing λ to also decline. As a consequence, [P*] will be higher than would otherwise be predicted from our modeling analysis. However, as P is leached from the sediments over time, net sedimentation (and λ) should increase again, while [P*] would approach the distribution predicted in our analysis. Because there is no clear basis for modeling trends in the distribution of λ, our analysis is based on its observed distribution from 1975 to 1996.

The long-term record strongly supports the conclusion that P concentrations in Lake Mendota are tightly coupled to external P loadings. In-lake P concentrations declined during the drought years of 1987–1988 and increased following periods of high runoff, especially in 1993. Annual P loads were similar during 1989–1992, and April P concentrations were stable during that period. Consequently, a large reduction in P loadings realized by an aggressive nonpoint pollution abatement program should produce measurable water quality benefits, particularly in the form of reduced blue-green algal densities, within a few years. However, because future P loading reductions will be insufficient to cause average loadings to be below the "excessive" loading threshold proposed by Vollenweider (1976), Lake Mendota will continue to experience algal blooms.

In summary, our modeling analyses indicate that there is no "law of diminishing returns" for reducing blue-green blooms over a wide range of management goals. In other words, Lake Mendota should experience proportional improvements in water quality per unit reduction in P loading for any abatement program that is implemented. The ultimate goal emphasized by our modeling analysis is the reduced frequency (or probability) of extreme events — dense blue-green algal blooms — that are very noticeable to the public, especially when decaying algae accumulate on lake shorelines. This finding should help convince local lake managers and politicians that reducing algal blooms is not an intractable problem.

Acknowledgments

We were able to make long-term annual P loading estimates for Lake Mendota because of monitoring programs sustained by local, state, and federal agencies. The Dane County Regional Planning Commission (DCRPC), with technical advice from many agency and university scientists, initiated and has continued to coordinate the cooperative stream and storm sewer monitoring program since it began in the mid-1970s. Many staff at the USGS district field office in Madison have been responsible for carrying out the flow monitoring program since its inception and the stream P sampling program since 1981. The USGS provided 50% federal cost-sharing monies that were matched with local monies for this work. U.S. Environmental Protection Agency funds to the DCRPC as part of the Dane County Water Quality Plan were used to help develop and support the monitoring network in the first few years of operation. The cities of Middleton and Madison provided the bulk of the local cost-sharing monies for the long-term monitoring at the Pheasant Branch Creek and Spring Harbor storm sewer stations, respectively. Grants

© 1998 NRC Canada

from the WDNR to Dane County provided funding in later years for the Yahara River station as well as P monitoring at the Pheasant Branch Creek station. The in-lake P data collection was funded principally by the WDNR. For the preparation of our report, Becky Hayes compiled the flow and P loading data for the lake outlet. Dave Armstrong, Tara Reed, and Kathy Webster made many helpful comments on an earlier draft. We also wish to thank Roger Bachmann and an anonymous reviewer for their helpful comments on the final draft. Our analysis was supported in part by the WDNR, Andrew W. Mellon Foundation, and North Temperate Lakes LTER Program.

References

Barker, F., Soh, Y.C., and Evans, R.J. 1988. Properties of the geometric mean functional relationship. Biometrics, **44**: 279–281.

Betz, C.R., Lowndes, M.L., and Porter, S. 1997. Nonpoint source control plan for the Lake Mendota Priority Watershed Project. Wis. Dep. Nat. Resour. Publ. No. WT-481-97.

Brock, T.D. 1985. A eutrophic lake: Lake Mendota, Wisconsin. Springer-Verlag, New York.

Canfield, D.E., Jr., and Bachmann, R.W. 1981. Prediction of total phosphorus concentrations, chlorophyll *a*, and Secchi depths in natural and artificial lakes. Can. J. Fish. Aquat. Sci. **38**: 414–423.

Cooke, G.D., Welch, E.B., Peterson, S.A., and Newroth, P.R. 1993. Restoration and management of lakes and reservoirs. Lewis Publishers, Boca Raton, Fla.

Dillon, P.J., and Rigler, F.H. 1974*a*. A test of a simple nutrient budget model predicting the phosphorus concentration in lakewater. J. Fish. Res. Board Can. **31**: 1771–1778.

Dillon, P.J., and Rigler, F.H. 1974*b*. The phosphorus–chlorophyll relationship in lakes. Limnol. Oceanogr. **19**: 767–773.

Gelman, A., Carlin, J.B., Stern, H.S., and Rubin, D.B. 1995. Bayesian data analysis. Chapman and Hall, New York.

Havens, K.E. 1994. Relationship of annual chlorophyll *a* means, maxima, and algal bloom frequencies in a shallow eutrophic lake (Lake Okeechobee, Florida, U.S.A.). Lake Reservoir Manage. **10**: 133–138.

Havens, K.E., Hanlon, C., and James, R.T. 1994. Seasonal and spatial variation in algal bloom frequencies in Lake Okeechobee, Florida, U.S.A. Lake Reservoir Manage. **10**: 139–148.

Henrich, E.W., and Daniel, D.N. 1983. Drainage area data for Wisconsin streams. U.S. Geol. Surv. Open-File Rep. 83-933.

James, R.T., and Havens, K. 1996. Algal bloom probability in a large subtropical lake. Water Resour. Bull. **32**: 1–12.

Lathrop, R.C. 1979. Appendix H: Lake management. *In* Dane County water quality plan. Vol. 2. Dane County Regional Planning Commission, Madison, Wis.

Lathrop, R.C. 1992. Nutrient loadings, lake nutrients, and water clarity. *In* Food web management: a case study of Lake Mendota, Wisconsin. *Edited by* J.F. Kitchell. Springer-Verlag, New York. pp. 69–96.

Lathrop, R.C. 1998. Water clarity responses to phosphorus and *Daphnia* in Lake Mendota. Ph.D. thesis, University of Wisconsin, Madison, Wis.

Lathrop, R.C., and Carpenter, S.R. 1992. Phytoplankton and their relationship to nutrients. *In* Food web management: a case study of Lake Mendota, Wisconsin. *Edited by* J.F. Kitchell. Springer-Verlag, New York. pp. 97–126.

Lathrop, R.C., Carpenter, S.R., and Rudstam, L.G. 1996. Water clarity in Lake Mendota since 1900: responses to differing levels of nutrients and herbivory. Can. J. Fish. Aquat. Sci. **53**: 2250–2261.

National Research Council. 1992. Restoration of aquatic ecosystems. National Academy Press, Washington, D.C.

Paerl, H.W. 1988. Nuisance phytoplankton blooms in coastal, estuarine and inland waters. Limnol. Oceanogr. **33**: 823–847.

Reckhow, K.H., and Chapra, S.C. 1983. Engineering approaches for lake management. Vol. 1: Data analysis and empirical modeling. Butterworth Publishers, Boston, Mass.

Reckhow, K.H., Beaulac, M.N., and Simpson, J.T. 1980. Modeling phosphorus loading and lake response under uncertainty: a manual and compilation of export coefficients. EPA 440/5-80-011. U.S. Environmental Protection Agency, Washington, D.C.

Ripley, B.D. 1987. Stochastic simulation. Wiley, New York.

Sas, H. (*Editor*). 1989. Lake restoration by reduction of nutrient loading: expectations, experiences, extrapolations. Academia-Verlag, Richarz, St. Augustine, Germany.

Schindler, D.W. 1977. Evolution of phosphorus limitation in lakes: natural mechanisms compensate for deficiencies of nitrogen and carbon in eutrophied lakes. Science (Washington, D.C.), **195**: 260–262.

Soranno, P.A. 1997. Factors affecting the timing of surface scums and epilimnetic blooms of blue-green algae in a eutrophic lake. Can. J. Fish. Aquat. Sci. **54**: 1965–1975.

Soranno, P.A., Hubler, S.L., Carpenter, S.R., and Lathrop, R.C. 1996. Phosphorus loads to surface waters: a simple model to account for spatial pattern of land use. Ecol. Appl. **6**: 865–878.

Soranno, P.A., Carpenter, S.R., and Lathrop, R.C. 1997. Internal phosphorus loading in Lake Mendota: response to external loads and weather. Can. J. Fish. Aquat. Sci. **54**: 1883–1893.

Stauffer, R.E., and Lee, G.F. 1973. The role of thermocline migration in regulating algal blooms. *In* Modelling the eutrophication process. *Edited by* E.J. Middlebrooks. Ann Arbor Science Publishers Inc., Ann Arbor, Mich.

Stow, C.A., Carpenter, S.R., and Lathrop, R.C. 1997. A Bayesian observation error model to predict cyanobacterial biovolume from spring total phosphorus in Lake Mendota, Wisconsin. Can. J. Fish. Aquat. Sci. **54**: 464–473.

Vollenweider, R.A. 1968. Scientific fundamentals of the eutrophication of lakes and flowing waters, with particular reference to nitrogen and phosphorus as factors in eutrophication. Rep. No. DAS/CSI/68.27, Organization for Economic Cooperation and Development, Paris.

Vollenweider, R.A. 1969. Possibilities and limits of elementary models concerning the budget of substances in lakes. Arch. Hydrobiol. **66**: 1–36.

Vollenweider, R.A. 1975. Input–output models with special reference to the phosphorus loading concept in limnology. Schweiz. Z. Hydrol. **37**: 53–84.

Vollenweider, R.A. 1976. Advances in defining critical loading levels for phosphorus in lake eutrophication. Mem. Ist. Ital. Idrobiol. **33**: 53–83.

Walker, W.W., Jr. 1985. Statistical bases for mean chlorophyll *a* criteria. Lake Reservoir Manage. **4**: 57–62.

© 1998 NRC Canada

Modeling foraging in the northern anchovy (*Engraulis mordax*): individual behavior can predict school dynamics and population biology

Peter Nonacs, Paul E. Smith, and Marc Mangel

Abstract: Many economically important oceanic fishes travel in large schools, but the foraging behaviors of these schools and the life history consequences of these behaviors have rarely been addressed. The availability of extensive information on bioenergetics of the northern anchovy (*Engraulis mordax*) allows us to use this species as a case study. We modeled two types of potential behavior that fish could use to exploit a patchy environment: (*i*) maximizing growth rate or (*ii*) maximizing survivorship to adulthood and reproduction, which is a function of both growth and avoiding predation. Patterns from existing data sets on gut contents and growth rates from the field for juvenile *E. mordax* were consistent only with the prediction of maximizing survivorship. The model makes further testable predictions about (*i*) expected swimming velocities between zooplankton patches, (*ii*) patterns of size segregation in the formation of schools, (*iii*) the proportion of zooplankton patches that schools consume, and (*iv*) reactions to decreases in environmental quality. Overall, the model predicts that anchovies spend at least 25% of their time in schools that are too large to be energetically economical and suggests further research on several variables that could affect populations of schooling fishes.

Résumé : De nombreaux poissons d'importance commerciale se déplacent en grands bancs, mais le comportement de recherche de nourriture de ces bancs et les conséquences de ce comportement sur le cycle vital ont rarement été étudiés. La disponibilité d'information détaillée sur la bioénergétique de l'anchois du Pacifique (*Engraulis mordax*) nous a permis d'utiliser cette espèce dans une étude de cas. Nous avons modélisé deux types de comportement potentiel que le poisson peut utiliser pour exploiter un milieu inégal, soit : (*i*) maximiser son taux de croissance ou (*ii*) maximiser sa survie jusqu'au stade adulte et à la reproduction, ce qui est fonction de la croissance et de l'évitement de la prédation. Les tendances dans les séries de données disponibles sur les contenus stomacaux et les taux de croissance des juvéniles de *E. mordax*, données recueillies sur le terain, ne correspondaient qu'à l'hypothèse de la maximisation de la survie. Le modèle fait d'autres prédictions vérifiables sur : (*i*) la vitesse prévue de nage entre les nuées de zooplancton, (*ii*) les tendances de la répartition par taille dans la formation des bancs, (*iii*) la proportion des nuées de zooplancton que les bancs consomment et (*iv*) les réactions à une baisse de la qualité de l'environnement. En général, le modèle prédit que l'anchois passe au moins 25 % de son temps en bancs trop gros pour être efficaces au plan énergétique et indique d'autres pistes de recherche sur plusieurs variables qui pourraient influer sur les populations de poissons se déplaçant en bancs.
[Traduit par la Rédaction]

Introduction

Oceanic schooling fishes are a vital resource for human populations, and for this reason alone there should be considerable interest in understanding their behavior and responses to environmental changes (Gates 1993). To predict the population consequences of a particular set of environmental conditions, we need to connect the fishes' behavioral response to their physical surroundings. Although parameters such as prey abundance, water temperatures, school sizes, and biomass of stocks have often been measured or estimated, less is known about the interaction between foraging tactics, growth, and survivorship. As a starting point, we can construct a predictive foraging model based on data covering a species in its natural environment. Such models have an excellent track record of both explaining the functional bases for observed behaviors and identifying key variables that need future study (Stephens and Krebs 1986; Mangel and Clark 1988). An excellent species among schooling fish for such an approach is the northern anchovy (*Engraulis mordax*). There is a wealth of natural historical data that includes the bioenergetics of swimming and feeding (Blaxter and Hunter 1982; Butler 1989; Boggs 1991),

Received April 15, 1997. Accepted October 21, 1997.
J13967

P. Nonacs.[1] Department of Biology, 621 Circle Dr. South, University of California, Los Angeles, CA 90095, U.S.A.
P.E. Smith. Southwest Fisheries Science Center, La Jolla Laboratory, National Marine Fisheries Service, NOAA, La Jolla, CA 92038, U.S.A.
M. Mangel. Department of Environmental Studies and Institute of Marine Sciences, University of California, Santa Cruz, CA 95064, U.S.A.

[1] Author to whom all correspondence should be addressed.
e-mail: PNonacs@biology.ucla.edu

© 1998 NRC Canada

schooling behavior, feeding methods, and diet (Blaxter and Hunter 1982), and patchiness of its prime prey item, zooplankton (Koslow 1981; Star and Mullin 1981; Smith et al. 1989).

Nonacs et al. (1994) constructed behavioral and population models of *E. mordax* living in the California Current. Although their model predicted a life history trade-off of reduced growth for reduced predation rate, it was based on a single school size (i.e., the "average" school). In general, however, anchovies live in schools that are much larger the average size. The mean diameter across all schools is 29.1 m, but over half the population of anchovies are in schools of diameter >70 m (Smith 1981). Schooling in fishes can increase survivorship by diminishing detection by predators (Brock and Riffenburgh 1960; Swartzman 1991) and confusing predators by complex coordinated maneuvers (Eshel 1978). However, an upper limit to school size must be set by the spatial distribution of food and productivity of the habitat (Duffy and Wissel 1988).

Using state variable dynamic models (see Mangel and Clark 1988), we examine anchovies behaving in one of two broadly defined ways: (*i*) strictly maximizing growth rate, which is equivalent to maximizing the net rate of calorie intake over time, or (*ii*) maximizing lifetime egg production, which often can require a trade-off between feeding in zooplankton patches (which increases fish size and therefore fecundity) and reducing predation rates (which are assumed to be highest in the zooplankton patches). Thus, the behavior of energy-maximizing animals will not be affected by predation risk, while animals that maximize lifetime reproduction will often exhibit predation risk sensitive behavior. That fish are capable of a growth rate / predation risk trade-off has been experimentally demonstrated in a wide array of species (e.g., Werner et al. 1983; Dill and Fraser 1984; Abrahams and Dill 1989; Fraser and Gilliam 1992). Further model predictions include the maximum size of *E. mordax* schools able to capture enough food to maintain a positive energy balance and the consequences of depleted food resources on growth and behavior.

Methods

The summary points of our model are the following. (*i*) Zooplankton are found in high densities in discrete patches in the ocean (Koslow 1981; Star and Mullin 1981). These patches are taken as circular and anchovies feed by biting at zooplankters. (*ii*) Between patches, there are no large zooplankters and the fish feed only by filtering small zooplankton and phytoplankton. (*iii*) In the zooplankton patches, fish can be up to 20 times more susceptible to predation per unit of time than they are between the patches. We do not specify the mechanism that increases the predation risk. (Potential factors that could increase susceptibility to predation could include loss in tactical evasion ability due to inattentiveness while feeding, increased range at which predators can detect the school due to wider spacing of individuals, uncoordinated movements of feeding fish drawing attention, or the inability to effectively respond to attacks due lowered school cohesion.) (*iv*) As they grow, fish become less vulnerable to predators. (*v*) Schools encounter zooplankton patches randomly. The average patch has a radius of 634 m and the average gap between patches is 2553 m (Smith et al. 1989).

Specifically, in the model the size range of fish is 5–12.98 cm, with steps of 0.02 cm. This far exceeds the size range of late juveniles so as to eliminate "edge" effects from the model (i.e., if a fish is constrained such that it cannot grow larger than 8.5 cm, then as it approaches that size, feeding will be artifactually devalued because further growth is not possible). We use caloric expenditures in *E. mordax* as measured by Boggs (1991) such that basal metabolism = $0.4683L^{2.4}$ cal/day and swimming metabolism = $0.00094L^{2.14}v^{1.44}$ cal/h where L is length (centimetres) and v is swimming velocity (centimetres per second).

The behaviors of the fish that we consider are how fast they swim both between patches and inside the patches. The rate of swimming between patches (v_0) directly determines the rate at which new patches are encountered. The range of swimming velocities between patches is 1–59 cm/s. Anchovies filter-feed for a third of the time they are swimming between patches, and it is assumed that they swim at a constant rate of 10 cm/s while filter-feeding. Thus, the average rate of swimming between patches (=$(10 + 2v_0)/3$) has a range of 4–42.7 cm/s. Blaxter and Hunter (1982) found that faster-moving schools were more elongate. From their relationship, the width of a school is estimated to be $25.3A^{0.5}v_0^{-0.42}$ m where A is the surface area of the school. The faster a school swims, the smaller is the volume of water experienced by the school (i.e., more fish will swim through the same water). Therefore, moving rapidly between patches reduces the gain (averaged for all fish in the school) from filter-feeding. Spacing between fish, the density of microplankton between patches, and the stomach capacity of fish are all constants in this model and are given values that are estimated from the field (Nonacs et al. 1994). Fish at the front of a moving school have been observed to feed more than those in the rear (Krause 1993; DeBlois and Rose 1996), but it is assumed that the leading fish will change over time with perhaps the hungriest leading the schools (see Krause 1993).

A zooplankton patch is assumed to occupy a cylindrical volume with a depth of 10 m and a radius of 634 m (Smith et al. 1989). A fish school upon encountering a zooplankton patch expands to fill the entire volume with an equal number of fish per cubic metre and, after feeding, contracts to its original size and exits the patch in a randomly chosen direction (such as for Atlantic cod (*Gadus morhua*), see DeBlois and Rose 1995). Therefore, the average distance a fish from a school travels in entering and exiting a patch is equal to twice the average chord length of the circular surface area of the patch, which is 2.401 times the radius of the patch. This is the minimum distance a fish swims in a food patch if it swims only in straight lines. However, it is likely that a fish's movement will have both a forward component (v_f: to move through the patch) and a lateral movement component (v_s: to search for prey). The true velocity of the fish in the patch is a function of both: $v_p = (v_f^2 + v_s^2)^{1/2}$. The model allows fish to choose integer values of v_f and v_s, subject to the constraint that $v_p \leq 50$ cm/s. The actual time fish spend in a patch is directly proportional to v_f, which has a minimum value of 1 cm/s (i.e., all schools eventually do leave patches).

The anchovy–zooplankton expected time to encounter within a patch (Z) is determined by a Gerritsen–Strickler equation (Gerritsen and Strickler 1977) such that

$$(1) \qquad Z = 1 + 2/\{R^2d/3)[(u^2 + 3v_p^2)/v_p]\}\ \text{s}$$

where R is the reactive distance of the fish, d is the density of zooplankton (number per cubic metre), and u and v_p are the swimming velocities of the zooplankton and fish, respectively ($v_p > u = 5$ cm/s, the swimming velocity of a copepod). The model assumes a 50% failure rate per encounter due to either the prey escaping or interference with other fish in the school plus a 1-s handling time per prey. Interference between foraging fish is likely to increase with fish density, but the model's results are not very sensitive to a wide range of capture efficiencies (Nonacs et al. 1994). The energetic cost of capturing a prey item is calculated as the cost of swimming at a velocity that captures a prey item swimming directly away from an approaching anchovy 1 s after it enters the fish's reactive distance. The R is best estimated from numerous studies on other species (see Nonacs

© 1998 NRC Canada

et al. 1994) as equal to $13.4xL$ where x and L are the lengths (centimetres) of the prey item and the anchovy.

Note that hunger or gut fullness in the anchovies is not a state variable in this model. This is not to say that hunger does not motivate fish behavior. However, in our model, swimming velocity directly determines patch encounter rates (i.e., a hungry fish could alter its swimming speed). Therefore, having a hunger state variable would be redundant to our swimming speed variables. We also assume that the fish's habitat is globally nondepleting. Therefore, the consumption of an encountered patch does not reduce the likelihood of future patch encounters. This is equivalent to assuming a steady state where the rate of blooming of new zooplankton patches equals the rate at which they are being consumed.

The model translates captured prey into calories accumulated and available for growth. Assimilation efficiency (65%) and stomach emptying rates ($e^{-0.106t}$ where t is the time (hours) since the food was ingested) are estimated from direct measurements by Boggs (1991) on captive *E. mordax*. Nonacs et al. (1994) analyzed the sensitivity of the model to errors in these estimates and found that the predictions were robust to a large range of values. Therefore, we do not vary these values in this paper. If fish reached satiation (i.e., completely filled their stomachs), feeding rate was constrained to be no greater than the emptying rate. In practice, however, the model rarely predicted feeding to satiation (see Results section).

A dynamic state variable model requires estimating a terminal fitness at the endpoint interval being considered. We use a 1-year time interval, with reproduction occurring only in the last 90 days. The terminal fitness function is then the fecundity of the fish, based on a size–fecundity relationship measured from fish caught in the field (Hunter and Leong 1981). Thus, in our model, the fitness of any behavior at any time is defined by its eventual payoff in egg production. We constructed a simplified version of the model for the reproductive period of the last 90 days because of the added complication of investing in eggs versus investing in somatic growth. This model produced a robust result across many assumptions of growth/egg production trade-offs, which is that fitness is linearly related to fish size. From that terminal function, we backward iterated 270 days in 10-day time steps to find the optimal behavioral trajectories for fish of a given size at a given time. Predictions of growth trajectories are derived using forward iterations (Mangel and Clark 1988) for fish that are 6 cm on day 1. This time period, both in our model and in the field, appears to encompass the stage known as "late juvenile" (=6–8.5 cm in length: Smith 1985; Butler et al. 1993), which is the dominant size-class in *E. mordax* (Smith 1985; Nonacs et al. 1994). It is also the size at which complex differentiation and metamorphosis seen in smaller fry no longer occur but at which no reproduction occurs (reproduction is rare in fish under 9 cm in length: Hunter and Leong 1981). Therefore, the simplification of assuming only somatic growth for the first 180 days is fully justified.

Thus, fitness is defined as a function of the size the fish achieves through growth multiplied by the probability of surviving to reproduction. The survival probability is a function of size and where the fish spend their time; the daily instantaneous mortality rate (IMR) is

$$\text{IMR} = 0.003e^{-a(L-5)}[p(m-1)+1] \quad (2)$$

where p is the proportion of the day spent inside the zooplankton patch and m measures how much more risky the patch is than the surrounding ocean ($1 < m < 20$), L is the length of the fish (centimetres), and a measures the benefit of larger size in reducing mortality (we use $a = 0.01$). A 6-cm fish that never entered a zooplankton patch would thus have an IMR of close to 0.003, which is estimated as that of the next larger life stage (Smith 1985; Butler et al. 1993). When $m = 1$, a fish is equally at risk inside and outside zooplankton patches. Thus, if $m < 1$, then the zooplankton patch will be best both for growth and avoiding predators. The optimal strategy, then, must be the one that maximizes growth rate and will be insensitive to overall predation risk.

A substantial advance in this model from the one in Nonacs et al. (1994) is that here, we include school size variability as observed in nature. To do so, we used five school diameters of 14.5, 28.6, 56.2, 110, and 217 m, each of which represents the mean school size for 20% of the population biomass (as cumulative population biomass is plotted against increasing school size: Smith 1981). We assumed that an average fish in any given 10-day time period spends 20% of its total time in each of the five size-classes of schools. In this model, we do not consider how schools form or break up, and thus do not consider how fish move between schools of different sizes. In a separate analysis, we increased school size for fish of 6 and 8.5 cm until no possible combination of swimming velocities could maintain a positive energy balance for the average school member. We defined this as the maximum economic school size.

Each of the five school sizes could have different optimal swimming velocities, so that in total, fish make 15 independent behavioral choices of swimming velocities (v_0, v_p, and v_s for each school size) between patches and within patches. With this many variables (with each having at least 49 possible states), it becomes impossible to examine every possible combination of swimming velocities across all school sizes. Therefore, initially, we made a series of random guesses regarding possible combinations of swimming velocities (in step sizes of 5 cm/s) across the various school sizes. After 10 000 such guesses, we restricted the search for optimal values to the area around the best guess and a new series of guesses began, with smaller step sizes. After a number of such iterations, the region surrounding the best guess was rigorously examined. This methodology was repeated several times for the same starting conditions and the optima converged across runs. This indicates that although it is unlikely that the model found the globally optimal set of predicted swimming velocities, it was close to that set and not erroneously climbing local peaks of fitness.

Results

If zooplankton patches have a radius of 634 m and an average distance of 2553 m between patches, the maximum school size that can maintain a positive energy balance has a diameter of 108 or 123 m for 6- or 8.5-cm fish, respectively. Larger fish can form larger maximum-sized schools because the interfish distances are greater, resulting in fewer fish per cubic metre of water (Graves 1977). Nevertheless, about 25–30% of *E. mordax* found in nature (Smith 1981) are in schools that are larger than is energetically economic (Fig. 1). These large-size schools are not able to move through the ocean fast enough (or would expend too much energy moving) to encounter sufficient quantities of zooplankton to maintain a positive energy balance.

Although fish are in negative energy balance in the largest schools, they can maintain rapid growth by compensating in smaller schools. If fish ignore differential predation risk in zooplankton patches and maximize net caloric intake rate ($m = 1$), then we predict a growth rate that appears to be substantially faster than observed in nature (Fig. 2). However, fish that respond to both food and predation risk show a growth rate that is more similar to estimates from the field. The predicted growth rates also decline as the zooplankton patch increases from 2 to 20 times more risky than areas between patches.

Assuming that fish maximize growth rate also produces very different predictions about how fast fish are swimming between patches and within them (Fig. 3). Predation-sensitive behavior predicts across all school sizes, times of year, and fish size a slow rate of swimming between patches (the

© 1998 NRC Canada

Fig. 1. Cumulative biomass (solid circles) of a northern anchovy population contained in schools of a given diameter or less (from Smith 1981). The curve fit to the relationship is $y = D^2/(D^2 + D_0^2)$ where D is the school diameter and D_0 is a constant (=65). The open circles are the predicted maximum school sizes for fish of length 6 or 8.5 cm for which energy budgets are positive. School sizes to the right of the broken lines are thus bioenergetically uneconomical.

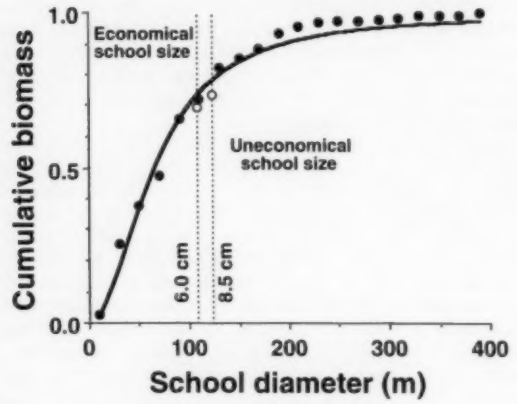

Fig. 2. Predicted growth rates of northern anchovy under an assumption that anchovies are net energy intake rate maximizers or are predation sensitive (with zooplankton patches varying from 2 to 20 times more risky than the surrounding water). The heavy line is the mean size of anchovy juveniles caught in the field as the season progresses (Butler 1989).

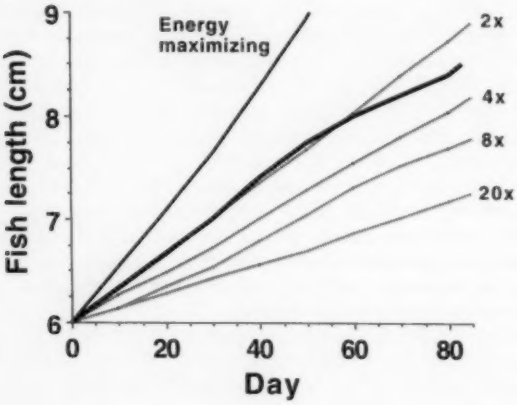

average rate is <7 cm/s). In contrast, energy-maximizing behavior predicts rapid movement between patches in all school sizes except the largest class. Fish in small schools (the 10 and 30% size-classes) move between 20 and 30 cm/s and in medium schools (50 and 70%) generally range between 30 and 40 cm/s.

As the season progesses, predation-sensitive behavior predicts that smaller schools may start moving more quickly between patches, but larger schools remain slow moving. Predation-sensitive behavior also predicts that smaller juveniles (<7.25 cm) swim more rapidly than larger juveniles (>7.25 cm). Conversely, energy-maximizing behavior predicts no consistent effect of time or fish size except in the 70% size-class school where larger fish tend to swim more rapidly than smaller fish.

Both assumptions of fish behavior predicted generally similar behavior in the zooplankton patches, i.e., rapid movement through them. In all cases, predation-sensitive fish move forward as rapidly as possible (v_f = 49 cm/s, the maximum velocity allowed in the model). A wider range of velocities (33–49 cm/s) is predicted for energy-maximizing fish in schools in the 70% or less size-classes. The only exception to the prediction of rapid movement was in the 90% size-class where the model predicted v_f's of 3–9 cm/s.

Energy-maximizing fish will spend more time in zooplankton patches feeding than predation-sensitive fish. This allows us to compare the patch depletion associated with different behaviors (Table 1). Schools in the 50th percentile or greater in size uniformly will consume all the zooplankton. However, predation-sensitive small schools will leave patches that still contain about 40% of the initial zooplankton population. Energy-maximizing schools will take a far higher proportion.

The assumptions of energy maximization and predation sensitivity thus predict different rates of encounter of zooplankton patches and different levels of exploitation of those patches. This translates into fish having different levels of stomach fullness and, if the population of fish were to be sampled, a different distribution of gut contents. The model allows us to predict the distribution of gut contents as if a hypothetical population were sampled. We generated the expected distributions by estimating the average fish's gut contents at the time it left a zooplankton patch based on the number of prey per fish (which was a function of the school size) and how long it searched in the patches (based on the assumption of either energy maximization or predation sensitivity). The gut is assumed to empty at the rate that Boggs (1991) estimated for fed *E. mordax*, prorated by the time between patch encounters. The gut is assumed to fill at a linear rate from the minimum content at patch encounter to the previously estimated fullness at departure. We divided this patch encounter / patch use cycle into equal time steps and then randomly sampled 250 000 fish in equal proportion across time steps and across the five school size-classes and recorded their gut contents.

This sampling regime assumed that each fish in a school had equal success, but clearly, there is likely to be within-school variability in prey capture rates. To estimate the effect of such variance, we used the estimates of the mean proportion of the gut that was filled at any given time and supplied variance around that mean (assuming a normal distribution of success probabilities). Therefore, we randomly choose a time step in the cycle and then randomly choose a fish from a normal distribution of stomach fullness. (For the sampling regime, we arcsin transformed into degrees the predicted proportion of gut fullness and gave the distribution standard deviations of 10, 20, or 30 degrees.)

The expected distribution of stomach contents (=gut fullness) from a randomly sampled population under an assumption of energy maximization is bimodal, with a large proportion of fish having fairly full stomachs, even when within-school capture success is highly variable (Fig. 4). In

© 1998 NRC Canada

Fig. 3. Mean predicted velocity of northern anchovy schools of various sizes as a function of fish size and time of season. Predation risk in the zooplankton patches is assumed to be either equal to the surrounding waters or 4 times greater. When the risk is equal, fish act like net energy intake rate maximizers (see text). The percentages correspond to school diameters of 14.5 m (10%), 28.6 m (30%), 56.2 m (50%), 110 m (70%), and 217 m (90%).

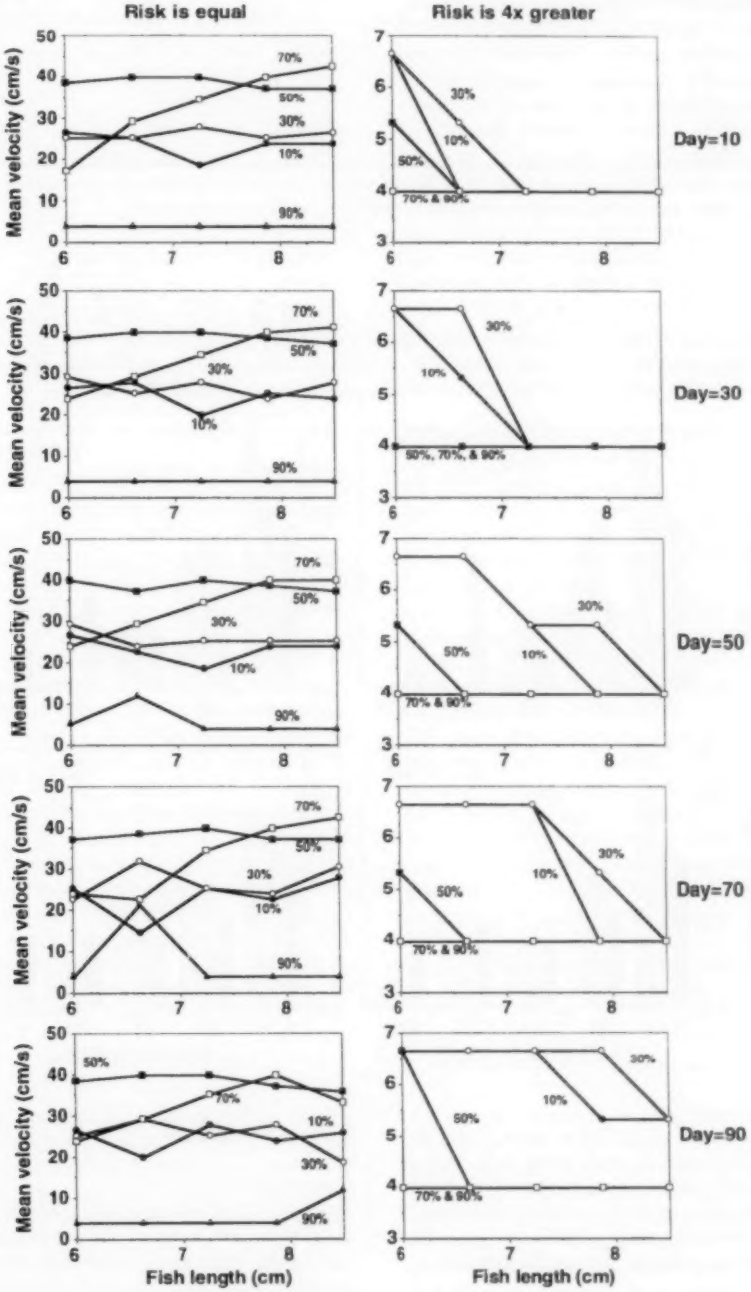

© 1998 NRC Canada

Table 1. Proportion of zooplankton consumed by northern anchovy schools of various diameters.

	Risk			
School diameter (m)	1	2	4	8–20
14.5	0.960	0.597	0.597	0.593
28.6	0.863	0.614	0.614	0.611
56.2	1	1	1	1
110	1	1	1	1
217	1	1	1	1

Note: Risk refers to how much more risky a zooplankton patch is for a fish than the water surrounding the patch. When risk = 1, then the fish act as net energy intake rate maximizers (see text).

Fig. 4. Predicted stomach contents of randomly sampled northern anchovy when they are assumed to be either net energy intake rate maximizers or predation sensitive. Risk in the zooplankton patch ranges from equal to the surrounding waters to 8 times greater. When risk is equal, fish behave so as to maximize overall growth rates. The columns are given by their midrange values.

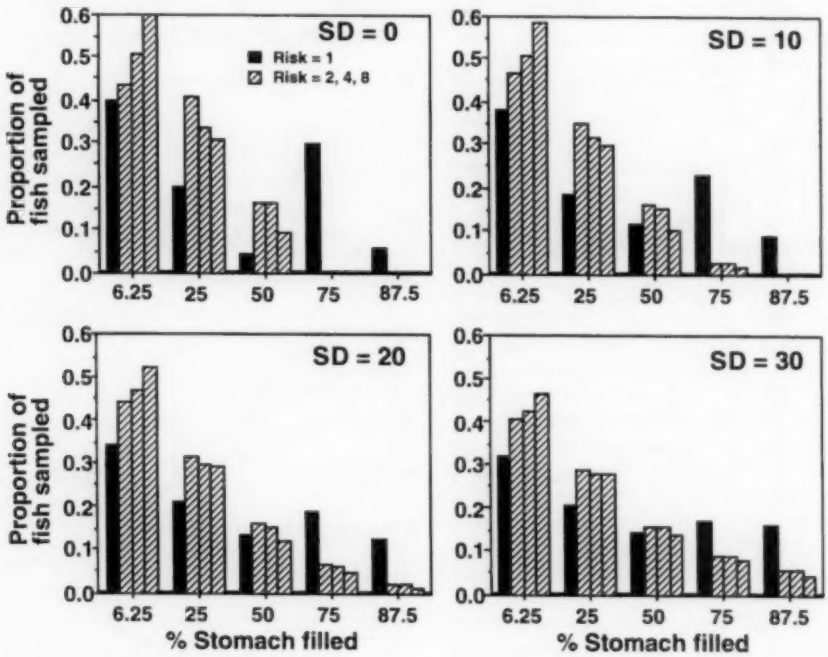

contrast, under an assumption of predation sensitivity, the distributions are always unimodal, with most fish having guts that are <25% full. The effect of increasing relative risk in the patch exaggerates this relationship, but qualitatively, the effect is the same. Within-school variability makes the differences less clear, but the patterns still appear distinct.

Discussion

The results of this model are valuable in two ways: (*i*) to generate testable predictions and (*ii*) to identify critical assumptions for which data need to be collected.

Testing predictions

Gut contents

A population of energy-maximizing fish should show a bimodal distribution in stomach contents, with a significant fraction of the fish having rather full stomachs. In contrast, the assumption of predation risk sensitivity predicts a unimodal distribution, with the large majority of fish having very little in their stomachs at any given time (Fig. 4). Loukashkin (1970) measured the stomach contents of sampled *E. mordax* from several populations. His estimates of content were divided into five categories: (*i*) empty or almost empty (0%

© 1998 NRC Canada

Fig. 5. Stomach contents of four populations of northern anchovy sampled by Loukashkin (1970). He categorized stomach fullness as either empty or almost empty, 25% full, 50% full, 75% full, and almost or totally to capacity.

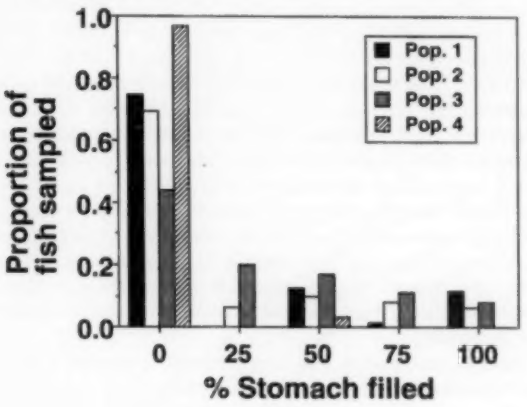

full), (*ii*) 25% full, (*iii*) 50% full, (*iv*) 75% full, and (*v*) full to almost bursting. From four populations where a large sample was taken, it is clear that most fish had very little in their stomachs, and in only one population (No. 1) was there a suggestion of a bimodal distribution in gut contents (Fig. 5). Therefore, these data are clearly more consistent with the assumption of risk sensitive behavior.

An indirect piece of evidence comes from Arthur (1976), who summarized measurements of feeding incidence (defined as the percentage of fish with food in their stomachs) in clupeoid fish larvae. Larvae are much smaller than the juveniles considered in our models and thus may differ in behavior for size-based reasons. Nevertheless, for several *Engraulis* species, Arthur (1976) reported feeding incidences rarely in excess of 30% and often quite a bit lower. Interestingly, Pacific sardine (*Sardinops sagax*) and jack mackerel (*Trachurus symmetricus*) larvae of the same size as anchovy larvae and feeding on the same prey items had considerably higher levels of feeding incidence (at times, over 90% in the mackerel). Sardines born at the same time as anchovies in the same waters show higher growth rates than anchovies, and mackerel grow faster than either sardines or anchovies (Blaxter and Hunter 1982).

Growth rates

The highest growth rates predicted by our model are physiologically possible for anchovy juveniles. Fish kept in the laboratory and fed ad libitum exhibit growth rates equal to or exceeding our predicted maximal rate (Blaxter and Hunter 1982; Boggs 1991). We can also compare the model's predictions with field data. Butler (1989) sampled *E. mordax* in the California Current at various times of the year and found a population with a continuously increasing mean size (Fig. 2). These data cannot be considered a true measure of growth rate because if smaller fish are more likely to be eaten, then samples later in the season reflect both growth and differential predation. Therefore, the data are likely to slightly overestimate the true growth rate of the surviving fish. Thus, the predicted growth rate under an assumption of energy maximization seems to far outstrip the rate of fish in the field. In contrast, fish showing risk sensitivity to zooplankton patches that are 2-4 times more risky than the surrounding waters have growth rates very similar to the progression shown in Butler's (1989) samples. This again suggests that anchovies in nature respond to both prey densities and their own predators.

Sudden bursts of apparent accelerated growth have occasionally been observed in natural populations of *E. mordax*. Fiedler et al. (1986) recorded an increased growth rate (by as much as 0.2 mm/day over a 2-month period) from the 1982 and 1983 age-classes during the autumn of 1984. As it is unlikely that there could have been an improvement in the food supply at this time of the year, it may be that the anchovies were responding to the withdrawal of exotic, tropical predators such as tropical tunas, skipjack tuna (*Katsuwonus pelamis*), and yellowfin tuna (*Thunnus albacares*) at the end of an El Niño cycle. A reduction in the risk associated with feeding would predict increased use of zooplankton patches and thus an increased growth rate.

Swimming speeds and behavior

The model predicts that the swimming behavior of fish that are energy maximizing or predation risk sensitive will be quite different. Energy-maximizing fish should swim rapidly, and all but the largest schools should rarely stay in one area very long, particularly in the absence of encountering high-density zooplankton patches. In contrast, predation-sensitive fish should be observed to swim very rapidly in zooplankton patches and rather slowly between encounters of patches. Schools would be expected to linger in areas even in the absence of zooplankton patches, as long as they are not attracting predators. Such behavior would increase survival in two ways: fish reduce time spent in the more dangerous zooplankton patch, and if anchovies and their predators also follow a Gerritsen–Strickler encounter model (Gerritsen and Strickler 1977), then swimming slowly on the part of the prey (the anchovies in this case) would reduce encounter rates (this latter effect was not considered in the model, but see Swartzman 1991). Furthermore, smaller schools of predation-sensitive fish of the same size are predicted to swim more rapidly later in the season. This is likely due to food (i.e., growth) becoming more important to the fish as time passes. For example, a 7-cm fish at day 1 of the model has 270 days in which to reach reproductive size. In contrast, a 7-cm fish at day 90 has only 180 days and thus has to sacrifice safety to increase growth rate.

Composition and movement of fish schools

Bioenergetically, the cost of swimming is easily offset by foraging gains in the zooplankton, and the per gram costs of swimming decrease with increasing size. Thus, if fish are energy maximizing, all fish should move rapidly at most times so as to encounter more zooplankton patches. If there are any differences in swimming speed, it should be the larger fish that sometimes swim faster between patches than smaller fish (i.e., from a bioenergetic standpoint, swimming is less costly per unit biomass for larger fish). If fish are predation risk sensitive, however, it should be smaller fish that tend to swim faster between patches, especially in smaller schools. Intuitively, this result reflects the trade-off of

© 1998 NRC Canada

Fig. 6. Combinations of growth rates and the mean IMR for fish that are net energy intake rate maximizers (squares) or predation sensitive (circles). The heavy line is the set of values from a Lefkovitch population matrix that predicts a stable population (Nonacs et al. 1994). Values above and to the left of the line predict declining populations, while values below and to the right predict possibly increasing populations. The open triangle is the predicted combination for predation-sensitive fish in a scenario of climate change (see text) and with zooplankton patches being 4 times riskier than their surrounding waters.

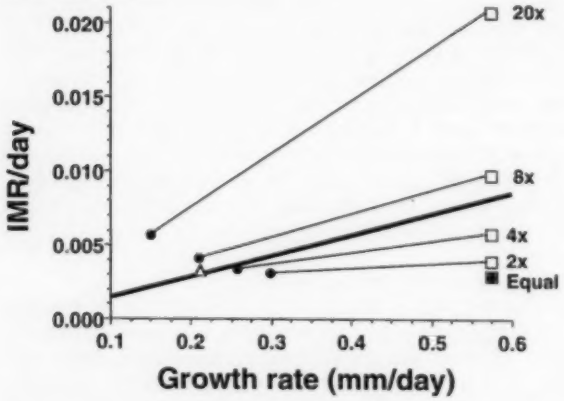

growth versus safety such that faster growth maximizes fitness more for smaller fish than it does for larger fish. Different optimal swimming speeds for different sizes of fish suggest that mixed size schools are not stable for all size-classes, and we should see significant size segregation across schools. For example, if fish are predation sensitive, then smaller schools may divide due to their members swimming between patches at different velocities. However, large schools may be more diverse in fish sizes because the optimal velocities are predicted to be minimal for all sizes.

Exploitation of zooplankton patches

Our model predicts that anchovy behavior can have different consequences for the zooplankton patches. For energy-maximizing fish, encountered patches of zooplankton should almost always be completely consumed. Conversely, predation-sensitive fish in smaller schools should leave with perhaps as much as 40% of the zooplankton still uneaten. To our knowledge, no study has directly examined how long fish stay in zooplankton patches or the state of the patch once the school leaves.

Population and species effects

It is also possible to gain insight into how the behavior of schools can affect the population dynamics of the species. The life cycle of *E. mordax* can be divided into nine size-based stages (Smith 1985; Butler et al. 1993). We used a Lefkovitch matrix (Lefkovitch 1965) to predict population growth, stability, or decline based on possible combinations of growth and mortality rates for each stage (see Nonacs et al. 1994 for details). In Fig. 6, these combinations are plotted as the heavy line, where combinations of growth rate and average daily IMR for the late juvenile life stage to the left and above the line result in declining populations and combinations to the right and below can result in increasing populations. The combination of growth rates and IMR's with an assumption of predation sensitivity plot into the region of population growth until the risk in the zooplankton patches more than exceeds 4 times that of the surrounding water. The model predicts that as the patches get relatively more risky, fish sacrifice growth rate more than survivorship (i.e., predation risk sensitivity increases). The exact location of the growth rate/IMR points from our model vis-à-vis the prediction from the Lefkovitch population model partially depends on the assumption of the baseline mortality rate of a fish while not in a zooplankton patch (a maximum mortality rate of 0.003/day). A proportionally lower baseline estimate would move all the points down a similar proportion on the y-axis. Conversely, a higher estimate would move them up. Therefore, in Fig. 6, it is the location of the points relative to each other that is likely the more robust result rather than their absolute position in relation to the population model.

Energy-maximizing fish do not sacrifice growth rate and thus incur higher IMR's as the relative risk of the zooplankton patch increases (squares in Fig. 6). Under our assumptions of predation risk, population growth with energy-maximizing fish would be positive until the risk in the zooplankton patches is between 4 and 8 times greater than in the surrounding waters. Thus, at the population level, multiple strategies may co-occur in the same habitat if zooplankton patches are not that much riskier. For example, anchovies, sardines, and mackerel may coexist in the same waters even if as larvae and juveniles they respond differently to predators. However, if patches are much riskier (e.g., 20 times), then the cost of ignoring the predation becomes much more severe and energy-maximizing populations may be much less likely to persist than predation-sensitive ones.

Implications for future research

Our model relies on a combination of data and assumptions. While the assumptions we make are to our knowledge the most reflective of natural conditions, it is also clear that aspects of the biology of *E. mordax* need to be better understood, particularly predation risk, school formation and dynamics, comparison with other species of schooling fish, and environmental stability.

Predation risk

First and foremost, it would be particularly valuable to determine whether fish are more at risk while feeding in zooplankton patches than when swimming between them. If zooplankton patches are not more risky than the water between, or in fact are safer, then there is no trade-off between foraging gain and avoiding predation risk and we would predict that all fish should act like energy maximizers. Second, we need to have more accurate size-dependent predation rates for both the behavioral and population models. For example, Nonacs et al. (1994) examined various assumptions about the predation risk functions used in these models and found that behavior was strongly affected by how rapidly growth reduced predation risk. Not surprisingly, the more likely fish were to "outgrow" their predators, the more closely they behaved like net energy rate maximizers. Therefore, anchovy behavior should be affected by the relative attack rates of predators that they cannot outgrow (e.g., seabirds, dolphins) and those that

© 1998 NRC Canada

Fig. 7. Predicted growth rates of northern anchovy under present-day conditions (solid lines) and under a scenario where zooplankton patches are 50% smaller and 50% further apart (broken lines). Fish are assumed to be either net energy intake rate maximizers or predation sensitive in a scenario where the zooplankton patches have 4 times the predation risk of the surrounding waters. The heavy gray lines are the mean size of anchovy juveniles caught in the field as the season progresses in a non-El Niño year (top line) and in an El-Niño year (Butler 1989).

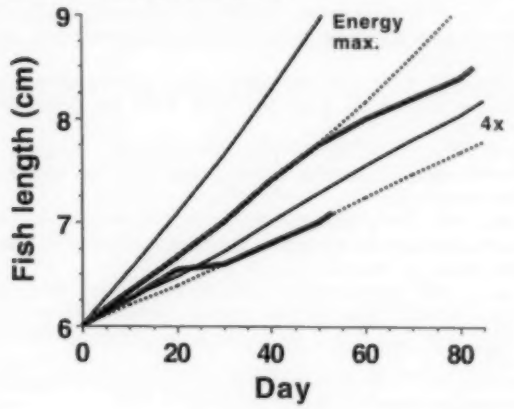

they can outgrow (e.g., smaller piscivores such as adult anchovies). Growth rate / predation risk trade-offs could be adapted to the predominant type of search and tactical predation experienced by the fish. Sustained predation by one suite of predators may result in tactical adaptation in the schooling behavior of their prey to the nature of the attack (Neill and Cullen 1974). For example, fish schools continually attacked from the air by visual predators may compact and move to greater depths, or schools attacked by acoustically guided predators may move towards the surface where acoustic returns can be more ambiguous. Also, if attacks tend to correlate with specific ambient characteristics (e.g., day versus night, or in cloudy rather than clear water), appropriate avoidance behaviors could be expected to evolve.

School formation and dynamics

Habitat richness and the costs of swimming must combine to set a maximum school size beyond which anchovies would be in a negative energy balance. Applying our bioenergetics model to observed school sizes argues that at least 25% of the anchovy population is in a negative energy balance. This suggests that the largest schools form for reasons besides foraging.

Our model assumed that predation risk was independent of school size. However, if the per capita mortality rate of fish declines with increasing school size, large schools may be safer for fish and may be particularly favored by fish that have had recent bouts of good foraging. Conversely, it is possible that very large schools are especially easy for predators to find, and thus the largest schools might provide neither increased foraging nor increased safety. The question of whether schools are effective as antipredator devices is quite complicated and attack abatement from predators may be a function of both avoiding predators and diluting individual risk (Turner and Pitcher 1986). Very large schools may also form spontaneously for nonadaptive reasons, such as coalescing into a single school when encountering each other. Thus, large schools might be transitory and more likely to occur in waters where schools are likely to intersect each other. Overall, the pattern of school formation and breakup in *E. mordax* could be very important to understanding the benefits of the schooling.

Other species of schooling fish

Anchovies, sardines, and mackerel are all found off the California coast and as juveniles feed on the same prey items, but exhibit different growth rates. Our model would predict both higher growth rates and higher mortality rates for mackerel and sardines if their behavior were less predation risk sensitive than that of anchovies. Therefore, comparative studies are needed of foraging behavior of each species. In one such study (Holliday 1977), one anchovy school and two jack mackerel schools were followed for a distance of 1 km. Overall, the mackerel swam faster than the anchovies, which would be consistent with net energy rate maximization in mackerel.

Environmental stability

We repeated model simulations with a scenario of a poorer environment in which zooplankton patch size was decreased by 50% and the distance between patches was increased by 50%. Even with an assumption of a rather substantial decline in large zooplankton, maximal possible growth rates can still match the growth rate inferred from Butler's (1989) samples (Fig. 7). It is interesting to note that growth rates observed in an environmentally stressful El Niño year were considerably reduced and they closely resemble the predation-sensitive prediction with a habitat affected by climate change (Fiedler et al. 1986).

Predation-sensitive fish in environments where zooplankton patches are 4 times riskier than the surrounding waters still express a combination of growth rate and IMR that is very close to values predicted for a stable population (triangle in Fig. 6). The largest bioenergetically economic schools in this changed environment would have diameters of 50 or 59 m for 6- or 8.5-cm fish, respectively, so that in relation to present-day school sizes, anchovies will be in net negative energy balance about 50% of the time. This would predict that if school size is directly affected by fish hunger levels, poorer environments should result in smaller schools. For species that need rapid growth rates to reach breeding size in a short period of time (e.g., sardines and jack mackerel, see above), less available food could have much more severe population consequences, either through increased mortality rates or increased time to maturation.

Therefore, *E. mordax* populations may not be severely affected by dramatic changes in their zooplankton prey, given that all other variables remain constant. However, it is unlikely that this last assumption holds. For example, changes in zooplankton patches could increase predation rates if predators accumulate at these patches, or could decrease predation rates if predators have more difficulty in encountering these patches than do anchovy schools. The former would decrease anchovy populations and the latter would increase them. If in a poorer environment, fish tend to form smaller schools, then,

© 1998 NRC Canada

at least as far as energetic limitations are concerned, growth rates would be very much less affected than our model predicts. On the other hand, if the new distributions of zooplankton patches tend to concentrate fish into larger schools, then growth rates would be even more reduced than our model now predicts. Also, a change in the average size of fish schools could have a significant impact on the cost-effectiveness of fishers harvesting those schools. In sum, if environmental change brings a correlated change in anchovy behavior or the behavior of anchovy predators, the population-level effects could be dramatic and unpredictable from our current state of knowledge. Therefore, it may be very important to observe behavioral responses to varied and changing environmental conditions.

Acknowledgments

We thank A. Bouskila and B. Luttbeg for their help with designing the models in their larval life stages and E.M. DeBlois, S. Gilboa, and an anonymous reviewer for many helpful comments on the manuscript. This work was supported by NSF grant OCE 90-16895 to M. Mangel. This is contribution 100 of the U.S. GLOBEC program, funded jointly by NOAA and NSF.

References

Abrahams, M.V., and Dill, L.M. 1989. A determination of the energetic equivalence of the risk of predation. Ecology, **70**: 999–1007.

Arthur, D.K. 1976. Food and feeding of larvae of three fishes occurring in the California Current, *Sardinops sagax*, *Engraulis mordax*, and *Trachurus symmetricus*. Fish. Bull. U.S. **74**: 517–529.

Blaxter, J.H.S., and Hunter, J.R. 1982. The biology of the clupeoid fishes. *In* Advances in marine biology. Vol. 20. *Edited by* J.H.S. Blaxter, F.S. Russell, and R. Yonge. Academic Press, New York.

Boggs, C.H. 1991. Bioenergetics and growth of northern anchovy *Engraulis mordax*. Fish. Bull. U.S. **89**: 555–566.

Brock, V.E., and Riffenburgh, R.H. 1960. Fish schooling: a possible factor in reducing predation. J. Cons. Cons. Int. Explor. Mer, **25**: 307–317.

Butler, J.L. 1989. Growth during the larval and juvenile stages of the northern anchovy, *Engraulis mordax*, in the California current during 1980–84. Fish. Bull. U.S. **87**: 645–652.

Butler, J.L., Smith, P.E., and Lo, N.C.H. 1993. The effect of natural variability of life-history parameters on anchovy and sardine population growth. Calif. Coop. Oceanic Fish. Invest. Rep. **34**: 55–62.

DeBlois, E.M., and Rose, G.A. 1995. Effect of foraging activity on the shoal structure of cod (*Gadus morhua*). Can. J. Fish. Aquat. Sci. **52**: 2377–2387.

DeBlois, E.M., and Rose, G.A. 1996. Cross-shoal variability in the feeding habits of migrating Atlantic cod (*Gadus morhua*). Oecologia (Heidelb.), **108**: 192–196.

Dill, L.M., and Fraser, A.H.G. 1984. Risk of predation and the feeding behavior of juvenile coho salmon (*Oncorhynchus kisutch*) Behav. Ecol. Sociobiol. **16**: 65–71.

Duffy, D.C., and Wissel, C. 1988. Models of fish school size in relation to environmental productivity. Ecol. Model. **40**: 201–211.

Eshel, I. 1978. On a prey–predator nonzero-sum game and the evolution of gregarious behavior of evasive prey. Am. Nat. **112**: 787–795.

Fiedler, P.C., Methot, R.D., and Hewitt, R.P. 1986. Effects of California El Niño 1982–1984 on the northern anchovy. J. Mar. Res. **44**: 317–338.

Fraser, D.F., and Gilliam, J.F. 1992. Nonlethal impacts of predator invasion: facultative suppression of growth and reproduction. Ecology, **73**: 959–970.

Gates, D.M. 1993. Climate change and its biological consequences. Sinauer Associates, Sunderland, Mass.

Gerritsen, J., and Strickler, J.R. 1977. Encounter probabilities and community structure in zooplankton: a mathematical model. J. Fish. Res. Board Can. **34**: 73–82.

Graves, J. 1977. Photographic method for measuring spacing and density within pelagic fish schools at sea. Fish. Bull. U.S. **75**: 230–234.

Holliday, D.V. 1977. Two applications of the doppler effect in the study of fish schools. Rapp. P.-v. Réun. Cons. Int. Explor. Mer, **170**: 21–30.

Hunter, J.R., and Leong, R. 1981. The spawning energetics of female northern anchovy, *Engraulis mordax*. Fish. Bull. U.S. **79**: 215–229.

Koslow, J.A. 1981. Feeding selectivity of schools of northern anchovy *Engraulis mordax*, in the Southern California Bight. Fish. Bull. U.S. **79**: 131–142.

Krause, J. 1993. The relationship between foraging and shoal position in a mixed shoal of roach (*Rutilus rutilus*) and chub (*Leuciscus cephalus*): a field study. Oecologia (Heidelb.), **93**: 356–359.

Lefkovitch, L.P. 1965. The study of population growth in organisms grouped by stages. Biometrics, **21**: 1–18.

Loukashkin, A.S. 1970. On the diet and feeding behavior of the northern anchovy, *Engraulis mordax* (Girard). Proc. Calif. Acad. Sci. **37**: 419–458.

Mangel, M., and Clark, C.W. 1988. Dynamic modeling in behavioral ecology. Princeton University, Princeton, N.J.

Neill, S.R. St. J., and Cullen, J.M. 1974. Experiments on whether schooling by their prey affects the hunting behaviour of cephalopods and fish predators. J. Zool. (Lond.), **172**: 549–569.

Nonacs, P., Smith, P.E., Bouskila, A., and Luttbeg, B. 1994. Modeling the behavior of the northern anchovy, *Engraulis mordax*, as a schooling predator exploiting patchy prey. Deep-Sea Res. **41**: 147–169.

Smith, P.E. 1981. Fisheries on coastal pelagic fish. *In* Marine fish larvae: morphology, ecology, and relation to fisheries. *Edited by* R. Lasker. University of Washington, Seattle, Wash. pp. 1–32.

Smith, P.E. 1985. Year-class strength and survival of O-group clupeoids. *In* Proceedings of the Symposium on the Biological Characteristics of Herring and Their Implications for Management. *Edited by* J.R. Brett. Can. J. Fish. Aquat. Sci. **42**(Suppl. 1): 69–92.

Smith, P.E., Ohman, M.D., and Eber, L.E. 1989. Analysis of the patterns of zooplankton aggregations from an acoustic doppler current profiler. Calif. Coop. Oceanic Fish. Invest. Rep. **30**: 88–103.

Star, J.L., and Mullin, M.M. 1981. Zooplanktonic assemblages in three areas of the North Pacific as revealed by continuous horizontal transects. Deep-Sea Res. **28**: 1303–1322.

Stephens, D.W., and Krebs, J.R. 1986. Foraging theory. Princeton University, Princeton, N.J.

Swartzman, G. 1991. Fish school formation and maintenance: a random encounter model. Ecol. Model. **56**: 63–80.

Turner, G.F., and Pitcher, T.J. 1986. Attack abatement: a model for group protection by combined avoidance and dilution. Am. Nat. **128**: 228–240.

Werner, E.E., Gilliam, J.F., Hall, D.J., and Mittelbach, G.G. 1983. An experimental test of the effects of predation risk on habitat use in fish. Ecology, **64**: 1540–1548.

© 1998 NRC Canada

Predictions on the effect of common carp (*Cyprinus carpio*) exclusion on water quality, zooplankton, and submergent macrophytes in a Great Lakes wetland

Vanessa L. Lougheed, Barb Crosbie, and Patricia Chow-Fraser

Abstract: We conducted a study to examine the relationship between common carp (*Cyprinus carpio*) exclusion, water quality, zooplankton, and submergent macrophytes. Twelve 50-m^2 in situ experimental enclosures were installed in degraded Cootes Paradise Marsh during the carp spawning period in 1995. Enclosures were stocked with two or three carp of similar size, ranging from 13 to 59 cm and in total biomass from 23 to 2100 kg/ha. Turbidity, total phosphorus, and total ammonia concentrations increased predictably with total carp biomass in the enclosures. Although carp had no direct effect on zooplankton community structure, increased turbidity and nutrient load associated with carp activity resulted in reduced total zooplankton biomass. We developed a relationship between species richness and water turbidity for 19 wetlands in the Great Lakes basin which indicated that above an apparent threshold of 20 NTU, there were less than five species of submergent plants, while a more diverse community existed in less turbid systems. We predict that water turbidity in Cootes Paradise Marsh may not be reduced below this threshold value of 20 NTU following carp exclusion. We emphasize the need to consider other factors that may contribute to increases in water turbidity and nutrient concentrations, including wind resuspension and substrate characteristics.

Résumé : Nous avons étudié la relation entre l'exclusion des carpes (*Cyprinus carpio*), la qualité de l'eau, le zooplancton et les macrophytes submergés. Douze enclos expérimentaux in situ de 50 m^2 ont été aménagés dans le marais Cootes Paradise, un marais dégradé, durant la période de fraye des carpes en 1995. Nous avons placé dans les enclos deux ou trois carpes de tailles similaires allant de 13 à 59 cm, pour une biomasse totale de 23 à 2 100 kg/ha. La turbidité et les concentrations de phosphore total et d'ammoniac total se sont accrues comme prévu avec l'accroissement de la biomasse totale de carpes dans les enclos. Bien que les carpes n'aient eu aucun effet direct sur la structure de la communauté zooplanctonique, l'accroissement de la turbidité et de la charge de nutriants lié à l'activité des carpes a eu pour effet de réduire la biomasse totale de zooplancton. Nous avons établi une relation entre la diversité des espèces et la turbidité de l'eau pour 19 milieux humides du bassin des Grands Lacs, relation qui a montré qu'au-dessus d'un seuil apparent de 20 NTU, il y avait moins de cinq espèces de plantes submergées, alors qu'une communauté plus diverse était présente dans des milieux moins turbides. Nous prévoyons que la turbidité de l'eau au marais Cootes Paradise pourrait ne pas être réduite sous ce seuil de 20 NTU après exclusion des carpes. Nous mettons l'accent sur la nécessité de considérer d'autres facteurs pouvant contribuer aux accroissements de la turbidité de l'eau et des concentrations de nutriants, comme la remise en suspension des sédiments sous l'action du vent et les caractéristiques du substrat.
[Traduit par la Rédaction]

Introduction

Many authors have described the existence of two alternative stable states within shallow lakes or wetlands: one with clear water, dominated by submergent vegetation, and the other with turbid water, dominated by phytoplankton. Moss (1990) and Scheffer (1990) suggested that restoration of either state requires identifying and removing the stressor(s) that initiated the switch. To restore macrophytes, this could involve reducing nutrient levels to decrease phytoplankton biomass (e.g., Perrow et al. 1994; Mjelde and Faafeng 1997), adding piscivores and (or) removing planktivores and benthivores to reduce algae through trophic cascade effects (e.g., Brönmark and Weisner 1992; Hanson and Butler 1994), or removing benthivorous fish to increase water clarity (Meijer et al. 1990). Wetland managers in the Great Lakes basin are now attempting to restore degraded turbid, algal-dominated marshes to clear-water, macrophyte-dominated systems (e.g., Hamilton Harbour Remedial Action Plan (HHRAP) 1992; Whillans 1996); however, in many of these marshes where the nutrient levels are high, and the fish community is dominated by both planktivores and common carp (*Cyprinus*

Received April 3, 1997. Accepted November 26, 1997.
J13949

V.L. Lougheed,[1] B. Crosbie, and P. Chow-Fraser. Department of Biology, McMaster University, 1280 Main St. W., Hamilton, ON L8S 4K1, Canada.

[1] Author to whom all correspondence should be addressed.
e-mail:loughevl@mcmaster.ca

© 1998 NRC Canada

Fig. 1. Map of Cootes Paradise Marsh showing (*a*) remnant aquatic vegetation (shaded areas) and the enclosure site and (*b*) the location of the enclosures relative to each other.

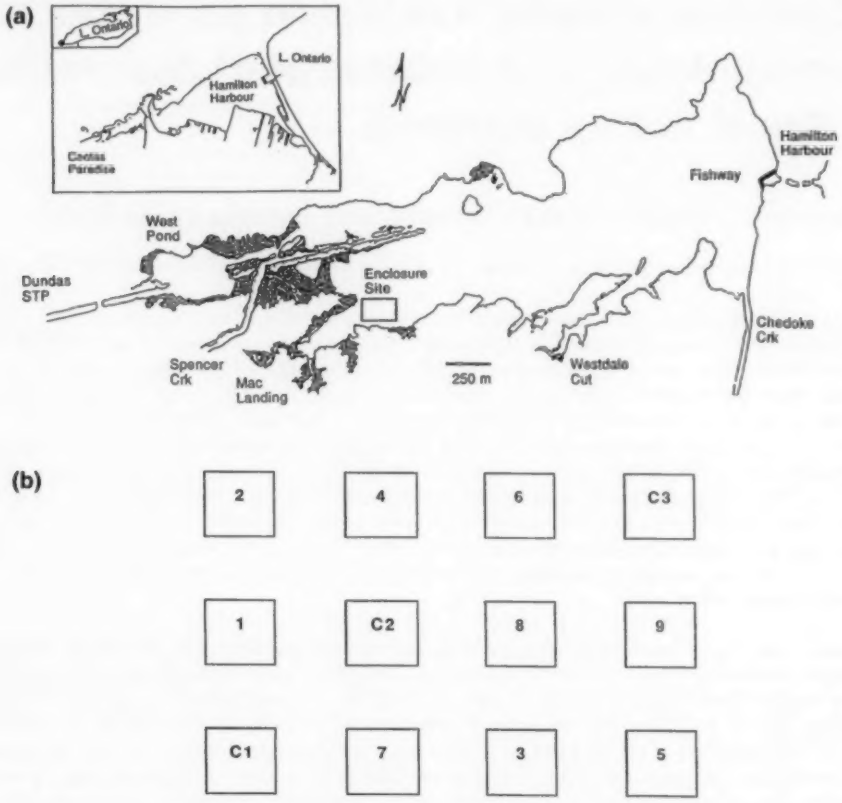

carpio), the key strategy that must be implemented to initiate such a switch is often difficult to identify.

The mechanical damage of submergent aquatic vegetation by carp is well documented (Robel 1962; Crivelli 1983). Macrophyte growth may also be hindered by shading from high algal biomass (Brönmark and Weisner 1992) and elevated turbidity (Skubinna et al. 1995), both of which have been shown to increase in the presence of carp and other benthivorous fish (Meijer et al. 1990; Qin and Threlkeld 1990; Richardson et al. 1990; Breukelaar et al. 1994). In some of these studies, benthivores were also found to increase nutrient levels (Meijer et al. 1990; Breukelaar et al. 1994; Cline et al. 1994), although this has not been consistently observed for both phosphorus and nitrogen (Meijer et al. 1990; Qin and Threlkeld 1990; Richardson et al. 1990; Cline et al. 1994). Carp may also indirectly lead to elimination of large-bodied zooplankton such as *Daphnia*, since high turbidity inhibits their ingestion of phytoplankton (e.g., Kirk and Gilbert 1990; Kirk 1991), and loss of plant refugia permits them to be readily consumed by planktivores (e.g., Schriver et al. 1995). However, studies that included analysis of zooplankton community response to carp manipulation have been in plantless outdoor tanks and have been inconclusive, showing either a suppression of (Richardson et al. 1990) or no effect on (Qin and Threlkeld 1990; Cline et al. 1994) large zooplankton.

Although the direct physical destruction of natural communities of submersed vegetation by carp is well documented, the indirect effects, through sediment resuspension, and increased nutrient and algal concentrations are not well understood. Although the manipulation of benthivorous fish communities appears well studied, it has been suggested that different benthivorous species have different levels of benthic activity (Meijer et al. 1990; Breukelaar et al. 1994). To date, no studies exist that document the impact of a range of carp biomass on water quality and the zooplankton community in situ, in the absence of macrophytes. Moreover, there is little field evidence that clearly links improvement in water clarity to increased diversity of submersed aquatic vegetation, a condition that must be met if carp exclusion is to be promoted as an general management strategy. The primary objective of this paper is to address these deficiencies in the literature and to provide a basis for improved decisions about wetland restoration and carp management in the Great Lakes.

Study site

Cootes Paradise Marsh (Fig. 1) is located in the Hamilton Harbour watershed at the western end of Lake Ontario. It is a severely degraded, 250-ha drowned river-mouth marsh, with

© 1998 NRC Canada

Table 1. Sex ratio, mean fork length, and biomass of carp added to each enclosure on May 19, 1995 (day 1).

Enclosure	Sex ratio (F:M)	Type	Mean fork length (cm)	Total biomass (kg/enclosure)	Total biomass (kg/ha)
C1	—	Control	0	0	0
C2	—	Control	0	0	0
C3	—	Control	0	0	0
1	2:1	Immature	9.7	0.11	22.8
2	2:1	Immature	13.3	0.22	45.6
3	2:1	Mature	33.3	2.88	596
4	2:1	Mature	41.8	3.94	816
5	1:1	Mature	43.2	3.48	721
6	2:1	Mature	47.2	6.40	1326
7	2:1	Mature	52.3	8.18	1695
8	2:1	Mature	55.3	9.97	2066
9	1:1	Mature	59.3	10.10	2093

an estimated carp density of 3500 individuals/ha in the near marsh areas during spawning, compared with 400 individuals/ha outside of spawning season (T. Theismeijer, McMaster University, Hamilton, Ont., personal communication). In the early 1900s, 90% of the marsh was covered with diverse emergent vegetation interspersed with smaller patches of submergents. Since the 1940s, the marsh has receded to less than 15% cover, consisting mainly of cattails (*Typha* sp.) and manna grass (*Glyceria* sp.). The loss of emergents has been attributed primarily to increased water levels, while submergent loss was likely due to decreased water clarity, resulting from reduced wind protection and increased carp disturbance, as well as increased nutrient load from the developing watershed (Chow-Fraser et al. 1998). Cootes Paradise Marsh is being restored as part of the HHRAP to create spawning and nursery habitat for warmwater fish species, mainly largemouth bass (*Micropterus salmoides*), smallmouth bass (*Micropterus dolomieu*), and northern pike (*Esox lucius*), in the Hamilton Harbour ecosystem (HHRAP 1992). To accomplish this, the HHRAP calls for exclusion of large carp (>30 cm) to improve water quality and to reestablish submergent aquatic vegetation.

Methods and materials

Experimental design

Twelve 50-m^2 in situ enclosures were built in a shallow (40–70 cm), nonvegetated area of the marsh (Fig. 1*a*) where the sediment was composed of fine sand and silt and the mean summer phosphorus content of the sediment was about 0.921 mg soluble reactive phosphorus (SRP)/g dry weight. Each side of an enclosure was 7.3 m and consisted of three adjoining panels, sunk 10–30 cm into the sediment and connected with plastic cable ties. Each panel was constructed with welded-wire fencing attached with plastic cable ties to a frame of four cast-iron T-shape bars. Silt screen (estimated mesh size 10 μm) was hand-sewn to each frame, forming overlapping flaps where each panel met. The silt screen was chosen over less permeable plastic sheeting because it better resists tearing due to wind and wave action (V.L. Lougheed, personal observation) and, in a productive system like the study site, quickly becomes impermeable due to buildup of periphyton and sediment. To ensure buildup of detritus, the enclosures were left standing empty for 2 weeks prior to the start of the experiment.

On May 19, 1995 (day 1), after all fish were removed from the enclosures using a seine net, two or three carp of the same size were randomly placed in each of nine enclosures; three enclosures were randomly selected as controls and received no carp (Table 1; Fig. 1*b*). To encourage spawning, we intended to put two female and one male carp in each of our enclosures but two females perished due to handling stress; the final carp numbers (see sex ratio), mean length, and biomass in each enclosure are provided in Table 1. The size of the carp was chosen based on those readily caught in Cootes Paradise Marsh and surrounding areas. Although carp were not retrieved from the enclosures after the experiment, their presence was verified throughout the experiment by the presence of sediment clouds, a sign of carp activity.

Enclosure sampling methods

Plankton and water samples were collected from each enclosure and a nearby open-water site between 04:00 and 06:00 on a total of four dates from May 19 (day 1) to June 2, 1995 (day 15), the period when carp were spawning in the marsh. The open-marsh site was included to provide a water quality reference that could be used to quantify enclosure effects. Water samples were taken at middepth with a peristaltic pump (capacity 1.4 L/min) which was located in a canoe outside the enclosures; samples were delivered through plastic tubing (inner diameter 6.4 mm) installed so as to withdraw water from the center of the enclosures and thus avoid edge effects.

Water samples were analyzed for total phosphorus (TP), SRP, nitrate nitrogen (NO_3-N), ammonia nitrogen (NH_3-N), suspended solids, and dissolved oxygen (Winkler method). Analyses were performed according to standard methods (American Public Health Association 1992), using Hach protocols and Hach chemicals as required. Turbidity was measured using a portable Hach turbidimeter (model 2100P). Chlorophyll *a* was extracted using 90% acetone and a 1-h extraction period. Absorbance measurements were made with a Milton Roy spectrophotometer and results were corrected for phaeopigments by acidification.

Zooplankton were pumped into a 5-L beaker, filtered through 63-μm-mesh Nitex screen, backwashed into 60-mL bottles, and preserved in 4% sugar–formalin. Samples collected on days 7, 11, and 15 were enumerated and identified and dry weights were estimated as described in Lougheed and Chow-Fraser (1998). The earliest sampling date was not analyzed to allow zooplankton 1 week to respond to the different treatments. Zooplankton were grouped into

© 1998 NRC Canada

Table 2. Location and summary of depth, mean turbidity, and number of common submergent plants for the 19 wetlands.

Wetland	Latitude	Longitude	Carp present (Y/N)	Depth (cm)	Mean turbidity (NTU)	No. of submergent plants
15 Mile Creek	43°10′00″	43°10′00″	Y	35	81	2
Big Creek	42°57′20″	80°26′50″	Y	105	4	9
Christie Lake	44°47′00″	76°28′00″	N	40	21	10
Cootes Paradise Marsh	43°16′00″	79°55′00″	Y	20	83	1
Harris Lake	45°42′00″	80°82′00″	N	78	2	10
Hay Bay	44°10′30″	76°55′30″	Y	30	3	15
Holiday	42°02′05″	83°03′00″	Y	30	276	0
Humber River	43°38′00″	79°29′00″	Y	25	68	1
Joe's Lake	45°08′00″	76°41′00″	N	80	1	10
Jordan Harbour	43°11′00″	79°23′00″	Y	46	56	2
Martindale Pond	43°10′07″	79°16′00″	Y	128	44	1
Presqu'ile Marsh	44°00′00″	77°43′00″	N	75	1	11
Sawguin Marsh	44°06′00″	77°23′00″	Y	80	4	9
Shebeshekong River	45°24′30″	80°19′00″	N	80	6	8
Stump Lake	44°56′48″	76°38′12″	N	53	2	12
Tay River Marsh	44°52′45″	76°10′30″	N	50	1	14
Tobies Bay	44°51′00″	79°47′00″	N	123	3	7
Turkey Creek	42°14′08″	83°05′07″	Y	28	11	11
Waterford Pond	42°56′10″	80°18′45″	Y	44	23	4

size-specific functional groups for all analyses (i.e., herbivorous rotifers, microcladocerans (<300 μm), medium-sized cladocerans (300–600 μm), macrocladocerans (600 μm), nauplii and copepodids, cyclopoid copepods, and predaceous rotifers), although medium- and macrocladocerans were not visible in the graphical output due to their low levels.

Wetland sampling

Nineteen wetlands located mainly in the Great Lakes basin were sampled twice each in the ice-free seasons of 1995 or 1996 for various factors including turbidity and submergent macrophyte richness (Table 2; Crosbie 1997). These wetlands ranged from pristine to severely degraded and were chosen to ensure a large gradient of disturbance. Ontario Wetland Evaluation reports (Ontario Ministry of Natural Resources) as well as personal observations were used to determine whether carp were present in each marsh. We recorded every species of submergent plant encountered within a 3-m radius of a randomly selected vegetated site. In wetlands with less than two species, the sparse distribution of individual plants (estimated as <5 plants/m^2) necessitated surveying the shoreline for about 100 m. Keys by Fassett (1940) were used to identify the submergent macrophytes species. Turbidity readings were taken in triplicate from the middle of the water column, about 3 m from aquatic vegetation, using a portable Hach turbidimeter (model 2100P).

Statistical analysis

All calculations and statistical analyses were performed using SAS.JMP software (SAS Institute Inc. 1982), and graphical analysis was performed using Cricket Graph III. For all enclosure analyses, we excluded data from enclosure 1 (carp biomass = 0.11 kg/enclosure) because a patch of sago pondweed (*Potamogeton pectinatus*) developed in this enclosure whereas all other control and experimental enclosures were devoid of plants. In the presence of submergent plants, turbulence created by the water pump dispersed sediment and epiphytes from plant surfaces and contaminated water samples. Simple linear regressions were performed on means of all sampling dates for both enclosure and wetland survey data. For analysis of zooplankton – water quality relationships, zooplankton biomass and water quality parameters were transformed using a $\log(x + 1)$ relationship. To describe changes in the zooplankton community through time, an ANOVA was constructed on arcsin-transformed percent biomass data for each functional taxon using enclosures as replicates for the three sampling dates. A Tukey–Kramer test was performed to confirm the significance tests of all combinations of dates. For wetlands, turbidity data entered into the Student *t*-test, the multipair comparisons, and the regression against submergent plant species were log-transformed to ensure equal variances. Historical data from Cootes Paradise Marsh in 1948 and 1973 (Chow-Fraser et al. 1998) were also included in the wetland regression of number of submergent species versus log turbidity.

Results

Water quality characteristics

To determine the overall impact of carp on water quality parameters, we calculated mean values for each enclosure over the four sampling dates and plotted these against carp biomass (Figs. 2 and 3). There was a highly significant relationship between water turbidity and carp biomass (p = 0.0023) that explained 76% of the variation (Fig. 2*a*); variation explained by this relationship increased to 83% (p = 0.0047) when a second-order polynomial was used. Relationships between other water quality parameters and carp biomass were similar but weaker. Both total suspended solids (TSS) and inorganic suspended solids (ISS) varied significantly with carp biomass (Figs. 2*b* and 2*c*), with about 50% of the variation explained by a linear relationship and 70% explained by a nonlinear relationship, in both cases. NH_3-N also increased linearly with carp biomass (r^2 = 0.50; Fig. 3*a*) whereas NO_3-N showed no significant relationship (Figs. 3*a*

© 1998 NRC Canada

Fig. 2. Relationship between carp biomass and mean (*a*) turbidity, (*b*) TSS, and (*c*) ISS in enclosures over 2 weeks during the carp spawning season.

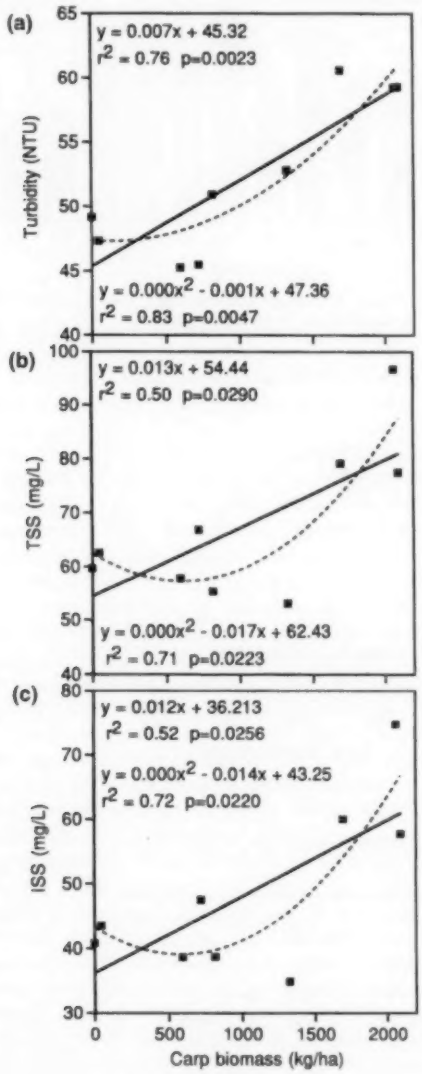

and 3*b*). By contrast, TP and SRP (Figs. 3*c* and 3*d*) concentrations varied nonlinearly with carp biomass (no significant linear relationship was found, $p > 0.05$); TP concentrations peaked at intermediate carp biomass whereas SRP concentrations were lowest at this biomass. Chlorophyll *a* was not significantly related to carp biomass or nutrient levels during this study. Mean turbidity at the open marsh site was 80 NTU, as compared with 45–60 NTU measured in the enclosures, which corresponds to a 25–45% reduction in turbidity within the enclosures. This is consistent with earlier experiments showing that exclusion of carp from similar silt-screened enclosures reduced turbidity by about 50% (P. Chow-Fraser, unpublished data).

Zooplankton

Seasonal succession was evident in the enclosures over the study period as rotifers such as *Brachionus*, *Keratella*, *Filinia*, and *Asplanchna* were replaced by small-bodied cladocerans such as *Bosmina*, cyclopoid nauplii, and small numbers of medium-sized cladocerans as the temperature increased from 13 to 22°C over the 15-day period. These differences between sampling dates were significant (ANOVA, $p < 0.05$; Table 3). There were, however, no obvious differences among enclosures in terms of overall zooplankton community composition (Fig. 4).

Mean total zooplankton biomass decreased significantly with both TSS and ISS, with about 50% of the variation explained by a linear relationship and 60% explained by a nonlinear relationship (Figs. 5*a* and 5*b*). Zooplankton biomass also declined significantly with increasing TP and NO_3-N (Figs. 5*c* and 5*d*). We observed that, regardless of carp biomass, the community was dominated by small-bodied cladocerans, herbivorous rotifers, and cyclopoid copepods and their nauplii.

Water clarity, submergent growth, and presence of carp

When sorted by presence or absence of carp, the number of submergent species differed significantly between groups of wetlands ($n = 19$; *t*-test, $t = 2.65$, $p = 0.0169$), with an average of five or fewer species in wetlands that supported carp, compared with 10 or more species in wetlands that did not. There were also highly significant differences ($n = 19$; *t*-test, $t = 4.58$, $p = 0.0003$) between groups with respect to turbidity, with a mean turbidity of 26.1 NTU in marshes with carp, compared with 2.1 NTU in those without.

We found that the number of submergent species decreased significantly with mean seasonal water turbidity in the 19 wetlands and two historical Cootes Paradise Marsh samples, explaining 81% of the variation in the data (Fig. 6). Above an apparent threshold of 20 NTU, species richness of aquatic vegetation was reduced to less than five species. In the highly turbid systems, *Potamogeton pectinatus*, a species known to be tolerant of high water turbidity, was the only submerged macrophyte.

According to our enclosure experiments, removing large carp from Cootes Paradise Marsh would at most reduce turbidity from existing levels of 80 NTU (open marsh site) to a low of 45 NTU (based on enclosures with no carp). This level of turbidity corresponds to less than five species of submergents (Fig. 6), far fewer than the 10+ species that existed in Cootes Paradise Marsh during a 1948 census when water clarity was only 5 NTU, and no improvement over 1973 conditions (Chow-Fraser et al. 1998).

Discussion

Recent studies of mixed fish assemblages, which compared control and fish treatments (Richardson et al. 1990; Qin and Threlkeld 1990; Breukelaar et al. 1994; Cline et al. 1994) or total lake benthivore biomass before and after biomanipulation (Meijer et al. 1990), suggested that carp play an important role in increasing turbidity and sometimes nutrient levels. Our data confirm that water turbidity and nutrient levels increased predictably with the biomass of spawning carp. Carp activity clearly resulted in increased sediment

© 1998 NRC Canada

Fig. 3. Relationship between carp biomass and (*a*) NH_3-N, (*b*) NO_3-N, (*c*) TP, and (*d*) SRP.

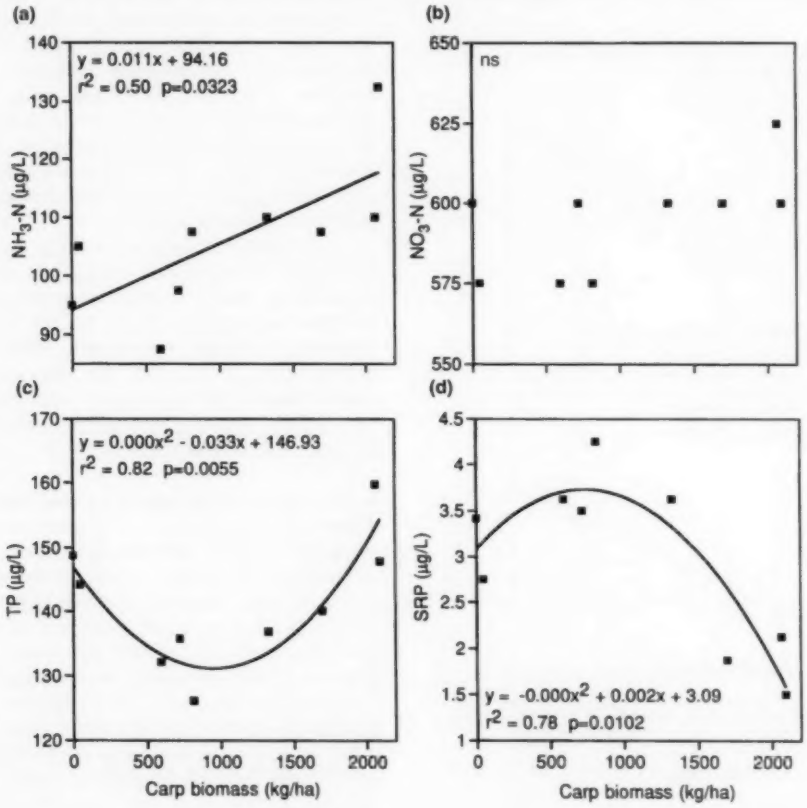

Table 3. Characteristics of the ANOVA of arcsin-transformed percent biomass data for each functional taxon compared for three sampling dates (days 7, 11, and 15).

Taxon	r^2	*F*-ratio	*p*-value	Significant differences
Herbivorous rotifers	0.94	232.13	0.0000	Day 7 > 11 > 15
Microcladocerans	0.07	35.18	0.0000	Day 15 > 11 > 7
Medium-sized cladocerans	0.37	8.78	0.0010	Day 15 > 11 and 7
Macrocladocerans	0.13	2.23	0.1249	—
Nauplii and copepodids	0.43	11.35	0.0002	Day 15 > 11 and 7
Cyclopoid copepods	0.08	1.29	0.2897	—
Predaceous rotifers	0.63	25.29	0.0000	Day 11 > 7 and 15

Note: The degrees of freedom for the regression and the residual were 2 and 30, respectively. The significant differences between dates were confirmed with a Tukey-Kramer test.

resuspension. The increase in phosphate and ammonia levels with carp biomass likely reflected both resuspension of nutrient-laden sediments and a proportionate increase in excretion rates by larger fish. Although benthivorous fish excrete mostly SRP and NH_3-N (Brabrand et al. 1990), bioavailable phosphorus can be easily removed from the water column by adsorption to particles under aerobic conditions, forming phosphate-rich inorganic particles (Holdren and Armstrong 1980). In our study, the resuspension of sediment by the larger spawners may have provided more surfaces for phosphate adsorption, therefore resulting in a reduction in SRP with a concomitant increase in TP.

Although levels of turbidity and nutrients generally increased with carp biomass, surprisingly high levels were

© 1998 NRC Canada

Fig. 4. Mean percent biomass of zooplankton functional groups in all enclosures (except enclosure 1; see text for details).

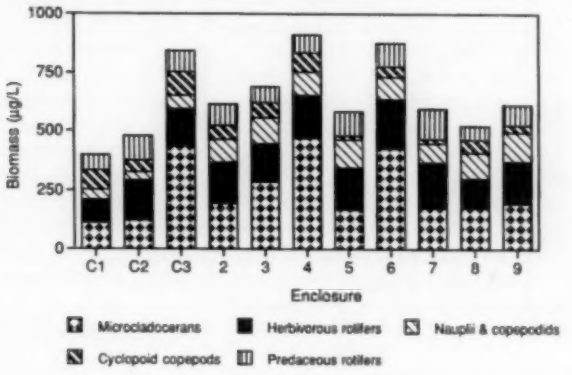

still found in enclosures containing small carp (enclosure 2) and no carp (i.e., controls) (Figs. 2 and 3). Levels of turbidity and nutrients measured in these enclosures far exceeded those values reported by other researchers studying small benthivores (Horpilla and Kairesalo 1990; Qin and Threlkeld 1990; Richardson et al. 1990). Wind speed and fetch increase sediment resuspension (Sager 1996) as well as nutrient release in shallow systems (Hamilton and Mitchell 1997) and may have played an important role in reducing water clarity and increasing nutrient load in the enclosures located on the edges of the site (including C1, C3, and enclosure 2) which were exposed to relatively high winds (3 m/s) at this shallow (40–70 cm) and exposed location. In addition, reduced benthivorous fish levels, as was the case in the control enclosures and those enclosures containing smaller carp, may result in an increased benthic invertebrate population that has the potential to increase phosphorus release by bioturbation (Holdren and Armstrong 1980; Phillips et al. 1994).

Phosphorus release from sediment is not only dependent on resuspension and bioturbation but also on the characteristics of the sediment, such as iron, aluminum, organic, and TP content (Holdren and Armstrong 1980; Ostrofsky et al. 1989; Phillips et al. 1994), which can vary greatly among systems (Nürnberg 1988). For example, clay particles have a greater capacity for forming complexes with phosphorus; however, even within systems containing clay particles, there exists variation in nutrient release. Meijer et al. (1990) and Breukelaar et al. (1994), working in systems with mainly sand and clay substrate, both found significant relationships between suspended sediment and carp and bream (*Abramis brama*) biomass; however, whereas Breukelaar et al. (1994) found an associated increase in phosphorus load, Meijer et al. (1990) did not. This discrepancy may be attributed to differences in sediment characteristics and deserves further investigation. The inclusion of substrate descriptions in future studies would permit more accurate predictions regarding nutrient regeneration related to benthivorous feeding activities.

Unlike other studies where zooplankton community composition changed with removal of carp (Richardson et al. 1990), there were no obvious between-enclosure differences in zooplankton community structure in this study. In addition to residual effects, the time period of this study, corresponding to carp spawning season, was an obvious limitation to these results in that the study was restricted to only 2 weeks in the spring, when zooplankton in the marsh were typically composed of low to moderate numbers of small animals (Lougheed and Chow-Fraser 1998) which are less sensitive than the larger grazers to changes in water clarity (Kirk and Gilbert 1990; Kirk 1991). Overall, a reduction in total zooplankton biomass was associated with increased levels of suspended solids, as well as TP and NO_3-N, that were presumably due to carp activity. We therefore predict that by excluding spawning carp from Cootes Paradise Marsh, and thereby reducing the suspended solid and nutrient levels, total zooplankton biomass should increase, and that if suitable macrophyte habitats became available, previous work (Lougheed and Chow-Fraser 1998) suggested that this increased biomass would consist of larger grazers. A larger population of macrograzers may lead to further increases in clarity due to zooplankton grazing (Hanson and Butler 1994; Schriver et al. 1995); however, it appears that an increased biomass of smaller grazers will have no impact on algae, as indicated by chlorophyll *a* in this study.

Scheffer (1990) theorized that in shallow lakes of homogeneous depth, submergent plants will disappear suddenly when a threshold turbidity is exceeded, which renders most of the lake unsuitable for plant growth. We found support for this theory in wetlands where above an apparent threshold of 20 NTU, there were less than five species of submergents whereas a more diverse community of macrophytes existed in clearer water. It is noteworthy that marshes where carp were absent had uniformly clear water (<6 NTU) and a relatively diverse (more than seven species) and dense (estimated as >20 plants/m^2) submergent flora; however, whereas carp-free systems were always macrophyte dominated, macrophyte-dominated systems were not always carp free (i.e., Big Creek, Hay Bay, Sawguin, and Turkey Creek). An obvious limitation to these results was the absence of data on carp biomass, which is known to be related to submergent plant cover (Robel 1962; Crivelli 1983). In addition, the presence of established submerged macrophytes could stabilize sediment and maintain water clarity (Hamilton and Mitchell 1997) in the presence of carp. Nonetheless, because these four wetlands were significantly clearer than other wetlands containing carp and were not significantly different from carp-free wetlands (ANOVA, $p = 0.0000$, $F = 62.6$, df = 2 and 16; confirmed with Tukey–Kramer), we suggest that this is additional evidence that water turbidity in Great Lakes marshes must be affected by factors other than carp, such as wind resuspension of sediment, high algal concentration, and fine substrate composition.

Further remedial actions will likely be necessary to promote the restoration of Cootes Paradise Marsh, as the increase in water clarity that will result from carp removal in the marsh is unlikely to be sufficient to allow the establishment of a diverse community of submergent vegetation. Carp-free enclosures had a mean turbidity of 45 NTU throughout the experimental period which was much higher than the 20 NTU required for submergent growth. We must acknowledge, however, that there are limitations to this prediction. Whole systems and enclosed systems behave differently, especially as it pertains to flow, turbulence, and the settling of particles (Bloesch et al. 1988; Horpilla and

© 1998 NRC Canada

Fig. 5. Relationship between total zooplankton biomass (ZB) and (*a*) TSS, (*b*) ISS, (*c*) TP, and (*d*) NO_3-N.

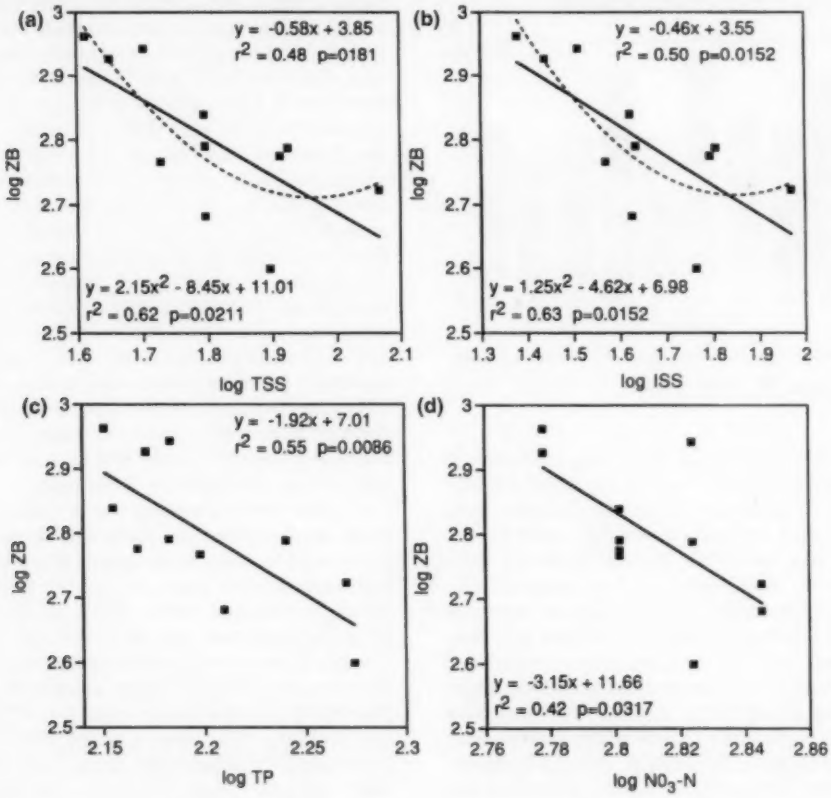

Fig. 6. Relationship between the number of submergent plant species versus turbidity (log scale) for 18 marshes in the Great Lakes basin (solid squares) and Cootes Paradise Marsh from 1948, 1973, and 1996 (open squares). Also indicated is the predicted water clarity following carp removal (45 NTU) in Cootes Paradise Marsh.

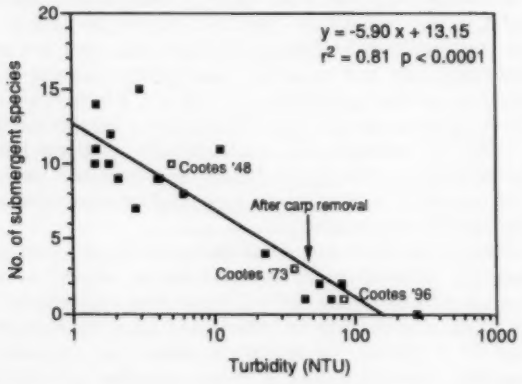

Kairesalo 1990). In addition, the plantless enclosures may have inhibited carp activity during the spawning season, as carp tend to spawn near plants (Balon 1995), notably in Cootes Paradise Marsh where they congregated near the cattails at levels eight times higher than outside of the spawning season (T. Theismeijer, McMaster University, Hamilton, Ont., personal communication). The 25–45% reduction in turbidity in the enclosures compared with the open marsh may, in part, reflect these limitations.

This study provides promising management applications towards predicting the extent of improvement in water quality from carp reduction schemes, as well as indicating the required improvement in water clarity for diverse submergent plant growth. At first glance, these results may appear discouraging for Cootes Paradise Marsh; however, acknowledging that there is more than one stressor maintaining the marsh in its turbid state is an important step towards restoration. Although the ability to extrapolate across systems is useful, we must emphasize the need to accurately identify the stressor(s) that are degrading each specific system. We suggest that the relative impact of reductions in carp biomass on turbidity will be identical for most wetlands in the Great Lakes; however, the ambient conditions in each marsh will determine the ultimate result of any manipulation. Although carp activity is likely one of the primary agents degrading many of the Great Lakes wetlands, managers must consider all factors that may contribute to increases in water turbidity and nutrient concentrations, including wind resuspension, benthic bioturbation, algal concentrations, internal nutrient loading, and substrate type, to ensure that the desired response from carp reduction or exclusion will be obtained in marsh restoration programs.

© 1998 NRC Canada

Acknowledgements

This project was funded by the McMaster Eco-Research Program for Hamilton Harbour and an operating grant and NSERC Women's Faculty Award to PC-F. We greatly appreciate the work of many volunteers who built and stocked the enclosures, especially J. Hautopp and H. Mitcheson, as well as the advice of V. McLean and D. Johnson, among others, during the planning stages of the experiment. We also thank the summer students of 1995 (B. Schuur, T. Frayn, K. Price, J. Wood, L. Lindsay, and M. Climenhaga) and M. Doyle for assisting with field work and water chemistry analysis. We are thankful to J. Brazner, M.A. Hanson, K. Havens, and an anonymous reviewer for helpful suggestions on the manuscript.

References

American Public Health Association. 1992. Standard methods for the examination of water and wastewater. 18th ed. American Public Health Association, Washington, D.C.

Balon, E.K. 1995. The common carp, *Cyprinus carpio*: its wild origin, domestication in aquaculture, and selection as colored nishigoi. Guelph Ichthyol. Rev. **3**: 1–54

Bloesch, J., Bossard, P., Buhrer, H., Burgit, H.R., and Uehlinger, U. 1988. Can results from limnocorral experiments be transferred to in situ conditions. Hydrobiologia, **159**: 297–308.

Brabrand, A., Faafeng, B.A., and Nilssen, J.P. 1990. Relative importance of phosphorus supply to phytoplankton production: fish excretion versus external loading. Can. J. Fish. Aquat. Sci. **47**: 364–372.

Breukelaar, A.W., Lammens, E.H.R.R., Breteler, J.G.P.K., and Tatrai, I. 1994. Effects of benthivorous bream (*Abramis brama*) and carp (*Cyprinus carpio*) on sediment resuspension and concentrations of nutrients and chlorophyll *a*. Freshwater Biol. **32**: 113–121.

Brönmark, C., and Weisner, S.E.B. 1992. Indirect effects of fish community structure on submerged vegetation in shallow, eutrophic lakes: an alternative mechanism. Hydrobiologia, **243/244**: 293–301.

Chow-Fraser, P., Lougheed, V., Le Thiec, V., Crosbie, B., Simser, L., and Lord, J. 1998. Long-term response of the biotic community to fluctuating water levels and changes in water quality in Cootes Paradise Marsh, a degraded coastal wetland of Lake Ontario. Wetland Ecol. Manage. In press.

Cline, J.M., East, T.L., and Threlkeld, S.T. 1994. Fish interactions with the sediment–water interface. Hydrobiologia, **275/276**: 301–311.

Crivelli, A.J. 1983. The destruction of aquatic vegetation by carp. Hydrobiologia, **106**: 37–41.

Crosbie, B. 1997. An evaluation of the pollutants entering Ontario's wetlands: how landuse impacts wetland health. M.Sc. thesis, Department of Biology, McMaster University, Hamilton, Ont.

Fassett, N.C. 1940. A manual of aquatic plants. McGraw-Hill Book Company Inc., New York.

Hamilton, D.P., and Mitchell, S.F. 1997. An empirical model for sediment resuspension in shallow lakes. Hydrobiologia, **317**: 209–220.

Hamilton Harbour Remedial Action Plan (HHRAP). 1992. Stage 2 report. Goals, options and recommendations. Canada–Ontario publication. Remedial Action Planning Team, Hamilton, Ont.

Hanson, M.A., and Butler, M.G. 1994. Responses of plankton, turbidity and macrophytes to biomanipulation in a shallow prairie lake. Can. J. Fish. Aquat. Sci. **51**: 1180–1188.

Holdren, G.C., Jr., and Armstrong, D.E. 1980. Factors affecting phosphorus release from intact sediment cores. Environ. Sci. Technol. **14**: 79–86.

Horpilla, J., and Kairesalo, T. 1990. A fading recovery: the role of roach (*Rutilus rutilus* L.) in maintaining high phytoplankton productivity and biomass in Lake Vesijarvi. Hydrobiologia, **200/201**: 153–165.

Kirk, K.L. 1991. Inorganic particles alter competition in grazing plankton: the role of selective feeding. Ecology, **72**: 915–923.

Kirk, K.L., and Gilbert, J.J. 1990. Suspended clay and the population dynamics of planktonic rotifers and cladocerans. Ecology, **71**: 1741–1755.

Lougheed, V.L., and Chow-Fraser, P. 1998. Factors that regulate the zooplankton community structure of a turbid, hypereutrophic Great Lakes wetland. Can. J. Fish. Aquat. Sci. **55**: 150–161.

Meijer, M-L., de Haan, M.W., Breukelaar, A.W., and Buiteveld, H. 1990. Is reduction of the benthivorous fish an important cause of high transparency following biomanipulation in shallow lakes? Hydrobiologia, **200/201**: 303–315.

Mjelde, M., and Faafeng, B.A. 1997. *Ceratophyllum demersum* hampers phytoplankton development in some small Norwegian lakes over a wide range of phosphorus concentrations and geographical latitude. Freshwater Biol. **37**: 335–365.

Moss, B. 1990. Engineering and biological approaches to the restoration from eutrophication of shallow lakes in which aquatic plant communities are important components. Hydrobiologia, **200/201**: 367–377.

Nürnberg, G. 1988. Prediction of phosphorus release rates from total and reductant-soluble phosphorus in anoxic lake sediments. Can. J. Fish. Aquat. Sci. **45**: 453–461.

Ostrofsky, M.L., Osborne, D.A., and Zebulske, T.J. 1989. Relationship between anaerobic sediment phosphorus release rates and sedimentary phosphorus species. Can. J. Fish. Aquat. Sci. **46**: 416–419.

Perrow, M.R., Moss, B., and Stansfield, J. 1994. Trophic interactions in a shallow lake following a reduction in nutrient loading: a long-term study. Hydrobiologia, **275/276**: 43–52.

Phillips, G., Jackson, R., Bennett, C., and Chilvers, A. 1994. The importance of sediment phosphorus release in the restoration of very shallow lakes (The Norfolk Broads, England) and the implications for biomanipulation. Hydrobiologia, **275/276**: 445–456.

Qin, J., and Threlkeld, S.T. 1990. Experimental comparison of the effects of benthivorous fish and planktivorous fish on plankton community structure. Arch. Hydrobiol. **119**: 121–141.

Richardson, W.B., Wickham, S.A., and Threlkeld, S.T. 1990. Food-web response to the experimental manipulation of a benthivore (*Cyprinus carpio*), zooplanktivore (*Menidia beryllina*) and benthic insects. Arch. Hydrobiol. **119**: 143–165.

Robel, R.J. 1962. The relationship of carp to waterfowl food plants on a western marsh. Utah Dep. Fish Game Inf. Bull. 62-4.

Sager, E.P.S. 1996. Factors limiting the light environment in Cootes Paradise, Hamilton Harbour and other coastal marshes of Lake Ontario. Water Qual. Res. J. Can. **31**: 553–575.

SAS Institute Inc. 1982. User's guide: statistics, 1982 edition. SAS Institute Inc., Cary, N.C.

Scheffer, M. 1990. Multiplicity of stable states in freshwater systems. Hydrobiologia, **200/201**: 475–486.

Schriver, P., Bogestraand, J., Jeppesen, E., and Sondergaard, M. 1995. Impact of submerged macrophytes on fish–zooplankton–phytoplankton interactions: large-scale enclosure experiments in a shallow eutrophic lake. Freshwater Biol. **33**: 255–270.

Skubinna, J.P., Coon, T.G., and Batterson, T.R. 1995. Increased abundance and depth of submersed macrophytes in response to decreased turbidity in Saginaw Bay, Lake Huron. J. Great Lakes Res. **21**: 476–488.

Whillans, T.H. 1996. Historic and comparative perspectives on rehabilitation of marshes as habitat for fish in the lower Great Lakes basin. Can. J. Fish. Aquat. Sci. **53**(Suppl. 1): 56–66.

© 1998 NRC Canada

Anaerobic capacity and swim performance of juvenile salmonids

D.G. McDonald, W.J. McFarlane, and C.L. Milligan

Abstract: This study describes the development of procedures for the assessment of anaerobic capacity and swim performance in juvenile Atlantic salmon (*Salmo salar*), rainbow trout (*Oncorhynchus mykiss*), and brook trout (*Salvelinus fontinalis*). Three exercise tests, with exhaustion as an end point, were evaluated: a fixed-duration, high-intensity exercise; a fixed-velocity exercise; and an incremental-velocity exercise. Muscle (or whole body) lactate, phosphocreatine (PCr), and ATP were used to calculate, in ATP equivalents, the anaerobic energy expenditure (AEE, in $\mu M \cdot g^{-1}$ or μmoles) and to document the recovery from exhaustion. AEE was maximal in the first of these tests and submaximal in the second. Recovery was characterized by rapid restoration of PCr, slower recovery of ATP and lactate, and even slower recovery of glycogen. Mathematical expressions were developed to express the rates of recovery and thereby permit intra- and inter-species comparisons. Body size was the most important determinant of performance. Anaerobic capacity (AEE in the fixed duration test), sprint duration at fixed velocity, and maximum swimming speed scaled as length L^4 to L^5, L^4 to L^5, and $L^{1.3}$, respectively. Each of these tests are effective measures for evaluating intra- and inter-specific differences in anaerobic capacity and swimming performance providing correction is made for the large scaling coefficients.

Résumé : On décrit la mise au point de procédures pour évaluer la capacité anaérobie et la performance de nage des juvéniles du saumon atlantique (*Salmo salar*), de la truite arc-en-ciel (*Oncorhynchus mykiss*) et de l'omble de fontaine (*Salvelinus fontinalis*). Trois épreuves d'effort, avec l'épuisement comme point final, ont été évaluées : l'une d'intensité élevée de durée fixe, l'autre à une vitesse fixe et la dernière à une vitesse différentielle. La teneur musculaire (ou corporelle totale) en acide lactique, en phosphocréatine et en ATP a servi à calculer, en équivalents ATP, la consommation d'énergie anaérobie (en $\mu M \cdot g^{-1}$ ou μM) et à documenter le rétablissement après l'épuisement. La consommation d'énergie anaérobie était maximale lors de la première épreuve et sous-maximale lors de la deuxième. Le rétablissement était caractérisé par une remontée rapide de la teneur en phosphocréatine, une remontée plus lente de la teneur en ATP et en acide lactique, et une remontée encore plus lente de la teneur en glycogène. Des formules mathématiques ont été établies pour exprimer les taux de rétablissement et donc permettre de faire des comparaisons interspécifiques et intraspécifiques. La taille était le premier facteur déterminant de la performance. La capacité anaérobie (la consommation d'énergie anaérobie dans l'épreuve de durée fixe), la durée de la nage rapide à vitesse fixe et la vitesse maximale de nage ont été établies à L^4 à L^5, L^4 à L^6 et $L^{1,3}$ respectivement par rapport à la longueur *L*. Chacune de ces épreuves est un moyen efficace d'évaluer les différences intraspécifiques et interspécifiques de la capacité anaérobie et de la performance de nage, pourvu que l'on tienne compte des coefficients de proportionnalité indiqués. [Traduit par la Rédaction]

Introduction

This study examines the exercise responses of juvenile salmonids with the view to developing and refining tests of anaerobic capacity and swim performance. While the focus of this study is on Atlantic salmon (*Salmo salar*), juvenile rainbow trout (*Oncorhynchus mykiss*), and brook trout (*Salvelinus fontinalis*) have been included for reference because, generally speaking, their swim performance is better characterized. Specifically we addressed the following questions: what are the behavioral and physiological responses of Atlantic salmon to various exercise tests; what is their capacity for anaerobic energy expenditure; what is the nature of their recovery from exhaustive exercise; how does performance scale with body size; and how does their performance compare with other salmonids, specifically rainbow trout and brook trout?

Measuring the swim performance of Atlantic salmon is problematic compared with other salmonids, because Atlantic salmon are able to remain stationery while in current. They do not swim readily but rather cling to the substrate by keeping their pectoral and anal fins in direct contact with the substrate and by using their large pectoral fins as depressors (Rimmer et al. 1985; Arnold et al. 1991). Depending on substrate, their performance is therefore a combination of current avoidance and swimming. Consequently, they exhibit a much wider variability in performance in swimming trials than other salmonids (McNeish and Hatch 1978).

With this in mind we employed three different procedures for stamina assessment and tested them on Atlantic salmon, using the other two salmonid species for reference.

Received May 5, 1997. Accepted October 20, 1997.
J14003

D.G. McDonald[1] **and W.J. McFarlane.** Department of Biology McMaster University, 1280 Main Street West, Hamilton, ON L8S 4K1, Canada.
C.L. Milligan. Department of Zoology, University of Western Ontario, London, ON N6A 5B7, Canada.

[1] Author to whom all correspondence should be addressed. e-mail: mcdonad@mcmail.mcmaster.ca

© 1998 NRC Canada

(1) Fixed-duration exercise test. In this high-intensity test, fish are continuously stimulated to exercise for a fixed period, with stimulation continued beyond the point where the fish become refractory. This approach has been widely used to study anaerobic metabolism in salmonids (see Wood and Perry 1985; Goolish 1991; Milligan 1996 for reviews). We evaluated performance in this test from depletion of anaerobic fuels (glycogen, phosphocreatine (PCr), and ATP) and by the rate of recovery of these fuels and tested the hypothesis that this test produces maximum exertion, i.e., is a measure of anaerobic capacity.
(2) Fixed-velocity test. In this test, fish are swum at a constant velocity until exhausted (Hammer 1995). We evaluated performance from time to exhaustion and anaerobic energy expenditure. This test simulates the natural experience of salmon, which dart briefly into high velocity currents for prey capture. Test velocities were typical of those in natal streams (30–60 $cm \cdot s^{-1}$; Gibson 1993).
(3) Incremental-velocity test. In this test, fish are exposed to increasing velocity increments of a constant amount and duration until exhaustion is reached. Such a test has been used to measure critical holding velocity in juvenile Atlantic salmon (Rimmer et al.1985; Graham et al. 1996) and is the approach used on other salmonids to measure critical swimming speed or maximum sustainable swimming speed (cf. Beamish 1978; Hammer 1995).

All three tests were modified from previous studies to improve their utility as performance tests; in all three, fish were swum in groups rather than singly, and in test 3 the duration of each increment was reduced to 5 min from the usual increment of 20–60 min.

Materials and methods

Experimental animals

Experiments were carried out at the Cardigan Salmonid Enhancement Centre (Cardigan, P.E.I.) on fish reared from eggs collected from wild broodstock (Atlantic salmon and brook trout) or from a domesticated hatchery-reared strain (rainbow trout). Atlantic salmon were fingerlings (age 0^+) and yearlings (age 1^+) of fork length 4–14 cm, while brook trout and rainbow trout were fingerlings of 6–9 cm and 11–16 cm, respectively. Fish were reared in 2.4- or 7.3-m circular "Swede" tanks under natural photoperiod and temperature and were hand fed dry hatchery pellets to satiation at least four times per day. Experiments were carried out in August and September of 1994–1996. Temperature was 11–13°C. Additional trials on 0^+ rainbow trout (6–9 cm) was carried out at McMaster University on fish obtained from Rainbow Springs Trout Hatchery, Thamesford, Ont. All fish handling was carried out humanely following Canadian Council of Animal Care guidelines.

Performance tests

Maximum-exertion, fixed-duration test

Fish were transferred in groups of 5 or 10 (depending on body size) to a 15 cm diameter cylinder containing 10 L and immediately forced to activity for 8 min by continuous mechanical stimulation by hand. At the end of 8 min, fish were removed as a group and were either immediately sampled or allowed to recover for up to 4 h (sampling at 30 min, 1 h, 2 h, and 4 h). For tissue sampling, fish were terminally anaesthetized in tricaine methanesulphonate (MS-222, 2 $g \cdot L^{-1}$, neutralized to pH 7.5) and length and mass recorded. For fish of ≤2 g body mass, the whole fish was immediately freeze-clamped in liquid N_2 (LN_2) using a pair of aluminum plates (1 cm thickness), a section of white muscle tissue was removed and each fraction ground and stored separately. For larger fish, 0.5–1.0 g white muscle was removed from above the lateral line and anterior to the dorsal fin, and freeze-clamped in LN_2. Frozen tissue was ground to a powder in LN_2, and stored in LN_2 for later analysis of glycogen, lactate, PCr, and ATP and activities of the two glycolytic enzymes: phosphofructokinase (PFK) and lactate dehydrogenase (LDH).

Design of swim flume

Fish were exercised in an open, recirculating swim flume of 100 L total volume, constructed, according to the design recommendations of Vogel (1981), of PVC pipe (15 cm I.D.) connected to a rectangular swim section of 11 × 20 × 74 cm (W × H × L) constructed of PVC plate (0.64 cm thickness). The bottom of the working section was rounded with a half section of 10 cm i.d. PVC pipe to eliminate eddy currents. Water flow was generated by a propeller (13 cm diameter) driven by a 373-W DC motor controlled by a solid state controller with internal feedback. The swim flume was calibrated with a Marsh–McBirney Model 2000 electromagnetic flow meter and had a practical upper speed of 72 $cm \cdot s^{-1}$. Higher speeds could be obtained with higher motor rpm but flow became turbulent. Temperature was maintained by partial replacement from holding tanks.

Fixed-velocity test

For all tests, fish were transferred to the swim flume in groups of 10 and allowed to adjust to the chamber and orient to low-speed current (1–2 body lengths $(BL) \cdot s^{-1}$) for 5 min. For each test, initial trials were performed to determine the velocity which produced exhaustion of the majority within 30 min (typically >7 $BL \cdot s^{-1}$). For each trial, velocity was increased continuously over 5 min until the test velocity was reached and timing was begun. Once the test velocity was chosen, at least three trials (10 different fish each) were done at that velocity. Fish maintained station in the flume, either by contact with the bottom (Atlantic salmon) or by continuous swimming (brook trout and rainbow trout, see Results), but as they tired, they fell to the back screen.

Fish were lightly prodded with a thin metal rod to resume swimming. If this was ineffective the fish were removed.

Once fish became exhausted, or after 60 min exercise, whichever came first, they were removed from the flume, terminally anaesthetized, length and mass recorded, tissues were freeze clamped and ground (as above) and stored in LN_2 for later analysis. For analysis of sprint perfomance for each group the times to exhaustion from each trial were pooled, and the time to 50% fatigue was estimated by log-probit analysis (cf. Brett 1967).

Incremental-velocity test

These tests were performed on groups of 10 fish per trial. Each test began with a 5 min orientation period at 14 $cm \cdot s^{-1}$, followed by an increase to 38 $cm \cdot s^{-1}$ over 13 min, and then increments of 5 $cm \cdot s^{-1}$ every 5 min until all fish were exhausted. On each group, at least three trials (10 per trial) were performed. Final velocity (or maximum swimming speed (MSS) in $cm \cdot s^{-1}$) was calculated according to the following expression from Brett (1964):

$$(1) \qquad MSS = V_p + \left(\left(\frac{t_f}{t_i} \right) + V_i \right)$$

where V_i is the velocity increment ($cm \cdot s^{-1}$), V_p is the penultimate velocity at which the fish swum before fatigue, t_f is the elapsed time from the velocity increase to fatigue, and t_i is the time between velocity increments.

Analysis of tissue metabolites

For tissue glycogen analysis, glycogen was first isolated from 100 mg of frozen tissue powder by the digestion–precipitation method of Hassid and Abraham (1957). Glycogen in the redissolved precipitate was digested with amyloglucosidase, and the resultant

© 1998 NRC Canada

glucose was analyzed enzymatically according to procedures in Bergmeyer (1983). For analysis of lactate, ATP and PCr, ~100 mg of frozen tissue powder was homogenized on ice in 1.0 mL of 8% perchloric acid, and the supernatant was analyzed enzymatically according to procedures in Bergmeyer (1983).

Activities of glycolytic enzymes

For measurement of the activities of the glycolytic enzymes l-lactate dehydrogenase (LDH, EC 1.1.1.27) and phosphofructokinase (PFK, EC 2.7.1.11), frozen muscle powder (~50 mg) was homogenized in 10 volumes of 50 mM Tris–HCl buffer (pH 7.5) at 2°C. Homogenates were centrifuged for 5 min at 12 500 × *g* at 4°C, and the supernatants were collected, stored on ice, and used immediately for enzyme assays. Assays were performed in thermostatted cuvettes at 15°C using substrate concentrations giving maximal velocities. Enzyme activity was measured in a Perkin-Elmer LS-50 spectrofluorometer (excitation 340 nm; emission 460 nm) based on the decrease in fluorescence due the hydrolysis of NADH. All activities are expressed as moles of NADH converted to NAD^+ per minute per gram wet tissue mass at the measurement temperature of 15°C.

LDH activity was assayed in the pyruvate reductase direction, i.e., the direction of an anaerobically functioning tissue. The assay medium contained, in a total volume of 2.0 mL, 50 mM glycylglycine buffer (pH 8.2), 4 mM Na pyruvate, 5 mM $MgCl_2$, 100 mM KCl, and 0.6 mM NADH. The assay was started by addition of 10 µL of a 1:6 dilution of the above supernatant. PFK activity was assayed with the fructose-1,6-diphosphate coupled assay of Shonk and Boxer (1964). The assay medium contained, in a total volume of 2.0 mL, 50 mM glycylglycine buffer (pH 8.2), 2 mM ATP, 2 mM fructose-6-phosphate, 40 mg·dL^{-1} of bovine serum albumin, 1 U·mL^{-1} of aldolase, 1 U·mL^{-1} of glycerol-3-phosphate dehydrogenase, 1 U·mL^{-1} of triosphosphate isomerase, 5 mM $MgCl_2$, 100 mM KCl, and 0.1 mM NADH. The assay was started by addition of 40 µL of the above supernatant.

Calculations

The anaerobic energy expenditure in ATP equivalents (AEE or anaerobic ATP turnover; Pearson et al. 1990) was calculated according to the following formula:

$$\text{(2)} \qquad \text{AEE} = (\Delta\text{Lactate}) \times 1.5 + \Delta\text{ATP} + \Delta\text{PCr}$$

where Δ is the difference between values for resting animals and those at exhaustion, 1.5 ATP are produced per lactate; 1 PCr = 1 ATP. Additional energy during anaerobic metabolism is derived from the hydrolysis of ADP to AMP, but this term was ignored since the contribution is small (less than 10% of AEE; Pearson et al. 1990).

Statistical analysis

Means ± one standard error of the mean (SE) are reported throughout. Analysis of variance was used to test significance of regressions. Differences at $P < 0.05$ were considered significant.

Results

Fixed duration test

Forced exercise for 8 min produced significant changes in muscle glycogen, ATP, PCr, and lactate in Atlantic salmon, rainbow trout, and brook trout. Although glycogen, ATP and PCr were not completely depleted by this procedure, in any of the three species, the depletion was essentially maximal, since the fish became refractory to electrical or mechanical stimulation within 3–5 min of the start of the protocol. This was confirmed in trials on rainbow trout sampled at 1, 2, 4, 6, and 8 min of forced activity (Fig. 1A) which showed that each metabolite reached plateau values within 4–6 min of the 8-min protocol. Thus AEE (eq. 2) in the forced exercise test can be regarded as a measure of the realized or effective anaerobic capacity (AC).

There was a clear trend of increasing anaerobic capacity with increasing body size in all three species (e.g., Fig. 2A). The best fit to the data was with the power relation:

$$\text{(3)} \qquad Y = aX^b$$

where Y is anaerobic capacity (in µM·g^{-1} white muscle) and X is fork length (L) in centimetres. In Atlantic salmon (Fig. 2A) the scaling was to $L^{1.2}$ ($r^2 = 0.931$, $N = 25$); in rainbow trout, to $L^{1.2}$ ($r^2 = 0.379$, $N = 27$); and in brook trout, to $L^{1.6}$ ($r^2 = 0.665$, $N = 10$). When AC is expressed in micromoles (whole body value, calculated assuming that white muscle constitutes 60% of the body weight; Goolish 1989) the corresponding exponents are $L^{4.3}$ (Atlantic salmon), $L^{4.1}$ (rainbow trout), and $L^{4.7}$ (brook trout).

Most of the scaling of anaerobic capacity is due to the scaling of lactate production. In Atlantic salmon, lactate production scaled as $L^{4.6}$ ($r^2 = 0.990$), very similar to the scaling of AC ($L^{4.3}$), while the scaling of ATP depletion was smaller ($L^{3.2}$, $r^2 = 0.503$). In contrast, there was no scaling of PCr depletion. Similar results were obtained for brook trout and rainbow trout, although they were not as clear because of the more limited size range analyzed in both these species.

The large effect of body size on anaerobic capacity made it necessary to apply a size correction before comparing groups of differing sizes. The approach adopted was to scale the data to a common reference length (RL in cm) using the following equation:

$$\text{(4)} \qquad \text{AC}_c = \frac{\text{AC } (\mu\text{M} \cdot \text{g}^{-1})}{\left(\dfrac{\text{length (cm)}}{\text{RL (cm)}}\right)^b}$$

where AC_c is the anaerobic capacity corrected to a reference length and b is the scaling exponent from eq. 3. Anaerobic capacity, when corrected to a reference length of 10 cm, was not significantly different between Atlantic salmon and brook trout (40.5 ± 1.3 and 41.7 ± 2.1 µM·g^{-1}, respectively) but was significantly lower in rainbow trout (35.9 ± 1.2 µM·g^{-1}).

Anaerobic capacity was not correlated with the quantity of anaerobic fuels in white muscle (glycogen, ATP, PCr) in any of the three species. In 0^+ brook and rainbow trout there were no size-related variations in any of these variables. Similarly, in Atlantic salmon, muscle glycogen and ATP levels were nearly the same in 0^+ and 1^+ fish, while PCr levels were actually lower in the 1^+ fish (Fig. 2B).

Anaerobic capacity was, however, correlated with muscle lactate dehydrogenase (LDH) activity, at least in Atlantic salmon (Table 1). Moreover, LDH activity scaled according to body size ($L^{4.7}$, $r^2 = 0.832$, $N = 56$) with a very similar exponent to that for lactate production ($L^{4.6}$). In contrast, PFK activity in Atlantic salmon, which was ≤5% of LDH activity, was unchanged with body size (Table 1).

Recovery from exhaustive exercise

Recovery from exhaustion was characterized in all three species by rapid restoration of PCr, slower recovery of ATP and lactate, and even slower restoration of glycogen (see Fig. 1B for Atlantic salmon example). Moreover, the patterns of

© 1998 NRC Canada

Fig. 1. Changes in muscle glycogen, lactate, PCr (phosphocreatine), and ATP in $\mu M \cdot g^{-1}$ (wet mass) of white muscle in (A) fingerling (age 0^+) rainbow trout during 8 min of exhaustive exercise and in (B) 0^+ Atlantic salmon following 8 min of exhaustive exercise. Note the difference in time scales between (A) and (B). Values are means ± 1 SE. $N = 5$ per point. Rainbow trout were 16.1 ± 0.6 g; Atlantic salmon were 4.3 ± 0.3 g.

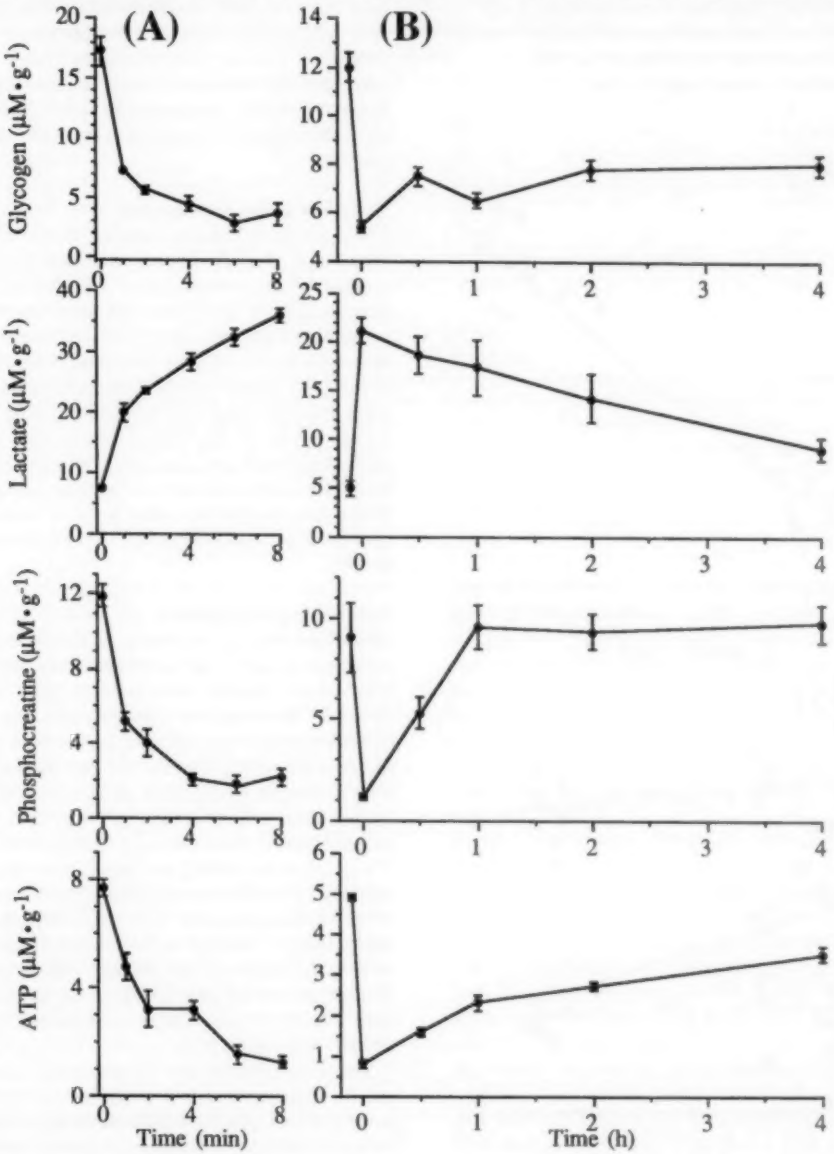

recovery (Fig. 1B) were sufficiently uniform amongst the three species to suggest that the rates of recovery could be described mathematically. For each set of data, various equations were tested; those that provided the best fit to the data for all three species are reported here.

For lactate removal, an exponential relationship ($Y = ae^{bX}$ where Y is lactate concentration, and X is time in h) provided the best fit, and the equation was used to express lactate removal rate (LRR) in terms of percent removal per hour (Table 1). For glycogen recovery, a linear relationship ($Y = bx + a$, where Y is glycogen, and x is time) was used to express glycogen recovery rate (GRR, in $\mu M \cdot g^{-1} \cdot h^{-1}$; Table 1), although for 1^+ salmon and 0^+ rainbow trout, there was no significant recovery of glycogen over the 4-h post-exercise period (Table 1). For ATP recovery, a logarithmic relationship ($Y = aX^b$, where Y is time and X is ATP concentration expressed as percent of rest value) gave the best fit to the data. The resulting equation was used to calculate the time (h) for 50% recovery of ATP (RT_{50} ATP; Table 1). PCr recovery was so rapid that there were not sufficient data points (e.g., Fig. 1) to fit a mathematical expression, so recovery has been expressed qualitatively only (Table 1).

© 1998 NRC Canada

Fig. 2. Effect of body size expressed as fork length (in cm) on (A) anaerobic energy expenditure (AEE) and (B) muscle energy stores (glycogen, ATP, and PCr) in 0^+ and 1^+ Atlantic salmon (5–7 and 10–14 cm, respectively). AEE was determined by eq. 2 (see Materials and methods) on fish sampled immediately after 8 min of exhaustive exercise. The equation for the line in A is AEE = $2.6\,L^{1.2}$, $r^2 = 0.931$, where L is fork length (in cm).

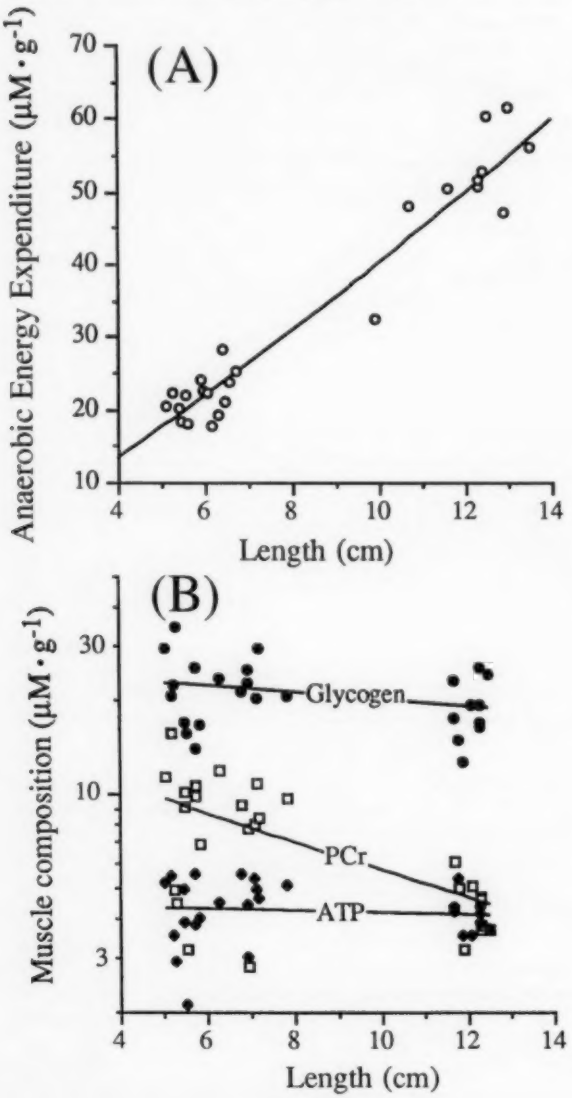

Lactate recovery rate showed a declining trend in Atlantic salmon with increasing body size (from $22\%\cdot h^{-1}$ in 0^+ to $15\%\cdot h^{-1}$ in 1^+), which suggests a possible relation to AEE, i.e., increasing lactate burdens may inhibit lactate metabolism. However, based on interspecific comparisons, there is apparently no fixed relationship between lactate burden and recovery. The LRR for 0^+ rainbow trout was almost double that of 1^+ Atlantic salmon despite the fact that both species exhibited a similar AEE (Table 1).

A clearer trend is evident for the recovery of ATP where within and among species the time to recover 50% of ATP (RT_{50}) increased with increasing AEE. The longer recovery time may, in part, be attributable to a greater reduction in ATP (Table 1). However, the increased depletion of ATP with body size in Atlantic salmon (Table 1) was small compared with the increase in time for recovery of ATP (Table 1). Recovery of PCr was typically faster than ATP recovery but also lengthened in proportion to AEE, at least in Atlantic salmon.

Behavior in swimming tests

The behavior of Atlantic salmon in swimming tests was different from that of rainbow trout and brook trout. Both trout species swam continuously, maintaining station againt the current, usually at midpoint in the swim flume and near one or the other side but always off the bottom, while the salmon showed a more complex behavior. With increasing velocity, salmon alternated between swimming in position, darting forward near the front and holding out near the bottom of the flume. While in the latter position their pectoral fins were splayed outward, and may have been in physical contact with the bottom, although this was not easy to observe from above. While near the bottom, their level of exertion, based on frequency of tail beats, appeared lower than that of the other two species.

Fixed-velocity sprint test

This difference in swimming behavior was reflected in performance in sprint tests at least between the salmon and rainbow trout. Atlantic salmon were able to swim longer at $38\ cm\cdot s^{-1}$ than rainbow trout despite being smaller (Fig. 3A). In both species, fatigue time scaled with body size and the power relation (eq. 3) gave the best fit to the data with Y as time to fatigue (sprint time (ST) in s) and X as body length in centimetres. The unexplained variation was greater in the salmon than in the trout ($r^2 = 0.404$, $N = 30$ vs. $r^2 = 0.635$, $N = 21$), but the scaling exponents were similar and high (5.0 and 3.8 for salmon and rainbow trout, respectively). Brook trout did not exhaust at $38\ cm\cdot s^{-1}$, because they were larger than salmon (7–10 cm vs. 5–7 cm for salmon) so both species were sprinted at a higher velocity ($50\ cm\cdot s^{-1}$). At this speed, all fish exhausted and brook trout, in contrast to rainbow trout, showed comparable swimming performance with Atlantic salmon (Fig. 4).

The large effect of size on sprint performance again necessitated applying a size correction (eq. 4) before comparing groups of differing size. The corrected sprint time (ST_c) was then used in log-probit analysis of time versus percent fatigue data. The resulting relationship (e.g., Fig. 3B) typically gave a good linear fit ($r^2 > 0.98$). The correction of sprint times to a reference length (6 cm) emphasizes the substantial difference in sprint performance between salmon and rainbow trout. The time to 50% fatigue at $38\ cm\cdot s^{-1}$ was 69 ± 5 s in rainbow trout, and 453 ± 24 s in Atlantic salmon (Fig. 3B). In contrast, the size-corrected sprint performance for salmon and brook trout at $50\ cm\cdot s^{-1}$ (Fig. 4) was nearly identical with ST_{50}s of 132 ± 8 (45) s and 113 ± 8 (66) s, respectively after correction to a reference length of 7 cm.

Another major implication of the large scaling coefficient for sprint performance is that it sets a quite narrow limit on

© 1998 NRC Canada

Table 1. Anaerobic energy expenditure (AEE) resulting from exhaustive exercise and, following exercise, glycogen recovery rate (GRR), lactate removal rate (LRR), time to 50% recovery of ATP (RT_{50}), and time to full recovery of phosphocreatine (PCr) in Atlantic salmon fingerlings (0^+) and yearlings (1^+), 0^+ brook trout, and 0^+ rainbow trout.

	Atlantic salmon		Brook trout	Rainbow trout
Age	0^+	1^+	0^+	0^+
Mass (g)	1.9±0.1	20.1±1.3	5.9±0.7	15.9±0.3
Length (cm)	5.7±0.1	12.1±0.4	8.4±0.3	13.4±0.4
AEE ($\mu M \cdot g^{-1}$)	20.8±0.7	51.1±2.6	29.8±3.1	48.0±2.3
% of AEE due to Δlactate	66.6±2.3	88.7±2.1	65.4±4.8	59.3±3.0
GRR ($\mu M\ g^{-1} \cdot h^{-1}$)	ns	0.4	0.6	ns
ΔATP ($\mu M \cdot g^{-1}$)	3.0±0.1	3.7±0.03	4.7±0.1	5.8±0.1
RT_{50} ATP (h)	0.7	3.6	1.4	3.6
Time to full recovery of PCr (h)	0.5	>4	1	1
LDH activity ($nM\ min \cdot g^{-1}$)	350±32	1428±117	—	839±61
PFK activity ($nM\ min \cdot g^{-1}$)	14.5±6.3	17.1±4.0	—	8.0±2.5

Note: AEE was calculated (eq. 2) with the data from 20 fish (10 before exercise and 10 at $t = 0$); lactate recovery rate (LRR), glycogen recovery rate (GRR), and time to 50% recovery (RT_{50}) for ATP were calculated with equations described in the text using all post-exercise measurements ($T = 0$, 0.5, 1, 2, and 4 h; $N = 30$). Δlactate and ΔATP refer to differences pre-exercise and immediately post-exercise in muscle lactate and ATP levels, respectively. ns, regressions were not significant.

the range of body lengths that can be tested at any one sprint velocity. At the low end of the range of sizes, fish will exhaust too quickly for reliable estimation of sprint duration, while at the upper end a threshold size is quickly reached beyond which fish will not exhaust. For example, at a test velocity of 38 $cm \cdot s^{-1}$ the testable size range for Atlantic salmon was approximately 4.5–6.5 cm, with sprint times varying from under 1 min to over 10 min (see Fig. 3). Only slightly beyond 6.5 cm in length, fish did not exhaust in this test, at least within 60 min. Those fish not exhausting had an average body length of 6.6 ± 0.1 cm ($N = 11$, 3.04 ± 0.1 g).

Effect of sprint speed on the scaling of sprint performance

The 0^+ salmon were sprinted at three different velocities (38, 50, and 62 $cm \cdot s^{-1}$) and while the time to 50% fatigue declined with increasing velocity (291, 77, and 39 s, respectively, uncorrected for body size variations) the scaling exponents were relatively uniform ($L^{5.0}$, $L^{4.6}$, $L^{5.4}$, respectively) as was the unexplained variation ($r^2 = 0.404$, 0.356, 0.449, respectively).

Is sprint performance reproducible in Atlantic salmon?

The superior sprint performance of Atlantic salmon could be more a function of their ability to avoid swimming rather than greater stamina. Consequently, the fraction of time avoiding current could vary from trial to trial, and thus their apparent endurance could be unpredictable. Certainly, a larger amount of unexplained variation in sprint performance (i.e., lower r^2) was characteristic of salmon compared with the trout species. This unpredictability was tested by repeated sprinting a group of twenty 0^+ Atlantic salmon (Fig. 5). On the basis of their initial sprint performance (not shown) the 20 were subdivided into an upper and lower performance group of 10 each. Then each group was sprinted daily for four successive days. As shown (Fig. 5) the performance of the two groups remained separated over time confirming that, despite the variability, sprint performance was, in fact, reproducible. The improvement in performance over time in the upper group is consistent with recent observations on rainbow trout (W.J. McFarlane and D.G. McDonald, unpublished data), although the change was modest in the salmon compared with the trout.

Anaerobic energy expenditure during fixed-velocity sprint tests

In the fixed-velocity tests, fish were removed and sampled when they could no longer be stimulated into resuming swimming, although brief muscular contractions could still be evoked. AEE (in μmoles) in these tests scaled according to size in a fashion similar to that for forced exercise, but AEE was typically submaximal and was more variable. This is illustrated for Atlantic salmon in Fig. 6 for the fixed-duration test versus a fixed-velocity test at 62 $cm \cdot s^{-1}$. Scaling coefficients were $L^{4.0}$ versus $L^{3.9}$ and r^2 values were 0.907 versus 0.382 for the forced-exercise and fixed-velocity tests, respectively.

All salmon exhausted at 62 $cm \cdot s^{-1}$ but not at 38 $cm \cdot s^{-1}$ (5.8 $BL \cdot s^{-1}$). Those that did not exhaust at the latter velocity exhibited virtually no AEE (–0.1 ± 1.4 $\mu M \cdot g^{-1}$, $N = 11$) when sampled at 60 min, the end of the test. This suggests that anaerobic expenditure only occurred with the onset of exhaustion.

Incremental-velocity test

Maximum swimming speed (MSS), as determined by the incremental-velocity test, scaled with body size (Fig. 7) but with a much smaller exponent ($L^{1.4}$ in salmon; $L^{1.3}$ in brook trout) than sprint performance in the fixed-velocity test ($L^{\sim 5.0}$). The unexplained variability in performance of Atlantic salmon was also much larger in the incremental-velocity test than in the fixed-velocity test ($r^2 = 0.171$, $N = 50$

© 1998 NRC Canada

Fig. 3. (A) Scaling of sprint times to body size in Atlantic salmon (open symbols, $N = 30$) and rainbow trout (solid symbols, $N = 21$) sprinted at 38 cm·s^{-1}. Curves are $Y = 0.06X^{5.0}$, $r^2 = 0.404$ and $Y = 0.09X^{3.8}$, $r^2 = 0.635$ for salmon and trout, respectively. Scaling exponents were then used to correct sprint times to a reference length of 6 cm using eq. 4. (B) Log-probit regressions for corrected sprint times from Fig. 3A. Atlantic salmon (open symbols), rainbow trout (solid symbols). Equations are $Y = 0.20X + 1.64$, $r^2 = 0.987$; $Y = 0.16X + 1.06$, $r^2 = 0.962$, for salmon and trout, respectively.

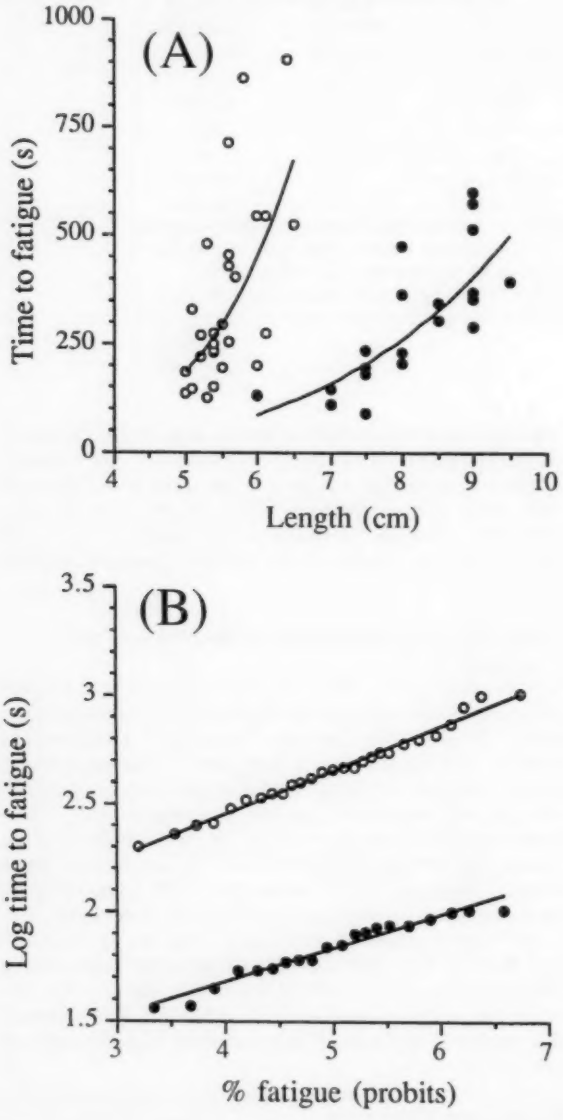

compared with $r^2 = 0.404$, $N = 30$, Fig. 3A) and was also substantially larger than that seen in brook trout (Fig. 7; $r^2 = 0.692$, $N = 50$). In this test, Atlantic salmon showed significantly better performance compared with brook trout, in contrast to the fixed-velocity test (Fig. 4) where the performance of the two species was similar. Corrected to a reference length of 7 cm, the MSS of salmon was 60 ± 1 cm·s^{-1} compared with 46 ± 1 cm·s^{-1} in brook trout.

Fig. 4. Scaling of sprint times to body size in 0$^+$ Atlantic salmon (open symbols, broken line, $N = 58$) and 0$^+$ brook trout (solid symbols, solid line, $N = 35$) sprinted to exhaustion at 50 cm·s^{-1}. Equations are $Y = 0.018X^{4.6}$, $r^2 = 0.356$ and $Y = 0.001X^{6.2}$, $r^2 = 0.810$ for salmon and trout, respectively.

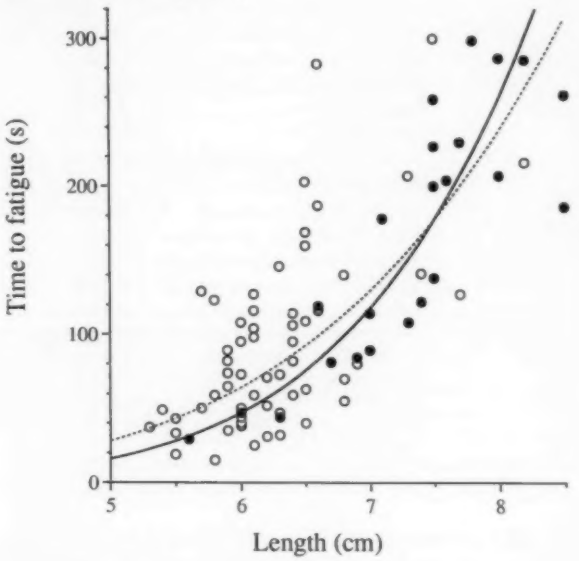

Discussion

Although scaling relationships have been widely reported for anaerobic metabolism (e.g., Somero and Childress 1980, 1990; Childress and Somero 1990; Goolish 1989, 1991; Ferguson et al. 1993) and for swimming performance (e.g., Beamish 1978; Hammer 1995 for reviews), this study is the first to compare the outcomes of the various tests with one another in three different species. As a result of this approach, we are now able to make a number of recommendations for the assessment of exercise performance in juvenile salmonids, including which test to use, as well as incorporating corrections for scaling effects especially when comparing groups of different size. These recommendations should improve our ability to determine intrinsic species differences as well as assess variations within species attributable to either rearing environment or genetics.

Fixed-duration test

In this test, fish were exercised manually for a fixed period (8 min), and the measures of performance were the utilization of anaerobic fuels (summarized by the calculation of AEE) and the rates of recovery of lactate, ATP, and PCr.

The procedure passed an important criterion for a performance test, in that it produced a uniform result. Lactate production and the depletion of glycogen, ATP, and PCr were all uniform within and amongst species even though the test was administered to groups of 10 fish at a time rather than singly as in previous studies. Furthermore, AEE scaled more

© 1998 NRC Canada

Fig. 5. Time to 50% fatigue (estimated by log-probit regression, see Fig. 3B) for 0+ Atlantic salmon sprinted twice daily for four successive days. Salmon were subdivided into two groups (upper and lower, $N = 10$ each) based on their individual performance in the first sprint (not shown).

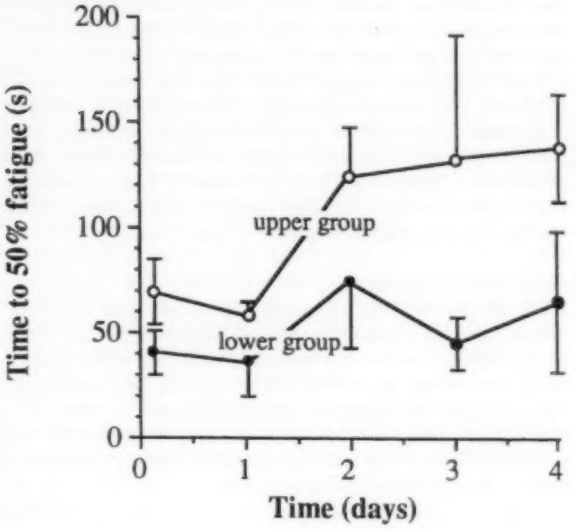

Fig. 6. Comparison of anaerobic energy expenditure (AEE in micromoles) in 0+ Atlantic salmon between the fixed duration (8 min) maximum exertion test (solid symbols) and the fixed velocity sprint test at 62 $cm \cdot s^{-1}$ (open symbols). For the fixed-duration test, the equation is $Y = 0.027X^{4.0}$, $r^2 = 0.907$ ($N = 14$); for the fixed-velocity test, the equation is $Y = 0.018X^{3.9}$, $r^2 = 0.382$ ($N = 21$).

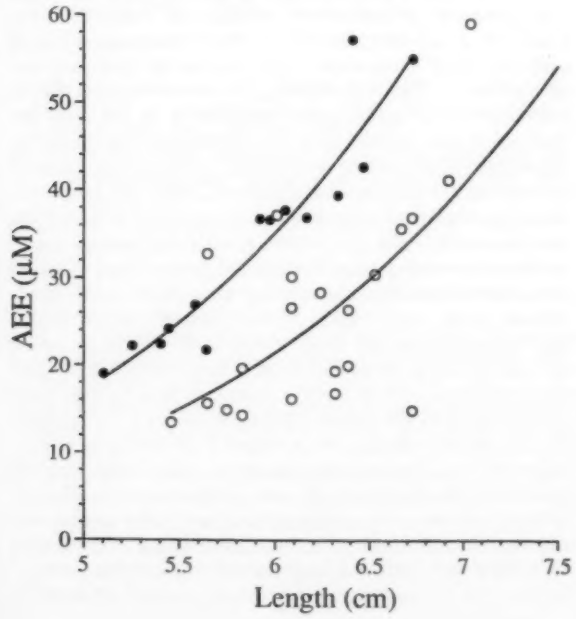

Fig. 7. Incremental-velocity test on 0+ Atlantic salmon (open symbols) and brook trout (solid symbols). Equations are $Y = 4.10X^{1.36}$, $r^2 = 0.171$ ($N = 50$) and $Y = 3.53X^{1.33}$, $r^2 = 0.692$ ($N = 50$) for salmon and trout, respectively.

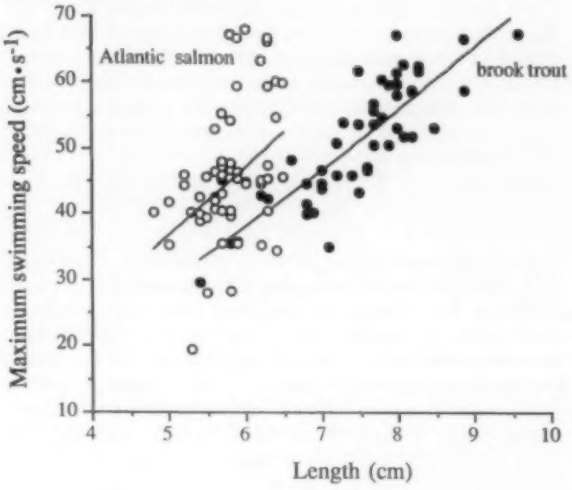

closely with body size (i.e., with a higher r^2) in this maximum exertion test than did AEE in the fixed-velocity tests (Fig. 6), where cessation of swimming activity was voluntary. This finding supports the conclusion that fuel depletion was maximum, a conclusion confirmed by the sequential sampling of white muscle through the 8-min forced exercise period (Fig. 1A). Hence we are able to conclude that the AEE calculated in this test is, in effect, a measure of anaerobic capacity.

Body size was the major factor determining anaerobic capacity in all three species. Moreover, the corresponding coefficients for the scaling of AC (in μmoles of ATP equivalents in white muscle) were relatively uniform ($L^{4.3}$, $L^{4.1}$, and $L^{4.7}$, for Atlantic salmon, rainbow trout, and brook trout, respectively).

Much of the scaling, at least in Atlantic salmon, was due to lactate production ($L^{4.6}$). Since glycogen did not scale to body size, the increase in lactate production must be due to greater anaerobic glycolysis, which in turn, would be related to the activities of the glycolytic enzymes and (or) the capacity of the muscle to buffer acidic end products.

Lactate dehydrogenase is likely to have played a key role in anaerobic scaling, since its scaling coefficient in salmon was virtually identical to that of lactate production ($L^{4.7}$ vs. $L^{4.6}$, respectively). But LDH is not the rate-limiting enzyme in glycolysis, and the activity of PFK, which is regarded as the rate-limiting enzyme (Bonen et al.1989), was independent of body size (Table 1). However, PFK is highly allosterically regulated in vivo (Su and Storey 1994), regulation that would not be apparent in the in vitro assays performed here.

In other species, there has been some evidence of scaling of muscle buffering capacity as well: in the marine pelagic teleost, *Paralax clathratus* (Somero and Childress 1990) but not in rainbow trout (Ferguson et al. 1993). Obviously, the mechanism underlying anaerobic scaling in salmonids is more complex than that presented here. Nonetheless, the results indicate that LDH activity is a good surrogate for

© 1998 NRC Canada

anaerobic capacity in salmonid muscle especially since it is probably the easiest of the glycolytic enzymes to measure.

Once scaling corrections are applied, the fixed-duration test can be used to evaluate intra- and inter-specific differences. Such comparisons reveal, for example, that the domestic rainbow trout had a lower anaerobic capacity than either salmon or brook trout, which correlated with its lower performance in the fixed-velocity sprint tests (see below). Furthermore, the similarity of AC between the salmon and brook trout was reflected in their similar performance in fixed-velocity tests (Fig. 4).

The analysis of the recovery from the test suggests some clear possibilities for other measures of performance. The rates of recovery of glycogen, ATP, and lactate were sufficiently uniform amongst and within species (Fig. 1B) that the rates could be captured with simple mathematical expressions (Table 1). Furthermore, the different rates are, at least to some extent, independent of one another. For example, rainbow trout exhibited a relatively high rate of lactate recovery but no significant glycogen recovery, while 1^+ salmon showed a relatively low rate of lactate recovery, but significant glycogen recovery. Thus, the possibility exists that each could serve as a performance measure. Certainly, from an ecological standpoint the speed of recovery from anaerobic activity is likely to be just as significant to predator avoidance and prey capture as anaerobic capacity.

Fixed-velocity test

This test also met important criteria for a performance test; it was rapid (velocities can be chosen that will produce exhaustion quickly, and the test can be performed on groups of fish), the outcome was predictable (most of the variability was explained by scaling with body size, especially in the trout species where $r^2 > 0.6$), and sprint times were reproducible. Although the large scaling coefficient necessitated correcting sprint times to a reference length to compare fish of different size, the scaling coefficient was relatively insensitive to test velocity or to species. In Atlantic salmon, the exponent varied little over a range in sprint speeds from 38 to 62 $cm \cdot s^{-1}$ ($L^{5.0}$–$L^{5.4}$). Moreover, amongst the three species the scaling coefficients all fell within the range $L^{4.0}$–$L^{6.0}$. There is only one other study of which we are aware that has examined the scaling of endurance time to body size for sprints at constant velocity, and that was by Boyar (1961). He showed that sprint duration in immature Atlantic herring (*Clupea harengus*) scaled as L^4 and that the exponent was the same for the three test velocities employed. This relative uniformity in scaling both within and amongst species simplifies the task of correcting size differences between comparison groups. In any case, using a exponent of 4–6 to correct sprint times to a reference length (eq. 4) is preferable to that used in previous studies where either no scaling correction was applied (e.g., Houlihan and Laurent 1987) or sprint times were scaled directly to mass (as $s \cdot g^{-1}$; e.g., Nahhas et al. 1982; Mitton and McDonald 1994). If either of the latter approaches is used then comparisons between groups that differ even slightly in body size could be misleading.

Probably the major limitation of this test is the limited range of body sizes that can be tested at any one velocity, a product of the large scaling coefficient. For example, the useful size range was only 4.5–6.5 cm fork length for Atlantic salmon tested at 38 $cm \cdot s^{-1}$. This means that if groups of differing sizes are being compared, they should at least partially overlap in size range and a test velocity chosen that produces exhaustion over the entire size range of the two groups.

AEE was less than maximal in the fixed-velocity sprint test. Nonetheless, it scaled to body size in a similar fashion to that seen in the fixed-duration test (Fig. 6). Therefore, performance in this test can be used as a nondestructive approximation of anaerobic capacity. However, the fraction of the maximal AEE or anaerobic capacity utilized in a sprint to exhaustion may vary from species to species and with variations in rearing conditions. Thus, in any detailed application of the sprint test, it would be worthwhile to first examine the relationship between anaerobic capacity in the fixed duration test and AEE in voluntary sprints to exhaustion.

Incremental-velocity test

Although this test took longer to administer than the fixed-velocity test; it overcomes the size range limitations of the fixed-velocity test. In any case, the limitation in the present study was not the test per se but the upper speed of the swim flume. Furthermore, the test met an important criterion for a practical screening tool in that it could be performed on groups of fish and still produce uniform results (especially in brook trout; Fig. 7).

Again, the major determinant of performance in this test was body size. Furthermore, the scaling to body size was very similar for Atlantic salmon and brook trout; $L^{1.4}$ and $L^{1.3}$, respectively. These are large exponents in comparison with those obtained in more conventional versions of the incremental velocity test where each increment is $\geq$20 min in duration and fish are exercised singly. For the latter tests, most of the scaling exponents fall within the range of $L^{0.4}$–$L^{0.6}$ (see Beamish 1978; Videler and Wardle 1991; Hammer 1995 for reviews). We interpret our higher values as indicating that our test is measuring a different end point from the conventional tests. Maximum swimming speed (or U_{crit}) in the conventional incremental-velocity test is assumed to be a measure of aerobic capacity. In other words, once U_{crit} is achieved, oxygen consumption has reached its maximum sustainable value. The steeper scaling in our test suggests that, in contrast, there is an anaerobic contribution to the endpoint. This conclusion follows from the observation that anaerobic metabolism scales with a much larger exponent than aerobic metabolism (cf. Somero and Childress 1980). We also conclude that the endpoint in this test is, in turn, different from that measured in the fixed-velocity test. This conclusion is based on two observations. Firstly, fish swam longer at higher speeds in the incremental-velocity trials than in the fixed-velocity trials. For example, 50% of Atlantic salmon fingerlings had exhausted by about 2 min in the 50 $cm \cdot s^{-1}$ sprint but did not exhaust in the incremental-velocity trial until speeds in excess of 60 $cm \cdot s^{-1}$ were reached, having spent 5 min at each of the increments below 60 $cm \cdot s^{-1}$. Secondly, the incremental-velocity test revealed a difference in performance between brook trout and salmon (Fig. 7) that was not apparent in the fixed-velocity test on these species (Fig. 4). Although we have not attempted to quantify the aerobic and anaerobic contributions to performance in each of these tests we suggest that there is a larger aerobic contribution to performance in the incremental-velocity test compared with the

© 1998 NRC Canada

fixed-velocity test. This discriminates the short duration increment incremental-velocity test from the fixed-velocity test and, in turn, from the more conventional version of the incremental-velocity test.

Conclusions

We therefore conclude that each of the tests in this study measures a different aspect of swim performance in salmonids. The fixed-duration test is especially useful for assessing the maximum anaerobic fuel reserves (which may not be entirely exploited in voluntary sprints to exhaustion) and for assessing rates of recovery, while the fixed-velocity and incremental-velocity tests are useful for assessing anaerobic and aerobic performance in voluntary swims to exhaustion. Furthermore, the latter tests are nondestructive and thus can be used as screening or selection tools. Since body size explained only 40–70% of the variation in swim performance in these tests, the remaining variation probably reflects real interindividual physiological differences. Thus, the tests could be used to select individuals for high or low swim performance. Such selection would have applications in a variety of contexts, including experimental hatchery-rearing programs (McDonald et al. 1998) and studies of the relationship between swim performance and performance in other physiological processes such as growth, osmoregulation, and stress resistance.

Acknowledgments

The authors thank Dr. Tina Kieffer and Mrs. Vandy Thomas for excellent technical assistance and the manager and staff of Cardigan Salmonid Enhancement Centre for their help and hospitality. This work was supported by grants from Natural Sciences and Engineering Research Council of Canada (NSERC) and Department of Fisheries and Oceans Canada (DFO) to D.G.M. and C.L.M. under the NSERC operating grant and DFO–NSERC Science Subvention programs.

References

Arnold, G.P., Webb, P.W., and Holford, B.H. 1991. The role of the pectoral fins in station holding of Atlantic salmon parr (*Salmo salar* L.). J. Exp. Biol. **156**: 625–629.

Beamish, F.W.H. 1978. Swimming capacity. *In* Fish physiology. Vol. 7. *Edited by* W.S. Hoar and D.J. Randall. Academic Press, New York. pp. 101–187.

Bergmeyer, H.U. 1983. Methods of enzymatic analysis. Verlag Chemie, Basel, Switzerland.

Bonen, A., McDermott, J.C., and Hutber, C.A. 1989. Carbohydrate metabolism in skeletal muscle: an update of current concepts. Int. J. Sports Med. **10**: 385–401.

Boyar, H.C. 1961. Swimming speeds of immature Atlantic herring with reference to the Passamaquoddy Tidal Project. Trans. Am. Fish. Soc. **90**: 21–26.

Brett, J.R. 1964. The respiratory metabolism and swimming performance of young sockeye salmon. J. Fish. Res. Board Can. **21**: 1183–1226.

Brett, J.R. 1967. Swimming performance of sockeye salmon (*Oncorhynchus nerka*) in relation to fatigue time and temperature. J. Fish. Res. Board Can. **24**: 1731–1741.

Childress, J.J., and Somero, G.N. 1990. Metabolic scaling: a new perspective based on the scaling of glycolytic enzyme activities. Am. Zool. **30**: 161–173.

Ferguson, R.A., Kieffer, J.D., and Tufts, B.L. 1993. The effects of body size on the acid–base and metabolite status in the white muscle of rainbow trout before and after exhaustive exercise. J. Exp. Biol. **180**: 195–207.

Gibson, R.J. 1993. The Atlantic salmon in fresh water: spawning, rearing and production. Rev. Fish Biol. Fish. **3**: 39–73.

Goolish, E.M. 1989. The scaling of aerobic and anaerobic muscle power in rainbow trout, (*Salmo gairdneri*). J. Exp. Biol. **147**: 493–505.

Goolish, E.M. 1991. Aerobic and anaerobic scaling in fish. Biol. Rev. Camb. Philos. Soc. **66**: 33–56.

Graham, W.D., Thorpe, J.E., and Metcalfe, N.B. 1996. Seasonal current holding performance of juvenile Atlantic salmon in relation to temperature and smolting. Can. J. Fish. Aquat. Sci. **53**: 80–86.

Hammer, C. 1995. Fatigue and exercise tests with fish. Comp. Biochem. Physiol. **112A**: 1–20.

Hassid, W.Z., and Abraham, S. 1957. Chemical procedures for analysis of polysaccharides. *In* Methods in enzymology. *Edited by* S.P. Colowick and N.O. Kaplan. Academic Press, New York. pp. 34–37.

Houlihan, D.F., and Laurent, P. 1987. Effects of exercise training on the performance, growth and protein turnover of rainbow trout. Can. J. Fish. Aquat. Sci. **44**: 1614–1621.

McDonald, D.G., Milligan, C.L., McFarlane, W., Croke, S., Currie, S., Hooke, B., Angus, R., Tufts, B.L., and Davidson, K. 1998. Condition and performance of juvenile Atlantic salmon (*Salmo salar*): effects of rearing conditions on hatchery fish and comparison to wild fish. Can. J. Fish. Aquat. Sci. **55**. This issue.

McNeish, J.D., and Hatch, R.W. 1978. Stamina tunnel tests on hatchery-reared Atlantic salmon. Prog. Fish Cult. **40**: 116–117.

Milligan, C.L. 1996. Metabolic recovery from exhaustive exercise in rainbow trout. Comp. Biochem. Physiol. **113A**: 51–60.

Mitton, C.J.A., and McDonald, D.G. 1994. Effects of electroshock, air exposure and enforced exercise on swim performance in rainbow trout (*Oncorhynchus mykiss*). Can. J. Fish. Aquat. Sci. **51**: 1799–1803.

Nahhas, R., Jones, N.V., and Goldspink, G. 1982. Some aspects of sustained training of rainbow trout, *Salmo gairdneri* Richardson. J. Fish Biol. **20**: 351–358.

Pearson, M.P., Spriet, L.L., and Stevens, E.D. 1990. Effect of sprint training on swim performance and white muscle metabolism during exercise and recovery in rainbow trout. J. Exp. Biol. **149**: 45–60.

Rimmer, D.M., Saunders, R.L., and Paim, U. 1985. Effects of temperature and season on the position holding performance of juvenile Atlantic salmon *Salmo salar*. Can. J. Zool. **63**: 92–96.

Shonk, C.E., and Boxer, G.E. 1964. Enzyme patterns in human tissue. I. Methods for the determination of glycolytic enzymes. Cancer Res. **24**: 709–724.

Somero, G.N., and Childress, J.J. 1980. A violation of the metabolism-size scaling paradigm: activities of glycolytic enzymes increase in larger-size fish. Physiol. Zool. **53**: 322–337.

Somero, G.N., and Childress, J.J. 1990. Scaling of ATP-supplying enzymes, myofibrillar proteins and buffering capacity in fish muscle: relationship to locomotory habit. J. Exp. Biol. **149**: 319–333.

Su, J.Y., and Storey, K.B. 1994. Regulation of rainbow trout white muscle phosphofructokinase during exercise. Int. J. Biochem. **4**: 519–528.

Videler, J.J., and Wardle, C.S. 1991. Fish swimming stride by stride: speed limits and endurance. Rev. Fish Biol. Fish. **1**: 23–40.

Wood, C.M., and Perry, S.F. 1985. Respiratory, circulatory and metabolic adjustments to exercise in fish. *In* Comparative physiology and biochemistry—current topics and trends. *Edited by* R. Gilles. Springer-Verlag, Berlin. pp 1 –21.

Vogel, S. 1981. Life in moving fluids: the physical biology of flow. Princeton University Press, Princeton, N.J. pp 297–302.

© 1998 NRC Canada

Condition and performance of juvenile Atlantic salmon (*Salmo salar*): effects of rearing practices on hatchery fish and comparison with wild fish

D.G. McDonald, C.L. Milligan, W.J. McFarlane, S. Croke, S. Currie, B. Hooke, R.B. Angus, B.L. Tufts, and K. Davidson

Abstract: This study examined the effects of various modifications of rearing practices on hatchery-reared Atlantic salmon (*Salmo salar*) fingerlings and compared condition and performance of hatchery fingerlings (age 0^+) and yearlings (age 1^+) with those of wild-reared Atlantic salmon. Reduced fish density (and increased ration) in rearing tanks promoted increased growth and condition factor and significant changes in muscle composition, including increased muscle lipid content and glycolytic enzyme activity, specfically phosphofructokinase and lactate dehydrogenase. However, these changes had no effect on anaerobic capacity. Moreover, swimming performance was poorer in fingerlings reared at low compared with normal density. Raising the water velocity from 0 to 4 $cm \cdot s^{-1}$ (~0.7 body length$\cdot s^{-1}$) had overall beneficial effects, most notably increased endurance in fixed velocity sprint tests and a reduction of ion loss in an epinephrine challenge test. Increasing velocity to 9 $cm \cdot s^{-1}$ had no further effects. Wild fingerlings were larger with better fin quality and superior anaerobic capacity and swim performance. Even larger differences were seen between hatchery-reared and wild yearlings. It is concluded that significant changes in morphology, physiology, and muscle biochemistry of juvenile Atlantic salmon can be brought about by changing hatchery rearing conditions, but these changes are of limited effectiveness in reducing the difference between hatchery-reared and wild fish.

Résumé : On examine dans la présente études les effets de diverses modifications de méthodes d'élevage sur des juvéniles de saumon atlantique (*Salmo salar*) d'élevage, et on compare la condition et la performance de juvéniles (0^+) et de saumoneaux de 1 an (1^+) à celles de saumons atlantiques sauvages. La réduction de la densité des poissons (et une augmentation de la ration) dans les bassins d'élevage a donné lieu à une hausse de la croissance et du coefficient de condition, ainsi qu'à des changements marqués dans la composition masculaire, notamment un acroissement de la teneur en lipide et de l'activité des enzymes de la glycolyse, notamment la phosphofructokinase et la lacticodéshydrogénase. Mais ces changements n'avaient aucun effet sur la capacité anaérobie. De plus, la performance de nage était moins bonne chez les juvéniles élevé à de faibles densités que chez ceux élevés à des densités normales. Une augmentation de la vitesse du débit de 0 à 4 $cm \cdot s^{-1}$ (~0,7 longueur de corps$\cdot s^{-1}$) a eu des effets globalement bénéfiques, notamment une endurance accrue dans les épreuves de sprint à vitesse fixe et une réduction de la perte d'ions dans un test à l'épinéphrine. Une augmentation de la vitesse du débit à 9 $cm \cdot s^{-1}$ n'avait aucun effet additionnel. Chez les juvéniles sauvages, qui étaient plus gros, les nageoires étaient en meilleur état; en outre, la capacité anaérobie et la performance de nage étaient supérieures. Les différences étaient encore plus marquées chez les aaumoneauz d'un an selon qu'ils étaient d'élavage ou sauvages. On conclut que l'on peut apporter des changements importants dans la morphologie, la physiologie et la biochimie musculaire des jeunes saumons atlantiques en changant les conditions d'élevage, main l'efficacité de ces changements est limitée pour ce que est de réduire la différence entre le poisson d'élevage et le poisson sauvage.
[Traduit par la Rédaction]

Received May 5, 1997. Accepted December 19, 1997.
J14004

D.G. McDonald,[1] **W.J. McFarlane, and S. Croke.** Department of Biology, McMaster University, 1280 Main St. West, Hamilton, ON L8S 4K1, Canada.
C.L. Milligan and B. Hooke. Department of Zoology, University of Western Ontario, London, ON N6A 5B7, Canada.
S. Currie and B.L. Tufts. Department of Biology, Queen's University, Kingston, ON K7L 3N6, Canada.
R.B. Angus. Department of Fisheries and Oceans, Cardigan Salmonid Enhancement Centre, R.R. 3, Cardigan, PE C0A 1G0, Canada.
K. Davidson. Department of Fisheries and Oceans, Gulf Fisheries Centre, P.O. Box 5030, Moncton, NB E1C 9B6, Canada.

[1] Author to whom all correspondence should be addressed. e-mail: mcdonald@mcmail.mcmaster.ca

© 1998 NRC Canada

Introduction

Hatchery supplementation programs are widely used for the rehabilitation and enhancement of native salmonid populations (Coux 1994; Stickney 1994). Nonetheless, it is widely recognized that hatchery-reared salmonids perform less well in the wild than wild-reared fish. Decreased performance manifests as reduced survival to reproductive age and much reduced marine returns (as little as 25% the return rates of wild smolts; Coux 1994). Stickney (1994) argued that radical changes in fish cultural practices are required, in essence, to rear wild fish in a hatchery environment. Such a program requires providing the appropriate genetic diversity and rearing environment for nurturing wild-type behaviors and physiology. The present study is confined to the cultural aspects of such a program, improving condition and performance of hatchery-reared fish through altering rearing practices.

This task requires a detailed knowledge of how the physiological systems of hatchery-reared fish and wild fish differ from one another, how and to what extent rearing practices modify those systems, and the development of techniques to assess condition and performance. The present study has two interrelated objectives: to determine the manner and extent to which alterations in rearing practices can alter morphology, biochemical composition, and (or) physiology of the juvenile Atlantic salmon (*Salmo salar*) and to evaluate whether the observed change can be interpreted as a change in either condition or performance and therefore be relevant to survival in the wild. We addressed the latter objective by using, as a benchmark for comparison, wild-reared Atlantic salmon from the same brood stock and of the same age as hatchery fish, reasoning that wild-reared fish are, by definition, better conditioned for life in the wild. Condition was assessed largely on the basis of biochemical measures (muscle metabolites, glycolytic enzyme activities, whole-body electrolytes). Performance was assessed on the basis of responses to tests of anaerobic capacity and swim performance, developed and refined in a companion study (McDonald et al. 1998), and to an integrated test of acute stress response (an epinephrine challenge test).

Rearing experiments consisted of examining the effects of rearing density and velocity. The principal effect of reducing density in Atlantic salmon is to stimulate growth, an effect thought to result from the reduction of intraspecific agression (Fenderson and Carpenter 1971) and possibly freer movement and therefore greater food availability (Refstie and Kittelsen 1976). Rearing in currents of $\geq$1 body length (BL)·s^{-1} has more complicated effects, but again, increased growth rates are a common observation in Atlantic salmon (Totland et al. 1987; Jørgensen and Jobling 1993) and other salmonids (reviewed by Davison 1989; Jobling et al. 1993). It is also believed to reduce stress in part through a reduction in negative social interactions (East and Magnan 1987; Jørgensen and Jobling 1993). Whether it also improves swim performance is less certain. This relationship has not been studied in Atlantic salmon, and in other salmonids, there has been no consistent response. Some studies report beneficial effects on endurance, or maximum sustainable swimming speed or rates of recovery (reviewed in Davison 1989), while others report virtually no change in performance, even though the exposure to elevated current was over several months (e.g., Kiessling et al. 1994).

Materials and methods

Experimental animals

Experiments were carried out in the summers of 1994–1996 at Cardigan Salmonid Enhancement Centre, Cardigan, P.E.I., a Department of Fisheries and Oceans facility rearing Atlantic salmon from wild-caught brood stock for stocking in Prince Edward Island rivers. The Morell River (0.27 mM NaCl, 0.53 mM Ca^{2+}) in Prince Edward Island was the source of the brood stock and the Cardigan River (0.2 mM Na^+, 0.14 mM Cl^-, 0.49 mM Ca^{2+}) the source of water for the hatchery. Wild Atlantic salmon fingerlings (age 0$^+$) and yearlings (age 1$^+$) were obtained by electrofishing. Fingerlings (N = 117) were obtained from the Morell River and yearlings (N = 69) from the Valleyfield River (0.11 mM Na^+, 0.17 mM Cl^-, 0.53 mM Ca^{2+}). The Valleyfield River was sampled in late August 1994 and 1996; temperature was 11–14°C and flow in midchannel was 40–60 cm·s^{-1}. The Morell River was sampled in late August 1995 and 1996; fingerlings were in a shallow, rocky riffle, flow varied from 30 to 145 cm·s^{-1}, and temperature was 14–15°C. Fish were transferred to holding in the laboratory for 1 week prior to use. Water velocities were measured with a Marsh–McBirney model 2000 electromagnetic flowmeter with an accuracy of ±2%.

Atlantic salmon in the hatchery were hatched from late fall egg collections from brood stock collected from the Morell River. Median hatch date in the hatchery was 10 April; Atlantic salmon in Prince Edward Island rivers typically hatch about 2 weeks later. Atlantic salmon are normally reared in the hatchery for about 1 year and are then transferred to seminatural rearing ponds in mid-June for smoltification and release the following spring. A subset of about 10 000 age 1$^+$ fish was held back at the hatchery each year until September for experimentation.

Rearing trials

The experimental rearing trials consisted of modifying existing rearing practice, with existing practice acting as control (i.e., normal density, normal velocity: NDNV). The current practice at Cardigan is to transfer fingerlings, when they reach about 1 g body mass, from early rearing units to 3 × 3 m rounded-corner "Swede" tanks (Isaksson 1991). Swede tanks are centre drain, with a bottom surface area of 9.3 m^2 and filled to a depth of 47 cm. Normally, tanks are stocked with about 10 000 fish per tank, and flow to tanks is adjusted to 32 L·min^{-1}. Flow into the tank is normally directed to the side of the tank to create a circular current, averaging 4.3 cm·s^{-1}. Average velocity was computed from measurements taken along concentric circles from planes 10 and 30 cm from tank bottoms and a simple arithmetic mean of all measurements was calculated. Fish in the hatchery were hand-fed to satiation at least four times a day. The duration of each feeding time was about 10 min per tank, and food was offered to the point at which uneaten food would just begin to appear on the tank bottom. Each tank was fed in the same fashion, irrespective of rearing trial, and the ration that each tank received was not recorded, nor was any attempt made to standardize the feeding rates among various rearing trials.

Three modifications of normal rearing practice (i.e., NDNV) were made, a lower density (LD) and two different current regimes: "zero" velocity (0V) and high velocity (HV). For the LD treatment, tanks were stocked with 5000 instead of 10 000 fish. For the 0V treatment, the flow into the tank was kept at about 32 L·min^{-1} but was directed straight down. For the HV treatment, flow to the tank was increased to 91 L·min^{-1} which created an average flow of 9 cm·s^{-1}. Fish were sampled after $\geq$50 days of rearing under these conditions. In 1994 the treatments were NDNV, ND0V, NDHV, and LDNV, in 1995 the treatments were NDNV, ND0V, NDHV, LDNV, LD0V, and LDHV; and in 1996 the treatments were NDNV and LDNV.

Whenever fish were sampled, all fish in the rearing tank were gently crowded by seine net into a small section of the tank and then sampled by dip net. This was done to minimize sampling stress (fish

© 1998 NRC Canada

were not chased when sampling) and to ensure random sampling of the population. The water temperature at the time of sampling was 9–12°C. All fish handling was done in accordance with the Canadian Council of Animal Care guidelines.

Measures of condition

Condition factor

Condition factor (CF) was calculated according to the following formula:

$$(1) \qquad CF = \frac{Mass}{FL^{exp}} \times 100.$$

Mass was measured to the nearest 0.1 g and fork length (FL) to the nearest millimetre. A different exponent was used in calculating condition factor for fingerlings and yearlings. The exponents were derived from the length–mass relationships on hatchery-reared 0^+ and 1^+ Atlantic salmon:

0^+: mass (g) = 0.008 length (cm)$^{3.18}$ (N = 1244, r^2 = 0.960)
1^+: mass (g) = 0.018 length (cm)$^{2.82}$ (N = 268, r^2 = 0.962).

Normally, condition factor is calculated with an exponent of 3 (e.g., Busacker et al 1990). However, condition factor will vary with body mass if the exponent is not the same as the length versus mass exponent, and in this study, comparisons are being made among groups of differing body mass.

Pectoral fin condition

Erosion of the fins, particularly the pectoral fins, is a common feature of hatchery-reared Atlantic salmon (e.g., Soderberg and Meade 1987). The degree of fin erosion relative to wild-caught fish was assessed as follows. On wild fish (6.2–16.0 cm FL, ages 0^+ and 1^+) the leading edge of the right pectoral fin and FL were measured to the nearest millimetre. The following linear relationship was found in wild fish between pectoral fin length (PFL, centimetres) and body length (FL, centimetres):

$$(2) \qquad PFL = 0.083FL + 0.61.$$

This relationship (N = 182, r^2 = 0.894) was then used to calculate the expected PFL from FL measurements on hatchery fish. The measured PFL was then expressed as percent normal.

Whole-body electrolytes

Fish were terminally anaethetized in tricaine methanesulphonate (MS 222, Syndel Laboratories, Vancouver, B.C., 2 g·L^{-1}, neutralized to pH 7.5), length and mass recorded, and digested for ≥48 h in 1 volume of 0.5 M H_2SO_4. Digests were centrifuged at 12 500 × g for 5 min and the supernatants decanted and analyzed in triplicate for Na^+ and Cl^-. Na^+ was measured on a Varian model 1275 atomic absorption spectrophotometer (AAS) on 40-µL aliquots diluted 1:250 in deionized water; Cl^- was measured in a Radiometer CMT-10 chloride titrator on undiluted 40-µL aliquots.

Muscle chemistry

For sampling, fish were terminally anaesthetized as above and length and mass recorded. For fish of ≤2 g mass, the whole fish was then immediately freeze-clamped using aluminum blocks chilled in liquid nitrogen (LN_2), a section of white muscle tissue was removed, and each fraction ground and stored separately. For larger fish, a 0.5- to 1.0-g quantity of white muscle was removed from above the lateral line and anterior to the dorsal fin and freeze-clamped in LN_2. Frozen tissue was then ground to a fine powder under LN_2 and stored in LN_2 for later analysis.

For analysis of protein, about 30 mg of frozen muscle tissue powder was homogenized on ice in 1 mL of TES buffer (20 mM *N*-tris(hydroxymethyl)methyl-2-aminoethanesulphonic acid in 250 mM sucrose, pH 4.4). The homogenate was analyzed for protein using the Coomassie Blue reaction of Bradford (1976). For analysis of lipid, about 50 mg of tissue was homogenized in 3 mL of chloroform–methanol (2:1, v/v), centrifuged, and 0.5 mL of the lower chloroform layer evaporated to dryness under N_2. The precipitate was analyzed for lipid using the sulphophosphovanillin method of Barnes and Blackstock (1973). For analysis of glycogen, the digestion–precipitation method of Hassid and Abraham (1957) was used to isolate glycogen from 100 mg of frozen tissue powder. Glycogen in the redissolved precipitate was digested to glucose with amyloglucosidase and the glucose analyzed enzymatically according to procedures in Bergmeyer (1983). For analysis of lactate, ATP, and phosphocreatine (PCr), about 100 mg of frozen tissue powder was homogenized on ice in 1.0 mL of 8% perchloric acid and the supernatant analyzed enzymatically according to procedures in Bergmeyer (1983).

Muscle glycolytic enzyme activity

For measurement of the activities of the glycolytic enzymes l-lactate dehydrogenase (LDH, EC 1.1.1.27) and phosphofructokinase (PFK, EC 2.7.1.11), frozen muscle powder (~50 mg) was homogenized on ice in 10 volumes of 50 mM Tris–HCl buffer (pH 7.5). Homogenates were centrifuged for 5 min at 12 500 × g at 4°C and the supernatants collected, stored on ice, and used immediately for enzyme assays. Assays were performed in thermostatted cuvettes at 15°C using substrate concentrations giving maximal velocities. Enzyme activity was measured in a Perkin-Elmer LS-50 spectrofluorometer (excitation 340 nm, emission 460 nm) based on the decrease in fluorescence due the hydrolysis of NADH. All activities are expressed as international units (micromoles of NADH converted to NAD^+ per minute) per gram of tissue at the measurement temperature of 15°C.

LDH is the terminal enzyme in anaerobic glycolysis and thus provides a good index of a tissue's capacity for anaerobic metabolism (Somero and Childress 1980). LDH activity was assayed in the pyruvate reductase direction, i.e., the direction of an anaerobically functioning tissue. The assay medium contained, in a total volume of 2.0 mL, 50 mM glycylglycine buffer (pH 8.2), 4 mM sodium pyruvate, 5 mM $MgCl_2$, 100 mM KCl, and 0.6 mM NADH. The assay was started by addition of 10 µL of a 1:6 dilution of the above supernatant.

PFK has long been assumed to be central to the regulation of carbohydrate metabolism because it is considered to be the rate-limiting enzyme in the glycolytic pathway (Bonen et al. 1989). PFK activity was assayed with the fructose 1,6-diphosphate coupled assay of Shonk and Boxer (1964). The assay medium contained, in a total volume of 2.0 mL, 50 mM glycylglycine buffer (pH 8.2), 2 mM ATP, 2 mM fructose 6-phosphate, 40 mg bovine serum albumin·dL^{-1}, 1 U aldolase·mL^{-1}, 1 U glycerol-3-phosphate dehydrogenase·mL^{-1}, 1 U triosphosphate isomerase·mL^{-1}, 5 mM $MgCl_2$, 100 mM KCl, and 0.1 mM NADH. The assay was started by addition of 40 µL of the above supernatant.

Measures of performance

Anaerobic capacity test

This is a maximum-exertion, fixed-duration test described in detail in McDonald et al. (1998). Fish were transferred in groups of five or 10 (depending on body size) to a 10-L volume in a cylindrical tank (15 cm in diameter) and then immediately forced to activity for 8 min. Fish were then removed as a group and either immediately sampled or allowed to recover for up to 4 h (sampling at 30 min and 1, 2, and 4 h). Anaerobic capacity (AC, anaerobic energy expenditure resulting from maximum exertion) was assessed from measurements of ATP, PCr, and lactate at time 0 (see below).

Fixed-velocity tests

For all fixed-velocity tests, fish were transferred to a 100-L swim flume (with a maximum laminar velocity of 72 cm·s^{-1}; see McDonald et al. 1998 for details) in groups of 10 and allowed to

© 1998 NRC Canada

adjust to the chamber and orient to low-speed current (1–2 BL·s^{-1}) for 5 min. For each trial, velocity was increased continuously over 5 min until the test velocity was reached and then timing was begun. The test velocities were 38, 50, and 62 cm·s^{-1} for fingerlings (5–9 cm FL) and 50 and 62 cm·s^{-1} for yearlings (11–15 cm FL). At least three trials (5–10 fish each) were done on each group at the test velocities.

Once fish became exhausted, or after 60 min of exercise in the 38 cm·s^{-1} test or 10 min in the 50 and 62 cm·s^{-1} tests, whichever came first, fish were removed from the flume, anaesthetized, and length and mass recorded. For analysis of sprint perfomance for each group, the times to exhaustion from each trial were pooled and the time to 50% fatigue (ST_{50}) was estimated by log-probit analysis following the recommendations of Brett (1967).

Incremental-velocity tests

These tests were performed on groups of 10 fish per trial. Each test began with a 5-min orientation period at 14 cm·s^{-1}, followed by an increase to 38 cm·s^{-1} over 13 min, and then increments of 5 cm·s^{-1} every 5 min until all fish were exhausted. At least three trials (10 per trial) were performed on each group. Final velocity (or maximum swimming speed (MSS), centimetres per second) was calculated according to the following expression (after Brett 1964):

$$\text{(3)} \qquad \text{MSS} = V_p + \left(\left(\frac{t_f}{t_i} \right) + V_i \right)$$

where V_i is the velocity increment (centimetres per second), V_p is the penultimate velocity at which the fish swam before fatigue, t_f is the elapsed time from the velocity increase to fatigue, and t_i is the time between velocity increments.

Epinephrine challenge test

This test consisted of examining losses of Na^+ following a single intraperitoneal injection of epinephrine (as the bitartrate salt) at a dose of 0.08 μg·g^{-1}, a dose calculated to produce a blood concentration of 300 nM epinephrine and near maximal stimulation of adrenergic receptors (Gonzalez and McDonald 1992). After the injection the fish were immediately transferred to small-volume cylinders containing 250 mL of aerated water at the experimental temperature. The purpose of this test is to provide a "snapshot" of the stress response and is based on the principle that epinephrine evokes branchial and cardiovascular changes that result in an increased branchial permeability to electrolytes (Gonzalez and McDonald 1992; McDonald and Milligan 1997). The test is therefore an integrated measure of adrenergic sensitivity and the integrity of the gills at resisting stress-induced ion losses. The response to the injection is rapid and short-lived and can easily be detected by measuring appearance of Na^+ in the water. The amount lost over 1 h was calculated (microequivalents per gram per hour) and then expressed as a percent of the whole-body Na^+ content (microequivalents per gram).

Calculations

Effects of body size

McDonald et al. (1998) documented significant effects of body size on the following variables (Var): AC, ST_{50}, and MSS. Scaling of variables for the effects of body size was done according to the following equation:

$$\text{(4)} \qquad \text{Var}_c = \frac{\text{Var}}{\left(\frac{\text{Length (cm)}}{\text{RL (cm)}} \right)^b}$$

where RL is the reference length. The b value for AC and ST_{50} was 5 and for MSS was 1.36.

Anaerobic energy expenditure

Anaerobic energy expenditure in ATP equivalents (AEE ≅ anaerobic ATP turnover; Pearson et al. 1990) in sprints was calculated according to the following formula:

$$\text{(5)} \qquad \text{AEE} = \Delta\text{Lactate} \times 1.5 + \Delta\text{ATP} + \Delta\text{PCr}$$

where Δ is the difference between values for resting animals and those at exhaustion and 1.5 ATP are produced per lactate; 1 PCr = 1 ATP.

Metabolic recovery

McDonald et al. (1998) showed that recovery of muscle metabolite levels from exhaustive exercise could be characterized mathematically and made recommendations for the calculation of constants for lactate removal and for the recovery of ATP and glycogen. For lactate removal, an exponential relationship ($Y = ae^{bX}$, where Y is lactate concentration and X is time (hours)) was fitted to the data and the equation used to express lactate recovery in terms of percent removal per hour. For ATP, a logarithmic relationship ($Y = aX^b$, where Y is time and X is ATP concentration (percentage of rest value)) was fitted to the data and the resulting equation used to calculate the time for 50% recovery of ATP. For glycogen recovery a linear relationship ($Y = bX + a$, where Y is muscle glycogen concentration (micrograms per gram) and X is time (hours)) was fitted to the data and the slope b used to express recovery rates (micromoles per gram per hour). Since PCr recovery was so rapid, there were not sufficient data points to fit a mathematical expression, so recovery has been expressed as the earliest time postexercise (hours) at which full recovery was observed.

Statistical analysis

Means ± 1 standard error of the mean (SEM) are reported throughout. Analysis of variance was used to test significance of regressions and to compare among treatment groups. If the latter comparisons were significant, Dunnett's t-test (Dunnett 1955) was used to compare treatment groups with the control. Differences between two regressions (e.g., lactate recovery rates, glycogen recovery rates, and sprint times estimated by log-probit regression) were tested by t-test according to procedures outlined in Steel and Torrie (1960). Differences at $P < 0.05$ were considered significant.

Results

Behavior of hatchery fingerlings in rearing treatments

Atlantic salmon distributed themselves uniformly across the bottom of the rearing tanks in all treatments, and once that territorial space was filled, they distributed uniformly up into the water column. Consequently, at the higher of the two rearing densities (1.0 versus 0.6 kg·m^{-2}), a greater proportion of the total number of fish in the tank was off the bottom. Those that were exposed to water currents at either rearing density responded by orienting into the current, while those in 0V showed no discernible orientation pattern. Fish in elevated velocities tended to remain stationary, either by extending their pectoral fins in contact with the bottom of the tank or by swimming movements against the current, while those at 0V tended to move around in the tanks. In the tanks with current, there was no apparent current preference, even though the velocities ranged from 0 to 6 in the 4 cm·s^{-1} treatment and from 0 to 14 in the 9 cm·s^{-1} treatment.

Fingerlings: measures of condition

Growth and condition factor

At the time of sampling (late August – early September), the hatchery-reared Atlantic salmon 0$^+$ fingerlings were ≥130 days posthatch, and the rearing trials had been running

© 1998 NRC Canada

Fig. 1. (A) Body mass, (B) condition factor (mass ÷ length$^{3.18}$ × 100), (C) fin condition (PFL as a percentage of wild; eq. 2, Materials and methods), and (D) whole-body Na^+ and Cl^- in hatchery-reared and wild Atlantic salmon fingerlings (age 0$^+$). Hatchery 0$^+$ were reared at two densities (ND and LD: 1.0 and 0.6 kg·m^{-2}, respectively) and at three different velocities (0, 4, and 9 cm·s^{-1}) for ≥50 days. Initial mass was about 1 g. Wild 0$^+$ were collected in August 1995 and 1996 from a fast-flowing riffle area in the Morell River, P.E.I. Values are means + 1 SEM. Different letters indicate means that are significantly different ($P < 0.05$) and N is indicated inside each bar.

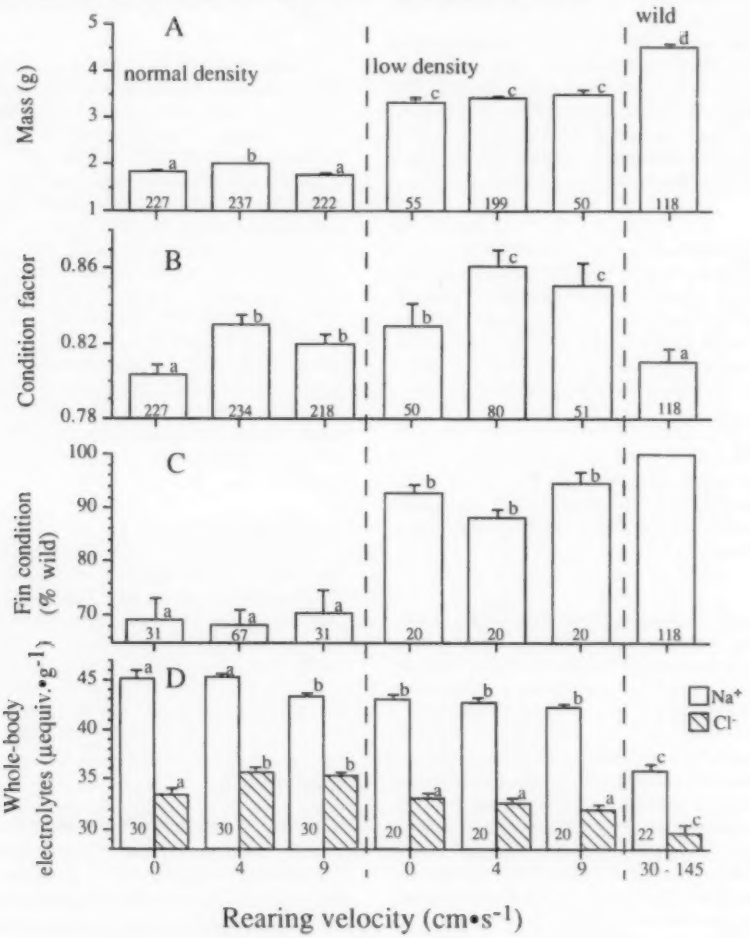

for ≥50 days. Of the two rearing variables, velocity and density, only the latter had a major effect on growth.

At the start of the rearing trials the fingerlings averaged about 1 g. Those reared at a ND (initially 1.0 kg·m^{-2}) doubled in mass over 50 days to about 2 g (Fig. 1A), a specific growth rate of 1.5%·day^{-1}. Those reared at LD (initially 0.6 kg·m^{-2}) showed substantially better growth. Over 50 days, mass had increased to about 3.4 g (Fig. 1A), a specific growth rate of 2.5%·day^{-1}. It is important to emphasize that this higher growth was not just an effect of lower density but also of higher ration, since all fish were fed to satiation rather than a fixed ration (see Materials and methods). The growth in wild fingerlings was even better; their mass at sampling averaged 4.4 g, or 27% greater than the LD fingerlings, despite hatching an average of 2 weeks later.

Rearing velocity had only a slight effect on growth and only at normal rearing density (Fig. 1A). Both the 0V and HV treatment groups showed a slight reduction in growth relative to the NDNV treatment group.

Rearing density also had a prominent effect on condition factor (Fig. 1B). Lowering the density increased the condition factor of hatchery fingerlings to significantly greater than that of wild fingerlings. There was also an effect of rearing velocity. Fish reared at 0V had a lower condition factor at both ND and LD.

The pectoral fins of hatchery fish were eroded compared with wild fish. In hatchery fingerlings reared at ND, the leading edge of the pectoral fin was, on average, eroded to about 70% of the length of that of the wild fingerlings (Fig. 1C). Lowering rearing density improved fin condition to about 91% of wild. There was, however, no effect of rearing velocity on fin condition at either of the rearing densities (Fig. 1C).

© 1998 NRC Canada

Table 1. Biochemistry of white muscle in hatchery-reared and wild Atlantic salmon fingerlings (age 0^+).

	Hatchery		
	ND	LD	Wild
Protein ($mg \cdot m^{-1}$)	108.9±2.6 (54) *a*	117.0±4 (35) *b*	150.6±3.3 (30) *c*
Lipid ($mg \cdot g^{-1}$)	94.6±3.7 (54) *a*	157.6±6.3 (35) *b*	68.5±3.1 (30) *c*
Glycogen ($\mu mol \cdot g^{-1}$)	22.3±2.2 (10) *a*	22.6±1.5 (8) *a*	12.0±1.2 (5) *b*
PCr ($\mu mol \cdot g^{-1}$)	8.9±1.2 (10) *a*	8.3±1 (8) *a*	9.1±1.7 (5) *a*
ATP ($\mu mol \cdot g^{-1}$)	4.3±0.4 (10) *a*	4.5±0.3 (8) *a*	4.9±0.1 (5) *a*
PFK ($nmol \cdot g^{-1} \cdot min^{-1}$)	14.5±6.3 (9) *a*	49.3±6.8 (15) *b*	34.0±9 (14) *a*
LDH ($nmol \cdot g^{-1} \cdot min^{-1}$)	349.7±31.7 (9) *a*	869.2±140.2 (15) *b*	1119.2±107.1 (14) *b*

Note: Hatchery 0^+ were reared at two densities (ND and LD: 1.0 and 0.6 $kg \cdot m^{-2}$, respectively) and at NV (4 $cm \cdot s^{-1}$) for ≥50 days. Values are means ± 1 SEM (*N*). Different letters indicate means that are significantly different ($P < 0.05$).

Table 2. Maximum-exertion, fixed-duration tests on hatchery-reared and wild Atlantic salmon fingerlings (age 0^+).

	Hatchery		
	ND	LD	Wild
Mass (g)	1.9±0.1 *a*	3.0±0.1 *b*	4.3±0.2 *c*
AC ($\mu mol \cdot g^{-1}$)	20.8±0.7 *a*	23.5±1.6 *a*	36.5±1.8 *b*
AC corrected to RL ($\mu mol \cdot g^{-1}$)	22.4±0.8 *a*	21.4±1.4 *a*	29.5±1.6 *b*
Lactate recovery rate ($\% \cdot h^{-1}$)	21.8±3.2 *a*	16.0±2.8 *b*	21.2±0.6 *a*
Time (h) to 50% recovery of ATP	0.7	1.0	1.4
Time (h) for full recovery of PCr	0.5	0.5	1.0
Glycogen recovery rate ($\mu mol \cdot g^{-1} \cdot h^{-1}$)	ns	ns	0.58

Note: Hatchery 0^+ were reared at two densities (ND and LD: 1.0 and 0.6 $kg \cdot m^{-2}$, respectively) and at NV (4 $cm \cdot s^{-1}$) for ≥50 days. Values are means ± 1 SEM. Different letters indicate means that are significantly different ($P < 0.05$). Tests were done on 25–30 fish for each treatment, with 5–10 fish for each of the following sampling intervals: before exercise and 0, 0.5, 2, and 4 h postexercise. AC (anaerobic energy expenditure in the maximum-exertion test) was calculated from the difference in lactate, ATP, and PCr between before exercise and 0 h (see Materials and methods). AC was corrected to a reference length (RL) of 6 cm using eq. 4. Lactate, ATP, PCr, and glycogen recovery rates were calculated from postexercise measurements (see Materials and methods). ns, nonsignificant regression of glycogen versus time.

Muscle composition and glycolytic enzyme activity

Rearing density also had major effects on muscle composition (Table 1; effects of rearing velocity were not evaluated). Muscle protein and, in particular, lipid levels were higher at LD than at ND (Table 1), the latter by 40%. LDH and PFK activities were about two- and threefold higher at LD, respectively, while glycogen, ATP, and PCr levels were the same (Table 1).

Wild fingerlings showed significantly higher muscle protein but significantly lower glycogen and lipid levels compared with hatchery fish reared at either density (Table 1). There were, however, no differences in either ATP or PCr content compared with hatchery fish (Table 1). LDH activity was similar in wild fingerlings compared with LD hatchery fingerlings, and PFK activity was intermediate between ND and LD fingerlings (Table 1).

Whole-body electrolytes

Rearing density had an effect on whole-body Na^+ and Cl^- (Fig. 1D). There was a significant reduction in Na^+ and Cl^- in the LD treatments compared with fish reared at ND (Fig. 1D). The difference amounted to, on average, 1.7 $\mu equiv. \cdot g^{-1}$ for Na^+ and 2.9 $\mu equiv. \cdot g^{-1}$ for Cl^-. Moreover, at ND, there was a reduction in Na^+ at HV relative to NV and a reduction in Cl^- at 0V relative to NV. In contrast, at LD, there was no effect of rearing velocity on electrolyte levels (Fig. 1D).

The most prominent difference was the lower electrolyte levels in wild fingerlings. The difference amounted to 9 $\mu equiv. \cdot g^{-1}$ for Na^+ and 6 $\mu equiv. \cdot g^{-1}$ for Cl^- compared with hatchery controls (NDNV).

Fingerlings: measures of performance

Anaerobic capacity

Lowering rearing density had no effect on AC, i.e., the anaerobic energy expenditure in the maximum-exertion test, but significantly reduced the rate of lactate recovery following maximal exertion (Table 2) (the effect of rearing velocity was

© 1998 NRC Canada

Table 3. Fixed-velocity sprint tests on hatchery-reared and wild Atlantic salmon fingerlings (age 0+).

Sprint speed ($cm \cdot s^{-1}$)	Parameter	Hatchery		
		NDNV	LDNV	Wild
38	*N*	30	30	18
	Length (cm)	5.5±0.1	6.3±0.1	7.3±0.1
	ST_{50} (s)	291±37	897±428	—
	DE (*N*)	0	11	18
50	*N*	66	70	19
	Length (cm)	6.3±0.1	8.7±0.1	7.7±0.2
	ST_{50} (s)	77±4 *a*	106±10 *a*	221±169
	DE (*N*)	2	10	11
	ST_{50c} (s) (RL = 7 cm)	132±8 *a*	38±4 *b*	—
62	*N*	17	39	9
	Length (cm)	6.6±0.2	8.9±0.1	7.5±0.3
	ST_{50} (s)	39±8 *a*	57±4 *a*	54±16 *a*
	DE (*N*)	0	0	0
	ST_{50c} (s) (RL = 7 cm)	54±13 *a*	17±2 *b*	33±19 *a*

Note: Hatchery 0+ were reared at two densities (ND and LD: 1.0 and 0.6 $kg \cdot m^{-2}$, respectively) and at NV (4 $cm \cdot s^{-1}$) for ~50 days. Values are means ± 1 SEM. Different letters indicate means that are significantly different ($P < 0.05$). Tests of significance were not performed if more than 30% of the fish in a trial did not exhaust. DE are fish that did not exhaust in the sprint period (60 min for 38 $cm \cdot s^{-1}$, 10 min for 50 and 62 $cm \cdot s^{-1}$). ST_{50} is the estimated time (by log-probit analysis) to 50% fatigue of the sprint population. ST_{50c} is the sprint time corrected to a reference length (RL) of 7 cm using eq. 4 (see Materials and methods).

Table 4. Fixed-velocity sprint tests at 38 $cm \cdot s^{-1}$ on hatchery-reared Atlantic salmon fingerlings (age 0+) reared at ND (1.0 $kg \cdot m^{-2}$) and at three velocities (0V, NV, and HV: 0, 4, and 9 $cm \cdot s^{-1}$, resoectively) for ≥50 days.

	0V	NV	HV
N	30	30	30
Length (cm)	5.4±0.1	5.5±0.1	5.2±0.1
Mass (g)	1.7±0.1	1.9±0.1	1.5±0.1
ST_{50c} (s)	192±23 *a*	291±37 *b*	238±20 *a*
ST_{50c} (s) (RL = 7 cm)	231±16 *a*	294±16 *b*	324±19 *b*

Note: Values are means ± 1 SEM. Different letters indicate means that are significantly different ($P < 0.05$). ST_{50} is the estimated time (by log-probit analysis) to 50% fatigue of the sprint population. ST_{50c} is the sprint time corrected to a reference length (RL) of 5.5 cm.

not evaluated). Moreover, there was a major difference in AC between hatchery-reared and wild fingerlings. Despite their lower muscle glycogen levels (Table 1), wild fingerlings had almost double the AC of ND and LD fingerlings (Table 2). This is partly attributable to the scaling of AC to body size (McDonald et al. 1998), since the wild fingerlings were substantially larger (4.3 versus 1.9 g). However, when AC was corrected to a common reference length (6 cm, eq. 4), it was still about 30% higher in the wild fingerlings (29.5 ± 1.6 versus 22.4 ± 0.7 $\mu mol \cdot g^{-1}$, Table 2).

Also, wild and hatchery fingerlings differed in the rate of recovery from maximum exertion. While lactate recovery rates were similar between wild and NDNV fingerlings (Table 2), ATP and PCr took longer to return to normal in wild fish compared with hatchery controls. However, there was significant recovery of muscle glycogen in wild fish over 4 h postexercise (0.6 $\mu mol \cdot g^{-1} \cdot h^{-1}$) but no significant recovery in hatchery fish (Table 2).

Sprint performance (fixed-velocity tests)

There was a large effect of rearing density on sprint performance in the fixed-velocity tests (Table 3). LD fingerlings showed superior performance at all three test velocities, 38, 50, and 62 $cm \cdot s^{-1}$, compared with ND fingerlings. Endurance, expressed as ST_{50}, was greater, and at the lower two test velocities, a larger fraction of the total did not exhaust (37% at 38 $cm \cdot s^{-1}$ and 14% at 50 $cm \cdot s^{-1}$, Table 3). However, this greater endurance was largely due to their larger size. When the sprint times are scaled to the same body length (7 cm) using eq. 4, the sprint performance of the ND fingerlings was, in fact, three- to fourfold better at the two upper test velocities compared with the LD group (Table 3). A scaling correction was not applied to the 38 $cm \cdot s^{-1}$ data because of the large fraction of the LD fish that did not exhaust (Table 3).

There was also an effect of rearing velocity on sprint performance, at least in the ND trials (the effects of rearing velocity at LD were not evaluated). Fingerlings reared at 0V exhibited significantly shorter fatigue times at 38 $cm \cdot s^{-1}$ than controls (NDNV), and this difference remained when the ST_{50} values were corrected to a common reference length (Table 4). In contrast, rearing at HV did not improve sprint performance relative to the controls (Table 4).

Wild fingerlings behaved differently from hatchery-reared fish in sprint tests. At speeds below about 50 $cm \cdot s^{-1}$, they

© 1998 NRC Canada

Fig. 2. MSS corrected to a reference body length of 6 cm (see eq. 4, Materials and methods) in hatchery-reared Atlantic salmon fingerlings (age 0^+) reared at two densities (ND and LD: 1.0 and 0.6 $kg \cdot m^{-2}$, respectively) and at three different velocities (0, 4, and 9 $cm \cdot s^{-1}$) for ≥50 days. Values are means + 1 SEM ($N = 30$). Different letters indicate means that are significantly different ($P < 0.05$).

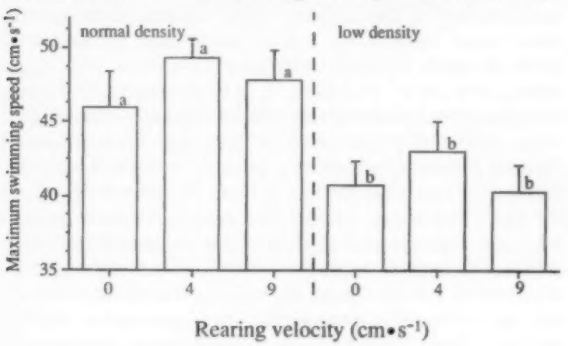

Table 5. Condition, body composition, and response to the epinephrine challenge test (ECT) of hatchery-reared and wild Atlantic salmon yearlings (age 1^+).

	Hatchery	Wild
Mass (g)	25.1±1.1 (152)	28.6±1.5 (69)
Condition factor	1.759±0.017 (152)	1.796±0.0225 (69)
Fin condition (%)	43.0±1.4 (132)	100
Muscle		
Protein ($mg \cdot g^{-1}$)	161.8±8.8 (40 *a*)	185.4±3.1 (30) *b*
Lipid ($mg \cdot g^{-1}$)	181.8±4.2 (49) *a*	83.2±5.3 (20) *b*
Glycogen ($\mu mol \cdot g^{-1}$)	19.2±1.3 (10) *a*	8.5±1.1 (10) *b*
PCr ($\mu mol \cdot g^{-1}$)	4.4±0.3 (10) *a*	3.2±0.5 (10) *a*
ATP ($\mu mol \cdot g^{-1}$)	4.1±0.2 (10) *a*	3.7±0.9 (10) *a*
Whole body		
Na^+ ($\mu equiv. \cdot g^{-1}$)	43.6±0.9 (20) *a*	43.9±1.7 (12) *a*
Cl^- ($\mu equiv. \cdot g^{-1}$)	35.9±0..8 (20) *a*	34.5±1.5 (12) *a*
Na^+ loss in ECT as % of body Na^+	4.1±0.7 (12) *a*	1.5±0.5 (6) *b*

Note: Hatchery yearlings were reared at a density of 1.7 $kg \cdot m^{-2}$ and a velocity of 4 $cm \cdot s^{-1}$. Values are means ± 1 SEM (N). Different letters indicate means that are significantly different ($P < 0.05$).

were, by comparison, virtually stationary in the current, very close to the bottom or "anchored" on the bottom with their pectoral fins and showing infrequent swimming movements. Consequently, when sprinted at 38 $cm \cdot s^{-1}$, none of the wild 0^+ exhausted in 60 min (Table 3). When sprinted at 50 $cm \cdot s^{-1}$, the ST_{50} was about double that of hatchery fish (Table 3) and only 40% of the fish exhausted in this 10-min test. Complete exhaustion was only seen at the highest test velocity, 62 $cm \cdot s^{-1}$. Here, the ST_{50}, when scaled to a reference length of 7 cm, was higher than that of the LD fingerlings but not significantly different from that of the ND hatchery fingerlings (Table 3).

Swim performance (incremental-velocity tests)

Lowering the rearing density also had a significant negative effect on performance in the incremental-velocity tests (Fig. 2). Despite the fact that LD fingerlings were larger, their MSS was identical to that of ND fish, 46.6 $cm \cdot s^{-1}$ in LD fish versus 46.7 $cm \cdot s^{-1}$ in ND fish. Consequently, when corrected to a common reference length (6 cm), the MSS of the LD fish was significantly less, irrespective of rearing velocity (Fig. 2). There was, by contrast, no effect of rearing velocity on MSS at either rearing density.

The assessment of the MSS of wild fingerlings was problematic because of their larger body size. As a result, four of the 20 fish tested did not exhaust at the maximum speed of the swim tunnel (72 $cm \cdot s^{-1}$), so their MSS could not be estimated. Also, none of the wild fish exhausted below 58 $cm \cdot s^{-1}$, while most of the hatchery controls had exhausted at this point. However, when MSS values were corrected to a common reference length of 6 cm, the MSS of wild and NDNV fish were virtually identical to one another (48 ± 1.5 versus 49.3 ± 1.2 $cm \cdot s^{-1}$, respectively).

Epinephrine challenge test

Intraperitoneal injection of epinephrine produced an immediate net loss of Na^+ in all fish tested ($N = 16$ per group), but the loss quickly waned so that by 1 h, net Na^+ loss had fallen virtually to zero. The injection proved to be a relatively mild challenge, as the amount lost was small, between 1 and 2% of whole-body Na^+. There was no significant effect of rearing density on Na^+ loss in this test (which was 1.6 and 1.7%, respectively, for ND and LD), but at ND, there was an inverse relationship between Na^+ loss and rearing velocity (2.1, 1.7, and 1.4% for 0, 4, and 9 $cm \cdot s^{-1}$, respectively).

Wild versus hatchery-reared yearlings: condition and performance

Hatchery-reared yearlings had the same mass, condition factor, and whole-body Na^+ and Cl^- as wild-reared yearlings, but their pectoral fin erosion was substantial; pectoral fin length was only 43% of wild (Table 5) compared with 70–90% of wild for hatchery fingerlings (Fig. 1). The muscle metabolic profile in hatchery yearlings was characteristic of hatchery versus wild fingerlings (Table 1). Wild yearlings had lower lipid and glycogen and higher protein than hatchery yearlings whereas PCr and ATP levels were similar in both groups (Table 5).

In the epinephrine challenge test, Na^+ losses were more than twofold greater in the hatchery yearlings compared with the wild yearlings despite similar whole-body electrolyte levels (Table 5).

The sprint performance of the wild yearlings was considerably better than that of hatchery-reared yearlings, about threefold better at 50 $cm \cdot s^{-1}$ and about twofold better at 62 $cm \cdot s^{-1}$ (Table 6). Moreover, a much larger fraction of the wild fish did not exhaust in the sprint tests, 47 versus 18% at 50 $cm \cdot s^{-1}$ and 27 versus 6% at 62 $cm \cdot s^{-1}$ (Table 6).

Discussion

Both density and water velocity had significant effects on hatchery-reared Atlantic salmon fingerlings. Moreover, the two treatments were largely independent of one another.

© 1998 NRC Canada

Table 6. Sprint tests on hatchery and wild Atlantic salmon yearlings (age 1^+).

Sprint speed ($cm \cdot s^{-1}$)	Parameter	Hatchery	Wild
50	*N*	39	15
	Length (cm)	12.1±0.2	12.3±0.3
	ST_{50} (s)	136±64 *a*	401±102 *b*
	DE (*N*)	7	7
62	*N*	36	15
	Length (cm)	13.4±0.3	13.5±0.3
	ST_{50} (s)	99±9 *a*	188±83 *b*
	DE (*N*)	2	4

Note: Values are means ± 1 SEM. Different letters indicate means that are significantly different ($P < 0.05$). ST_{50} is the estimated time (by log-probit analysis) to 50% fatigue of the sprint population. DE are fish that did not exhaust in the sprint period (10 min).

Density had similar effects at all three water velocities (e.g., effect on growth), while velocity had similar effects at both densities (e.g., effect on swim performance). However, the effects of density were somewhat more pronounced than those of velocity.

Effects of density

The most prominent effect of reducing density was stimulation of growth, an effect widely reported for Atlantic salmon (e.g., Refstie and Kittelsen 1976; Soderberg et al. 1993) and explained as a consequence of the need in this highly territorial species for discrete feeding territories for optimum growth and survival (cf. Keenleyside and Yamamoto 1962). However, the stimulation of growth produced in the present study (a twofold increase in specific growth rate (SGR) over 50 days) was substantially larger than the 10% increase over a similar time course reported in previous studies (Refstie and Kittelsen 1976; Soderberg et al. 1993). The higher growth is probably due mainly to a difference in feeding regime. In the present study the LD group received a higher ration because they would feed more readily when food was offered, while in previous studies, all treatment groups were offered the same ration.

Along with higher growth at LD was an increase in condition factor (Fig. 1B) and an increase in muscle lipid content (Table 1), both probably attributable to higher food consumption. However, there were other effects of lowering the rearing density that do not clearly follow from higher ration such as an improvement in fin condition (Fig. 1C), an increase in muscle PFK activity (Table 1), a minor reduction in whole-body electrolytes (Fig. 1D), and, most importantly, a reduction in performance in both the fixed-velocity (Table 3) and incremental-velocity swimming tests (Fig. 2) when correction was made for differences in body size between the two density treatment groups. These effects appear to be unrelated and their precise origin is unknown. Nonetheless, there is a clear implication that hatchery culture conditions that favor increased growth also act to compromise swim performance.

Effects of velocity

We obtained an almost negligible effect of current on growth (Fig. 1A) compared with previous studies, e.g., a 40% increase in SGR in juvenile Atlantic salmon with an increase in current from 0 to 1 $BL \cdot s^{-1}$ (Jørgenson and Jobling 1993). That study used a fivefold higher stocking density than the present study (20 versus 4 $kg \cdot m^{-3}$ in the ND treatment), and as a result, the SGR at zero current was much lower (0.75 versus 1.5%·day^{-1}). This suggests that in the present study, negative social interactions that might impact growth were relatively minor compared with previous studies. Imposing a current of 4 $cm \cdot s^{-1}$ (≤ 1 $BL \cdot s^{-1}$), in comparison with no current, generally had beneficial effects: slightly increased condition factor (Fig. 1B, at both ND and LD), increased endurance in the fixed-velocity sprint tests (Table 4, only ND fish tested), increased MSS in the incremental test (Fig. 2, at ND only), and a reduction of fractional Na^+ loss in the epinephrine challenge test. The latter can be interpreted explicitly as a measure of the stress reduction effects of continuous exposure to current. However, the improvements in condition and performance were limited to the increase in velocity from 0 to 4 $cm \cdot s^{-1}$ except for a further reduction in fractional Na^+ loss at 9 $cm \cdot s^{-1}$. These observations are consistent with those of Jørgenson and Jobling (1993) and suggest that it is the presence–absence of water current rather than its amplitude that is the key variable.

Differences between hatchery-reared and wild-reared fish

By comparing hatchery and wild fish, we can begin to determine which parameters, among all those measured in this study, qualify as measures of condition (i.e., correlate with or predict performance) and which performance tests are useful for assessing the success of hatchery rearing (i.e., that measure a reduction in the difference between hatchery and wild fish). Most important to this comparison is the fact that wild and hatchery fish were of the same age and were derived from the same parent population (i.e., sea-run adults returning in the fall to the Morell River). Hence, the comparison specifically addresses the relative quality of the wild and hatchery environments.

Fin condition

Pectoral fin condition was one of the most striking and obvious differences between wild and hatchery-reared Atlantic salmon and was quite sensitive to rearing environment. Lowering the rearing density led to a significant improvement in pectoral fin condition (Fig. 1C), while transferring yearlings to seminatural rearing ponds led to complete restoration of fin condition to the wild state within 2 months of the transfer (unpublished observations).

The disproportionately large pectoral fins of juvenile Atlantic salmon are important for station holding in current (Arnold et al. 1991). In the present study, wild Atlantic salmon exhibited greater attachment to the substrate and reduced swimming movements in the swim flume compared with hatchery Atlantic salmon, a response particularly noticeable at sprint speeds at or below 50 $cm \cdot s^{-1}$ (Table 3). Poor fin condition was obviously important to the lower swim performance of hatchery yearlings (Table 6) because they were otherwise similar in size and condition factor to wild yearlings (Table 5), but whether this can explain differences between wild and hatchery fingerlings is less clear. Even though the swim performance of the wild fingerlings was superior to that

© 1998 NRC Canada

of hatchery fingerlings, the difference between wild and hatchery controls (i.e., NDNV) disappeared when scaling corrections were applied, even though the fin condition of NDNV fish was only 70% of wild (Fig. 1C). Moreover, rearing at LD improved pectoral fin condition (Fig. 1) but worsened endurance time (Table 3) and MSS (Fig. 2) suggesting that fin condition was not the sole variable explaining these differences in swim performance.

Growth

Wild 0$^+$ Atlantic salmon exhibited superior growth compared with hatchery fish. A number of features of the wild environment could have contributed to the higher growth, but probably the most prominent are larger individual territories (wild fish were widely dispersed in a shallow rocky riffle with lots of available refugia), higher rearing temperature (at the time of collection the habitat of wild fish was about 3°C higher than the Cardigan River supplying the hatchery), and a continuous, rather than periodic, food supply. Nonetheless, it is clear from our hatchery studies that rearing practices that favor high growth rate cannot by themselves improve the performance of hatchery fish relative to wild fish. The most clear-cut example of that is the fact that increasing the growth rate through lowering density actually led to a reduction in swim performance relative to wild fish.

Muscle biochemistry

There are important differences in muscle composition and enzyme activity between wild and hatchery fish (Tables 1 and 5). However, none of these was an unambiguous predictor of AC or swim performance. Clearly, AC was not dependent on fuel quantity in muscle. The contents of fuels powering anaerobic activity in wild fish were either lower than (glycogen) or similar to those in hatchery fish (ATP and PCr). Moreover, AC was not related to glycolytic enzyme activity, for while there were major differences in enzyme activity among groups (Table 1), the differences were size related, not performance related. The largest difference in glycolytic enzyme activity was seen between the ND and LD treatment groups where there was a substantial difference in size but no significant difference in AC (Table 2). Furthermore, PFK activity, the rate-limiting enzyme in glycolysis, was actually lower in wild fish compared with LD fish (Table 1). The only muscle parameter that was related at all with AC was muscle lipid level, and it was a negative relationship. Lipid levels were lowest in wild fingerlings, intermediate in NDNV fish, and highest in LDNV fish. However, this was by no means a clear-cut relationship because there was a large difference in lipid between NDNV and LDLV fish (Table 1) but no significant difference in AC (Table 2). In any case, muscle lipid has no direct role to play in anaerobic metabolism per se, since it is an aerobic fuel only. However, it is possible that high muscle lipid levels may, in fact, act to inhibit muscle glycolysis (Dyck et al. 1993).

A more positive marker for swim performance is muscle protein content, which was higher in wild fingerlings and yearlings than in hatchery fish (Tables 1 and 5, respectively). This increase could lead to an increase in either muscle power or buffering capacity depending on the specific proteins affected. In either case, one could expect improvements in swim performance and (or) AC. However, muscle protein also went up significantly with LD rearing (Table 1) but swim performance declined (Table 3; Fig. 2) which raises a question concerning the physiological significance of the changes in muscle protein.

Endurance and maximum swimming speed

The main finding from both the fixed and incremental velocity tests was the lack of difference in swim performance between NDNV and wild fingerlings, once scaling corrections were applied, despite the eroded pectoral fin condition of the hatchery fish (Fig. 1C). When wild fish were forced into continous swimming for the entire trial (i.e., at 62 cm·s^{-1}), their endurance was quite similar to that of hatchery fish reared at ND (Table 3). Furthermore, the MSS of those wild fingerlings that exhausted in the incremental-velocity tests (Fig. 2) was virtually identical to that of NDNV fingerlings (48 versus 49 cm·s^{-1}, respectively), once scaling corrections were applied.

These findings are quite remarkable because previous studies by Rimmer et al. (1985) clearly demonstrated the superior swim performance of wild Atlantic salmon juveniles compared with hatchery-reared Atlantic salmon. MSS in wild fish, measured throughout the year at a range of temperatures from 1 to 15°C, was anywhere from 22 to 84% better than that of hatchery fish of similar size. However, the Rimmer et al. (1985) study was on yearlings (10–13 cm FL), while the above comparison is for fingerlings. This suggests that differences in swim performance may not develop until later, i.e., over the second year of hatchery rearing. Certainly, we can confirm that once hatchery fish have reached the yearling stage, their sprint endurance has significantly deteriorated compared with wild yearlings (Table 6) and this is an unambiguous difference because of the similarity in body size between the wild and hatchery fish.

Anaerobic capacity and recovery

Unlike swim performance, the AC measure did provide an unambigous difference between wild and hatchery fingerlings. Not only did wild fingerlings have a higher AC than either LD or ND hatchery fingerlings, but the difference remained after correction was applied for their larger body size (Table 2). Moreover, the wild fish showed a small but significant glycogen recovery postexercise that was not seen in the hatchery fish.

Given the higher AC of wild fingerlings, it is surprising that they did not exhibit superior endurance in the swimming trials over hatchery fish. However, this, in fact, could be seen as an adaptive strategy, as it would preserve anaerobic fuels for multiple sprints (e.g., repeated dashes into current for prey capture) and would be complementary to their increased ability to recover their anaerobic reserves. This conclusion suggests that an effect of rearing in the wild is to alter the point at which fish sense fatigue and cease further activity, i.e., fish become "less willing" to exert themselves in a swimming challenge, which would be expressed as a relatively lower anaerobic energy expenditure at exhaustion.

Conclusions

The results of the present study taken together now permit two general conclusions that bear on future efforts to rear wild fish in a hatchery environment. Firstly, we had relatively

© 1998 NRC Canada

little success in narrowing the gap between wild and hatchery fish through manipulations of density (and ration) and velocity. This may simply mean that the normal hatchery practice was fairly close to optimal already, but it does underscore the basic limitations of hatchery rearing over wild or seminatural rearing programs. Secondly, none of the 10 biochemical or morphological parameters measured in this study (Fig. 1; Tables 1 and 5) qualified as a measure of condition, i.e., no measurement, by itself, unambiguously predicted performance in any of the four performance tests used here (AC, sprint endurance, MSS, or epinephine challenge). This suggests that the future assessment of fitness of hatchery fish be based on performance testing only, perhaps even to the point of using nondestructive performance tests to select fish for stocking to the wild.

Acknowledgments

The authors thank Mike Murray, Francis Maclean, Dr. Tina Kieffer, and Vandy Thomas for excellent technical assistance. This work was supported by grants from the Natural Sciences and Engineering Research Council of Canada (NSERC) and the Department of Fisheries and Oceans (DFO) to D.G.M., C.L.M., and B.L.T. under the NSERC operating grant and DFO/NSERC Science Subvention programs.

References

Arnold, G.P., Webb, P.W., and Holford, B.H. 1991. The role of the pectoral fins in station-holding of Atlantic salmon parr (*Salmo salar* L.). J. Exp. Biol. **156**: 625–629.

Barnes, H., and Blackstock, J. 1973. Estimation of lipids in marine animals and tissues: detailed investigation of the sulphophosphovanillin method for "total" lipids. J. Exp. Mar. Biol. Ecol. **12**: 103–118.

Bergmeyer, H.U. 1983. Methods of enzymatic analysis. Verlag Chemie, Basel, Switzerland.

Bonen, A., McDermott, J.C., and Hutber, C.A. 1989. Carbohydrate metabolism in skeletal muscle: an update of current concepts. Int. J. Sports Med. **10**: 385–401.

Bradford, M.M. 1976. A rapid and sensitive method for the quantitation of microgram quantities of protein utilizing the principle of protein–dye binding. Anal. Biochem. **72**: 248–254.

Brett, J.R. 1964. The respiratory metabolism and swimming performance of young sockeye salmon. J. Fish. Res. Board Can. **21**: 1183–1226.

Brett, J.R. 1967. Swimming performance of sockeye salmon (*Oncorhynchus nerka*) in relation to fatigue time and temperature. J. Fish. Res. Board Can. **24**: 1731–1741.

Busacker, G.P., Adelman, I.R., and Goolish, E.M. 1990. Growth. *In* Methods for fish biology. *Edited by* C.B. Schreck and P.B. Moyle. American Fisheries Society, Bethesda, Md. pp. 363–388.

Coux, I.G. 1994. Stocking strategies. Fish. Manage. Ecol. **1**: 15–30.

Davison, W. 1989. Training and its effects on teleost fish. Comp. Biochem. Physiol. A Comp. Physiol. **94**: 1–10.

Dunnett, C.W. 1955. A multiple comparisons procedure for comparing several treatments with a control. J. Am. Stat. Assoc. **50**: 1096–1121.

Dyck, D.J., Putman, C.T., Heigenhauser, G.J.F., Hultman, E., and Spriet, L.L. 1993. Regulation of fat–carbohydrate interaction in skeletal muscle during intense aerobic cycling. Am. J. Physiol. **265**: E852–E859.

East, P., and Magnan, P. 1987. The effect of locomotor activity on the growth of brook charr, *Salvelinus fontinalis* Mitchill. Can. J. Zool. **65**: 843–846.

Fenderson, O.C., and Carpenter, M.R. 1971. Effects of crowding on the behaviour of juvenile hatchery and wild landlocked Atlantic salmon (*Salmo salar* L.). Anim. Behav. **19**: 439–447.

Gonzalez, R.J., and McDonald, D.G. 1992. The relationship between oxygen consumption and ion loss in a freshwater fish. J. Exp. Biol. **163**: 317–332.

Hassid, W.Z., and Abraham, S. 1957. Chemical procedures for analysis of polysaccharides. *In* Methods in enzymology. *Edited by* S.P. Colowick and N.O. Kaplan. Academic Press, New York. pp. 34–37.

Isaksson, A. 1991. Culture of Atlantic salmon. *In* Culture of salmonid fishes. *Edited by* R.R. Stickney. CRC Press, Boca Raton, Fla. pp. 85–130.

Jobling, M., Baardvik, B.M., Christiansen, J.S., and Jørgensen, E.H. 1993. The effects of prolonged exercise training on growth performance and production parameters in fish. Aquacult. Int. **1**: 95–111.

Jørgensen, E.H., and Jobling, M. 1993. The effects of exercise on growth, food utilisation and osmoregulatory capacity of juvenile Atlantic salmon, *Salmo salar*. Aquaculture, **116**: 233–246.

Keenleyside, M.H.A., and Yamamoto, F.T. 1962. Territorial behavior of juvenile Atlantic salmon (*Salmo salar*). Behaviour, **19**: 139–169.

Kiessling, A., Gallaugher, P., Thorarensen, H., Kolok, A., Eales, J.G., Sweeting, R., Gong, B., McKeown, B.A., Dosanjh, B., Farrell, A.P., and Higgs, D.A. 1994. Influence of sustained exercise and endurance training on growth, muscle physiology, cardiovascular parameters, and plasma levels of metabolic hormones of seawater adapted all-female chinook salmon. *In* High performance fish. *Edited by* D.D. MacKinlay. American Fisheries Society, Vancouver, B.C. pp. 300–305.

McDonald, D.G., and Milligan, C.L. 1997. Ionic, osmotic and acid–base regulation in stress. *In* Fish stress and health in aquaculture. *Edited by* G.K. Iwama, A.D. Pickering, J.P. Sumpter, and C.B. Schreck. Cambridge University Press, Cambridge, U.K. pp. 119–144.

McDonald, D.G., McFarlane, W., and Milligan, C.L. 1998. Anaerobic capacity and swim performance of juvenile salmonids. Can. J. Fish. Aquat. Sci. **55**. This issue.

Pearson, M.P., Spriet, L.L., and Stevens, E.D. 1990. Effect of sprint training on swim performance and white muscle metabolism during exercise and recovery in rainbow trout. J. Exp. Biol. **149**: 45–60.

Refstie, T., and Kittelsen, A. 1976. Effect of density on growth and survival of artificially reared Atlantic salmon. Aquaculture, **8**: 319–326.

Rimmer, D.M., Saunders, R.L., and Paim, U. 1985. Effects of temperature and season on the position holding performance of juvenile Atlantic salmon (*Salmo salar*). Can. J. Zool. **63**: 92–96.

Shonk, C.E., and Boxer, G.E. 1964. Enzyme patterns in human tissue. I. Methods for the determination of glycolytic enzymes. Cancer Res. **24**: 709–724.

Soderberg, R.W., and Meade, J.W. 1987. Effects of rearing density on growth, survival, and fin condition of Atlantic salmon. Prog. Fish-Cult. **49**: 208–283.

Soderberg, R.W., Meade, J.W., and Redell, L.A. 1993. Growth, survival and food conversion of Atlantic salmon reared at four different densities with common water quality. Prog. Fish-Cult. **55**: 29–31.

Somero, G.N., and Childress, J.J. 1980. A violation of the metabolism–size scaling paradigm: activities of glycolytic enzymes increase in larger-size fish. Physiol. Zool. **53**: 322–337.

© 1998 NRC Canada

Steel, R.G.D., and Torrie, J.H. 1960. Principles and procedures of statistics with special reference to the biological sciences. McGraw-Hill, Toronto, Ont.

Stickney, R.R. 1994. Use of hatchery fish in enhancement programs. Fisheries (Bethesda), **19**(5): 6–13.

Totland, G.K., Kryvi, H., Jødestøl, K., Christiansen, E.N., Tangerås, A., and Slinde, E. 1987. Growth and composition of the swimming muscle of adult Atlantic salmon (*Salmo salar* L.) during long-term sustained swimming. Aquaculture, **66**: 299–313.

© 1998 NRC Canada

Fine-scale mapping of fish distribution from commercial catch and effort data using maximum entropy tomography

M. Vignaux, G.A. Vignaux, S. Lizamore, and D. Gresham

Abstract: We present a technique for mapping the spatial distribution of fish using commercial catch and effort data. The relative fish density can be estimated at scales smaller than the length of the unit of effort, such as a tow, by using a Bayesian maximum entropy method. This can take advantage of the fact that the tows cross to give information about the density in those areas. This is a novel application of a well-tested technique that has been used in other fields such as astronomical imaging. Its utility and robustness is demonstrated both on simulated data and on real data from the trawl fishery on spawning hoki off the west coast of the South Island of New Zealand.

Résumé : Nous décrivons une technique de représentation de la distribution des poissons d'après les captures et l'effort de pêche. La méthode de l'entropie maximum bayésienne permet d'estimer la densité relative de poissons à des échelles beaucoup plus petites que la longueur d'une unité d'effort telle que le trait de chalut. Il est ainsi possible de tirer parti du fait que les traits se croisent pour obtenir de l'information sur la densité de poissons dans les zones de croisement. La technique est tout à fait éprouvée, mais il s'agit d'une nouvelle application qui été utilisée dans d'autres domaines, dont celui de l'imagerie astronomique. Nous en démontrons l'utilité et la robustesse, tant avec des données simulées qu'avec les données réelles recueuillies sur la pêche au chalut du hoki en fraye, au large de la côte ouest de l'île du Sud, en Nouvelle-Zélande.
[Traduit par la Rédaction]

Introduction

The fine-scale structure of fish distribution is difficult to measure using CPUE data although it is important for interpreting it. The spatial dimensions of effort (tens of kilometres) may be large compared with the dimensions of the spatial structure of interest (kilometres). To map the fishery, catch and effort data are typically aggregated into blocks of size comparable with or larger than the spatial dimensions of effort. However, there may be spatial correlations on scales smaller than this that can significantly affect catch rates and that may be interesting in their own right. This is the case in the trawl fishery for New Zealand hoki, as shown in Vignaux (1996*a*).

Despite this, it is possible to infer information about the distribution of fish on a finer scale than the length of the tow (typically 10–20 nautical miles). This is achieved because many individual tows cross and the catch data from such tows can be used to infer the density of the fish in the small region in common to them. Two tows that pass through an area of high fish density will share a higher than average catch. Transforming from information about catches to information about the location of dense patches of fish is complicated. This transformation involves optimization because the catch rate data are typically very noisy and one cannot solve the resulting equations exactly.

This problem of transforming data from one space into information or an image in another space (sometimes known as the inverse problem) is common to many fields of science, and the method of maximum entropy (known as MaxEnt) has been found to be a useful technique in many such applications. One familiar form of the inverse problem is the Fourier transform, and MaxEnt has been used effectively for problems in spectral analysis (Buck and Macaulay 1990), nuclear magnetic resonance analysis (Sibisi 1983), and radio astronomy (Gull and Daniell 1978). An even closer analogy to the problem of fish density estimation is the general technique of tomography. In medical X-ray tomography for example, X-ray scans are passed through the body in different directions and the total absorption in each pass is measured. The density of absorption centres at different locations in the body are mapped by transforming the information from a large number of scans in many different directions.

Applications of MaxEnt in tomography problems in other fields include detecting cracks in rods (such as fuel pins) by X-ray (Freiden and Zoltani 1985), using radio waves to investigate the electrical properties of rocks in situ (Pendock and Wedepohl 1991), and astronomical imaging of binary stars (Marsh and Horne 1989).

In the novel application described here, the area of the fishery corresponds to a body being scanned by X-rays, the mass of fish per unit volume corresponds to the density of the bones and flesh within the body, the commercial fishing tows

Received January 3, 1997. Accepted October 27, 1997.
J13814

M. Vignaux. National Institute of Water and Atmospheric Research, Wellington, N.Z.
G.A. Vignaux,[1] S. Lizamore, and D. Gresham. ISOR, Victoria University, Wellington, N.Z.

[1] Author to whom all correspondence should be addressed.
e-mail: Tony.Vignaux@vuw.ac.nz

© 1998 NRC Canada

are equivalent to X-ray scans through it, and the fish catches are equivalent to the reduction of density of the X-ray film. The work is therefore a straightforward application of a well-known technique to a completely new type of data.

On the other hand, there are a few differences. First, the number and location of scans in medical tomography have been chosen by the operator to give the most easily transformable and unambiguous data for preparing the image. For example, they may be chosen to follow a strict grid or along regularly spaced radii. In fishing, the tows are chosen by the fishers to maximise their catches with, unfortunately, little regard to their information content for mapping purposes. Despite this, we have been able to obtain useful images.

A second difference is that the fish distribution is likely to change as fish move during the season. In this study, the season was divided into periods that were short compared with the persistence of the fish aggregates (Vignaux 1996*a*) and each period was studied separately.

A third difference is that the catches in the tows from which we obtained our information are not simple measurements and are highly variable. In particular, there are coarse scale differences between tows made by different vessels and at different times of day and these have effects on catch rates that are not related to the density distribution of the fish. It was important in our studies to remove as much as possible of this uninteresting variation. We used the same linear model that was used for standardizing the CPUE to estimate year to year changes in fish abundance to measure the size and importance of each of these effects. The catches in each tow were standardised using this fitted model to calculate a standardised catch expected in each tow if the tows had been done under identical conditions.

Even when these systematic effects have been removed, we would still expect large variations between tows. Experience shows, however, that the algorithm used to find the maximum entropy image appears to be relatively robust to such variability.

Method

In this section we outline the theory of maximum entropy fitting for images and then show how we tested its use in our situation by simulating random tows through a known density pattern. Finally, we describe the standardization of the real data using a CPUE model.

Theory

The ocean area of interest is divided into n blocks with an unknown average density of fish, f_j, in each of the $j = 1, 2, ..., n$ blocks. Information is provided via the catches in each of p tows which pass through some of the blocks, where D_i is the catch in the ith tow.

Because each fish in D_i must have been caught in one of the blocks through which tow i passed, the total catch can be written as a sum of sub-catches in each of the blocks. Allowing for random error,

$$D_i = \sum_{j=1}^{n} R_{ij} f_j + \epsilon_i. \tag{1}$$

Here R_{ij} is the distance that tow i passed in block j (in nautical miles) in which fish were present at a relative linear density f_j (in kg/nautical mile). ϵ_i is a random error mean 0 for the ith tow. It is assumed to include a variety of unmeasurable effects such as variable catchability and observational errors.

Although this equation may not be able to be inverted to find the values of f_j directly, the D_i values can be used to find the most plausible values of f_j that are consistent with the data D_i. This is done using a Bayesian method in which the posterior probability of a particular set of f_j values (known as a candidate image) is based on both the prior probability (the plausibility of the image based on what we know about the fishery generally) and on the likelihood of obtaining the data if the trial image was in fact the true image.

The MaxEnt method uses the information entropy (also known as the configurational entropy) of a trial image to establish its prior probability. An image that varies a great deal is defined to have a lower prior probability than a smooth image. This is because the density distribution is expected to be smooth, perhaps even uniform, over the area of sea in the absence of data to the contrary. This bias towards smoothness means that all structure seen in the final image must have come from the data and cannot be an artifact (see Daniell 1991).

In MaxEnt (e.g., Buck and Macaulay 1990), the prior probability of a candidate image $\mathbf{f}'$ is given by

$$P(\mathbf{f}'|m) \propto \exp(\alpha S(\mathbf{f}', \mathbf{m})), \tag{2}$$

where $\mathbf{f}' = \{f'_1, f'_2, ..., f'_n\}$ is the vector of f'_j values, $\mathbf{m}$ is the vector of m_i, representing what is called the null model for the density distribution in the absence of data (taken in this case to be uniform), α is a constant, and $S(\mathbf{f}', \mathbf{m})$ is the information entropy of the trial image $\mathbf{f}'$ relative to the null model $\mathbf{m}$:

$$S(\mathbf{f}', \mathbf{m}) = \sum_i \left[f'_i - m_i - f'_i \log\left(\frac{f'_i}{m_i}\right)\right]. \tag{3}$$

The likelihood of obtaining the dataset $\mathbf{D}$ if the true image was $\mathbf{f}'$ and assuming normal errors is

$$P(\mathbf{D}|\mathbf{f}') \propto \prod_i \exp\left(-\frac{(F'_i - D_i)^2}{2\sigma^2}\right) = \exp(-L(\mathbf{f}')). \tag{4}$$

where the

$$F'_i = \sum_{j=1}^{n} R_{ij} f'_j \tag{5}$$

are the predicted catches given the trial image, and σ is an estimate of the variance of the expected noise. The likelihood therefore depends on the size of the discrepancy between the set of predicted catches given the trial image and the true set of catches. If the trial image was very good (i.e., it fitted the data well), the likelihood would be large. Hence, using Bayes' theorem, the posterior probability of the trial image $\mathbf{f}'$ is

$$P(\mathbf{f}'|\mathbf{D}) \propto P(\mathbf{D}|\mathbf{f}') \times P(\mathbf{f}'|\mathbf{m}). \tag{6}$$

To find the most plausible image (i.e., to maximise the Bayesian posterior), we begin with a trial image $\mathbf{f}'$ and in a series of iterations move towards the $\mathbf{f}'$, which maximises $\exp(\alpha S(\mathbf{f}', \mathbf{m}) - L(\mathbf{f}'))$. The algorithm for this is as described in Skilling and Bryan (1984) and a particularly clear exposition of the method is given by Sivia (1996).

The assumed noise parameter σ of eq. 4 is provided by the user. If σ is set too low, the algorithm is expecting the catches D to be fitted so precisely that it will never find an acceptable solution. If σ is set too high, the algorithm will allow quite a poor fit between D and F' and may terminate abruptly without trying a number of solutions. For values between these, the algorithm will iterate to find the most probable solution. Because σ is unknown in this application, the algorithm was run a number of times to find the minimum value of σ for which convergence is still possible.

The null model, $\mathbf{m}$, which is also known as the Lebesque measure (Sivia 1996), expresses the idea of a pre-prior density. In most cases this will be uniform over the region so that all m_i are the same constant but this choice depends on the details of the application. Here we assumed a completely uniform density.

The parameter α describes the trade-off between optimising the entropy of the prior and optimising the fit of the image given the data. We have used the usual approach of setting it so that the misfit

© 1998 NRC Canada

Fig. 1. Example images of the artificial "face"pattern. (*a*) The original face, (*b*) a set of 150 "tows" generated at random, (*c*) an image reproduced by the MaxEnt method from these tows, (*d*) to (*g*) images reproduced when random noise is added to the "catches," (*h*) the set of tows with a "cross" of extra "tows" concentrating effort in one block, and (*i*) a resulting image with a cross added to the tows.

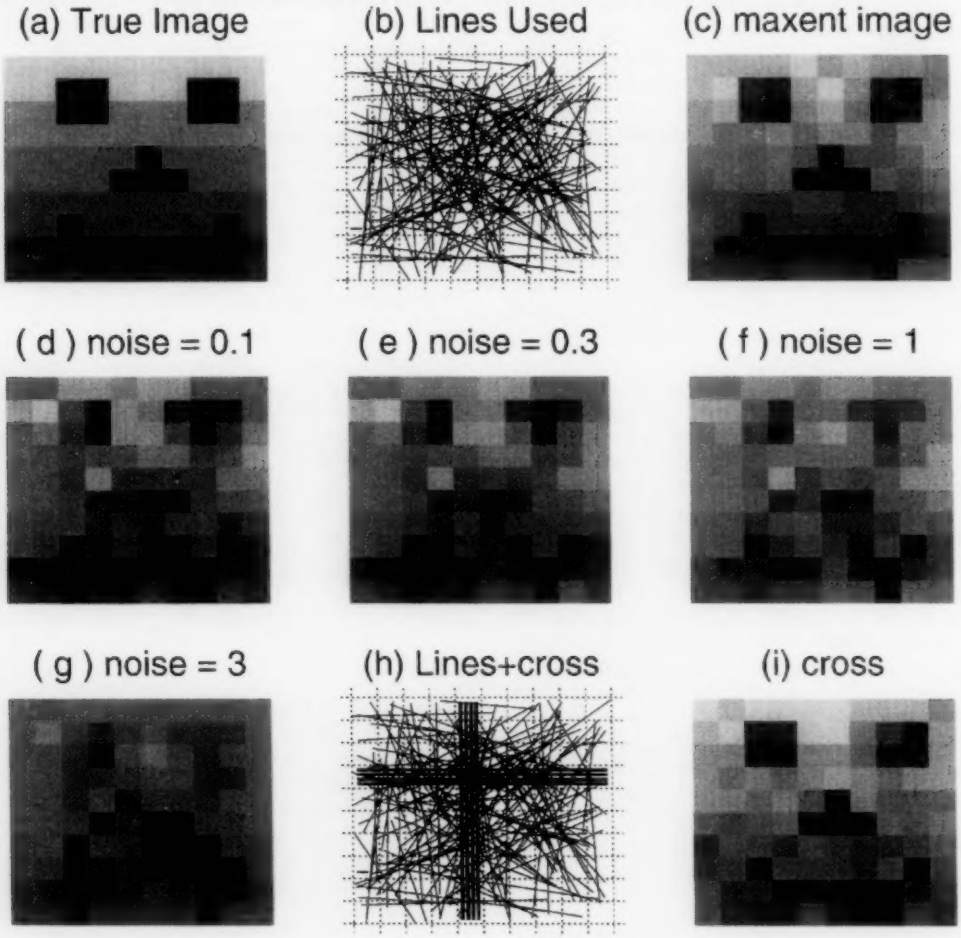

of the image (the logarithm of the likelihood or $\sum_i (F_i' - D_i)^2/2\sigma^2$) is equal to the number of records in the dataset, since that is approximately the number of degrees of freedom in the problem. The reasons for this choice are described in Sivia (1996).

All data manipulation and the production of figures and images in this study were carried out using S-PLUS functions, which extracted the data sets, set up the parameter files for the final inversion, called the optimization programs, read back the solution files, and plotted the graphs and images. The actual optimization of the trial image f' was done with separate C programs based on Macaulay's (1992) modifications of the original published algorithm by Skilling and Bryan (1984).

Testing the method

The MaxEnt tomography method has been used and tested in other areas of application but the differences here were sufficient to persuade us to test the method with randomly distributed tomography lines and to investigate its sensitivity to the choice of other parameters. A 10 by 10 square artificial pattern of varying density between 1 and 9 in the figure of a face was generated (Fig. 1*a*). The mean level of the image is 3.94 (standard deviation 2.36). Then 150 lines, representing tows, were passed across the image from random start to random finish points within the image (Fig. 1*b*). The mean line length was 5.44 units (standard deviation 5.50). Because all of the points were generated within the image, the edge blocks of the figure have fewer lines passing through them and we would expect a poorer fit of the image there. To simulate the "catch" in each tow, the density was integrated along each line giving a mean of 22.30 (standard deviation 11.57). Of this variance, 64% would be generated even with a constant density image because of the variation in line lengths.

The simulated "catches" and locations of the lines were passed to the maximum entropy tomography algorithm, which was able to regenerate the figure of the face (Fig. 1*c*). A number of runs were made, varying the control parameter, σ, to find the smallest value that would still produce a solution. The algorithm would be unable to terminate with a value of σ smaller than this. This choice of σ should therefore give an image with maximum contrast. The sum of squares of the densities of the original image was 2106. After optimization in this way, the sum of squares of differences between the fitted image and the original was 51, explaining 97.58% of the sum of squares.

A number of further runs were made, in each case adding normal

© 1998 NRC Canada

Fig. 2. Density differences between the true face image blocks and a MaxEnt reproduction versus the total length of "tows" passing through each block (the effort). The horizontal line indicates zero differences between original and image blocks.

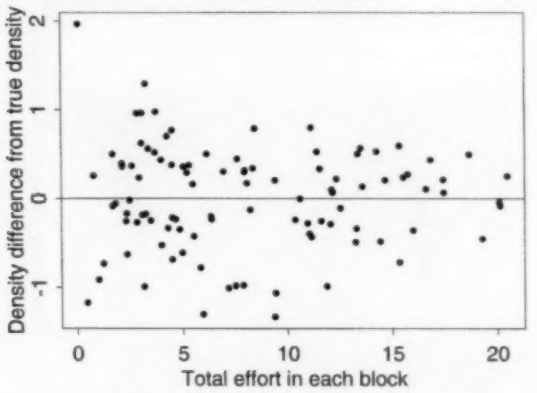

variate noise (mean 0) to the catches. Figures 1*d* to 1*g* show the images for noise standard deviations of 0.1, 0.3, 1.0, and 3.0, respectively. As noise is added, the image degenerates, becoming less and less intense as the added noise increases until it relapses into a uniform field. This demonstrates one of the advantages of the method: that it does not invent patterns that do not exist. Further testing could have been done with non-normally distributed noise.

Because the fishery data have the additional disadvantage that the locations of the tows are very uneven, we tested the behaviour of the method when there were many more tows through certain squares than through others. We wanted to ensure that extra effort in a block would not, in itself, cause the system to conclude that there was a greater density in that block. We added a cross of 12 vertical and 12 horizontal lines passing through one square, as shown in Fig. 1*h*. The added lines should even improve the fit of the resulting image as extra information is being provided to the algorithm. Figure 1*i* shows this. The final fitted image is improved with a residual sum of squares of 36.7 (fitted correlation of 0.9826) compared with 51 (0.9758) for the image without the cross (Fig. 1*c*). Examining the resulting image closely shows that densities are indeed closer to the original for those rows and columns containing the cross.

To emphasise this point, the density difference between the true image and the fitted image for the 100 blocks in the face image were plotted against the total length of tomography lines in the square, corresponding to the effort in that region (Fig. 2). The cross was not used in this example. Although the variance decreases as the length increases (as the density in the square becomes better defined with more data), those blocks with more lines running through them have the same zero average difference in density as those with few lines.

Data standardization

As stated previously, the quantity of fish caught in a tow depends not only on the density of fish but also on the size of the net, characteristics of the ship towing it, and other factors. A linear multiplicative model was fitted to standardise the catches so that data from tows would be more comparable:

$$(7) \qquad \frac{D'_i}{R_i} = k_{1,i}k_{2,i}k_{3,i}\ldots\exp(e_i).$$

Here D'_i is the observed catch in tow i, R_i is the length of that tow, $k_{1,i}$, $k_{2,i}$, $k_{3,i}$, etc., are fitted regression terms reflecting the effect of other factors on the catch. e_i is the residual from the fitted model and represents fluctuations in catch rate that cannot be explained by other factors. Some of this residual may be explained by spatial variation in fish density on a local scale. The expression is made additive by a logarithmic transformation.

The model was fitted using stepwise regression. The variables included were time within the season, vessel nationality (a surrogate for many behavioural factors), time of day, year, vessel length, latitude, and headline height. The most significant variable is a seasonal effect, modelled as a cubic continuous variable on the day of the season. The second most important variable is nationality, followed by the time of day and year. The last is a surrogate for changes in total biomass from year to year. Vessel size, net size, and tow latitude are minor variables. All of the variables explain only about a quarter of the total variance. Apart from any variation due to spatial fluctuations in fish density, there will also be a great deal of noise and variations due to other undocumented changes in fishing efficiency such as net configuration and water currents. The model is described in more detail by Vignaux (1996*a*).

A standardized catch is defined as

$$(8) \qquad D_i = \frac{D'_i}{k_{1,i}k_{2,i}k_{3,i}\ldots} = R_i\exp(e_i) = \sum_{j=1}^{n} R_{ij}f_j + \epsilon_i.$$

This is the equivalent of eq. 1.

Although all factors should be fitted in the regression model, it is not necessary to use all factors ($k_{1,i}k_{2,i}k_{3,i}$, ...) in the standardization of eq. 8. For example, it might be better not to remove variability due to seasonal and spatial effects in the D_i by standardization but to allow the MaxEnt model to fit these.

Results

Hoki (*Macruronus novaezelandiae*) is a gadid species widely distributed in New Zealand waters. The largest stock, known as the western stock, is thought to have feeding grounds in the Sub-Antarctic region south of New Zealand and to migrate to the West Coast of the South Island to spawn in July and August each year (Sullivan et al. 1995). The 1994 stock assessment estimated the biomass in 1995 of this stock to be 1.54 million tonnes, with a virgin biomass of 1.69 million tonnes and a long-term average yield of about 185 000 t·year^{-1} (Sullivan et al. 1995).

There is a concentrated trawl fishery on the spawning aggregations consisting mainly of large foreign vessels chartered by New Zealand companies. In 1993 there were 61 vessels in the fishery, in an area about 130 nautical mile long by 30 nautical mile wide. The vessels ranged from 25 to 105 m overall length and come from a number of countries, including Japan, Korea, and Norway. They use mid-water or bottom trawl nets in depths of 300–700 m. All vessels fishing in New Zealand waters are required to report both their catch and effort on forms submitted to the Ministry of Agriculture and Fisheries. Most of the larger vessels must include details about each tow.

We applied the method to CPUE residuals data from hoki seasons 1991 through 1993. The area of the fishery chosen for analysis was a 96 by 160 nautical mile rectangle with the lower left-hand corner at point 169°22.5′E, 43°4.5′S. It was divided into rectangular blocks for each of which we would estimate a fish density. Several block sizes were tested (see Lizamore 1995) and a block size of 8 by 8 nautical miles was finally used for the analyses reported here. This accords well with Vignaux (1996*a*), who gave evidence for spatial correlation in this fishery up to 11 nautical miles. Apart from choosing an appropriate block size, we assumed no spatial correlation between blocks, though one would hope for better

© 1998 NRC Canada

Fig. 3. Weekly tows and corresponding MaxEnt density images for the test area for weeks 5 to 8 (19 July to 15 August) of the 1991 hoki season. The area shown is a 96 by 160 nautical mile rectangle with the lower left-hand corner at point 169°22.5′E, 43°4.5′S. The rectangle is divided into 8 × 8 nautical mile blocks for calculation of the relative density.

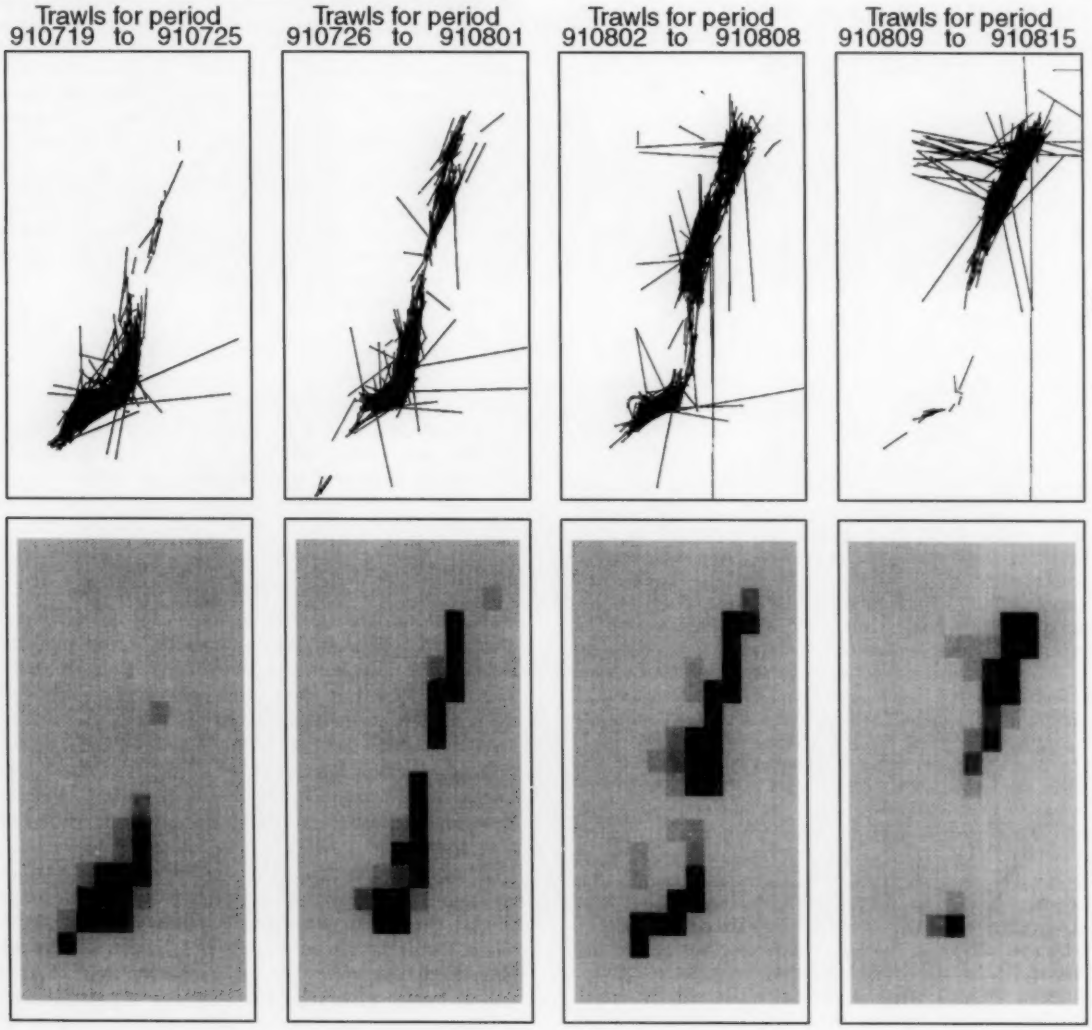

fitted images if such information was incorporated into the model. Work is progressing to incorporate spatial correlation as well as other information into the model.

The data for a season was divided into time periods and each period was analysed independently. One would choose the shortest period possible balanced by the need for sufficient trawls to generate a useful image. Periods of a day, a week, and a month were all tested and, for this paper, 7-day periods were used. Vignaux (1996*a*) gave evidence of temporal correlations up to 14 days. It was therefore assumed that within a 7-day period the pattern of fish distribution would be relatively stable. No further temporal correlation was included in the model. Each period was analysed independently with the possible loss of some quality of image generation. Work to incorporate temporal correlation into the model is continuing.

The null model, **m**, was set to be a uniform distribution over the area, that is, the pre-prior probability of fish in each of the squares was assumed to be the same.

Figure 3 shows a sequence of density plots for 1-week periods in 8 × 8 nautical mile squares for part of the 1991 season. The top row of Fig. 3 shows the tows recorded for each period. Obviously anomalous tows appear in some of the periods. The effect of their removal is described in the sensitivity studies outlined later in this section (Fig. 4). The bottom row of Fig. 3 shows the results of the tomographic fit in the form of densities in 8 × 8 nautical mile squares. The greatest density of fish is represented by the blackest squares. Each period is analysed and normalised independently.

The squares are blank where there are no tows as no information about density is provided where there is no effort.

© 1998 NRC Canada

Fig. 4. Images of the fish density for the week of 19–25 July 1993 (week 6 of the season). The left-hand figure shows the density with all reported tows, the right-hand picture shows it with all tows with the straightness ratio outside the range 0.7 to 1/0.7 removed. The white area indicates those blocks for which there is no information. The densities are on a common density range but the original densities are scaled using a square-root scaling to better display the detail of the images and the zone of no information.

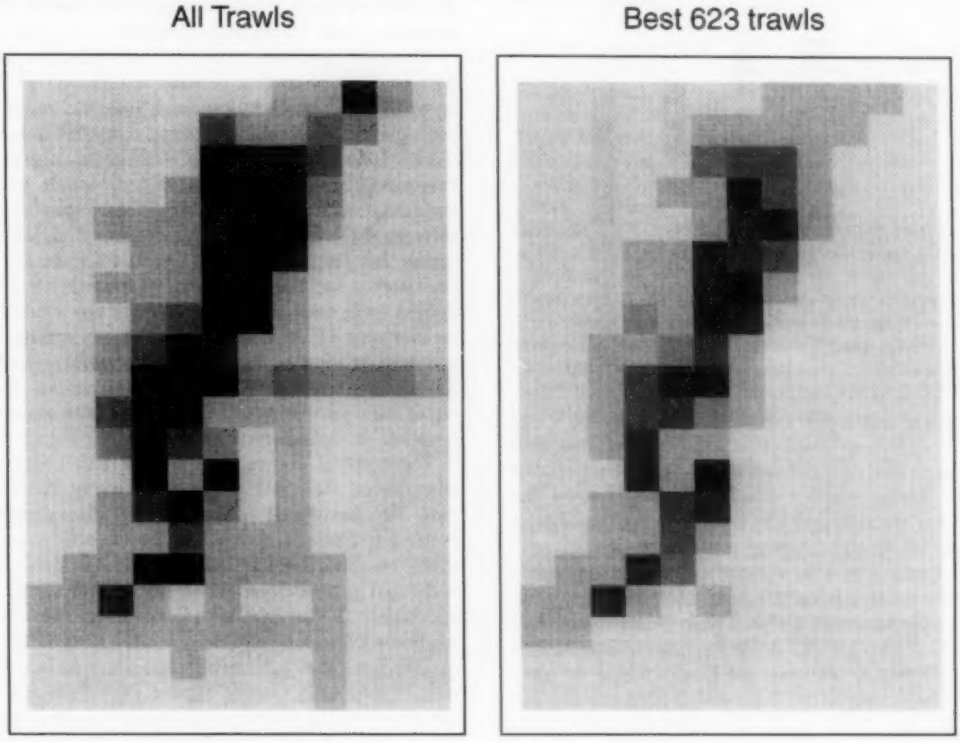

This highlights the fact that the data come from the activities of the commercial fishers who are hoping to concentrate their effort in high density locations and avoid low density areas. However, Vignaux (1996*b*) has produced evidence that fishers are not entirely successful at this and often do not put greatest effort into the areas with greatest fish density. This is probably because they do not have enough information to know where these areas are.

Even though each picture is obtained from a completely independent set of trawl data, the density patterns seem to change in a smooth way from one week to the next, suggesting that interpreting the dense areas as patches of fish would not be unreasonable.

Interpreting the images for a complete season of 11 weeks in this way suggests a high density conglomeration of fish in the south at the start of the season which grows, spreads north, and then splits into two. The southern concentration of fish remains throughout the season but seems to contract. Figure 3 shows a sequence of 4 weeks from the season.

If patches of fish move on time scales of weeks, we might expect that from one day to the next there be relatively little movement. This would suggest that the images taken from two days should be relatively similar. However, on a daily scale there will be few tows in many of the squares so we might expect poor quality images of density. We extracted 14 consecutive 1-day data sets from the 1993 season to investigate this. We took all squares where there were data available on two consecutive days and calculated the correlation in the densities. A high correlation would indicate that a square that had high image density on one day is more likely to have a high image density on the next and vice versa. Although the images on this level display a large degree of variation, a small but statistically significant correlation was found between the data on consecutive days. The nonparametric rank order correlation coefficient was 16.4%, which with 435 degrees of freedom has a t value of 3.48 ($p = 0.0003$) showing that this result is significant at the 1% level. However, pairs two days apart have a correlation coefficient of only 6.9%, which with 363 degrees of freedom has a t value of only 1.31. The probability of obtaining a t value as large as this under the null hypothesis that the two patterns are independent is 9.5%. That is, after two days the daily data are not good enough to detect any correlation (at a 5% significance level). There is too much noise and there are too few records when we use the data from only one day.

The model assumes that the tows are straight lines between the start and end positions entered on the fisher's form. However, if the displacement between the start and end positions of the tow is compared with the distance that a vessel could travel given the recorded speed and start and end times it is clear that while most tows go directly from start to end position (within the errors associated with the start and end

© 1998 NRC Canada

Fig. 5. Correlation between the original image and a series of images recalculated with 50, 100, ..., 250 tows removed from the dataset at random. The original dataset (giving the base image) is for 1993 week 6 and contains the 623 straightest tows.

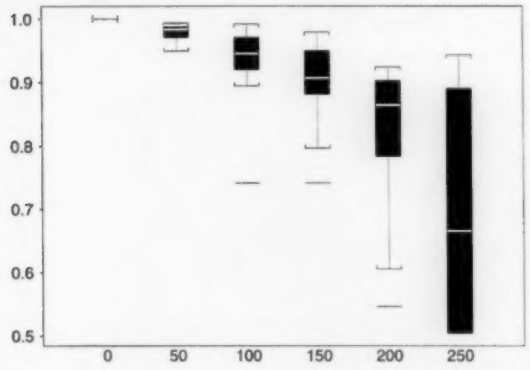

positions, start and end times, and particularly with the speed of the tow), a significant number of tows achieve less than half the displacement possible and therefore probably travel a curved path. There is also a smaller number of tows that apparently travel much longer distances than are possible in the time. These are clearly reporting errors.

The two images in Fig. 4 show the effect of removing those tows that deviate most from the straight tow assumption, those whose displacement to distance ratio is less than 0.7 or greater than 1/0.7. This left 623 of an original 1007 tows. The figures also differentiate between the blocks where no tows passed (white) and those where there was at least one tow but no inferred density (light grey). The densities have been adjusted by a square root scaling before plotting to produce a better contrast between the light grey (no density) areas and those where a density is inferred by the algorithm. The density pattern is similar in the two diagrams but some of the outlying dark areas have disappeared. The correlation between the two images is 0.62 (using the 77 blocks in common).

To test the robustness of the images produced, we randomly removed tows from the dataset, starting from the set of 623 "straight" tows, and recalculated the image. We then calculated the correlation between the old and the new dataset using only blocks where there was effort in both datasets. This process was repeated ten times at each level of removals. The results are shown in Fig. 5 with a boxplot at each number of removals. The average observed correlation falls slowly as the tows are removed and does not drop below 0.9 until 100 are removed (i.e., about 16% of the original 623 tows). This shows that the main features of the image are robust, although details may be sensitive to some features of the data. The ultimate safeguard is that, as the information is reduced, the image becomes less and less intense, asymptotically reducing to uniformly grey. This is demonstrated by the simulation experiments.

Discussion

Tomography is a well known technique in a variety of different fields, and the MaxEnt algorithm for solving the tomography equations is well tested. It has not (to our knowledge) been previously applied in this novel way. However, there is an elegant analogy between X-ray beams probing the density distribution inside a body and tows probing the density distribution of a fishery. This means that the mathematical structure of the fishing situation maps neatly into the mathematical structure of the tomography problem.

Thus MaxEnt tomography is a useful technique that allows fine-scale maps of fish density distribution to be generated from CPUE data. The tomography method requires data consisting of totals of some quantity accumulated over a distance. Trawl, long-line, or dredge CPUE are examples of datasets that would be appropriate for this purpose. It is desirable that the data be dense, with numbers of tomography lines passing through the same squares, so that the fish density in each square can be determined in a robust way from a large number of data values. Data from an intense fishery, such as a fishery on a spawning stock, is therefore ideal. The inherent noisiness of CPUE data and the non-uniformity and nonrandomness of the tow locations do not seem to have prevented the method from producing valid images (as shown by the significant correlations of the images from consecutive days, based on independent datasets).

The method allows mapping of fish distributions from commercial data where there are many vessels collecting data. This has the advantage that there is a great deal of data coming in from many areas at the same time, so you do not need to assume that the fish distribution is static over the time scale that it takes a single vessel to sample the whole area adequately. It can take significant time, even using a rapid method such as acoustics, to cover the whole fishery area, and in this time the fish distribution may have changed. The images that are produced from CPUE data are, in contrast, largely synoptic. However, because it relies on commercial data, produced by fishers who are unlikely to search the entire extent that the fish may occupy, the picture will have gaps in those areas where fishers did not operate. Also, because the data originate from many different vessels and under different conditions, the method requires that the catches be standardized, using a linear or GLM model to ensure comparability.

Once this is done, the tomography method allows fish distribution to be mapped at finer spatial scales than the size of a tow, producing higher resolution maps than you would expect were possible. Vignaux (1996*a*) showed that it is possible to detect such fine-scale density distributions using CPUE data, but this tomography method is necessary to produce images at the fine scale. The resolution of the image produced by this method is only limited by the number of tows and the noise in the data. Another advantage of the general method is that data from different sources such as trawls and acoustic surveys can be combined to produce a single density map. Work is continuing to follow up on this idea.

Mapping fish distribution is an essential first step in any study of a fishery (Caddy and Garcia 1986; Hilborn and Walters 1992). We have shown that images during the season can be generated so that fish distribution and movements can be visualised. These images give insight into the fishery that cannot be obtained simply by looking at crude maps of CPUE or maps of the effort distribution.

However, determining the spatial distribution is also essential for understanding the relationship between CPUE and abundance (Cooke 1985). Hilborn and Walters (1987) point

© 1998 NRC Canada

out that when fish distribution is heterogeneous, skippers can manipulate their CPUE by appropriate choice of fishing area, altering the relationship between CPUE and abundance. Even fine-scale spatial distribution can be important in the relationship between CPUE and abundance because, even on a fine-scale, skippers are making decisions about where to fish (Vignaux 1996*b*).

Of course, the location of the fish is of great interest to the fishers themselves. In principle, if you built a linear model to standardise the CPUE data based on a large data set from a number of years, you would not expect the model or the parameter estimates to change markedly with the addition of a few extra records. You might therefore use the model to rapidly standardise the data as it arrived, allowing images to be constructed week by week. This would allow visualization of the fish distribution during the season itself for anyone who had immediate access to tow by tow data from a large number of vessels.

Our results are preliminary but show promise of development. Work is proceeding on testing the effects of including spatial correlation and uncertainty of trawl tracks and combining trawl data with acoustic survey data (see Gresham 1997).

Acknowledgements

We thank Chris Francis and two referees for useful comments and Valerie Chan for her contributions.

References

Buck, B. and Macaulay, V.A. 1990. Maximum entropy in action. Clarendon Press, Oxford.

Caddy, J.F., and Garcia, S. 1986. Fisheries thematic mapping — a prerequisite for intelligent management and development of fisheries. Oceanogr. Trop. **21**: 31–52.

Cooke, J.G. 1985. On the relationship between catch per unit effort and whale abundance. Rep. Int. Whal. Comm. **35**: 511–519.

Daniell, G.J. 1991. Of maps and monkeys: an introduction to the maximum entropy method. *In* Maximum entropy in action. Chapt. 1. *Edited by* B. Buck and V. Macaulay. Clarendon Press, Oxford. pp. 1–18.

Freiden, B.R., and Zoltani, C.K. 1985. Maximum bounded entropy: application to tomographic reconstruction. Appl. Optics, **24**: 201–207.

Gresham, D. 1997. Techniques for fine resolution MaxEnt image analysis. Master's thesis, ISOR, Victoria University of Wellington, New Zealand.

Gull, S.F., and Daniell, G.J. 1978. Image reconstruction from incomplete and noisy data. Nature (London), **272**: 686–690.

Hilborn, R., and Walters, C.J. 1987. A general model for simulation of stock and fleet dynamics in spatially heterogeneous fisheries. Can. J. Fish. Aquat. Sci. **44**: 1366–1369.

Hilborn, R., and Walters, C.J. 1992. Quantitative fisheries stock assessment: choice, dynamics and uncertainty. Chapman and Hall, New York.

Lizamore, S.C. 1995. Topics in maximum entropy applications. Master's thesis, ISOR, Victoria University of Wellington, New Zealand.

Macaulay, V.A. 1992. Bayesian inversion with applications to physics. PhD thesis, Theoretical Physics, University of Oxford.

Marsh, T.R., and Horne, K. 1989. Maximum entropy tomography of accretion discs from their emission lines. *In* Maximum entropy and Bayesian methods. *Edited by* J. Skilling. Kluwer Academic Publishers, Dordrecht. pp. 339–345.

Pendock, N., and Wedepohl, E. 1991. Application of maximum entropy to radio imaging of geological features. *In* Maximum entropy and Bayesian methods. *Edited by* C. Smith. Kluwer Academic Publications, Dordrecht. pp. 397–402.

Sibisi, S. 1983. Two-dimensional reconstructions from one-dimensional data by maximum entropy. Nature (London), **301**: 134–136.

Sivia, D.S. 1996. Data analysis. Clarendon Press, Oxford.

Skilling, J., and Bryan, R.K. 1984. Maximum entropy image reconstruction: general algorithm. Mon. Not. R. Astronom. Soc. **211**: 111–124.

Sullivan, K.J., Cordue, P.L., and Ballara, S.L. 1995. A review of the 1992–93 hoki fishery and assessment of hoki stocks for 1994. New Zealand Fisheries Assessment Research Document 95/5, MAF Fisheries, N.Z. Ministry of Agriculture and Fisheries.

Vignaux, M. 1996*a*. Analysis of spatial structure in fish distributions using commercial catch and effort data from the New Zealand hoki fishery. Can. J. Fish. Aquat. Sci. **53**: 963–973.

Vignaux, M. 1996*b*. Analysis of vessel movements and strategies using commercial catch and effort data from the New Zealand hoki fishery. Can. J. Fish. Aquat. Sci. **53**: 2126–2136.

© 1998 NRC Canada

Influence of beaver ponds on the phosphorus concentration of stream water

R.L. Klotz

Abstract: A study of five beaver ponds in central New York State showed that the ponds differed in how they influenced streamwater P concentration. Processes in three of the ponds increased soluble reactive P (SRP) of the stream water during warmer months, and also dramatically increased SRP in one of these ponds (Black Warrior) during an extended period of ice cover. The remaining two ponds were consistent in reducing SRP in stream water at all times of the year. Total soluble P trends essentially followed those of SRP at each of the ponds, while total P differed from SRP at four of the sites. Microbial respiration created anaerobic conditions within the pond sediments which influenced biogeochemical cycling of P. Anaerobic conditions and H_2S production occurred at Black Warrior pond during the extended winter ice cover, resulting in SRP release. My results showed that elevated levels of P may occur for only short distances downstream of ponds before equilibrium processes reduce the concentration.

Résumé : Une étude portant sur cinq étangs à castors du centre de l'État de New York a révélé que ces retenues d'eau différaient dans la manière dont elles modulaient la teneur en P dans l'eau du ruisseau. Dans trois des étangs, les processus ont donné lieu à une augmentation de la teneur en P soluble réactif (PSR) de l'eau pendant les mois chauds, ainsi qu'à une augmentation spectaculaire de la teneur en PSR dans l'un de ces étangs (Black Warrior), pendant une période prolongée de couverture de glace. Les deux autres étangs, de façon régulière, réduisaient la teneur en PSR de l'eau à n'importe quel moment de l'année. Les tendances des teneurs en P soluble total suivaient pour l'essentiel celles du PSR dans chacun des étangs, tandis que les teneurs en P total étaient différentes de celles en PSR dans quatre des étangs. La respiration microbienne créait des conditions anaérobies dans les sédiments des étangs, ce qui influait sur le cycle biogéochimique du P. Des conditions anaérobies et la production de H_2S se sont manifestées dans l'étang Black Warrior pendant la longue période hivernale où la retenue d'eau était couverte de glace, ce qui a causé la libération de PSR. Les résultats révèlent que les teneurs élevées en P ne se manifestent que sur de courtes distances en aval des étangs car les processus d'équilibre les font rapidement baisser. [Traduit par la Rédaction]

Introduction

Beaver (*Castor canadensis*) influence free-flowing streams by cutting trees and building dams, activities that alter stream morphology, hydrology, organic matter transport, nutrient cycling, and species composition and diversity (Naiman et al. 1986, 1988; Hammerson 1994). Anaerobic zones created within the sediments of beaver ponds may result in the cycling of nutrients into soluble forms which enhance the productivity of the stream (Dahm et al. 1987). The entire stream ecosystem may be impacted, since stream ecosystem theory holds that modification of the upstream reaches where dams are typically constructed will impact ecological processes downstream (Vannotte et al. 1980).

The cycling of P in beaver impounded streams has received only limited attention. In a Wyoming stream, total P (TP) was found to accumulate in the impounded area, a phenomenon attributed to the trapping of particles in the pond (Maret et al. 1987). The deeper of two beaver ponds studied in the Precambrian shield area of Canada showed a net release of TP downstream, while the other showed no significant trends (Devito et al. 1989). Ice cover during the winter was associated with high levels of P in the anoxic surface water in a central Ontario beaver pond (Devito and Dillon 1993). This same pond exhibited seasonal trends in P retention that were inversely correlated with runoff.

Studies of nutrient cycling in swamps and other wetlands may provide insight into how beaver ponds influence the cycling of P in streams, although one direct comparison of swamps versus beaver ponds showed that they were different in terms of total N and TP retention (Devito et al. 1989). Wetland sediments retain P by chemical precipitation and adsorption reactions and by incorporation into biomass (Gehrels and Mulamoottil 1989). However, processes that lead to the release of P from sediments also occur in wetlands simultaneously with retention (Gehrels and Mulamoottil 1989). Richardson (1985) concluded that while wetlands may initially remove large amounts of P, this would be followed by large exports of P in a few years.

This study assessed how beaver ponds influenced the concentration of P in stream water. The results are important because P is an element that often limits the growth and metabolism of stream organisms (Elwood et al. 1981). If the concentration of this element is altered, then downstream reaches will be changed.

Received May 30, 1997. Accepted September 30, 1997.
J14029

R.L. Klotz. Department of Biological Sciences, State University of New York, Cortland, NY 13045, U.S.A.
e-mail: klotz@snycorva.cortland.edu

© 1998 NRC Canada

Fig. 1. Map of the five beaver pond sites located in Cortland County, New York State.

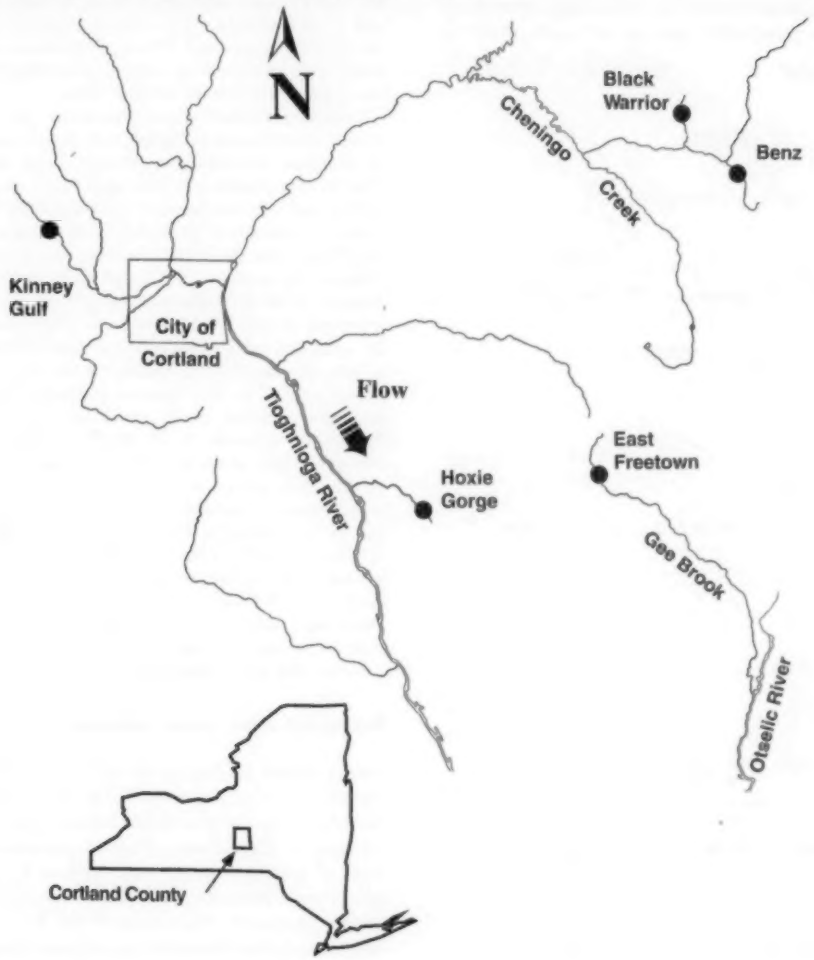

Table 1. Characteristics of beaver ponds.

Site	Age (years)	Pond area (m^2)	Pond volume (m^3)	Watershed area (km^2)
Black Warrior	6	36 400	19 500	3.0
Benz	7	5 400	3 050	3.1
Hoxie Gorge	7	1 800	810	1.1
East Freetown	4	12 500	6 900	3.7
Kinney Gulf	1	7 700	3 500	5.0

Study area

The streams and beaver ponds studied were located in Cortland County in central New York State (Fig. 1). The soils surrounding each of the sites were of the silt loam type (USDA 1961). Morphometric characteristics of the ponds, all located on first-order streams, are presented in Table 1. Each pond had just one inlet and one outlet stream. The inlet streams for the Black Warrior, Benz, East Freetown, and Kinney Gulf sites were 2 m wide with streambeds of cobblestones interspersed with coarse-grained sediments. At the Hoxie Gorge site, the inlet was 1 m wide with fine-grained, darker sediments and fewer cobbles. The watersheds surrounding the ponds were a mixture of forest and old field habitat with a small amount of agricultural activity at the East Freetown and Kinney Gulf sites.

© 1998 NRC Canada

Fig. 2. SRP, TSP, and TP concentrations upstream (solid circles) and downstream (open triangles) of Black Warrior beaver pond over 12 months. Error bars represent SE.

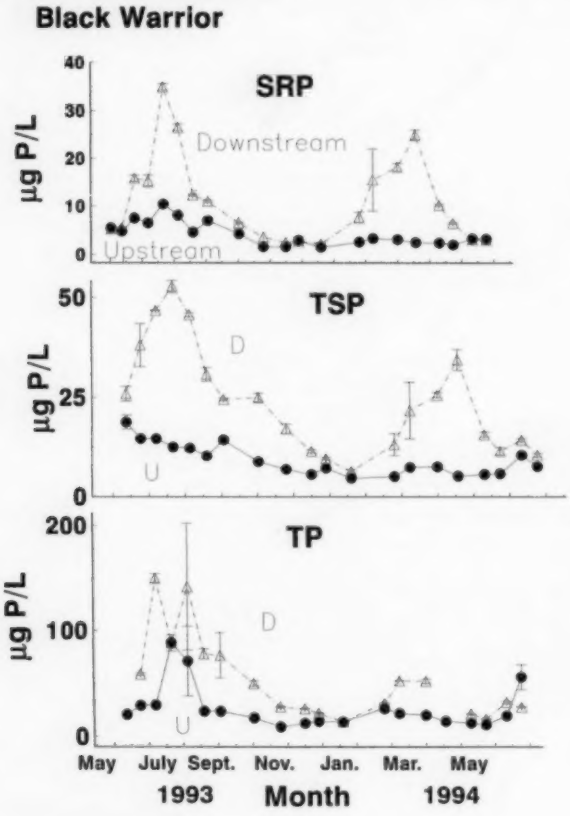

The winter period during this study was cold with significant snow. Ice formed on the ponds around 20 December 1993 and thickened significantly before being covered by a 60-cm snowfall on 4 January 1994 and again by a 60-cm snowfall on 3 March. Ice was about 38 cm thick on the ponds on 26 January and increased to 56 cm by 7 March. There were no midwinter thaws. Ice-out occurred on Kinney Gulf pond by the end of March, on East Freetown and Hoxie Gorge ponds in the first part of April, on Benz pond in the middle of April, and on Black Warrior pond by the end of April.

Methods

Stream water samples for this study were collected in duplicate at about biweekly intervals from May 1993 thru May 1994 at the Black Warrior, Benz, East Freetown, and Hoxie Gorge sites and from December 1993 to December 1994 at the Kinney Gulf site. These biweekly collections were taken from free-flowing locations just upstream of each pond and also downstream just below the beaver dam. On three dates in 1994, water samples were collected from five locations in Black Warrior pond to determine P levels in pond areas isolated from the stream channel. Collections were made in acid-cleaned, 1-L polyethylene bottles and stored on ice until returned to the laboratory. Samples were filtered (0.45-µm Millipore type HA, acid cleaned) in the laboratory within 3 h of collection. Soluble reactive P (SRP) was determined the day of collection by the ascorbic acid method (APHA 1985). Total soluble P (TSP) was determined on filtered aliquots and TP was determined on unfiltered aliquots within 24 h of collection utilizing persulfate digestion followed by the ascorbic acid method (APHA 1985).

Duplicate samples were collected from the top 5 cm of sediments at each upstream site and pond, each sample being a composite from 10 locations. Samples were seived (2-mm mesh) and either used fresh for determination of zero equilibrium phosphate concentration (EPC_0) and electron transport system activity (ETSA) or dried and stored for subsequent measurement of various sediment characteristics. EPC_0 is the phosphate concentration in solution at which no net sorption nor desorption of phosphate by sediments occurs and was determined by the technique described in Klotz (1988). ETSA, an indication of microbial biomass and respiration, was measured as the reduction of 2-(*p*-iodophenyl)-3-(*p*-nitrophenyl)-5-phenyltetrazolium chloride (INT) to INT-formazan (Broberg 1985). Since INT can be reduced by both aerobes and anaerobes, the total microbial respiratory activity in the sediments was measured. Anaerobic ETSA was assumed to be unaffected by the procedures used (Songster-Alpin and Klotz 1995). Several characteristics considered potentially important in regulating P adsorption by or release from sediments were determined on dried sediments. Exchangeable Al and Fe and sediment P were determined as described by Klotz (1988) and expressed on a dry weight basis. Organic matter content was estimated by weight loss of dried sediments at 500°C in a muffle furnace. Sediment density was determined by weighing 1-mL subsamples after drying overnight at 80°C. Pond morphometries were determined by making depth soundings and using Sigma Scan software with aerial photographs.

Results and discussion

Beaver ponds in this study differed in how they influenced streamwater P concentration. The influence of the ponds was determined by comparing the P concentrations at the upstream versus downstream sites at each pond location. SRP is an estimate of orthophosphorus, the form of P readily available for uptake by organisms and directly involved in ecological processes. Therefore, this form of P was focused on in this study. Processes in the Black Warrior, Hoxie Gorge, and East Freetown ponds consistently increased the SRP of the stream water during the warmer months (June–October for Black Warrior and Hoxie Gorge (Figs. 2 and 3) and June–August for East Freetown (Fig. 4)). Of these three sites, there was also a significant increase in SRP downstream of Black Warrior pond during the period of ice cover (December–April; Fig. 2). SRP did not consistently increase from upstream to downstream of the other four ponds during this ice-cover period (Figs. 3–6). Processes in two of the beaver ponds resulted in consistently lower SRP from upstream to downstream; SRP decreased on 19 of 22 collections at Benz pond (Fig. 5) and on 20 of 21 collections at Kinney Gulf pond (Fig. 6). TSP trends (Figs. 2–6) essentially followed those of SRP at each of the sites. TP mirrored SRP trends at Black Warrior (Fig. 2), but at Benz, an opposite trend was detected during warmer months, with TP concentration higher downstream relative to upstream, while SRP was lower (Fig. 5). TP was similar to SRP at Hoxie Gorge in that concentrations were higher downstream during warmer months, but differed during cold months when TP values were elevated downstream (Fig. 3). No consistent trends were found for TP at the East Freetown and Kinney Gulf sites (Figs. 4 and 6).

© 1998 NRC Canada

Fig. 3. SRP, TSP, and TP concentrations upstream (solid circles) and downstream (open triangles) of Hoxie Gorge beaver pond over 12 months. Error bars represent SE.

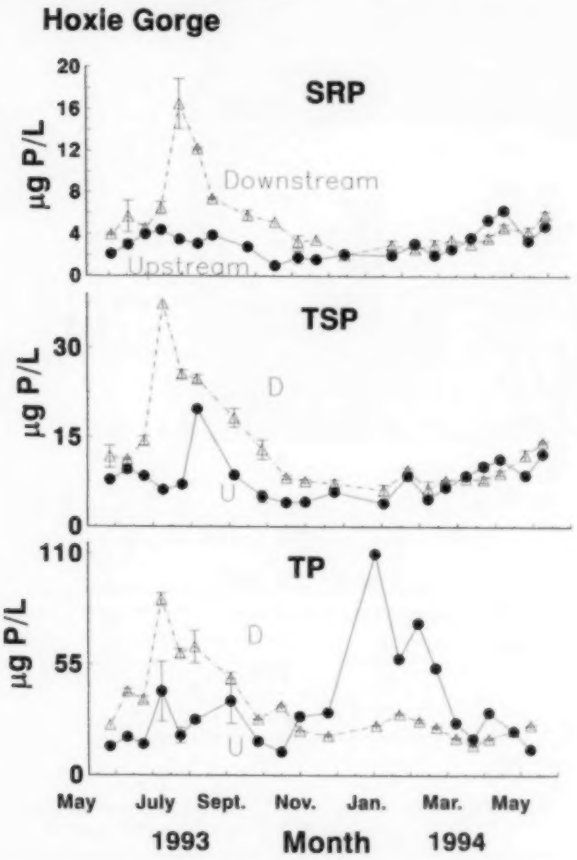

Fig. 4. SRP, TSP, and TP concentrations upstream (solid circles) and downstream (open triangles) of East Freetown beaver pond over 12 months. Error bars represent SE.

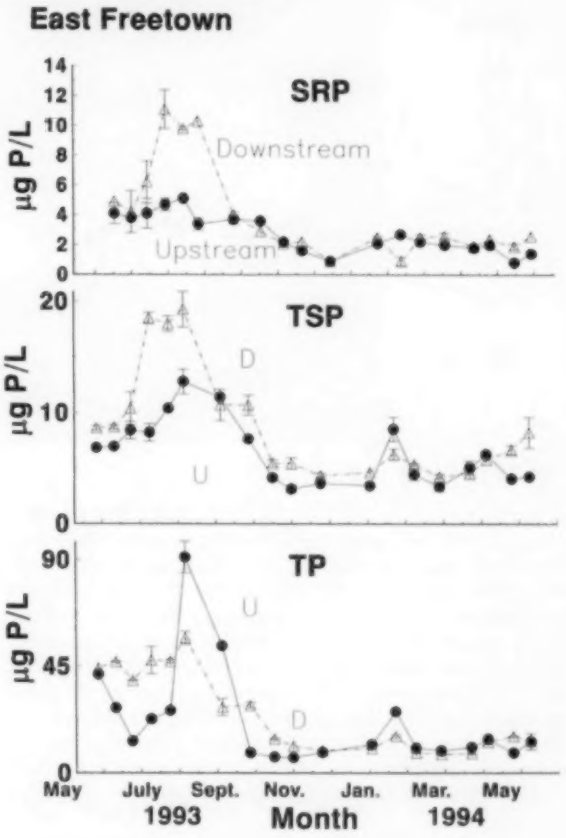

Seasonal trends in the export of P from wetlands and beaver ponds have been found in other studies, but the timing was different from that found in this study. Greater release of orthophosphorus from wetlands occurred in the fall due to higher water levels creating anaerobic conditions and the leaching of P from decaying vegetation (Gehrels and Mulamoottil 1989). The beaver ponds in this study that released SRP (Black Warrior, Hoxie Gorge, and East Freetown; Figs. 2–4) typically did so during the warm summer growing season with no elevation of SRP downstream of the ponds in the fall.

The shape of the Black Warrior pond led to anaerobic conditions during the ice-cover period (December 1993 – April 1994), a phenomenon that coincided with high levels of SRP (Figs. 2 and 7). The location of the stream channel at one edge of the pond prevented aerated water of the inlet stream from mixing with much of the pond water (Fig. 7). Beginning in March, there was a strong odor of H_2S when holes were drilled through the pond ice, indicating anaerobic conditions. Since ice cover prevented reaeration from the atmosphere, large portions of the pond became anaerobic. It can be seen from Fig. 7 that these shallow, isolated areas had the highest P concentrations. Others have shown that anaerobic conditions in the winter can cause a release of P from beaver ponds in Canada (Devito and Dillon 1993). The P released from the Black Warrior pond during the winter was at least partly due to P release from the sediments. There was a decrease in the P content of sediments in Black Warrior pond after H_2S was noticed (Table 2; 7 March – 12 May).

Various mechanisms have been given for the release of P from sediments under anaerobic conditions. Mortimer (1941, 1942) hypothesized that P was released into solution from Fe compounds when Fe was reduced under anaerobic conditions. Golterman (1995) showed that a large quantity of H_2S is needed to reduce sufficient amounts of ferric oxyhydroxides (Fe(OOH)) to measure P release. Jensen et al. (1995) found that maximal P release from marine sediments was linked to sulfate reduction and formation of sulfide. The odor of H_2S was intense at the outlet of Black Warrior, but not at the other ponds, during March. Perhaps the combination of high H_2S and anaerobic conditions led to P release under ice cover at Black Warrior (Fig. 2). Some research suggests that storage and release of P by sediment bacteria are redox-dependent processes, with anaerobic conditions leading to rapid release of P from living cells (Gachter et al. 1988). Other possible mechanisms for P release under anaerobic conditions include

© 1998 NRC Canada

Fig. 5. SRP, TSP, and TP concentrations upstream (solid circles) and downstream (open triangles) of Benz beaver pond over 12 months. Error bars represent SE.

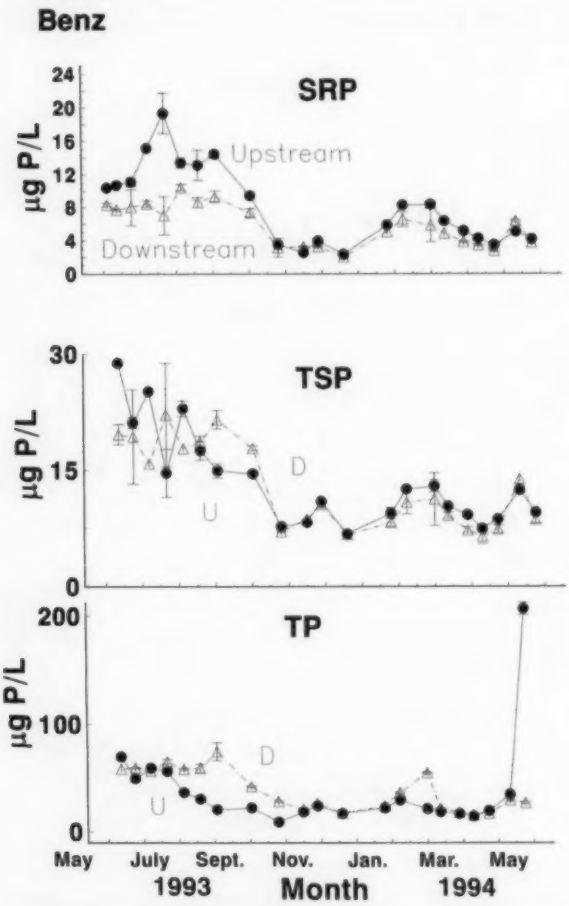

Fig. 6. SRP, TSP, and TP concentrations upstream (solid circles) and downstream (open triangles) of Kinney Gulf beaver pond over 12 months. Error bars represent SE.

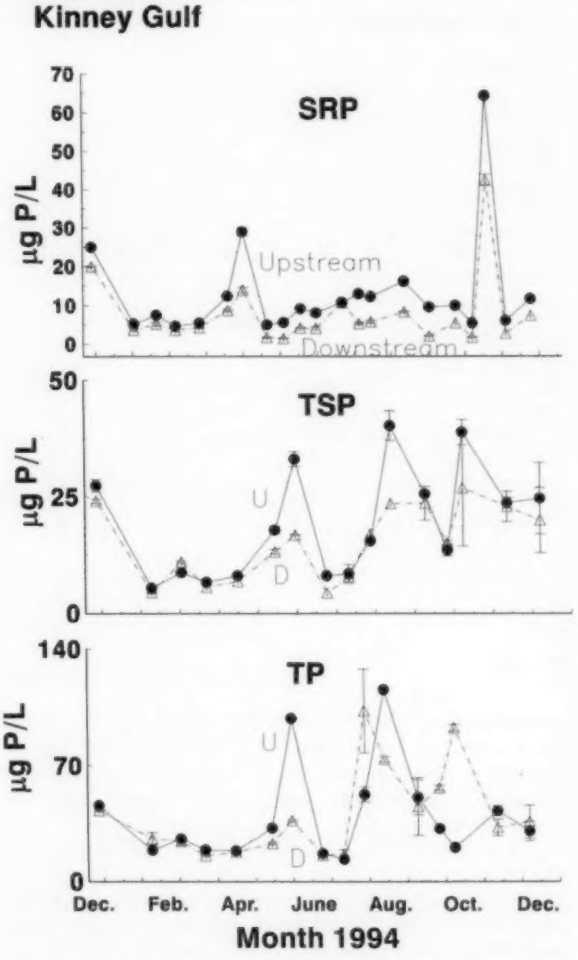

bacterial lysis (De Montigny and Prairie 1993), mineralization of organic P, and solubilization of apatite due to decreased pH (Golterman 1995). Another factor that possibly led to higher P in the Black Warrior outlet stream was the release of P from decaying aquatic plants, perhaps stimulated by the anaerobic conditions. On 7 March 1994, green particles were found in the water of Black Warrior pond that appeared to be from the breaking up of dense stands of the green alga *Chara*.

Ponds other than Black Warrior did not exhibit higher levels of SRP downstream versus upstream in winter (Figs. 3–6). The stream channels passed through the middle of these other ponds, bringing aerated water to most of the pond area, thus preventing the creation of sizeable anaerobic zones. It should be emphasized that only one of five ponds released P during the unusually long ice-cover period of this study. The results for Black Warrior and the pond studied by Devito and Dillon (1993) may not be typical.

There are a number of factors associated with the P cycle that influence P release and sorption by sediments (Wetzel 1983) that may have resulted in the differences in P behavior between the ponds studied here. The differences may have been due to conditions in the overlying water and sediments of the ponds that alter the P exchange equilibria. The oxygen content of the sediment–water interface and the thickness of the oxygenated microzone are important. A small difference of a few millimetres in depth to the anaerobic level can determine whether the sediments will release P or not. Turbulence can affect this process. The distribution, composition, growth, and decay of the aquatic plants in the ponds may also result in differences in the timing and extent of P retention and export. Maturational processes that occur as beaver ponds accumulate sediments, at different rates for different ponds, may also lead to differences in P cycling. Future research is necessary to isolate the most important mechanisms.

The plots for Black Warrior (Fig. 2) show higher downstream values for all forms of P during a large part of the year. Since a pond cannot export P forever, there must be an unmeasured source of P. One explanation for this source is that P may have accumulated in the sediments/soil of the

© 1998 NRC Canada

Fig. 7. SRP (μg P/L) at five locations (A, B, D, E, and H) in Black Warrior beaver pond on three dates in 1994: (*a*) 11 March (ice covered), (*b*) 20 May, and (*c*) 6 July.

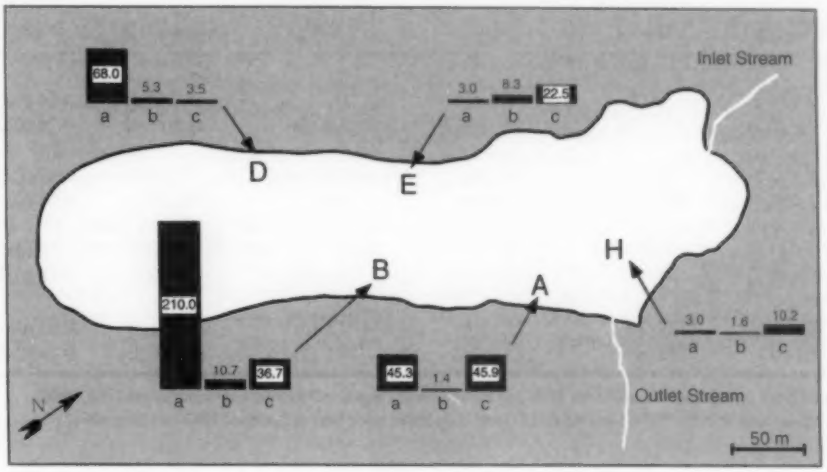

Table 2. Sediment P levels (mean (SE)) in Black Warrior pond during and after ice cover in winter 1994.

Date	Sediment P (μg P/g sediment)
26 January	188 (4)
7 March	214 (2)
12 May	164 (8)

Table 3. Changes in SRP and TSP (mean (SE)) in a stream reach below Black Warrior dam on 11 March 1994.

Site	SRP (μg P/L)	TSP (μg P/L)	Temperature (°C)
Upstream	2.5 (0)	5.1 (0.3)	0
At dam	24.9 (1.1)	34.3 (2.6)	0
60 m below dam	13.4 (0.2)	19.7 (0.2)	0

ponded area in previous years, and maturational processes (Richardson 1985) led to a release of the stored P during this study. A second explanation is that my sampling regime may not have included large storm-related inputs of P to the pond.

The increased concentration of P that sometimes results from beaver activities may occur for only short distances downstream of the pond. In March 1994, stream water SRP and TSP decreased from a point just below the dam at Black Warrior to a site 60 m downstream (Table 3). At this time the pond was anaerobic and releasing large amounts of P. The primary factor leading to the downstream P reduction was probably abiotic sorption by the sediment. Previous studies showed that the P concentration of stream water in this region was controlled by equilibrium processes with the sediments, and any input of P to stream water was removed rapidly by the sediments (Klotz 1988). The fact that these measurements were made when the water temperature was 0°C indicates that biological processes were probably minimal. The frozen landscape as well as the short distance over which the decrease was noted would rule out dilution as a reason for the concentration decrease. The oxidation of ferrous Fe as the previously anoxic water traveled downstream may also have led to the removal of dissolved P by precipitation. Stream sediments do not provide a limitless sink for P, and therefore, renewal of sorption sites is important. This renewal is accomplished by storm events that wash out streambed sediments and bring in new material from the stream banks (Meyer 1979).

The results of various analyses for upstream versus pond sediments are presented in Table 4. EPC_0 and sediment density were lower in the pond sediments at each of the sites studied, while sediment P, exchangeable Fe and Al, percent organic content, and ETSA were all higher in the pond sediments. Previous studies showed that streamwater P was significantly positively correlated with EPC_0 in Hoxie Gorge Creek (Klotz 1988). The SRP of the streamwater was hypothesized to be regulated by Fe and Al compounds in the sediments; the higher the concentration of these compounds, the lower the EPC_0 and streamwater P. If beaver ponds responded the same way as streams, then one would predict from Table 4 that SRP would be lower downstream of each of the ponds. This was not the case. The reason for the descrepancy is that EPC_0 was measured under aerobic conditions that are typically found in sediments of flowing streams, while beaver ponds create anaerobic patches in the stream (Dahm et al. 1987). These anaerobic conditions in pond sediments were created by higher microbial activity as measured by ETSA (Table 4; Songster-Alpin and Klotz 1995). If the beaver pond is replaced by a free-flowing stream when the dam washes out, these sediments would likely become more aerobic and would all be expected to absorb P.

Although wetlands have generally been considered to be nutrient sinks, Gehrels and Mulamootil (1989) concluded

© 1998 NRC Canada

Table 4. Zero equilibrium P concentration (EPC_0) and other sediment characteristics (mean (SE)) at four sites.

Site	EPC_0 (μg/L)	Sediment P (μg/L)	Exchangeable Fe (μg/g)	Exchangeable Al (μg/g)	Organic (%)	Density (mg/mL)	ETSA[a] ($\mu g\ O_2 \cdot g^{-1} \cdot h^{-1}$)
Black Warrior							
Upstream	3.9 (0.1)	83 (3)	3.5 (0)	0	5.7 (0.2)	1.06 (0.05)	18 (2)
Pond	2.4 (0.1)	159 (39)	159 (5)	74.8 (5)	42.6 (1.0)	0.26 (0.02)	263 (29)
Benz							
Upstream	8.3 (0.2)	145 (6)	15.8 (8)	0	6.3 (0)	1.12 (0.06)	29 (3)
Pond	2.4 (0.3)	189 (1)	71.2 (4)	28.2 (6)	18.0 (0.6)	0.34 (0.02)	221 (23)
East Freetown							
Upstream	3.5 (0.1)	57 (2)	0	0	3.2 (0)	1.62 (0.09)	11 (2)
Pond	0.6 (0.1)	94 (0)	44.3 (2)	14.5 (10)	9.1 (0.5)	0.66 (0.02)	258 (66)
Hoxie							
Upstream	2.9 (0.2)	138 (13)	3.5 (0)	7.4 (3)	11.3 (1.4)	0.63 (0.05)	65 (11)
Pond	1.1 (0.1)	282 (0)	123 (16)	20.2 (2)	19.7 (0.5)	0.26 (0.02)	227 (24)

Note: Black Warrior and Benz were sampled on 24 June 1993 and East Freetown and Hoxie Gorge were sampled on 1 July 1993.
[a]ETSA, electron transport system activity. Values are means of seven collections made between August 1993 and May 1994.

from their own study and a review of the literature that wetlands have a limited capacity to retain orthophosphorus. Beaver are currently creating new wetlands in many areas. From this study, we can begin to understand how beaver pond wetlands influence SRP concentrations in streams. Of the five ponds studied, two led to consistently lower SRP concentrations downstream (Figs. 5 and 6), while the other three exhibited seasonal summer release of SRP to their stream systems (Figs. 2–4). This release of SRP during the summer growing season may be great enough to influence nutrient limitation and act as a stimulus for increased stream production under certain conditions. While heterotrophic microbial production and breakdown rates of leaves were found to be greater in streams with higher P and N (Weyers and Suberkropp 1996), it should be noted that summer SRP release from the ponds in this study did not correspond to the fall period when leaves are present in greatest amount in the streams. P limitation of autotrophs decreased as SRP increased from 0.7 to 1.1 and 3.4 μg/L at three stream sites studied by Bothwell (1989). The SRP changes resulting from beaver activity were frequently much greater than the range studied by Bothwell, indicating that beaver ponds may affect nutrient limitation. Along with the nutrient changes, beaver ponds dramatically increase the unshaded water surface area, allowing sunlight to reach aquatic primary producers. In ponds where SRP increases, the combination of sufficient light and higher P should lead to greater primary production. If sunlight is sufficient at the downstream reaches, then primary production should increase in streams draining these ponds. Increased production will probably occur only short distances downstream as equilibrium processes in the sediments reduce streamwater P concentrations.

Acknowledgements

I thank K. Cameron, M. Songster-Alpin, and T. Roote for assistance with the field and laboratory analyses and Dr. David Miller for assisting with morphometric measurements. This research was supported by a grant to R.L. Klotz from the National Science Foundation (DEB-9205279).

References

American Public Health Association (APHA), American Water Works Association, and Water Pollution Control Federation. 1985. Standard methods for the examination of water and wastewater. 16th ed. APHA, Washington, D.C.

Bothwell, M.L. 1989. Phosphorus-limited growth dynamics of lotic periphytic diatom communities: areal biomass and cellular growth rate responses. Can. J. Fish. Aquat. Sci. **46**: 1293–1301.

Broberg, A. 1985. A modified method for studies of electron transport system activity in freshwater sediments. Hydrobiologia, **120**: 181–187.

Dahm, C.N., Trotter, E.H., and Sedell, J.R. 1987. Role of anaerobic zones and processes in stream ecosystem productivity. *In* Chemical quality of water and the hydrologic cycle. *Edited by* R.C. Averett and D.M. McKnight. Lewis Publishers, Chelsea, Mich. pp. 157–178.

De Montigny, C., and Prairie, Y. 1993. The relative importance of biological and chemical processes in the release of phosphorus from a highly organic sediment. Hydrobiologia, **253**: 141–150.

Devito, K.J., and Dillon, P.J. 1993. Importance of runoff and winter anoxia to the P and N dynamics of a beaver pond. Can. J. Fish. Aquat. Sci. **50**: 2222–2234.

Devito, K.J., Dillon, P.J., and LaZerte, B.D. 1989. Phosphorus and nitrogen retention in five Precambrian shield wetlands. Biogeochemistry, **8**: 185–204.

Elwood, J.W., Newbold, J.D., Trimble, A.F., and Stark, R.W. 1981. The limiting role of phosphorus in a woodland stream ecosystem: effects of P enrichment on leaf decomposition and primary producers. Ecology, **62**: 146–158.

Gachter, R., Meyer, J.S., and Maris, A. 1988. Contribution of bacteria to release and fixation of phosphorus in lake sediments. Limnol. Oceanogr. **33**: 1542–1558.

Gehrels, J., and Mulamoottil, G. 1989. The transformation and export of phosphorus from wetlands. Hydrol. Processes, **3**: 365–370.

Golterman, H.L. 1995. The role of the ironhydroxide–phosphate–sulphide system in the phosphate exchange between sediments and overlying water. Hydrobiologia, **297**: 43–54.

Hammerson, G.A. 1994. Beaver (*Castor canadensis*): ecosystem alterations, management, and monitoring. Nat. Areas J. **14**: 44–57.

Jensen, H.S., Mortensen, P.B., Andersen, F.O., Rasmussen, E., and Jensen, A. 1995. Phosphorus cycling in a coastal marine sediment, Aarhus Bay, Denmark. Limnol. Oceanogr. **40**: 908–917

© 1998 NRC Canada

Klotz, R.L. 1988. Sediment control of soluble reactive phosphorus in Hoxie Gorge Creek, New York. Can. J. Fish. Aquat. Sci. **45**: 2026–2034.

Maret, J.J., Parker, M., and Fanny, T.E. 1987. The effect of beaver ponds on the nonpoint source water quality of a stream in southwestern Wyoming. Water Res. **21**: 263–268.

Meyer, J.L. 1979. The role of sediments and bryophytes in phosphorus dynamics in a headwater stream ecosystem. Limnol. Oceanogr. **24**: 365–375.

Mortimer, C.H. 1941. The exchange of dissolved substances between mud and water in lakes (Parts I and II). J. Ecol. **29**: 280–329.

Mortimer, C.H. 1942. The exchange of dissolved substances between mud and water in lakes (Parts III, IV, summary, and references). J. Ecol. **30**: 147–201.

Naiman, R.J., Melillo, J.M., and Hobbie, J.E. 1986. Ecosystem alteration of boreal forest streams by beaver (*Castor canadensis*). Ecology, **67**: 1254–1269.

Naiman, R.J., Johnston, C.A., and Kelley, J.C. 1988. Alteration of North American streams by beaver. BioScience, **38**: 753–762.

Richardson, C. 1985. Mechanism controlling phosphorus retention capacity in freshwater wetlands. Science (Washington, D.C.), **228**: 1424–1427.

Sonster-Alpin, M.S., and Klotz, R.L. 1995. A comparison of electron transport system activity in stream and beaver pond sediments. Can. J. Fish. Aquat. Sci. **52**: 1318–1326.

United States Department of Agriculture (USDA). 1961. Soil survey, Cortland County, New York. Ser. 1957, No. 10. Soil Conservation Service, USDA, Washington, D.C.

Vannote, R.L., Minshall, G.W., Cummins, K.W., Sedell, J.R., and Cushing, C.F. 1980. The River Continuum Concept. Can. J. Fish. Aquat. Sci. **37**: 130–137.

Wetzel, R.G. 1983. Limnology. W.B. Saunders, Philadelphia, Pa.

Weyers, H.S., and Suberkropp, K. 1996. Fungal and bacterial production during the breakdown of yellow poplar leaves in 2 streams. J. North Am. Benthol. Soc. **15**: 408–420.

© 1998 NRC Canada

Estimation of growth and mortality parameters from size frequency distributions lacking age patterns: the red sea urchin (*Strongylocentrotus franciscanus*) as an example

Barry D. Smith, Louis W. Botsford, and Stephen R. Wing

Abstract: We present a maximum likelihood procedure for estimating population growth and mortality parameters by simultaneously analysing size frequency and growth increment data. The model uses von Bertalanffy growth with variability among individuals in the two parameters that determine growth rate, and size-dependent mortality. Analyzing growth increments together with size frequencies reduces the statistical confounding of the natural mortality rate with von Bertalanffy's K parameter. We assume steady-state (constant recruitment) conditions for the size distributions; hence the method does not depend on age modes in the distribution. We evaluate the bias and precision of estimates obtained for growth-dominated distributions typical of the red sea urchin (*Strongylocentrotus franciscanus*) in northern California, although the method and its evaluation could be applied as easily to mortality-dominated or bimodal distributions. The method provides good estimates with sample sizes as low as 200 individuals in a size distribution and 30 growth increments. Results are robust to random variability in recruitment, measurement error, and sampling selectivity up to the size where about one third of the distribution is affected. Estimation of the fishing mortality rate could require size distributions from both an unharvested and a harvested population. Estimates of growth and mortality rates depend critically on reliable growth data.

Résumé : Nous présentons une méthode du maximum de vraisemblance servant à estimer les paramètres de croissance et de mortalité d'une population par l'analyse simultanée de données sur les fréquences de taille et les incréments de croissance. Le modèle fait appel à la fonction de croissance de von Bertalanffy avec variabilité entre les individus dans les deux paramètres qui déterminent le taux de croissance, et à la mortalité dépendante de la taille. Le fait d'analyser les incréments de croissance en combinaison avec les fréquences de taille réduit la possibilité de confondre statistiquement le taux de mortalité naturelle ave le paramètre K de von Bertalanffy. Nous supposons des conditions stables (recrutement constant) pour la distribution des tailles, de sorte que la méthode ne dépend pas des modes d'âge dans la distribution. Nous évaluons le biais et la précision des estimations obtenues pour des distributions ayant la croissance comme facteur dominant, typiques de l'oursin rouge (*Strongylocentrotus franciscanus*) dans le nord de la Californie, mais la méthode et son évaluation pourraient être appliquées avec autant de facilité aux distributions dont le facteur dominant est la mortalité ou aux distributions bimodales. La méthode fournit de bonnes estimations avec des échantillons de 200 individus seulement pour la distribution des tailles et avec 30 incréments de croissance. Les résultats sont robustes par rapport à la variabilité aléatoire du recrutement, aux erreurs de mesure et à la sélectivité de l'échantillonnage jusqu'à une taille où environ un tiers de la distribution est touché. Pour avoir une estimation du taux de mortalité par pêche, il faudrait peut-être obtenir des distributions des tailles dans une population non exploitée et dans une population exploitée. Les estimations des taux de croissance et de mortalité dépendent de façon critique de la fiabilité des données sur la croissance.
[Traduit par la Rédaction]

Received January 6, 1997. Accepted December 5, 1997.
J13818

B.D. Smith.[1] Environment Canada, Canadian Wildlife Service, Pacific Wildlife Research Centre, 5421 Robertson Road, Delta, BC V4K 3N2, Canada.
L.W. Botsford and S.R. Wing.[2] Department of Wildlife, Fish and Conservation Biology and Center for Population Biology, University of California, Davis, CA 95616, U.S.A.

[1] Author to whom all correspondence should be addressed. e-mail: barry.smith@ec.gc.ca
[2] Present address: Department of Marine Science, University of Otago, 304 Castle Street, Dunedin, New Zealand.

Introduction

Estimation of population parameters such as mortality, recruitment, and growth rates from age distributions is common practice. Methods are well developed for analyses of either single cohorts (e.g., Pope 1972) or several cohorts simultaneously (Fournier and Archibald 1982; Deriso et al. 1985; see review in Megrey 1989). A significant component of the cost of those procedures is the determination of age for a large number of individuals. Individual size is easier and less expensive to determine, and measurement of size is a necessary alternative when individuals of a species do not have permanent anatomical structures that record the passage

© 1998 NRC Canada

of time. However, methods for the estimation of population parameters from size distributions are not as completely developed. Most early methods for estimating parameters from a single size distribution were related to Beverton and Holt's (1956) estimate of the ratio of the growth parameter, usually represented by K in the von Bertalanffy equation, to total instantaneous mortality in terms of moments of the size distribution (see Weatherall et al. 1987). Others have estimated mortality rate from a known growth pattern and moments of a size distribution (e.g., Ebert 1981).

Modern methods deal with the structure of the size distribution, rather than just the moments. However, with few exceptions (e.g., Van Sickle 1977; Ebert 1981), these methods are still in part age based in that they depend on the modes in size distributions that result from annual pulses of recruitment (Macdonald and Pitcher 1979; Schnute and Fournier 1980; Pauly and David 1981; Fournier and Breen 1983; Fournier et al. 1990; Smith and McFarlane 1990) or moulting of invertebrate instars (Smith and Jamieson 1989). These methods descend from Petersen's (1892) technique for separating age modes in size distributions (see Grant et al. 1987 for other descendants). They are limited by the fact that age modes are not present in all size distributions, and if they are present, they typically occur only at smaller sizes.

An extant, challenging problem is the estimation of growth and mortality rates from single size frequency distributions that lack age patterns. Such distributions would be typical of species that either do not have annual recruitment pulses or have enough variability in growth patterns to obscure age modes in their size distributions (Barry and Tegner 1990; Ebert et al. 1993; Botsford et al. 1994). Tropical and subtropical species are more likely to be characterized by size frequency distributions lacking age patterns, but such distributions are also characteristic of some temperate species. Here, we present a method for estimating growth and mortality from size distributions that do not exhibit dominant age modes by including an auxiliary source of information, growth increments. Growth increments are the changes in sizes of individuals over a measured time period; hence, they require greater effort to collect than size measurements alone. However, the ages of individuals do not have to be determined. Including growth increment data allows unequivocal estimation of population growth and mortality parameters (e.g., Barry and Tegner 1990).

We use size distributions and growth increments obtained for the red sea urchin (*Strongylocentrotus franciscanus*) population of northern California to demonstrate the use of this method. Red sea urchin frequency distributions of test diameters typically lack the modes at small sizes that would indicate recent recruitment. Size distribution data are available from both harvested and unharvested sites in northern California. Growth increments, on the other hand, are scarce, primarily because urchins are difficult to tag. Here, we use growth increments from individuals held in the laboratory at natural temperatures and fed natural foods to demonstrate the estimation method. Because we use data from laboratory-grown urchins in this demonstration, the estimates obtained will not necessarily represent those of wild red sea urchins. We are in the process of obtaining growth increments for wild urchins using passive integrated transponder (PIT) tags. Our use of laboratory-grown urchins allows us to demonstrate the importance of having reliable growth data when estimating mortality rates with this method.

Our interest in the red sea urchin results from its commercial exploitation (Tegner 1989) and a concern that recent exploitation rates exceed those necessary for a sustainable fishery. The northern California fishery began in the mid-1980s, with landings peaking at 13.6×10^3 t in 1988 and then declining every year since to a level of 2.6×10^3 t in 1994. We used the method developed here to obtain preliminary estimates of urchin growth and mortality for an analysis of rotating spatial harvest schemes (Botsford et al. 1993). Subsequent investigation of growth and mortality rates indicated the need to characterize bias and precision in these estimates. This provided the motivation for this paper where we (*i*) derive a method for estimating growth and natural and fishing mortality rates from combinations of size frequency and growth increment data, (*ii*) evaluate the statistical characteristics of that method and its limitations, and (*iii*) demonstrate the method using laboratory growth increments and northern California size frequency data from both unharvested and harvested sites. We have used this method to interpret size distributions of other species (Smith and Botsford 1998) and are using it in a comprehensive description of the spatial variability of growth and mortality rates in the red sea urchin in northern California.

Estimation method

Size frequency model

Estimation of growth and mortality parameters from size frequencies and growth increments requires models for size distributions and growth increments that contain those parameters. Such models facilitate the statistical evaluation of parameter estimates with respect to those data using a criterion such as maximum likelihood.

We use the size-structured von Foerster equation

$$(1) \qquad \frac{\partial n(l,t)}{\partial t} = -\frac{\partial}{\partial l}\left[n(l,t)g(l)\right] - D(l)n(l,t)$$

to describe how the density $n(l,t)$ of individuals in a size frequency distribution changes with size l and time t, when governed by growth and mortality functions $g(l)$ and $D(l)$, respectively (Botsford et al. 1994; Smith and Botsford 1998). If sampled distributions show no modes at small sizes, then we assume that recruitment is constant. This steady-state condition means that a size distribution will not change appreciably in form over time given that growth and mortality rates also do not change. Under steady-state conditions, eq. 1 yields (Botsford et al. 1994)

$$(2) \qquad \frac{\partial n(l)}{\partial l} = -\frac{n(l)}{g(l)}\left[\frac{\partial g(l)}{\partial l} + D(l)\right].$$

Integrating this expression over size provides a size distribution corresponding to the specified $g(l)$ and $D(l)$. Van Sickle (1977) noted that if the growth pattern is known, the mortality pattern can be obtained from eq. 2.

We assumed a von Bertalanffy growth function because our observed growth increments for the red sea urchin decline approximately linearly with size:

© 1998 NRC Canada

$$g(l) = K(L - l) \quad (3)$$

where K is the instantaneous rate of change in growth rate and L is asymptotic test diameter. Total mortality is the sum of natural and fishing mortalities:

$$D(l) = Ze^{-bl} + F(l) \quad (4)$$

where Z is the instantaneous natural mortality rate at $l = 0$, $b > 0$ allows the natural mortality rate to decline with size, and $F(l)$ is the instantaneous fishing mortality rate at size l. A positive value for b can result in a bimodal size distribution.

Previous assessments of red sea urchin test diameter frequency distributions indicated that variability in growth was required to produce size frequency distributions similar to those observed from field-collected red sea urchins (Botsford et al. 1994). Variability in individual growth can be described in two ways: (*i*) as variability in inherent growth patterns among individuals and (*ii*) as random independent variability in each individual's growth over time (cf. Kirkpatrick 1984; Deriso and Parma 1988). Both growth models can produce the growth increment patterns we see in our urchin data.

We introduced variability in growth rate by admitting random variability in the von Bertalanffy parameters L and K (Sainsbury 1980). Equation 2 with variable growth can describe three generic types of size distributions observed in field collections: growth dominated (a single mode composed of larger individuals), mortality dominated (a single mode composed of smaller individuals), and bimodal (modes of both smaller and larger individuals), each depending on the relative values of K and the mortality rate (Botsford et al. 1994; Smith and Botsford 1998). Sampled distributions typically underrepresent the smallest individuals in a population because they are more difficult to collect. Thus, to complete our model, we chose a cumulative Gaussian selectivity curve defined by its mean (μ_ψ) and SD (σ_ψ).

Growth increment model

Following Sainsbury (1980), we chose L to be Gaussian in distribution and K to be gamma-distributed. We defined the growth parameters to be μ_L (mean of L), σ_L (SD of L), μ_K (mean of K), and σ_K (SD of K). Variability in L produces the mode at large sizes (i.e., the difference between the dashed and the solid lines in fig. 1*a* of Botsford et al. 1994). Variability in K, on the other hand, has little discernible effect on a steady-state size distribution (Botsford et al. 1994), but can dramatically affect the appearance of growth increment plots (Smith and Botsford 1998).

Sainsbury (1980) derived the mean and variance of the growth increments that would result from von Bertalanffy growth with random L and K. Specifically, the expected value of a growth increment, I_j, conditional on initial size l_j and time interval Δt is

$$\mu_{I_j} = (\mu_L - l_j)(1 - E[e^{-\mu_K \Delta t}]) \quad (5)$$

where μ_{I_j} is the expected increment of indivdual j. When K is gamma-distributed

$$E[e^{-\mu_K \Delta t}] = \left(1 + \frac{\Delta t \sigma_K^2}{\mu_K}\right)^{-\frac{\mu_K^2}{\sigma_K^2}}. \quad (6)$$

The variance of the distribution of increments conditional on initial test diameter l and time interval Δt is

$$\sigma_{I_j}^2 = \eta \sigma_L^2 + (\mu_L - l_j)^2 V[e^{-\mu_K \Delta t}] + \sigma_{M,I_j}^2 \quad (7)$$

where

$$V[e^{-\mu_K \Delta t}] = \left(1 + \frac{2\Delta t \sigma_K^2}{\mu_K}\right)^{-\frac{\mu_K^2}{\sigma_K^2}} - \left(1 + \frac{\Delta t \sigma_K^2}{\mu_K}\right)^{-\frac{2\mu_K^2}{\sigma_K^2}} \quad (8)$$

$$\eta = 1 - 2\left(1 + \frac{\Delta t \sigma_K^2}{\mu_K}\right)^{-\frac{\mu_K^2}{\sigma_K^2}} + \left(1 + \frac{2\Delta t \sigma_K^2}{\mu_K}\right)^{-\frac{\mu_K^2}{\sigma_K^2}} \quad (9)$$

and σ_{M,I_j}^2 represents the variance of error in measuring an increment I_j. Negative growth in sea urchin test diameters can occur, particularly if urchins are starved (Levitan 1988). Negative growth cannot result from this model, but measurement error can cause negative growth increments.

Maximum likelihood estimation

Maximum likelihood parameter estimates are obtained by minimizing the sum of the negative ln-likelihood of each datum. For our model, two likelihood functions are required, one for the size distribution data and another for the growth increments. The likelihood function for a simultaneous analysis of these data is the product of the likelihood function (or the sum of the negative ln-likelihood) for each data type if the growth increment and size frequency data are independent. This independence occurs when no individual (sea urchin) that provides growth increments also occurs as a member of the size distribution data.

Growth increments

We assumed a Gaussian distribution of observed growth increments (I_j) with mean μ_{I_j} and variance $\sigma_{I_j}^2$. Strictly speaking, the distribution of increments would be a combination of the Gaussian and gamma distributions of L and K, respectively, with the distribution tending to be truncated as l approaches L. However, the choice of a gamma distribution is arbitrary, having been made only to constrain $K > 0$ (Sainsbury 1980). If growth rates are always positive, then the distribution of increments must be truncated for values of l within the domain of the distribution of L (see fig. 5 of Sainsbury 1980 and fig. 6 of Smith and Botsford 1998). We deal with truncation by reshaping the Gaussian distribution of increments conditional on l and Δt to incorporate this truncation. If there is no measurement error, then our choice of a negative ln-likelihood function for growth increments is

$$\Theta_1(\mu_L, \sigma_L, \mu_K, \sigma_K | l, \Delta t) = \sum_{j=1}^{v} \ln\left(\sqrt{2\pi}\sigma_{I_j}\right) + \frac{(I_j - \mu_{I_j})^2}{2\sigma_{I_j}^2} + \ln(1 - \zeta_l) \quad (10)$$

which is modified from the strictly Gaussian function of Smith and McFarlane (1990) to incorporate truncation. The

© 1998 NRC Canada

term $1 - \zeta_l$ is the cumulative probability density of the Gaussian distribution of positive growth increments at size l. Equation 10 assures that the expected value of an increment remains greater than zero while the variance of the distribution of increments decreases as l approaches and exceeds μ_L.

We found that our urchins grown in the laboratory often yielded negative growth increments. Since these well-fed urchins were unlikely to have undergone negative growth, we attributed the negative increments to measurement error. Incorporation of measurement error in the likelihood function involves convolving the truncated Gaussian distribution (eq. 10) of true increments (l_j) with a Gaussian distribution representing measurement error for each increment. Measurement error variance for a growth increment l_j is

$$(11) \qquad \sigma^2_{M,l_j} = \sigma^2_{M,l_j} + \sigma^2_{M,l_j+l_j}.$$

For the red sea urchin, measurement error appeared to be proportional to test diameter; hence:

$$(12) \qquad \sigma_{M,l_j} = \sqrt{(0.01 l_j \sigma_{M,l=100})^2 + (0.01(l_j + l_j)\sigma_{M,l=100})^2}$$

where we have introduced the parameter $\sigma_{M,l=100}$ as the SE of measurement at 100 mm, or percent measurement error. True test diameters can never be known exactly; therefore, we show by simulation that the model error introduced by (*i*) assuming that the initial measurement of l_j is error free and (*ii*) using μ_{l_j} as a surrogate for l_j in eq. 12 tends to be small and unimportant for measurement error less than 5% of l.

The revised negative ln-likelihood function is thus

$$(13) \qquad \Theta_2(\mu_L, \sigma_L, \mu_K, \sigma_K, \sigma_{M,l=100} | l, \Delta t) = \sum_{j=1}^{v} \ln(2\pi\sigma_{M,l_j}\sigma_{l_j}) \times \int_{l_j=0}^{l_j=\infty} \frac{(\tilde{l}_j - l_j)^2}{2\sigma^2_{M,l_j}} + \frac{(l_j - \mu_{l_j})^2}{2\sigma^2_{l_j}} + \ln(1 - \zeta_l).$$

In eq. 13, we distinguish a true growth increment (l_j) from a growth increment measured with error ($\tilde{l}_j$). Although measurement error ($\sigma_{M,l=100}$) is an estimable parameter, in practice, it would be preferable to provide a value for measurement error ($\sigma_{M,l=100}$) obtained from measurement experiments performed independently of the measurement of growth increments.

Size distributions

We used the separation statistic of Schnute and Fournier (1980), without their factor 2,

$$(14) \qquad \Theta_3(\mu_L, \sigma_L, \mu_K, \sigma_K, Z, b, F(l), \mu_\psi, \sigma_\psi) = \sum_{i=1}^{m} O_i \ln\left[\frac{O_i}{P_i}\right] \text{ for all } O_i > 0$$

to evaluate the fit of estimated size frequency distributions to observed distributions. Equation 14 measures the discrepancy between the observed (O_i) and predicted (P_i) numbers of individuals within each size frequency cell i and is the negative ln-likelihood function for a multinomial distribution (i.e., the probability distribution corresponding to a size distribution) without the additive constant (Schnute and Fournier 1980).

Minimization

We used the software of Mittertreiner and Schnute (1985) to minimize Θ_2 when using only growth increments, Θ_3 when using only size distribution data, and $\Theta_2 + \Theta_3$ when using both types of data. The SEs of the maximum likelihood parameter estimates were calculated using their approximate numerical method. Model parsimony was achieved by fixing nonsignificant parameters at zero. Diagnostics of model fit for the distribution of growth increment residuals and the distribution of size frequency data were based on chi-square probabilities (p) calculated using the Monte Carlo method of Roff and Bentzen (1989). Their diagnostic evaluates the probability of the observed data given the model and parameter estimates. A satisfactory diagnostic would be a probability value that suggests that the data are reasonably likely given the model. This diagnosis is the antithesis to null hypothesis testing where one generally tests to reject the null model. Thus, higher values of p will be associated with more likely models.

Evaluation of model performance

Approach

We evaluated performance of the method by calculating the bias and precision of estimates obtained for data simulated using known parameter values. These known parameter values were chosen based on the results of preliminary analyses of red sea urchin size frequencies and growth increments (μ_L = 120 mm, σ_L = 11 mm, μ_K = 0.3 year^{-1}, σ_K = 0 year^{-1}, Z = 0.1 year^{-1}). A growth-dominated size structure is typical of the northern California red sea urchin distributions to which we plan to apply this method, so we choose that distributional form for rigorous statistical evaluation. We subjected the model to a variety of imperfect data and conditions that could be encountered by practitioners (Table 1). Specifically, we tested the robustness of our assumption of constant recruitment by evaluating the way in which random variability in recruitment affects parameter estimates. The influences of practical values for sample size, measurement error, bin size, and size selectivity on parameter estimates were also evaluated. We also estimated parameters using only growth increments under various conditions.

Additionally, to address the concern that the expeditious use of laboratory data (or any other data that could misrepresent true growth rates) would give misleading results for wild urchins, we tested the consequence of analyzing simulated growth data that overrepresented true growth rates by 1.5, 2, and 3 times. We analyzed these growth data in combination with a typical steady-state growth-dominated distribution experiencing a fishing mortality rate of $F(l)$ = 0.3 year^{-1} for $l \geq 76$ mm, the minimum legal size. It should be noted that this is not a test of the efficacy of the model's estimation ability; it is an assessment of the effect of misrepresentative growth data on the estimates of other parameters, particular the mortality parameters.

We focused all of our evaluations on the key parameters describing growth (μ_L, σ_L, μ_K), natural mortality (Z), fishing mortality ($F(l)$), and measurement error ($\sigma_{M,l=100}$). We did not evaluate estimation of variability in K (σ_K) because our

© 1998 NRC Canada

Table 1. Percent bias and precision (in parentheses) expressed as percent SE. These are calculated using the results of 30 replicates of each of the simulation cases considered.

Consideration	μ_L	σ_L	μ_K	Z	ME ($\sigma_{M,l=100}$)
Baseline distribution					
400 frequencies, 60 increments	**0.7** (1.2)	1.5 (5.8)	**–1.8** (3.7)	**–12.5** (13.8)	—
Frequency data only[a]					
400 frequencies	**0.8** (1.3)	–1.0 (8.6)	–0.4 (17.5)	—	—
Increment data only					
60 increments	0.3 (3.0)	–2.0 (8.8)	–0.8 (6.6)	—	—
60 increments, $\sigma_K = 0.1$ (not estimated)	**–14.0** (5.4)	**49.0** (***15.1***)	**36.7** (20.0)	—	—
60 increments, 2% ME (estimated)	**1.5** (***4.9***)	0.2 (***20.1***)	**–2.9** (9.0)	—	1.3 (17.4)
60 increments, 2% ME (estimated)	2.9 (10.0)	**19.9** (45.8)	**–2.1** (15.6)	—	**–3.8** (13.1)
Frequency and increment data					
100 frequencies, 30 increments	0.6 (2.1)	0.1 (9.9)	**–2.7** (5.7)	**–18.3** (26.7)	—
200 frequencies, 30 increments	**1.0** (1.6)	–2.8 (8.5)	–1.4 (5.1)	–4.6 (19.6)	—
400 frequencies, 30 increments	**1.0** (1.2)	**–2.8** (6.7)	0.9 (4.7)	**–7.9** (14.2)	—
200 frequencies, 60 increments	**0.6** (***1.5***)	**4.6** (7.4)	–0.5 (4.3)	**–10.9** (19.1)	—
800 frequencies, 120 increments	**0.7** (0.8)	–0.6 (4.2)	**–1.0** (2.6)	**–5.1** (9.8)	—
Nonzero σ_K					
$\sigma_K = 0.1$ (not estimated)	**–3.2** (1.3)	**36.8** (6.9)	**10.8** (***5.7***)	**–11.2** (16.0)	—
Measurement error					
2%	0.4 (1.4)	**7.0** (7.8)	–1.2 (4.3)	–5.8 (14.8)	**–7.4** (14.3)
5% (not estimated)	**–7.4** (1.6)	**71.2** (***9.6***)	**31.3** (8.7)	**–44.0** (21.0)	—
5% (estimated)	–0.2 (2.1)	**50.5** (13.2)	–0.9 (9.1)	**–9.3** (18.4)	0.1 (10.2)
Monthly recruitment variability					
RV = 2	–0.4 (***1.2***)	**4.4** (6.1)	0.5 (3.9)	**–15.8** (***14.4***)	—
RV = 4	–0.7 (***1.3***)	**–6.4** (6.4)	0.1 (4.0)	**–17.8** (***14.9***)	—
Combination cases					
RV = 4, 5% ME (not estimated)	**–8.1** (***1.7***)	**83.9** (***10.7***)	**34.4** (9.6)	**–45.2** (***18.4***)	—
RV = 4, 5% ME (estimated)	–0.9 (***1.0***)	**23.4** (***5.6***)	1.2 (5.8)	–10.2 (***13.8***)	–3.1 (11.3)
Size selectivity					
$\mu_\psi = 10$ mm; $\sigma_\psi = 5$ mm	0.2 (1.2)	–0.2 (***6.7***)	–0.8 (3.8)	–4.9 (15.7)	—
$\mu_\psi = 20$ mm; $\sigma_\psi = 10$ mm	–0.0 (1.3)	–0.9 (6.7)	0.5 (3.9)	–1.3 (***19.6***)	—
$\mu_\psi = 40$ mm; $\sigma_\psi = 20$ mm	0.5 (1.6)	–0.5 (6.9)	–0.5 (4.1)	14.2 (48.7)	—
Bin size					
2 mm	–0.0 (1.2)	**2.4** (6.0)	0.4 (3.8)	**–8.7** (14.4)	—
10 mm	0.3 (1.2)	**2.4** (6.1)	–1.2 (3.8)	**–8.3** (14.2)	—

Note: These cases address concerns that the bin size, large measurement error, poor size selectivity, or failure of the constant recruitment assumption might result in seriously biased estimates of the tabled parameters. We use bold type to indicate that the bias is significant (t-test, $\alpha = 0.05$, df = 29), although possibly small. Similarly, we use italic bold type to indicate if the SD of the 30 estimates is significantly different from the mean of the 30 SEs of those estimates provided by Mittertreiner and Schnute's (1985) numerical method. The baseline case has $\mu_L = 120$ mm, $\sigma_L = 11$ mm, $\mu_K = 0.3$ year^{-1}, $\sigma_K = 0$ year^{-1}, $Z = 0.1$ year^{-1}, ME = 0, RV = 0, 400 size frequencies, 60 growth increments, a bin size of 5 mm, and no size selectivity. All other cases are modifications, as indicated, of this growth-dominated case. RV, coefficient of monthly recruitment variability; ME, percent measurement error.

[a]For this case with just size frequency data, μ_K refers to the ratio μ_K/Z.

previous work (Botsford et al. 1994) indicated that variability in K is not likely to be at detectable levels in constant-recruitment size frequency distributions of the red sea urchin. However, we did test whether the presence of variability in the growth parameter K (i.e., $\sigma_K > 0$) affected the estimates of other parameters.

The bias and precision associated with each parameter were measured by conducting 30 replications of each simulation. To measure bias, we compared the simulated true value with the mean of the 30 replicates. To measure precision, we calculated the SD of those 30 replicates (i.e., the SE from simulation) and compared it with the SE of the estimate provided by Mittertreiner and Schnute's (1985) numerical method.

Simulations

Growth increments were simulated by choosing an initial test diameter l_j and then drawing a random value for L_j from a Gaussian distribution with mean μ_L and variance σ_L^2. If the value for l_j exceeded L_j, then it was rejected and the draw repeated until $L_j > l_j$. A random value of K_j was then drawn from a gamma distribution with mean μK and variance σ_K^2. A simulated increment was calculated using

© 1998 NRC Canada

$$(15) \qquad l_j = (L_j - l_j)(1 - e^{-K_j \Delta t}).$$

Measurement error was added to l_j as

$$(16) \qquad \bar{l}_j = l_j + \sigma_{M,l_j} \epsilon_j,$$

where ϵ_j is an independent standard Gaussian deviate. For each replicate, growth increments were drawn until there were equal numbers of individuals for each of 30 initial sizes spaced 5-mm apart and ranging from 17.5 to 162.5 mm.

Size distributions were simulated by sampling the continuous distributions generated by integrating solutions to eq. 2 over the range of values of L and K and then summing the results in proportion to the probability densities of L and K. Measurement error was added to the sampled distributions according to eq. 12. Recruitment variation was imposed by assuming monthly lognormal recruitment variability having a specified coefficient of variation (RV). Distributions were randomly sampled as many times as required to produce the sampled distributions of 1-mm bins. These bins were then summed to create bins of 2, 5, or 10 mm as required.

Results

The estimation method yielded acceptable estimates, even when challenged with small sample sizes, imperfect data (i.e., measurement error), and compromised model assumptions (Table 1). In some cases, bias was shown to be significant, but it was typically less than 10%. The SEs were generally on the order of 1–20% and were almost always not significantly different from the SE estimated numerically (Mittertreiner and Schnute 1985). For the baseline case, bias and precision of the parameters other than mortality are very low when compared with estimates of vital rates in general, and even though a bit higher, the bias and precision in the estimate of mortality are in the low range of many estimates. The method appears to be useful in estimating parameters from size frequency data only, except that μ_K and Z cannot be independently estimated (Barry and Tegner 1990; Botsford et al. 1994). The model can also be used to analyze just growth increment data, as long as measurement error is also estimated or known.

The method is robust to a variety of sampling conditions. The one case with a larger sample size than the baseline provided better estimates than the baseline, while the cases with fewer samples provided generally poorer estimates. However, even the smallest sample sizes provided adequate estimates. Using different bin sizes in the size frequency had almost no effect on the estimates. Size selectivity at lower sizes had an effect mainly on the estimate of natural mortality, with Z tending to be less well estimated as mean selectivity increased. This result is intuitively reasonable. Mortality is estimated by formally comparing the abundance of older (larger) and younger (smaller) individuals in the distribution. If smaller individuals are not well represented in the distribution, then natural mortality cannot be as confidently estimated. The method tolerated incomplete sampling of the smallest individuals in a size distribution for sizes up to about one third of μ_L.

The method also yielded reasonable estimates when there was variability in the data due to either measurement error or variable recruitment. The method was robust to practical variability in measurement error, so long as it was estimated. The primary effect of measurement error was to increase the bias in σ_L. Levels of recruitment variability typical of what we have observed for the red sea urchin increased the negative bias in the estimate of mortality, but did not substantially degrade the estimates. The presence of both measurement error and recruitment variability, when measurement error is estimated, led to a better estimate of mortality. This occurs because some of the recruitment variability was absorbed in the estimate of measurement error, although the bias in σ_L increased. Measurement error was well estimated by this method.

The method appears to depend critically on accurate growth increment data to reliably estimate Z and F. Measured growth rates higher than true growth rates led to seriously biased estimates of K, Z, and F (Fig. 1). This result makes sense in the context of eq. 2 in that to maintain the form of the steady-state size distribution when individuals grow faster, both natural and fishing mortality would have to increase proportionately. Despite this obvious concern for practitioners, it is important to recognize that this bias originates with the data and not with the model.

Red sea urchin example

Growth increments only

To demonstrate the use of our method, we estimated growth rate using 215 growth increment records obtained from well-fed red sea urchins held in tanks of flowing seawater at the Bodega Bay Marine Laboratory from 18 July 1991 until 23 July 1992. During this period, nine series of sequential measurements of test diameter provided growth data for eight time periods ranging in length from 23 to 83 days (Fig. 2). We chose smaller rather than larger urchins for this experiment, since smaller urchins provide better information on the value of μ_K than do larger, slow-growing urchins. In contrast, size distribution data provide no data on μ_K, but very good information on μ_L (cf. Smith and McFarlane 1990).

The growth rates that we estimated from our laboratory-grown urchins (Table 2) seem fast when compared with results others have obtained for wild urchins (Ebert and Russell 1992; 1993). We note that our estimate for μ_K is 1.14 year^{-1}. The estimate for μ_L of 72.1 mm seems low, possibly because selecting smaller, faster-growing individuals for the growth increment experiment resulted in the increment data containing less information about the value of μ_L (Smith and McFarlane 1990). Our estimate of measurement error of 2.4% (SE 0.2%) is close to the estimate of 1.8% (SE 0.3%) that we obtained independently by blindly measuring three times the test diameters of 39 urchins ranging in test diameter from 26 to 78 mm. The p-value of 0.02 for this model indicates that the model is an imperfect fit to the data. This imperfect fit occurs because we chose not to omit a few outlier data points.

Growth increments with size frequency data: estimating F

We followed the analysis of growth increments alone with an analysis of size frequency data alone collected from an unharvested site, the Point Cabrillo Marine Reserve, in 1989 (Kalvass et al. 1991). Then, we simultaneously analyzed the growth increments and these size frequency data. The results

© 1998 NRC Canada

Table 2. Parameter estimates (with SEs in parentheses) for those analyses illustrating the use of (*i*) growth increments alone, (*ii*) size frequencies alone and size frequencies with growth increments for the unharvested site (Point Cabrillo Marine Reserve), and (*iii*) size frequencies with growth increments for the harvested site (near Fort Bragg, Mendocino County).

Analysis	p	μ_L (mm)	σ_L (mm)	μ_K (year^{-1})	σ_K (year^{-1})	Z (year^{-1})	F (year^{-1})	$\sigma_{M,l=100}$ (%)	μ_ψ (mm)	σ_ψ (mm)
Growth increments (Fig. 2)	0.02	72.1 (6.0)	18.3 (2.3)	1.14 (0.19)	0 (—)	—	—	2.4 (0.2)	—	—
Unharvested site (Fig. 3)										
Size frequencies only[a]	>0.1	113.1 (1.5)	14.4 (0.9)	4.9 (1.2)	—	—	—	—	13.2 (2.4)	7.4 (2.4)
Size frequencies and increments	>0.1	110.4 (1.7)	16.5 (1.2)	0.61 (0.2)	—	0.064 (0.03)	—	3.4 (0.3)	11.4 (2.3)	6.6 (2.1)
Harvested site (Fig. 3)										
Size frequencies and increments (unconditional)	>0.1	78.3 (3.8)	19.7 (0.9)	0.98 (0.08)	—	0.80 (0.61)	0 (—)	2.4 (0.2)	1576 (1058)	164 (83)
Size frequencies and increments (conditional)	>0.1	110.4 (—)	16.5 (—)	0.61 (—)	—	0.064 (—)	0.36 (0.04)	3.4 (—)	43 (6)	26 (5)

Note: For the harvested site, one analysis attempts to estimate all parameters (unconditional) and the other is conditional upon the growth and natural mortality estimates. Note that F refers to $F(l)$ where $l \geq 76$ mm, the minimum legal size.

[a]For this case with just size frequency data, μ_K refers to the ratio μ_K/Z.

(Table 2; Fig. 3, top panel) illustrate the benefit of analyzing growth increments and size frequency data together. This latter analysis relies mainly on the size frequency data to estimate μ_L and σ_L, while the growth increments are used to estimate μ_K. The simultaneous analysis can also provide an estimate for natural mortality, $Z = 0.064$ year^{-1}.

The similarity of the size distributions from the unharvested (Point Cabrillo Marine Reserve) and heavily harvested (near Fort Bragg in Mendocino, Calif.) sites for urchins larger than 76 mm test diameter (Fig. 3) suggests that it would be difficult to estimate fishing mortality using only a harvested distribution, even though our simulations showed that, in principle, this is feasible. Indeed, when we first attempted to estimate all parameters from the harvested distribution (Fig. 3), we found that F need not exceed zero to explain the form of the size distribution ($p = 0.18$, Table 2). We also obtained an unrealistically high and uncertain estimate for natural mortality ($Z = 0.8$ year^{-1}) and dissatisfying estimates for the selectivity parameters.

We therefore suggest a two-step procedure in which parameters are first estimated for the unharvested distribution (i.e., $F(l) = 0$) and then fishing mortality is estimated for the harvested distribution conditional on estimates for the unharvested distribution. With this procedure, only fishing mortality above the minimum legal size limit of 76 mm plus the two size selectivity parameters are estimated. This two-step analysis yielded satisfactory estimates of all parameters. Despite the method providing reliable estimates of growth and mortality for those data analyzed, we caution that our estimate of μ_K (0.61 year^{-1}) for urchins grown under ideal laboratory conditions might be 2–3 times higher than would be obtained for wild urchins. Estimates of Z and F may therefore be similarly inflated (Fig. 3).

Discussion

Size distributions lacking age structure are quantitatively less informative about growth and mortality than are size distributions with age patterns (Macdonald and Pitcher 1979; Schnute and Fournier 1980; Fournier and Breen 1983). Here, we have demonstrated using simulation and an example that estimation of growth, natural mortality, and fishing mortality from size frequency distributions lacking age patterns is feasible and practical when information on growth rate is also available. Reliable estimates can be obtained even when the fundamental assumption of constant recruitment cannot be strictly met. Bias is typically less than 10% for all parameters except mortality, while SEs are on the order of 1–20%. Mortality estimates are the most uncertain resulting in higher biases and SEs for them. Additionally, the SEs of the parameter estimates provided by Mittertreiner and Schnute's (1985) numerical method were generally in good agreement with the SDs of the parameter estimates obtained from the 30 replicates for each simulation.

In principle, fishing mortality should be estimable using only growth increments and the harvested distribution, as we did using simulated data (Fig. 1). The growth increments are necessary to resolve the ambiguity between the mortality rates and von Bertalanffy's K parameter, both of which affect the slope of the size distribution in the same way (our eq. 2; Barry and Tegner 1990; Botsford et al. 1994). However, in

© 1998 NRC Canada

Fig. 1. Effect of misrepresentative growth increments on the mean percent bias (histograms, mean of 30 replicates) and the percent SE from simulation (error bars, mean of 30 replicates) for estimates of the mean of L (μ_L), the SD of L (σ_L), the mean of K (μ_K), the natural mortality rate (Z), and fishing mortality rate (F). Estimates were obtained for simulated growth-dominated size distributions with 400 individuals and 60 simulated growth increments (μ_L = 120 mm, σ_L = 11 mm, μ_K = 0.3 year^{-1}, σ_K = 0 year^{-1}, Z = 0.1 year^{-1}, $F(l)$ = 0 year^{-1} for l < 76 mm, $F(l)$ = 0.3 year^{-1} for $l \geq$ 76 mm).

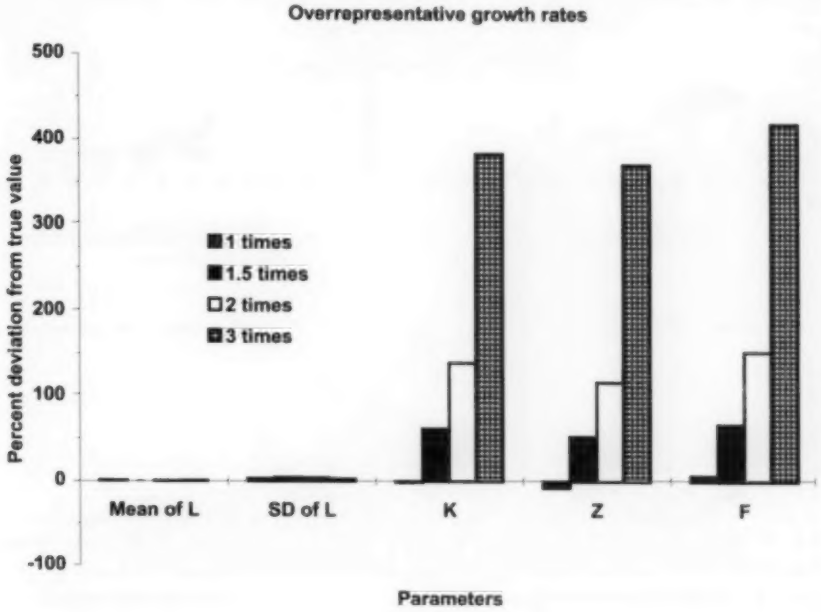

practice the available size distribution data are not likely to be as ideal as simulated data. Thus, as in our example (Fig. 3), we suggest that to obtain estimates of growth and natural and fishing mortality from a harvested size distribution, a third source of information should be used, a comparable unharvested size distribution. This distribution would first be analyzed to estimate growth and natural mortality parameters and then the harvested distribution would be analyzed to estimate fishing mortality conditional on those growth and natural mortality parameter estimates.

Even if the cost of these two additional data requirements is considered, use of the method presented here to estimate fishing mortality would be justified in many cases. For example, since invertebrates typically cannot be reliably aged, invertebrate populations that do not display age modes in their size distributions would require such a method. For populations that can be aged, but only at considerable expense, this method may still be the most feasible. We foresee this analytical approach having utility for many invertebrate species that are difficult to age but for which high-quality growth-at-size and size distribution data can be collected rather easily and inexpensively. Although our example was for the growth-dominated distributional form, the method and its evaluation are equally valid for the mortality-dominated and bimodal distributional forms (Botsford et al. 1994; Smith and Botsford 1998).

We assumed constant recruitment, but the relative robustness of the method to failure of this assumption would make it suitable for many populations with undramatic monthly or annual recruitment variability. We note that our simulation with a monthly RV of 4 corresponds to an annual RV slightly greater than 1. For populations that only occasionally present an age mode, we are considering development of a method that uses growth increments in combination with size distributions obtained sequentially in time and that estimates annual recruitment. Another approach would filter recruitment that occurs as uncorrelated periodic, say monthly, events.

One consideration when using this method to estimate fishing mortality is the comparability of vital rates for harvested and unharvested distributions. Harvested and unharvested sites should be chosen with habitat comparability in mind. Practitioners must also consider if density-dependent processes could cause marked differences in growth and mortality rates between the unharvested and harvested sites. For our example of the red sea urchin, the protection of small urchins from mortality by a spine canopy of adult urchins has received much study as a population regulation mechanism involving predation and recruitment of small sea urchins to the adult population (Tegner and Dayton 1981, 1991; Tegner and Levin 1983; Tegner 1989). If adults are harvested, then the relationship between size and mortality for smaller urchins (eq. 4) might change.

There are few size-based estimation methods with which we can compare our method. Ebert (1980) and Ebert and Russell (1992, 1993) have collected red sea urchin growth increments and have estimated growth and mortality rates in a variety of ways. However, they have presented no statistical

© 1998 NRC Canada

Fig. 2. Laboratory-obtained growth increments (points) for well-fed red sea urchins held in tanks at the Bodega Bay Marine Laboratory from 18 July 1991 until 23 July 1992. Estimated von Bertalanffy growth models (lines) are also presented for eight time periods between measurements (Table 2). Note that the different slopes are due to the variable number of days between successive measurements of test diameters.

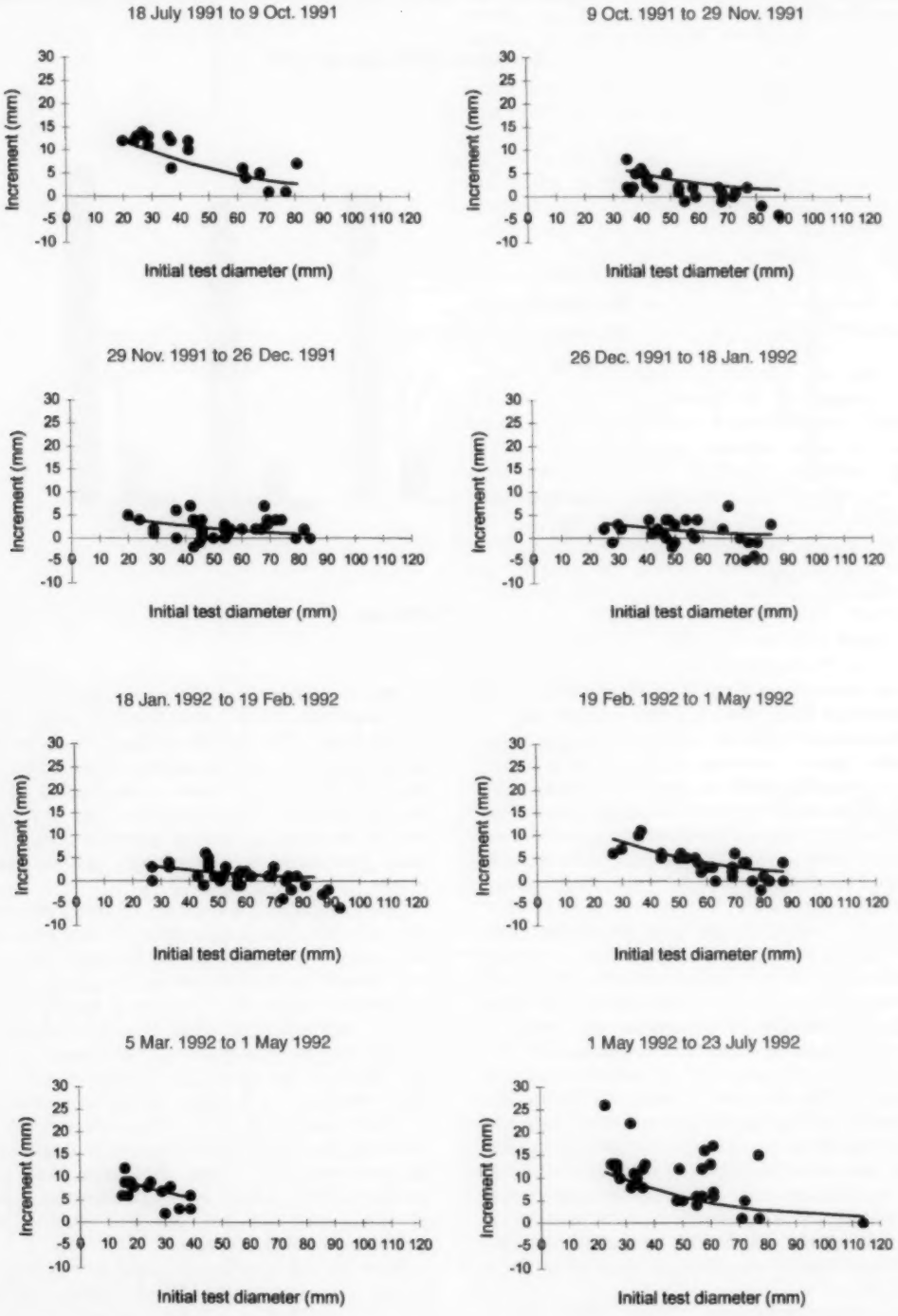
18 July 1991 to 9 Oct. 1991
9 Oct. 1991 to 29 Nov. 1991
29 Nov. 1991 to 26 Dec. 1991
26 Dec. 1991 to 18 Jan. 1992
18 Jan. 1992 to 19 Feb. 1992
19 Feb. 1992 to 1 May 1992
5 Mar. 1992 to 1 May 1992
1 May 1992 to 23 July 1992
Increment (mm)
Initial test diameter (mm)

© 1998 NRC Canada

Fig. 3. Histograms of red sea urchins collected from harvested (near Fort Bragg, Mendocino County) and unharvested (Point Cabrillo Marine Reserve) sites in northern California in 1989. Top panel: unharvested site (n = 868). The line indicates the estimated unharvested size distribution (Table 2). Bottom panel: harvested site (n = 1337). The heavy line draws the estimated harvested size distribution (conditional estimate) conditional on the growth and natural mortality estimates obtained for Point Cabrillo Marine Reserve (Table 2). Only fishing morality (F), the mean of size selectivity (μ_ψ), and the SD of size selectivity (σ_ψ) were estimated. The light line projects the form of the corresponding unharvested distribution (conditional projection, F = 0). The broken line draws the harvested distribution obtained by estimating all parameters (unconditional estimate).

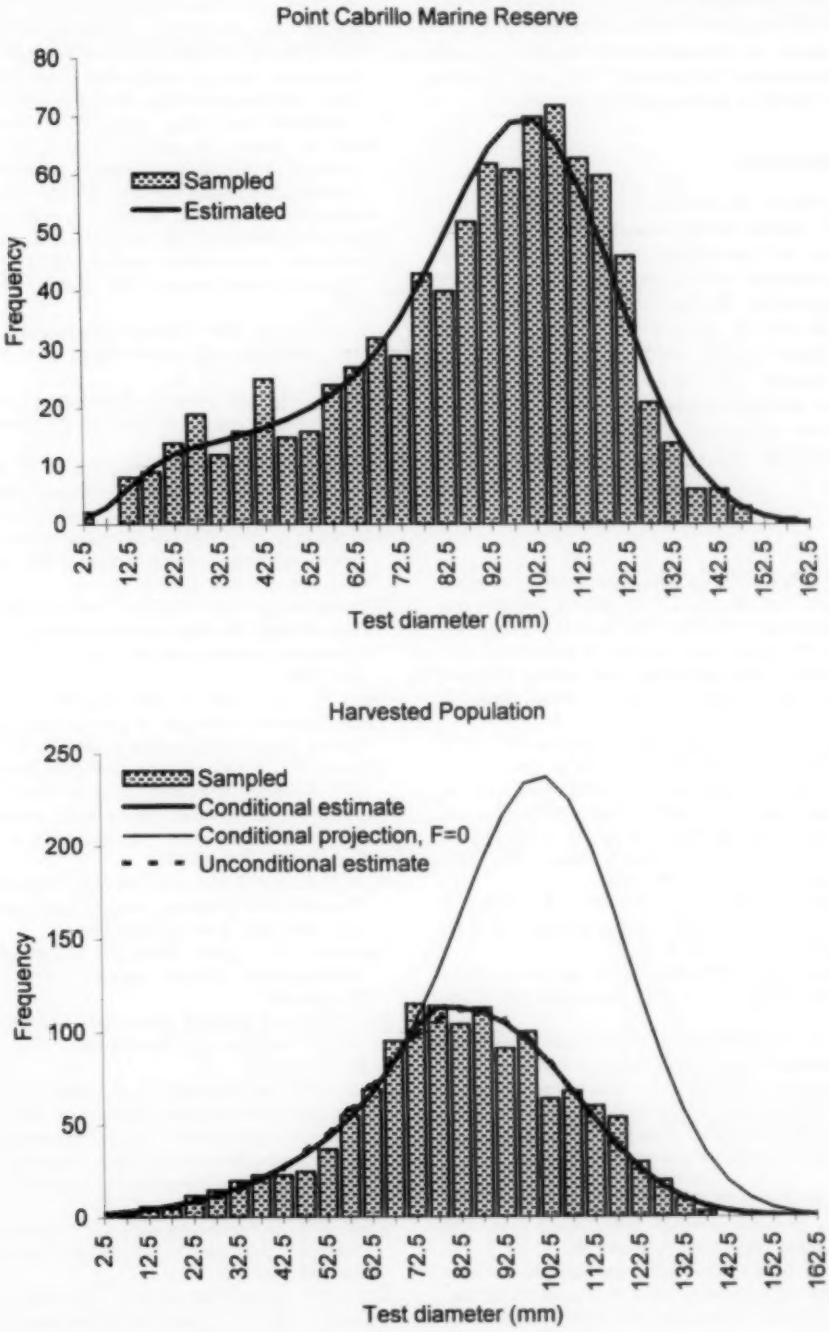

© 1998 NRC Canada

evaluation of their methods similar to the evaluation conducted here. They interpreted the asymptotic approach of the growth increment prediction to the abscissa of initial test diameter for a given time period at large as indicating a Richards growth curve. We find that Sainsbury's (1980) assumptions regarding statistical variability provide a more satisfactory explanation of variability in positive growth increments than does a Richards curve. One limitation of our implementation of Sainsbury's (1980) assumptions is that negative growth cannot be accommodated. Negative growth of urchins has been reported by Levitan (1988), and we have observed negative growth in starved red sea urchins.

Acknowledgments

We wish to thank John G. Brittnacher for help with the simulations and James F. Quinn for advice early in this study. This paper was is funded by a grant from the National Sea Grant College Program, National Oceanic and Atmospheric Administration, U.S. Department of Commerce, under grant No. NOAA NA89AA-D-SG138, project No. R/F-136, through the California Sea Grant College, and in part by the California State Resources Agency. The views expressed herein are those of the authors and do not necessarily reflect the views of NOAA or any of its subagencies. The U.S. Government is authorized to reproduce and distribute for governmental purposes.

References

Barry, J.P., and Tegner, M.J. 1990. Inferring demographic processes from size–frequency distributions: simple models indicate specific patterns of growth and mortality. Fish. Bull. U.S. **88**: 13–19.

Beverton, R.J.H., and Holt, S.J. 1956. A review of methods for estimating mortality rates in fish populations, with special reference to sources of bias in catch sampling. Rapp. P.-v. Réun. Cons. Int. Explor. Mer, **140**: 67–83.

Botsford, L.W., Quinn, J.F., Wing, S.R., and Brittnacher, J.G. 1993. Rotating spatial harvest of a benthic invertebrate, the red sea urchin, *Strongylocentrotus franciscanus*. *In* Proceedings of the International Symposium on Management Strategies for Exploited Fish Populations. *Edited by* G. Kruse, D.M. Eggers, R.J. Marasco, C. Pautzke, and T.J. Quinn II. Alaska Sea Grant College Program AK-SG-93-02. pp. 409–428.

Botsford, L.W., Smith, B.D., and Quinn, J.F. 1994. Bimodality in size distributions: the red sea urchin *Strongylocentrotus franciscanus* as an example. Ecol. Appl. **4**: 42–50.

Deriso, R.B., and Parma, A.M. 1988. Dynamics of age and size for a stochastic population model. Can. J. Fish. Aquat. Sci. **45**: 1054–1068.

Deriso, R.B., Quinn, T.J., II, and Neal, P.R. 1985. Catch-age analysis with auxiliary information. Can. J. Fish. Aquat. Sci. **42**: 815–824.

Ebert, T.A. 1980. Estimating parameters in a flexible growth equation, the Richards function. Can. J. Fish. Aquat. Sci. **37**: 687–692.

Ebert, T.A. 1981. Estimating mortality from growth parameters and a size distribution when recruitment is periodic. Limnol. Oceanogr. **26**: 764–769.

Ebert, T.A., and Russell, M.P. 1992. Growth and mortality estimates for red sea urchin *Strongylocentrotus franciscanus* from San Nicolas Island, California. Mar. Ecol. Prog. Ser. **81**: 31–41.

Ebert, T.A., and Russell, M.P. 1993. Growth and mortality of subtidal red sea urchins (*Strongylocentrotus franciscanus*) at San Nicolas Island, California, USA: problems with models. Mar. Biol. **117**: 79–89.

Ebert, T.A., Schoeter, S.C., and Dixon, J.D. 1993. Inferring demographic processes from size–frequency distributions: effect of pulsed recruitment on simple models. Fish. Bull. U.S. **91**: 237–243.

Fournier, D., and Archibald, C.P. 1982. A general theory for analyzing catch at age data. Can. J. Fish. Aquat. Sci. **39**: 1195–1207.

Fournier, D.A., and Breen, P.A. 1983. Estimation of abalone mortality rates with growth analysis. Trans. Am. Fish. Soc. **112**: 403–411.

Fournier, D.A., Sibert, J.R., Majkowski, J., and Hampton, J. 1990. MULTIFAN, a likelihood-based method for estimating growth parameters and age composition from multiple length frequency data sets illustrated using data for southern bluefin tuna (*Thunnus maccoyii*). Can. J. Fish. Aquat. Sci. **47**: 301–317.

Grant, A., Morgan, P.J., and Olive, P.J.W. 1987. Use made in marine ecology of methods for estimating demographic parameters from size/frequency data. Mar. Biol. **95**: 201–208.

Kalvass, P., Taniguchi, I., Buttolph, P., and DeMartini, J. 1991. Relative abundance and size composition of red sea urchin, *Strongylocentrotus franciscanus*, populations along the Mendocino and Sonoma County coasts, 1989. Calif. Fish Game Admin. Rep. 91-3.

Kirkpatrick, M. 1984. Demographic models based on size, not age, for organisms with indeterminate growth. Ecology, **65**: 1874–1884.

Levitan, D.R. 1988. Density-dependent size regulation and negative growth in the sea urchin *Diadema antillarum* Philippi. Oecologia (Heidelb.), **76**: 627–629.

Macdonald, P.D.M., and Pitcher, T.J. 1979. Age groups from size–frequency data: a versatile and efficient method of analyzing distribution mixtures. J. Fish. Res. Board Can. **36**: 987–1001.

Megrey, B.A. 1989. Review and comparison of age-structured stock assessment models from theoretical and applied points of view. Am. Fish. Soc. Symp. **6**: 8–48.

Mittertreiner, A., and Schnute, J. 1985. Simplex: a manual and software package for easy nonlinear parameter estimation and interpretation in fishery research. Can. Tech. Rep. Fish. Aquat. Sci. No. 1384.

Pauly, D., and David, N. 1981. ELEFAN I, a BASIC program for the objective extraction of growth parameters from length frequency data. Meeresforschung, **28**: 205–211.

Petersen, C.G.J. 1892. Fiskensbiologiske forhold I Holboek Fjord, 1890–91. Beret. Dan. Biol. St. **1**(1890(91)): 121–183.

Pope, J.G. 1972. An investigation of the accuracy of virtual population analysis using cohort analysis. Int. Comm. Northwest Atl. Fish. Res. Bull. **9**: 65–74.

Roff, D.A., and Bentzen, P. 1989. The statistical analysis of mitochondrial DNA polymorphisms: χ^2 and the problem of small samples. Mol. Biol. Evol. **6**: 539–545.

Sainsbury, K.J. 1980. Effect of individual variability on the von Bertalanffy growth equation. Can. J. Fish. Aquat. Sci. **37**: 241–247.

Schnute, J., and Fournier, D.A. 1980. A new approach to length frequency analysis: growth structure. Can. J. Fish. Aquat. Sci. **37**: 1337–1351.

Smith, B.D., and Botsford, L.W. 1998. Interpretation of growth, mortality, and recruitment patterns in size-at-age, growth increment, and size frequency data. *In* Proceedings of the North Pacific Workshop on Invertebrate Stock Assessment and Management. *Edited by* G.S. Jamieson and A. Campbell. Can. Spec. Publ. Fish. Aquat. Sci. No. 125. pp. 125–139.

Smith, B.D., and Jamieson, G.S. 1989. Growth of male and female Dungeness crabs near Tofino, British Columbia. Trans. Am. Fish. Soc. **118**: 556–563.

Smith, B.D., and McFarlane, G.A. 1990. Growth analysis of Strait of Georgia lingcod by use of length-frequency and length-increment data in combination. Trans. Am. Fish. Soc. **119**: 802–812.

© 1998 NRC Canada

Tegner, M.J. 1989. The feasibility of enhancing red sea urchin, *Strongylocentrotus franciscanus*, stocks in California: an analysis of the options. Mar. Fish. Rev. **51**(2): 1–22.

Tegner, M.J., and Dayton, P.K. 1981. Population structure, recruitment and mortality of two sea urchins (*Strongylocentrotus franciscanus* and *S. purpuratus*) in a kelp forest. Mar. Ecol. Prog. Ser. **5**: 255–268.

Tegner, M.J., and Dayton, P.K. 1991. Sea urchins, El Niños, and the long term stability of southern California kelp forest communities. Mar. Ecol. Prog. Ser. **77**: 49–63.

Tegner, M.J., and Levin, L.A. 1983. Spiny lobsters and sea urchins: analysis of a predator–prey interaction. J. Exp. Mar. Biol. Ecol. **73**: 125–150.

Van Sickle, J. 1977. Mortality rates from size distributions. Oecologia (Heidelb.), **27**: 311–318.

Weatherall, J.A., Polovina, J.J., and Ralston, S. 1987. Estimating growth and mortality in steady-state fish stocks from length–frequency data. *In* Length-based methods in fisheries research. *Edited by* D. Pauly and G.R. Morgan. ICLARM Conference Proceedings 13. Int. Cent. Living Aquat. Resourc. Manage., Manila, Philippines, and Kuwait Inst. Sci. Res., Safat, Kuwait. pp. 53–74.

© 1998 NRC Canada

Estimating trends in fishing mortality at age and length directly from research survey and commercial catch data

Alan F. Sinclair

Abstract: Relative fishing mortality (R) is estimated directly as the ratio of commercial catch divided by a research vessel survey index of relative population abundance. If the survey is conducted near the middle of the fishing year, its catchability is constant, and the rate of catch reporting remains constant, R will be proportional to the actual fishing mortality (F). Trends in R will reflect trends in F. A case study is presented where R at age and length are compared with estimates obtained with sequential population analysis (SPA). They were found to be of similar magnitude and trend. This new method would be useful for stocks where SPA is not possible. It would also be a useful addition to analytical assessments where SPA is used; it provides estimates of relative F at length, it is insensitive to changes in natural mortality provided the research survey occurs close to the middle of the fishing year, and it provides useful diagnostics for interpreting SPA results.

Résumé : La mortalité par pêche relative (R) est estimée directement comme étant le rapport des prises commerciales sur un indice calculé par le navire de recherche à partir d'un relevé de l'abondance relative de la population. En supposant que l'étude soit réalisée environ au milieu de la saison de pêche, que le potentiel de capture soit constant et que le taux de déclaration des captures demeure constant, la valeur R sera proportionnelle à la valeur réelle de la mortalité par pêche actuelle (F). Les tendances observées dans la valeur R refléteront celles de F. On présente une étude de cas dans laquelle les valeurs de R à un certain âge et à une certaine longueur sont comparées avec des estimations obtenues grâce à une analyse séquentielle de population (ASP). On a trouvé qu'elles étaient de grandeurs semblables et qu'elles suivaient la même tendance. Cette nouvelle méthode serait utile pour les stocks où il n'est pas possible d'appliquer l'ASP. Elle représenterait également un ajout utile aux évaluations obtenues grâce à une ASP; elle fournit des estimations de la valeur F relative à une certaine longueur; elle est sensible aux changements dans la mortalité naturelle pourvu que l'étude soit réalisée environ au milieu de la saison de pêche, et elle offre un diagnostic utile pour l'interprétation des résultats de l'ASP.
[Traduit par la Rédaction]

Introduction

Fish stock assessment techniques such as virtual population analysis (Gulland 1965) and cohort analysis (Pope 1972) are commonly used to obtain information for fisheries management. These techniques, which are referred to hereafter as sequential population analysis (SPA), use catch-at-age data from the fishery to obtain absolute estimates of population numbers (N) and the instantaneous rate of fishing mortality (F) at age. Pope's (1972) cohort approximation to Gulland's (1965) virtual population analysis is shown here as an example, but the general characteristics of SPA are the same for both methods. The abundance of any cohort at age (a) = b is estimated as the sum of two components, its abundance at the maximum age in the data (N_s), and the sum of the annual catches (C) of the cohort, both adjusted for the instantaneous rate of natural mortality (M):

$$(1) \qquad N_b = N_s e^{M(s-b)} + \sum_{a=s-1}^{b} C_a e^{M/2}$$

Received July 31, 1997. Accepted December 5, 1997.
J13588

A.F. Sinclair. Department of Fisheries and Oceans, Gulf Fisheries Centre, P.O. Box 5030, Moncton, NB E1C 9B6, Canada.

In almost all cases, M cannot be estimated annually from the data; rather, it is assumed constant across years and in many cases it is assumed constant across ages. To simplify notation I did not subscript M for age. When a cohort has passed completely through the population, i.e., $N_s = 0$, its abundance is estimated only from the catch-at-age data. The abundance of cohorts still alive in the final year of the data are determined by a calibration process. Gavaris (1993) describes a nonlinear estimation technique that minimizes residuals between SPA estimates of the population and those obtained from fishery-independent indices such as research vessel (RV) surveys. Other SPA calibration methods are described by Winters (1988) and Mohn and Cook (1993). Calibrating an SPA is relatively complex and requires the estimation of several parameters from sparse data. The power of SPA is that as the sum of M-adjusted catches becomes large, the influence of N_s on N_b gets smaller, and thus population estimates converge to stable values. This converged part of the analysis forms the basis of the calibration process.

While SPA may be the preferred assessment method, it is not always possible. The technique requires several years of data, in the order of 10 years, to establish a reliable calibration base. Fishing mortalities need to be relatively high compared with natural mortality. Pope (1972) suggests that a cumulative F of 2.0 on a cohort is required for convergence. The technique is age based and catch-at-age estimates from the

© 1998 NRC Canada

commercial fishery are required on an annual basis. Interruptions in the commercial catch-at-age time series, resulting from a break in the catch sampling or periods of unreliable catch reporting, are problematic. Errors in one year will affect population estimates in previous years as well as the overall calibration process. Nonstationarity in M or the abundance index has complex effects on parameter estimates.

This study presents a simple method for estimating trends in F. Relative F (R) is estimated directly from research survey and commercial catch data. This method may be used as an alternative to SPA in situations where the more complex analysis is not possible. It may be used to follow trends in F at length. It also provides useful diagnostics that, when used in conjunction with SPA, may help to detect changes in natural mortality, survey catchability, and the rate of catch reporting. These characteristics are demonstrated with simulations and a case study where SPA estimates are compared with the direct estimates. Of the over 40 Northwest Atlantic fish stocks assessed annually by Canada and the Northwest Atlantic Fisheries Organization, some 35 have relatively long (15 years or more) data sets, which are suitable for this new type of analysis. Yet, only six use age-based SPA, and few of the remaining cases provide estimates of trends in F. This new method could be applied in all cases.

Methods

The theory

The basic approach uses the following well accepted relationship between F, C, and mean population abundance ($\bar{N}$), where F and M are spread proportionally throughout the year (type-2 fishery of Ricker 1975):

$$F = \frac{C}{\bar{N}} \tag{2}$$

$$\bar{N} = \frac{N(1 - e^{-Z})}{Z} \tag{3}$$

where Z is the instantaneous rate of total mortality, the sum of F and M. Annual RV surveys have been used in many areas to obtain relative indices of population abundance (A). If the survey is conducted when the population is at its mean abundance for the year, the ratio of C divided by A is an estimate of R:

$$R = \frac{C}{A} = \frac{F}{k} \tag{4}$$

Trends in R will be proportional to trends in F, and the ratio between F and R would be equal to the catchability (k) of the RV survey. It is, of course, impractical to conduct a survey exactly when a population is at its mean abundance because the population reaches its mean abundance earlier when Z is higher.

The timing of the survey relative to the timing of the fishery has an important effect on the ratio of C/A. If we assume that the survey catchability is constant, then if the survey is conducted at the beginning of the year:

$$A_{pre} = kN \tag{5}$$

and the ratio of catch divided by the survey estimate is proportional to the exploitation rate. I refer to this as the pre-ratio. If the survey is conducted at the middle of the year:

$$A_{mid} = kNe^{-0.5Z} \tag{6}$$

and the ratio is approximately proportional to the fishing mortality. I call this the mid-ratio. The trends will not be exactly proportional, because there is a difference between mean ($\bar{N}$) and midyear ($Ne^{-0.5Z}$) population numbers. The midyear population size is about 1, 4, 10, and 18% less than the mean population size at Zs of 0.5, 1.0, 1.5, and 2.0, respectively. Total mortality rarely exceeds 1.5 in commercial fisheries. If the survey is conducted at the end of the year:

$$A_{post} = kNe^{-Z} \tag{7}$$

I call it the post-ratio. It follows that $R_{pre} < R_{mid} < R_{post}$

The pre-, mid-, and post-ratios have different functional forms relative to M. Catch is defined as

$$C = \frac{N(1 - e^{-Z})F}{Z} \tag{8}$$

Substituting this and eq. 5 into eq. 4 we have

$$R_{pre} = \frac{(1 - e^{-(M+F)})F}{k(M + F)} \tag{9}$$

Plotting eq. 9 as a function of M indicates a continuously decreasing function (Fig. 1); thus, one would expect R_{pre} to decline if M increases (all other things equal). Substituting eqs. 6 and 8 into eq. 4, we see that R_{mid} is relatively insensitive to changes in M, increasing slightly over a range of $0.1 \leq M \leq 2.0$.

$$R_{mid} = \frac{(e^{0.5(M+F)} - e^{-0.5(M+F)})F}{k(M + F)} \tag{10}$$

Therefore, R_{mid} is the preferred index of relative F. The post-ratio can be rewritten by substituting eqs. 7 and 8 into eq. 4 to obtain

$$R_{post} = \frac{(e^{(M+F)} - 1)F}{k(M + F)} \tag{11}$$

This is an increasing function of M. One would expect R_{post} to increase if M increased. This divergent behaviour of R_{pre} and R_{post} may be a useful diagnostic for changes in M and warrants further research. The relative insensitivity of R_{mid} to changes in M is explored further in the following simulations, where it is compared with F estimates from SPA. It should be possible to recombine catch samples to estimate catch at age by a half year relative to the timing of the RV survey, and thus calculate pre-, mid-, and post-fishery ratios for any type-2 fishery. The assumption of constant catchability is met, since the same survey estimates are used in all three ratios.

All three ratios (R_{pre}, R_{mid}, R_{post}) increase in response to increased F. However, R_{pre} increases at a slower rate, and R_{post} at a faster rate than the true F (Fig. 2).

Estimates of C and A may be either age- or length-based thus producing either age- or length-based estimates of R.

Estimates of R are obtained directly from annual catch and RV data and are thus independent from one year to the next. This is in contrast to F estimates from SPA, which are based on the catch at that age and year, the catches of the same cohort at older ages, the assumed value of M, and the calibrated abundance of the cohort at age s.

Simulations

Simulations were used to investigate the sensitivity of SPA estimates of F and direct estimates of R to changes in M, F, k, and the rate of catch under-reporting (d). A "true" population with 13 age groups and constant recruitment was generated over a period of 10 years. Fishing mortality was age dependent. Ages 7+ were fully recruited and experienced the same F in any year while ages 1–6 were partially recruited with Fs in proportions of 0.01, 0.10, 0.35, 0.55, 0.725, and 0.875, respectively of the fully recruited F. Two scenarios of M were investigated; constant at 0.2 in all years and ages, and constant at 0.2 for the first 7 years, then increasing to 0.4, 0.6, and 0.8 over years 8–10, respectively (referred to as M up). Two scenarios of fully recruited F were used; constant at 0.4 in all years, and constant for the first 7 years then increasing to 0.6, 0.8, and 1.0 over years 8–10, respectively (referred to as F up). Three scenarios of k and d were used. These were constant at 1.0, constant at 0.5, and a step from 1.0

© 1998 NRC Canada

Fig. 1. Relationship between R and M. F is constant at 0.4. R_{pre} is calculated from population numbers at the beginning of the fishing year and declines as M increases. R_{mid} is calculated from midyear population numbers and is relatively insensitive to changes in M. R_{post} is calculated from end of the year population numbers and increases as M increases.

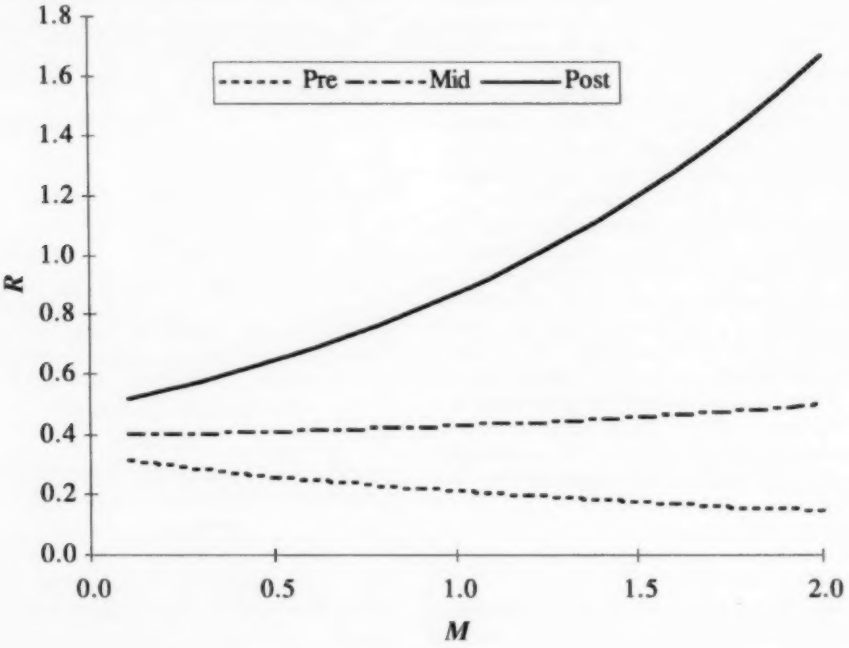

Fig. 2. Relationship between R and F. M is constant at 0.2. R_{pre} is calculated from beginning of year population numbers and increases at a slower rate than F. R_{mid} is calculated from midyear population numbers and increases approximately proportionally to F. R_{post} is calculated from end of the year population numbers and increases faster than F.

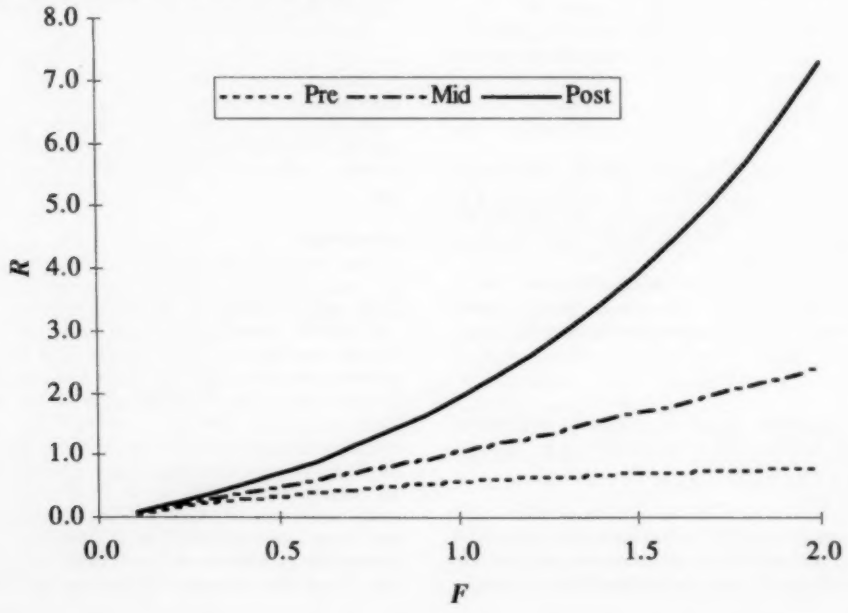

© 1998 NRC Canada

Table 1. Monte Carlo simulation scenarios for comparing direct estimates of R and SPA estimates of F.

	$k = 1, d = 1$	$k = 0.5, d = 1$	k step, $d = 1$	$k = 1, d = 0.5$	$k = 1, d$ step
$F = 0.4, M = 0.2$	×	×	×	×	×
$F = 0.4, M$ up	×	×	×	×	×
F up, $M = 0.2$	×	×	×	×	×
F up, M up	×	×	×	×	×

Note: Comparisons were made between characteristics of the populations (fishing mortality (F) and natural mortality (M)) and characteristics of the sampling programs (survey catchability (k) and rate of catch under-reporting (d)). Thirty replicates were made of each scenario.

for the first 5 years to 0.5 for the last 5 years (referred to as k step and d step).

Stock assessment data were generated from the true data. Log-normal errors were added to approximate sampling errors. For catches, the stock assessment data ($\hat{C}$) were calculated from the true values (C) in the following manner:

$$\hat{C} = Ce^{\phi} \tag{12}$$

where ϕ was a random variable with mean 0 and SD 0.1. The abundance index was simulated from the true mean population

$$\hat{A} = \bar{N}e^{\gamma} \tag{13}$$

where γ was a random variable with mean 0 and SD 0.25. F was estimated for all ages and years with the ADAPT calibration method (Gavaris 1993) assuming a constant M of 0.2. R was estimated for all ages using eq. 4 and substituting $\hat{C}$ and $\hat{A}$ for C and A, respectively. Thirty replicates were made for each of the scenarios described in Table 1. The means and variances of the age 7–12 estimates of R and F were compared graphically.

Examination of residual patterns from a multiplicative analysis of the RV data may be useful for diagnosing changes in M, F, k, or d. The model used has been described by Shepherd and Nicholson (1991) and is of the form:

$$\ln A_{ij} = \beta_0 + \beta_1 \mathbf{I} + \beta_2 \mathbf{J} + \epsilon \tag{14}$$

where A_{ij} is the RV index at age i and year-class j, $\mathbf{I}$ is a matrix of 0 and 1 indicating age, and $\mathbf{J}$ is a matrix of 0 and 1 indicating year-class. Age and year-class are assumed to be separable main effects with no interactions. Violations of this assumption should show up as residuals. Possible violations include a temporal change in the mortality schedule of a year-class caused by a change in M or F, and a change in the catchability of the survey. Temporal patterns in the residuals of multiplicative analyses of the simulated RV data were examined for potentially useful diagnostic patterns.

Case study

How well does this new method of estimating trends in F perform? This was tested with a case study of the southern Gulf of St. Lawrence Atlantic cod (*Gadus morhua*) stock. The stock status is assessed annually using SPA, and data are available to calculate R at age and length (see Sinclair et al. (1996) for the most recent assessment). In the case study, F estimates from SPA are compared with both age- and length-based estimates of R.

This stock has been surveyed annually, in September, since 1971. This analysis concentrated on the time period 1982–1995, during which time there was no change in the regulated mesh size in the commercial fishery. Approximately 60% of the annual commercial catch was taken before the survey, and I have assumed that the survey has occurred close to the period of mean population abundance. The research vessel E.E. Prince was used from 1971 to 1985 and the Lady Hammond from 1986 to 1991. A third vessel, the Alfred Needler, has been used since 1992. Comparative fishing experiments were conducted between vessels each time there was a change and conversion factors were applied when warranted (see Nielsen (1994), Swain et al. (1995), and Sinclair et al. (1995) for details).

Stratified mean catches per tow at length and age were calculated according to the stratified random survey design (Halliday and Koeller 1981). Population estimates were obtained by applying a conversion factor of 1.729×10^6, corresponding to the number of Alfred Needler trawlable units in the survey area. These estimates are considered to be a relative index rather than an absolute estimate of abundance. The RV mean numbers per tow at age were obtained from Sinclair et al. (1996). The RV population estimates at length are presented in Table 2.

The size and age composition of the commercial catches were obtained using the method described by Zwanenburg and Smith (1983). The necessary data were obtained from port and at-sea sampling. The sampling was stratified by quarter and gear sector. The catch at age was obtained from Sinclair et al. (1996), and the length frequency of the catches was obtained from the intermediate steps in the calculation of catch at age (Table 3).

The Wilcoxon signed-rank test was used to test for difference in annual estimates of R and SPA F on an age-by-age basis and overall. In addition, linear regression of R as a function of F was used to compare age-by-age trends. The null hypothesis was that the estimates were independent, and the alternative hypothesis was that the relationship had zero intercept and a slope of 1.0.

Catches outside the 39–71 cm length range were not included in statistical analyses, but some data are presented for illustration. The ranges of lengths observed in the 1982–1995 RV surveys and commercial catches were 4–133 and 13–139 cm, respectively. However, the majority of the commercial catch was between 39 and 71 cm. For analytical purposes, catches were combined in 3-cm length groups within this length range.

The objective of the analysis of R at length (l) was to develop an overall measure of trend in F from length-frequency data and to examine trends for specific length groups. These trends were then compared to estimates of R and F obtained from catch-at-age data. Initial analysis indicated that $\ln R_{ly}$ could be cast as a cubic function of length, and the annual curves were estimated using an analysis of covariance described below.

$$\ln R_{ly} = \beta_0 + \beta_1 L + \beta_2 L^2 + \beta_3 L^3 + \beta_4 \mathbf{Y} + \beta_5 \mathbf{Y}L + \beta_6 \mathbf{Y}L^2 + \beta_7 \mathbf{Y}L^3 + \epsilon \tag{15}$$

where L is a continuous variable for length; $\mathbf{Y}$ is a matrix of 0 and 1 designating the year of the observation; the coefficients β_1, β_2, and β_3 are scalar; and β_4, β_5, β_6, and β_7 are vectors. The variable length (L) was centered to the mean length in the series (L = length – 60.53) to avoid problems associated with multicolinearity (Neter et al. 1983).

Residuals were tested for normality, and the main effects were tested for significance using type III sums of squares.

The final step in this analysis was to compare trends in the different estimates of R and F. Separate time series were constructed from the age- and length-based analyses. For R and F at age, annual mean

© 1998 NRC Canada

Table 2. Population estimates (thousands) at length from research surveys for southern Gulf of St. Lawrence cod, 1982–1995.

Length (cm)	1982	1983	1984	1985	1986	1987	1988	1989	1990	1991	1992	1993	1994	1995
4	284	11	96	8	14	21	0	0	0	0	0	0	52	0
7	284	0	784	87	193	528	191	28	34	351	287	59	1 007	5 368
10	24	27	0	444	533	48	772	174	279	1 452	535	780	802	7 434
13	457	3 184	129	10 489	4 736	292	932	650	1 125	715	955	680	826	951
16	3 671	5 659	145	12 378	5 680	310	4 146	7 730	1 114	2 172	1 669	181	349	10 685
19	2 828	4 602	1 135	4 199	4 888	1 482	3 112	16 431	1 062	2 507	763	838	486	18 961
22	8 197	13 487	8 544	6 935	14 279	5 673	4 283	15 114	1 672	3 508	1 443	3 088	1 124	12 155
25	31 133	19 576	9 545	11 430	33 968	12 287	14 594	23 427	4 971	8 958	3 510	6 946	1 284	11 564
28	37 173	21 802	10 642	15 339	24 567	15 667	31 017	23 967	12 131	11 609	6 136	5 386	2 238	13 558
31	16 211	47 861	15 853	26 964	17 886	23 821	54 404	16 842	21 954	10 777	11 829	5 843	7 557	6 547
34	11 312	55 882	27 225	32 278	28 612	20 454	68 454	24 709	29 559	19 251	12 769	11 805	9 431	5 589
37	16 560	35 538	43 734	47 085	40 803	20 112	62 604	28 665	26 705	30 814	10 237	16 042	9 019	10 795
40	18 209	20 584	45 917	77 148	58 674	34 905	61 305	33 757	24 997	31 260	11 209	18 282	13 539	13 932
43	25 688	23 639	29 436	96 549	66 152	49 100	70 401	43 800	27 008	27 167	12 212	15 846	14 490	15 409
46	50 357	22 457	22 381	64 923	49 393	47 429	61 899	45 896	24 852	17 885	9 820	12 678	12 075	13 956
49	58 087	26 240	18 439	33 336	29 254	30 696	45 139	36 214	19 979	12 670	6 342	8 836	8 930	11 017
52	42 057	25 785	14 907	16 197	12 496	13 582	19 852	19 966	12 522	7 067	3 197	4 265	5 005	5 877
55	25 845	18 932	11 955	12 134	7 490	6 364	8 853	9 540	5 872	3 569	1 298	1 802	3 055	2 935
58	13 226	9 663	7 947	6 233	3 625	2 613	2 807	3 442	2 051	1 463	688	845	1 318	1 653
61	6 236	4 768	4 431	3 811	2 333	1 139	1 047	1 482	977	665	281	365	744	804
64	2 088	3 409	2 698	1 852	1 713	378	381	697	458	331	161	134	361	500
67	914	1 814	1 287	1 481	772	188	266	346	145	150	22	137	335	314
70	816	1 139	549	659	550	95	134	166	52	184	30	48	241	221
73	484	696	536	814	282	124	174	86	131	45	20	54	65	151
76	371	752	347	650	309	142	115	8	83	47	43	61	64	125
79	404	410	215	144	328	40	133	12	59	11	31	41	34	106
82	175	213	72	126	299	170	125	0	20	38	29	33	11	152
85	88	274	101	357	110	161	187	30	17	17	10	9	8	57
88	244	350	75	162	223	41	120	45	17	0	23	17	13	62
91	166	60	112	115	161	132	33	55	9	31	10	5	21	0
94	44	110	73	334	130	95	79	28	69	50	10	9	21	34
97	93	135	125	40	168	25	53	122	17	0	10	9	15	12
100–133	297	1 232	471	655	648	272	725	586	159	66	10	77	23	9
Total	374 020	370 183	279 905	485 356	411 268	288 387	518 339	354 014	220 102	194 828	95 591	115 203	94 542	170 930

© 1998 NRC Canada

Table 3. Commercial catch at length (thousands) of southern Gulf of St. Lawrence cod, 1982–1995.

Length (cm)	1982	1983	1984	1985	1986	1987	1988	1989	1990	1991	1992	1993	1994	1995
4	—	—	—	—	—	—	—	—	—	—	—	—	—	—
7	—	—	—	—	—	—	—	—	—	—	—	—	—	—
10	—	—	—	—	—	—	—	—	—	—	—	—	—	—
13	—	—	—	—	—	—	—	1	—	—	—	—	0	0
16	—	—	—	—	—	—	—	2	—	—	—	—	0	0
19	—	—	—	—	—	—	—	1	—	—	—	—	0	1
22	—	—	—	—	—	—	—	—	—	—	—	—	1	12
25	—	1	6	—	—	7	5	2	—	1	—	—	2	32
28	—	3	3	11	21	32	—	3	—	0	4	—	3	33
31	—	5	11	45	106	41	37	22	45	21	42	17	10	28
34	22	22	63	200	373	174	183	161	72	191	137	64	15	40
37	206	144	206	839	1 399	859	713	744	422	791	753	217	27	79
40	1 397	773	977	3 496	4 670	3 798	3 009	3 528	2 464	3 870	3 960	385	56	113
43	3 223	2 582	3 031	7 712	9 471	10 056	8 237	8 996	7 692	8 253	8 451	564	100	143
46	7 259	5 483	4 544	9 893	11 131	12 244	12 357	12 874	11 056	9 373	8 710	686	119	137
49	9 613	8 701	5 839	8 190	10 053	9 441	11 121	11 290	11 853	8 961	6 846	603	143	124
52	8 012	9 853	6 659	6 452	7 222	5 660	6 774	7 130	7 852	6 361	4 473	465	116	81
55	5 979	8 187	5 696	5 103	4 719	3 292	3 489	3 869	4 939	3 832	2 949	381	92	60
58	4 002	5 335	4 082	3 717	2 899	1 942	1 721	1 975	2 173	2 156	1 512	270	75	43
61	2 217	2 833	2 680	2 266	1 912	1 038	835	993	1 061	1 092	787	200	63	28
64	1 010	1 551	1 558	1 376	1 138	637	439	470	493	560	490	137	49	22
67	598	806	945	742	644	351	231	270	200	329	237	84	41	15
70	611	420	571	437	423	246	153	143	100	184	140	39	22	12
73	292	242	372	268	251	212	150	77	70	100	87	20	11	8
76	173	158	285	173	171	126	83	52	40	73	43	10	5	5
79	102	114	222	118	120	86	56	38	21	49	35	8	3	4
82	79	72	133	81	99	89	47	25	10	26	20	7	1	3
85	40	51	129	52	61	70	53	17	11	15	16	7	1	2
88	30	34	68	48	49	62	39	14	6	27	4	4	1	2
91	25	38	53	37	27	41	37	13	1	7	4	6	0	1
94	8	18	35	21	22	29	35	6	3	10	3	2	0	1
97	7	8	25	17	14	27	39	5	2	3	2	1	0	1
100–133	8	51	68	42	31	65	95	16	24	16	10	4	0	0
Total	44 916	47 484	38 259	51 337	57 026	50 626	49 938	52 737	50 611	46 302	39 716	4 182	958	1 028

© 1998 NRC Canada

Fig 3. Comparison of *R* (left column) and SPA *F* (right column) estimates from simulated datasets where the "true" values of *F* and *M* varied. If *F* or *M* was constant, the value is shown. *F* up refers to a simulation where *F* was constant at 0.4 in years 1–7, then increased to 0.6, 0.8, and 1.0 in years 8–10, respectively. *M* up refers to a simulation where *M* was constant at 0.2 in years 1–7, then increased to 0.4, 0.6, and 0.8 in years 7–10, respectively. The variable *k* (RV catchability) was constant at 1.0 and *d* (rate of catch under-reporting) was constant at 0.0. Thirty simulated replicates were used for each series, and the error bars show 1 SD.

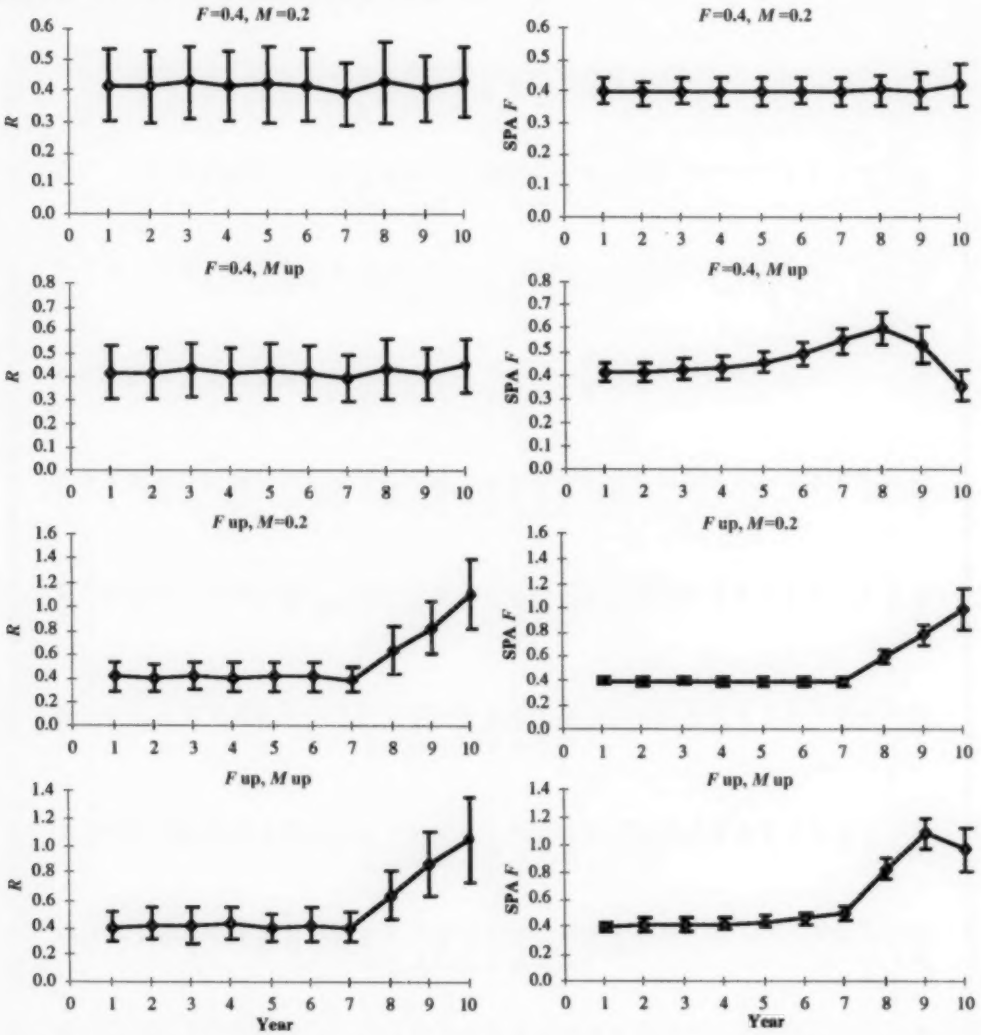

values for ages 7–12 were calculated. For the length-based analysis, the annual predicted *R* at 40, 49, and 58 cm were estimated. The five time series were compared with correlation analysis.

Results

Simulations

The SPA estimates of *F* and the direct estimates of *R* were of similar magnitude and trend when *M* was held constant and *k* = 1.0 (Fig. 3; *F* = 0.4, *M* = 0.2, and *F* up, *M* = 0.2). The mean estimates of *R* for ages 7–12 were slightly above the "true" value, partially because of the skewed distribution of *R* and the difference between mean and midyear population abundance. The mean SPA *F* estimates were virtually identical to the true values. The standard deviations of the *R* estimates were about three times higher than those of the SPA *F* estimates. This was expected, since each *R* is affected by variability in both the catch and index while the SPA essentially smooths variability in catch-at-age data by basing estimates on the cumulative catches of a cohort. The SPA estimates of *F* in the final year of the simulations were more sensitive to the variability in the index. This is evident in the standard deviations of the *F* estimates which, in year 6, were approximately 60% those in year 10. The standard deviations of *R* were constant over the simulation period.

When *M* was constant for the first 7 years, then increased in years 8, 9, and 10, the SPA estimates of *F* showed a biased trend while *R* was unaffected (Fig. 3, *F* = 0.4, *M* up and *F* up, *M* up). Even though the true *F* was constant, the SPA

© 1998 NRC Canada

Fig. 4. Comparison of R (left column) and SPA F (right column) estimates from simulated data sets where the "true" values of F, M, and k varied. Two scenarios of k were used, a fixed value of 0.5, and a step from 1.0 to 0.5 in year 6. Thirty simulated replicates were used for each series, and the error bars show 1 SD.

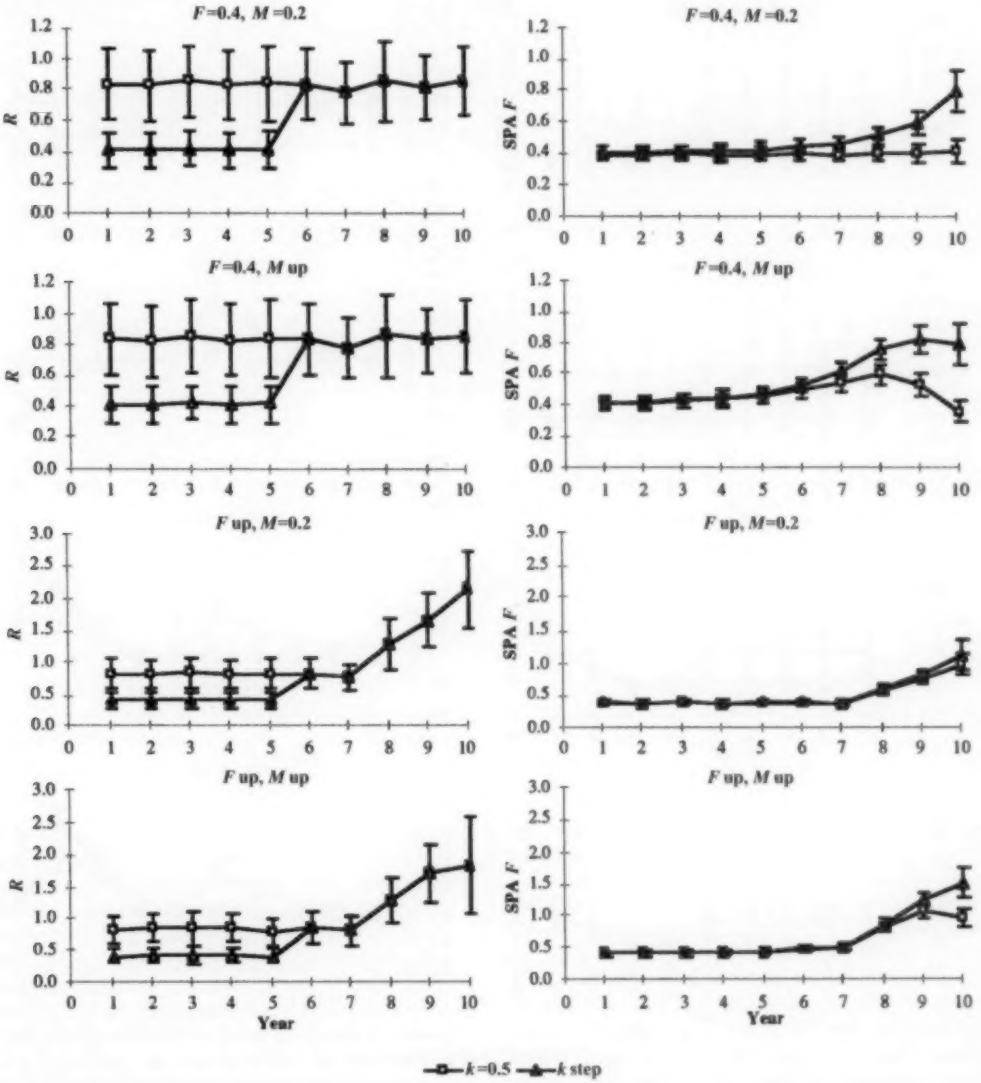

estimates increased from year 1 to year 8, then declined steeply. This was caused by the incorrect M assumption in the SPA calculations and because the true M changed during the simulation period. If the true M was constant but different than the assumed value, the SPA F estimates were biased but showed no trend.

Changes in survey catchability (k) had different effects on R and SPA F (Fig. 4) . If k was constant throughout the simulation but had a value of 0.5, R estimates doubled and were approximately twice the true F. The trend in R reflected the trend in true F regardless of the value of k. If there was a step in k, this appeared as a step in the R estimates. With the exception of the spurious step in the R estimates, trends in true F were still well estimated. SPA F estimates agreed with the true F if RV catchability was constant during the simulation period (Fig. 4, cases where $k = 0.5$ and $M = 0.2$). If there was a step in k, however, the SPA F estimates showed a spurious trend. There was an increasing trend in SPA F estimates if $M = 0.2$ and k was reduced to 0.5 in years 6–10. The effects of a step in k and an increase in M on the SPA F estimates was additive. However, the effects of a step in k and an increase in true F seemed to cancel, since there was little difference between the true F and the SPA estimates (Fig. 4, F up, $M = 0.2$, k step).

Changes in the rate of catch under-reporting (d) had similar effects on R as changes in k (Fig. 5). If d was constant

© 1998 NRC Canada

Fig. 5. Comparison of *R* (left column) and SPA *F* (right column) estimates from simulated datasets where the true values of *F*, *M*, and *d* varied. Notation for changes in *F* and *M* are explained in Fig. 3. Two scenarios of *d* were used, a fixed value of 0.5 and a step from 0.0 to 0.5 in year 6. Thirty simulated replicates were used for each series, and the error bars show 1 SD.

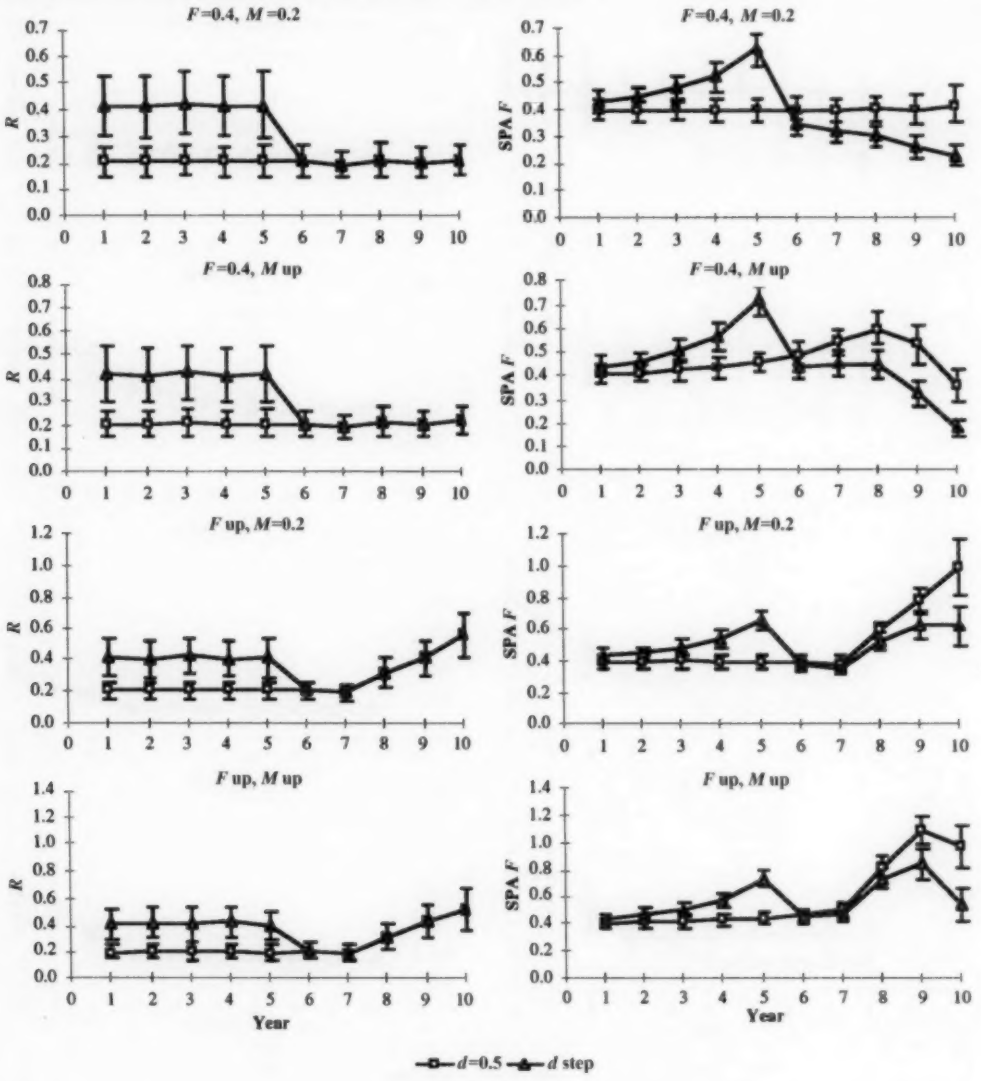

through the simulation period, *R* estimates reflected trends in true *F*. If *d* stepped to 0.5, there was a proportional reduction in *R*. If *d* was constant at 0.5 throughout the simulation, SPA *F* estimates were close to the true *F*. However, the SPA *N* estimates were biased downward, since the estimated catch was lower than the true catch. When there was a step in *d*, the SPA *F* estimates had spurious trends. When *F* and *M* were constant, the SPA *F* increased in the first 5 years of the simulation, and the estimates were generally greater than the true values. There was a large decline in *F* in year 6, followed by a declining trend. The effects of changes in *M* and changes in *d* were additive.

Residuals from multiplicative analyses of the RV data and from SPA calibration showed different temporal patterns depending on the simulation scenario. There were no temporal trends in either set of residuals if *F*, *M*, *k*, and *d* were constant throughout the simulations (Fig. 6). If *M* increased in the latter part of the simulation series (*M* up), there was a trend in residuals from both analyses, increasing to year 7 then declining. If *F* increased, only the residuals from the multiplicative analysis had a trend.

A step in *k* produced distinctive patterns in the residuals from multiplicative analyses and SPA calibration (Fig. 7). There were clear temporal steps in the residuals. The residuals increased for 5 years, decreased in year 6, then increased again until year 10 in the case of the multiplicative analyses.

© 1998 NRC Canada

Fig. 6. Residual from multiplicative analyses of simulated RV data (left column) and SPA calibrations (right column) using simulated data sets where F and M varied. Notation for changes in F and M are explained in Fig. 3. k was constant at 1.0 and d was constant at 0.0 in each scenario. Thirty simulated replicates were used for each series, and the error bars show 1 SD.

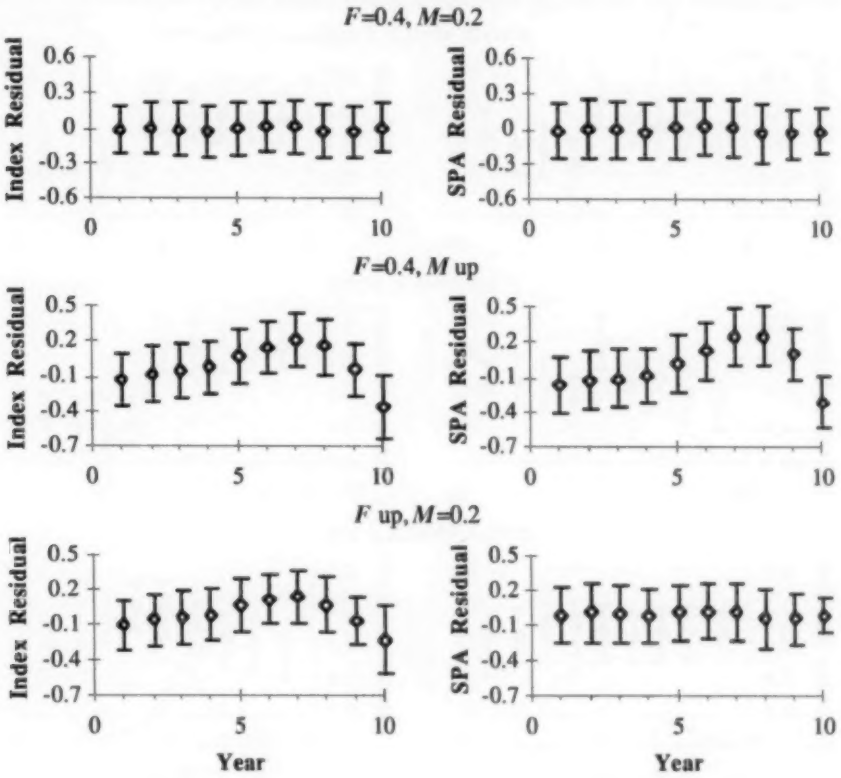

The SPA residuals were stable but positive in the first 5 years, decreased in year 6, and then increased to year 10. The residual patterns from the F up, k step scenario were interesting. The multiplicative analysis residuals increased in the first 5 years, then declined and were relatively stable in years 6–10. In the SPA, the residuals were high and stable in the first 5 years, then low and stable in the last 5 years. What is interesting is that the SPA calibration resulted in relatively good estimates of the true population size, but the residual patterns would indicate a problem and cast doubt on the results. The residual patterns from the multiplicative analyses showed no trend when M, F, and k were constant, but there was a step in d (Fig. 7). This would be expected given that these analyses did not use commercial catch data. The SPA residuals were dome shaped in this scenario.

Case study

Age-by-age comparisons of R and F estimates for the southern Gulf of St. Lawrence cod stock indicated that they were of similar magnitude and trend. Signed-rank tests were conducted separately for each age. The differences between F and R estimates were statistically significant at the 0.05 level only for age 3 (Table 4). Linear regressions of annual estimates of R as a function of F were highly significant ($p < 0.01$) for all ages (Table 5). None of the estimated intercepts were significantly different than 0.0 and only the age-3 slope was significantly different than 1.0.

Comparing annual RV survey and commercial catch length frequencies reveals important events in this fishery (Fig. 8). The above-average 1979 and 1980 year-classes recruited to the commercial fishery in 1985. They were apparent in the RV survey as modes at 28, 34, 40 , and 43 cm in 1982–1985, respectively. The size composition of the commercial catch shifted towards smaller fish in 1985 as these year-classes entered the commercial size range. The year-classes produced in the 1980s were smaller, and the abundance of commercial sized fish declined in the late 1980s and early 1990s. However, the commercial catches remained relatively stable (an example is shown for 1991) indicating that fishing mortality increased during this period. The cod-directed fishery was closed in September 1993 when stock abundance had declined to a very low level. This is shown by the 1994 length frequencies, where the RV survey estimates were very low compared with previous years, and the commercial catch length frequency was indistinguishable from the x axis.

Annual estimates of R at selected lengths indicated similar patterns for the period of the case study (Fig. 9). R was relatively stable during 1982–1989. This was followed by a rapid increase to a peak in 1992. With the closure of the fishery in 1993, the estimates declined to minimal values. There

© 1998 NRC Canada

Fig. 7. Residual from multiplicative analyses of simulated RV data (left column) and SPA calibrations (right column) using simulated data sets where *F*, *M*, *k*, and *d* varied. Notation for changes in *F* and *M* are explained in Fig. 3. *k* step refers to a simulation where *k* was constant at 1.0 in years 1–5 then it decreased to 0.5 in years 6–10. *d* step refers to a simulation where *d* was constant at 0.0 in years 1–5 then it changed to 0.5 in years 6–10. Thirty simulated replicates were used for each series, and the error bars show 1 SD.

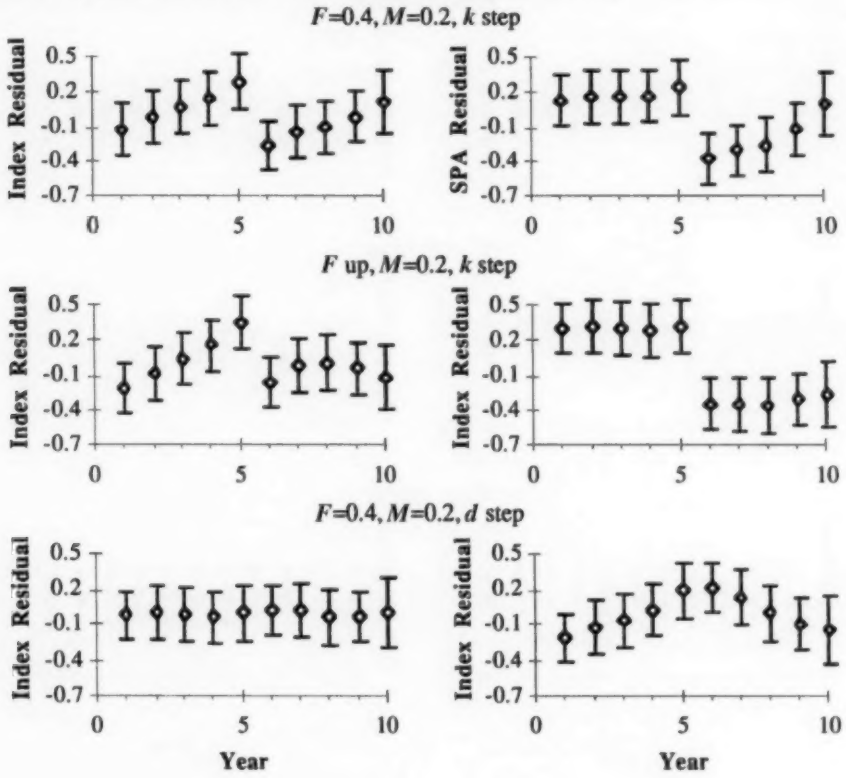

was a slight divergence in the trends during 1982–1985, with *R* at 40 cm declining while there was an increase for the 49- and 58-cm groups. The fishery may have been targeting the abundant and larger fish (>40 cm) that were present in the population at that time, and avoiding the smaller fish (see Fig. 8).

The analysis of covariance of *R* as a function of length and year suggested that a cubic model provided the best fit. In addition, the analysis supported the estimation of separate slopes and intercepts for each year (Table 6). The regression explained 99% of the variation in observed *R* at length, and there was very little difference between the observed and predicted values. The trends in predicted *R* at selected lengths were the same as those shown in Fig. 5.

Estimates of *R* were dome shaped with respect to length; the maximum values were in the 65–75 cm length range (Fig. 10). This may reflect size segregation in the population with the larger animals inhabiting deeper water than the smaller ones (Sinclair 1993; Swain 1993). The fishery may select larger concentrations of midsized fish to maximize catch rates. The trend of *R* at age is flat-topped with high values at ages 7 and above (Fig. 11). The difference between the pattern at length and at age is due to a skewed distribution of length at age. The mean lengths at ages 7–12 were below the length of maximum *R*, but the upper tails of the distributions were above the length of maximum *R* (Fig. 12). This observation suggests that, for this stock, there is an intermediate length range where the vulnerability to fishing is the highest. Slower growing fish may remain in this length range for a longer period of time and experience a higher cumulative mortality than faster growing fish. Examination of the distribution of *F* at age would not reveal this phenomenon.

The reduction of *F* that occurred when the directed fishery was closed in 1993 is clearly shown in both *R* at length and age (Figs. 10 and 11). The annual trends in relative and absolute fishing mortality obtained from age- and length-based data were compared using correlation analysis. Comparisons were made among mean SPA *F* and *R* at ages 7–12, and the predicted *R* at lengths 40, 49, and 58 cm from the analysis of covariance (*R*40, *R*49, and *R*58, respectively). Correlations between age- and length-based estimates were highly significant ($p < 0.01$) (Table 7). The highest correlations were among the direct age and length-based estimates (0.91–0.98). The correlation coefficients between the assessment *F* estimates and all the direct estimates of *R* ranged from 0.76 to 0.89. The weakest correlation was between the assessment *F* and *R*40.

© 1998 NRC Canada

Fig. 8. RV (solid line) and commercial (broken line) catch length frequencies for southern Gulf of St. Lawrence cod, 1982–1985, 1991, and 1994.

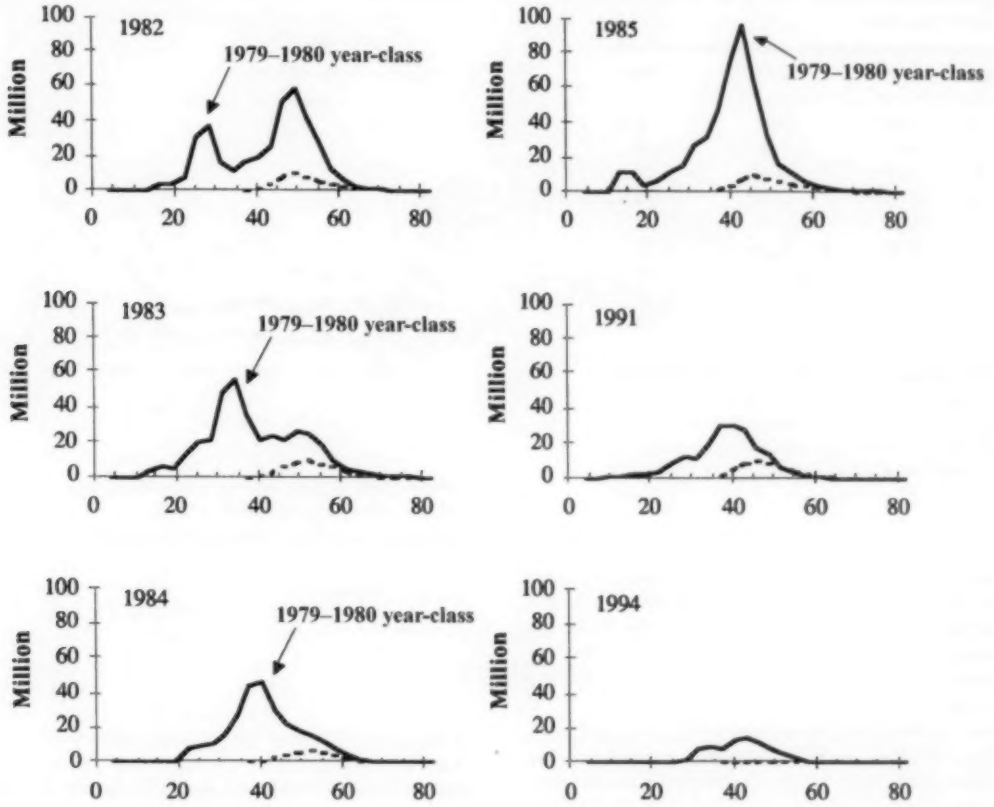

Table 4. Summary of Wilcoxon signed-rank tests comparing annual estimates of R and F at age for southern Gulf of St. Lawrence cod, 1982–1995.

Age	Mean arithmetic difference	Mean logarithmic difference
3	–0.00**	–0.37*
4	–0.00	–0.16
5	–0.00	0.03
6	0.01	0.09
7	0.01	0.06
8	–0.00	0.01
9	–0.05	–0.11
10	0.08	0.05
11	0.09	0.15
12	0.24	0.31
All ages	0.04	0.04

Note: Values are mean differences in the arithmetic and natural logarithmic scales. *, Significant at the 0.05 level; **, significant at the 0.01 level, both using a Wilcoxon signed-rank test.

Discussion

The direct method for estimating R is a simple and useful addition to the fish stock assessment toolbox. Describing trends in F is an important component of fish stock assessment. Age-based SPA methods are commonly used for this purpose, but such analyses are not always possible. The basic requirements for estimating R include a temporally consistent index of population abundance at age or length and accurate estimates of commercial catch at age or length. R is estimated as the ratio of catch divided by the index and, provided the index represents conditions close to the middle of the fishing season, the ratio is approximately proportional to F. The population index used in the case study was obtained from a research vessel survey for which we are reasonably confident that catchability has remained constant. Alternatively, a commercial catch per unit effort index could be used; however, it would be necessary to verify that fishing power remained constant and that the index was proportional to stock size. Through simulations and a case study, it was demonstrated that R estimates compared well with trends in both the true fishing mortality and estimates obtained from traditional SPA assessments. R estimates are likely to have higher variance than SPA F estimates, mainly because the latter

© 1998 NRC Canada

Table 5. Estimated R^2, intercepts, and slopes from linear regression of R at age as a function of F at age for southern Gulf of St. Lawrence cod, 1982–1995.

Age	R^2	Intercept	Slope
3	0.88**	–0.00	1.76**
4	0.87**	0.00	1.08
5	0.81**	–0.03	1.22
6	0.76**	–0.06	1.17
7	0.80**	–0.09	1.19
8	0.79**	–0.15	1.32
9	0.76**	–0.03	1.15
10	0.53**	0.04	0.82
11	0.52**	0.03	0.82
12	0.55**	–0.04	0.77

Note: The results of statistical tests of the regression, the difference of the intercept from 0.0, and the difference of the slope from 1.0 are as follows: **, significant at the 0.01 level.

Fig. 9. Trends in R for the 40-, 49-, and 58-cm length groups for southern Gulf of St. Lawrence cod, 1982–1995.

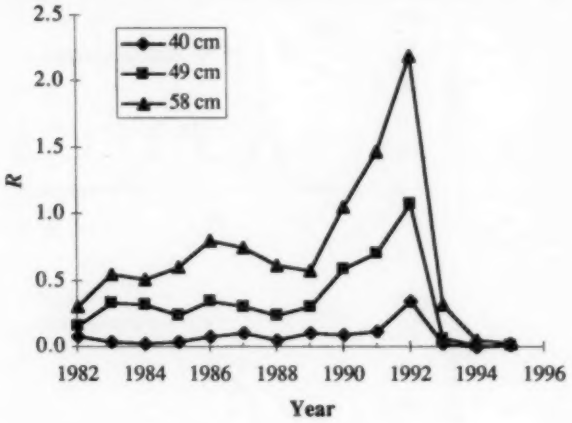

Table 6. Results of an analysis of covariance of R at length as a function of length and year ($R^2 = 0.99$).

Source	df	SS	F	$P > F$
L	1	9.60	493	<0.0001
$L2$	1	0.60	31	<0.0001
$L3$	1	0.20	10	0.0021
Year	13	56.29	222	<0.0001
Year × L	13	6.08	24	<0.0001
Year × $L2$	13	1.48	6	<0.0001
Year × $L3$	13	2.01	8	<0.0001

smoothes population estimates of cohort abundance by using cumulative catch rather than annual catch. The variance of R could be estimated using Monte Carlo techniques if one has reliable estimates of the variance of C and A. For the case study, estimates of the variance of A were available, but this was not the case for C.

The direct method has advantages over traditional SPA methods for estimating F. SPA requires a continuous time series of commercial data. Errors or omissions in the commercial data will affect both the direct and SPA estimates in the year where the problems occur. However, these effects will be spread over several years in SPA, because the population estimates are based on the cumulative catch of a cohort. The effects may also be spread by the calibration process depending to the influence of the affected input data on the calibrated SPA parameters. The direct estimates of R are independent from one year to the next. If it is determined that certain years of commercial catch data are unreliable, these years could be ignored, and R could be estimated in adjacent years without bias. R is insensitive to changes in M provided the index is taken near midyear while SPA F estimates are highly sensitive to changes in M. This characteristic is especially useful if there is doubt about the effects of fishing on stock trajectories. The direct estimates of R agreed with the SPA estimates of F in the case study, thus confirming that F increased substantially on the southern Gulf of St. Lawrence cod stock in the early 1990s leading to a drastic decline in stock abundance (Sinclair et al. 1995). This technique could be useful for other stocks where there is doubt about the role of fishing in stock decline. However, there are several outputs of SPA that are not available from the direct method, for example, absolute estimates of F and population size, stock production, and catch projections.

The direct method may be used to estimate temporal trends in F from length-based data. Several length-based SPA techniques may also be used for this purpose; however, they all require some information on size at age (i.e., growth) either determined by a limited amount of age determination of from interpretation of modes in length frequencies. This is difficult with many fish stocks, since modes often become indistinguishable at moderate ages. The direct method does not require any information or assumptions about size at age. Age-based estimates might be preferred, since fish have the same nominal age throughout the year and there is reasonable assurance that the commercial catch and the research survey catch may be identified to a specific cohort. This is not the case for length-based estimates, since fish grow throughout the year. However, the high correlation between the age- and length-based estimates in the case study indicated that length-based estimates would provide a reliable index of trends in F and would be particularly useful for stocks where length-based data exist, but age-based data do not. R also provides information on how fishing mortality is distributed over age- and length-classes. Rivard (1984) describes a similar method for estimating relative fishing mortality at age. However, he did not exploit the information on temporal trends in F.

The method may be used in conjunction with SPA to diagnose possible data problems. If trends in R and SPA F are consistent, as was found in the case study, this suggests that M, k,

© 1998 NRC Canada

Fig. 10. Scatterplot of ln *R* at length for the period 1982–1995. Points from the period 1982–1993 are shown as circles, and those from 1994–1995, after the directed fishery was closed, are shown as squares. Mean values of ln *R* at length for the two time periods are joined with a solid line. The trend ln *R* at length for the two time periods is dome shaped with maximum values in the 65- to 75-cm range. There was a marked decline in *R* at length after the commercial fishery was closed.

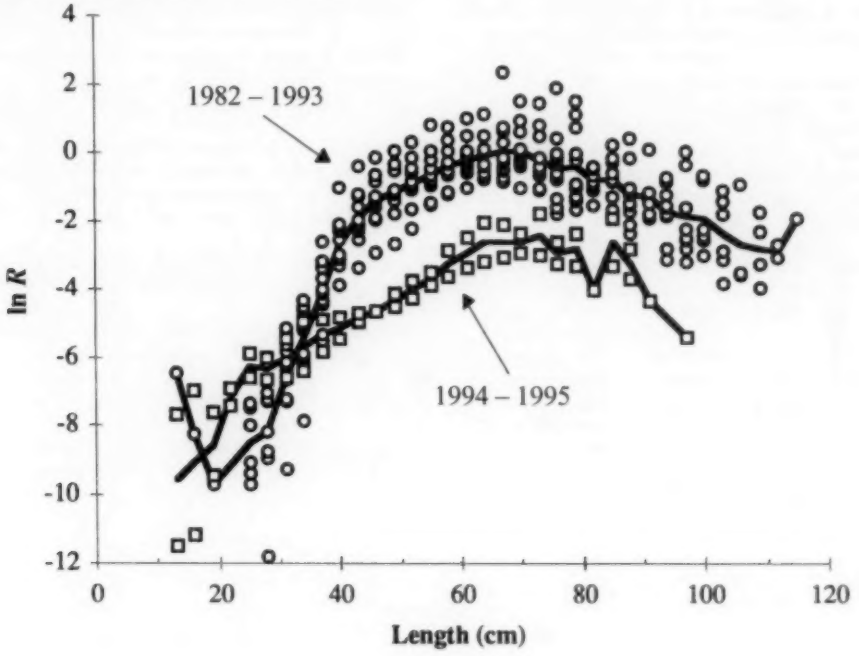

Fig. 11. Scatterplot of ln *R* at ages 3–12 for the period 1982–1995. Points from the period 1982–1993 are shown as circles, and those from 1994–1995, after the directed fishery was closed, are shown as squares. Mean values of ln *R* at age for the two time periods are joined with a solid line. The general pattern of ln *R* at age for the two time periods is flat topped with maximum values at ages 7 and above. There was a marked decline in *R* at age after the commercial fishery was closed.

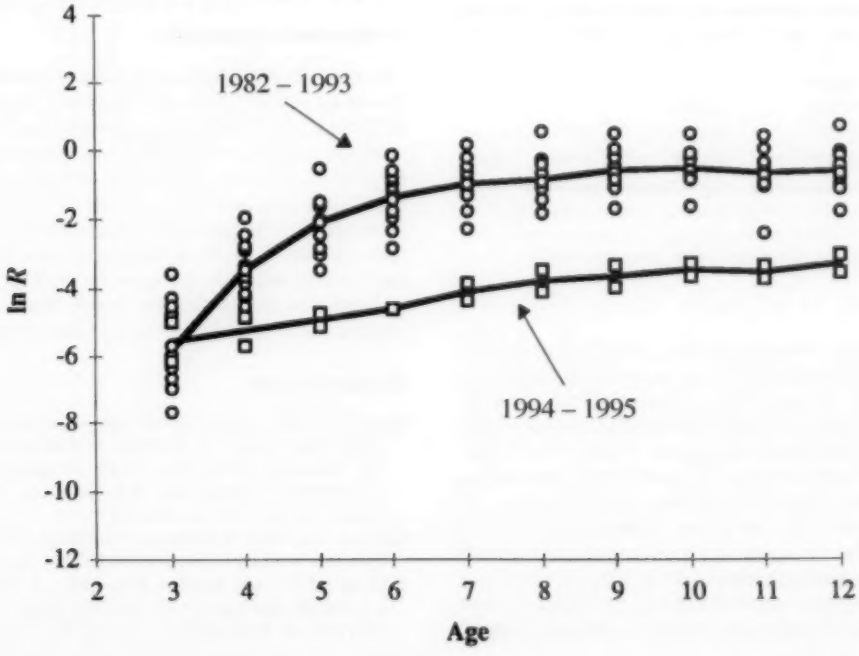

© 1998 NRC Canada

Fig. 12. The distribution of length at age for southern Gulf of St. Lawrence cod, 1982–1995. The vertical line gives the range, the boxes denote the 10th and 90th quantiles, the short horizontal line indicates the medians, and the mean values are shown with a star. The distributions were highly skewed for ages 6–12. The mean values of length at age for ages 7–12 were close to but below the length of maximum ln *R* (Fig. 10), but the range of observations extended well above the length of maximum ln *R*.

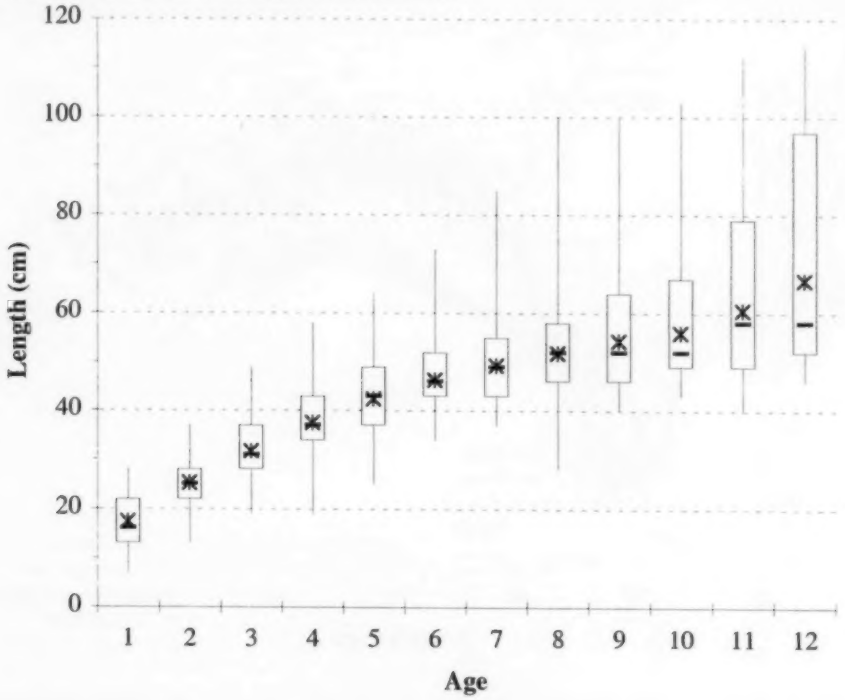

Table 7. Correlations among estimates of annual fishing mortalities obtained from various sources.

	Assessment	Direct age	*R*40	*R*49
Direct age	0.86**			
*R*40	0.76**	0.91**		
*R*49	0.89**	0.96**	0.92**	
*R*58	0.86**	0.95**	0.92**	0.98**

Note: The assessment and direct age estimates were the average ages 7–12 SPA *F* and *R*, respectively. The *R*40, *R*49, and *R*58 estimates were obtained from an analysis of covariance of *R* at length. **, $p < 0.01$.

and *d* were stationary. If the trends differ, further investigation using simulation of *R* and SPA *F* may be useful in diagnosing the source of the inconsistency. I have not presented an exhaustive examination of all possible combinations of events that could lead to differences in trends in *R* and SPA *F*. However, the examples presented here suggest that the two estimators have different sensitivities to data inconsistencies. An increase in *M* had no effect on *R*, but it introduced a skewed trend in SPA *F* (Fig. 3). A step in *k* resulted in a proportional step in *R* and an increasing trend in SPA *F* (Fig. 4). A step in *d* resulted in a proportional step in *R* and caused first an increase in SPA *F* followed by a step down and then a decreasing trend. Thus, direct estimates of relative *F* would be a useful addition to analytical assessments where SPA is used.

Acknowledgments

The idea for this study came from the final meeting of the Canadian Atlantic Fisheries Scientific Advisory Committee (CAFSAC) Groundfish Subcommittee held in May 1993. We needed a way to provide useful management advice on the status of two Scotian Shelf haddock stocks for which only length-based data were available. I'd like to thank K. Zwanenburg and P. Hurley for providing the original haddock data and for their comments on the general approach. R. Mohn provided helpful comments on the manuscript. I am also grateful to L. Currie for assembling the length-based data used in the southern Gulf of St. Lawrence cod case study.

References

Gavaris, S. 1993. Analytical estimates of reliability for the projected yield from commercial fisheries. *In* Risk evaluation and biological reference points for fisheries management. *Edited by* S.J. Smith, J.J. Hunt, and D. Rivard. Can. Spec. Publ. Fish. Aquat. Sci. No. 120. pp. 185–191.

Gulland, J.A. 1965. Estimation of mortality rates. Annex to Arctic Fisheries Working Group Report. ICES, C.M. 1965: 3.

Halliday, R.G., and Koeller, P.A. 1981. A history of Canadian groundfish trawling surveys and data usage in ICNAF divisions 4TVWX. *In* Bottom trawl surveys. *Edited by* W.G. Doubleday

© 1998 NRC Canada

and D. Rivard. Can. Spec. Publ. Fish. Aquat. Sci. No. 58. pp. 27–41.

Mohn, R.K., and Cook, R. 1993. Introduction to sequential population analysis. NAFO Sci. Coun. Stud. No. 17.

Neter, J., Wasserman, W., and Kutner, M.H. 1983. Applied linear regression models. Richard D. Irwin, Inc., Homewood, Ill.

Nielsen, G.A. 1994. Comparison of the fishing efficiency of research vessels used in the southern Gulf of St. Lawrence groundfish abundance surveys from 1971 to 1992. Can. Tech. Rep. Fish. Aquat. Sci. No. 1952.

Pope, J.G. 1972. An investigation of the accuracy of virtual population analysis using cohort analysis. ICNAF Res. Bull. **9**: 65–74.

Ricker, W.E. 1975. Computation and interpretation of biological statistics of fish populations. Bull. Can. Fish. Res. Board No. 191.

Rivard, D. 1984. Estimating partial recruitment from catches and a research survey index: a Monte-Carlo simulation. CAFSAC Res. Doc. No. 84/70.

Shepherd, J.G., and Nicholson, M.D. 1991. Multiplicative modelling of catch-at-age data, and its application to catch forecasts. J. Cons. Cons. Int. Explor. Mer, **47**: 284–294.

Sinclair, A.F. 1993. Partial recruitment considerations in setting catch quotas. Can. J. Fish. Aquat. Sci. **50**: 734–742.

Sinclair, A., and Chouinard, G. 1992. Application of a multiplicative model to research survey data from two cod stocks. CAFSAC Res. Doc. No. 92/66.

Sinclair, A. F., Chouinard, G., Swain, D., Nielsen, G., Hanson, M., Currie, L., Hurlbut, T., and Hébert, R. 1995. Assessment of the southern Gulf of St. Lawrence cod stock, March 1995. DFO Atl. Fish. Res. Doc. No. 95/39.

Sinclair, A.F., Chouinard, G.A., and Currie, L. 1996. Assessment of the southern Gulf of St. Lawrence cod fishery, March 1996. DFO Atl. Fish. Res. Doc. No. 96/52.

Swain, D.P. 1993. Age- and density-dependent bathymetric pattern of Atlantic cod (*Gadus morhua*) in the southern Gulf of St. Lawrence. Can. J. Fish. Aquat. Sci. **50**: 1255–1264.

Swain, D.P., Nielsen, G.A., and McKay, D.E. 1995. Incorporating depth-dependent differences in fishing efficiency among vessels in the research survey time series for Atlantic cod (*Gadus morhua*) in the southern Gulf of St. Lawrence. Can. MS Rep. Fish. Aquat. Sci. No. 2317.

Winters, G.H. 1988. The development and utility of sequential population analysis in stock assessments. *In* Collected papers on stock assessment methods. *Edited by* D. Rivard. CAFSAC Res. Doc. No. 88/61. pp. 111–134.

Zwanenburg, K.C.T., and Smith, S.J. 1983. Comparison of finfish length-frequency distributions estimated from samples taken at sea and in port. *In* Sampling commercial catches of marine fish and invertebrates. *Edited by* W.G. Doubleday and D. Rivard. Can. Spec. Publ. Fish. Aquat. Sci. No. 66. pp. 189–193.

© 1998 NRC Canada

Microsatellite gene diversity analysis in anadromous arctic char, *Salvelinus alpinus*, from Labrador, Canada

Louis Bernatchez, J. Brian Dempson, and Sylvain Martin

Abstract: We analysed six loci among 257 Arctic char (*Salvelinus alpinus*) representing seven locations in Labrador and Newfoundland to provide a first assessment of microsatellites gene diversity in anadromous char and to determine the geographic scale of population structuring within the species. The number of alleles per locus varied between 9 and 48, and gene diversity ranged from 0.190 to 0.968. Significant F_{ST} and differences in allele frequencies were observed among most samples, as well as heterozygous deficiency, which was indicative of a Wahlund's effect. These results implied the existence of genetically distinct populations on a microgeographic scale (less than 10 km) and that our samples represented an admixture of char from those populations that interchange among rivers for owerwintering, in congruence with tagging investigations. These results indicate that microsatellites potentially offer more sensitivity than allozymes and mitochondrial DNA to infer fine-scale population structure in anadromous arctic char.

Résumé : Nous avons analysé six loci parmi 257 ombles chevalier *(Salvelinus alpinus)* provenant de sept sites au Labrador et à Terre-Neuve dans le but d'établir l'utilité des microsatellites pour la quantification du partage de variance génétique parmi les populations anadromes et pour documenter l'échelle de structuration génétique chez cette espèce. Les microsatellites se sont révélés modérément à hautement variables, avec un nombre d'allèles par locus variant entre 9 et 48 et une hétérozygotie attendue variant entre 0.190 et 0.968. Des valeurs de F_{ST} significatives, de même qu'une hétérogénéité des fréquences alléliques ont été observées entre la plupart des échantillons. Nous avons observé un déficit en hétérozygote associé à un effet Wahlund dans tous les échantillons, sauf un. Ces résultats traduisent l'existence de populations génétiquement différenciées sur une échelle microgéographique (inférieure à 10 km), de même qu'un mélange de ces populations dans les tributaires d'hivernage, corroborant ainsi les études de marquage. Nous concluons que les microsatellites offre une sensibilité supérieure aux marqueurs traditionnels pour l'étude de structures populationelles fines.

Introduction

Explaining the extent, causes, and consequences of biotic distribution in space is fundamental to our understanding of how species evolve to cope in particular environments, as well as for their conservation and management. In the past decade, the member–vagrant hypothesis has provided an important conceptual framework for studying the role of ecological processes in determining spatial patterns of abundance in aquatic species (Sinclair and Iles 1988). One prediction of this hypothesis is that the number of populations composing a given species will primarily be determined by the number of environmental settings (either geographic, physical, or oceanographic) allowing the closure of a species life cycle. Thus, the member–vagrant hypothesis predicts that anadromous fish species, typically homing to a given river for spawning, and into which juvenile fish grow until moving down to sea where they live until sexual maturation, should be composed of numerous populations determined by the number of rivers available to the species. This has been corroborated by both ecological and genetic studies in species of the genus *Salmo* and *Oncorhynchus* (e.g., Davidson et al. 1989; Sinclair and Iles 1988). Predicting population structure from such theoretical framework may, however, be more complicated in species exhibiting complex migratory behavior, for instance, involving sporadic coastal movements at both juvenile and adult stages and (or) overwintering migration in different rivers, and for which homing behavior has not been documented.

Anadromous arctic char (*Salvelinus alpinus*) represents an extreme in complexity of migratory behavior among anadromous fishes. Periodic migrations of adult and juvenile fish to the sea enable anadromous populations to take advantage of marine food resources (reviewed in Dempson 1995). The seaward movement coincides with spring runoff and ice breakup in coastal rivers and consists of both first-time and repeat migrants. First-time migrants have spent 1–8 years in fresh water. Repeat migrants include adults (maturing and nonmaturing) and juveniles. Arctic char are not known to

Received June 11, 1997. Accepted December 11, 1997.
J14056

L. Bernatchez[1] **and S. Martin.** Groupe interuniversitaire de recherches océanographiques du Québec, Département de biologie, Pavillon Vachon, Université Laval, Sainte-Foy, QC G1K 7P4, Canada.
J.B. Dempson. Science Branch, Department of Fisheries and Oceans, P.O. Box 5667, St. John's, NF A1C 5X1, Canada.

[1] Author to whom all correspondence should be addressed. e-mail: louis.bernatchez@bio.ulaval.ca

© 1998 NRC Canada

Table 1. Sample locations with their abbrevaiations, date of sampling, and life-history stage sampled (A, adult; J, juvenile).

Region and river	Latitude (N)	Longitude (W)	Date	Stage	*N*
Labrador					
Pangertok Inlet River (PI)	58°21′	63°10′	08/1991	A	30
Sachem Bay Pond (SB)	56°41′	61°48′	08/1988	A	41
Fraser River (FR)	56°39′	63°10′	07/1988	A	39
Reid Brook (RB)	58°18′	62°05′	08/1996	A, J	46
Ikadlivik Brook (IB)	58°18′	62°10′	08/1996	A	30
Kogluktokluk Brook (KOB)	58°18′	62°07′	08/1996	J	30
Newfoundland					
Gander Lake (GL)	48°55′	54°35′	07/1995	A, J	40

overwinter at sea and reenter freshwater yearly at the end of the summer and early fall.

Such complexity in migratory behaviour and the lack of clear information about the extent of homing behaviour makes it difficult to predict the population structure in Arctic char. Namely, it is not clear if the fact that the species use more than one river to complete its life cycle should result in populations structured by region rather than by river. Tagging studies revealed that summer coastal movements are geographically localized and indicated that char from different geographic areas may be considered different population units (Dempson 1995). On a smaller scale, tagging studies revealed the propensity of char to move among different rivers emptying within a same bay from year to year (Dempson and Kristofferson 1987). These observations are compatible with the hypothesis that char populations may be structured by region rather than by river. On the other hand, it is not known whether straying fish only comprised nonspawning, overwintering components of the populations or also included mature fish, therefore precluding to refute the hypothesis that the species may be genetically structured by river.

In theory, allele frequency data from neutral loci may provide the best approach to assess genetic population structure. Thus far, the usefulness of allozymes and mitochondrial DNA (mtDNA) to characterize genetic structure in arctic char has been hampered bythe extremely reduced polymorphism generally observed in the species (e.g., Wilson et al. 1996). In addition, there are increasing concerns that the non-neutrality of enzymatic loci may, in some cases, mask the identity of existing population differentiation (e.g., Verspoor and Jordan 1989).

Microsatellites are a class of highly polymorphic and presumably neutral nuclear loci that are receiving increasing attention (Jarne and Lagoda 1996). The usefulness of microsatellites for addressing fine-scale population structure has been demonstrated in *Salvelinus* species (Angers and Bernatchez 1998). In the only use of microsatellites in arctic char published thus far, a recent study on European populations from central alpine lakes clarified the species population structure on a mesogeographic scale where other markers failed to detect significant genetic diversity partitioning (Brunner et al. 1998).

In this study we performed a gene diversity analysis among arctic char from Labrador and Newfoundland to assess the scale of population structuring in anadromous species using more than one river to complete their life cycle. This study also provides an assessment of the potential usefulness of microsatellites to infer fine-scale population structure in species exhibiting extremely reduced genetic diversity at both allozymes and mtDNA, such as observed in arctic char. We also document the usefulness of comparing data analyses based on the consideration, or not, of mutational differences among alleles to infer genetic structure among closely related populations. Finally, we discuss the importance of the observed population structure in the context of environmental impacts.

Materials and methods

Samples and microsatellite loci

A total of 257 arctic char were collected to cover different geographic scales from six sampling sites along the Labrador coast and from an inland lake in Newfoundland, as a reference population to ensure that statistically significant genetic divergence can indeed be quantified among populations known a priori not to be currently connected by gene flow (Table 1). Three of the most important tributaries of Voisey's Bay that support arctic char were surveyed (Fig. 1). Ikadlivik Brook is a tributary of Kogluktokoluk Brook, which empties into the head of Voisey's Bay. Reid Brook's mouth essentially empties at the same location as the Kogluktokoluk River (Fig. 1) and is normally considered as an extended tributary of the Kogluktokoluk–Ikadlivik river system. The other samples represent char originally assigned to several different management stock complexes distinct from Voisey's Bay (Dempson and Kristofferson 1987). Reid Brook samples were captured either in Reid Brook itself or in Reid Pond located about 15 km upstream of Reid Brook's mouth. Tissues used for DNA extraction consisted of either adipose fins, white muscle, or liver first kept at –20°C and then fixed in 95% ethanol for shipment from Newfoundland to Québec City for genetic analysis. Genetic diversity at six microsatellite loci was screened using primers originally developed for other salmonids to amplify homologous microsatellite loci in *S. alpinus* (Table 2). The methods used for DNA extraction, PCR reactions, electrophoresis, autoradiography and allele scoring were as outlined in Brunner et al. (1998).

Genetic diversity

Genetic polymorphism for each sample (=location throughout the text) was estimated as the mean number of alleles per locus (*A*),

© 1998 NRC Canada

Fig. 1. Location map showing sampling sites for Arctic char from northern Labrador and Newfoundland.

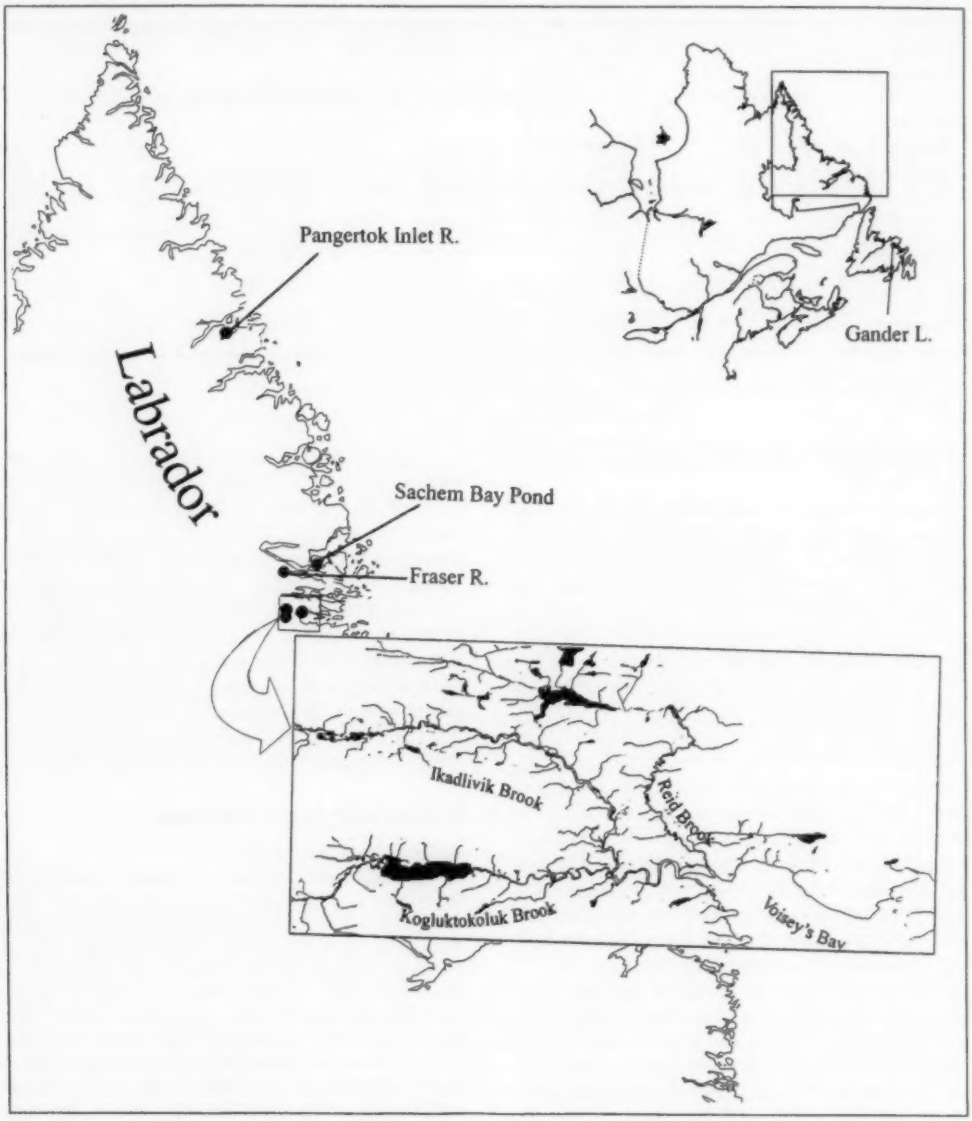

Table 2. Source species, reference, annealing temperature, allelic size range, number of fish successfully analyzed per locus (N), number of alleles per locus (A), and overall gene diversity (H_e) for six microsatellite loci used in this study.

Locus	Species	Reference	Temperature (°C)	Size range (bp)	N	A	H_e
MST85	*Salmo trutta*	Presa and Guyomard 1996	55	170–220	248	16	0.521
Pupupy	*Oncorhynchus mykiss*	Morris et al. 1996	60	387–492	247	9	0.411
Cocl-3	*Coregonus clupeaformis*	Bernatchez 1996	50	219–289	240	33	0.760
Ssa-85	*Salmo salar*	O'Reilly et al. 1996	60	115–255	257	46	0.911
Sfo-8	*Salvelinus fontinalis*	Angers et al. 1995	60	216–316	234	33	0.916
Sfo-23	*Salvelinus fontinalis*	Angers et al. 1995	60	159–289	237	48	0.907

© 1998 NRC Canada

observed heterozygosity (H_o), and gene diversity (H_e), using the version 3.0 of GENEPOP (Raymond and Rousset 1995). GENEPOP was also used to assess heterogeneity in allele frequencies among pairwise comparisons of samples and to test for deviations from Hardy–Weinberg (HW) equilibrium within samples for every single locus and over all loci. Values of significance were estimated by Fisher's exact test in cases of five alleles per locus or less, and a Markov chain method to obtain unbiased estimates of the exact test through 1000 iterations when the number of alleles was higher. As discussed by Rousset and Raymond (1997), exact tests share several properties that make them one of the most powerful method to circumvent potential problems imposed to the use of more traditional statistical procedures by high number alleles relative to the sample size, a typical situation with microsatellites. Briefly, exact tests do not require the use of an asymptotic distribution (exactness) and rely on probability distribution independent of unknown parameters under the null hypothesis. Together, this leads to the use of particular conditional distributions that is independant of unknown frequencies. It has been shown that the power of exact tests remains high at elevated heterozygosities (>0.70) and that power increases and asymptotic variance around genetic parameters estimates decreases with the number of alleles (Rousset and Raymond 1997, and references therein).

The population genetic structure was quantified using an analysis of variance framework, which involves computing correlation of a pair of alleles drawn from the same subpopulation relative to that randomly drawn from a group of subpopulations (Weir and Cockerham 1984). Fixation indices were also computed in an analysis of molecular variance framework (AMOVA), using information on the mutational differences among alleles, which was entered as a matrix of Euclidian squared distances (Michalakis and Excoffier 1996). Comparing the extent of population structure depicted from allele frequency and mutational information may allow to assess the relative role of long-term separation and contemporary genetic drift in population differentiation (Bernatchez and Martin 1996). By this procedure, genetic structure indices were computed at three hierarchical levels: within individuals, among individuals within samples (F_{IS}), and among samples (F_{ST}) using the program ARLEQUIN (Schneider et al. 1997). The significance of the variance components associated with the different levels of genetic structure was tested using nonparametric permutation procedures (1000 permutations in the present case). Pairwise F_{ST} estimates among all population combinations were also computed in the same manner.

Population relationships

Because of the uncertainty regarding what constitutes the most appropriate method for quantifying population differences based on microsatellite polymorphism, two measures of genetic distance were performed; chord distance (D_{CE}; Cavalli-Sforza and Edwards 1967), assuming pure genetic drift, and the $(\delta\mu)^2$ genetic distance, which takes into account size differences between alleles and theoretically fits linearity with time better than non-SMM based distance measures when microsatellites follow a strict stepwise mutation model (SMM) (Goldstein et al. 1995). Simulation and empirical studies recently demonstrated that the use of chord distance generally leads to a higher probability of obtaining the correct tree topology under either the infinite allele model (IAM) or SMM assumptions, whereas branch lengths may be better approximated from SMM-based methods with microsatellites (Takezaki and Nei 1996; Angers and Bernatchez 1998). Therefore, only the D_{CE} distance matrix was used to obtain the topology of neighbour-joining phenograms. Branch lengths obtained from both D_{CE} and $(\delta\mu)^2$ were then compared by imposing the D_{CE} topology when using the $(\delta\mu)^2$ distances with the user tree option in PHYLIP, version 3.5 (Felsenstein 1993). Comparisons of both phenograms may then provide insight into the relative role of genetic drift and mutations on population divergence. Bootstrap values on branching patterns were obtained by 1000 resamplings of loci and individuals within samples using a program developed by J.M. Cornuet (Institut national de la recherche agronomique, Laboratoire de neurobiologie comparée des invertébrés, Bures-sur-Yvette, France).

Results

Overall and intrapopulation gene diversity

All six microsatellite loci used were moderately (*MST-85**, *Pupupy**, *Cocl-3**) or highly (*Sfo-8**, *Ssa-85**, *Sfo-23**) polymorphic, with the total number of alleles per locus varying between 9 and 48 and overall heterozygosity at each locus ranging between 0.411 and 0.916 (Table 2). The intrapopulation diversity was also generally high for all populations with gene diversity (H_e) ranging between 0.190 and 0.968 depending on locus and population (Table 3). *F* statistics revealed highly significant positive F_{IS} estimates based either on allelic or molecular variance analysis with a higher component observed in the latter case (Table 4), which indicates an overall departure from HW genotypic frequency expectations due to heterozygous deficiency in one or more samples. Indeed, global F_{IS} estimates were positive for each sample except for FR (abbreviations are given in Table 1), although only two of these values (GL and PI) were statistically significant (Table 1). However, when RB was split into Reid Brook and Reid Pond, a highly significant F_{IS} value was observed in Reid Brook ($F_{IS} = 0.108$, $P = 0.005$), whereas char from Reid Pond appeared to be in HW equilibrium ($F_{IS} = -0.014$, $P = 0.9079$). Overall tests revealed that three loci (*MST-85**, *Pupupy**, and *Cocl-3**) were globally responsible for the significant F_{IS} values observed ($0.00001 < P < 0.003$). Significant values were not consistently observed for the same loci in all populations, and a significant value was also observed at *Sfo-8** in one population (Table 3). Significant genotypic phase disequilibrium was also detected for one different locus pair in each sample except for GL and PI: RB (*MST-85*/Cocl-3**, $P < 0.00001$), IB (*Cocl-3*/Sfo-8**, $P = 0.01$), KOB (*MST85*/Pupupy**, $P = 0.035$), SB (*Pupupy*/Ssa-85**, $P < 0.00001$), which suggested the absence of physical linkage. Globally, highly significant F_{IS} and (or) genotypic phase disequilibrium estimates are indicative of either small population sizes, the presence of null alleles, or Wahlund's effect (see Discussion).

Population structure

Population structure analysis led to rejection of the null hypothesis of no differentiation among samples, indicating the existence of two or more genetically distinct populations among the samples analysed. *F* statistics revealed an overall moderate but highly significant interpopulation component based either on allelic or molecular variance analysis, with a higher value obtained in the latter case (Table 4). Pairwise population analysis based on allelic variance revealed significant F_{ST} values in all comparisons, except between FR and PI ($P = 0.120$) (Table 5). A different scenario was observed in the analysis based on molecular variance where only comparisons involving GL and KOB populations remained highly significant. In those cases, F values were largely increased, whereas they were reduced for the others. Both analyses, as expected, were congruent in showing a high differentiation of GL from other populations, and interestingly enough, a higher differentiation between KOB and its

© 1998 NRC Canada

Table 3. Total number of alleles scored for each sample and locus (N), number of different alleles (A), observed heterozygosity (H_o), gene diversity (H_e), and significant ($P < 0.05$) exact probability or unbiased estimate of type-I error for Hardy-Weinberg (HW) departure proportions per locus and population.

	GL	IB	KOB	RB	FR	SB	PI
MST-85							
N	80	60	60	92	60	78	60
A	7	8	7	9	9	6	7
H_o	0.400	0.400	0.733	0.608	0.467	0.436	0.467
H_e	0.696	0.475	0.622	0.706	0.408	0.415	0.508
HW	$<10^{-5}$ns	ns	0.014	ns	ns	0.043	
Pupupy							
N	80	60	60	92	54	82	60
A	4	5	5	7	4	4	3
H_o	0.400	0.200	0.133	0.478	0.519	0.561	0.500
H_e	0.443	0.533	0.190	0.659	0.545	0.646	0.538
HW	ns	0.002	0.042	ns	ns	0.007	ns
Cocl-3							
N	80	60	60	88	48	80	58
A	10	12	16	18	13	15	13
H_o	0.875	0.700	0.833	0.750	0.750	0.725	0.690
H_e	0.873	0.835	0.877	0.884	0.890	0.844	0.835
HW	ns	0.023	ns	ns	ns	ns	ns
Ssa-85							
N	80	60	60	92	74	82	60
A	26	25	18	22	34	25	20
H_o	0.925	1.000	0.900	0.870	1.000	0.854	0.833
H_e	0.950	0.957	0.913	0.929	0.965	0.929	0.893
HW	ns	ns	ns	ns	ns	ns	ns
Sfo-8							
N	78	60	60	90	34	82	68
A	14	15	14	19	15	11	21
H_o	0.821	1.000	0.966	0.956	0.880	0.829	0.862
H_e	0.871	0.898	0.896	0.902	0.919	0.831	0.940
HW	$<10^{-5}$ns	ns	ns	ns	ns	ns	
Sfo-23							
N	72	60	56	90	60	70	60
A	34	20	20	23	23	22	18
H_o	0.833	0.933	0.964	0.978	0.967	0.800	0.867
H_e	0.968	0.930	0.935	0.922	0.902	0.837	0.924
HW	0.043	ns	ns	ns	ns	ns	ns
F_{IS} (overall)	0.118***	0.084	0.078	0.081	–0.084	0.086	0.091***

Note: Abbreviations for populations are given in Table 1. ns, not significant. *** Significant ($P < 0.00001$) overall F_{IS} estimates, using the Fisher's method and following sequential Bonferroni corrections ($k = 7$).

Table 4. Fixation indices based on allelic (F_{ST}) and molecular (Φ) variance analysis.

	F_{ST}	P*	Φ	P*
F_{IS}	0.0574	$<10^{-5}$	0.1412	$<10^{-5}$
F_{ST}	0.0586	$<10^{-5}$	0.1082	$<10^{-5}$
F_{IT}	0.1126	$<10^{-5}$	0.2341	$<10^{-5}$

*P, Probability of difference from zero.

tributary, IB, than between the latter one and the neighbouring RB population.

Concomitant with F-statistic results, the existence of more than one population in the system was also supported by significant differences in allele frequency between all pairwise sample comparisons. The number of significant comparisons (out of 21 per locus) varied between 14 and 20 depending on locus. Most samples were characterized by the presence of specific alleles or striking differences in frequencies. For instance, GL population was characterized by high

© 1998 NRC Canada

Table 5. Pairwise differentiation estimates based on allelic (F_{ST}; below diagonal) and molecular (Φ; above diagonal) variance analysis.

	GL	IB	KOB	RB	FR	SB	PI
GL		0.2525*	0.2609*	0.1640*	0.1417*	0.2324*	0.2758*
IB	0.0927*		0.1409*	0.0020	0.0235	0.0000	0.0000
KOB	0.0845*	0.0329*		0.1300*	0.1500*	0.1280*	0.1002*
RB	0.0765*	0.0161*	0.0471*		0.0000	0.0117	0.0156
FR	0.1155*	0.0225*	0.0725*	0.0255*		0.0258	0.0439
SB	0.1244*	0.0397*	0.0790*	0.0370*	0.0266*		0.0000
PI	0.1111*	0.0339*	0.0711*	0.0359*	0.0091	0.0300*	

Note: Abbreviations refer to populations in Table 1.

*Statistically significant ($\alpha = 0.05$) following adjustment for multiple tests with the sequential Bonferroni method ($k = 21$).

frequencies of alleles *MST-85*196* and *MST-85*204* (relative frequency (RF) > 0.325), which were found at low frequencies elsewhere (RF < 0.083). Within Voisey's Bay, KOB char were characterized by a relatively high frequency of allele *MST-85*208* (RF = 0.217) compared with IB and RB (RF < 0.05). Similarly, allele *Pupupy*459* was frequent in those two populations (RF > 0.239) compared with KOB (RF < 0.033). Allele *Cocl-3*225*, which was relatively abundant elsewhere (RF > 0.136), was not observed in IB population. Northern populations (PI and SB) differed by a relatively high frequency of allele *SSa-85*189*, which was absent or observed at very low frequency among more southern populations. Allele *Sfo-23*183* was abundant in the FR population (RF = 0.283) but relatively rare elsewhere (RF < 0.10). Many additional differences were observed at all loci (data not shown but available upon request).

Such differences in allele frequencies resulted in relatively large genetic distances among samples (Fig. 2). Gander Lake population was the most distant, as expected from its physical isolation. All Voisey's Bay samples clustered together, although supported by a relatively low bootstrap value (either based on locus or individual bootstraping) and FR clustered closer to PI than SB samples, thus not correlating with the geographic distance separating them. The most striking difference observed between the D_{CE} and $(\delta\mu)^2$ phenograms was the much longer branch length differentiating the KOB char from all other anadromous samples in the latter one. The $(\delta\mu)^2$ phenogram also increased the divergence of the GL population relative to anadromous ones.

Discussion

Microsatellite diversity in anadromous arctic char

High level of polymorphism of microsatellite loci used in this study is in sharp contrast with the extremely low levels of variation detected in arctic char with other genetic markers. For instance, average heterozygosity ($H_e = 0.737$) and number of alleles per locus ($A = 30.8$) observed in microsatellites largely exceeds values generally reported in allozyme studies in which average heterozygosity and number of alleles for polymorphic loci do not exceed 0.05 and 2.0 (e.g., Osinov et al. 1996). Levels of mtDNA diversity detected by either RFLP or sequencing in arctic char are also much lower than for microsatellites, with overall haplotypic diversity and the total number of haplotypes reported never exceeding 0.40 and 10, respectively (e.g., Wilson et al. 1996). The extent of microsatellite variation among arctic char from Labrador and Newfoundland is, however, comparable with that recently reported in a study on European arctic char populations from central alpine lakes (Brunner et al. 1998), indicating that microsatellites potentially offer more sensitivity than traditional markers to infer fine-scale population structure in arctic char.

The scale of population structure in anadromous arctic char

All genetic measures employed in this study led to the rejection of the null hypothesis of absence of genetic differentiation among arctic char samples, implying the existence of genetically differentiated populations among which gene flow has been restricted and on which mutation and drift may independently act to enhance genetic divergence. The overall F_{ST} (0.059) and F (0.108) values observed were, however, relatively low, suggesting only mild genetic differentiation among char from different locations, as generally reported in anadromous fishes (Ward et al. 1994). Such levels of interpopulation genetic divergence in anadromous species most likely reflect the long-term combined effect of their general propensity for homing to natal sites and the potential of straying in absence of firm physical barriers to gene flow.

Results of this study indicated various levels of genetic divergence among samples. As expected, landlocked arctic char from Gander Lake, represented the most distinct population. While this can certainly be attributed to its physical isolation from anadromous populations, the magnitude of its genetic differentiation could also be potentially due to historical factors, namely to a distinct postglacial origin (e.g., Wilson et al. 1996). The significant genetic differentiation observed among anadromous char from the four different geographic areas surveyed in is congruent with limited movements observed in tagging studies (Dempson and Kristofferson 1987). These involved the tagging of more than 7500 char, of which 1886 (nearly 25%) were subsequently recaptured. Results indicated that dispersal at sea was very limited by comparison with either Atlantic (*Salmo salar*) or various Pacific salmon (*Oncorhynchus* sp.) species. Thus, 95% of all recaptures of fish tagged in Nain Bay were within 70 km from tagging sites and only 2.3% were recaptured 100 km away or more. Consequently, results of these tagging experiments also

© 1998 NRC Canada

Fig. 2. Neighbour-joining phenogram showing relationships among char populations from Labrador and Newfoundland. Values along branches indicate bootstrap values in percent either based on locus (above) or individual. (A) Phenogram based on chord distance; (B) $(\delta\mu)^2$ phenogram built by imposing tree topology obtained from chord distance.

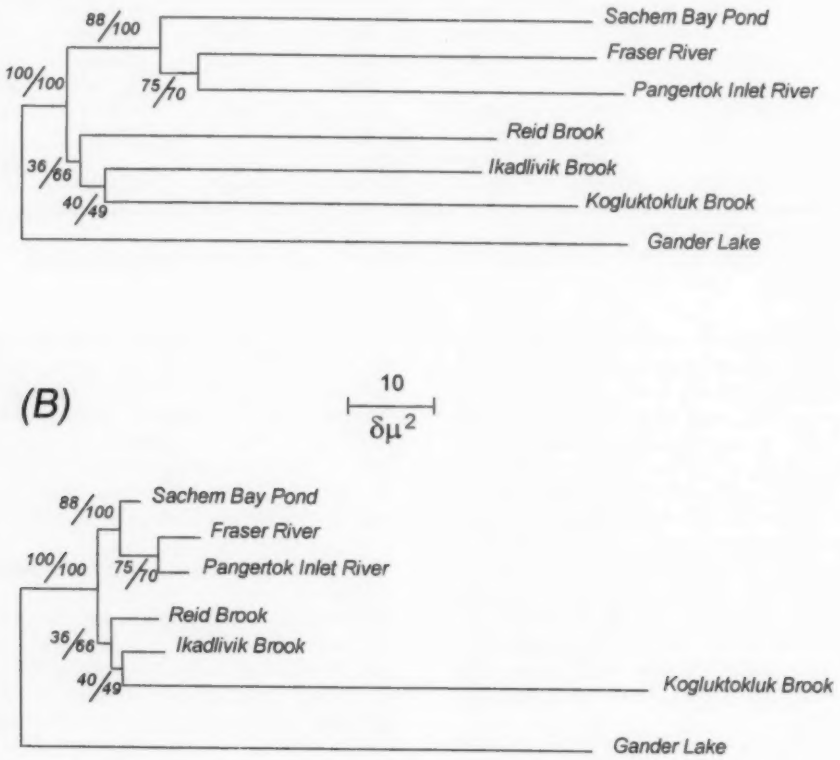

revealed little straying over a time frame of 7 years among widely distributed areas along 300 km of the northern Labrador coast. For instance, only 1.3% (including juvenile, sexually immature, and mature fish) of char tagged in Nain Bay and Voisey's Bay were subsequently recaptured in more northern sites such as Saglek Fjord. In the present study, gene flow estimates based on the theoretical relationships between fixation index and gene flow ($Nm = [(1/F_{ST}) - 1]/4$) varied between 4.6 and 27.5 effective number of migrants per generation among the four major regions surveyed. Although the veracity of these absolute values may be biased by not satisfying theoretical assumptions, namely that populations are in equilibrium with respect to genetic drift and migration, and that their population structure fit an island model, they nevertheless corroborate tagging results by indicating limited intermixing among char populations from different areas at each generation.

The exact definition of population genetic composition and their association to specific tributaries was partly hampered in this study by the fact that fish could not be sampled on spawning grounds and evidence that our samples represented a mixture of nonrandomly mating fish (see below). Nevertheless, the results obtained were sufficient to refute the hypothesis of a single panmictic population within a same area, such as Voisey's Bay. The magnitude of genetic divergence (F_{ST} and genetic distance) among the three char samples from Voisey's Bay, captured less than 10 km apart, was within the range of that observed among wide geographic areas. This, and the observation of tributary specific alleles, is not compatible with the hypothesis of a single panmictic population, therefore being indicative of the existence of more than one reproductive unit among tributaries draining in proximity one of each other. These results, therefore, reinforce the view that anadromous Arctic char may possess strong homing capability (Johnson 1980), perhaps comparable with that of Atlantic salmon as suggested by F_{ST} values similar to those quantified in that species using similar markers (e.g., Fontaine et al. 1997).

The salient feature of this study, however, was the demonstration of a more pronounced genetic differentiation between char from Kogluktokluk Brook and those from its tributary, Ikadlivik Brook, than that observed between Ikadlivik Brook and the neighbouring Reid Brook. In fact, the magnitude of differentiation of Kogluktokluk Brook char exceeded that observed among other char from wide geographic areas. At present, the possible causes of such differentiation are only hypothetical. If the potential for straying was the primary cause of the extent of their genetic differentiation, one would intuitively conclude that gene flow should be more important among tributaries draining into the same river, which was

© 1998 NRC Canada

clearly not the case for Kogluktokluk and Ikadlivik brooks. Instead, the observed population structure could be the result of differential ecological selection acting to maintain local adaptation (discussed in Tessier et al. 1997). Alternatively, the higher differentiation of the Kogluktokluk Brook compared with other anadromous populations could partly be explained by historical rather than ecological factors. For instance, the development of reproductive isolation between populations that evolved in separate glacial refugia and subsequently came into secondary contact have been documented in other fishes (e.g., Bernatchez 1997). At present, the hypothesis that a similar scenario could be involved in Voisey's Bay arctic char is indirectly supported by the striking frequency differences of several alleles between Kogluktokluk Brook and all other anadromous populations, and by the fact that, as for Gander Lake, the extent of differentiation of the Kogluktokluk Brook population increased substantially when molecular rather than allelic variance was considered. This suggests an important mutational component, likely implying long-term separation, whereas pure genetic drift may mainly be responsible for differentiation among other populations.

Evidence for straying among rivers

Heterozygous deficiency in all but one sample was indicative of a Wahlund's effect, implying that our samples were often composed of a mixture of char from different populations. Alternative explanations could conceivably result in the same pattern, but those appear less parsimonious in the present context. Stochastic departures from HW equilibrium are expected to occur in small populations. Such processes, however, are considered negligible when effective population size (N_e) is greater than 500 (Hartl and Clark 1989). Although we cannot estimate effective sizes for char populations, it is obvious from commercial landings data that their current census (N) must be relatively large. For instance, more than 10 000 char per year have been harvested from the Voisey stock complex over the period 1977–1994 (Dempson and Shears 1995). Although there may be important discrepancies between a population census and its effective population size, anadromous char populations appear sufficient to consider stochastic processes negligible among cohorts of a same generation, given the fact the ratio of N:N_e reported in other salmonids are usually smaller than 20:1 (e.g., Hedrick et al. 1995). In addition, stochastic departures from HW equilibrium would be expected to equally imply both excess and deficiency of heterozygotes, which was not the case here.

The occurrence of null alleles has also been regularly reported as a major explanation for observed heterozygous deficiency (discussed in Brookfield 1996). Several lines of evidence suggest that the occurrence of null alleles would not affect HW equilibrium importantly in this study. Heterozygous deficiency was due to different loci in different populations, which would imply both the occurrence of null alleles at many loci and the differential absence of those alleles depending on populations. In addition, heterozygous deficiency has not been observed in other studies where the same loci were used, including arctic char (e.g., Angers and Bernatchez 1998; Tessier et al. 1997; Brunner et al. 1998), suggesting that the occurrence of null alleles would be confined to char populations from Labrador and Newfoundland. While those factors could still partly explain the observed heterozygous deficiencies, it appears more plausible that these mainly reflect the effect of population admixture. Further evidence of population admixture was also provided by significant genotypic phase disequilibrium, which cannot easily be explained by the effects of null alleles unless those were linked with alleles at other loci. Since char captured at most sites comprised both spawning and nonspawning fish, it is likely that our samples represented a mixture of both local spawners returning to their natal site and fish reentering rivers at the end of the summer for overwintering. The hypothesis of genetically mixed samples is also compatible with knowledge on movements obtained from tagging studies. For instance, multiple recaptures within the same river revealed that some char did not reenter the river for 2 years before the second recovery, and char tagged in a given river were also subsequently recaptured in a different tributary (Dempson and Kristofferson 1987). Gyselman (1994) has also reported that some char returning to Nauyuk Lake, Northwest Territories, do so following an absence of 1 or 2 years, and that part of the Nauyuk Lake population is likely composed of immigrants from other river systems. Altogether, the observed pattern of gene diversity partitioning in anadromous populations from Labrador lends support to the hypothesis that arctic char have the capacity to home to their natal rivers but that the behavioural pattern does not appear to be rigid (e.g., Johnson 1980). Straying has been proposed as an evolutionary alternative strategy to homing (Quinn 1984). Arctic char may utilize this tactic in seeking alternative overwintering and perhaps spawning localities. There may be several advantages to this strategy for a species living in areas where environmental conditions can be unpredictable and extreme. For instance, homing may ensure distribution of reproductive effort in "successful areas," whereas straying and overwintering in alternate systems may allow for the colonization of new systems (Johnson 1980).

Implications for conservation and management

These results has several implications for conservation and management. They first indicate that more than one management units may occur in anadromous char on a very fine geographic scale. Proposed development following the discovery of rich mineral deposits in the watershed of Reid Brook within Voisey's Bay raised concerns about the potential for detrimental impacts due to habitat disturbance on char populations. In this context, our results imply that severe habitat perturbation, such as destruction of spawning grounds, a toxic contaminant spill, etc., could lead to a net loss of genetic diversity within the species. The fact that Reid Brook may also be used as an overwintering site by char from other Voisey's Bay rivers implies that any habitat disturbance that would lead to loss of overwintering grounds could also have effects on the demography of other populations within Voisey's Bay.

Acknowledgments

This study was supported by the Department of Fisheries and Oceans Voisey's Bay Ecological Characterization Program, and an Natural Sciences and Engineering Research Council operating grant to L.B. M. Shears, G. Furey, and C. Pennell assisted with the collection of Arctic char specimens. We also

© 1998 NRC Canada

thank D. Scruton, J. Brattey, and two anonymous referees for reviewing the manuscript critically and providing editorial advice.

References

Angers, B., and Bernatchez, L. 1998. Combined use of SMM and non-SMM methods to infer fine structure and evolutionary history of brook charr (*Salvelinus fontinalis*, Salmonidae) populations from microsatellites. Mol. Biol. Evol. **15**: 143–159.

Angers, B., Bernatchez, L., Angers, A., and Desgroseillers, L. 1995. Specific microsatellite loci of brook charr (*Salvelinus fontinalis* Mitchill) reveals strong population subdivision on microgeographic scale. J. Fish Biol. **47**(Suppl. A): 177–185.

Bernatchez, L. 1996. Réseau de suivi environnemental du complexe La Grande. Caractérisation génétique des formes naines et normales de grand corégone du réservoir Caniapiscau et du lac Sérigny à l'aide de marqueurs microsatellites. Rapport présenté par l'université Laval à la Vice-présidence Environnement et Collectivités d'Hydro-Québec.

Bernatchez, L. 1997. Mitochondrial DNA analysis confirms the existence of two glacial races of rainbow smelt *Osmerus mordax* and their reproductive isolation in the St. Lawrence River estuary (Québec, Canada). Mol. Ecol. **6**: 73–83.

Bernatchez, L., and Martin, S. 1996. Mitochondrial DNA diversity in anadromous rainbow smelt, *Osmerus mordax* Mitchill: a genetic assessment of the member–vagrant hypothesis. Can. J. Fish. Aquat. Sci. **53**: 424–433

Brookfield, J.F.Y. 1996. A simple new method for estimating null allele frequency from heterozygote deficiency. Mol. Ecol. **5**: 453–455.

Brunner, P., Douglas, M., and Bernatchez, L. 1998. Microsatellite and mitochondrial DNA assessment of population structure and stocking effects in arctic charr *Salvelinus alpinus* (Teleostei: Salmonidae) from central alpine lakes. Mol. Ecol. **7**: 209–223.

Cavalli-Sforza, L.L., and Edwards, A.W.F. 1967. Phylogenetic analysis: models and estimation procedures. Am. J. Hum. Gen. **19**: 233–257.

Davidson, W.S., Birt, T.P. , and Green, J.M. 1989. A review of genetic variation in Atlantic salmon, *Salmo salar* L., and its importance for stock identification, enhancement programmes and aquaculture. J. Fish Biol. **34**: 547–560.

Dempson, J.B. 1995. Trends in population characteristics of an exploited anadromous arctic charr, *Salvelinus alpinus*, stock in northern Labrador. Nord. J. Freshwater Res. **71**: 197–216.

Dempson, J.B., and Kristofferson, A.H. 1987. Spatial and temporal aspects of the ocean migration of anadromous Arctic charr. Am. Fish. Soc. Symp. **1**: 340–357.

Dempson, J.B., and Shears, M. 1994. Status report for northern Labrador arctic charr stocks in 1994. Dep. Fish. Oceans Atl. Fish. Res. Doc. No. 95/76.

Felsenstein, J. 1993. PHYLIP (Phylogeny inference package), version 3.5c edition. Department of Genetics, SK-50, University of Washington, Seattle.

Fontaine, P.-M., Dodson, J.J., Bernatchez, L., and Slettan, A. 1997. A genetic test of metapopulation structure in Atlantic salmon (*Salmo salar*) using microsatellites. Can. J. Fish. Aquat. Sci. **54**: 2434–2442.

Goldstein, D.B., Linares, A.R., Cavalli-Sforza, L.L., and Feldman, M.W. 1995. An evaluation of genetic distances for use with microsatellite loci. Genetics, **139**: 463–471.

Gyselman, E.C. 1994. Fidelity of anadromous Arctic charr (*Salvelinus alpinus*) to Nauyuk Lake, N.W.T., Canada. Can. J. Fish. Aquat. Sci. **51**: 1927–1934.

Hartl, D.L., and Clark, A.G. 1989. Principles of population genetics. Sinauer Associates Inc, Sunderland, Mass.

Hedrick, P.W., Hedgecock, D., and Hamelberg, S. 1995. Effective population size in winter-run chinook salmon. Conserv. Biol. **9**: 615–624.

Jarne, P.J., and Lagoda, J.L. 1996. Microsatellites, from molecules to populations and back. TREE, **11**: 424–429.

Johnson, L. 1980. The arctic charr, *Salvelinus alpinus*. *In* Charrs: salmonid fishes of the genus *Salvelinus*. *Edited by* E.K. Balon. Dr. W. Junk, The Hague, Netherlands. pp. 15–98.

Michalakis, Y., and Excoffier, L. 1996. A generic estimation of population subdivision using distances between alleles with special reference for microsatellite loci. Genetics, **142**: 1061–1064.

Morris, D.B., Richard, K.R, and Wright, J.M. 1996. Microsatellites from rainbow trout (*Oncorhynchus mykiss*) and their use for genetic study of salmonids. Can. J. Fish. Aquat. Sci. **53**: 120–126.

Nei, M. 1987. Molecular evolutionary genetics. Columbia University Press, New York.

O'Reilly, P.T., Hamilton, L.C., McConnell, S.K., and Wright, J.M. 1996. Rapid analysis of genetic variation in Atlantic salmon (*Salmo salar*) by PCR multiplexing of dinucleotide and tetranucleotide microsatellites. Can. J. Fish. Aquat. Sci. **53**: 2292–2298.

Osinov, A.G., Pavlov, S.D., and Maksimov, V.A. 1996. Allozyme variation and genetic differentiation in populations of Arctic charr *Salvelinus alpinus* from the Baltic Sea – Taimyr part of the range. Russ. J. Gen. **32**: 474–485.

Presa, P., and Guyomard, R. 1996. Conservation of microsatellites in three species of salmonids. J. Fish Biol. **49**: 1326–1329.

Quinn, T.P. 1984. Homing and straying in Pacific salmon. *In* Mechanisms of migration in fishes. *Edited by* J.D. McCleave, G.P. Arnold, J.J. Dodson, and W.H. Neill. Plenum, New York. pp. 357–362.

Raymond, M., and Rousset, F. 1995. GENEPOP (version 1.2): population genetics software for exact test and ecumenism. J. Hered. **86**: 248–249.

Rousset, F., and Raymond, M. 1997. Statistical analyses of population genetic data: new tools, old concepts. TREE, **8**: 313–317.

Sinclair, M., and Iles, T.D. 1988. Population richness of marine fish species. Aquat. Living Resour. **1**: 71–83.

Schneider, S., Kueffer, J.-M., Roessli, D., and Excoffier, L. 1997. ARLEQUIN version 1: an exploratory population genetics software environment. Genetics and Biometry Laboratory, University of Geneva, Geneva, Switzerland.

Takezaki, N., and Nei, M. 1996. Genetic distances and reconstruction of phylogenetic trees from microsatellite DNA. Genetics, **144**: 389–399.

Tessier, N., Bernatchez, L., and Wright, J.M. 1997. Population structure and impact of supportive breeding inferred from mitochondrial and microsatellite DNA analyses in landlocked Atlantic salmon (*Salmo salar* L.). Mol. Ecol. **7**: 735–750.

Verspoor, E., and Jordan, W.C. 1989. Genetic variation at the *Me*-2 locus in the Atlantic salmon within and between rivers: evidence for its selective maintenance. J. Fish Biol. **35**: 205–213.

Ward, R.D., Woodwark, M., and Skibinski, O.F. 1994. A comparison of genetic diversity levels in marine, freshwater, and anadromous fishes. J. Fish Biol. **44**: 213–232.

Weir, B.S., and Cockerham, C.C. 1984. Estimating *F*-statistics for the analysis of population structure. Evolution, **38**: 1358–1370.

Wilson, C.C., Hebert, P.D.N., Reist, J.D., and Dempson, J.B. 1996. Phylogeography and postglacial dispersal of arctic charr *Salvelinus alpinus* in North America. Mol. Ecol. **5**: 187–197.

© 1998 NRC Canada

Consequences of prey fish community dynamics on lake trout (*Salvelinus namaycush*) foraging efficiency in Lake Superior

Doran M. Mason, Timothy B. Johnson, and James F. Kitchell

Abstract: We used a size-structured model, indexed by age, that combines bioenergetics and foraging theory to evaluate the effects of prey fish community structure (species dominance, size structure, and density) on the diet and net foraging efficiency of lake trout (*Salvelinus namaycush*) in Lake Superior. Prey size structure was important for young lake trout but decreased in importance for older lake trout, especially with increasing prey density. The model predicted that rainbow smelt (*Osmerus mordax*) should dominate the diet of young lake trout due to the size-dependent capture limitations of larger prey. In contrast, lake herring (*Coregonus artedi*) should dominate the diet of oldest lake trout owing to a higher net energy return than rainbow smelt. Model results are consistent with age-specific diet and size-at-age of lake trout during the last 40 years. Diets of intermediate-sized lake trout do not reflect the recent resurgence of lake herring populations. Absence of a dietary switch is probably due to higher capture probability for rainbow smelt. Lake trout growth and production will likely be highest with a mixed prey species assemblage of young rainbow smelt and older lake herring.

Résumé : Un modèle structuré selon la taille, indexé sur l'âge, qui combine la bioénergétique avec la théorie de la recherche de nourriture, a servi à évaluer les effets de la structure des communautés de poissons proies (dominance des espèces, structure des tailles et densité) sur l'alimentation du touladi (*Salvelinus namaycush*) et son efficacité nette de recherche de nourriture dans le lac Supérieur. La structure des tailles des proies était importante pour le jeune touladi, mais elle diminuait en importance chez le touladi plus âgé, en particulier lorsque la densité des proies augmentait. Selon le modèle, l'éperlan de lac (*Osmerus mordax*) devait être l'espèce dominante dans l'alimentation du jeune touladi à cause des limites à la capture imposées par la taille des grosses proies. Par contre, le cisco de lac (*Coregonus artedi*) devait dominer dans l'alimentation du touladi plus âgé en raison du rendement énergétique net plus élevé du cisco de lac par rapport à l'éperlan. Les résultats du modèle concordent avec les données sur l'alimentation selon l'âge et la longueur selon l'âge du touladi recueillies au cours des 40 dernières années. L'alimentation du touladi de taille intermédiaire ne reflète pas la remontée récente des populations de cisco de lac. Le fait que le touladi n'ait pas modifié son alimentation pour se prévaloir de cette nouvelle abondance du cisco de lac peut être imputé à la probabilité plus élevée de capturer de l'éperlan de lac. La croissance et la reproduction du touladi atteindront probablement leur maximum en présence d'un assemblage mixte d'espèces proies composé de jeunes éperlans de lac et de ciscos de lac âgés. [Traduit par la Rédaction]

Introduction

The primary goal of fish community restoration in Lake Superior is to build the population of native fishes to levels similar to those prior to sea lamprey (*Petromyzon marinus*) invasion (Busiahn 1990). However, the fish community now includes a number of exotics that have established self-sustaining populations such as chinook salmon (*Oncorhynchus tshawytscha*), coho salmon (*Oncorhynchus kisutch*), steelhead (*Oncorhynchus mykiss*), and pink salmon (*Oncorhynchus gorbuscha*), which also prey heavily on the exotic rainbow smelt (*Osmerus mordax*) (Negus 1995). Lake trout (*Salvelinus namaycush*) and lake herring (*Coregonus artedi*) previously dominated the native fish assemblage. Thus, fish community restoration must account for the role of exotics and their interactions with native species.

Lake trout, a target species for restoration, have established self-sustaining populations and appear to be recovering in Lake Superior following several decades of sea lamprey control, lake trout stocking, and commercial fishery regulation (Hansen et al. 1995). As a result, resource managers have made a recommendation to cease stocking lake trout in nine of the 13 U.S. management zones of Lake Superior (M. Hansen, University of Wisconsin-Stevens Point, personal communication). However, analysis of predatory demand by Negus (1995) and Ebener (1995) indicated that current

Received April 23, 1997. Accepted October 28, 1997.
J13984

D.M. Mason,[1] T.B. Johnson, and J.F. Kitchell. Center for Limnology, University of Wisconsin, 680 North Park Street, Madison, WI 53706-1492, U.S.A.

[1] Author to whom all correspondence should be addressed. Present address: Department of Forestry and Natural Resources, Purdue University, 1159 Forestry Building, West Lafayette, IN 47907-1159, U.S.A.
e-mail: doran@fnr.purdue.edu

© 1998 NRC Canada

populations of lake trout and other stocked salmonines may exceed the carrying capacity of forage fish stocks in Lake Superior and thereby impair lake trout restoration.

The principal prey of adult lake trout are lake herring and rainbow smelt (Dryer et al. 1965; Negus 1995). Lake herring and rainbow smelt also support an important commercial fishery (MacCallum and Selgeby 1987) and dominate the pelagic planktivorous fish community, despite undergoing large fluctuations in abundance (Lawrie 1978; MacCallum and Selgeby 1987). Prior to the 1950s, lake herring dominated the pelagic forage base of Lake Superior, but declined sharply in the 1950s due to overfishing (Selgeby 1982). Coincident with the lake herring decline was an exponential increase in the abundance of the rainbow smelt which dominated the system by the early 1960s (Lawrie 1978; Selgeby et al. 1978). Rainbow smelt peaked in abundance in the late 1960s and early 1970s and represented 90–99% of the pelagic fish community in the late 1970s (Heist and Swenson 1983). Aggressive stocking programs for lake trout and Pacific salmon (chinook, coho, and steelhead) rebuilt the piscivore populations in the 1970s and 1980s (Hansen et al. 1995; Negus 1995). In the early 1980s, rainbow smelt abundance decreased about 10-fold, while the lake herring population increased to their former dominance (MacCallum and Selgeby 1987). Lake herring continue to dominate the pelagic prey fish community. These historical fluctuations in prey fish abundance and dominance were also accompanied by changes in the age and size structure of the pelagic planktivore community (Anderson and Smith 1971; Lawrie 1978).

The diet of lake trout generally mirrored the changes in the prey fish community. Prior to the 1950s, lake herring were the primary prey of lake trout in Lake Superior. As lake herring populations declined and rainbow smelt numbers increased in the 1950s, rainbow smelt became more important and dominated the lake trout diet by the early 1960s (Dryer et al. 1965). However, in the 1980s, rainbow smelt remained the primary prey of lake trout despite the shift in dominance from rainbow smelt back to lake herring (Negus 1995). In light of the progress in lake trout restoration, fluctuations and limitations in the prey base, and shifts in lake trout diets, improved understanding of the foraging ecology of lake trout is needed. Moreover, knowledge of the relative importance of lake herring and rainbow smelt as food for lake trout is required for sustained long-term management of this multispecies predator–prey system (Busiahn 1985).

Relative importance of a given prey in a fish's diet determined through gut analysis, when combined with bioenergetics models, provides a mechanism to quantify the importance of various prey types through effects on predator growth rate (Hewett and Johnson 1992 and references within). Predator–prey relationships can also be evaluated using foraging theory, where intrinsic and extrinsic constraints on a predator are used to rank the importance of various prey types (Stephens and Krebs 1986). Each approach emphasizes a different mechanism to evaluate predator choice: predator physiology and energetics (bioenergetics) and predator behavior and physical constraints (foraging theory). We combined bioenergetics with foraging theory to evaluate the predator–prey interactions occurring in Lake Superior. Our objectives were to (*i*) evaluate age-specific net foraging efficiency of lake trout on lake herring and rainbow smelt, (*ii*) determine the optimal size structure of each prey species for lake trout, and (*iii*) provide an estimate of the forage fish assemblage that might maximize lake trout growth and production.

Methods

We developed a size-structured model, indexed by age, to evaluate the net foraging efficiency of lake trout preying on a two-species, size-structured prey assemblage for a fixed foraging duration (Table 1). The model was based on fish bioenergetics and foraging theory, independent of field observations of lake trout in Lake Superior. We defined net foraging efficiency F_e as the ratio of energy ingested to energetic costs for a single day during the growing season:

$$(1) \quad F_e = \frac{e_I}{M + P}$$

where e_I is total energy ingested (joules), M is metabolic costs for routine maintenance (joules), and P is energy expended while foraging (joules). Because we combined bioenergetics with F_e, F_e can be interpreted in terms of growth. When $F_e < 1.0$, fish operate in an energetic deficit and lose mass whereas when $F_e > 1.0$, fish have a net energetic gain and positive growth.

Model simulations were run on a population of 9000 lake trout uniformly distributed among nine age-classes (2, 4, 6, 8, 10, 12, 14, 16, and 18 years). Individual foraging was simulated for three fixed durations (0.5, 1.0, and 2.0 h) on three prey population densities (0.1, 0.01, and 0.001·m^{-3}) and four prey mean ages (0.25, 1.0, 2.0, and 4.0 years; 4.0 years for the lake herring population only).

Mean prey densities of about 0.01 individual·m^{-3} have been observed in western Lake Superior (Heist and Swenson 1983), so we bounded this estimate plus and minus one order of magnitude. Mean prey ages were used to construct the size distribution of the prey fishes (see below). Mixed prey species assemblages were modeled based on equal numerical densities and scaled to total densities of 0.1, 0.01, and 0.001 individuals·m^{-3}. Age-specific F_e of lake trout feeding on lake herring and rainbow smelt was then determined for all combinations of total densities and prey age structures.

Lake trout randomly encountered prey in a single-species and mixed-species assemblage of varying ages and sizes. Encountered prey were ranked according to total energy content (as per foraging theory, Stephens and Krebs 1986). Vulnerability of prey to capture was determined for each encountered prey based on prey to predator size ratio. Most profitable vulnerable prey were sequentially ingested until the predator was satiated (see below). Energy expended by each lake trout was determined for the duration of the foraging bout and for daily routine maintenance. While we do not know the actual foraging patterns of lake trout, we assumed that one foraging bout occurs per day and that rates of prey capture are bounded by satiation or starvation over a 100-fold range of prey densities.

Energy ingested

We modeled energy ingested as the combined processes of search, encounter, and capture:

$$(2) \quad I_{ij} = \frac{E_{ij} N_{ij} t}{1 + h_t (E_i N_i + E_j N_j)}$$

where I is number of prey encountered, E is volume searched (cubic metres per second), N is prey density (number per cubic metre), h_t is mean time (seconds) discounted from prey inspection, unsuccessful attack, or handling of prey, and t is length of the foraging bout (seconds). The subscripts "i" and "j" represent two different prey species. Volume searched by the predator was modeled as

$$(3) \quad E = \left(\frac{\pi R^2}{3}\right)\left(\frac{3v^2 + u^2}{v}\right) \text{ for } v > u$$

where R is reaction distance (metres), v is swimming velocity of

© 1998 NRC Canada

Table 1. Symbol definitions and values used in the foraging efficiency model.

Symbol	Definition	Value	Units	Reference(s)[a]
e_I	Total energy ingested		J	
I	Number of prey encountered			
E	Search volume		$m^3 \cdot s^{-1}$	
N	Prey density	0.1, 0.01, 0.001	No.$\cdot m^{-3}$	
h_t	Time depreciation during prey encounter	1	s	
C	Size-dependent capture probability			
C_{opt}	Capture probability on optimal size prey	0.4,0.8		1, 2
e_i	Energy density, lake herring	6900	$J \cdot g^{-1}$	3
e_j	Energy density, rainbow smelt	5320	$J \cdot g^{-1}$	3
t	Length of foraging bout	1800, 3600, 7200	s	
M	Routine metabolism		J	
P	Foraging costs		J	
R	Reaction distance	0.4	m	
u	Swimming velocity, prey		$m \cdot s^{-1}$	
v	Swimming velocity, predator		$m \cdot s^{-1}$	
w	Mass		g	
S_{max}	Maximum prey to predator length ratio	0.5		4, 5, 6, 7
S_{min}	Ambient prey to predator length ratio			
S_{opt}	Optimum prey to predator length ratio	0.25		2, 7
η	Constant	1.42		8
β	Constant	2.42		8
L	Length		cm	
ρ_w	Density of water	1.0	$g \cdot cm^{-3}$	
μ	Viscosity of water	0.01	$g \cdot cm^{-1} s^{-1}$	

[a] 1, Savitz and Bardygula (1989); 2, Jones et al. (1993); 3, Vondracek et al. (1996); 4, Hyatt (1979); 5, Folkvard and Hunter (1986); 6, Hargreaves and LeBrasseur (1986); 7, Power (1987); 8, Ware (1978).

predator (metres per second), and u is swimming velocity of prey (metres per second) (Gerritsen and Strickler 1977). Assuming that reaction distance is similar and constant for all prey (Breck 1993), eq. 3 reduces to

$$E = bv\left(3 + \frac{u^2}{v^2}\right) \quad (4)$$

where $b = \pi R^2/3$. Thus, comparison of predator encounter rates between prey species requires estimates of relative swimming velocities of predator and prey.

Mean swimming velocity of lake trout was taken as $0.183w^{0.05}$ at 11°C (Stewart et al. 1983) and for lake herring as $0.072w^{0.25}$ (Rudstam et al. 1994) where w is mass (grams). Rainbow smelt, by contrast, swim very slowly and spend much of their time motionless (Savitz and Bardygula 1989; Lantry and Stewart 1993). We assumed that mean swimming velocity of rainbow smelt was negligible relative to lake trout and was set to zero. Swimming velocity for each species was varied by selecting from a Gaussian distribution of mean swimming velocity with an arbitrary standard deviation of 0.05. Standard deviation was set to create an overlap in the swimming velocities of rainbow smelt and lake herring. The Gaussian distribution was truncated at zero to prevent negative swimming velocity.

Size structure of encountered prey was reconstructed from a Poisson distribution given mean age of the corresponding prey population. Populations with older mean ages had an age/size structure skewed to larger individuals and vise versa for young mean ages. Age was converted to length using the von Bertalanffy growth equation and then converted to mass (Table 2). Age-specific lake trout mass was also determined using a von Bertalanffy growth equation and length–mass relationship (Table 2). Probability of capture was then calculated for each prey encountered based on prey and predator lengths.

We assumed that probability of capture is highest for prey of optimal size, 25% of predator length (Power 1987), and decreases to zero for prey ≥50% of predator length (Hyatt 1979; Hargreaves and LeBrasseur 1986; Power 1987). This assumption creates a dome-shaped relationship for capture probability such as that estimated by Folkvord and Hunter (1986) and used by Jones et al. (1993). We used the size-dependent capture probability function with capture success decreasing to zero for prey at the gape limit threshold and zero at minimum size:

$$C = C_{opt} k^2 e^{2(1-k)}$$
$$k = \frac{(S_{max} - S_{ratio})}{(S_{max} - S_{opt})} \quad (5)$$

where C_{opt} is capture probability of optimal-size prey, S_{max} is maximum prey to predator length ratio, S_{ratio} is ratio of prey length encountered to predator length, and S_{opt} is the optimum prey to predator length ratio. Vulnerability to capture was determined using a Bernoulli distribution. A Bernoulli trial is a probabilistic experiment that can only have two outcomes, success (1) or failure (0); the probability of success is defined by eq. 5.

We ran two different capture probability scenarios. For the first, the greatest capture probability of lake herring and rainbow smelt was assumed to be 40% (Folkvord and Hunter 1986; Savitz and Bardygula 1989). In the second scenario, we accounted for the lower activity of rainbow smelt by increasing the capture probability of rainbow smelt to 80% while keeping lake herring at 40%. In experimental studies, capture probabilities of salmonines foraging on rainbow smelt may be as high as 100% (Savitz and Bardygula 1989).

© 1998 NRC Canada

Table 2. Age (years), length (TL, cm), and mass (w, g) relationships for lake herring, rainbow smelt, and lake trout.

Species	Reference
Lake herring	
$TL = 39.37\ (1 - e^{-0.195(age+0.484)})$	Johnson et al. 1998
$\log_{10} w = 3.056 \log_{10}(10 \cdot TL) - 5.279$	Johnson et al. 1998
Rainbow smelt	
$TL = 25.63\ (1 - e^{-0.282(age+1.401)})$	Johnson et al. 1998
$\log_{10} w = 3.119 \log_{10}(10 \cdot TL) - 5.453$	Johnson et al. 1998
Lake trout	
$TL = 105.41\ (1 - e^{-0.095(age+0.206)})$	Ebener 1995
$\log_{10} w = 3.266 \log_{10}(10 \cdot TL) - 5.792$	Eby et al. 1995

While we do not know the actual probabilities in the lake, our estimates are consistent with available evidence and provide a basis for comparisons. Moreover, although prey may behaviorally reduce encounter rates by schooling or diel migration, our modeling approach provides an estimate of relative vulnerability only during the period of active foraging by the predator.

Energy ingested e_I was determined by ranking vulnerable prey by total energy content ($w \times e_i$, where e_i is energy density (joules per gram)) and ingesting the most profitable prey first until satiated. Gut capacity was defined as the 1.5 × maximum daily consumption (C_{max}) for lake trout where $C_{max} = 0.079368w^{-0.307}$ (Stewart et al. 1983).

Energetic costs

Energetic costs were calculated for energy expended during active foraging and for the nonforaging part of the day. Swimming costs while foraging at a constant velocity are given by

$$(6) \qquad P = \alpha L^{\eta}(0.01v)^{\beta}t$$

where P is the power (joules) required to overcome the drag on a fish of length L (centimetres) swimming at a velocity $0.01v$ (centimetres per second) for a specific foraging duration t, v is swimming velocity (metres per second), η and β are constants, and $\alpha = 1.06 \times 10^{-6}\ (\rho_w/(\rho_w/\mu)^{0.58})$ where ρ_w is the density of water (1.0 g·cm^{-3}) and μ is the viscosity of water (0.01 g·cm^{-1}·s^{-1}) (Ware 1978). The costs associated with nonforaging activity (resting metabolism, excretion, egestion, and specific dynamic action) were determined using the bioenergetics equations and parameters established for lake trout by Stewart et al. (1983). Total energy cost was the sum of foraging and nonforaging costs.

Results

Single prey species

F_e of lake trout increased with increased foraging duration for both lake herring and rainbow smelt prey but varied according to lake trout age, prey age structure, and prey type (Fig. 1). The youngest lake trout (2 years) maximize F_e by feeding on the youngest rainbow smelt, while older lake trout maximize F_e by feeding on lake herring. In addition, simulations for all prey age structures, from younger to older, produced a complete reversal in importance of prey size structure at about 6 years of age for lake trout feeding on rainbow smelt. A similar reversal occurred at ages 8–18 years when lake trout fed exclusively on lake herring. F_e decreased with lake trout age when lake trout fed on both rainbow smelt and the youngest lake herring (Fig. 1). Age 2 lake trout had higher growth efficiency when preying on younger rainbow smelt than on younger lake herring.

F_e generally increased with increasing prey density for all ages of lake trout (Fig. 2). However, F_e remained inversely related to prey age structure for younger lake trout (2–4 years) and directly related to prey age structure for older lake trout (18 years). High prey density weakened the effect of age structure on older lake trout (Fig. 2*c*), but prey size structure remained important for the youngest lake trout (Fig. 2*a*). At the highest prey densities, F_e was always <1.0 for the youngest lake trout foraging on lake herring. For lake trout >4 years, high density satiated the F_e response.

Mixed prey species assemblage

For mixed prey species assemblages, various prey densities and capture probabilities produced similar patterns in F_e, but the overall effect of increasing prey density was to decrease variability in F_e (Fig. 3). Age 2 lake trout showed similar variability in F_e at both prey densities (Fig. 3*a*). At the higher density, F_e was most variable for age 2 lake trout and quickly converged for lake trout ≥4 years (Fig. 3). However, the improved capture success on rainbow smelt reduced this variability. Greatest variability for the youngest and oldest lake trout reflected the importance of prey size structure and prey type. A higher capture probability for rainbow smelt caused F_e to increase for all age-classes and to be less variable at a prey density of 0.01 prey·m^{-3}.

At intermediate and equal prey density (0.01 prey·m^{-3}; 0.005 lake herring and 0.005 rainbow smelt·m^{-3}), F_e of age 2 lake trout was highest with a young-aged rainbow smelt population and a diet exclusively of rainbow smelt (Figs. 4 and 5). Young lake trout had the lowest net F_e when mean ages of the prey populations were older, reflecting size dependence in capture ability. The opposite relationship held for the oldest lake trout: F_e was greatest for the oldest rainbow smelt and lake herring with the diet being dominated by lake herring (Figs. 4 and 5). At higher prey density (0.1 prey·m^{-3}), prey size varied inversely with growth efficiency for age 2 lake trout (Fig. 4*d*), while the oldest lake trout did well across all prey age structures (Fig. 4*f*). Once again, rainbow smelt dominated the diet of young lake trout, while older lake trout grew better on lake herring (Figs. 5*d* and 5*f*).

Increasing capture probability increased F_e for the youngest lake trout and increased the importance of rainbow smelt in the diet of all lake trout. The clearest example of the shift in diet was observed for age 4 lake trout, which shifted from a diet dominated by lake herring to one dominated by rainbow smelt at the highest prey density (Figs. 4*e* and 5*e*).

Discussion

Prey community structure (species dominance, size structure, and density) and lake trout size interacted to determine diet selection and net foraging efficiency of lake trout in Lake Superior. We therefore expect rainbow smelt to dominate the diet of young lake trout and lake herring to dominate the diet of older lake trout in the wild. Further, we expect growth rate of the youngest piscivorous lake trout to be greatest for those feeding on the youngest rainbow smelt. In contrast, we expect older lake trout to maximize growth when foraging on older, larger lake herring. The lake trout population as a whole

© 1998 NRC Canada

Fig. 1. Age-specific F_e of lake trout on rainbow smelt and lake herring at 0.01 prey·m^{-3} and with foraging durations of 0.5, 1.0, and 2.0 h. Symbols represent mean age of the prey fish population (open circles, 0.25 years; solid circles, 1 year; asterisks, 2 years; open diamonds, 4 years). The horizontal dotted line indicates where energy ingested equals energy expended (i.e., growth rate equals zero).

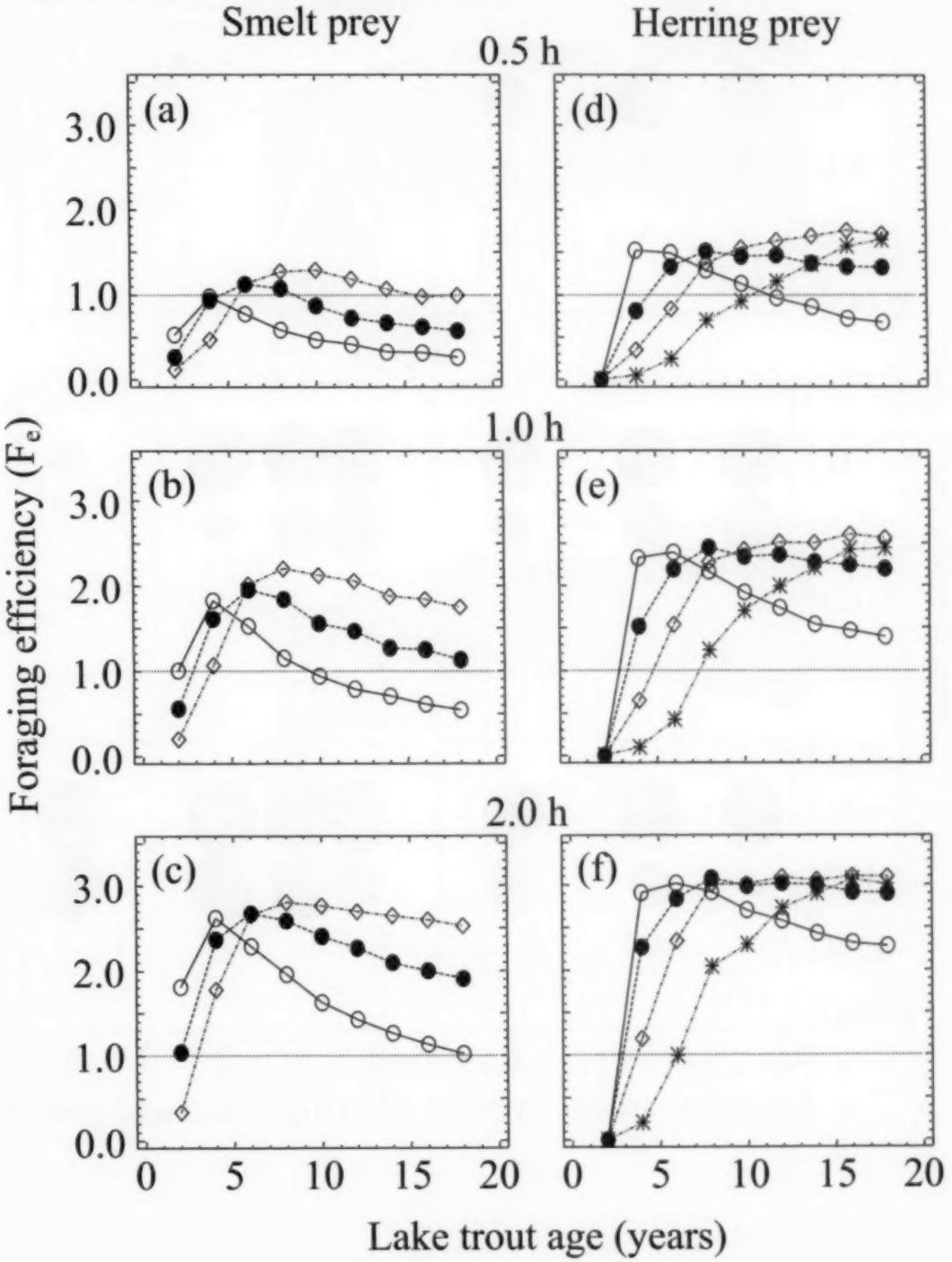

© 1998 NRC Canada

Fig. 2. Effects of prey age structure and prey density on the F_e of 2-, 4-, and 18-year-old lake trout with a foraging duration of 2 h. The size of the circle is proportional to the F_e of lake trout, with solid circles having values ≥1.0.

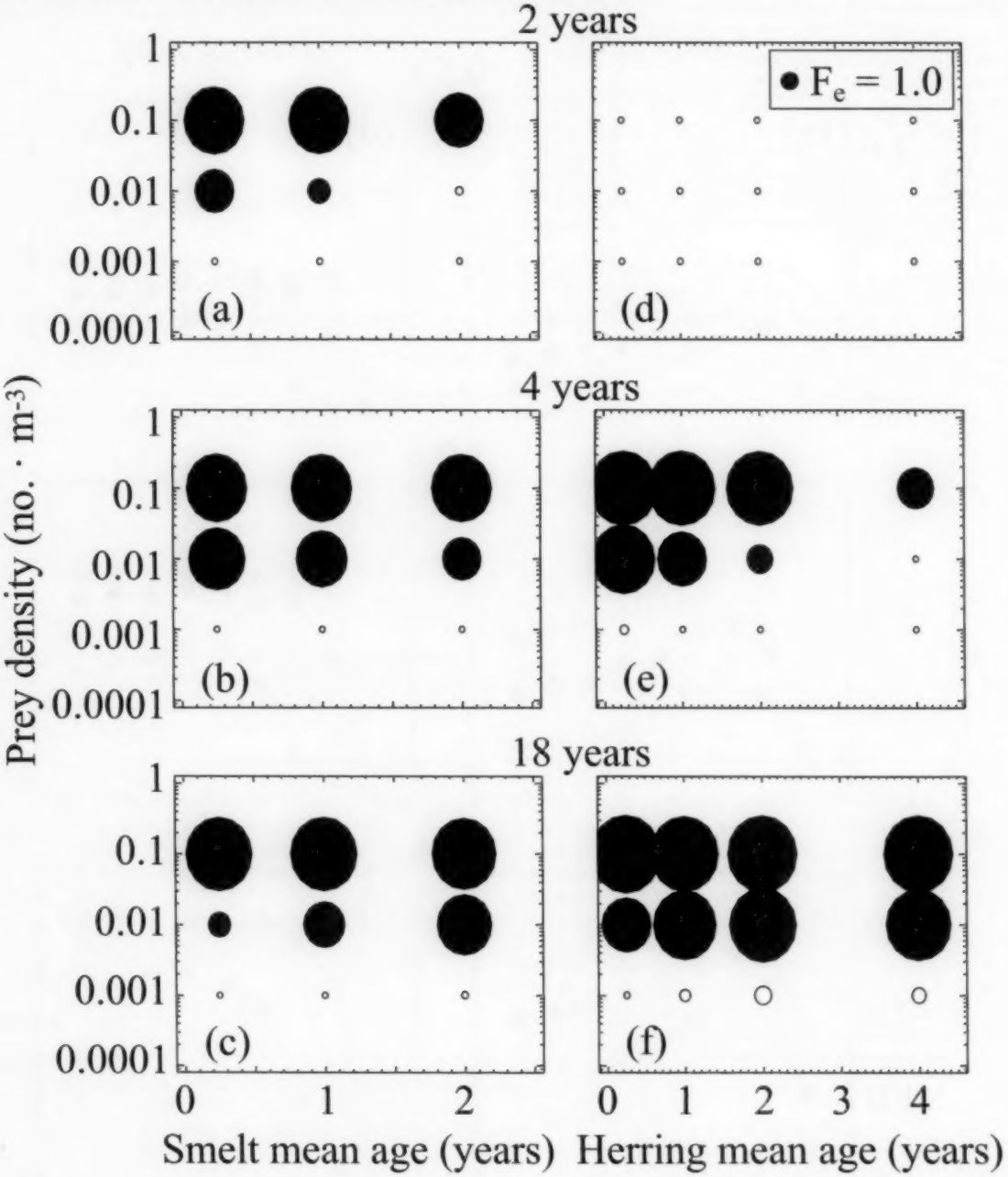

© 1998 NRC Canada

Fig. 3. Age-specific F_e of lake trout for a mixed prey species assemblage (rainbow smelt and lake herring) at two densities (solid line, 0.10 prey·m^{-3}; dotted line, 0.01 prey·m^{-3}) across all age-structure scenarios and a foraging duration of 2 h. (*a*) C_{opt} = 40% for rainbow smelt and lake herring; (*b*) C_{opt} = 80% for rainbow smelt and 40% for lake herring.

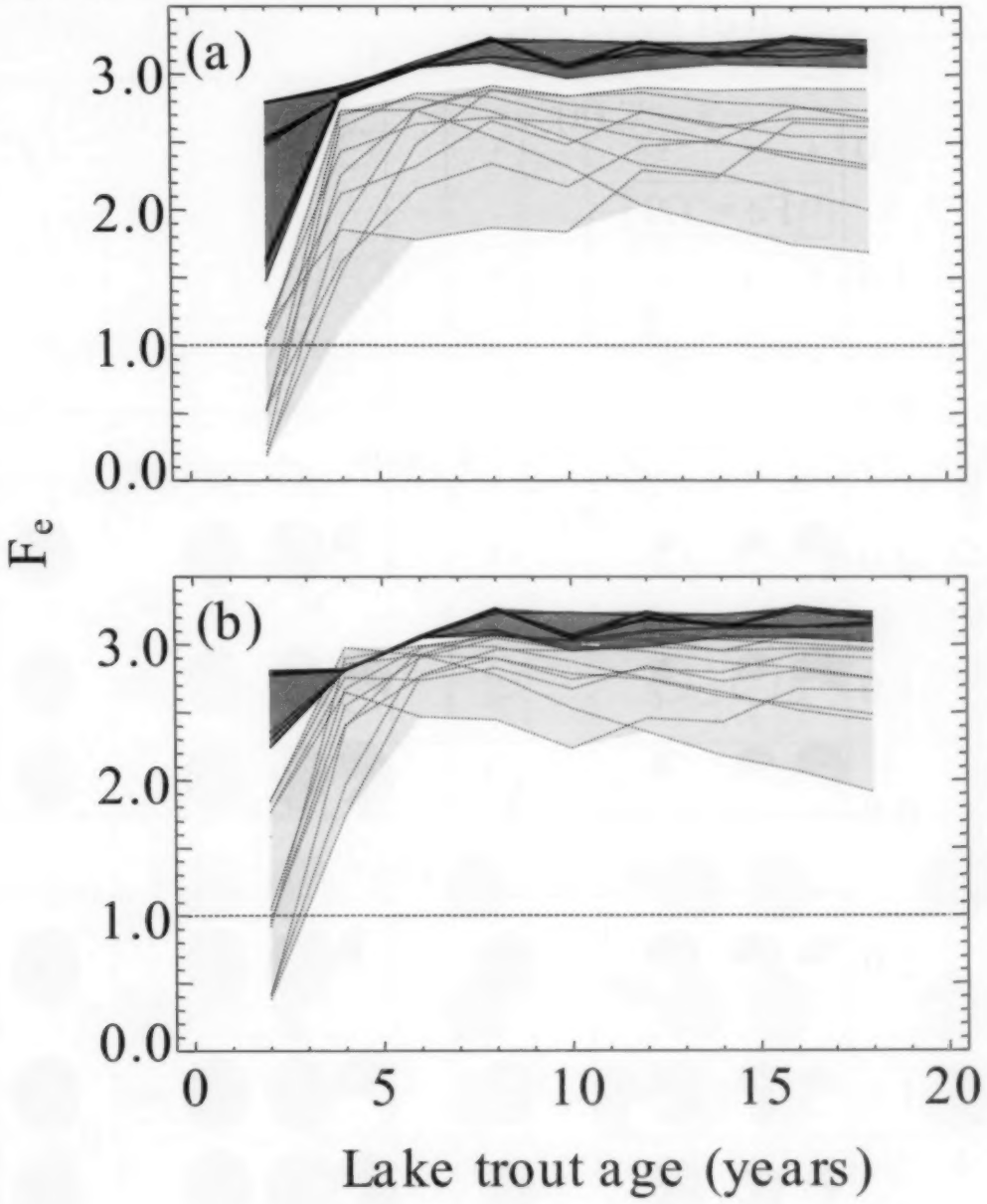

© 1998 NRC Canada

Fig. 4. Diet composition (mass) and F_e of 2-, 4-, and 18-year-old lake trout feeding on mixed prey assemblage at prey densities of 0.01 and 0.1 prey·m^{-3} and a foraging duration of 2 h; C_{opt} = 40% for rainbow smelt. The size of the circle is proportional to the net F_e of lake trout, with black being the proportion of lake herring and white the proportion of rainbow smelt in the diet.

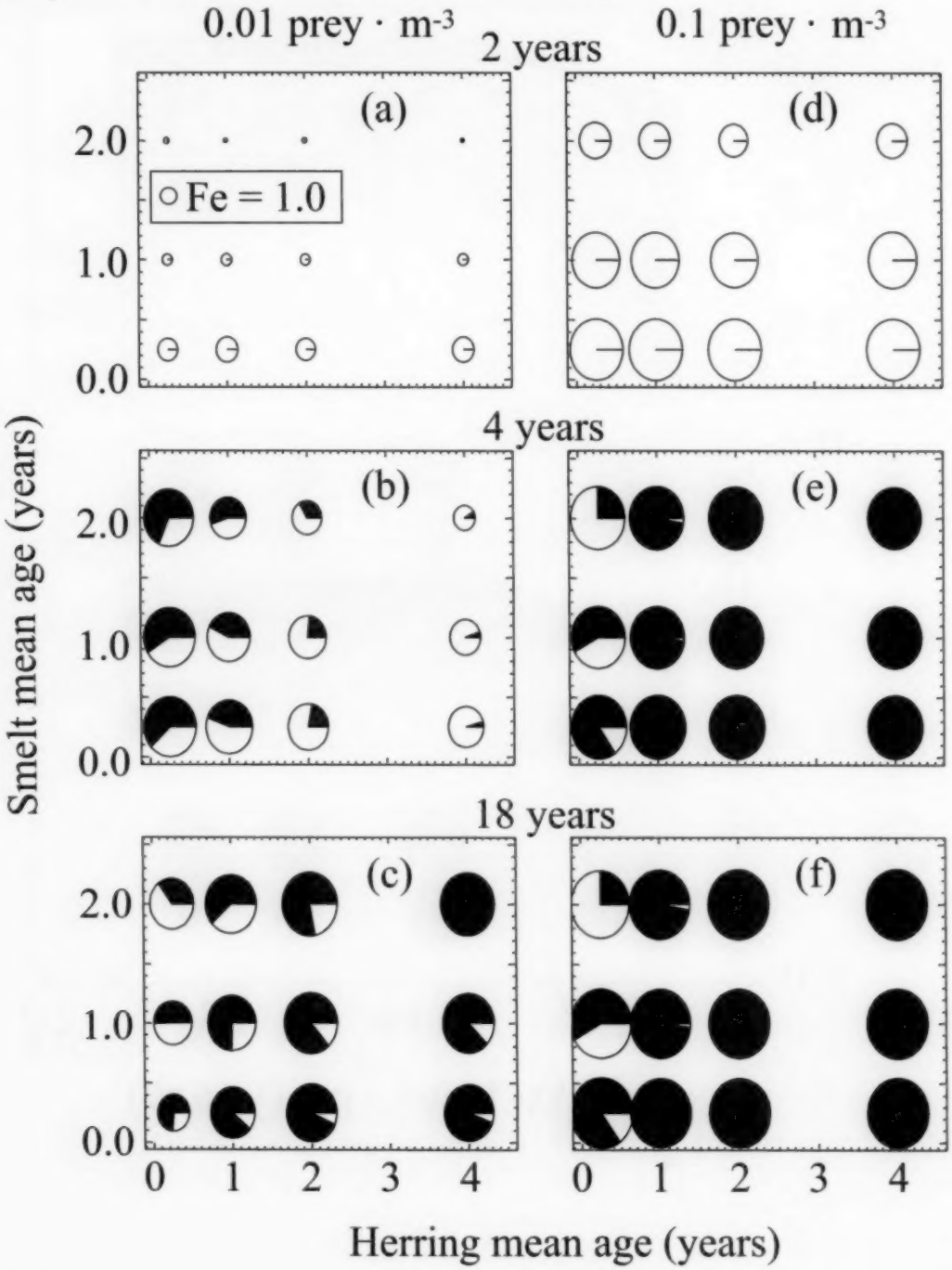

© 1998 NRC Canada

Fig. 5. Same as Fig. 4 except that C_{opt} = 80% for rainbow smelt.

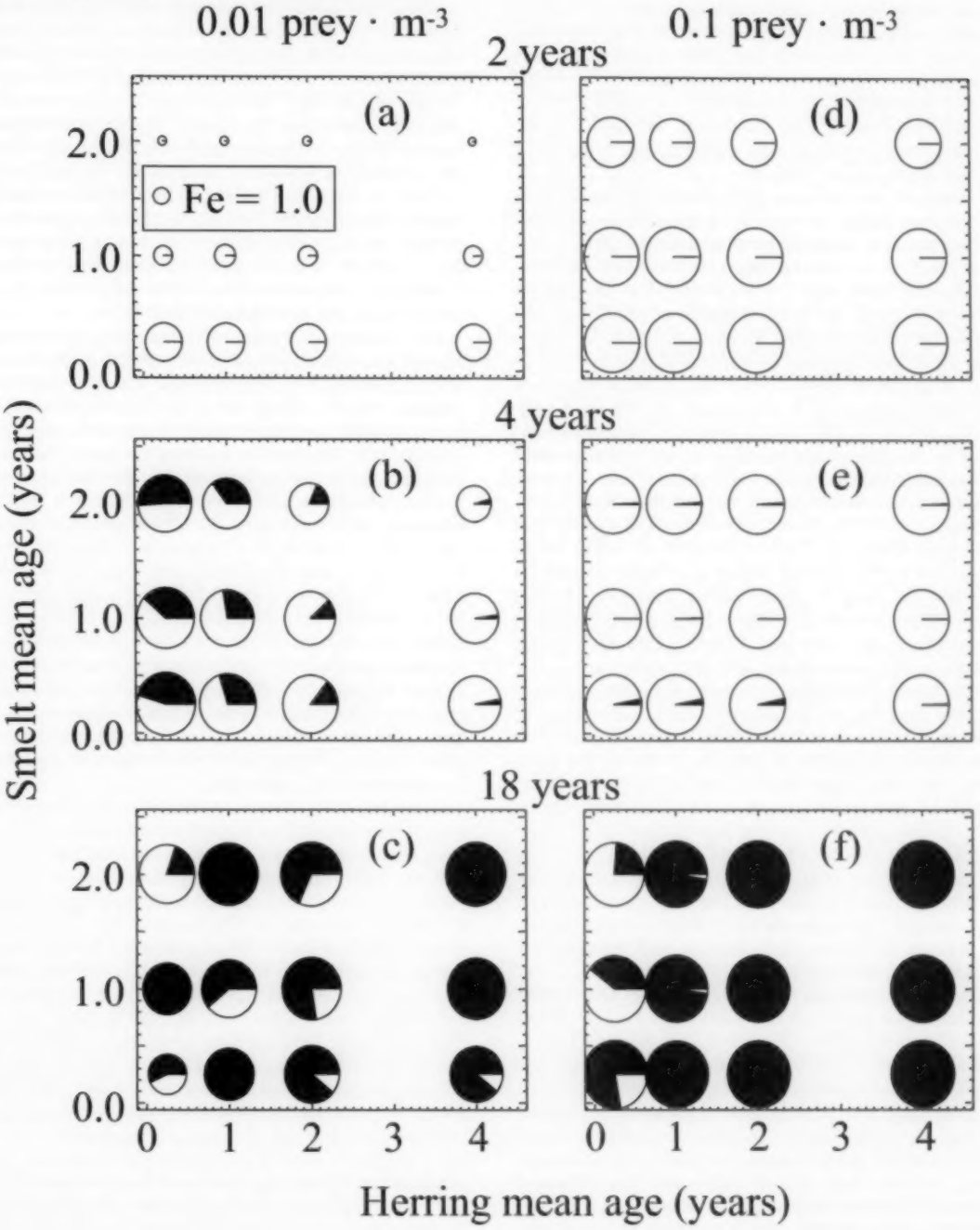

should grow best on a mixed prey species assemblage made up of young, small rainbow smelt and old, large lake herring.

Our predictions are consistent with age-specific diets and historical changes in size-at-age of lake trout in Lake Superior. In the mid-1980s to early 1990s, the fish component of diets of 2- to 3-year-old lake trout was 61–100% rainbow smelt (Ebener 1995). Older lake trout (4–11 years old) gradually shifted from a diet dominated by rainbow smelt to a diet with equal proportions of lake herring and rainbow smelt (Ebener 1995). Lake herring dominated the diet of lake trout older than 12 years (Ebener 1995). Young lake trout were also larger at age in the 1980s and 1990s, when rainbow smelt

© 1998 NRC Canada

dominated the diet, than in the pre-1960s (Ferreri and Taylor 1996) when lake herring was the dominate prey. In contrast, older lake trout were larger at age in the early 1950s on a lake herring diet than in the 1980s and 1990s with a mixed lake herring and rainbow smelt diet (Ferreri and Taylor 1996). Similarly, Busiahn (1985) found that the growth rate of commercially harvested adult lake trout was lower in the 1970s with a rainbow smelt dominated diet than in the 1950s with a lake herring dominated diet.

The increased size-at-age of young lake trout on a rainbow smelt diet may reflect the timing of the shift to piscivory rather than absolute energetic gains from lake herring versus rainbow smelt. In our lake herring – rainbow smelt comparison, young lake trout (age 2) were restricted to foraging on young rainbow smelt and were incapable of consuming lake herring due to gape limitations. Dryer et al. (1965) found that rainbow smelt first appeared in the diet of lake trout 15.2–17.5 cm in length (about 1–2 years old), while coregonines appeared at lengths of 27.9–30.2 cm (about 3–4 years old). Similarly, Ebener (1995) found that rainbow smelt first appeared in the diet of age 0 lake trout, while coregonines first appeared in the diet of age 4 lake trout. Moreover, prior to rainbow smelt dominance, aquatic and terrestrial invertebrates represented 70% by volume of the total diet of lake trout <2 years of age (≤17.5 cm) (Dryer et al. 1965), but in the 1980s and 1990s, diets of similar-aged fish contained up to 80% rainbow smelt by mass (Ebener 1995). An obvious shift from an invertebrate-dominated diet to a fish-dominated diet occurred for young lake trout following the establishment of rainbow smelt in the food web of Lake Superior.

The mechanism regulating size-at-age for older lake trout is less clear than for young lake trout. Historical changes in size-at-age of lake trout in Lake Superior are complicated by potential density-dependent growth during the 1970s when stocking rates were high. Ferreri and Taylor (1996) found that observed changes in growth rate of lake trout can be attributed to compensatory mechanisms but that other mechanisms may have also been important. Fish growth is highly pliant and integrates both density-dependent and density-independent (i.e., prey quality and size structure) factors. It is likely that both factors regulate lake trout growth and size-at-age, but the degree to which each of these mechanisms operates has yet to be resolved.

Following the rainbow smelt decline in the 1980s, intermediate-aged lake trout did not switch back to a diet dominated by coregonines. This may reflect the high capture success of rainbow smelt. Gape limitations explain why the youngest lake trout consumed only rainbow smelt; however, intermediate-aged lake trout continued to consume rainbow smelt when they were capable of consuming prey of higher energetic value (i.e., lake herring). Predator avoidance by the prey may influence lake trout diet selection. We accounted for potential differences in predator avoidance capabilities of the prey by increasing the capture probability of rainbow smelt. Capture probability is one of the least understood, but perhaps most important, parameters in foraging models of piscivorous fishes (Breck 1993). Coregonines and rainbow smelt may have different predator avoidance and escape strategies. Rainbow smelt tend to remain motionless, thereby decreasing encounter rates with predators and making themselves less conspicuous, while coregonines are active swimmers (Savitz and Bardygula 1989). However, when detected, rainbow smelt are easily captured, while coregonines may be captured only 40% of the time (Savitz and Bardygula 1989). The result of increasing rainbow smelt capture probability in the model was to increase the proportion of rainbow smelt in the diet for all ages of lake trout, with the most dramatic changes occurring in the younger to intermediate-aged lake trout. These increases occurred at high prey densities when prey availability should not be limiting. The high proportion of rainbow smelt in the diet of intermediate-aged lake trout may be the result of higher capture success when feeding on rainbow smelt. Another effect of increasing capture probability on rainbow smelt in a mixed prey species assemblage was to improve performance (i.e., reduce variability of F_e) over a greater range of prey fish densities and sizes.

The timing and duration of spatial overlap between predator and prey are critical to understanding predator and prey interactions and thus lake trout diet and growth. Obviously, predator and prey must occur at the same location at the same time to interact, and the duration of their interaction is dependent on the duration of the overlap (Mason and Patrick 1993). Lake herring, adult rainbow smelt, and lake trout all have similar bathymetric distributions (Selgeby and Hoff 1996). However, little is known of the diel migratory behavior and relative activity levels of these species in Lake Superior. Evidence suggests that lake herring may be pelagic both day and night, as this species is rarely collected in day bottom trawls but is common in overnight gillnet sets (Selgeby and Hoff 1996). In contrast, Lake Michigan rainbow smelt are common in bottom trawls by day and are known to vertically migrate at night (Brandt et al. 1991). If lake trout are primarily visual predators and remain near the bottom, rainbow smelt may be more available as prey during the daylight hours. Future work must focus on the space–time component of predator–prey interactions in Lake Superior.

Our model predictions appear relatively robust given the uncertainties in the foraging and metabolic parameters. Handling time is an important parameter in foraging models, as it sets the upper limit on feeding rate; however, a 30-fold increase in h_t produced negligible changes in our results and no change in conclusions. The insensitivity of the model to h_t is consistent with the conclusions of Breck (1993), who found that the handling time for piscivores is a relatively unimportant component of foraging. Metabolic costs for lake trout are well understood (Stewart et al. 1983), but the energy expended while foraging may be underestimated. However, any errors in the energy expended while foraging should produce a consistent shift in F_e for all simulations and not change any of the general relationships or conclusions based on comparisons.

Implications for management and future research

Our analysis provides an interpretation of observed diets of lake trout and a tenable explanation for the evidence that predation and growth rates are not simply direct functions of "forage" abundance. A predominance of small rainbow smelt in the diets of adult lake trout may also indicate suboptimal conditions for lake trout growth and production. This suggests that fisheries managers might consider managing for both prey community structure and prey size structure for an optimal prey base for lake trout. Management actions may

© 1998 NRC Canada

include size regulations on commercial fisheries for prey fishes and stocking policies for predator species that preferentially focus on certain sizes of some prey species. However, one must also exercise caution, as exotic rainbow smelt may interfere with the recruitment dynamics of lake herring and have unknown effects on the Lake Superior food web (e.g., Selgeby et al. 1978). Also, the combination of a low-cost monitoring program of lake trout diets with traditional fisheries assessment can provide valuable information for the management of Lake Superior fish populations.

Our analysis will help to improve understanding of the predator–prey dynamics in Lake Superior, although there is still much we need to learn. Future research should include the role of space and time in predator and prey interactions (e.g., Mason and Patrick 1993; Walters and Juanes 1993) and separate the roles of food quality and quantity from compensatory responses. Furthermore, our analysis focused on lake trout and their prey; this approach should be expanded to include other salmonid species if we are to gain a better understanding of the entire fish community. Until we gain a better understanding of the spatial overlap and dynamics of both predators and prey, we will be limited in our ability to describe the intensity of predator–prey interactions and to make predictions of community responses to management actions.

Acknowledgments

We thank Jim Breck, Mike Hansen, Sture Hansson, Chris Harvey, Tom Hrabik, Ed Rutherford, Jason Stockwell, and two anonymous reviewers for critical review and helpful comments on the manuscript and Jay Kirsch and Jiangang Luo for programming advice. This work was funded by the University of Wisconsin Sea Grant Institute under grants from the National Sea Grant College Program, National Oceanic and Atmospheric Administration, U.S. Department of Commerce, and from the State of Wisconsin. Federal grant No. NA46RG0481, project Nos. R/LR-45 and R/LR-72.

References

Anderson, E.D., and Smith, L.L., Jr. 1971. Factors affecting abundance of lake herring (*Coregonus artedii* Lesueur) in western Lake Superior. Trans. Am. Fish. Soc. **100**: 691–707.

Brandt, S.B., Mason, D.M., Patrick, E.V., Argyle, R.L., Wells, L., Unger, P., and Stewart, D.J. 1991. Acoustic measures of the abundance and size of pelagic planktivores in Lake Michigan. Can. J. Fish. Aquat. Sci. **48**: 894–908.

Breck, J.E. 1993. Foraging theory and piscivorous fish: are forage fish just big zooplankton? Trans. Am. Fish. Soc. **122**: 902–911.

Busiahn, T.R. 1985. Predator responses to fish community changes in Lake Superior. *In* Presented papers from the Council of Lake Committees plenary session on Great Lakes predator–prey issues, March 20, 1985. *Edited by* R.L. Eshenroder. Great Lakes Fish. Comm. Tech. Rep. 85-3. pp. 41–56.

Busiahn, T.R. 1990. Fish community objectives for Lake Superior. Great Lakes Fish. Comm. Spec. Publ. 90-1.

Dryer, W.R., Erkkila, L.F., and Tetzloff, C.L. 1965. Food of lake trout in Lake Superior. Trans. Am. Fish. Soc. **94**: 169–176.

Ebener, M.H. 1995. Bioenergetics of predator fish in western US waters of Lake Superior. Report prepared for the Red Cliff Band of Lake Superior Chippewas. Red Cliff Fisheries Dept., Bayfield, Wis.

Eby, L.A., Rudstam, L.G., and Kitchell, J.F. 1995. Predator responses to prey population dynamics: an empirical analysis based on lake trout growth rates. Can. J. Fish. Aquat. Sci. **52**: 1564–1571.

Ferreri, C.P., and Taylor, W.W. 1996. Compensation in individual growth rates and its influence on lake trout population dynamics in the Michigan waters of Lake Superior. J. Fish Biol. **49**: 763–777.

Folkvord, A., and Hunter, J.R. 1986. Size-selective vulnerability of northern anchovy, *Engraulis mordax*, larvae to predation by fishes. Fish. Bull. U.S. **84**: 859–869.

Gerritsen, J., and Strickler, J.R. 1977. Encounter probabilities and community structure in zooplankton: a mathematical model. J. Fish. Res. Board Can. **34**: 73–82.

Hansen, M.J., Peck, J.W., Schorfhaar, R.G., Selgeby, J.H., Schreiner, D.R., Schram, S.T., Swanson, B.L., MacCallum, W.R., Burnham-Curtis, M.K., Curtis, G.L., Heinrich, J.W., and Young, R.J. 1995. Lake trout (*Salvelinus namaycush*) populations in Lake Superior and their restoration in 1959–1993. J. Gt. Lakes Res. **21**(Suppl. 1): 152–175.

Hargreaves, J.B., and LeBrasseur, R.J. 1986. Size selectivity of coho (*Oncorhynchus kisutch*) preying on juvenile chum salmon (*O. keta*). Can. J. Fish. Aquat. Sci. **43**: 581–586.

Heist, B.G., and Swenson, W.A. 1983. Distribution and abundance of rainbow smelt in western Lake Superior as determined from acoustic sampling. J. Gt. Lakes Res. **9**: 343–353.

Hewett, S.W., and Johnson, B.L. 1992. Fish bioenergetics model 2. Univ. Wis. Sea Grant Inst. Tech. Rep. WIS-SG-92-250.

Hyatt, K.D. 1979. Feeding strategy. *In* Fish physiology. Vol. 8. *Edited by* W.S. Hoar, D.J. Randall, and J.R. Brett. Academic Press, New York. pp. 71–119.

Johnson, T.B., Mason, D.M., Bronte, C.R., and Kitchell, J.F. 1998. Estimation of invertebrate production from patterns of fish predation in western Lake Superior. Trans. Am. Fish. Soc. **127**: 496–506.

Jones, M.L., Koonce, J.F., and O'Gorman, R. 1993. Sustainability of hatchery-dependent salmonine fisheries in Lake Ontario: the conflict between predator demand and prey supply. Trans. Am. Fish. Soc. **122**: 1002–1018.

Lantry, B.F., and Stewart, D.J. 1993. Ecological energetics of rainbow smelt in the Great Lakes: an interlake comparison. Trans. Am. Fish. Soc. **122**: 951–976.

Lawrie, A.H. 1978. The fish community of Lake Superior. J. Gt. Lakes Res. **4**: 513–549.

MacCallum, W.R., and Selgeby, J.H. 1987. Lake Superior revisited 1984. Can. J. Fish. Aquat. Sci. **44**(Suppl. 2): 23–36.

Mason, D.M., and Patrick, E.V. 1993. A model for the space–time dependence of feeding for pelagic fish populations. Trans. Am. Fish. Soc. **122**: 884–901.

Negus, M.T. 1995. Bioenergetics modeling as a salmonine management tool applied to Minnesota waters of Lake Superior. N. Am. J. Fish. Manage. **15**: 60–78.

Power, M.E. 1987. Predator avoidance by grazing fishes in temperate and tropical streams: importance of stream depth and prey size. *In* Predation: direct and indirect impacts on aquatic communities. *Edited by* W.C. Kerfoot and A. Sih. University Press of New England, Hanover, N.H. pp. 333–351.

Rudstam, L.G., Binkowski, F.P., and Miller, M.A. 1994. A bioenergetics model for analysis of food consumption patterns of bloater in Lake Michigan. Trans. Am. Fish. Soc. **123**: 344–357.

Savitz, J., and Bardygula, L. 1989. Analysis of the behavioral basis for changes in salmonid diets. Illinois–Indiana Sea Grant Rep. IL-IN-SG-R-89-3.

Selgeby, J.H. 1982. Decline of lake herring (*Coregonus artedii*) in Lake Superior: an analysis of the Wisconsin herring fishery, 1936–78. Can. J. Fish. Aquat. Sci. **39**: 554–563.

Selgeby, J.H., and Hoff, M.H. 1996. Seasonal bathymetric distribu-

© 1998 NRC Canada

tions of 16 fishes in Lake Superior, 1958–75. Biol. Sci. Rep. 7, National Biological Service, Washington, D.C.

Selgeby, J.H., MacCallum, W.R., and Swedbery, D.V. 1978. Predation by rainbow smelt (*Osmerus mordax*) on lake herring (*Coregonus artedii*) in western Lake Superior. J. Fish. Res. Board Can. **35**: 1457–1463.

Stephens, D.W., and Krebs, J.R. 1986. Foraging theory. Princeton University Press, Princeton, N.J.

Stewart, D.J., Weininger, D., Rottiers, D.V., and Edsall, T.A. 1983. An energetics model for lake trout, *Salvelinus namaycush*: application to the Lake Michigan population. Can. J. Fish. Aquat. Sci. **40**: 681–698.

Vondracek, B., Giese, B.D., and Herny, M.G. 1996. Energy density of three fishes from Minnesota waters of Lake Superior. J. Gt. Lakes Res. **22**: 757–764.

Walters, C.J., and Juanes, F. 1993. Recruitment limitations as a consequence of natural selection for use of restricted feeding habitats and predation risk taking by juvenile fishes. Can. J. Fish. Aquat. Sci. **50**: 2050–2070.

Ware, D.M. 1978. Bioenergetics of pelagic fish: theoretical change in swimming speed and ration with body size. J. Fish. Res. Board Can. **35**: 220–228.

© 1998 NRC Canada

Quantifying cutthroat trout (*Oncorhynchus clarki*) predation on sockeye salmon (*Oncorhynchus nerka*) fry using a bioenergetics approach

Margaret A. Cartwright, David A. Beauchamp, and Mason D. Bryant

Abstract: Although some sockeye salmon (*Oncorhynchus nerka*) enhancement programs achieve production goals in Alaskan lakes, others like the Margaret Lake project fall well below expected levels. We used bioenergetics model simulations, coupled with field sampling of predator diet and distribution, to quantify the intensity of cutthroat trout (*Oncorhynchus clarki*) predation on stocked sockeye salmon fry in Margaret Lake during 1993 and 1994. Model results indicated that, by September, cutthroat trout consumed an estimated 34–51 and 32–100% of the 200 000 and 100 000 sockeye salmon fry stocked in May 1993 and 1994, respectively. September hydroacoustic survey results estimated a 82–87% decline of fry in 1993 and 90–93% in 1994. Stomach fullness and evacuation estimates of total consumption were 59% of model estimates after the first fry release in 1994 and 120% of the model estimates after the second release. All approaches to estimating cutthroat trout predation on stocked fry suggested that piscivores played a substantial role in the decline of sockeye salmon fry in Margaret Lake. The ability to estimate consumption is valuable in isolating predator influence on food web dynamics, especially in manipulated systems.

Résumé : Bien que certains programmes d'amélioration des stocks de saumon rouge (*Oncorhynchus nerka*) atteignent leurs objectifs de production dans les lacs de l'Alaska, d'autres comme le projet du lac Margaret obtiennent une production bien en deçà des niveaux attendus. Grâce à des modélisations bioénergétiques, alliées à un échantillonnage sur le terrain pour déterminer le régime et la distribution des prédateurs, nous avons quantifié l'intensité de la prédation exercée par la truite fardée (*Oncorhynchus clarki*) sur les alevins de saumon rouge ensemencés dans le lac Margaret au cours de 1993 et 1994. Les résultats de la modélisation indiquent que, dès septembre, la truite fardée avait consommé entre 34 et 51 % et entre 32 et 100 % des 200 000 et 100 000 alevins de saumon rouge ensemencés en mai 1993 et en 1994, respectivement. Selon les résultats d'un relevé hydroacoustique effectué en septembre, il y a eu réduction estimative de 82 à 87 % des alevins en 1993 et de 90 à 93 % en 1994. Des estimations de la consommation totale obtenues grâce à une évaluation de la plénitude et de l'évacuation gastriques correspondaient à 59 % des estimations du modèle après le premier lâcher d'alevins en 1994 et à 120 % des estimations du modèle après le deuxième lâcher. Selon toutes les méthodes d'estimation de la prédation exercée par la truite fardée sur les alevins ensemencés, les piscivores jouaient un rôle substantiel dans la réduction du nombre d'alevins du saumon rouge dans le lac Margaret. La capacité d'estimer la consommation est utile pour isoler l'effet des prédateurs sur la dynamique du réseau trophique, en particulier dans les systèmes aménagés.
[Traduit par la Rédaction]

Introduction

For several decades, aquatic ecologists have been interested in factors that regulate the biomass and production of fishes in freshwater lakes. The extent to which bottom-up and top-down forces interact to regulate biomass at each trophic level is important to fisheries resource managers interested in predicting the outcome of manipulating the nutrient levels, forage base, or top predators in lake systems to enhance a fishery. Sockeye salmon (*Oncorhynchus nerka*) enhancement programs are a good example of how the duality of food limitation and predator–prey interactions can produce variable results in studies designed to increase smolt biomass and adult salmon returns to commercial, sport, and subsistence fisheries. Koenings and Burkett (1987) developed a bottom-up model to predict sockeye salmon smolt and adult production based on the euphotic volume of the lake, the product of euphotic zone depth (1% incident light level), and the area of the lake. In Alaska, this model is combined with zooplankton production estimates to determine the number of sockeye salmon fry that can be supported in lakes targeted for enhancement.

Although some sockeye salmon enhancement programs

Received September 29, 1996. Accepted December 12, 1997. J13668

M.A. Cartwright[1] **and D.A. Beauchmap.** Utah Cooperative Fish and Wildlife Research Unit, Department of Fisheries and Wildlife, Utah State University, Logan, UT 84322-5255, U.S.A.
M.D. Bryant. USDA Forest Service, Forestry Sciences Laboratory, 2770 Sherwood Lane, Suite 2A, Juneau, AK 99801-8545, U.S.A.

[1] Author to whom all correspondence should be addressed. Present address: Alaska Department of Fish and Game, 304 Lake Street, Suite 103, Sitka, AK 99835, U.S.A.

© 1998 NRC Canada

have been successful in Alaska, others like the Margaret Lake project have failed to reach expected smolt production levels. Six years of hydroacoustic surveys indicated that only 5–34% of the stocked sockeye salmon fry survived 1 month after initial stocking in Margaret Lake. Poor adult sockeye salmon returns ranging from 75 to 350 fish between 1991 and 1994 support these low acoustic estimates of fry and smolt abundance (Bryant et al. 1995). Mortality due to handling and transportation of sockeye salmon fry from the hatchery to Margaret Lake was negligible (Cartwright and Beauchamp 1995). Previous Margaret Lake studies confirmed that the zooplankton forage base was sufficient to support 350 000 sockeye salmon fry, based on the euphotic volume model (DeCino 1992). We hypothesized that intense predation by resident piscivores could account for a rapid decline in sockeye salmon fry abundance. Several studies have shown that fish predators can significantly reduce juvenile sockeye salmon populations (Ruggerone and Rogers 1992; Beauchamp 1994; Beauchamp et al. 1995).

In Margaret Lake, we examined the diets of all potential predators including cutthroat trout (*Oncorhynchus clarki*), Dolly Varden (*Salvelinus malma*), coho salmon (*O. kisutch*) smolts, and kokanee (*O. nerka*) during 1990–1994. Of these, resident cutthroat trout was the only predator on sockeye salmon fry (Bryant and Frenette 1993; Frenette and Bryant 1994; Cartwright and Beauchamp 1995). The objective of this study was to quantify cutthroat trout predation on stocked juvenile sockeye salmon fry in Margaret Lake during 1993 and 1994.

Study site

Margaret Lake is located in southern Southeast Alaska about 48 km northwest of Ketchikan, Alaska. The 62-ha lake lies within a 30.6-km^2 drainage at 41 m in elevation with a maximum depth of 39 m and a mean depth of 10.9 m. The lake is dimictic, stained, and oligotrophic with seasonally variable Secchi depth transparencies of 2.5–8.5 m. Mean summer epilimnetic temperatures range from 15 to 18°C. Resident fishes include cutthroat trout, Dolly Varden, threespine stickleback (*Gasterosteus aculeatus*), prickly sculpin (*Cottus asper*), and kokanee (resident sockeye salmon). Anadromous species include steelhead trout (*O. mykiss*), coho salmon, pink salmon (*O. gorbuscha*), stocked sockeye salmon, and Pacific lamprey (*Lampetra tridentata*).

Methods

Piscivore diet and distribution sampling

The stomach samples of piscivorous species were examined to identify potential sockeye salmon predators. Stomach samples were taken from all captured cutthroat trout, kokanee, and rainbow/steelhead trout (snout to fork length (FL) ≥ 140 mm) in 1993 and 1994. The stomachs of all resident Dolly Varden (FL ≥ 140 mm) and coho salmon smolts captured in May and June were examined for fish parts. Dolly Varden were periodically examined throughout the rest of the season.

Sampling of potential piscivore diet and distribution was stratified along dimensions of space, time, and body size. Spatial dimensions were divided between two lake habitats, shore slope and offshore, and depth of capture for predators within each habitat. Shore slope habitat was defined as the littoral area of the lake out to a water column depth of 0–5 m and within 0–2 m of the shore slope below the 5-m isobath. The offshore habitat or the pelagic area of the lake included depths from the surface to 30 m deep but ≤2 m off the bottom, excluding the littoral area.

Temporal components of sampling were stratified by season and within a 24-h period. Three seasonal predation periods were defined in relation to the fry stocking date on May 19 in both years: prestock (April 1 – May 18), acute poststock (May 19 – June 20), and summer. Acute poststock and summer periods were further divided according to the number of stomach samples collected within periods of varying environmental conditions and prey availabilities (Tables 1 and 2). Within a 24-h period, four diel periods were delineated: day, dusk, night, and dawn.

Because the age structure of the cutthroat trout population in Margaret Lake was unknown, size categories were determined by length frequency histograms and the size at which cutthroat trout became piscivorous in other lakes (Beauchamp et al. 1992, 1995). For diet analysis, we partitioned cutthroat trout into three size categories in 1993 (140–200, 200–250, and 250–350 mm) and four size categories in 1994 (140–200, 200–250, 250–300, and 300–400 mm).

Fish were captured in the shore slope area using fyke nets, large minnow traps, horizontal gill nets, and angling. Offshore capture methods included vertical gill nets, angling, large suspended minnow traps, and trolling simultaneously at depths of 0.5, 4.5, 8.5, 12.5, and 16.5 m with downriggers. The vertical gill net was 30 m deep and consisted of two 2.5-m-wide panels of 50- and 90-mm stretch mesh. The horizontal gill nets (2 × 40 m) consisted of four panels: one 16-m-wide panel with 20-mm stretch mesh and three 8-m-wide panels with 50-, 80-, and 100-mm stretch mesh. Large 3-mm-mesh cylindrical minnow traps (3.1 m^3) were set individually and in sets of five: one every 5 m in both shore slope and offshore habitats. Fyke nets, covered with 3-mm-mesh nylon netting, were set in the littoral zone and a lead wing was attached to the shore. Gear sets coincided with changes in diel light regime. For example, nets were pulled and reset just before and just after crepuscular periods to obtain diet data for discrete diel periods.

Captured fish were enumerated by species, measured to the nearest millimetre (FL), and weighed to the nearest 0.1 g. A nondestructive gastric evacuation method was used to extract stomach contents (Foster 1977). Samples were individually preserved in a 16% buffered formalin–alcohol solution.

Diet analysis

Stomach samples from resident and sea-run Dolly Varden, kokanee, and coho salmon smolts were examined visually for fish parts. All cutthroat trout stomach samples were examined under a dissecting microscope. Fish prey were separated by species, insects grouped together, and miscellaneous prey such as fish eggs, plankton, mollusks, annelids, and the occasional amphibian and lamprey recorded as "other." Each group was weighed to the nearest 0.01 g wet weight.

Temporal and spatial patterns of piscivory were incorporated into a weighted average diet composition for each predator size-class and for each predation period throughout the season. For each predator size-class, diet compositions (wet weight proportions of each prey category) were averaged across shore slope and offshore habitats and were summed over all diel periods for each predation period for input to the bioenergetics model (Tables 1 and 2). Weekly temperature profiles were taken at 1-m intervals over 0–30 m with a YSI model 57 thermistor. An average Secchi depth was also measured weekly.

Cutthroat trout and sockeye salmon fry abundance estimates

Abundance estimates of cutthroat trout were estimated with a multiple mark–recapture sampling design using Schnabel and Schumacher–Eschmeyer estimators (see Bryant and Frenette 1993 for detailed description of methods). In 1993, 200 000 (gravimetric method) 0.21-g sockeye salmon fry were released into Margaret Lake at noon on May 19 (B. Halloran, Southern Southeast Regional Aquaculture Association (SSRAA), 2721 Tongass Ave, Ketchikan,

© 1998 NRC Canada

Table 1. Cutthroat trout 1993 diet composition used in the bioenergetics model.

Size-class (mm)	Predation period	Dates	Model days	Sockeye salmon	Threespine stickleback	Cottids	Coho salmon	Insects	Cutthroat trout	Unidentified fish parts	Others	*N*
cal/g[a]				1251–1255	1000	1304	1377	1195	1377	1255	500	
140–200	Prestock	Apr. 1 – May 8	1–47	0.00	0.25	0.16	0.00	0.59	0.00	0.00	0.01	61
	Postacute	May 19–25	48–54	0.10	0.00	0.00	0.00	0.86	0.00	0.00	0.04	44
		May 26–30	55–59	0.45	0.09	0.00	0.24	0.20	0.00	0.00	0.01	43
		June 1–20	60–80	0.00	0.01	0.00	0.00	0.84	0.00	0.05	0.10	21
	Summer	June 21 – July 2	81–92	0.08	0.07	0.03	0.29	0.51	0.00	0.04	0.01	51
		July 3–28	93–118	0.00	0.00	0.00	0.07	0.91	0.00	0.00	0.02	18
		July 29 – Sept. 7	119–149	0.00	0.49	0.01	0.00	0.28	0.00	0.08	0.14	32
200–250	Prestock	Apr. 1 – May 8	1–47	0.00	0.13	0.00	0.00	0.21	0.00	0.66	0.00	20
	Postacute	May 19–25	48–54	0.74	0.00	0.00	0.00	0.15	0.00	0.94	0.10	47
		May 26–30	55–59	0.01	0.02	0.00	0.01	0.94	0.00	0.00	0.20	31
		June 1–20	60–80	0.06	0.35	0.00	0.03	0.39	0.17	0.00	0.00	24
	Summer	June 21 – July 2	81–92	0.00	0.46	0.01	0.33	0.14	0.00	0.00	0.06	33
		July 3–28	93–118	0.00	0.40	0.02	0.00	0.41	0.00	0.00	0.17	45
		July 29 – Sept. 7	119–149	0.00	0.63	0.12	0.00	0.29	0.00	0.02	0.39	49
250–350	Prestock	Apr. 1 – May 8	1–47	0.00	0.38	0.00	0.51	0.10	0.00	0.00	0.00	11
	Postacute	May 19–25	48–54	0.46	0.08	0.01	0.00	0.42	0.00	0.01	0.02	45
		May 26–30	55–59	0.09	0.06	0.00	0.00	0.64	0.00	0.00	0.22	14
		June 1–20	60–80	0.06	0.27	0.01	0.00	0.55	0.00	0.02	0.09	16
	Summer	June 21 – July 2	81–92	0.01	0.75	0.16	0.00	0.03	0.00	0.00	0.05	20
		July 3–28	93–118	0.00	0.38	0.00	0.16	0.56	0.00	0.00	0.06	24
		July 29 – Sept. 7	119–149	0.00	0.78	0.00	0.00	0.15	0.00	0.04	0.03	34

Note: April 1 is day 1 of the simulation.

[a]Energy density estimated from weight-dependent function in Beauchamp et al. (1989): cal/g = 150 + 1.851*W*.

© 1998 NRC Canada

Table 2. Cutthroat trout 1994 diet composition used in the bioenergetics model.

Size-class (mm)	Predation period	Dates	Model days	Sockeye salmon	Threespine stickleback	Cottids	Pink salmon	Insects	Sockeye salmon smolts	Unidentified fish parts	Others	*N*
140–200	Prestock	Apr. 1 – May 18	1–47	0.00	0.16	0.00	0.00	0.76	0.00	0.06	0.07	67
	Postacute I	May 19–22	48–51	0.09	0.00	0.00	0.00	0.56	0.06	0.24	0.05	111
		May 23–27	52–56	0.24	0.23	0.00	0.00	0.59	0.00	0.00	0.16	37
	Postacute II	May 28–31	57–60	0.40	0.00	0.00	0.00	0.55	0.00	0.00	0.05	41
		June 1–4	61–64	0.00	0.00	0.00	0.00	0.84	0.00	0.00	0.16	6
	Midsummer	June 5–20	65–80	0.23	0.00	0.00	0.00	0.68	0.00	0.01	0.07	52
		June 21 – July 16	81–106	0.06	0.01	0.00	0.00	0.78	0.00	0.02	0.13	34
	Late summer	July 17 – Aug. 16	107–137	0.00	0.33	0.00	0.00	0.60	0.00	0.00	0.07	15
		Aug. 17 – Sept. 10	138–162	0.00	0.35	0.00	0.00	0.24	0.00	0.34	0.06	12
200–250	Prestock	Apr. 1 – May 18	1–47	0.00	0.05	0.00	0.01	0.90	0.00	0.00	0.04	30
	Postacute I	May 19–22	48–51	0.14	0.21	0.00	0.00	0.48	0.09	0.03	0.02	102
		May 23–27	52–56	0.01	0.01	0.00	0.00	0.79	0.00	0.00	0.18	35
	Postacute II	May 28–31	57–60	0.58	0.00	0.01	0.00	0.39	0.00	0.00	0.01	90
		June 1–4	61–64	0.00	0.05	0.00	0.00	0.95	0.00	0.00	0.00	15
	Midsummer	June 5–20	65–80	0.08	0.05	0.00	0.00	0.76	0.05	0.01	0.05	89
		June 21 – July 16	81–106	0.19	0.01	0.01	0.00	0.68	0.00	0.00	0.02	30
	Late summer	July 17 – Aug. 16	107–137	0.00	0.30	0.41	0.00	0.22	0.00	0.00	0.06	43
		Aug. 17 – Sept. 10	138–162	0.00	0.38	0.00	0.00	0.46	0.00	0.14	0.03	11
250–300	Prestock	Apr. 1 – May 18	1–47	0.00	0.02	0.00	0.06	0.90	0.00	0.01	0.01	15
	Postacute I	May 19–22	48–51	0.48	0.00	0.11	0.00	0.26	0.00	0.04	0.03	47
		May 23–27	52–56	0.34	0.05	0.00	0.00	0.48	0.05	0.01	0.07	25
	Postacute II	May 28–31	57–60	0.25	0.07	0.00	0.00	0.64	0.00	0.00	0.02	26
		June 1–4	61–64	0.00	0.09	0.00	0.00	0.78	0.00	0.01	0.13	6
	Midsummer	June 5–20	65–80	0.22	0.20	0.09	0.00	0.47	0.00	0.00	0.01	37
		June 21 – July 16	81–106	0.00	0.81	0.01	0.00	0.18	0.00	0.00	0.01	11
	Late summer	July 17 – Aug. 16	107–137	0.01	0.66	0.00	0.00	0.18	0.00	0.00	0.15	23
		Aug. 17 – Sept. 10	138–162	0.04	0.20	0.00	0.00	0.53	0.00	0.00	0.23	7
300–400	Prestock	Apr. 1 – May 18	1–47	0.00	0.40	0.00	0.00	0.60	0.00	0.00	0.00	2
	Postacute I	May 19–22	48–51	0.85	0.03	0.00	0.00	0.11	0.00	0.00	0.00	8
		May 23–27	52–56	0.00	0.00	0.00	0.00	0.00	0.00	0.00	0.00	1
	Postacute II	May 28–31	57–60	0.03	0.22	0.00	0.00	0.74	0.00	0.00	0.01	3
		June 1–4	61–64	0.00	0.00	0.00	0.00	0.00	0.00	0.00	0.00	2
	Midsummer	June 5–20	65–80	0.02	0.28	0.48	0.00	0.21	0.00	0.00	0.02	10
		June 21 – July 16	81–106	0.00	0.40	0.00	0.00	0.60	0.00	0.00	0.00	1
	Late summer	July 17 – Aug. 16	107–137	0.00	0.40	0.00	0.00	0.60	0.00	0.00	0.00	4
		Aug. 17 – Sept. 10	138–162	0.00	0.40	0.00	0.00	0.60	0.00	0.00	0.00	1

Note: April 1 is day 1 of the simulation.

© 1998 NRC Canada

AK 99901, U.S.A., personal communication). In 1994, an estimated 50 000 0.3-g sockeye salmon fry were released in the lake at noon on May 19 (SSRAA, personal communication). An additional 50 000 0.3-g sockeye salmon fry were held in situ in a 227-m^3 net pen with 3-mm mesh and released at midnight on May 28 as 0.4-g fry.

The seasonal abundance of juvenile sockeye salmon was estimated by serial hydroacoustic surveys and midwater trawls (2-m^2 opening and 3-mm knotless mesh) conducted by the Alaska Department of Fish and Game (ADF&G) on June 23, July 24, and September 2 in 1993, on May 24, June 1, June 18, and September 2 in 1994, and on April 26 in 1995. The duration-in-beam method (Thorne 1988) was used to enumerate the number of fish targets collected with a 70-kHz Simrad EY-M scientific echo sounder and recorded in digital format from 10 randomly chosen transects selected for each survey. Species and age composition of acoustic targets were determined by sampling the pelagic area with midwater trawl gear.

Consumption model

The importance of predation versus other sources of mortality can only be evaluated explicitly by quantifying predation and comparing it with total mortality. The bioenergetics approach to modeling (Kitchell et al. 1977) is less labor intensive than the stomach fullness–evacuation approach (Elliot and Persson 1978) and offers fine-scale temporal resolution of piscivory not possible with the production-based method (Ney 1990).

We used the Wisconsin bioenergetics model 2 (Hewett and Johnson 1992) modified for cutthroat trout (Beauchamp et al. 1995) to estimate daily consumption rates (grams per day) by cutthroat trout for each prey type and for each specific predator size-class for the 1993 and 1994 seasons. April 1 of each year was designated as day 1 in the model runs, and May 10 (day 40) was defined as the spawning date in the adult cutthroat trout species file. Spawning weight loss was estimated at 8% (D.A. Beauchamp, unpublished data). Prey caloric densities (Table 1) were obtained from the literature (Cummins and Wuycheck 1971; Hewett and Johnson 1992; Beauchamp et al. 1995). Because prey caloric densities of prey can change over a season, we calculated salmonid prey caloric density as a function of weight (Beauchamp et al. 1989).

The bioenergetics model estimates average individual predator consumption (grams per day), given population-specific data on growth, diet composition (Tables 1 and 2), and thermal experience of the predator. We calculated a weighted mean thermal experience for cutthroat trout based on their vertical distribution and concurrent vertical temperature profiles (Table 3). Information on predator growth was derived from length and weight data collected during population estimates of cutthroat trout during April, June, and October (Frenette and Bryant 1994; Bryant et al. 1995) (Table 4).

Daily sockeye salmon fry consumption estimates (grams per day) for individual cutthroat trout were divided by the mean body mass of fry sampled from the lake at that time to estimate the number of fry consumed per individual cutthroat trout. Individual consumption was multiplied by size-structured population estimates (±95% confidence interval (CI)) of cutthroat trout to estimate the total sockeye salmon fry biomass consumed by the entire cutthroat trout population during 1993 and 1994. The consumption estimate was then compared with hydroacoustic survey estimates of the number of sockeye salmon fry remaining in the lake throughout the season for each year.

To compare our model results with a more direct measurement of consumption, we calculated the daily ration of the mid-sized cutthroat trout (196–265 mm) using the stomach fullness–evacuation rate method (Elliott and Persson 1978) coupled with diet data collected over ecologically important feeding periods (day, dusk, night, and dawn). Data were pooled for three days immediately following the two fry releases: May 20–22 and May 28–30 in 1994. Mean stomach fullness with error bounds was calculated for these two periods. A fish evacuation rate (Elliott 1991) and an invertebrate evacuation rate (Elliott 1972) were calculated using temperatures taken May 22 and 29 and weighted by the average proportional weekly depth distribution of mid-sized cutthroat trout (Table 3). A final consumption estimate was weighted by the proportion of fish and insects in the diet during each 3-day period.

Sensitivity and error analyses

Sensitivity analysis of the internal parameters of the cutthroat trout model has been performed for similar salmonid models (Beauchamp et al. 1989; Ruggerone and Rogers 1992), so here, we will focus only on effects of error in our field inputs to the model. Error bounds (2 SE) were calculated as a percentage of the mean weights to estimate the 95% CI around the nominal weight values (Table 5). The average ratio of 95% CI/mean weight across all cutthroat trout size classes was 3.2% in 1993 and 5.5% in 1994. The model was rerun using these weight error bounds to calculate a range of consumption estimates (Table 5). Other field parameters were perturbed using only data from 1993. Prey caloric densities were changed ±10% from their nominal values. Temperature was changed ±1°C from nominal values to evaluate the sensitivity of our simulations to uncertainty in thermal experience.

To evaluate the collective effect of variation of several field values on the model consumptions estimates, an error analysis (Bartell et al. 1986) was performed on cutthroat trout consumption of sockeye salmon fry using 120 randomly generated values of growth, temperature, and diet composition (sockeye salmon and "other") from the 1994 data between May 19 and 27. Because the editing capabilities of the Wisconsin bioenergetics model are cumbersome, we only performed the error analysis on the mid-sized cutthroat trout (196–220 mm), the size category with the largest number of diet samples and the highest abundance in the population estimates. Growth and temperature values were generated from a normal distribution. A binomial distribution was used to simulate random proportions of sockeye salmon fry and "other" prey around mean field values. The "other" diet category was assigned the insect caloric density value of 1195 cal/g (1 cal = 4.1868 J) because insects were the most dominate prey item in the diet of the trout in Margaret Lake.

Results

Stomach samples were taken from all captured cutthroat trout (N = 694 in 1993, N = 1049 in 1994) and kokanee (FL ≥ 140 mm; N = 12 in 1993, N = 7 in 1994) from April to mid-September in 1993 and 1994. Stomach samples were taken from resident Dolly Varden (FL ≥ 140 mm; N = 110 in 1993, N = 55 in 1994) during April–June of both years and periodically for the remainder of each year (N = 28 in 1993, N = 61 in 1994) after it became apparent that they did not consume sockeye salmon fry. In 1994, coho salmon smolts (N = 17) emigrating to the ocean in late May and early June and two sea-run Dolly Varden entering the lake in September were also sampled for diet composition. Cutthroat trout were the only piscivore examined that contained sockeye salmon fry in the stomach samples.

Predator and prey abundance

The estimated cutthroat trout population (FL > 140 mm) declined from 3000 (95% CI = 2600–3600) in October 1992 to 1600 (95% CI = 1300–2000) in October 1993 with an instantaneous daily mortality rate of –0.00177. The cutthroat trout population continued to decline throughout 1994 with an instantaneous daily mortality rate of –0.00085 and a nominal number of 1200 fish (95% CI = 600– 4000) by October 15, 1994.

Hydroacoustic estimates of sockeye salmon fry abundance

© 1998 NRC Canada

Table 3. Temperature (°C) model inputs for each cutthroat trout size class in 1993 and 1994.

Year	Model day	Small cutthroat trout, 10–200 mm	Medium cutthroat trout, 200–250 mm	Medium to large cutthroat trout, (250–300 mm)	Large cutthroat trout, 250–350 mm (300–400 mm)
1993	1	7.1	9.6		10.1
	48	7.1	9.6		10.1
	55	8.0	11.4		12.4
	64	9.2	13.5		15.0
	78	7.5	11.1		11.2
	85	8.4	11.1		11.1
	103	8.0	12.5		12.7
	115	8.0	13.3		12.7
	124	8.0	13.0		12.5
	142	8.0	13.7		13.0
	160	8.0	13.3		13.0
	168	8.0	12.7		12.4
	181	8.0	10.1		9.9
	190	8.0	10.1		9.9
	203	8.0	8.3		8.3
	365	8.0	9.6		10.0
1994	1	5.3	5.3	5.2	5.2
	38	7.9	8.0	7.7	7.7
	49	11.8	11.8	11.1	11.2
	52	11.0	10.6	10.0	10.3
	58	8.6	8.5	8.3	8.3
	64	8.1	8.0	7.8	7.9
	71	11.4	11.4	10.8	11.2
	78	12.5	12.2	12.1	12.0
	94	13.1	12.6	12.7	12.3
	101	12.1	11.6	11.8	11.4
	107	15.1	14.8	14.3	14.4
	115	16.7	16.3	15.8	15.7
	122	15.8	15.5	15.2	15.1
	128	16.3	14.9	16.1	15.0
	134	18.9	17.0	18.8	17.2
	141	18.1	16.3	17.8	16.9
	148	15.1	14.0	14.9	13.7
	155	13.9	13.1	13.7	12.8
	164	13.1	12.4	12.9	12.1
	171	10.9	10.7	10.9	10.7
	365	5.3	5.3	5.2	5.3

Note: April 1 is day 1 of the simulations. Model days represent the date the temperature profiles were taken. Temperatures describe a weighted average proportional to the weekly distribution of the cutthroat trout size-class in the water column. Size intervals in paretheses are 1994 only.

declined dramatically during the first month after stocking in both 1993 and 1994. In 1993, 34 800 (±6200) fry out of 200 000 remained 1 month after stocking. Sockeye salmon fry mortality slowed considerably during the remainder of the growing season, and the acoustic estimate in September was 31 100 (±5567) fry. Although 50% fewer fish were stocked in 1994, the estimated number of fry remaining 1 month after stocking (32 900 ± 3000) was similar to that of June 1993. However, the September 1994 estimate of 8600 fry (±1100) indicated a substantial decline in fry numbers (8.5% survival) during the remainder of the growing season when compared with 1993 (15.6% survival). The hydroacoustic survey conducted in April 1995 estimated that 5800 (±1300) fry from the 1994 stocking cohort survived to age 1. The 68% overwinter survival rate is consistent with the standard survival assumption of 70% from fall fry to spring smolt developed for sockeye salmon in Southeast Alaska (T. Zadina, ADF&G, 2030 Sea Level Dr., Ketchikan, AK 99901, U.S.A., unpublished data).

Cutthroat trout experienced warmer temperatures on average in 1994 than in 1993 during the initial acute predation period which began on May 19 both years (Table 3).

© 1998 NRC Canada

Table 4. Average initial wet weights for each cutthroat trout length interval and cohort modeled in 1993 and 1994 and in the spring of 1995.

Year	Cohort	Model days	Length interval (mm)	Initial weight (g) (2 SE)
1993	J2	75–183	91–160	24.5 (2.1)
	J3	184–365	131–190	39.7 (3.4)
	J4	1–74	151–195	43.5 (1.2)
	J5	75–183	161–210	54.1 (1.5)
	J6	184–365	191–220	79.3 (2.2)
	A1	1–74	196–215	79.5 (2.1)
	A2	75–183	211–240	108.1 (8.1)
	A3	184–365	221–255	119.2 (8.9)
	A4	1–74	216–225	114.6 (5.2)
	A5	75–183	241–275	150.0 (6.8)
	A6	184–365	256–305	209.3 (9.5)
	A7	1–74	256–350	205.5 (17.7)
	A8	75–183	276–350	214.5 (18.5)
	A9	184–365	306–380	290.7 (25.1)
1994	J2	75–183	135–170	33.1 (2.7)
	J3	184–365	125–175	33.3 (2.7)
	J4	1–74	151–195	46.6 (1.8)
	J5	75–183	171–200	55.2 (2.1)
	J6	184–365	226–290	211.7 (15.8)
	A1	1–74	196–220	71.7 (3.2)
	A2	75–183	201–250	89.4 (4.0)
	A3	184–365	221–265	123.1 (5.5)
	A4	1–74	221–265	111.9 (8.4)
	A5	75–183	251–275	156.1 (11.7)
	A6	184–365	226–290	211.7 (25.8)
	A7	1–74	226–310	175.1 (14.9)
	A8	75–183	276–310	216.2 (18.4)
	A9	184–365	291–320	287.5 (24.5)
	A10	1–74	311–350	300.5 (41.1)
	A11	75–183	311–400	314.7 (43.0)
	A12	184–365	321–350	371.0 (50.7)
1995	J4	1–74	131–180	33.4 (2.7)
	J7	1–74	181–230	74.3 (2.8)
	A4	1–74	231–270	132.3 (5.9)
	A7	1–74	271–300	206.2 (15.5)
	A10	1–74	301–330	272.7 (23.3)
	A13	1–74	330–370	381.6 (52.2)

Note: April 1 is day 1 of the simulations. Cohort letter initials indicate whether juvenile (J) or adult (A) physiological parameters were used, and the number represents the cohort interval. The initial weight of the next cohort is the end weight of the preceding cohort. For example, the end weight of J3 is J4, the weight gained overwinter.

However, this thermal pattern was reversed by May 26, 1994, due to an intense and prolonged rainstorm. The storm caused the lake level to rise 2–3 m and remain in flood condition for 10 days, creating a dramatic decline in temperature and near-isothermic conditions during the acute predation period of the study in 1994. Although temperature regimes in 1993 were considerably different among cutthroat trout size-classes, all three groups occupied increasingly warmer temperatures between May 19 (model day 49) and June 3 (model day 64) (Table 3). During the same period in 1994, thermal experience was similar among the four cutthroat trout size groups and dropped 2.0–2.3°C between May 22 and May 28 (Table 3).

Bioenergetics model estimates

For 1993 and 1994, bioenergetics model simulations estimated that roughly half the sockeye salmon fry stocked were consumed by cutthroat trout (Fig. 1). The nominal consumption estimate from the model was 82 800 fry in 1993 (Fig. 1A). Sockeye salmon fry consumption ranged from 67 800 to 101 000 fry based on 95% CI around cutthroat trout population estimates. In 1994, model simulations predicted that cutthroat trout consumed 51 400 fry (32 100 – 130 300, 95% CI) of the 100 000 fry released into the lake (Fig. 1B). In 1993, most predation occurred during the first 2 weeks after stocking whereas predation in 1994 proceeded at a more gradual rate throughout the summer (Fig. 1).

Although the two smaller cutthroat trout size groups consumed fewer grams of sockeye salmon per individual than the larger size groups, at the population level, they consumed as many or more sockeye salmon fry than the larger cutthroat trout in 1994 (Fig. 2). Insects dominated the diet of cutthroat trout during most of the growing season both years (Fig. 2; Tables 1 and 2). The increased proportion of threespine stickleback in the diet of all sizes of cutthroat trout during summer reflected the availability and vulnerability of newly emerging young-of-the-year in July.

Direct measurement of consumption

Using the stomach fullness–evacuation method (Elliott and Persson 1978), the mean (95% CI) total daily consumption estimate for 196- to 265-mm cutthroat trout was 1.98 g (1.23–2.72 g) per predator during May 20–22, 1994. When compared with the bioenergetics model estimate of consumption during the same time period, the direct measurement mean estimate was 59% of the nominal model estimate (3.36 g) with a range of 37–81% (Fig. 3). After the second release of sockeye salmon fry on May 27, 1994, the direct consumption estimate was 3.71 g (2.60–4.34 g) per predator during May 28–30, 1994 (Fig. 3). During this period, the direct estimate was 20% higher than the mean model estimate (2.98 g), but within the upper and lower 95% CI error bounds (Fig. 3).

Sensitivity analysis

Individual parameter perturbations of 1993 field values for growth, caloric density, temperature, and cutthroat trout population estimates showed cutthroat trout consumption estimates of juvenile sockeye salmon to be most sensitive to changes in predator abundance estimates (±19% of nominal value, Fig. 1) and least sensitive to changes in estimated growth (3.1–5.5%) between cutthroat trout size-classes (Table 5). In 1993, changes in cutthroat trout initial and end mean weights for each size-class and predation period produced an estimated range of 80 200 – 87 400 sockeye salmon fry consumed (Table 5). In 1994, model simulations encompassing the 95% CI around mean cutthroat trout growth resulted in consumption ranging between 46 150 and 54 300 fry. Changes in prey caloric densities had an inverse effect on fry consumption estimates; lowering prey caloric density increased the estimated number of fry consumed. In 1993, a

© 1998 NRC Canada

Table 5. Sensitivity analysis results of cutthroat trout consumption estimates of sockeye salmon fry in 1993.

Parameter	Amount parameter perturbed	Deviation from nominal value	% change in consumption	Consumption estimate
Cutthroat abundance	Lower 95% CI	19%	−18.0	67 853
	Upper 95% CI	19%	+22.0	101 047
Cutthroat weight (g)	−2 SE	−2595	−3.1	80 203
	+2 SE	+4569	+5.5	87 367
Prey caloric density (cal/g wet weight)	−10%	+9019	+10.9	91 817
	+10%	−8051	−10.8	74 747
Temperature (°C)	−1	5599	−7.8	77 199
	+1	5045	+6.8	87 843

Note: Nominal values of all other field input values and model parameters were used. The nominal consumption value was 82 798 sockeye salmon fry.

Fig. 1. Comparison of bioenergetics model estimates of cutthroat trout consumption (broken lines) with hydroacoustic measurement of stocked (age 0) sockeye salmon fry decline (solid line) for (A) 1993 and (B) 1994. The range of consumption estimates is based on 95% CI around cutthroat trout population estimates.

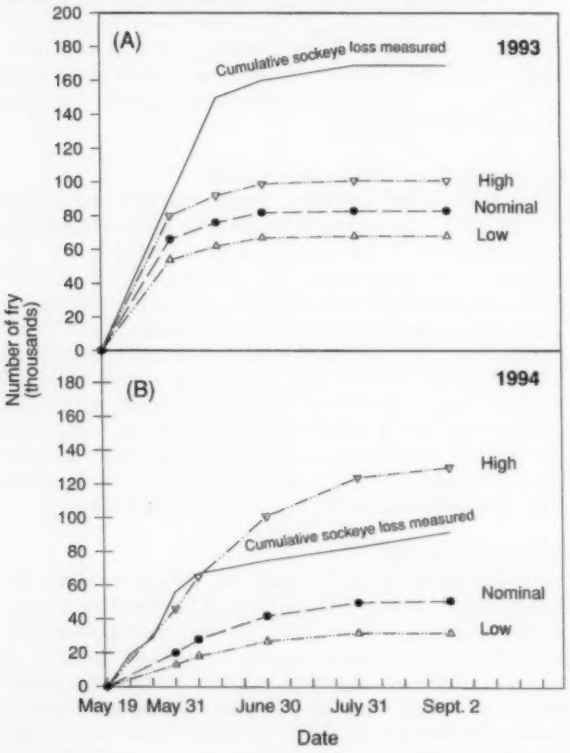

10% reduction in prey caloric densities resulted in a mean of 91 817 sockeye salmon fry consumed (Table 5). Conversely, a 10% increase in prey caloric densities resulted in a mean of 74 747 fry eaten in the 1993 growing season (Table 5). Raising and lowering the temperature by 1°C resulted in a 7.8% change in the number of sockeye salmon fry consumed. Higher temperatures increased consumption estimates to a mean of 87 800 fry, and lower temperatures reduced consumption estimates to a mean of 77 200 fry (Table 5).

The error analysis of field values for growth, temperature, and diet for the 196- to 220-mm cutthroat trout (N = 137) generated a mean (95% CI) daily consumption of 2.44 g (2.22–2.66 g) of sockeye salmon fry per predator and a coefficient of variation of 52%. This translated into a mean daily consumption of 7.4 (6.7–8.1) 0.33-g sockeye salmon fry per predator during May 19–27, 1994.

Discussion

Results from the bioenergetics modeling of cutthroat trout consumption suggest that cutthroat trout predation is a significant contributor to the decline of sockeye salmon fry in Margaret Lake. Although half as many fry were stocked in 1994, consumption estimates and hydroacoustic estimates showed similar rates of sockeye salmon fry decline in both years. Cutthroat trout abundance estimates, stratified by size, produced large confidence intervals around mean abundance estimates. Population-level consumption estimates were sensitive to cutthroat trout abundance, and estimates of predation intensity accounted for 34–51% of the observed fry mortality in 1993 and 32–100% in 1994.

It appears that cutthroat trout in Margaret Lake are capable of sustaining a constant rate of predation even as the prey biomass declines until some low threshold is reached. Between 1990 and 1994, the number of fry stocked ranged from 100 000 to 518 000 (T. Zadina, ADF&G, 2030 Sea Level Dr., Ketchikan, AK 99901, U.S.A., unpublished data). The fall hydroacoustic surveys consistently showed that sockeye salmon fry were driven to low numbers (5000 – 75 000 fry, 2.5–16.7% of total number stocked). This suggests that cutthroat trout were efficient predators and exhibited a modified type II functional response to the introduction of stocked juvenile salmonids (Peterman and Gatto 1978). The functional response of the predators was not diminished when low numbers of fry were stocked in 1994. Because this broad range of stocking strategies did not improve sockeye salmon fry survival in Margaret Lake, stocking was discontinued after 1994.

We attempted to address several of the criticisms directed towards field inputs of previous bioenergetics model studies. Diet composition errors in this study are most likely minimal

© 1998 NRC Canada

Fig. 2. Seasonal 1994 patterns of individual daily consumption of major prey by size-class of cutthroat trout (top) and size-class population-level consumption of sockeye salmon fry (bottom). Predation stanza date codes: Pre, prestock, April 1 – May 18; Acute, acute poststock, May 19 – June 4; Jun, June 5–20; Sum, summer, June 21 – September 10.

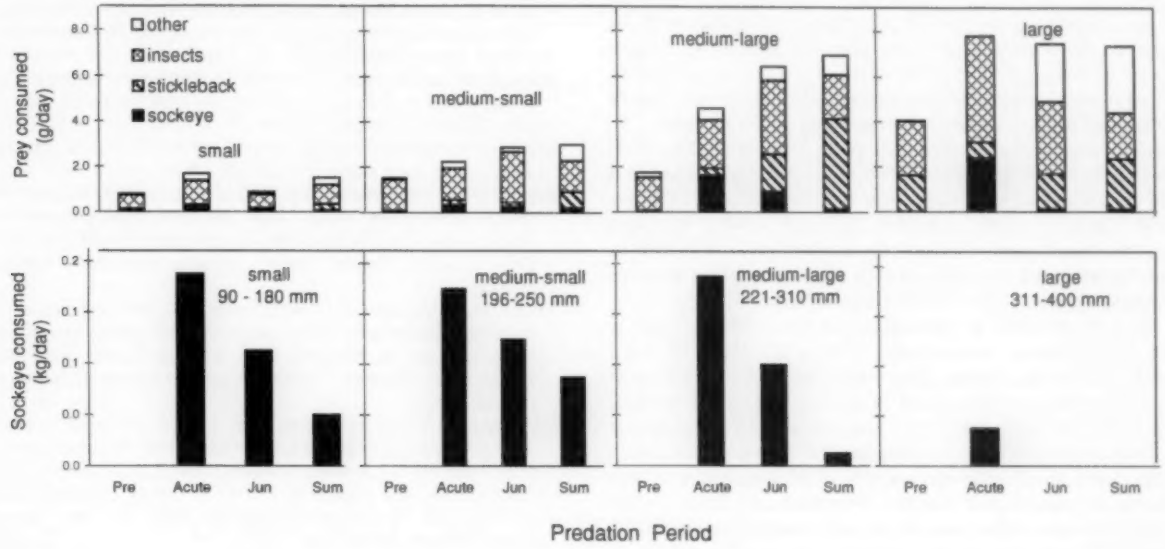

Fig. 3. Daily total consumption per predator estimated by the bioenergetics model and the stomach fullness–evacuation model for a 3-day period following the first fry release (May 20–22) and the second fry release (May 28–30) in 1994. The stomach fullness–evacuation model error bars were derived from the 95% CI around the mean stomach fullness values.

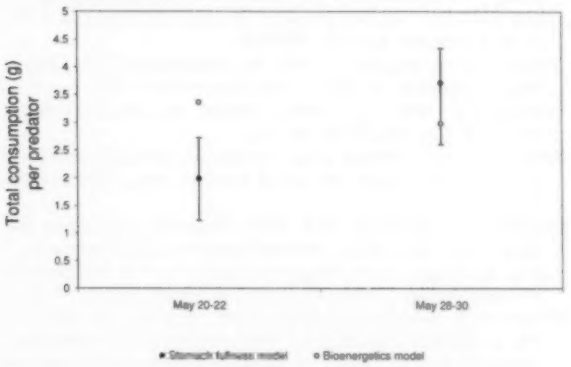

because stomach samples were collected on a fine-grained temporal and spatial scale. Temperature values were assigned according to the proportion of cutthroat trout distributed in the water column. Although this approach is not as accurate as telemetry studies of fish movement, it does include field data on distribution of the cutthroat trout not considered in the more common assumption of behavioral thermoregulation.

One criticism of the Wisconsin bioenergetics model is its inability to accurately represent energetic costs associated with activity (Boisclair and Leggett 1989; Hansen et al. 1993). Most studies reporting a wide variation in activity costs were conducted on juvenile planktivorous fish (Boisclair and Leggett 1989; Post 1990; Madon and Culver 1993; Tang and Boisclair 1995), which have very different energetic demands than insectivorous and piscivorous adults. Germane to this study, the difference between activity costs measured in the Wisconsin model and by other methods appears to less important for adult fish compared with more active juvenile fish (Post 1990), especially nonspawning adults (Rowan and Rasmussen 1996). In addition, sensitivity analysis of the Wisconsin model indicates only modest errors in consumption estimates associated with activity parameters (Bartell et al.1986; Beauchamp et al. 1989).

Comparing bioenergetics model consumption estimates with estimates derived from an independent source is essential to the credibility of model outputs. Hydroacoustic abundance estimates of sockeye salmon fry throughout the season provided independent estimates of sockeye salmon fry abundance and mortality for comparison with model estimates of predation-induced mortality from cutthroat trout. Both the bioenergetics model and acoustic estimates showed a sharp reduction in fry numbers immediately after stocking and a more gradual decline of sockeye salmon fry in 1994 than in 1993 for the rest of the season. Consumption estimates from the bioenergetics model were also reasonably close to consumption estimates derived by the "direct" stomach fullness–evacuation method. Contradictory results in the comparison of model and direct measurement consumption estimates between the first (May 20–22) and second fry releases (May 28–30) may have been confounded by the dramatically fluctuating thermal experience of the predator during a heavy rainstorm after the second release of fry in 1994.

The density of cutthroat trout in Margaret Lake (16 fish/ha, FL ≥175 mm) was similar to the average densities estimated in other Southeast Alaska lakes. The Sport Fish Division of

© 1998 NRC Canada

the ADF&G has estimated that cutthroat trout (FL ≥180 mm) densities range 2–38 fish/ha for several Southeast Alaska lakes (see summary in Der Hovanisian and Marshall 1995). However, survival of stocked sockeye salmon fry in Margaret Lake was low compared with other stocked populations in the region. For example, after stocking 556 000 fry in Badger Lake on May 16, 1985, 65% of the fry survived to June 24 (Zadina and Haddix 1989) compared with 17% fry survival in Margaret Lake 1 month after stocking in 1993. The 2.5–16.7% range of fry to smolt survival in Margaret Lake is well below the 28–65% range for other Southeast Alaska lakes and on the lower end of a wide range reported for other Alaskan and Canadian lakes, 2.8–66% (Foerster 1968). Bradford (1995) placed sockeye salmon fry to smolt survival at 22% in northwestern lakes compared with 8% estimated for sockeye salmon fry stocked in 1994 in Margaret Lake.

Despite evidence in other lakes that piscivores are capable of compromising enhancement efforts, the Margaret Lake study is the only Alaskan lake where resident cutthroat trout densities and the associated predatory impact on stocked juvenile salmonids have been determined. The detrimental effects of resident trout on introduced sockeye salmon fry in Margaret Lake provide one example of the importance of predation in manipulated systems (Peterman and Gatto 1978). How piscivores affect juvenile sockeye salmon recruitment in other lakes may depend on a complex suite of physical (basin morphometry, water transparency, temperature, oxygen, etc.) and biological (density, distribution, and size structure of predators, availability of alternative prey, trophic state) conditions present in different lakes. Therefore, similar investigations in other lakes would provide valuable insights into the importance of piscivory across a range of different physical and biological conditions and may improve our ability to predict the relative importance of top-down or bottom-up control in different waters.

Acknowledgements

Funding was provided by the USDA Forest Service Forestry Sciences Laboratory, Utah Cooperative Fish and Wildlife Research Unit, and the Ecology Center at Utah State University. BioSonics, Inc. analyzed the hydroacoustic survey tapes. Special thanks are extended to Fredrik Norssell for his long hours in the field and laboratory and uncompromising attention to detail. We thank Gary Thiede, Nick Bouwes, Brian Frenette, John Troxler, Todd Teisler, and John Hudson for their field assistance and Jane Chen for laboratory assistance. This paper benefitted from reviews by Daniel Boisclair, James Haefner, Peter Rand, Phillip Symons, and Wayne Wurtsbaugh.

References

Bartell, S.M., Breck J.E., Gardner R.H., and Brenkert, A.L. 1986. Individual parameter perturbation and error analysis of fish bioenergetics models. Can. J. Fish. Aquat. Sci. **43**: 160–168.

Beauchamp, D.A. 1994. Spatial and temporal dynamics of piscivory: implications for food web stability and the transparency of Lake Washington. Lake Reservoir Manage. **9**: 151–154.

Beauchamp, D.A., Stewart, D.J., and Thomas, G.L. 1989. Corroboration of a bioenergetics model for sockeye salmon. Trans. Am. Fish. Soc. **118**: 597–607.

Beauchamp, D.A., Vecht, S.A., and Thomas, G.L. 1992. Temporal, spatial, and size-related foraging of wild cutthroat trout in Lake Washington. Northwest Sci. **66**: 149–159.

Beauchamp, D.A., LaRiviere, M.G., and Thomas, G.L. 1995. Evaluation of competition and predation as limits to juvenile kokanee and sockeye salmon production Lake Ozette, Washington. N. Am. J. Fish. Manage. **15**: 193–207.

Boisclair, D., and Leggett, W.C. 1989. The importance of activity in bioenergetics models applied to actively foraging fishes. Can. J. Fish. Aquat. Sci. **46**: 1859–1867.

Bradford, M.J. 1995. Comparative review of Pacific salmon survival rates. Can. J. Fish. Aquat. Sci. **52**: 1327–1338.

Bryant, M.D., and Frenette, B.J. 1993. Assessment of resident cutthroat trout, Dolly Varden char and introduced anadromous salmonid in Margaret Lake. Progress Report for 1992. USDA-PNW Research Station, Forestry Sciences Laboratory, Juneau, Alaska.

Bryant, M.D., McCurdy, S.J., and Frenette, B.J. 1995. Assessment of resident cutthroat trout, Dolly Varden char and introduced anadromous salmonid in Margaret Lake. Progress Report for 1994. USDA-PNW Research Station, Forestry Sciences Laboratory, Juneau, Alaska.

Cartwright, M.A., and Beauchamp, D.A. 1995. Piscivory on juvenile sockeye salmon in Margaret Lake, Alaska. 1994 Progress Report. U.S. Forest Service, Forestry Sciences Laboratory, Juneau, Alaska.

Cummins, K.W., and Wuycheck, J.C. 1971. Caloric equivalents for investigations in ecological energetics. Mitt. Int. Ver. Theor. Angew. Limnol. **18**: 1–151.

DeCino, R.D. 1992. Investigation on the effects of introduced sockeye salmon on growth, abundance, and utilization of forage resources in a small oligotrophic lake located in Southeast Alaska. M.S. thesis, Utah State University, Logan, Utah.

Der Hovanisian, J.A., and Marshall, R.P. 1995. Abundance and size of cutthroat trout at Baranof Lake, Southeast Alaska, 1994. Alaska Dep. Fish Game Fish. Data Ser. No. 95-27.

Elliott, J.M. 1972. Rates of gastric evacuation in brown trout, *Salmo trutta* L. Freshwater Biol. **2**: 1–18.

Elliott, J.M. 1991. Rates of gastric evacuation in brown trout, *Salmo trutta*. Freshwater Biol. **25**: 297–305.

Elliott, J.M., and Persson, L. 1978. The estimation of daily rates of food consumption for fish. J. Anim. Ecol. **47**: 977–991.

Foerster, R.E. 1968. The sockeye salmon, *Oncorhynchus nerka*. Bull. Fish. Res. Board Can. No. 162.

Foster, J.R. 1977. Pulsed gastric lavage: an efficient method of removing the stomach contents of live fish. Prog. Fish-Cult. **39**: 166–169.

Frenette, B.J., and Bryant, M.D. 1994. Assessment of resident cutthroat trout, Dolly Varden char and introduced anadromous salmonids in Margaret Lake. Progress Report for 1993. USDA-PNW Research Station, Forestry Sciences Laboratory, Juneau, Alaska.

Hansen, M.J., Boisclair, D., Brandt, S.B., Hewett, S.W., Kitchell, J.F., Lucas, M.C., and Ney, J.J. 1993. Applications of bioenergetics models to fish ecology and management: where do we go from here? Trans. Am. Fish. Soc. **122**: 1019–1030.

Hewett, S.D., and Johnson, B.J. 1992. Fish bioenergetics model 2. Univ. Wisc. Sea Grant Tech. Rep. WIS-SG-(2-250).

Kitchell, J.F., Stewart, D.J., and Weininger, D. 1977. Applications of a bioenergetics model to yellow perch (*Perca flavescens*) and walleye (*Stizostedion vitreum vitreum*). J. Fish. Res. Board Can. **34**: 1922–1935.

Koenings, J.P., and Burkett, R.D. 1987. Population characteristics of sockeye salmon (*Oncorhynchus nerka*) smolts relative to temperature regimes, euphotic volume, fry density, and forage base within Alaskan lakes. *In* Sockeye salmon (*Oncorhynchus nerka*) population biology and future management. *Edited by* H.D. Smith, L. Margolis, and C.C. Wood. Can. Spec. Publ. Fish. Aquat. Sci. No. 96. pp. 216–234.

© 1998 NRC Canada

Madon, S.P., and Culver, D.A. 1993. Bioenergetics model for larval and juvenile walleyes: an *in situ* approach with experimental ponds. Trans. Am. Fish. Soc. **122**: 797–813.

Ney, J.J. 1990. Trophic economics in fisheries: assessment of demand–supply relationships between predators and prey. Rev. Aquat. Sci. **2**: 55–81.

Peterman, R.M., and Gatto, M. 1978. Estimation of functional responses of predators on juvenile salmon. J. Fish. Res. Board Can. **35**: 797–808.

Post, J.R. 1990. Metabolic allometry of larval and juvenile yellow perch (*Perca flavescens*): in situ estimates and bioenergetic models. Can. J. Fish. Aquat. Sci. **47**: 554–560.

Rowan, D.J., and Rasmussen, J.B. 1996. Measuring the bioenergetic cost of fish activity in situ using a globally dispersed radiotracer (^{137}Cs). Can. J. Fish. Aquat. Sci. **53**: 734–745.

Ruggerone, G.T., and Rogers, D.E. 1992. Predation on sockeye salmon fry by juvenile coho salmon in Chignik Lakes, Alaska: implications for salmon management. North Am. J. Fish. Manage. **12**: 87–102.

Tang, M., and Boisclair, D. 1995. Relationship between respiration rate of juvenile brook trout (*Salvelinus fontinalis*), water temperature, and swimming characteristics. Can. J. Fish. Aquat. Sci. **52**: 2138–2145.

Thorne, R.E. 1988. An empirical evaluation of the duration-in-beam technique for hydroacoustic estimation. Can. J. Fish. Aquat. Sci **45**: 1244–1248.

Zadina, T., and Haddix, M. 1989. Fry stocking program in Southeast Alaska. *In* Proceedings of the 1989 Alaska Sockeye Culture Workshop, Soldotna, Alaska. *Edited by* T. Ellis. Alaska Dep. Fish and Game, Juneau, Alaska.

© 1998 NRC Canada

PERSPECTIVE

Sonar systems and aquatic organisms: matching equipment and model parameters[1]

John K. Horne and Clarence S. Clay

Abstract: Acoustic technology is an accepted and important component of aquatic research and resource management. Despite the widespread use of echosounders, few guidelines aid in the choice of appropriate sonar system parameters for acoustic surveys. Choice of acoustic carrier frequency is analogous to the choice of spotlight colour used to illuminate a painting. Three primary biological factors influence the scattering of sound by aquatic organisms: swimbladder presence, organism length, and organism behaviour. We illustrate the influence of these factors on the amplitude of backscattered echoes using a Kirchhoff-ray mode scattering model to quantify fish and zooplankton backscatter as a function of carrier frequency, fish length, and swimbladder aspect. Model results illustrate that echo amplitudes from aquatic organisms are largely dependent on the presence or absence of a swimbladder. Target strengths generally increase with increasing carrier frequency and organism length. Swimbladder angle relative to the incident sound wave affects scattering amplitudes at all frequencies. Measurements of backscatter from swimbladdered fish are relatively robust when the ratio of fish length to acoustic frequency wavelength ranges between 2 and 10. As fish length to frequency wavelength ratios increase, echo amplitudes become more dependent on aspect and peak when the swimbladder is perpendicular to the acoustic wavefront.

Résumé : La technologie acoustique est un élément accepté et important de la recherche et de la gestion des ressources aquatiques. Malgré l'utilisation répandue des échosondeurs, il existe peu de lignes directrices qui aident à choisir les paramètres du système sonar convenant aux relevés acoustiques. Le choix de la fréquence porteuse est analogue au choix de la couleur d'un projecteur utilisé pour éclairer une peinture. Trois facteurs biologiques majeurs influent sur la diffusion du son par les organismes aquatiques : la présence d'une vessie natatoire, la longueur de l'organisme visé et son comportement. Nous illustrons l'effet de ces facteurs sur l'amplitude des échos rétrodiffusés à l'aide d'un modèle de diffusion des modes de rayonnement de Kirchhoff pour quantifier la rétrodiffusion due aux poissons et au zooplancton en tant que fonction de la fréquence porteuse, de la longueur des poissons et de l'aspect de la vessie natatoire. Les résultats du modèle indiquent que l'amplitude de l'écho provenant d'organismes aquatiques dépend largement de la présence ou de l'absence d'une vessie natatoire. L'intensité de cible augmente généralement en fonction de l'augmentation de la fréquence porteuse et de la longueur de l'organisme. L'angle de la vessie natatoire relativement à l'onde sonore incidente affecte l'amplitude de diffusion à toutes les fréquences. Les mesures de la rétrodiffusion provenant des poissons avec vessie natatoire sont relativement robustes lorsque le rapport entre la longueur des poissons et la longueur d'onde de la fréquence acoustique se situe entre les valeurs 2 et 10. À mesure que ce rapport augmente, l'amplitude des échos dépend de plus en plus de l'aspect de la vessie et atteint un maximum lorsque celle-ci est perpendiculaire au front d'onde acoustique.
[Traduit par la Rédaction]

Introduction

Recent advances in sonar technology have increased the use of acoustic data in aquatic ecosystem research and in the management of harvestable resources. Federal governments, including Canada (cf. McFarlane and Kieser 1993), are increasing resources for use in acoustic research and surveys. These surveys quantify distributions, densities, and sizes of

Received March 24, 1997. Accepted December 5, 1997.
J13926

J.K. Horne.[2] Great Lakes Center, State University of New York at Buffalo State College, 1300 Elmwood Avenue, Buffalo, NY 14222-1095, U.S.A.
C.S. Clay. Department of Geology and Geophysics, University of Wisconsin–Madison, 1215 West Dayton Street, Madison, WI 53706, U.S.A.

[1] Contribution No. 581 of the Geophysical and Polar Research Center, University of Wisconsin, Madison, WI.
[2] Author to whom all correspondence should be addressed. Present address: Cooperative Institute for Limnology and Ecosystems Research, 2205 Commonwealth Boulevard, Ann Arbor, MI 48105, U.S.A. e-mail: horne@glerl.noaa.gov

© 1998 NRC Canada

Table 1. Summary of acoustic scattering models and measures of aquatic organisms or anatomical structures.

Organism or structure	Geometric form or measurement	Reference(s)
Zooplankton	Fluid-filled spheres	Anderson 1950; Johnson 1977*a*; Greenlaw 1977; Holliday and Pieper 1980
	Fluid-filled cylinders	Stanton 1988, 1989, 1990
	Bent, fluid-filled cylinders	Stanton 1988; Foote et al. 1990; Chu et al. 1993
Fish body	Gas-filled sphere	Hersey and Backus 1962; Andreeva and Chindinova 1964; Chapman and Marshall 1966
	Array of point scatterers	Huang and Clay 1980; Clay and Heist 1984
Fish swimbladder	Gas-filled spherical bubbles	Minnaert 1933; Andreeva 1964; Haslett 1965; Batzler and Pickwell 1970
	Gas-filled spheroid bubbles	Strasberg 1953; Devin 1959; Weston 1967; McCartney and Stubbs 1971; Love 1977, 1978; Furusawa 1988
	Gas-filled cylinders	Haslett 1965, 1966
Whole fish	Gas-filled swimbladder	Foote 1985; Ye and Farmer 1994
	Gas- and fluid-filled cylinders	Clay 1991, 1992
Empirical models	Literature review	Love 1971
	Caged	McCartney and Stubs 1971; Johannesson and Losse 1977; Foote 1983, 1986; Foote et al. 1990
	Tethered	Smith 1954; Hasimoto and Maniwa 1956; Harden Jones and Pearce 1958; Nakken and Olsen 1977; Foote 1983
	In situ	Traynor and Ehrenberg 1979; Foote 1987; Foote and Traynor 1988; Rose and Leggett 1988
	Statistical	Craig and Forbes 1969; Ehrenberg 1972; Peterson et al. 1976; Robinson 1978; Clay 1983

organisms through the entire water column over large geographic areas. Accurate conversions of acoustic data to population estimates require an understanding of the acoustic scattering properties of fish and invertebrates. Population estimates are based on theoretical, empirical, and statistical models of backscattering cross section or target strengths of aquatic organisms. We propose that the integration of theoretical acoustic models with empirical measures of backscatter forms a logical approach to understanding the biological scattering of sound.

Models and measures of acoustic scattering by zooplankton, fish and their swimbladders are continuously evolving (Table 1). Zooplankton have been modeled as fluid-filled spheres and bent, fluid-filled cylinders. Early swimbladder models were based on gas-filled spherical or spheroid bubbles and gas-filled cylinders. The fish body was first modeled as a gas-filled sphere, which ignored the shape of the animal. Arrays of point scatterers have also been used to model the fish body form. More anatomically correct models use fluid-filled cylinders for zooplankton or a combination of gas- and fluid-filled cylinders for fish. Empirical scattering models of fish and zooplankton are derived using backscattered echo measurements and scattering lengths of caged, tethered, or free-ranging organisms. Statistical models of fish backscatter assume a theoretical, or tabulate an empirical, probability density function (PDF) of scattering amplitudes within an insonified beam.

The diversity of acoustic backscatter models and the range of commercially available sonar frequencies emphasizes the need for a general acoustic model of aquatic organisms. Simple geometric shapes regularly used in theoretical acoustic models inadequately represent asymmetrically shaped swimbladders (Foote 1985). Moreover the presence, structure, and orientation of swimbladders in fish is species dependent

© 1998 NRC Canada

(cf. Jones and Marshall 1953; Whitehead and Blaxter 1964; Alexander 1970). An ideal, general model must accurately represent anatomical structures of a large number of fish and zooplankton species, be applicable over wide ranges of organism lengths and acoustic frequencies, and include low-frequency resonance for species containing a swimbladder or other gas filled organ.

Despite the long awareness of frequency-dependent scattering by aquatic organisms (e.g., Hersey and Backus 1954; McNaught 1968, 1969), few general guidelines aid in the selection of sonar frequencies and other system parameters for bioacoustical research. One rule of thumb commonly used by fisheries scientists is "the smaller the organism, the higher the frequency." This strategy is based on observations that echo amplitudes from zooplankton decrease rapidly when the wavelength of sound, λ, is greater than the circumference of the organism (Anderson 1950; McNaught 1968, 1969; Greenlaw 1979). This results in larger echo amplitudes at high frequency (i.e., short λ) compared with echo amplitudes from the same organism observed at low frequency (i.e., long λ).

Aquatic organisms scatter sound in a complicated matter, and this general guideline is not without caveats. Simply increasing the carrier frequency will not avoid additional complications caused by frequency-dependent scattering. Martin et al. (1996) showed that target strengths of decapod shrimp decreased 10 dB when the carrier frequency was increased from 400 to 500 kHz. To address this problem, Greenlaw (1977) and Holliday and Pieper (1980) used simple theoretical models and measures of zooplankton backscatter to demonstrate that multiple frequency sonar data can be used to measure sizes of individuals and identify constituent species within zooplankton aggregations. A second limitation is the ability of an echosounder to resolve individual targets within the sonar beam. Increasing the carrier frequency of an echosounder reduces the wavelength and potentially increases target resolution. Unfortunately, an increase in frequency without an increase in transmission power reduces the effective range of the echosounder. Assuming negligible transducer motion, the ability to separate echoes from a pair of targets is dependent on the effective ping duration of the sonar system and the speed of sound in water. The minimum resolvable distance between two targets is equal to one-half the effective ping duration multiplied by the sound speed. Minimum ping duration of a sonar system is determined by the resonant frequency of the transducer and a quality factor of the transducer, Q. Most transducers are like bells, they transmit 10–20 cycles of sound at their resonant frequency with decreasing amplitude after being excited. High-frequency transducers typically have shorter minimum ping durations than low-frequency transducers. However, if two echosounders have different frequencies but the same effective ping duration then the resolution of the two systems is the same.

Sound-scattering characteristics of swimbladdered fish differ from those of similar sized zooplankton. Gas-filled swimbladders resonate sound at wavelengths, λ, that are many times larger than the length of the fish, L. The backscattering cross section, σ_{bs}, from any fish is dependent on acoustic carrier frequency over a large range of L/λ. Furusawa (1991) recommends that a value of $L/\lambda \geq 2$ provides relatively robust measures of sound scatter by aquatic organisms.

Logistic constraints, such as the size of a transducer or the required depth of observations, may influence the choice of acoustic carrier frequency, but we believe that organism morphology and behaviour should be included in the criteria used to select carrier frequency. Sonar carrier frequencies commercially available for fisheries research range from 12 to 420 kHz. Low carrier frequencies are primarily limited by transducer dimensions, while sound absorption in sea water often limits the maximum carrier frequency. In this paper, we use a Kirchhoff-ray mode model (Clay and Horne 1994) as a representative scattering model to demonstrate the dependence of echo amplitude on acoustic carrier frequency, organism length, body morphology, and angle of swimbladder relative to the incident sound wave. This model is used to calculate species-, angle-, and frequency-dependent acoustic backscatter from aquatic organisms and to guide the choice of carrier frequencies and system parameters for acoustic measurements.

Quantifying acoustic scattering

Returned echoes received at a sonar transducer are measured as pressures. Transducers used in fisheries research typically use the same elements to transmit and receive sound. Echoes returning to the transducer are said to be backscattered sound. The pressure of backscattered sound p_{scat} (units μPa) is calculated as

$$(1) \qquad p_{scat} = D_t D_r \frac{[p_0 R_0]}{R^2} l_{bs}$$

where D_t is the transmitting beam pattern or directivity of the transducer, D_r is the receiving beam pattern of the transducer, p_0 is the on-axis source sound pressure at a reference range, R_0, of 1 m; R is the range (units m) to the scattering object, and l_{bs} is the scattering length (units m) of the scattering object. The combination of terms $(p_0 R_0)$ is the source calibration of the sonar. Equation 1 is a form of the sonar equation and can be rearranged to provide a solution for scattering length l_{bs}:

$$(2) \qquad l_{bs} = \frac{p_{scat} R^2}{D_t D_r [p_0 R_0]}$$

A variety of derived terms have been used to quantify the scattering of sound by aquatic organisms. Backscattering length, l_{bs}, is dependent on the acoustic frequency, f, or wave number, $k = 2\pi/\lambda$ (where λ is the wavelength, units m), the equivalent spherical radius of the organism, a (units m), L (units m), and the angle of the organism relative to the sonar beam χ (units degrees). The square of the absolute scattering length is σ_{bs} (Clay and Medwin 1977):

$$(3) \qquad \sigma_{bs} = |l_{bs}|^2$$

The logarithmic transformation of back scattering cross section is the target strength, TS (units dB):

$$(4) \qquad TS = 10 \log_{10}(\sigma_{bs}/L_0^2) = 20 \log_{10}(|l_{bs}|/L_0)$$

where L_0 is the reference length, typically 1 m.

© 1998 NRC Canada

Fig. 1. Schematic diagram illustrating the geometric construction of Kirchhoff-ray mode acoustic models of an Atlantic cod (*Gadus morhua*) in (*a*) lateral and (*b*) dorsal view. The fish body and swimbladder are represented by a series ($j = 1, 2, ..., n$) of short, fluid- (body) and gas- (swimbladder) filled cylinders. χ is the aspect angle of the swimbladder measured relative to the longitudinal axis of the fish. (*c*) Coordinate systems used in model calculations. The ray path from the transducer and its normals form directions of the *x*, *y*, *z* coordinate system (solid lines). The *u*, *v*, *w* coordinate system is relative to the fish (broken lines).

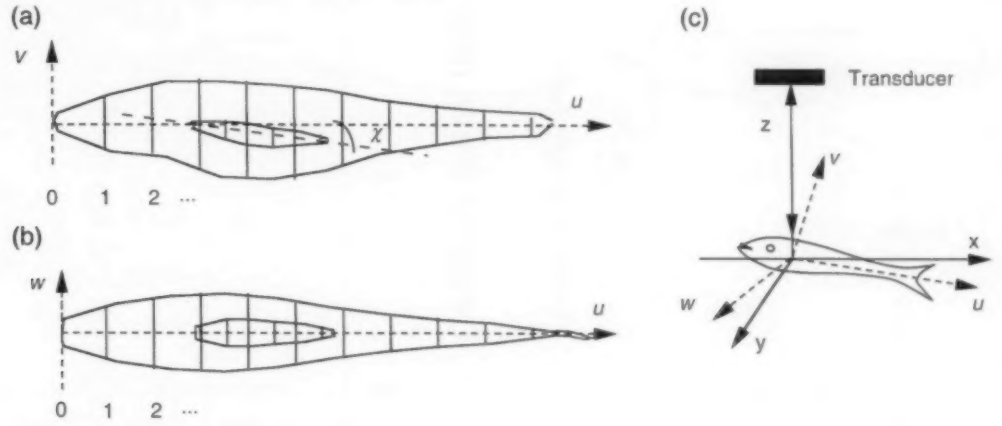

Fig. 2. (*a*) Lateral and (*b*) dorsal X-ray images of a 323-mm, 286-g Atlantic cod (*Gadus morhua*). The swimbladder is silhouetted in the body. Corresponding (*c*) lateral and (*d*) dorsal digitized images of the same cod used in the Kirchhoff-ray mode acoustic model.

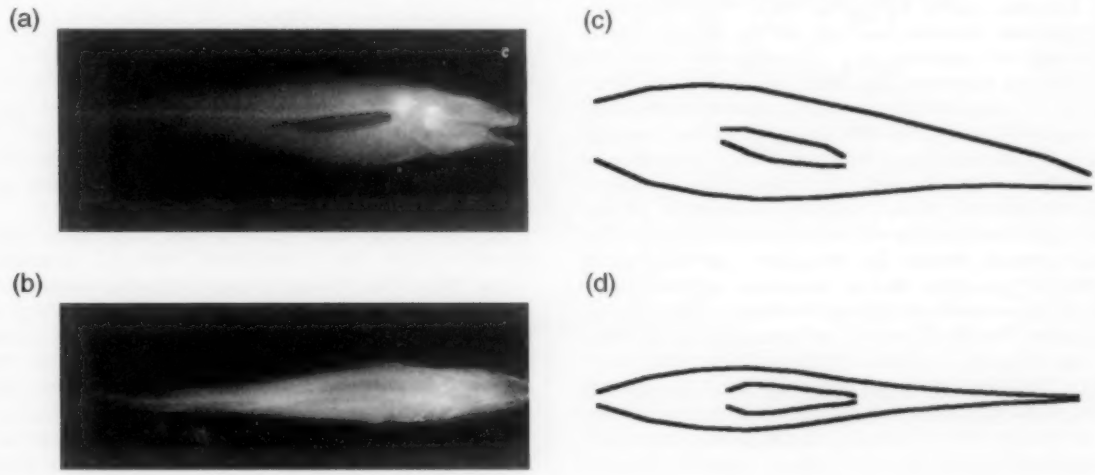

The following "reduced" quantities are convenient as scattering length is often proportional to L:

(5) Reduced scattering length = l_{bs}/L

(6) Reduced backscattering cross section = σ_{bs}/L^2

Reduced scattering lengths and reduced backscattering cross sections are dimensionless quantities. The reduced TS is calculated as

(7) $TS_{reduced} = 10 \log_{10}(\sigma_{bs}/L^2) = 20 \log_{10}(|l_{bs}|/L)$

We compute echo amplitudes as reduced scattering lengths to standardize the effect of organism length and then convert to TS (units dB) to provide familiar units to fisheries readers.

Model structure

Foote (1985) and Foote and Traynor (1988) developed an accurate and elaborate method to calculate the scattering of sound by swimbladdered fish. Clay and Horne (1994) simplified this technique by modeling a fish's body and swimbladder as a set of fluid- and gas-filled cylinders (Fig. 1). In the original model, fish bodies and swimbladders were digitized from dorsal and lateral X-ray images (Fig. 2) of Atlantic cod (*Gadus morhua*). Either a gas-filled prolate spheroid or a low-mode cylinder solution can be used to compute the scattering

© 1998 NRC Canada

Fig. 3. Reduced scattering lengths of a Kirchhoff-ray mode modeled swimbladder, fish body, and whole fish plotted as a function of fish length to wavelength ratio L/λ. Calculations were based on a 323-mm Atlantic cod (*Gadus morhua*).

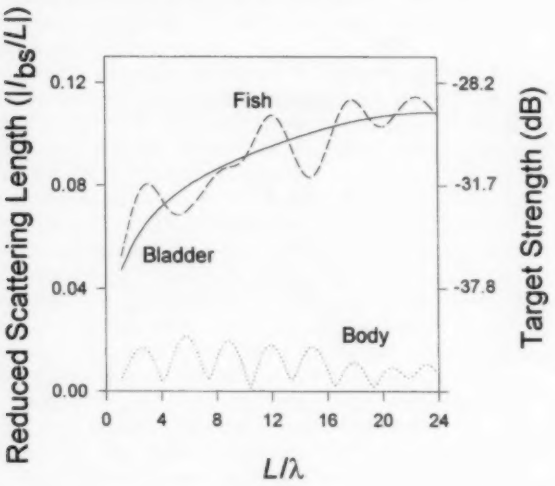

Fig. 4. Target strengths (dB) of a 323-mm Atlantic cod (*Gadus morhua*) scaled to 50, 100, 200, and 400 mm plotted as a function of frequency (kHz).

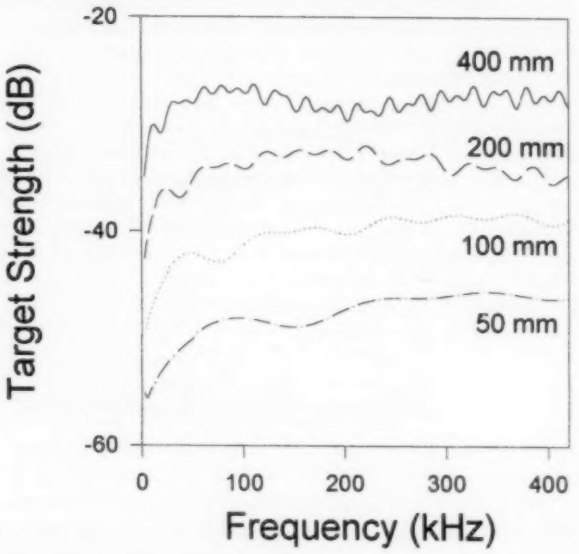

length of the swimbladder at the low-frequency, breathing-mode resonance (Love 1978; Clay 1992). Low-frequency, breathing-mode resonance has been used to identify species in ensembles of organisms (e.g., Greenlaw 1979; Holliday 1980; Zakharia and Sessarego 1982), but breath-mode resonance is very dependent on organism behaviour (Feuillade and Nero 1998) and recent depth history (Sand and Hawkins 1973). A low-mode solution for a gas-filled cylinder is used to compute the low-frequency, breathing-mode resonance. At high frequencies, $L/\lambda > 1$, sound is scattered by the top surface of the swimbladder and is independent of depth. The acoustic contrast between the top surface and the rest of swimbladder is so large that all anatomical structure below the top surface contributes little to the sound scattered by the swimbladder. We use Kirchhoff-ray approximations to compute high-frequency acoustic scattering (Foote 1985; Clay 1991) by the swimbladder and by the fish body. Backscatter from the swimbladder and fish body are then summed to estimate backscatter from the whole fish. Backscatter from non-swimbladdered aquatic organisms such as zooplankton can be estimated by omitting the backscatter from the swimbladder.

Biological influences on scattered sound

Aquatic organisms are complicated scatterers by nature of their shape (cylindrical or spheroid), deformation (curvature of the body and swimbladder), and composition (exoskeleton, muscle, bone, fat, presence and shape of swimbladder). The presence of a swimbladder is the most important factor affecting the amplitude of a returned echo. Swimbladders provide a large acoustic contrast to flesh or skeletal elements and form the major (≥90%; Foote 1980*a*) source of backscattered sound in teleost fish. For typical fish lengths (1–100 cm), swimbladders scatter sound over a range of three orders of frequency magnitude (hundreds of Hz to hundreds of kHz). Acoustic scattering by a swimbladder is four or more times greater than the scattering by fish bodies at any given frequency (Fig. 3). Frequency-dependent changes in the magnitude of backscatter for the entire fish are primarily due to the morphology of the swimbladder; oscillations in scattering magnitudes are primarily due to the fish body. As examined below, these frequency-dependent oscillations also depend on the aspect of the swimbladder relative to the incident sonar beam.

At low frequencies (ca. 100–1000 Hz), backscattered sound is largely due to resonance within the swimbladder (Clay 1991, 1992). Variability in swimbladder resonance due to differences in swimbladder size and morphology can potentially be used to help identify fish species in acoustic data. Empirical measures of resonance scattering by swimbladdered fish have been used to identify and estimate numbers of commercial fish species (e.g., Holliday 1972; Love 1993). This is not a common practice in fisheries research, as the resonance frequency region is lower than normal operating frequencies of fisheries echosounders. At high frequencies (>1000 Hz), sound is reflected from the upper surface of the swimbladder and is not significantly influenced by fish depth, stomach fullness, or gonad development.

A second factor influencing the amplitude of acoustic backscatter is organism length. Backscatter from a 323-mm X-rayed cod (Fig. 2), scaled from 50 to 400 mm, was calculated using the Kirchhoff-ray mode model, converted to target strengths, and plotted as a function of frequency. Clay and Horne (1994) found that for comparative purposes, cod could be linearly scaled to a common length. Target strength generally increases with increasing frequency and length of an animal (Fig. 4). The overall "shape" of the scattering curve is due to backscatter by the swimbladder. Transition from resonant to geometric scattering by the swimbladder occurs below 1 kHz. Comparison of the 50–400 mm scattering curves illus-

© 1998 NRC Canada

Fig. 5. Reduced scattering lengths of a 60-mm calanoid zooplankter scaled to (*a*) 10, (*b*) 20, and (*c*) 40 mm plotted as a function of frequency.

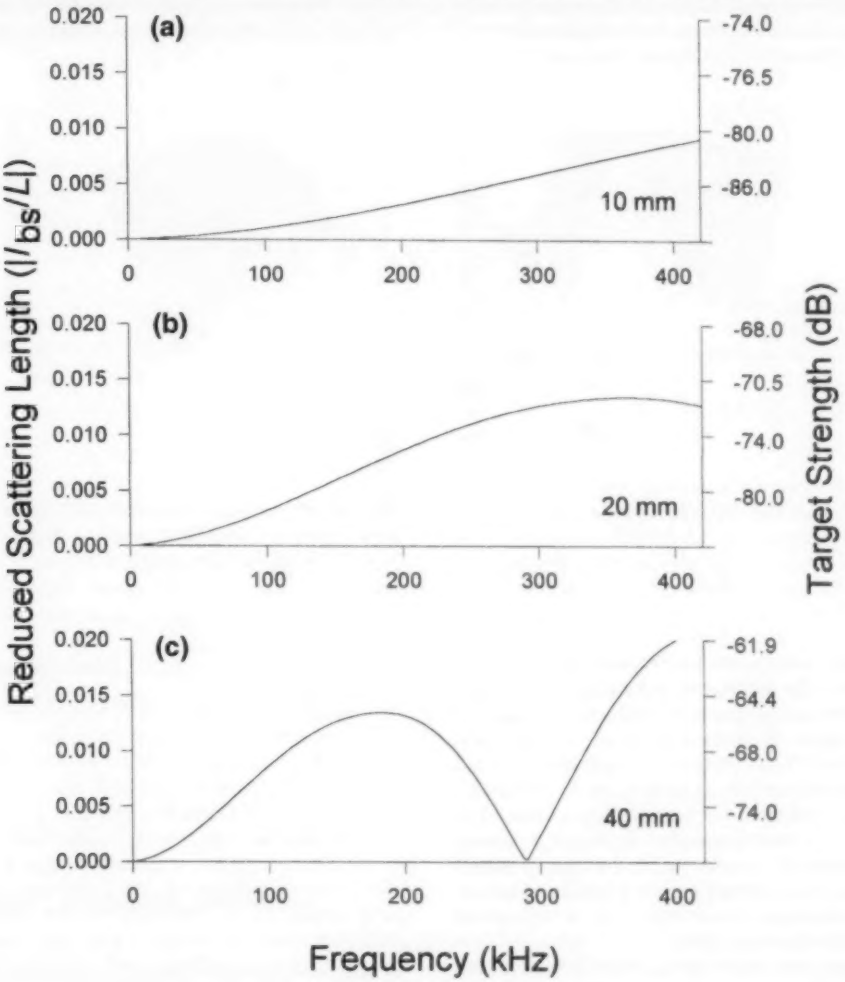

trates how the influence of the fish body on the scattering curve increases as fish length increases.

The frequency dependence of scattering amplitude on organism length is also observed among non-swimbladdered animals. The Kirchhoff-ray mode model can be used to estimate backscatter from non-swimbladdered fish or zooplankton. As an example, acoustic backscatter of a 60-mm decapod zooplankter was estimated at three lengths and plotted as a function of frequency (Fig. 5). Reduced scattering lengths of zooplankton are an order of magnitude lower than those of swimbladdered fish (Fig. 4) and do not contain frequency-dependent, small-amplitude oscillations present in the scattering curves of fish. The general monotonic increase in backscatter with increasing fish length does not occur across all frequencies for zooplankton.

The angle of an organism's swimbladder relative to the incident sound wave affects scattering amplitudes at all frequencies. Midttun (1984) reviews studies that cite the dependence of target strength on fish aspect angle. Olsen (1977) and Foote (1980*b*) have developed models to predict mean target strength of Atlantic cod based on fish aspect distributions and transducer beam patterns. Swimbladder angles typically differ from fish body aspects by 5–10° (see Fig. 1). For example, the swimbladder in the 323-mm cod deviates 5° from horizontal with the posterior end of the swimbladder pointed downward (Fig. 2). Reduced scattering lengths of the 323-mm cod scaled to 150 mm were computed for L/λ values of 1, 4, 12, and 20 and plotted as a function of aspect angles ranging from –25° to 15° (Fig. 6). The swimbladder is perpendicular to the incident sound wave at –5° from horizontal. At low L/λ values, scattering amplitudes are almost independent of aspect angle. As L/λ values increase, scattering lengths become more dependent on aspect and peak when the swimbladder is perpendicular to the acoustic wavefront. At $L/\lambda = 20$, scattering lengths range from 0.01 to 0.12, which is equivalent to a target strength change of 20 dB. Insonifying a single animal that varies its aspect or insonifying an aggregation of animals oriented at a variety of angles will result in a distribution of echo amplitudes.

In mobile surveys, it should be noted that the combination

© 1998 NRC Canada

Fig. 6. Reduced scattering lengths of a 323-mm Atlantic cod (*Gadus morhua*) scaled to 150 mm and plotted as a function of swimbladder deviation from horizontal for fish length to wavelength ratios: L/λ = 1 (solid line), 4 (broken line), 12 (dotted line), and 20 (dash-dot line).

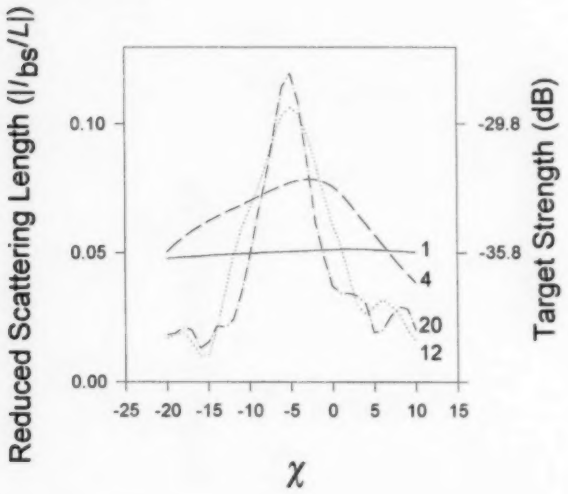

of narrow-beam transducers (<10°; Furusawa 1991), transducer motion, and aspect angle potentially bias acoustic data to smaller target strengths because of a reduction in apparent equivalent beam angle. With as little as 4° of transducer motion, Stanton (1982) found that echo amplitudes of a fish at 400 m deviated by as much as 64% for a 5° beamwidth transducer but only 1.4% for a 40° beamwidth transducer. For any individual fish, this bias diminishes at lower frequencies as L/λ decreases. It may be possible to use data from multiple or broadband sonars to determine aspect deviation of insonified targets by comparing target strengths to L/λ ratios (cf. Furusawa and Miyanohana 1990).

Repeated measures of a single fish at different aspects produces a PDF of scattering lengths. We tabulated the probability of reduced scattering lengths for a 323-mm cod over a uniformly distributed range of angles from –25° to 15° for the five common fisheries acoustic frequencies (Fig. 7). In general, the range of scattering lengths with a probability of occurring greater than 4% (arbitrary level) increases with an increase in acoustic carrier frequency. This is attributed to larger differences in scattering amplitudes as the swimbladder aspect deviates (positive or negative) from horizontal at higher frequencies (see Fig. 6). These empirical probability distributions could also be modeled using a theoretical Rician PDF. Clay and Heist (1984) use the mean backscattering cross section $\overline{\sigma_{bs}}$ and γ to parameterize Rician PDFs of fish backscatter. γ is the ratio of the concentrated or mean backscattering cross section $\overline{\sigma_{bs}}$ to the distributed or random component of the backscattering cross section σ_d:

$$(8) \qquad \gamma = \frac{\overline{\sigma_{bs}}}{\sigma_d}$$

The value of γ has been shown to depend on fish morphology, behaviour, and L/λ. Values of small fish are larger than those

Fig. 7. Probability of backscatter (%) from a 323-mm Atlantic cod (*Gadus morhua*) at (*a*) 38, (*b*) 70, (*c*) 120, (*d*) 200, and (*e*) 420 kHz plotted as a function of reduced scattering length.

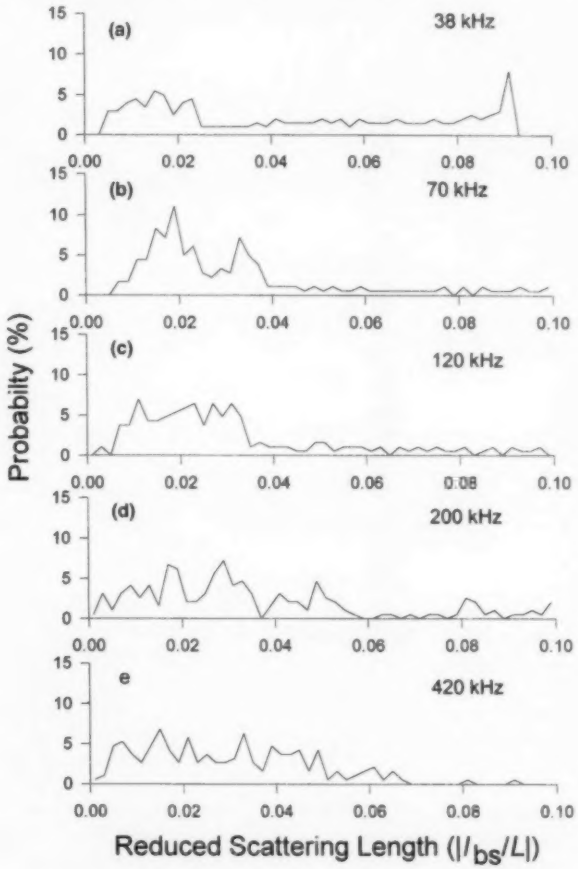

of large fish. As L/λ increases, γ decreases and tends to zero for $L/\lambda > 12$. Rician PDFs have been used to model the distribution of echo amplitudes in decapod shrimp (Wiebe et al. 1990) and to compare γ values from zooplankton (Stanton et al. 1993) and fish (Trevorrov 1996) aggregations. A reason for using theoretical PDFs for descriptions of echo amplitudes is that, if target species and behaviour are known, comparison of echo statistics such as γ from multiple frequencies may provide a way to differentiate among targets in acoustic survey data (Jech et al. 1995).

To summarize factors influencing acoustic backscatter of swimbladdered fish, target strengths of the scaled 150-mm Atlantic cod were plotted as a function of the ratio of organism length to acoustic wavelength and aspect angle (Fig. 8). Unless a fish's swimbladder is near orthogonal (90 ± 2°) to the face of the transducer, target strengths decrease as L/λ increases (Fig. 8*a*). The drop in target strengths is nonmonotonic and decreases three and one-third times the maximum (i.e., 20 dB) over a L/λ range of 1–20. The dependence of target strength on swimbladder aspect is emphasized by rotating the three-dimensional mesh diagram (Fig. 8*b*). As χ deviates from horizontal, target strengths decrease. Decreases

© 1998 NRC Canada

Fig. 8. (*a*) Modeled target strengths from a 323-mm Atlantic cod (scaled to 150 mm) plotted as a function of length to wavelength ratio, L/λ, and aspect angle, χ. (*b*) Plot was rotated to emphasize changes in target strength as fish aspect deviates from horizontal. Maximum target strength is at –5°, which corresponds to the aspect of the swimbladder relative to the longitudinal axis of the fish (see Figs. 2*a* and 2*c*).

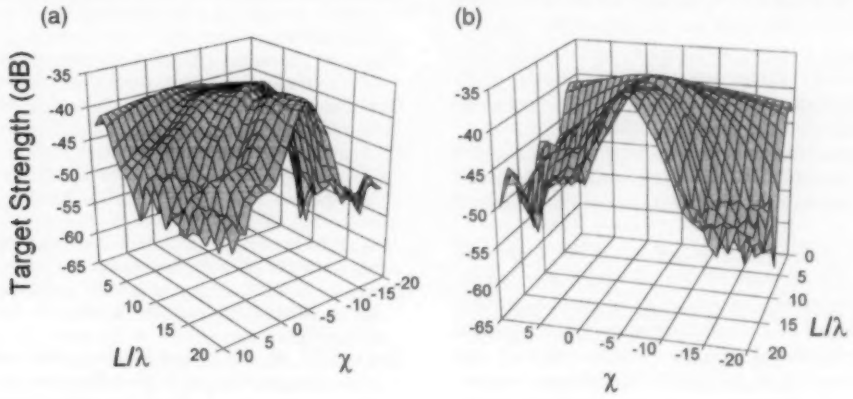

in target strengths are greater at higher values of L/λ. At high L/λ values, the curve is almost symmetric about the maximum scattering amplitude. Target strengths range 20 dB within 15° of horizontal. Fish length, carrier frequency, and fish aspect all interact to influence the magnitude of returned echoes.

Acoustic constraints

Organism behaviour combined with variation in morphology complicates the calculation of organism lengths from target strengths (Nakken and Olsen 1977; Huang and Clay 1980; Ehrenberg et al. 1981) and potentially influences precision in estimates of organism number or biomass (Hawkins 1981). Exclusive reliance on empirical backscatter measurements in a regression equation does not ensure accurate conversion of acoustic sizes to organism lengths. An implicit assumption in this approach is that animals insonified by the echosounder are within the same length range used to determine the statistical relationship between fish length and amplitude of returned echo. The range of target strengths that can be converted to fish lengths should not be extrapolated beyond the limits of data used to establish the relationship. A second common assumption is that statistical relationships between echo amplitudes and fish lengths are independent of acoustic frequency. We have shown that backscatter amplitudes are dependent on fish species, fish aspect, fish length, and acoustic carrier frequency. Theoretical acoustic models of swimbladdered and non-swimbladdered organisms are needed to explain variability in backscatter measurements, to improve estimation of animal length from acoustic target size, and to improve target recognition and discrimination among types of acoustic backscatterers (e.g., swimbladdered from non-swimbladdered organisms).

The conversion of single-frequency acoustic sizes to organism lengths is also constrained by the ability of sonars to resolve single targets. Resolution of single targets depends on effective pulse duration, sonar beam width, the speed of sound in water, and organism density. Many species of aquatic organisms shoal or school at densities too high to acoustically discriminate among individuals (Dickie et al. 1983). In this situation, individuals on the periphery of an aggregation are often used to tabulate a length-frequency distribution of the group. This frequency distribution is used in a regression equation to estimate lengths and densities of organisms within an aggregation (e.g., Haslett 1969; Holliday and Pieper 1980; Ehrenberg et al. 1981). This approach assumes that the type and length-frequency distribution of organisms at the periphery matches that of individuals within the aggregation. This may not always be the case. Rose (1993) found that aggregations of migrating Atlantic cod were structured by fish length.

One way to resolve and size organisms within aggregations is to use multifrequency or broadband sonars and high-resolution signal processing (Holliday et al. 1989). Multifrequency sonars measure scattering amplitudes over a range of discrete frequencies, while broadband systems measure backscatter over a continuous frequency range and decompose echos into spectral components. Resolution of a target is based on the frequency-dependent relationship between target size and magnitude of returned echo (Holliday 1972, 1980). Acoustic scatter models can be combined with multifrequency or broadband data in the inverse approach to estimate length distributions of acoustic targets (e.g., Horne and Jech 1998). The inverse approach uses backscatter amplitudes from a known population to model types and length distributions of acoustic scatterers. This reference set is then used to estimate the abundance of animals in the water column. Integrated multifrequency sounder data have been used with the inverse approach to determine length-frequency distributions of zooplankton (Greenlaw 1979; Holliday 1980; Holliday et al. 1989; Pieper et al. 1990) and small fish (Johnson 1977*b*; Holliday 1980), to separate fish length distributions from those of plankton (Sætersdal et al. 1984; Cochrane et al. 1991), and in an attempt to classify fish by species (Zakharia and Sessarego 1982).

The number and type of sonar frequencies chosen for fisheries research is often constrained by hardware that is currently available, or by funds available to purchase new equipment. The complexity of choosing the right equipment is compounded when the geographic area of interest contains

© 1998 NRC Canada

more than one fish species in single or multispecies aggregations. We suggest three primary factors be assessed when choosing carrier frequencies for bioacoustic research:

(1) Presence of a swimbladder. If the species of interest does not have a swimbladder then the frequency that robustly maximizes backscattering amplitudes should be used to survey distributions. The presence of a swimbladder shifts the focus of frequency choice to the expected length and aspect distributions of the species of interest.

(2) Organism length. To avoid bias in acoustic backscatter measures and to aid in species identification of acoustic targets, frequencies should be chosen to restrict values of L/λ from 2 to 10.

(3) Organism behaviour. Shoaling and aspect angle are two behaviours that have large effects on backscatter amplitudes. If organisms shoal or school in single or multispecies aggregations, then multifrequency or broadband sonar systems combined with the inverse approach can be used to resolve and identify individual acoustic targets. When using single-frequency systems, sampling should be conducted when organisms are dispersed in the water column. If the species of interest has a wide distribution of aspect angles, the organism length to wavelength ratio should approximate 2 to minimize the dependence of scattering amplitude on aspect angle.

Acknowledgments

This work was supported in part by the National Science Foundation (OCE-9415740), the Office of Naval Research (N00014-89J-1515), the New York Sea Grant Institute (NA46RG0090), and the Geophysical and Polar research Center, University of Wisconsin (C.S.C.). We thank Dr. R. Kieser for a thorough review that improved the manuscript.

References

Alexander, R.M. 1970. Functional design in fishes. 2nd ed. Hutchinson, London.

Anderson, V.C. 1950. Sound scattering from a fluid sphere. J. Acoust. Soc. Am. **22**: 426–431.

Andreeva, I.B. 1964. Scattering of sound by air bladders of fish in deep sound-scattering layers. Sov. Phys. Acoust. **10**: 17–20.

Andreeva, I.B., and Chindinova, Y.G. 1964. On the nature of deep-scattering layers. Okeanologiya No. 4.

Batzler, W.E., and Pickwell, G.V. 1970. Resonant acoustic scattering from gas bladder fish. *In* Proceedings of an International Symposium on Biological Sound Scattering in the Ocean, March 31 – April 2, Wamenton, Virginia. *Edited by* G.B. Farquhar. U.S. Government Printing Office, Washington, D.C. pp. 168–179.

Chapman, R.P., and Marshall, J.R. 1966. Reverberation from deep scattering layers in the western North Atlantic. J. Acoust. Soc. Am. **40**: 405–411.

Chu, D., Foote, K.G., and Stanton, T.K. 1993. Further analysis of target strength measurements of Antarctic krill at 38 and 120 kHz: comparison with deformed cylinder model and inference of orientation distribution. J. Acoust. Soc. Am. **93**: 2985–2988.

Clay, C.S. 1983. Deconvolution of the fish scattering PDF from the echo PDF for a single transducer sonar. J. Acoust. Soc. Am. **73**: 1989–1994.

Clay, C.S. 1991. Low-resolution acoustic scattering models: fluid-filled cylinders and fish with swimbladders. J. Acoust. Soc. Am. **89**: 2168–2179.

Clay, C.S. 1992. Composite ray-mode approximations for backscattered sound from gas-filled cylinders and swimbladders. J. Acoust. Soc. Am. **92**: 2173–2180.

Clay, C.S., and Heist, B.G. 1984. Acoustic scattering by fish—acoustic models and a two-parameter fit. J. Acoust. Soc. Am. **75**: 1077–1083.

Clay, C.S., and Horne, J.K. 1994. Acoustic models of fish: the Atlantic cod (*Gadus morhua*). J. Acoust. Soc. Am. **96**: 1661–1668.

Clay, C.S., and Medwin, H. 1977. Acoustical oceanography. Wiley, New York.

Cochrane, N.A., Sameoto, D., Herman, A.W., and Neilson, J. 1991. Multiple-frequency acoustic backscattering and zooplankton aggregations in the inner Scotian Shelf basins. Can. J. Fish. Aquat. Sci. **48**: 340–355.

Craig, R.E., and Forbes, S.T. 1969. Design of a sonar for fish counting. Fiskeridir. Skr. Ser. Havunders. No. 15. pp. 210–219.

Devin, C., Jr. 1959. Survey of thermal, radiation and viscous damping of pulsating air bubbles in water. J. Acoust. Soc. Am. **31**: 1654–1667.

Dickie, L.M., Kerr, S.R., and Boudreau, P.R. 1983. An echo counting and logging system (ECOLOG) for demersal fish size distributions and densities. Can. J. Fish. Aquat. Sci. **40**: 487–498.

Ehrenberg, J.E. 1972. A method for extracting the fish target-strength distribution from acoustic echoes. *In* Proceedings of the 1972 IEEE Conference on Engineering and the Ocean Environment, September 13–15, Newport, R.I., U.S.A. Vol. 1. pp. 61–64.

Ehrenberg, J.E., Carlson, T.J., Traynor, J.J., and Williamson, J.J. 1981. Indirect measurement of the mean backscattering cross section of fish. J. Acoust. Soc. Am. **69**: 955–962.

Feuillade, C., and Nero, R.W. 1998. A viscous-elastic swimbladder model for describing enhanced-frequency resonance scattering from fish. J. Acoust. Soc. Am. **103**: 3245–3255.

Foote, K.G. 1980*a*. Importance of the swimbladder in acoustic scattering by fish: a comparison of gadoid and mackerel target strengths. J. Acoust. Soc. Am. **67**: 2084–2089.

Foote, K.G. 1980*b*. Averaging of fish target strength functions. J. Acoust. Soc. Am. 67: 504–515.

Foote, K.G. 1983. Linearity of fisheries acoustics, with addition theorems. J. Acoust. Soc. Am. **73**: 1932–1940.

Foote, K.G. 1985. Rather-high-frequency sound scattered by swimbladdered fish. J. Acoust. Soc. Am. **78**: 688–700.

Foote, K.G. 1986. A critique of Goddard and Welsby's paper: "The acoustic target strength of live fish." J. Cons. Cons. Int. Explor. Mer, **42**: 212–220.

Foote, K.G. 1987. Fish target strengths for use in echo integrator surveys. J. Acoust. Soc. Am. **82**: 981–987.

Foote, K.G., and Traynor, J.J. 1988. Comparison of walleye pollock target strength estimates determined from in situ measurements and calculations based on swimbladder form. J. Acoust. Soc. Am. **73**: 1932–1940.

Foote, K.G., Everson, I., Watkins, J.L., and Bone, D.G. 1990. Target strengths of Antarctic krill (*Euphausia superba*) at 38 and 120 kHz. J. Acoust. Soc. Am. **87**: 16–24.

Furusawa, M. 1988. Prolate spheroidal models for predicting general trends of fish target strength. J. Acoust. Soc. Jpn. Ser. E, **9**: 13–24.

Furusawa, M. 1991. Designing quantitative echo sounders. J. Acoust. Soc. Am. **90**: 26–36

Furusawa, M., and Miyanohana, Y. 1990. Behaviour and target-strength observation through echo traces of individual fish. Rapp. P.-v. Réun. Cons. Int. Explor. Mer, **189**: 283–294.

Greenlaw, C.F. 1977. Backscattering spectra of preserved zooplankton. J. Acoust. Soc. Am. **87**: 16–24.

Greenlaw, C.F. 1979. Acoustical estimation of zooplankton populations. Limnol. Oceanogr. **24**: 226–242.

Harden Jones, F.R., and Pearce, G. 1958. Acoustic reflection experiments with perch (*Perca fluviatilis* L.) to determine the proportion

© 1998 NRC Canada

of the echo returned by the swimbladder. J. Exp. Biol. **35**: 437–450.

Hasimoto, T., and Maniwa, Y. 1956. Study of reflection loss of ultrasonic millimeter wave on fish body. Tech. Rep. Fishing Boats No. 8.

Haslett, R.W.G. 1965. Acoustic backscattering cross sections of fish at three frequencies and their representation on a universal graph. Br. J. Appl. Phys. **16**: 1143–1150.

Haslett, R.W.G. 1966. Acoustic backscattering from an air-filled cylindrical hole embedded in a sound-translucent cylinder. Br. J. Appl. Phys. **17**: 549–561.

Haslett, R.W.G. 1969. The target strengths of fish. J. Sound Vib. **9**: 181–191.

Hawkins, A.D. 1981. Some biological sources of error in the acoustical assessment of fish abundance. *In* Proceedings of the Meeting on Hydroacoustical Methods for the Estimation of Marine Fish Populations, June 25–29, 1979. Vol. 2. *Edited by* J.B. Suomala. Draper Laboratories, Cambridge, Mass. pp. 1983–2000.

Hersey, J.G., and Backus, R.H. 1954. New evidence that migrating gas bubbles, probably the swimbladders of fish, are largely responsible for scattering layers on the continental rise south of New England. Deep-Sea Res. **1**: 190–191.

Hersey, J.G., and Backus, R.H. 1962. Sound scattering by marine organisms. Ch. 13. *In* The sea. Vol. 1. *Edited by* M.N. Hill. John Wiley & Sons, New York. pp. 499–507.

Holliday, D.V. 1972. Resonance structure in echoes from schooled pelagic fish. J. Acoust. Soc. Am. **51**: 1322–1332.

Holliday, D.V. 1980. Use of acoustic frequency diversity for marine biological measurements. *In* Advanced concepts in ocean measurements for marine biology. *Edited by* F.P. Diemer. Belle W. Baruch Libr. Mar. Sci. No. 10. pp. 423–460.

Holliday, D.V., and Pieper, R.E. 1980. Volume-scattering strengths and zooplankton distributions at acoustic frequencies between 0.5 and 3 MHz. J. Acoust. Soc. Am. **67**: 135–146.

Holliday, D.V., Pieper, R.E., and Kleppel, G.S. 1989. Determination of zooplankton size and distribution with multifrequency acoustic technique. J. Cons. Cons. Int. Explor. Mer, **46**: 52–61.

Horne, J.K., and Jech, J.M. 1998. Multi-frequency estimates of fish abundance: constraints of rather high frequencies. ICES J. Mar. Sci. In press.

Huang, K., and Clay, C.S. 1980. Backscattering cross sections of live fish: PDF and aspect. J. Acoust. Soc. Am. **67**: 795–802.

Jech, J.M., Schael, D.M., and Clay, C.S. 1995. Application of three sound scattering models to threadfin shad (*Dorosoma petenense*). J. Acoust. Soc. Am. **98**: 2262–2269.

Johannesson, K.A., and Losse, G.F. 1977. Methodology of acoustic estimating of fish abundance in some UNDP/FAO resource survey projects. Rapp. P.-v. Réun. Cons. Int. Explor. Mer, **170**: 296–318.

Johnson, R.K. 1977*a*. Sound scattering from a fluid sphere revisited. J. Acoust. Soc. Am. **62**: 375–377.

Johnson, R.K. 1977*b*. Acoustic estimation of scattering-layer composition. J. Acoust. Soc. Am. **61**: 1636–1639.

Jones, F.R.H., and Marshall, N.B. 1953. The structure and function of the teleostean swimbladder. Biol. Rev. **28**: 16–83.

Love, R.H. 1971. Measurements of fish target strength: a review. Fish. Bull. U.S. **69**: 703–715.

Love, R.H. 1977. Target strength of an individual fish at any aspect. J. Acoust. Soc. Am. **62**: 1397–1403.

Love, R.H. 1978. Resonant acoustic scattering by swimbladder-bearing fish. J. Acoust. Soc. Am. **64**: 571–580.

Love, R.H. 1993. A comparison of volume scattering strength data with model calculations based on quasisynoptically collected fishery data. J. Acoust. Soc. Am. **94**: 2255–2268.

Martin, L.V., Stanton, T.K., Wiebe, P.H., and Lynch, J.F. 1996. Acoustic classification of zooplankton. ICES J. Mar. Sci. **53**: 217–224.

McCartney, B.S., and Stubbs, A.R. 1971. Measurement of the acoustic target strengths of fish in dorsal aspect, including swimbladder resonance. J. Sound Vib. **15**: 397–420.

McFarlane, G., and Kieser, R. 1993. Canada–Japan fisheries acoustic technology workshop. Department of Fisheries and Oceans Canada, Ottawa, Ont.

McNaught, D.C. 1968. Acoustical determination of zooplankton distributions. Proc. Conf. Great Lakes Res. **11**: 76–84.

McNaught, D.C. 1969. Developments in acoustic plankton sampling. Proc. Conf. Great Lakes Res. **12**: 61–68.

Midttun, L. 1984. Fish and other organisms as acoustic targets. Rapp. P.-v. Réun. Cons. Int. Explor. Mer, **184**: 25–33.

Minnaert, M. 1933. On musical air bubbles and the sounds of running water. Philos. Mag. **16**: 235–248.

Nakken, O., and Olsen, K. 1977. Target strength measurements of fish. Rapp. P.-V. Réun. Cons. Int. Explor. Mer, **170**: 52–69.

Olsen, K. 1977. Orientation measurements of the cod in Lofoten obtained from underwater photographs and their relation to target strength. ICES CM/B: 25.

Peterson, M.L., Clay, C.S., and Brandt, S.B. 1976. Acoustic estimates of fish density and scattering function. J. Acoust. Soc. Am. **60**: 618–622.

Pieper, R.E., Holliday, D.V., and Kleppel, G.S. 1990. Quantitative zooplankton distributions from multifrequency acoustics. J. Plankton Res. **12**: 433–441.

Robinson, B.J. 1978. In situ measurement of fish target strength. *In* Proceedings of 1978 Institute of Acoustics Specialists Meeting on Acoustics in Fisheries, September 26–27, 1978. Hull College of Higher Education, Hull, England.

Rose, G.A. 1993. Cod spawning on a migration highway in the north-west Atlantic. Nature (London), **366**: 458–461.

Rose, G.A., and Leggett, W.C. 1988. Hydroacoustic signal classification of fish schools by species. Can. J. Fish. Aquat. Sci. **45**: 597–604.

Sand, O., and Hawkins, A.D. 1973. Acoustic properties of the cod swimbladder. J. Exp. Biol. **58**: 797–820.

Sætersdal, G., Stromme, T., Bakken, B., and Piekutowski, L. 1984. Some observations on frequency-dependent backscattering strength. FAO Fish. Rep. No. 300. pp. 150–156.

Smith, P.F. 1954. Further measurements of the sound scattering properties of several marine organisms. Deep-Sea Res. **2**: 71–79.

Stanton, T.K. 1982. Effects of transducer motion on echo-integration techniques. J. Acoust. Soc. Am. **72**: 510–514.

Stanton, T.K. 1988. Sound scattering by cylinders of finite length. I. Fluid cylinders. J. Acoust. Soc. Am. **83**: 55–63.

Stanton, T.K. 1989. Sound scattering by cylinders of finite length. III. Deformed cylinders. J. Acoust. Soc. Am. **86**: 691–705.

Stanton, T.K. 1990. Sound scattering by zooplankton. Rapp. P.-v. Réun. Cons. Perm. Int. Explor. Mer, **189**: 353–362.

Stanton, T.K., Chu, K., Wiebe, P.H., and Clay, C.S. 1993. Average echoes from randomly oriented random-length finite cylinders: zooplankton models. J. Acoust. Soc. Am. **94**: 3463–3472.

Strasberg, M. 1953. The pulsation frequency of nonspherical gas bubbles in liquids. J. Acoust. Soc. Am. **25**: 536–537.

Traynor, J.J., and Ehrenberg, J.E. 1979. Evaluation of the dual beam acoustic fish target strength measurement method. J. Fish. Res. Board Can. **36**: 1065–1075.

Trevorrov, M.V. 1996. Multifrequency acoustic investigations of juvenile and adult fish in Lake Biwa, Japan. J. Acoust. Soc. Am. **100**: 3042–3052.

Weston, D.E. 1967. Sound propagation in the presence of bladder fish. *In* Underwater acoustics. *Edited by* V.M. Albers. Plenum, New York. pp. 55–88.

Whitehead, P.J.P., and Blaxter, J.H.S. 1964. Swimbladder form in clupeoid fishes. Zool. J. Linn. Soc. **97**: 299–372

Wiebe, P.H., Greene, C.H., Stanton, T.K., and Burczynski, J. 1990. Sound scattering by live zooplankton and micronekton: empirical

© 1998 NRC Canada

studies with a dual-beam acoustical system. J. Acoust. Soc. Am. **88**: 2346–2360.

Ye, Z., and Farmer, D.M. 1994. Acoustic scattering from swim-bladder fish at low frequencies. J. Acoust. Soc. Am. **96**: 951–956.

Zakharia, M., and Sessarego, J.P. 1982. Sonar target classification using a coherent echo processing. *In* Proceedings of the IEEE International Conference on Acoustics, Speech, and Signal Processing, Paris, France. May 3–5, 1982. Published by the IEEE ASSP Society, New York. pp. 331–334.

© 1998 NRC Canada

ASSIGNMENT OF COPYRIGHT

Ms. No._____

To: NATIONAL RESEARCH COUNCIL OF CANADA ("NRC") Research Press

From: _____

_____

_____

_____

(name and address of author signing this form)

This refers to the manuscript entitled: _____

_____

written by myself and the following additional author(s): _____

_____

for publication in: _____

1. I declare that the list of authors fairly conforms to academic conventions about who should be listed. I declare that the manuscript, or its equivalent, has not been submitted for publication elsewhere. If it is accepted for publication by the National Research Council of Canada, I will ensure that it, or its equivalent, is not submitted for publication elsewhere.

2. I declare that I am (check ONE):

☐ (a) the sole owner of the copyright relating to the manuscript,	and →	I **assign** to NRC the entire copyright.
☐ (b) a part owner of the copyright, in conjunction with interests held by co-authors or their employers,	and →	I **assign** to NRC my entire interest in the copyright, and I expect the co-authors to also sign a form like this one.
☐ (c) an agent of my employer with authority to assign the copyright owned by the employer, who is: _____,	and →	I **assign** to NRC, on behalf of my employer, my employer's entire interest in the copyright relating to the manuscript, and I expect the co-authors to also sign a form like this one.
☐ (d) a public servant in Canada (federal, provincial or territorial) or the United Kingdom, so that the copyright is owned by Her Majesty,	and →	I have obtained the approval of my employer, according to the terms of my employment, to grant NRC **non-exclusive permission** to publish the manuscript and administer the copyright.
☐ (e) a public servant of the United States of America, and subject to the law that creates no U.S. copyright for the manuscript,	and →	I **assign** to NRC, on behalf of my employer, my employer's entire interest in any copyright that may exist outside the U.S., and I expect the co-authors to sign a form like this one.

3. I understand that my submission of this document does not guarantee publication, and that publication will not occur until **all authors** have provided a copyright transfer. If the manuscript is not published within 2 years after I sign this, the assignment is revoked.

Signed at _____ on _____

(City and Province/State) (Date)

_____

(Signature)

[*Standard NRC form; alterations not acceptable.*]

Comments on Copyright Transfer
(with extracts from the *Copyright Act*, Revised Statutes of Canada 1985, chapter C-42, as amended)

The publisher is not permitted to publish the manuscript without permission or an assignment of ownership of copyright. For greatest flexibility, and to be prepared to deal with future uses of the published material, the publisher requires ownership.

The owner may assign the right, but that assignment must be in writing:

13.(4) The owner of the copyright in any work may assign the right, either wholly or partially, and either generally or subject to territorial limitations, and either for the whole term of the copyright or for any other part thereof, and may grant any interest in the right by licence, but no assignment or grant is valid unless it is in writing signed by the owner of the right in respect of which the assignment or grant is made, or by his duly authorized agent.

The owner may be the author, but in many cases, the owner is the author's employer:

13.(3) Where the author of a work was in the employment of some other person under a contract of service or apprenticeship and the work was made in the course of his employment by that person, the person by whom the author was employed shall, in the absence of any agreement to the contrary, be the first owner of the copyright, but where the work is an article or other contribution to a newspaper, magazine or similar periodical, there shall, in the absence of any agreement to the contrary, be deemed to be reserved to the author a right to restrain the publication of the work, otherwise than as part of a newspaper, magazine or similar periodical.

The only exception to taking ownership arises when the manuscript is covered by Crown copyright owned by a Canadian government.

12. Without prejudice to any rights or privileges of the Crown, where any work is, or has been, prepared or published by or under the direction or control of Her Majesty or any government department, the copyright in the work shall, subject to any agreement with the author, belong to Her Majesty and in that case shall continue for the remainder of the calendar year of the first publication of the work and for a period of fifty years following the end of that calendar year.

Governments, and in particular the federal government, do not have a simple mechanism for assigning ownership of this particular type of Crown asset. Therefore, when an author is a public servant so that there is Crown copyright in the manuscript, a simple permission to use is acceptable to the publisher, if it is granted by a person with appropriate authority.

CESSION DU DROIT D'AUTEUR

Document n° _____

Au : CONSEIL NATIONAL DE RECHERCHES DU CANADA («CNRC») - Presses scientifiques

De : _____

_____

_____

_____

(nom et adresse de l'auteur qui signe le présent formulaire)

La présente cession porte sur le document intitulé : _____

_____

rédigé par moi, en collaboration avec l'auteur/les auteurs suivant(s) : _____

_____

aux fins de publication dans : _____

1. Je déclare que la liste des auteurs ci-dessus respecte les pratiques usuelles de rédaction savante quant aux personnes dont le nom doit être cité. Je déclare que le document ou son équivalent n'a pas été soumis à quelque autre organisme aux fins de publication. Si le CNRC accepte de publier le document, je m'assurerai que celui-ci ou son équivalent n'est soumis à aucun autre organisme aux fins de publication sans en obtenir la permission préalable du CNRC.

2. Je déclare être (UN SEUL choix) :

☐	(a) le seul titulaire de droit d'auteur afférent au document,	et →	je **cède** le droit d'auteur intégral au CNRC.
☐	(b) un titulaire partite du droit d'auteur, de concert avec des coauteurs ou leurs employeurs,	et →	je **cède** ma part du droit d'auteur au CNRC et m'attends à ce que les coauteurs signent une entente comparable.
☐	(c) un agent de mon employeur ayant l'autorité de céder le droit d'auteur appartenant à l'employeur, nommément : _____,	et →	je **cède** au CNRC, au nom de mon employeur, la part entière du droit d'auteur afférent au document appartenant à mon employeur, et m'attends à ce que les coauteurs signent une entente comparable.
☐	(d) un fonctionnaire du Canada (fédéral, provincial ou territorial) ou du Royaume-Uni, donc le droit d'auteur appartient à Sa Majesté,	et →	j'ai obtenu de mon employeur, en vertu de mes conditions d'emploi, l'autorisation d'accorder au CNRC la **permission non exclusive** de publier le document et de gérer le droit d'auteur.
☐	(e) un fonctionnaire des États-Unis d'Amérique, donc sujet à la loi qui n'associe aucun droit d'auteur américain au document,	et →	je **cède** au CNRC, au nom de mon employeur, la part entière de quelque droit d'auteur en vigueur ailleurs qu'aux É.-U. appartenant à mon employeur, et m'attends à ce que les coauteurs signent une entente comparable.

3. Je comprends que la soumission du document ne garantit aucunement sa publication et que la publication ne pourra être réalisée tant que **tous les auteurs** n'auront pas signé une cession du droit d'auteur. Si le document n'est pas publié dans les deux années suivant ma signature des présentes, la cession sera automatiquement révoquée.

Signé à _____ (ville et province/état), le _____ (date)

_____

(signature)

[Formulaire normalisé du CNRC; aucune modification permise]

Commentaires sur la cession du droit d'auteur
(accompagnés d'extraits de la *Loi sur le droit d'auteur*, Lois révisées du Canada 1985, chapitre C-42 modifié)

L'éditeur ne peut publier un document sans la permission ou une cession du droit d'auteur. Pour des raisons de souplesse et en vue de l'utilisation future du document publié, l'éditeur doit devenir titulaire du droit d'auteur.

Le titulaire peut céder le droit, mais cette cession doit être faite par écrit :

13.(4) Le titulaire du droit d'auteur sur une oeuvre peut céder ce droit, en totalité ou en partie, d'une façon générale, ou avec des restrictions territoriales, pour la durée complète ou partielle de la protection; il peut également concéder, par une licence, un intérêt quelconque dans ce droit; mais la cession ou la concession n'est valable que si elle est rédigée par écrit et signée par le titulaire du droit qui en fait l'objet, ou par son agent dûment autorisé.

Le titulaire peut être l'auteur, mais dans plusieurs cas, le titulaire est l'employeur de l'auteur:

13.(3) Lorsque l'auteur est employé par une autre personne en vertu d'un contrat de louage de service ou d'apprentissage, et que l'oeuvre est exécutée dans l'exercice de cet emploi, l'employeur est, à moins de stipulation contraire, le premier titulaire du droit d'auteur; mais lorsque l'oeuvre est un article ou un autre contribution, à un journal, à une revue ou à un périodique du même genre, l'auteur, en l'absence de convention contraire, est réputé posséder le droit d'interdire la publication de cette oeuvre ailleurs que dans un journal, une revue ou un périodique semblable.

La seule exception dans la cession du droit d'auteur est lorsque le document est associé au droit d'auteur de la Couronne, qui appartient au gouvernement du Canada .

12. Sous réserve de tous les droits ou privilèges de la Couronne, le droit d'auteur sur les oeuvres préparées ou publiées par l'entremise, sous la direction ou la surveillance de Sa Majesté ou d'un ministère du gouvernement, appartient, sauf stipulation conclue avec l'auteur, à Sa Majesté et, dans ce cas, il subsiste jusqu'à la fin de la cinquantième année suivant celle de la première publication de l'oeuvre.

Les gouvernements, en particulier le gouvernement fédéral, ne disposent pas d'un mécanisme simple de cession de droit d'auteur pour ce genre de biens de la Couronne. C'est pourquoi lorsqu'un auteur est un fonctionnaire et que, par conséquent, le droit d'auteur appartient à la Couronne, une simple permission d'usage est suffisante pour l'éditeur, pour autant que celle-ci ait été octroyée par une personne jouissant de l'autorité nécessaire pour ce faire.

CCFFR Web-Site:
http://www.phys.ocean.dal.ca/ccffr/index.html

Canadian Conference for Fisheries Research (CCFFR)

Edmonton, Alberta
8–10 January, 1999

The major themes of the **1999 Conference** will be:

(1) Effects of land use on stream fish and their habitat

(2) Impacts of endocrine disruptors and contaminants

(3) Changes in climate and ecosystems

(4) Innovative applications of genetics in fishery management

(5) **Joint CCFFR/SCL Session**: (to be announced)

Papers addressing the major themes are encouraged, although submissions on other themes related to fisheries and aquatic habitat biology are also welcome.

The **DEADLINE for abstracts is 11 September 1998**. Submit abstracts to the Program Committee Chair:

Dr. Dick Beamish
Pacific Biological Station
Nanaimo, BC V9R 5K6
Tel.: 250-756-7029
Fax: 250-756-7053
e-mail: beamishr@dfo-mpo.gc.ca

Instructions overleaf

For general information contact the CCFFR Secretary Treasurer:

Dr. Howard Powles
Tel.: 613-990-0285
Fax: 613-954-0807
e-mail: powlesh@dfo-mpo.gc.ca

Conference Canadienne de la recherche sur les peches (CCRP)

Edmonton (Alberta)
les 8–10 janvier 1999

Les principaux thèmes abordés lors de la **Conférence de 1999** seront :

(1) Les impacts de l'utilisation des terres sur les poissons de rivière et leurs habitats

(2) Les impacts des disrupteurs endocrinaires et des contaminants

(3) Changements climatiques et écosystémiques

(4) Applications innovatrices des études génétiques dans la gestion des pêches

(5) **Session Conjointe CCRP/SCL** : (sera annoncée ultérieurement)

Des contributions reliées aux thèmes principaux sont particulièrement sollicitées, mais des contributions sur d'autres thèmes reliés aux sciences halieutiques et à la biologie des habitats aquatiques sont également bienvenues.

La **DATE LIMITE pour la soumission des résumés est le 11 septembre 1998**. Veuillez les soumettre au :

Dr. Dick Beamish
Pacific Biological Station
Nanaimo (C-B) V9R 5K6
Téléphone : 250-756-7029
Télécopieur : 250-756-7053
Adresse électronique : beamishr@dfo-mpo.gc.ca

Instructions au verso

Pour d'autres renseignements, prendre contact avec le Secrétaire-trésorier de la CCRP :

Dr. Howard Powles
Téléphone : 613-990-0285
Télécopieur : 613-954-0807
Adresse électronique : powlesh@dfo-mpo.gc.ca

Abstract preparation

(Deadline: September 11, 1998)
Please follow these guidelines carefully to facilitate work of the Program Committee and to ensure a final program of high quality.

E-mail copy of Abstract:

Follow the guidelines below and send an ASCII (text) version of your abstract (do NOT use Word, WordPerfect, or other word processing formats) by e-mail to:

beamishr@dfo-mpo.gc.ca

(1) Place an asterisk (*) after the name of the person presenting the paper.

(2) Indicate whether the presentation will be oral (O; only standard 5 × 5 cm slide projector and overhead projector will be provided free of charge) or poster (P) after the title.

(3) Two concurrent paper sessions will be held and the number of oral presentations will be limited. Please indicate, on a separate line after the end of your abstract, if your presentation COULD be a poster even if your preference is for oral presentation. Please also indicate on this line to which theme (1–5) your presentation is most closely related. This line will not appear in the program.

(4) Follow this format:

Relationships between sunspots and sea stars (O)
Gretzky*, W., and J. Villeneuve. Department of Epidemiology, Eastern University, Yoho, Saskatchewan

Sea stars shine increasingly brightly as the sunspot cycle progresses...

Could be poster; theme 3

Hard copy of Abstract
As CCFFR moves to an electronic process for developing the program, hard copy abstracts will not be accepted except under exceptional circumstances. Contact the Program Chair.

Préparation des résumés

(Date limite : le 11 septembre 1998)
Veuillez respecter ces lignes directrices afin de faciliter le travail du Comité du Programme et d'assurer que le programme final soit de haute qualité.

Copie du résumé envoyée par courrier électronique

Suivre les lignes directrices et envoyer une version de votre résumé en ASCII (texte)(ne PAS utiliser formats Word, WordPerfect, ou autres formats de traitement de textes) par courrier électronique à :

beamishr@dfo-mpo.gc.ca

(1) Placer un astérisque (*) à coté du nom de la personne qui fera la présentation

(2) Indiquer après le titre si la présentation sera orale (O; seuls les projecteurs à diapositives 5 × 5 cm et les rétroprojecteurs seront fournis sans frais) ou affiche (A).

(3) Il y aura deux sessions concurrentes et le nombre de présentations orales sera restreint. Veuillez indiquer sur une ligne à part après la fin de votre résumé si votre présentation POURRAIT être par affiche même si vous préférez une présentation orale. Indiquer également sur cette ligne à quel thème votre contribution est le plus reliée (1–5). Cette ligne n'apparaîtra pas dans le programme.

(4) Format :

Predation par les euphausiaces sur les bebes phoques (O)
Villeneuve*, J., et W. Gretzky. Departement de planctonologie, Université de Trois Pistoles, Trois Pistoles (Québec)

Une augmentation subite de la mortalité des bébés phoques s'est avérée...

Pourrait être affiche; thème 3

Copie du résumé sur papier
Puisque la CCRP est en train de développer un processus entièrement électronique pour la préparation du programme, les résumés sur papier ne seront acceptés que pour des raisons exceptionelles. Veuillez prendre contact avec le Président du Comité du programme.

Perspectives on Canadian Marine Fisheries Management

L.S. Parsons and/et W.H. Lear (*Editors/Directeurs scientifiques*)

446 pages
Hardcover/Édition reliée
November/Novembre1993
ISBN 0-660-15003-4
ISSN 0706-6503
NRC/CNRC 36176
$55.00/55,00 $

This volume, Canadian Bulletin of Fisheries and Aquatic Sciences 226, is a collection of 15 articles describing management approaches in different fisheries arising from the diversity and complexity of Canada's marine fisheries. Visit http://www.nrc.ca/cisti/journals/books/perspe_e.html at the NRC Research Press Web site to view the Table of Contents.

On décrit dans ce document, le Bulletin canadien des sciences halieutiques et aquatiques 226 (un recueil des 15 articles), des approches de gestion de diverses pêches axées sur la diversité et la complexité des pêches maritimes canadiennes. Visitez http://www.nrc.ca/cisti/journals/books/perspe_f.html au site Web des Press scientifiques du CNRC pour consulter la table des matières.

To order copies of this publication/Pour commander des exemplaires de ce livre

- Telephone: (613) 993-0151
- Fax: (613) 952-7656
- Mail orders: Monograph Orders, NRC Research Press, National Research Council Canada, Ottawa, Ontario K1A 0R6, Canada
- Internet e-mail: research.journals@nrc.ca
- World Wide Web: http://www.nrc.ca/cisti/journals/formmono.html

Canadian customers please add 7% GST. Orders from Quebec add a further 6.5% QST to the total price including GST. Make cheque or money order payable to "Receiver General for Canada, credit NRC". Note that for all orders outside Canada, rates are in U.S. Dollars. All sales are final.

- Téléphone : (613) 993-0151
- Télécopieur : (613) 952-7656
- Par la poste : Monographies, Presses scientifiques du CNRC, Conseil national de recherches Canada, Ottawa (Ontario) K1A 0R6, Canada
- Courrier électronique : research.journals@nrc.ca
- World Wide Web : http://www.nrc.ca/cisti/journals/formmofr.html

Les clients canadiens doivent ajouter la TPS de 7 %. Les clients du Québec doivent ajouter 6,5 % de TVQ au montant total, une fois la TPS additionnée. Libellez le chèque ou le mandat à l'ordre du «Receveur général du Canada, au crédit du CNRC». Pour les clients non canadiens, les prix sont en dollars américains. Aucun remboursement.

Please send me ____ copies of/Veuillez me faire parvenir ____ exemplaire(s) de *Perspectives on Canadian Marine Fisheries Management.*

NRC Research Press

Monograph Program

Presses scientifiques du CNRC

Programme de monographies

NRC·CNRC

PLEASE PRINT/LETTRES MOULÉES

☐ Payment enclosed/Paiement inclus ☐ Charge to/Imputer à ☐ Visa ☐ MasterCard

Account number/ N° de compte | Expiry date/ Date d'expiration

Name/Nom

Signature/Signature

Address/Adresse

City/Ville Province/Province

Postal code/Code postal Country/Pays

Telephone/Téléphone Fax/Télécopieur

e-mail/Courrier électronique Date of order/Date de la commande

Numerical Methods in Atmospheric and Oceanic Modelling

The André J. Robert Memorial Volume

Charles A. Lin, René Laprise and/et Harold Ritchie (Editors/Directeurs scientifiques)

634 pages
November/Novembre 1997
Hardcover/Édition reliée
ISBN 0-9698414-4-2
NRC/CNRC 41646
$79.95/79,95 $

This book, co-published with the Canadian Meteorological and Oceanographic Society, is a collection of papers by leading scientists in the field of numerical modelling, from the 1994 André J. Robert Memorial Symposium on Numerical Methods in Atmospheric and Oceanic Sciences. Visit http://www.nrc.ca/cisti/journals/41646/tc41646.html to view the Table of Contents.

Cet ouvrage, publié en collaboration avec la Société canadienne de météorologie and d'océanographie, est une collection d'articles, basés sur des conférences présentées par des scientifiques réputés lors du 1994 Symposium à la mémoire d'André J. Robert. Visitez http://www.nrc.ca/cisti/journals/41646/ftc41646.html pour afficher le table des matières du livre.

To order copies of this publication/Pour commander des exemplaires de ce livre

- Telephone: (613) 993-0151
- Fax: (613) 952-7656
- Mail orders: Monograph Orders, NRC Research Press, M-55, National Research Council Canada, Ottawa, Ontario K1A 0R6, Canada
- Internet e-mail : research.journals@nrc.ca
- World Wide Web: http://www.nrc.ca/cisti/journals/formmono.html

Canadian customers please add 7% GST. Orders from Quebec add a further 6.5% QST to the total price including GST. Make cheque or money order payable to "Receiver General for Canada, credit NRC". Note that for all orders outside Canada, rates are in U.S. dollars. Prepayment required. All sales are final.

- Téléphone : (613) 993-0151
- Télécopieur : (613) 952-7656
- Par la poste : Monographies, Presses scientifiques du CNRC, M-55, Conseil national de recherches Canada, Ottawa (Ontario) K1A 0R6, Canada
- Courrier électronique : research.journals@nrc.ca
- World Wide Web : http://www.nrc.ca/cisti/journals/formmofr.html

Les clients canadiens doivent ajouter la TPS de 7 %. Les clients du Québec doivent ajouter 6,5 % de TVQ au montant total, une fois la TPS additionnée. Libellez le chèque ou le mandat à l'ordre du «Receveur général du Canada, au crédit du CNRC». Pour les clients non canadiens, les prix sont en dollars américains. Toute commande doit être payée d'avance. Aucun remboursement.

Please send me _____ copies of/Veuillez me faire parvenir _____ exemplaires du *Numerical Methods in Atmospheric and Oceanic Modelling.*

NRC Research Press

Conference Proceedings

Presses scientifiques du CNRC

Comptes rendus de conférences

NRC·CNRC

PLEASE PRINT/LETTRES MOULÉES

☐ Payment enclosed/Paiement inclus ☐ Charge to/Imputer à ☐ Visa ☐ MasterCard

Account no./ N° de compte | Expiry date/ Date d'expiration

Name/Nom

Signature/Signature

Address/Adresse

City/Ville Province/Province

Postal code/Code postal Country/Pays

Telephone/Téléphone Fax/Télécopieur

e-mail/Courrier électronique Date of order/Date de la commande

Guide to the Parasites of Fishes of Canada. Part IV. Trematoda

David I. Gibson

373 pages
Softcover/Édition brochée
March/mars 1996
ISBN 0-660-16403-5
ISSN 0706-6481
NRC/CNRC 40083
$42.95/42,95 $
Canadian Special Publication of Fisheries and Aquatic Sciences/ Publication spéciale canadienne des sciences halieutiques et aquatiques 124

More than 80 keys leading to the identification of more than 220 species of trematode parasites of Canadian fishes and diagnoses of more than 80 family–group taxa and 130 genera are given. Each genus is illustrated. For each species a Canadian host list, locality data, and any relevant remarks are included. Visit http://www.nrc.ca/cisti/journals/40083/133to136.html at the NRC Research Press Web to view a short chapter of this book.

On retrouve plus de 80 clefs qui permettent d'identifier quelque 220 espèces de trématodes parasites des poissons du Canada et la description de plus de 80 taxums de famille/groupe et de 130 genres. Chaque genre y est illustré. À chaque espèce sont associées des données sur l'emplacement et des remarques particulières. Visitez http://www.nrc.ca/cisti/journals/40083/f133to6.html au site Web des Presses scientifiques du CNRC pour afficher un court chapitre du livre.

To order copies of this publication/Pour commander des exemplaires de ce livre

- Telephone: (613) 993-0151
- Fax: (613) 952-7656
- Mail orders: Monograph Orders, NRC Research Press, National Research Council Canada, Ottawa, Ontario K1A 0R6, Canada
- Internet e-mail: research.journals@nrc.ca
- World Wide Web: http://www.nrc.ca/cisti/journals/formmono.html

Canadian customers please add 7% GST. Orders from Quebec add a further 6.5% QST to the total price including GST. Make cheque or money order payable to "Receiver General for Canada, credit NRC". Note that for all orders outside Canada, rates are in U.S. dollars. All sales are final.

- Téléphone : (613) 993-0151
- Télécopieur : (613) 952-7656
- Par la poste : Monographies, Presses scientifiques du CNRC, Conseil national de recherches Canada, Ottawa (Ontario) K1A 0R6, Canada
- Courrier électronique : research.journals@nrc.ca
- World Wide Web : http://www.nrc.ca/cisti/journals/formmofr.html

Les clients canadiens doivent ajouter la TPS de 7 %. Les clients du Québec doivent ajouter 6,5 % de TVQ au montant total, une fois la TPS additionnée. Libellez le chèque ou le mandat à l'ordre du «Receveur général du Canada, au crédit du CNRC». Pour les clients non canadiens, les prix sont en dollars américains. Aucun remboursement.

Please send me ____ copies of/Veuillez me faire parvenir ____ exemplaire(s) de *Guide to the Parasites of Fishes of Canada: Part IV. Trematoda.*

NRC Research Press

Monograph Program

Presses scientifiques du CNRC

Programme de monographies

NRC·CNRC

PLEASE PRINT/LETTRES MOULÉES

☐ Payment enclosed/Paiement inclus ☐ Charge to/Imputer à ☐ Visa ☐ MasterCard

Account no./ N° de compte | | | | | | | | | | | | | | | | | | Expiry date/ Date d'expiration ____

Name/Nom

Signature/Signature

Address/Adresse

City/Ville Province/Province

Postal code/Code postal Country/Pays

Telephone/Téléphone Fax/Télécopieur

e-mail/Courrier électronique Date of order/Date de la commande

Margaret A. Cartwright, David A. Beauchamp, and Mason D. Bryant 1285–1295

Quantifying cutthroat trout (*Oncorhynchus clarki*) predation on sockeye salmon (*Oncorhynchus nerka*) fry using a bioenergetics approach

PERSPECTIVE

PERSPECTIVE

John K. Horne and Clarence S. Clay 1296–1306

Sonar systems and aquatic organisms: matching equipment and model parameters

Bruce M. Davis and Thomas N. Todd	**1140–1148**	Competition between larval lake herring (*Coregonus artedi*) and lake whitefish (*Coregonus clupeaformis*) for zooplankton
Eric T. Schultz, David O. Conover, and Amir Ehtisham	**1149–1157**	The dead of winter: size-dependent variation and genetic differences in seasonal mortality among Atlantic silverside (Atherinidae: *Menidia menidia*) from different latitudes
Kevin D. Friedland, David G. Reddin, Nobumichi Shimizu, Ruth E. Haas, and Alan F. Youngson	**1158–1168**	Strontium:calcium ratios in Atlantic salmon (*Salmo salar*) otoliths and observations on growth and maturation
Richard C. Lathrop, Stephen R. Carpenter, Craig A. Stow, Patricia A. Soranno, and John C. Panuska	**1169–1178**	Phosphorus loading reductions needed to control blue-green algal blooms in Lake Mendota
Peter Nonacs, Paul E. Smith, and Marc Mangel	**1179–1188**	Modeling foraging in the northern anchovy (*Engraulis mordax*): individual behavior can predict school dynamics and population biology
Vanessa L. Lougheed, Barb Crosbie, and Patricia Chow-Fraser	**1189–1197**	Predictions on the effect of common carp (*Cyprinus carpio*) exclusion on water quality, zooplankton, and submergent macrophytes in a Great Lakes wetland
D.G. McDonald, W.J. McFarlane, and C.L. Milligan	**1198–1207**	Anaerobic capacity and swim performance of juvenile salmonids
D.G. McDonald, C.L. Milligan, W.J. McFarlane, S. Croke, S. Currie, B. Hooke, R.B. Angus, B.L. Tufts, and K. Davidson	**1208–1219**	Condition and performance of juvenile Atlantic salmon (*Salmo salar*): effects of rearing practices on hatchery fish and comparison with wild fish
M. Vignaux, G.A. Vignaux, S. Lizamore, and D. Gresham	**1220–1227**	Fine-scale mapping of fish distribution from commercial catch and effort data using maximum entropy tomography
R.L. Klotz	**1228–1235**	Influence of beaver ponds on the phosphorus concentration of stream water
Barry D. Smith, Louis W. Botsford, and Stephen R. Wing	**1236–1247**	Estimation of growth and mortality parameters from size frequency distributions lacking age patterns: the red sea urchin (*Strongylocentrotus franciscanus*) as an example
Alan F. Sinclair	**1248–1263**	Estimating trends in fishing mortality at age and length directly from research survey and commercial catch data
Louis Bernatchez, J. Brian Dempson, and Sylvain Martin	**1264–1272**	Microsatellite gene diversity analysis in anadromous arctic char, *Salvelinus alpinus*, from Labrador, Canada
Doran M. Mason, Timothy B. Johnson, and James F. Kitchell	**1273–1284**	Consequences of prey fish community dynamics on lake trout (*Salvelinus namaycush*) foraging efficiency in Lake Superior

National Research Council Canada
Ottawa, Canada K1A 0R6

Conseil national de recherches Canada
Ottawa, Canada K1A 0R6

Postage paid at Ottawa
Publications mail
Registration No. 1240579

Port payé à Ottawa
Poste-publication
Enregistrement n° 1240579

Canadian Journal of Fisheries and Aquatic Sciences

Volume 55, Number 5, May 1998

Journal canadien des sciences halieutiques et aquatiques

Volume 55, numéro 5, mai 1998

ARTICLES		ARTICLES
Harry V. Leland and Steven V. Fend	**1051–1067**	Benthic invertebrate distribution in the San Joaquin River, California, in relation to physical and chemical factors
Dany Bussières, Marthe Monique Gagnon, Julian Dodson, and Peter V. Hodson	**1068–1077**	Does annual variation in growth and sexual maturation of white sucker (*Catostomus commersoni*) confound comparisons between pulp mill contaminated and reference rivers?
Richard Carignan, Anne-Marie Blais, and Chantal Vis	**1078–1084**	Measurement of primary production and community respiration in oligotrophic lakes using the Winkler method
Charles P. Madenjian, George E. Noguchi, Robert C. Haas, and Kathrin S. Schrouder	**1085–1092**	Sexual difference in polychlorinated biphenyl accumulation rates of walleye (*Stizostedion vitreum*)
Klaus P. Brodersen, Melbourne C. Whiteside, and Claus Lindegaard	**1093–1103**	Reconstruction of trophic state in Danish lakes using subfossil chydorid (Cladocera) assemblages
Nicola Urbani, Bernard Sainte-Marie, Jean-Marie Sévigny, David Zadworny, and Urs Kuhnlein	**1104–1113**	Sperm competition and paternity assurance during the first breeding period of female snow crab (*Chionoecetes opilio*) (Brachyura: Majidae)
Lisa Atwell, Keith A. Hobson, and Harold E. Welch	**1114–1121**	Biomagnification and bioaccumulation of mercury in an arctic marine food web: insights from stable nitrogen isotope analysis
Thomas P. Hurst and David O. Conover	**1122–1130**	Winter mortality of young-of-the-year Hudson River striped bass (*Morone saxatilis*): size-dependent patterns and effects on recruitment
Evan P. Dobson and Gerald L. Mackie	**1131–1139**	Increased deposition of organic matter, polychlorinated biphenyls, and cadmium by zebra mussels (*Dreissena polymorpha*) in western Lake Erie

Continued on inside back cover / Suite au verso

Canada

Printed in Canada by / Imprimé au Canada par
University of Toronto Press Inc.
Typesetting by / Typographie par
NRC Research Press / Presses scientifiques du CNRC

0706-652X(199805)55:5;1-X